Epidemiology and Pathophysiology of Clostridial Dermatitis (Cellulitis) in Turkeys

Megan Elizabeth Folk Lighty

Dissertation submitted to the faculty of the Virginia Polytechnic Institute and State University in partial fulfillment of the requirements for the degree of

Doctor of Philosophy
in
Biomedical and Veterinary Sciences

F. William Pierson, chairman
Tanya LeRoith, co-chairman
François Elvinger
Robert D. Evans
Nammalwar Sriranganathan

September 3, 2015
Blacksburg, VA

Keywords: clostridial dermatitis, cellulitis, turkeys, *Clostridium*

Epidemiology and Pathophysiology of Clostridial Dermatitis (Cellulitis) in Turkeys

Megan Elizabeth Folk Lighty

ABSTRACT

Clostridial dermatitis (CD) is a multifactorial disease of rapidly-growing turkeys. *Clostridium septicum* (Cs) has been identified as the primary cause, although *C. perfringens* (Cp) has also been implicated. Pathogenesis is not fully understood; however, it is hypothesized that *Clostridia* translocate from the gastrointestinal tract and spread hematogenously to capillary beds of skeletal muscles. Intense genetic selection has produced a rapidly growing bird that is heavier and less active. This may predispose birds to development of CD due to positional restriction of blood flow to the caudal breast and medial thigh. Subsequent reduction in oxygen tension within these tissues produces conditions conducive to germination, proliferation, and toxin production by previously trapped, non-replicative *Clostridia*.

Studies were undertaken to investigate the epidemiology and pathophysiology of CD. Retrospective epidemiologic investigations evaluated incidence, risk factors, and economic impact of CD. Cs and Cp qPCR were performed on blood and tissue samples to demonstrate hematogenous spread in asymptomatic birds. Studies assessed the effect of prolonged recumbency by measuring oxygen saturation and surface temperature in dependent tissues. Tissues from CD cases were evaluated for Cs and Cp alpha toxin mRNA (CsA and CpA). Analyses were conducted to determine associations between these toxins and severity of histopathologic lesions. Whole genome sequencing was performed on the Cs type strain to identify other toxin genes.

Flock type, breed, weight at time of processing, and stocking density affected disease incidence. Detection of *Clostridium* spp. in intestine, liver, and muscle from asymptomatic

turkeys without cutaneous trauma implies hematogenous spread from an endogenous source. Focal polyphasic myonecrosis in dependent muscles of asymptomatic turkeys suggests an underlying predisposition to development of CD. Recumbency appeared to be associated with decreased perfusion to these tissues. Cs DNA was present in asymptomatic birds without corresponding CsA mRNA expression suggesting that organisms were present in a quiescent form. CsA was associated with CD while CpA did not appear to be involved in pathogenesis. Genome sequencing identified several coding regions which may correspond to other potentially active Cs toxins. These results support the proposed mechanism of pathogenesis and provide targets for further investigation of disease pathophysiology and vaccine development.

DEDICATION

This work is dedicated to my parents, for always believing in me even when I didn't always believe in myself.

ACKNOWLEDGEMENTS

I shed a lot of blood, sweat, and tears while working on this PhD but I could never have completed this arduous process without the assistance of family, friends, advisors, co-workers, and members of the turkey industry. Words cannot express the depth of my gratitude to Mom, Dad, Grandma, Christopher, and Jeanne. Their encouragement, support, and generosity made it possible for me to get through this program. I would like to acknowledge the members of my PhD committee, Dr. F. William Pierson (advisor), Dr. Tanya LeRoith (co-advisor), Dr. François Elvinger, Dr. Robert Evans, and Dr. Nammalwar Sriranganathan for educating, encouraging, motivating, and supporting me. Thank you for putting up with the crazy scheduling and long disappearances from the lab that came with being dual-enrolled in the DVM program.

Funding for these studies was provided by Cargill Turkey Products, LLC in Harrisonburg, VA and Virginia Poultry Growers Cooperative in Hinton, VA. I am grateful to the veterinarians, flock supervisors, and growers of these companies, as well as Prestage Farms Inc. of Clinton, NC and Circle S Ranch of Monroe, NC, for sharing their wealth of knowledge and providing me with access to turkey flocks for data and sample collection. I would also like to acknowledge the National Turkey Federation, especially Drs. Michael Rybolt and Hilary Thesmar, for their cooperation in generating, distributing, and collecting the national cellulitis incidence and economic impact surveys.

I am indebted to the researchers at AgTech (Dupont) in Waukesha, WI, especially Tony Neumann, for providing me with a crash-course in anaerobic bacteriology and molecular diagnostics. Thanks to Dr. Miranda Vieson for her assistance identifying, describing, and taking photos of histopathology lesions. Thank you to Dr. William Huckle for taking the time to explain qPCR data analysis to a confused graduate student; his assistance with interpreting results and troubleshooting assays was invaluable. Thank you to Dr. Durelle Scott, Associate Professor in the Department of Biological Systems Engineering, for allowing me to borrow his thermal imaging camera. I am incredibly grateful for the efforts of Dr. Vivek Kapur, Robab Katani, and Lingling Li in the Department of Veterinary and Biomedical Sciences at Penn State for their help in making sense of my genome sequencing data. Chapter 6 would not have been possible without their insight. Thank you to Dr. Robert Wideman Jr., Professor of Physiology in the Department of Poultry Science at the University of Arkansas, for sharing ideas to refine my

proposed mechanism of pathogenesis and suggesting possible methods for testing those hypotheses. I appreciate the assistance of Dr. Rami Dalloul and Jon Salevsky of the Avian Immunology Lab in the Department of Animal and Poultry Sciences at Virginia Tech in designing the sample collection protocol for the mRNA toxin gene expression study and especially Jon for collecting samples for me while I was in vet school.

Thanks to the past and present members of the Avian Medicine Lab, especially Mary Mainous, Lori Settle, and Jessica Walters, for their friendship and assistance with sample collection, protocol development, troubleshooting, and editing. I am grateful for the efforts of Nancy Tenpenny and Kay Carlson who were always willing to answer questions and lend equipment and supplies. Thank you to the CMMID glassware ladies (Debby, Doris, and Allie) for their assistance and especially for putting up with my foul-smelling biohazardous waste. Thank you to everyone else at CMMID who made it such a great place to work. Thanks to Becky Jones for keeping all of the paperwork straight and for always being willing to listen and provide motherly advice and to Jill Kormendy for her assistance in keeping track of my advisor. Last, but certainly not least, I could not have gotten through this program without the support of my fellow graduate students, vet school classmates, and friends. Thanks for listening to me rant and making sure I took the time to have some fun along the way.

ATTRIBUTIONS

Several colleagues contributed to the study design, data analysis, writing, and editing of several chapters of this dissertation.

Chapter 2: A version of this chapter has been submitted to the *Journal of Applied Poultry Research* and is currently under review.

François Elvinger Dr.med.vet, PhD (Population Health Sciences) is currently a professor at VMCVM. Dr. Elvinger is a co-author on this manuscript and contributed to the study design, statistical analysis, writing, and editing.

Robert D. Evans, DVM, PhD is currently a veterinarian with Elanco. Dr. Evans is a co-author on this manuscript and contributed to the study design and provided access to flock records for the regional epidemiologic study.

Tanya LeRoith, DVM, PhD (Biomedical Sciences and Pathobiology) is currently an assistant professor at VMCVM. Dr. LeRoith is a co-author on this manuscript and contributed to the study design and editing.

Nammalwar Sriranganathan, BVSc, MVSc, PhD (Biomedical Science and Pathobiology) is currently a professor at VMCVM. Dr. Sriranganathan is a co-author on this manuscript and contributed to the study design.

F. William Pierson, MS, DVM, PhD, (Population Health Sciences) is currently a professor at VMCVM. Dr. Pierson is a co-author on this manuscript and contributed to the study design and editing.

Chapters 3 and 5:

Miranda Vieson, DVM (Biomedical Sciences and Pathobiology) is currently a pathology resident and PhD student at VMCVM. Dr. Vieson will be a co-author on the resulting manuscripts and assisted with obtaining histopathology images and interpretation of histopathology findings.

Tanya LeRoith will be a co-author on the resulting manuscripts and contributed to the scoring of skeletal muscle pathology and interpretation of histopathology findings.

Chapter 6:

Robab Katani is currently a PhD candidate in pathobiology at Penn State. Ms. Katani will be a co-author on the resulting manuscript and responsible for the genome assembly.

LingLing Li is a research assistant in the Department of Veterinary and Biomedical Science at Penn State. Ms. Li will be a co-author on the resulting manuscript and assisted with genome assembly.

Dr. Vivek Kapur, BVSc, PhD is currently a Professor of Veterinary and Biomedical Sciences at Penn State. Dr. Kapur will be a co-author on the resulting manuscript and assisted with genome assembly.

TABLE OF CONTENTS

LIST OF FIGURES

LIST OF TABLES

ABBREVIATIONS AND ACRONYMS

ATP	adenosine triphosphate
BHI	brain heart infusion broth
BLAST	Basic Local Alignment Search Tool
CD	clostridial dermatitis
CDS	coding sequence
CFU	colony forming unit
Cs	*C. septicum*
CsA	*C. septicum* alpha toxin
Cp	*C. perfringens*
CpA	*C. perfringens* alpha toxin
Cq	quantification cycle
CTM	chopped turkey meat broth
DNA	deoxyribonucleic acid
HRP	horseradish peroxidase
mPES	modified polyethersulfone
mRNA	messenger ribonucleic acid
MWCO	molecular weight cut-off
PBS	phosphate buffered saline
qPCR	quantitative (real-time) polymerase chain reaction
RAST	Rapid Annotation using Subsystem Technology
qRT-PCR	quantitative (real-time) reverse transcriptase polymerase chain reaction
SDS-PAGE	sodium dodecylsulfate-polyacrylamide gel electrophoresis
SpO_2	oxygen saturation
VMCVM	Virginia-Maryland College of Veterinary Medicine at Virginia Tech

Chapter 1 – Clostridial Dermatitis (Cellulitis) in Turkeys: A Review of Relevant Literature

1.0 Introduction

Increased mortality and subcutaneous necrosis in turkeys resulting from infection with *Clostridium* species is not a recent phenomenon, but until the early 1990s such findings were typically described in isolated reports [1, 2]. Within the last twenty years vertically integrated and large commercial turkey companies in the United States have experienced an increase in subcutaneous clostridial infections. Poultry veterinarians have ranked clostridial dermatitis (CD), also referred to as cellulitis, as a top concern facing the turkey industry [3, 4]. CD appears to be restricted to broad-breasted white turkeys that have been selected for rapid growth. While the condition occurs in both conventional and organic production systems there have been no reports to date in wild, heritage breed, or range-reared turkeys [5].

The turkey industry and several university research groups are interested in expanding our understanding of the etiology and pathogenesis of CD. Much of the information available concerning the incidence and factors contributing to the development of CD is anecdotal. It is generally accepted that the incidence of the condition varies by geographic region, company, and farm. Some companies have reported a seasonal increase in incidence during the summer and most state that the incidence is higher in toms than in hens [1, 6, 7]. However, to date there has been no formal study looking at incidence in or cost of the condition to the turkey industry. *Clostridium septicum* has recently been identified as the primary causative agent for CD in turkeys [8, 9]. *C. perfringens* has also been shown to be able to induce the disease in experimental models [9]. Other organisms including *C. sordellii*, *Staphylococcus aureus*, *Escherichia coli*, and *Streptococcus* species have been isolated from affected birds and may play

a role in the pathogenesis of the disease [10]. Many questions remain regarding the pathogenesis of CD in turkeys and the risk factors which contribute to the development of this condition.

1.1 Overview of *Clostridium* species

Organisms in the genus *Clostridium* are Gram positive, rod-shaped, spore-forming anaerobic bacteria which are unable to perform sulfate reduction [11]. While generally accepted to be Gram positive organisms, some isolates of *Clostridium* may appear Gram variable or Gram negative depending on the length of incubation or the presence of endospores [11, 12]. Bergey's Manual of Systematic Bacteriology recognizes 168 species belonging to the genus *Clostridium;* however, over 200 species have been proposed [12, 13]. Clostridia are ubiquitous; present in soil, dust, water, marine sediments, the gastrointestinal tracts of animals and humans, and decaying plant and animal matter [14, 15]. Currently only 35 *Clostridium* species are known to cause disease in animals or humans [16]. Fifteen *Clostridium* species are known to produce exotoxins, potent toxins excreted by the bacteria into the surrounding environment [13]. Pathogenic *Clostridium* species do not invade eukaryotic cells but rather exert damage from a distance via secreted exotoxins [17]. These toxins are antigenic proteins with bioactive properties that damage host tissues or interfere with biochemical processes in the host resulting in disease [14]. Exotoxins cause damage to host tissues either by blocking the action of an essential host enzyme system, therefore interfering with important metabolic pathways, or by acting as enzymes themselves [18]. The clostridial toxins are divided into two groups: the major toxins which induce damage to host cells at very low concentrations and the less potent minor toxins [17]. The toxins produced by a certain species of *Clostridium* were named, typically designated by a Greek letter, in the order of their discovery; therefore, the structure and activity

of the toxin of one species does not necessarily correlate with that of a similarly named toxin of a different species [14]. The major toxins of *C. septicum* and *C. chauvoei* are an exception to this generalization, given the close relationship between these two species.

The production of toxins and other related compounds by members of the genus *Clostridium* is highly variable throughout growth of the organism due to environmental conditions and nutrient availability. Production of toxins by *C. perfringens* peaks during the late log phase of growth [19, 20]. Through a process known as quorum sensing, individual bacterial cells are capable of both producing and detecting certain low-molecular mass signal molecules called autoinducing peptides [21, 22]. The concentration of these peptides is directly proportional to the size of the bacterial population. Quorum sensing allows a population of unicellular bacteria to act in concert allowing for the modulation of virulence factor production as well as adaptation to the metabolic demands of living as a community in a particular niche [22]. The presence of glucose in culture medium appears to be essential for the production of the alpha and delta toxins of *C. septicum in vitro* [23]. The production of a toxin *in vitro* does not necessarily correspond to activity of that toxin *in vivo*. Mariano *et al.* showed that while *C. perfringens* cultures grown in both brain heart infusion (BHI) and cooked meat medium (CMM) resulted in significant phospholipase C (PLC) activity in vitro, cultures grown in BHI demonstrated the greatest lethality *in vivo* [24]. The amount of these toxic compounds produced *in vitro* can be variable, even under ideal culture conditions. Multiple cultures of the same strain of *C. septicum* have been reported to produce variable amounts of neuraminidase despite the use of seemingly identical culture media and conditions [23]. Some factors present in certain types of culture media are capable of inactivating certain toxins. Production of hemolysin by *C. septicum* in cooked meat medium is equaled or exceeded by inactivation of the hemolysin by

lipids present in the medium [25, 26]. The variable nature of toxin production contributes to difficulty in correlating the results of *in vitro* analysis of *Clostridium* cultures with the pathogenesis of clostridial diseases *in vivo*.

Clostridium species are able to persist in the environment for long periods of time, even when conditions are unfavorable for vegetative growth, because of their ability to form spores. The formation of endospores provides the best protection against extremes of temperature and pH, lack of nutrients, desiccation, ultraviolet and ionizing radiation, antimicrobial compounds, toxic chemicals, phagocytosis and other environmental factors that are detrimental to the survival of vegetative cells [27-29]. The process of sporulation is typically initiated by a lack of suitable nutrients or other hostile conditions in the organism's environment [29, 30]. The resulting spores exist in a dormant state with no measurable metabolic activity [28]. When environmental conditions once again become favorable for vegetative growth, the spores germinate allowing the bacteria to resume normal metabolic and reproductive activity. Scientists have been able to successfully revive bacterial spores millions of years after their formation [31]. The ability of *Clostridium* species to form spores plays an important role in the pathogenesis of clostridial diseases.

1.1.1 Clostridium septicum and Clostridium chauvoei

C. septicum and *C. chauvoei* are very closely related organisms and considered by some to be subtypes of a single species [14, 15]. While the two organisms do share some somatic and spore antigens, therefore cross-agglutinating, they are distinct organisms biochemically, morphologically, pathologically, and serologically [14, 26, 32]. *C. septicum* is found as a normal inhabitant of both soil and the gastrointestinal tracts of humans and animals; however, *C.*

chauvoei is an obligate parasite of the gastrointestinal tract of animals [26, 32]. *C. septicum* and *C. chauvoei* are motile organisms which can swarm across the surface of solid culture media [14].

Both *C. septicum* and *C. chauvoei* produce four major toxins: a pore-forming alpha toxin which is lethal, necrotizing, hemolytic (oxygen-stable hemolysin) and has lecithinase activity; a beta toxin which is a DNase and leukocidin; a gamma toxin which is a hyaluronidase; and a delta toxin which is an oxygen-labile hemolysin [14, 15, 33, 34]. The alpha toxin of these organisms is initially secreted as an inactive protoxin. Binding of the toxin to its receptor on a target cell triggers cleavage by furin which allows aggregation of multiple toxin monomers to form a beta-barrel that is inserted into the cellular membrane of the host cell to form a pore [17]. Other cellular proteases including trypsin and proteinase K have also been shown to cleave the *C. septicum* alpha toxin into its active form [35]. The beta toxin is a heat-resistant deoxyribonuclease which is produced in an active form [32]. The gamma toxin is a heat-labile hyaluronidase [14]. This enzyme hydrolyzes the glycosidic bonds between the *N*-acetylglucosamine and glucuronic acid residues of hyaluronic acid which is a main component in the extracellular matrix of connective, epithelial, and neural tissues [36]. It is theorized by some that the activity ascribed to the gamma toxin is actually the result of several enzymes possessing hyaluronidase activity [26]. The delta toxin is an oxygen-labile hemolysin similar to the theta toxin of *C. perfringens* which produces more rapid hemolysis than the alpha toxin of *C. septicum* or *C. chauvoei* [14]. Although the delta toxin is very sensitive to inactivation by oxidation, this inactivation may be reversible in the presence of reducing agents such as sodium hydrosulfite, sodium thioglycolate, hydrogen sulfide, or cystein [14, 26].

C. septicum also produces several other potentially toxic compounds that exert activity on host cells including hemagglutinin, neuraminidase (sialidase), fibrinolysin, and chitinase [15, 26, 33]. Autolysis of the bacterial cell in four- to six-day old broth cultures of *C. septicum* releases a thermo-labile hemagglutinin [26]. It produces a neuraminidase which alters cell membrane glycoproteins rendering host cells more susceptible to the activity of other toxins produced by the bacteria [14]. The neuraminidase also aids in the spread of *C. septicum* through host tissues via its action on mucoproteins [14, 26]. A fibrinolysin has been identified in the cell-free filtrate of *C. septicum* isolates [15]. Some strains of *C. chauvoei* have also been demonstrated to produce a neuraminidase [32]. While the exact role of these other products in the virulence of these organisms remains unclear, they likely contribute to an increase in capillary permeability thus furthering the development of myonecrosis and toxemia [33].

C. septicum is pleomorphic, occurring in two forms: vegetative, short, motile rods and giant, filamentous, multinucleated, hyperflagellated swarm cells capable of rapid concerted migration across solid surfaces [37, 38]. These different forms of the organism play various roles in the pathogenesis of disease due to differences in their biochemical and metabolic properties. The short, motile, rod form of *C. septicum* produces higher amounts of alpha toxin thus exhibiting greater cytotoxicity toward epithelial cells and possesses a greater capacity for adhesion and invasion of epithelial cells [38]. The majority of the pathology associated with clostridial infections is due to the production of toxins and hydrolytic enzymes which act as spreading factors; however, the ability of the rod form of *C. septicum* to adhere to, invade, and proliferate within epithelial cells is important for virulence early in the course of disease when bacterial numbers are low and host tissues maintain higher oxygen tensions [38, 39]. When quorum sensing indicates that the number of vegetative cells of *C. septicum* in a particular

location reaches a certain critical mass, the short, motile rods at the periphery of the colony may undergo differentiation into long, filamentous, multinucleated, hyperflagellated swarm cells [21, 40]. Swarming allows for the coordinated movement of a population of bacteria large distances across solid surfaces, contributing to virulence of the organism by facilitating the spread of infection. Individual swarm cells join together to form rafts, aligning themselves along their long axis, which move as a result of coordinated flagellar activity [40, 41]. Swarm cells can revert to the short, motile rod form through a process known as consolidation [40]. *C. septicum* colonies can cycle through periods of vegetative growth, differentiation, swarm migration, and consolidation dependent on nutrient availability and population numbers [40, 41].

1.1.2 Clostridium perfringens

Clostridium perfringens, previously known as *C. welchii*, is the most commonly isolated clostridial pathogen [42]. *C. perfringens* isolates are capable of producing at least sixteen distinct toxins whose roles in pathogenesis include disruption of phospholipid membranes, hyaluronic acid, collagen, proteins, and DNA as well as inducing hemolysis and necrosis [14, 15]. The toxins produced by *C. perfringens* isolates are categorized as major lethal toxins, minor toxins (soluble antigens), and 'other' toxins [14]. There are four major toxins (alpha, beta, epsilon, and iota) and at least 9 minor toxins (delta, theta, kappa, lambda, mu, nu, gamma, eta, and neuraminidase) [14, 15, 42]. Another important toxin produced by many strains of *C. perfringens* is the enterotoxin. There is some dispute as to whether this toxin should be classified as a "major" toxin or an "other" toxin [14, 42]. More recently, a toxin associated with necrotic enteritis (netB) and second form of the beta toxin (beta 2) have been identified [43, 44]. Despite having similar biological activity to the beta toxin, the beta 2 toxin shares little sequence

homology with other clostridial toxins [45]. All the major toxins and many of the minor toxins of *C. perfringens* have been demonstrated to be lethal when injected into animal models [42].

Although *C. perfringens* is known to produce at least 17 distinct toxins, individual isolates are only capable of expressing certain combinations of toxins [46]. Isolates of *C. perfringens* are classified as one of five toxin types (A, B, C, D, or E) based on the presence or absence of each of the four major lethal toxins (alpha, beta, epsilon, and iota). Of the major lethal toxins, Type A isolates only produce the alpha-toxin; type B isolates produce the alpha, beta, and epsilon toxins; type C isolates produce the alpha and beta toxins; type D isolates produce the alpha and epsilon toxins; and type E isolates produce the alpha and iota toxins. Some earlier papers also include reference to a *C. perfringens* type F which also produces the alpha and beta toxins; however, this toxin type classification has largely been abandoned due to its similarity to type C [14, 15, 39]. *C. perfringens* type A is present as a normal inhabitant of the environment (soil) and within the gastrointestinal tracts of humans and many animal species while types B-E are obligate parasites, found primarily within the gastrointestinal tracts of domestic animals [39]. Only type A and type C isolates of *C. perfringens* have been implicated as causes of disease in poultry [43].

Type A strains of *C. perfringens* produce the alpha and kappa toxins, the neuraminidase and the enterotoxin. They may also produce the eta, theta, mu, and nu toxins. The alpha toxin of *C. perfringens* is the primary component responsible for the pathogenesis of lesions in gas gangrene [17]. It is a zinc metalloenzyme with phospholipase C activity which hydrolyzes phosphatidylcholine, lecithin, and sphingomyelin resulting in the degradation of phospholipid membranes [14, 17, 47]. The presence of *C. perfringens* alpha toxin in a clinical sample can be

verified by detection of lecithinase activity on egg yolk agar and a characteristic double zone of hemolysis on blood agar.

The phospholipase enzymatic action of the *C. perfringens* alpha toxin can directly trigger lysis of the cell it is interacting with. It can also indirectly result in the lysis of other cells through the upregulation of endogenous phospholipases. The phospholipid byproducts resulting from membrane degradation then trigger activation of the arachadonic cascade which results in inflammation and vasoconstriction [17, 45]. Low levels of toxin at the periphery of the gangrene lesion inhibit leukocyte migration by enhancing aggregation to the vascular endothelium. Phospholipase C also promotes platelet-platelet and platelet-neutrophil aggregation within the vasculature [17]. These intravascular aggregates cause blockage of the small blood vessels decreasing oxygen transport to the tissues surrounding the region of necrosis which expands the region of local anaerobic conditions to enable further spread of *C. perfringens*.

Strains of *C. perfringens* Type C produce two major toxins: the alpha toxin, as is present in strains of *C. perfringens* Type A, and the beta toxin. Type C isolates produce several minor toxins. These include the delta, theta, kappa, and nu toxins as well as the neuraminidase and enterotoxin; some isolates also produce the gamma, and mu toxins [14]. The beta toxin is a lethal, necrotizing, pore-forming, trypsin labile, thermolabile, highly oxygen-sensitive protein [13, 14]. Activity of the beta toxin is responsible for the enteric lesions seen in necrotic enteritis [17]. The beta toxin is extremely sensitive to protease activity; therefore, pathology due to the beta toxin is typically only seen in very young animals with low gastrointestinal tract protease activity or in animals on a low-protein diet which results in decreased trypsin activity [13].

Production of enterotoxin has been demonstrated by strains of *C. perfringens* Types A, C, and D [14]. The enterotoxin exhibits enterotoxic and cytotoxic properties [14, 42]. This toxin is

a spore-associated toxin that is not produced during normal growth conditions [42]. Presence of this toxin has been associated with cases of foodborne illness in the absence of large numbers of vegetative organisms [14, 42]. Enterotoxin also appears to play a role in non-foodborne gastrointestinal illness, possibly due to ingestion or inhalation of environmental isolates or transmission from person to person [45]. The enterotoxin binds to receptors on the surface of intestinal epithelial cells. The binding causes an increase in intracellular calcium levels which results in altered membrane permeability and ultimately cell death due to a loss of cellular fluids and ions [14].

1.2 Clostridial Diseases

Toxigenic clostridia are responsible for numerous clinically and economically important diseases of people and animals (Table 1.1) [14, 15, 48-53]. The course of many clostridial infections is typically acute, with sudden death often the first sign of illness [15, 50]. Rapid post-mortem decomposition is commonly seen with mortality due to clostridial infection [50]. Both of these factors contribute to difficulty in elucidating the pathogenesis of clostridial diseases. The diseases caused by these organisms can be classified as neurologic, enteric/hepatic, or soft tissue infections. Infection or intoxication due to *C. botulinum*, the causative agent of botulism, and *C. tetani*, the causative agent of tetanus, can cause fatal neurologic disease in mammals and birds [14, 15]. Strains of *C. difficile*, *C. novyi*, *C. coilinum*, *C. sordellii*, *C. perfringens*, and *C. septicum* cause enterotoxaemia as a result of oral ingestion of bacteria and/or pre-formed bacterial toxins. Some of these strains also cause hepatitis associated with liver fluke infestation [50]. Wound infections, and less commonly non-traumatic soft tissue infections, have been

associated with *C. chauvoe*i, *C. histolyticum*, *C. novyi*, *C. perfringens* (*C. welchii*), *C. septicum*, and *C. sordellii* [15, 50].

Clostridium species are pathogenic only under limited host environmental conditions [15]. These organisms are not capable of infecting normal, healthy tissue as the oxygen tension present in such tissues precludes the growth of anaerobic organisms. Loss of blood supply to a region, the presence of foreign material in a wound, necrotic tissue, hemorrhage, and growth of other types of bacteria are capable of producing localized areas of reduced oxygen tension creating an environment suitable for the germination and proliferation of *Clostridium* species [15]. Some clostridial diseases are the result of intoxication, rather than infection. The pathogenesis of these conditions does not rely on the presence of devitalized tissue as preformed soluble toxins, rather than proliferation of the organism itself, are responsible for the development of lesions. For diseases that result from clostridial infection, production of toxins by proliferating organisms leads to further devitalization of tissues resulting in rapid spread of the lesion. Mortality from these diseases is typically the result of toxins entering systemic circulation leading to shock and ultimately death [15].

Some *Clostridium* species, notably *C. septicum* and *C. perfringens,* are frequent post-mortem invaders. They spread rapidly from the gut where they are present as normal flora to other tissues as decomposition produces an environment favorable for anaerobic growth [46, 50]. Isolation of these species from tissues at necropsy does not necessarily represent a true clostridial infection. The diagnosis of clostridial infections is further complicated by the fact that *C. perfringens* is fairly oxygen tolerant and grows rapidly in culture thus making it easier to isolate than some other species of *Clostridium* which may lead to the false impression that *C. perfringens* was present in pure culture [50]. *C. septicum* and *C. sordellii* swarm across the

surface of solid media which can make it appear as if these organisms were present in overwhelming numbers in a diagnostic sample [50]. Accurate diagnosis of clostridial diseases requires integration of the microbiology report with historical and clinical information.

Table 1.1 Diseased caused by pathogenic *Clostridium* species

Disease	Causative Agent	Species Affected
Neurotrophic Diseases		
Tetanus	*C. tetani*	Mammals, birds
Botulism	*C. botulinum* Types A-G	Mammals, birds
Focal Symmetrical Encephalomalacia	*C. perfringens* Type D	Lambs, goats (rare)
Enteric Disease		
Foodborne illness	*C. perfringens* Type A	Humans
Necrotic Enteritis	*C. perfringens* Type A *C. perfringens* Type B *C. perfringens* Type C	Chickens, turkeys, other fowl Lambs, foals Chickens, turkeys, other fowl, humans, sheep, pigs, calves
Enterotoxemia	*C. perfringens* Type A *C. perfringens* Type B *C. perfringens* Type C *C. perfringens* Type E *C. spiroforme*	Cattle, goats, horses, dogs, alpacas, lambs (rare), others Sheep, goats, calves, foals, guinea pigs Lambs, calves, pigs, humans Calves, lambs, guinea pigs, rabbits Rabbits, laboratory rodents
Struck	*C. perfringens* Type C subtype 1	Adult sheep
Pulpy Kidney (Overeating) Disease	*C. perfringens* Type D	Sheep, goats (occasional), cattle (rare)
Ulcerative enteritis	*C. colinum*	Quail, chickens, turkeys, other game birds
Bacillary hemoglobinuria (Red Water Disease)	*C. haemolyticum* (*C. novyi* Type D)	Cattle, sheep, dogs (rare)
Braxy	*C. septicum*	Sheep, calves (rare)
Tyzzer's Disease	*C. piliforme*	Horses, rabbits, dogs (rare), cats (rare), calves (rare)
Infectious Necrotic Hepatitis (Black Disease)	*C. novyi* Type B	Sheep, cattle (occasional), pigs (rare), horses (rare)
Antibiotic-associated diarrhea	*C. difficile*	Humans
Spontaneous *C. difficile*-associated diarrhea	*C. difficile*	Horses, pigs, calves, dogs, cats, hamsters, guinea pigs, rats, rabbits
Soft Tissue Infections		
Gas Gangrene/Anaerobic Cellulitis	*C. chauvoei*, *C. histolyticum*, *C. novyi* *C. perfringens* Type A, *C. septicum*, *C. sordellii*, and *C. fallax* (rare)	Humans
Blackleg/Blackquarter	*C. chauvoei* and *C. septicum* (rare)	Even-toed ungulates, pigs (rare), horses (rare)
Malignant Edema	*C. septicum;* also *C. chauvoei*, *C. perfringens*, *C. novyi*, *and C. sordellii*	Cattle, sheep, horses, others
Big Head	*C. novyi*, *C. sordellii*, and *C. chauvoei (rare)*	Young rams
Gangrenous Dermatitis	*C. perfringens* Type A	Chickens, turkeys
Clostridial Dermatitis (Cellulitis)	*C. septicum*	Turkeys

1.2.1 Enteric Diseases

Multiple species of *Clostridium* can cause enteric disease in humans and animals. These diseases range in severity from uncomplicated food poisoning to fatal enterotoxemia. Clostridial enteric diseases occur when a host ingests either preformed toxins or vegetative cells or spores which subsequently produce toxins *in situ*. The action of exotoxins on the intestinal mucosa is responsible for the pathology associated with these conditions [54]. These diseases typically represent a primary intestinal pathology; however, they can also occur secondary to septicemia and bacteremia [50]. Certain *Clostridium* species can be found in the liver of healthy animals; damage to the liver parenchyma allows for the migration of these organisms via the blood stream or lymphatics to the gastrointestinal tract where they proliferate and produce toxins [48]. In sheep and cattle, black disease is seen secondary to hepatic necrosis caused by migration of the liver fluke, *Fasciola hepatica*, and bacillary hemoglobinuria occurs secondary to either liver fluke migration, migration of the tapeworm *Cysticercus tenuicollis*, or necrobacillosis caused by *Fusobacterium necrophorum* [48, 50]. Mechanical trauma to the abomasum following ingestion of frozen forage predisposes sheep to the development of braxy [48, 52]. Vegetative *Clostridium* cells are not able to survive the acidic conditions in the stomach; however, spores are able to pass through to the intestines where they germinate and colonize when disturbances in the resident microflora result in favorable conditions for clostridial growth [17]. Risk factors leading to clostridial colonization include ingestion of large numbers of enterotoxigenic *Clostridium*, young age with immature resident microflora, antibiotic use, rapid change in diet, overeating, ingestion of rough forage resulting in mechanical damage to the intestinal mucosa, and intestinal carcinoma [17, 48]. Some clostridial toxins produced within the gastrointestinal tract are capable of passing through the intestinal mucosa into systemic circulation. This condition, known as

enterotoxemia, produces systemic shock and frequently results in sudden death [17]. Enterotoxemia generally has a low incidence but high mortality in veterinary species [45].

The most notable clostridial enteric disease in poultry is necrotic enteritis caused by *C. perfringens* types A and C [14]. This disease primarily affects young chickens but can also be seen in turkeys, game birds, and wild birds. Two forms of necrotic enteritis can occur in poultry flocks: acute clinical and subclinical [55]. The classical acute clinical form is characterized by a rapid rise in flock mortality, often without any outward clinical signs. The alpha toxin of *C. perfringens* Type A and the beta toxin of *C. perfringens* Type C cause necrosis of the small intestinal mucous membrane [56]. Other toxins, including the beta 2 toxin and the net B toxin, produced by some strains of *C. perfringens* may play an important role in the pathogenesis of necrotic enteritis [43, 57]. Intestines of affected birds are often friable and distended with gas. The mucosal surface appears gray and thickened with a tightly adhering pseudomembrane, resulting in the classic "Turkish towel" appearance [56]. Lesions are typically restricted to the distal third of the small intestine [52]. While the beta toxin can induce hemorrhagic necrosis, hemorrhage is not a prominent feature of necrotic enteritis [56]. The intestinal lesions are often accompanied by hepatitis and cholecystitis [56, 58]. The subclinical form is typically not accompanied by a rise in mortality, but rather manifests as decreased production. The associated decreases in growth rate and feed conversion are the result of reduced digestion and absorption of nutrients and the increased condemnations at processing are due to hepatitis [43, 56, 59]. Damage to the intestinal mucosa facilitates adhesion of *C. perfringens* [60]. Adhesion is the first step in the sequence of colonization which ultimately leads to manifestation of disease [61]. This damage also results in the leakage of plasma proteins into the intestinal lumen; these proteins serve as a substrate for proliferation of *C. perfringens* [43]. The exact circumstances that trigger

toxin production within the gastrointestinal tract of birds remain unclear. However, studies have shown that coccidiosis, intestinal mucosal damage due to the use of high fiber litter, high stocking density, rapid changes in diet, high concentrations of cereal grains (wheat, rye, oat, and barley) in the diet, diets high in animal proteins (especially fish-meal), relatively high concentrations of dietary zinc, increased intestinal pH, and increased digesta viscosity with subsequent increased gut passage time predispose flocks to the development of necrotic enteritis [52, 56, 58, 60]. Many of these predisposing factors stimulate increased mucous production by the small intestine; this results in proliferation of mucolytic bacteria which in turn provide the substrates necessary for clostridial proliferation [56]. Immunosuppression due to management-related stress and/or previous or concurrent exposure to infectious bursal disease, chick infectious anemia virus, and Marek's disease also predisposes to the development of necrotic enteritis [60].

Ulcerative enteritis (quail enteritis), caused by *C. colinum,* is seen in young chickens, turkeys, and upland game birds and is characterized by a rapid peak in mortality [62]. Chronically infected birds serve as a source of the organism and its ability to form spores allows for persistence in the environment [58]. This condition can be differentiated from necrotic enteritis based on the presence of marked duodenal hemorrhagic enteritis. Early in the course of the disease, small yellow foci of necrosis surrounded by hemorrhage are present on the mucosal surface of the intestines. As the disease progresses the hemorrhagic border becomes less distinct as the lesions may coalesce to form large regions of diptheritic necrosis. In many cases the ulcers ultimately extend through the serosal surface of the intestines resulting in the development of peritonitis and intestinal adhesions [62]. Lesions can be found in any portion of the intestine and ceca but are most commonly found in the caudal third of the intestines [58, 62]. Lesions

within the ceca may present as foci with a central depression filled with dark material that cannot be rinsed off [62]. Splenic congestion, hemorrhage, and/or necrosis may be seen [58, 62]. As with necrotic enteritis, the intestinal lesions are often accompanied by hepatitis [62]. Previous gastrointestinal stress, such as coccidiosis, predisposes birds to the development of ulcerative enteritis [58].

1.2.2 Soft Tissue Infections

There are two main pathogeneses that can lead to clostridial infection of soft tissues. Contamination of wounds by *Clostridium* species is the most common method and results in gas gangrene in humans, malignant edema in sheep and cattle, and gangrenous dermatitis in chickens [14, 15]. In the absence of an external wound, soft-tissue infection can occur from the passage of spores, vegetative cells, or toxins from the gastrointestinal tract into the circulatory system. Organisms and/or toxins are then carried to distant sites where they cause disease. Nontraumatic clostridial infections include idiopathic gas gangrene in people and blackleg in ruminants [15]. Clostridial exotoxins play crucial roles in the pathogenesis of these clostridial soft-tissue infections. They induce disease through the lysis of host cells via destruction of cell membranes, by triggering the host inflammatory response in small blood vessels resulting in vasoconstriction and decreased oxygen concentrations in muscle and connective tissues, and by aiding the spread of bacteria throughout host tissues [17]. Various terms (dermatitis, cellulitis, fasciitis, and myositis) are used to describe these soft-tissue infections depending on which layer or layers are affected. The terminology used to describe these conditions is often confusing due to the use of multiple classification systems based on anatomical location, microbiology, and clinical presentation.

The pathogenesis of post-traumatic infections can vary greatly depending on the type and location of the precipitating injury. Deep penetrating injuries such as puncture or stab wounds can become contaminated by organisms from the skin's normal flora adhering to the instrument responsible for the initial injury. As the wound scabs over, an anaerobic environment is created which allows for the growth of anaerobic organisms such as *Clostridium*. Burns, blunt force injuries, and long-term pressure (i.e. bed sores) can also result in regions of devitalized or ischemic tissue. Tissue becomes ischemic when the vascular supply to the region is damaged or impaired and can occur through several mechanisms. Trauma causes direct damage to blood vessels. Tissue hypoxia can also result from peripheral vasoconstriction occurring in reaction to severe hemorrhage or severe dehydration [63]. Toxin-induced vascular occlusion due to aggregation of platelets and leukocytes can occur in response to the production of certain bacterial exotoxins (e.g. *C. perfringens* phospholipase C) [64]. The low oxygen tension of ischemic tissue also inhibits leukocyte bactericidal activity. If leukocytes are able to migrate to the site of infection, the lack of oxygen prevents production of reactive oxygen species and hypochlorous acid (HOCl) which are required for the effective destruction of certain bacterial species [63]. Localized tissue anoxia results in regional acidosis due to the production of lactic acid by the tissues themselves. This acidic environment promotes the activity of proteolytic enzymes produced by *Clostridium* species [65]. The proteolytic activity of certain clostridial exotoxins including hemolysin, hyaluronidase, and collagenase can damage tissue directly.

In human medicine, clostridial soft tissue infections are divided into three categories: simple wound contamination, anaerobic cellulitis, and gas gangrene [66]. Simple wound contaminations are the most common, with 30-80% of open traumatic wounds contaminated by *Clostridium* species [15, 67]. With simple wound contamination, the conditions within the

wound are barely suitable for the proliferation and elaboration of toxins by most *Clostridium* species; therefore infection does not spread to the underlying tissues [66]. Anaerobic cellulitis occurs when a contaminated wound contains a moderate amount of devitalized tissue resulting in an environment with decreased oxygen tension suitable for the proliferation of *Clostridium* species [67]. While gas production does extend along facial planes, clostridial invasion of healthy tissues and bacteremia are not present with anaerobic cellulitis. Anaerobic cellulitis is rarely fatal so long as devitalized tissues are promptly debrided [67]. Gas gangrene, also referred to as anaerobic myositis or clostridial myositis, is an anaerobic infections of muscle characterized by toxemia, localized edema, tissue necrosis, and crepitus [15]. In true gas gangrene there is clostridial invasion of healthy tissues that were not affected by the initial trauma [67]. Gas gangrene is most typically the result of coinfection by two or three species of *Clostridium*, often with involvement of other organisms including aerobic cocci and coliforms [66]. Reports of gas gangrene date back to the middle ages [15]. True gas gangrene is rare in civilian life and is estimated to be 10-100 times more common in war due to the severity of wartime injuries, heavy soil contamination of wounds, and delayed treatment [15, 66]. Prognosis for patients with gas gangrene is much better for wounds on the extremities than wounds on the trunk as aggressive surgical debridement is necessary to prevent further clostridial invasion of healthy tissues [67]. Mortality in patients with gas gangrene is not the direct result of toxin production by *Clostridium* species, but rather due to cardiovascular shock [26, 68].

Recurrent episodes of gas gangrene have been observed in patients that recovered from an initial episode of gas gangrene subsequent to a wound infection. *Clostridium* spores have been demonstrated to remain dormant within tissues for up to twenty years, germinating when localized conditions are favorable for anaerobic growth [65, 67, 69]. Spontaneous gas gangrene,

in the absence of trauma, can also occur. *C. septicum* is one of the more aerotolerant species of *Clostridium* and therefore is able to survive and proliferate within healthy tissues [67]. An endogenous source of *C. septicum* has been implicated in human cases of spontaneous non-traumatic gangrene, typically associated with an underlying malignancy [70-72]. Colonic carcinoma, gastrointestinal surgery, leukemia, lymphoproliferative disorders, cancer chemotherapy, radiation therapy, and AIDS have all been implicated as risk factors for the development of spontaneous gas gangrene [67]. In these conditions, cyclic neutropenia and/or underlying damage to the wall of the gastrointestinal tract allow for bacterial translocation into the bloodstream. Once the bacteria have begun to proliferate in tissues, suppression of the immune system as a result of malignancy and/or chemotherapy allows for continued proliferation and dissemination [72].

Similar clostridial wound infections and spontaneous clostridial soft tissue infections occur in many species of domestic animals. Malignant edema is the term used to describe traumatic clostridial wound infections in domestic animals, primarily cattle, sheep, and horses. These infections are most commonly caused by *C. septicum*; however, C. *chauvoei*, *C. perfringens*, *C. novyi*, and *C. sordellii* have also been implicated [48, 73]. Malignant edema typically presents as an acute, febrile episode with edematous and gangrenous inflammation of the skin and subcutaneous tissues [73]. These soft tissue infections typically present as a cellulitis, rarely progressing to the level of a myositis [48, 74]. Common causes of wounds leading to the development of malignant edema in domestic animals include: castration, tail-docking, dehorning, shearing, inoculation, penetrating stake wounds, injuries to the female genitalia during parturition, and umbilical infections [74, 75].

Blackleg, also referred to as blackquarter, is an example of a clostridial disease that occurs as a result of a spontaneous soft tissue infection. It is primarily a disease of cattle although it can occur in other species including sheep, goats, swine, mink, horses, and pigs [75]. While blackleg has a worldwide distribution, outbreaks tend to be localized to specific regions and to specific farms within those regions [74]. Blackleg may present as sudden death without any overt clinical illness [58]. Moribund animals present as febrile, anorexic and depressed with a rapidly progressing, edematous, necrotizing myositis [58, 75]. In blackleg, spores of *C. chauovei* or rarely *C. septicum* pass through the intestinal mucosa and enter circulation; the exact mechanism is not understood [50, 75]. The spores travel through the blood stream and localize in healthy skeletal muscle. These spores remain dormant until local conditions in the muscle are favorable for germination and proliferation of *C. chauovei* [58, 75]. Although the specific triggers for activation are not known, reduced oxygen tension and low pH likely contribute to this process. Impairment of capillary perfusion of tissues, possibly the result of increased pressure on dependent muscle groups, may contribute. Pressure placed on areas of healthy tissue as a result of inflammatory swelling or mechanical pressure can lead to ischemia with subsequent tissue necrosis [76]. The presence of a localized anaerobic environment allows the C*lostridium* to proliferate and begin production and secretion of various exotoxins. These toxins result in necrosis of healthy tissues at the margins of the lesion, thus creating additional areas of devitalized tissue enabling the organism to spread.

Gangrenous dermatitis is a disease of chickens and turkeys that typically presents as an acute increase in flock mortality. This condition can be caused by *C. perfringens* Type A or C, *C. septicum,* or *S. aureus* either alone or in combination [77, 78]. Lesions on affected birds include necrosis of the skin and subcutaneous tissues of the breast, abdomen, wing, and/or thigh.

Affected tissues are edematous and emphysematous. Gangrenous dermatitis is generally considered to be the result of secondary infection of a primary wound as lesions are typically associated with skin scratches [79]. While parenchymal organs are typically not affected swelling, infarction, necrotic foci in the liver, and/or bursal atrophy may be present [77, 79]. Prior immunosuppression is considered an essential component in the pathogenesis of this disease. Infections with infectious bursal disease virus, chicken infectious anemia virus, reticuloendotheliosis virus, or avian adenovirus have all been implicated in contributing to the development of gangrenous dermatitis [77]. High stocking densities, high production, aflatoxicosis, nutritional disturbances or imbalances, poor litter quality, improper drinker management, and poor ventilation have also been shown to increase susceptibility to the disease [77, 79]. A genetic component to susceptibility to gangrenous dermatitis has also been proposed as studies have shown that progeny from certain breeder flocks are more prone to development of the disease [77]. While there is some debate as to whether gangrenous dermatitis and CD (cellulitis) represent the spectrum of a single disease or two separate conditions, CD is different in that the lesions of this disease are not associated with skin scratches. CD is considered to be a "spontaneous" soft tissue infection with an endogenous source of *Clostridium* species.

While *Clostridium* species are generally accepted as the causative agents for these soft tissue infections, it is important to note that *Clostridium* species are rarely isolated in pure culture from these wounds [15]. Frequently, multiple species of *Clostridium* as well as other non-clostridial organisms are isolated. In humans, mixed clostridial infections seem to be more virulent than monoclostridial infection, especially when either *C. septicum* or *C. histolyticum* is present as part of the mixed culture [15]. It remains unclear whether the presence of other non-clostridial organisms merely represents subsequent contamination of the wound or if these

organisms actually play an important role in the pathogenesis of clostridial soft tissue infections. *Clostridium* species can also be present as wound contaminants, without representing a true clostridial infection. Additionally, pathogenic *Clostridium* species have been isolated from healthy tissues, likely the result of translocation of bacteria from the gastrointestinal tract [66].

1.3 Clostridial Dermatitis (Cellulitis) in Turkeys

Clostridial infection of subcutaneous tissues in turkeys was first described in the scientific literature in 1939 [2]. Although the term "clostridial dermatitis" is never explicitly used in this paper, the condition described is similar to the condition seen by turkey producers today. Fifty-two years passed before another mention of CD in turkeys appeared in the scientific literature [80]. For much of the twentieth century, reports of *Clostridium* infections in turkeys were sporadic with moderate increases in mortality. Recent increases in the incidence and severity of CD have driven research efforts into the etiology and pathogenesis of this condition.

In 2008 the Minnesota Turkey Research and Promotion Council held a Gold Medal Panel of turkey industry representatives and researchers to discuss CD. One outcome of the meeting was to officially rename the condition "clostridial dermatitis' (previously known as cellulitis) and to update the formal criteria required to diagnose CD in turkeys. For an individual bird to be diagnosed with CD based on the official definition developed by veterinarians and industry representatives, the bird must present with at least two of the following six signs: a) subcutaneous emphysema; b) serum/serosanguinous subcutaneous fluid; c) vesicles on the skin, especially on the breast-inguinal area; moist, dark, wrinkled skin, especially on the breast-inguinal area; d) cellular necrosis (microscopic); e) organ involvement (spleen/liver); and f) vesicles on the skin, moist, dark, wrinkled skin, or both on tail area [10]. A flock is diagnosed

with CD if the mortality with lesions characteristic of the disease is greater than or equal to 0.5 dead per 1000 birds over two consecutive 24 hour periods [10]. Personal communications with flock supervisors and company veterinarians suggest that elevated mortality with characteristic necrotic lesions on the breast and inguinal regions is the main criterion used in the field to identify CD-positive flocks; histopathology and bacteriological isolation are generally not performed as part of routine diagnostics. *C. septicum* has been identified as the primary agent responsible for the development of CD in turkeys [8]. *C. perfringens* and occasionally *C. sordellii* have also been associated with outbreaks of the disease but the role of these organisms remains unclear [7, 10]. The details of the pathogenesis of this disease are not fully understood. It is hypothesized that the natural route of infection is via hematogenous spread of organisms invading or leaking from the gastrointestinal tract [10, 81]. *C. septicum* has been identified in the blood of live asymptomatic turkeys supporting the possibility of hematogenous spread of the organism [82]. While veterinarians in some regions of the country consider the condition a true dermatitis [9], some veterinarians argue that the subcutaneous lesions of CD are not accompanied by skin lesions required to classify the infection as dermatitis.

Some laboratories have reported success in the development of an experimental challenge model to study CD [8, 9, 83, 84]. However, some question remains as to whether these models truly replicate field challenge. The limited success of oral challenge models in recreation of the disease has led some researchers to hypothesize that the natural route of infection is through skin scratches, similar to the pathogenesis of gangrenous dermatitis in chickens [10, 85]

When the Henle-Koch postulates were first developed it was believed that the presence of a specific pathogenic microorganism was responsible for the development of a particular disease (Table 1.2) [86]. However, scientists quickly realized that various host, organism, and

environmental factors can play an essential role in the development of disease. While *C. septicum* is recognized as the primary causative agent for the development of CD in turkeys, researchers have been unable to fulfill the third postulate since experimental oral inoculation with *C. septicum* does not repeatedly reproduce the disease [87]. CD in turkeys is a multifactorial disease; the presence of *C. septicum* alone is not sufficient to induce the disease. The causal relationship between *C. septicum* and CD in turkeys is better explained through Evan's Unified Concept for Consideration of Causality (Table 1.3) [86].

Table 1.2: The Henle-Koch Postulates [86, 88]

1. The parasite occurs in every case of the disease in question and under circumstances which can account for the pathological changes and clinical course of the disease.
2. It occurs in no other disease as a fortuitous and non-pathogenic parasite.
3. After being fully isolated from the body and repeatedly grown in pure culture, it can induce the disease anew.

Table 1.3: Evan's Criteria for Causation: A Unified Concept [86]

1. *Prevalence* of the disease should be significantly higher in those exposed to the putative cause than in cases controls not so exposed.[a]
2. *Exposure* to the putative cause should be present more commonly in those with the disease than in controls without the disease when all risk factors are held constant.
3. *Incidence* of the disease should be significantly higher in those exposed to the putative cause than in those not so exposed as shown in prospective studies.
4. *Temporally,* the disease should *follow* exposure to the putative agent with a distribution of incubation periods on a bell shaped curve.
5. *A spectrum* of host responses should follow exposure to the putative agent along a logical biological gradient from mild to severe.
6. *A measureable host response* following exposure to the putative cause should *regularly appear* in those lacking this before exposure (i.e., antibody, cancer cells) or should *increase* in magnitude if present before exposure; this pattern should not occur in persons so exposed.
7. *Experimental reproduction of the disease* should occur in higher incidence in animals or man appropriately exposed to the putative cause than in those not so exposed; this exposure may be deliberate in volunteers, experimentally induced in the laboratory, or demonstrated in a controlled regulation of natural exposure.
8. *Elimination or modification* of the putative cause or of the vector carrying it should decrease the incidence of the disease (control of polluted water or smoke or removal of the specific agent).
9. *Prevention or modification* of the host's response on exposure to the putative cause should decrease or eliminate the disease (immunization, drug to lower cholesterol, specific lymphocyte transfer factor in cancer).
10. The whole thing should make biological and epidemiological sense.

[a]The putative cause may exist in the external environment or in a defect in host response.

While many questions remain regarding the pathogenesis of CD in turkeys, we propose that the mechanism of pathogenesis is similar to that of blackleg in cattle and sheep (Figure 1.1). Low numbers of *C. perfringens* are considered normal flora in the intestinal tract of poultry [89, 90]. While it remains unclear whether *C. septicum* should be classified as normal flora versus transient flora in poultry, the organism has been isolated from the gastrointestinal tract, liver and blood of healthy birds [10, 82, 91]. Although there are no visible lesions in the gut of turkeys with CD, certain factors may alter the permeability of the gut wall allowing for translocation of *Clostridium* species. These factors include sudden changes in diet, coccidiosis, and any

disturbance in normal gastrointestinal flora. *Clostridium* species then travel through the blood stream and localize in the capillary beds of subcutaneous tissue or skeletal muscle where they remain dormant as spores. Isolation of *C. septicum* from the blood and liver of healthy birds provides support for the theory of hematogenous spread [82]. *Clostridium* spores remain dormant in muscle until conditions become favorable for anaerobic growth. Older birds are more susceptible to the development of CD; mortality and severity of lesions were more pronounced in 7 week old turkeys compared to 3 week old turkeys following experimental inoculation with *C. septicum* or *C. perfringens* [87]. The turkeys that develop CD are typically the biggest birds in a flock; these bigger birds frequently have musculoskeletal issues in their legs resulting in them spending prolonged periods of time sitting down. Pressure from sitting may result in localized anoxia to the dependent portions of the breast and thigh muscles. The resulting decrease in oxygen tension to these tissues would favor the germination and proliferation of *Clostridium* species. Localized toxin production results in the observed cellulitis and myositis and allows for the lesions to spread. Death ultimately follows as a result of systemic toxemia.

Figure 1.1: Proposed Mechanism of Pathogenesis for Clostridial Dermatitis in Turkeys

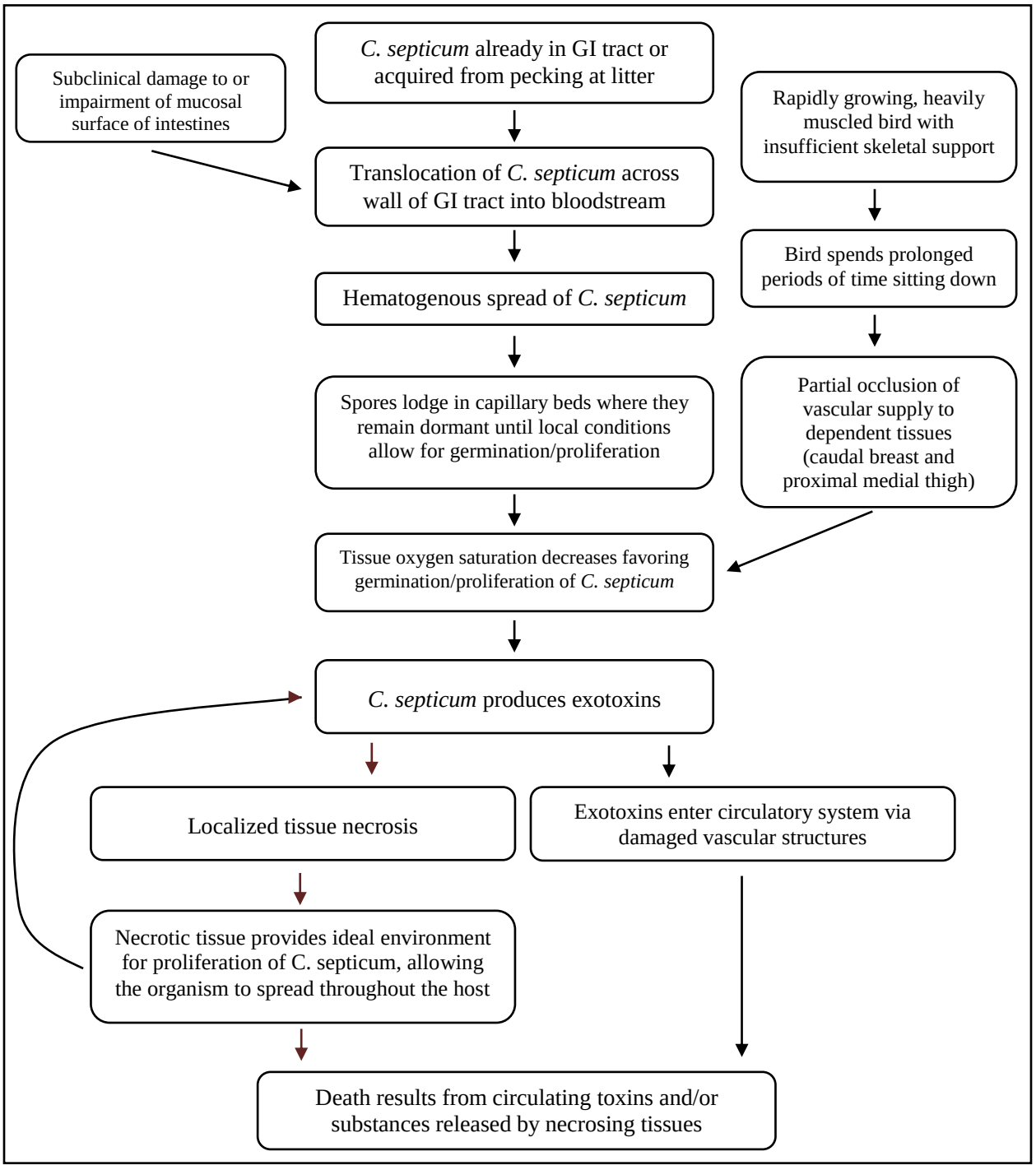

1.4 Treatment, Prevention, and Control of Clostridial Diseases

Infections caused by *Clostridium* species are typically rapidly progressive with acute mortality often being the first recognized sign of illness [33]. Therefore, prevention rather than treatment is an essential component of control programs for these diseases. Successful strategies to control against these diseases include reduction of the number of organisms in the host, reduction of the number of organisms in the host's environment, and enhancement of the host's immunity to the organism (e.g. vaccination) [10].

1.4.1 Treatment

Successful treatment of clostridial diseases depends on rapid diagnosis and implementation of appropriate therapies. However, the rapid course of these diseases often precludes successful treatment. In herd or flock outbreak situations, rapid diagnosis based on observed mortality and implementation of prophylactic therapies can reduce mortality and minimize further economic losses. Vegetative cells of *Clostridium* species are generally, but not universally, susceptible to the following antimicrobial agents: penicillin, amoxicillin, ticarcillin, piperacillin, cefazolin, cefoxitin, third generation cephalosporins, chloramphenicol, clindamycin, erythromycin, metronidazole, imipenem, meropenem, tetracycline, vancomycin, rifampin, and penicillins combined with betalactamase inhibitors [92-98]. For treatment of clostridial wound infections antibiotics should ideally be administered within the first 1-2 hours after injury [15]. This therapy is technically prophylaxis rather than treatment as the antibiotics are being administered before a true anaerobic myositis has had time to develop. For established infections, large doses of a long-acting antimicrobial administered both intravenously and intramuscularly around the site of infection are typically recommended [99]. The mortality rate

for nontraumatic clostridial infections is rather high as these infections are rarely diagnosed early enough for effective implementation of antibiotic therapy [15, 72].

While antibiotics are important in the treatment of clostridial soft tissue infections, the use of antibiotics alone is not enough to stop the spread of these soft tissue infections as antibiotics cannot protect against the activity of preformed toxins. Clostridial soft tissue infections require prompt surgical removal of devitalized tissue via wound excision and debridement. Primary wound closure and application of tight bandages are typically not advised as these would contribute to the creation of an anaerobic environment favorable for the growth of *Clostridium* species [15]. While surgical therapies are effective in humans and pets, such treatment methods are often not practical for use in livestock and poultry. Antibiotic therapy for clostridial infections in livestock and poultry is rarely of benefit [33]. Exceptions to this are Tyzzer's disease which is responsive to oxytetracyclin and necrotic enteritis and gangrenous dermatitis in chickens which are generally responsive to penicillin, macrolide, or tetracycline therapy [33]. While antibiotics are often not effective at treating animals with an already established clostridial infection, they can be useful in herd/flock situations to minimize further losses during an outbreak [10, 33]. Antibiotic therapy for treatment of turkey flocks with CD should be continued until no lesions or mortality typical of the disease are noted within the flock for at least three consecutive days [10].

Antisera (antitoxins) are commercially available against some clostridial toxins. In human cases of gas gangrene, the outcome of treatment is greatly improved by the use of antisera in conjunction with surgical excision of devitalized tissue [15]. These serological products can be administered to affected animals and potentially exposed animals in an outbreak situation to neutralize preformed toxins. Antitoxins should be administered as quickly as possible after

diagnosis of a clostridial outbreak in order to minimize additional losses. The use of antitoxins provides passive immunity against a specific clostridial toxin for up to three weeks following administration [33]. Antitoxin therapy is often used in combination with antimicrobial therapy in order to protect against both pre-formed toxins as well as bacterial growth leading to further production of toxins.

1.4.2 Prevention and Control

Many clostridial diseases can be effectively prevented through immunoprophylaxis, provided that the appropriate vaccines are used in an appropriate manner [50, 51]. Clostridial vaccines can be bacterins which contain inactivated bacterial cells, toxoids which contain inactivated toxin proteins, or combination bacterin-toxoids [45]. There is much debate regarding whether antibacterial or antitoxic immunity is more important in the prevention of clostridial diseases [46]. Early studies with *C. septicum* found that antitoxic immunity was not particularly effective and that antigens associated with the bacterial cell were more important in providing protective immunity [26]. Unfortunately, there do not appear to be any common immunogens across all strains of *C. septicum*; at least five protective antigens have been identified in various strains of the organism [26, 100]. A more recent study found that toxoid vaccines are most effective in providing protection against *C. septicum;* however, production of these vaccines is complicated by the fact that *C. septicum* produces low titers of lethal antigens in culture and native toxin filtrates are weakly immunogenic eliciting poor antibody responses in animals [101]. Most clostridial vaccines are multivalent, containing antigens from several *Clostridium* species in a single product; however, single antigen products are available against *C. hemolyticum, C. tetani,* and *C. perfringens* Type D [45, 102]. Antigens protective against *Clostridium* species

may also be included in combination products with antigens against other species of bacteria or viruses. Available clostridial vaccines are formulated for intramuscular or subcutaneous injection; most require a series of injections for initial protection with annual or semi-annual boosters [102, 103]. Vaccines requiring multiple injections to induce protective immunity are typically not practical for use in meat-type poultry. Vaccination, in combination with antibiotics and/or antisera, is commonly used in the face of an outbreak to minimize further losses in livestock species [48, 99]. In the United States, vaccines are commercially available to protect against multiple clostridial diseases in cattle, sheep, goats, and swine, tetanus in horses, and botulism in mink [48, 102, 103]. There are currently no clostridial disease vaccines approved for use in poultry in the United States. A *C. perfringens* Type A toxoid vaccine received conditional approval from USDA in 2005 for vaccination of pullets to protect against necrotic enteritis in hatched chicks; however, this product has never received full approval and is not commonly used in the US [103, 104]. Use of a commercially available *C. perfringens* toxoid, licensed for use in sheep, was not effective in protecting against development of CD in turkeys in a field setting [87]. At the time, this ineffectiveness was thought to be due to either genetic differences in the strains of *C. perfringens* responsible for causing disease in sheep and turkeys or the importance of other organisms in the pathogenesis of CD in turkeys [87, 105, 106]. Recent studies have concluded that *C. septicum* is the primary causative agent for development of this disease and that *C. perfringens* does not play a primary role in pathogenesis [8, 9, 107, 108]. Vaccination with a *C. perfringens* toxoid would not be expected to provide protective immunity against a disease caused by *C. septicum.*

Vaccination is only one component of a successful prevention and control program for clostridial diseases. Other methods of enhancing host immunity and strategies to reduce the

environmental load of *Clostridium* species are important in controlling these diseases, especially for the diseases for which vaccines are not readily available. Immunosuppression is known to play a role in the development of necrotic enteritis and gangrenous dermatitis in poultry. Prior or concurrent infection with diseases which suppress the immune system such as infectious bursal disease, chicken infectious anemia virus, reticuloendotheliosis virus, avian adenovirus infections, and Marek's disease in chickens and hemorrhagic enteritis virus in turkeys have been implicated as predisposing factors for the development of these clostridial diseases [56, 60, 77]. Non-specific stress is also known to contribute to immunosuppression which may make birds more susceptible to the development of clostridial diseases [10].

Effective control of enterotoxic clostridial infections requires maintenance of normal gastrointestinal health and nutritional management [45]. Since damage to the gastrointestinal mucosa and liver parenchyma can predispose animals to the development of clostridial diseases, controlling for the conditions that cause this initial damage can aid in the prevention of the associated clostridial diseases. Control of *Fasciola hepatica* infection reduces the incidence of black disease and bacillary hemoglobinuria in sheep and cattle [48]. Mucosal damage and changes in intestinal transport times associated with coccidiosis contribute to the development of necrotic enteritis in poultry [43, 60]. Use of anticoccidial drugs reduces the incidence of necrotic enteritis by minimizing these predisposing factors. Additionally, some ionophorous anticoccidial drugs have direct anticlostridial activity [60]. An increase in the incidence of clostridial diseases in poultry following the cessation of the use of growth promoting antibiotics in poultry feed has revealed the importance of these drugs in reducing the colonization and proliferation of *Clostridium* species [43, 60]. Abrupt changes in diet and high concentrations of rapidly fermentable carbohydrates favor the proliferation of *Clostridium* species; therefore gradual

changes in diet are recommended to minimize the incidence of struck and pulpy kidney disease in sheep and necrotic enteritis in poultry [45, 48]. The use of probiotics, competitive exclusion products, and prebiotics in poultry feed have all been shown to reduce the incidence of necrotic enteritis by reducing the colonization and proliferation of *C. perfringens* [43, 60]. Since an endogenous source for *C. septicum* and/or *C. perfringens* is proposed in the pathogenesis of CD, maintenance of normal gut health and microflora is suspected to play an important role in control of this disease in turkey flocks [10].

There are several strategies recommended to reduce environmental load of *Clostridium* species on livestock farms. *Clostridium* species are shed in the feces of livestock and poultry, and overcrowding increases the environmental load of these organisms leading to an increased incidence of clostridial diseases. Therefore, preventing overcrowding of animals and thorough cleaning and disinfecting barns aids in the control of clostridial diseases [10, 48]. Minimizing crowding is also important in controlling clostridial soft tissue infections that occur secondary to fighting, as with bighead in sheep and goats, or scratching, as with gangrenous dermatitis in poultry [48, 77]. During blackleg outbreaks, it is recommended to move animals from the contaminated pasture [99, 102]. Since it is extremely difficult to eliminate spores from contaminated soil, pastures known to be contaminated should ideally be used for alternative agricultural practices or only grazed with vaccinated livestock [99, 109]. Animals known or suspected to have the disease should be isolated from unaffected animals until at least two weeks after the last affected animal has recovered [109]. Carcasses of animals that have died as a result of blackleg or malignant edema should be burned or deeply buried [99]. Prompt disposal of affected turkey carcasses is also recommended to control outbreaks of CD [10].

1.5 Research Summary

CD emerged as a major problem for the turkey industry over twenty years ago. Currently, a poor understanding of the risk factors for development of CD and the mechanism of pathogenesis make prevention and treatment of the disease in turkey flocks challenging. Five research goals have been identified to address these concerns.

While *C. septicum* and *C. perfringens* have been identified as causative agents for CD in turkeys, many questions remain regarding the pathogenesis of this disease. Since these organisms are frequently isolated from the gastrointestinal tracts of healthy turkeys development of CD is likely multifactorial with various environmental, genetic, and/or management factors contributing to development of the disease. The first research goal is to determine the incidence of CD in turkey flocks and identify risk factors for the development of the disease through retrospective evaluation of flock production records and a survey of vertically integrated and large commercial turkey operations.

It is hypothesized that CD develops as a result of an endogenous (intestinal) source of *Clostridium* species. *C. septicum* has been found in the blood and liver of live asymptomatic turkeys; however, the organism has not yet been identified in the muscle of asymptomatic turkeys. The second research goal is to determine if *C. septicum* and *C. perfringens* are present in the blood, liver, and skeletal muscle of live asymptomatic turkeys on farms with a history of CD outbreaks to provide further evidence supporting the proposed hematogenous spread of *Clostridium* species from the gastrointestinal tract.

Healthy skeletal muscle is not the ideal environment for the growth and proliferation of anaerobic organisms like *Clostridium* species. Organisms that reach the capillary beds of skeletal muscle via hematogenous spread from the gastrointestinal tract would remain dormant in

the muscle until local conditions become favorable for growth. CD appears to affect the biggest, most rapidly-growing birds in a flock. These turkeys sometimes have issues with their skeletal development not keeping pace with muscle growth and will often spend prolonged periods of time sitting down. It is hypothesized that these prolonged periods of time sitting exert pressure on the capillary beds within the skeletal muscles on the lower breast and inguinal regions resulting in decreased perfusion to the muscles. The resulting decrease in oxygen tension to these muscles would provide an environment favorable for the germination and proliferation of *Clostridium* spores leading to the development of CD. The third research goal is to determine whether prolonged recumbency results in decreased perfusion to the skeletal muscle of the lower breast and inguinal regions.

The lesions and mortality associated with clostridial diseases are the result of the production of potent exotoxins by *Clostridium* species. While *C. septicum* produces at least four toxins and strains of *C. perfringens* are capable of producing at least seventeen toxins, expression of these toxins is highly variable depending on nutrient availability and environmental conditions. It remains unclear which toxins are being expressed leading to the development of and mortality associated with CD in turkeys. The fourth research goal is to identify which clostridial toxins are being produced during the course of CD infection through analysis of protein and messenger ribonucleic acid (mRNA) expression *in vitro* in a chopped turkey meat medium and *in vivo* during natural infection. The gene and protein sequence are currently known for the alpha toxin of *C. septicum;* however, the sequences of the beta, gamma, and delta toxins are unknown. The fifth research goal involves *de novo* sequencing of the whole genome of *C. septicum* in order to identify the gene sequences for these toxins.

1.5.1 Hypotheses

1. CD is a multifactorial disease; environmental, genetic, and/or management factors are important in development of the disease in turkey flocks.
2. *Clostridium* spores can be identified in the skeletal muscle of live asymptomatic turkeys on farms with a history of CD outbreaks supporting the proposed mechanism of pathogenesis.
3. Prolonged recumbency in turkeys results in decreased perfusion to and oxygen saturation of skeletal muscle in the breast and inguinal regions creating a region of localized anoxia that allows for the growth and proliferation of *Clostridium* species.
4. Clostridial mRNA expression *in vivo* and protein production *in vitro* in a chopped turkey meat broth culture system can identify which toxin proteins are being produced in infected turkey muscle contributing to the development of and mortality associated with CD.
5. *de novo* sequencing of the whole *C. septicum* genome will allow for identification of the gene sequences for the beta, gamma, and delta toxins which may further understanding of the pathogenesis of CD in turkeys and aid in the development of more effective vaccines against this disease.

1.6 References

1. Carr, D, D Shaw, DA Halvorson, B Rings and D Roepke. Excessive mortality in market-age turkeys associated with cellulitis. Avian Diseases 40:736-741. 1996.

2. Fenstermacher, R and BS Pomeroy. *Clostridium* infection in turkeys. Cornell Veterinary Journal 29:25-28. 1939.

3. Clark, SR, B Tilley and D Mills. Current health and industry issues facing the turkey industry. In: Proc. 112th Annual Meeting of the USAHA, Greensboro, NC. Richardson Printing, Kansas City, MO. pp 530-535. 2009.

4. Rives, D, D Mills and S Clark. Current health and industry issues facing the turkey industry. In: Report of the Committee on Transmissible Diseases of Poultry and Other Avian Species. Minneapolis, MN. 2006.

5. Menges, J. Health issues affecting organic-fed flocks. In: Pennsylvania Poultry Sales and Service Conference. State College, PA. September, 25 2014.

6. McComb, B. Upper midwest filed perspective of dermatitis in commercial turkeys. In: MTRPC Gold Medal Panel on [cellulitis] clostridial dermatitis. Bloomington, MN. pp 5-8. 2008.

7. USDA. Poultry 2010: Clostridial dermatitis on US turkey-grower farms. USDA-APHIS-VS-CEAH-NAHMS. 2012.

8. Tellez, G, NR Pumford, MJ Morgan, AD Wolfenden and BM Hargis. Evidence for *Clostridium septicum* as a primary cause of cellulitis in commercial turkeys. Journal of Veterinary Diagnostic Investigation 21:374-377. 2009.

9. Thachil, AJ, B McComb, MM Anderson, DP Shaw, DA Halvorson and KV Nagaraja. Role of *Clostridium perfringens* and *Clostridium septicum* in causing turkey cellulitis. Avian Diseases 54:795-801. 2010.

10. Clark, S, R Porter, B McComb, R Lippert, S Olson, S Nohner and HL Shivaprasad. Clostridial dermatitis and cellulitis: an emerging disease of turkeys. Avian Diseases 54:788-794. 2010.

11. Smith, LDS and BL Williams. The *Clostridia*. In: The Pathogenic Anaerobic Bacteria, 3rd ed. A. Balows, ed. Charles C Thomas Publisher, Springfield, IL, USA. pp 94-100. 1984.

12. Rainey, FA, BJ Hollen and A Small. Genus I. *Clostridium* Prazmowski 1880, 23^{AL}. In: Bergey's Manual of Systematic Bacteriology, 2nd ed. P. De Vos, G. Garrity, D. Jones, N. Kreig, W. Ludwig, F. Rainey, K. Schleifer and W. Whitman, eds. Springer, New York. pp 739-828. 2009.

13. Popoff, MR and P Bouvet. Clostridial toxins. Future Microbiology 4:1021-1064. 2009.

14. Hatheway, CL. Toxigenic *Clostridia*. Clinical Microbiology Reviews 3:66-98. 1990.

15. MacLennan, JD. The histotoxic clostridial infections of man. Bacteriological Reviews 26:177-275. 1962.

16. Stackebrandt, E and FA Raine. Phylogenetic relationships. In: The Clostridia: Molecular Biology and Pathogenesis J. Rood, B. McClane, J. Songer and R. Titball, eds. Academic Press, Inc, San Diego. pp 3-19. 1997.

17. Popoff, MR and BG Stiles. Clostridial toxins vs. other bacterial toxins. In: Handbook on *Clostridia*. P. Durre, ed. CRC Press: Taylor & Francis Group, Boca Raton, FL. pp 323-383. 2005.

18. Smith, LDS. Clostridia in gas gangrene. Bacteriological Reviews 13:233-254. 1949.

19. Fisher, DJ, ME Fernandez-Miyakwawa, S Sayeed, R Poon, V Adams, JI Rood, FA Uzal and BA McClane. Dissecting the contributions of *Clostridium perfringens* type C toxins to lethality in the mous intravenous injection model. Infection and Immunity 74:5200-5210. 2006.

20. Sayeed, S, ME Fernandez-Miyakawa, DJ Fisher, V Adams, R Poon, JI Rood, FA Uzal and BA McClane. Epsilon-toxin is required for most *Clostridium perfringens* type D vegetative culture supernatants to cause lethality in the mouse intravenous injection model. Infection and Immunity 73:7413-7421. 2005.

21. Daniels, R, J Vanderleyden and J Michiels. Quorum sensing and swarming migration in bacteria. FEMS Microbiology Reviews 28:261-289. 2004.

22. Sifri, CD. Quorum sensing: bacteria talk sense. Clinical Infectious Diseases 47:1070-1076. 2008.

23. Gadalla, MSA and JG Collee. The relationship of the neuraminidase of *Clostridium septicum* to the haemagglutinin and other soluble products of the organism. Journal of Pathology and Bacteriology 96:169-185. 1968.

24. Fernandez-Miyakawa, ME, R Marcellino and FA Uzal. *Clostridium perfringens* type A toxin production in 3 commonly used culture media. Journal of Veterinary Diagnostic Investigation 19:184-186. 2007.

25. Bernheimer, Alan W. and With the Technical Assistance of Margaret T. Spencer. Nutritional requirements and factors affecting the production of toxin of *Clostridium septicum*. The Journal of Experimental Medicine 80:321-331. 1944.

26. Smith, LDS and BL Williams. *Clostridium septicum*. In: The Pathogenic Anaerobic Bacteria, 3rd ed. A. Balows, ed. Charles C Thomas Publisher, Springfield, IL, USA. pp 180-190. 1984.

27. Durre, P. Sporulation in *Clostridia* (Genetics). In: Handbook on *Clostridia*. P. Durre, ed. CRC Press: Taylor & Francis Group, Boac Raton, FL. pp 659-669. 2005.

28. Setlow, P. I will survive: DNA protection in bacterial spores. Trends Microbiol 15:172-180. 2007.

29. Mallozzi, M, VK Viswanathan and G Vedantam. Spore-forming *Bacilli* and *Clostridia* in human disease. Future Microbiology 5:1109-1123. 2010.

30. Labbe, RG and N-J.R Shih. Physiology of Sporulation of *Clostridia*. In: The *Clostridia*: Molecular Biology and Pathogenesis. J. Rood, B. McClane, J. Songer and R. Titball, eds. Academic Press, Inc, San Diego, CA. pp 22-32. 1997.

31. Kennedy, MJ, SL Reader and LM Swierczyniski. Preservation records of micro-organisms: evidence of the tenacity of life. Microbiology 140:2513-2529. 1994.

32. Smith, LDS and BL Williams. *Clostridium chauvoei*. In: The Pathogenic Anaerobic Bacteria, 3rd ed. A. Balows, ed. Charles C Thomas Publisher, Springfield, IL, USA. pp 164-175. 1984.

33. Songer, JG and KW Post. The Genus *Clostridium*. In: Veterinary Microbiology: Bacterial and Fungal Agents of Animal Diseases. Elsevier Saunders, St. Louis, MO, USA. pp 261-282. 2005.

34. Timoney, JF, JA Gillespie, FW Scott and JE Barlough. The genus *Clostridium*. In: Hagan and Bruner's Microbiology and Infectious Diseases of Domestic Animals, 8th ed. Cornell University Press, Ithaca, New York. pp 214-240. 1988.

35. Tweten, RK. *Clostridium perfringens* beta toxin and *Clostridium septicum* alpha toxin: their mechanisms and possible role in pathogenesis. Veterinary Microbiology 82:1-9. 2001.

36. Csoka, TB, GI Frost and R Stern. Hyaluronidases in tissue invasion. Invasion and Metastasis 17:297-311. 1997.

37. Macfarlane, S, MJ Hopkins and GT Macfarlane. Toxin synthesis and mucin breakdown are related to swarming phenomenon in *Clostridium septicum*. Infection and Immunity 69:1120-1126. 2001.

38. Wilson, LM and GT Macfarlane. Cytotoxicity, adhesion and invasion of *Clostridium septicum* in cultured human epithelial cells (CACO-2, HEp-2): Pathological significance of swarm cell differentiation. Anaerobe 2:71-79. 1996.

39. Smith, LDS and BL Williams. *Clostridium perfringens*. In: The Pathogenic Anaerobic Bacteria, 3rd ed. A. Balows, ed. Charles C Thomas Publisher, Springfield, IL, USA. pp 101-136. 1984.

40. Sharma, M and SK Anand. Swarming: a coordinated bacterial activity. Current Science 83:707-715. 2002.

41. Fraser, GM and C Hughes. Swarming motility. Current Opinion in Microbiology 2:630-635. 1999.

42. Lyerly, DM and TD Wilkins. Toxins of anaerobes. In: Anaerobic microbiology: a practical approach. P. Levett, ed. IRL Press at Oxford University Press, Oxford. pp 163-181. 1991.

43. Van Immerseel, F, J De Buck, F Pasmans, G Huyghebaert, F Haesebrouck and R Ductalle. *Clostridium perfringens* in poultry: an emerging threat for animal and public health. Avian Pathology 33:537-549. 2004.

44. Keyburn, AL, JD Boyce, P Vas, TL Bannam, ME Ford, D Parker, A DiRubbo, JI Rood and RJ Moore. NetB, a new toxin that is associated with avian necrotic enteritis caused by *Clostridium perfringens*. PLoS Pathogens 4:e26. 2008.

45. McClane, BA, FA. Uzal, ME Fernandez Miyakawa, D Lyerly and T Wilkins. The enterotoxic *Clostridia*. Prokaryotes 4:698-752. 2006.

46. Songer, JG. Clostridial enteric diseases of domestic animals. Clinical Microbiology Reviews 9:216-234. 1996.

47. Rood, JI. Virulence Genes of *Clostridium perfringens*. Annual Review of Microbiology 52:333-360. 1998.

48. Lewis, CJ. Clostridial diseases. In: Diseases of Sheep. I. Aitken, ed. Blackwell Publishing, Oxford. pp 156-167. 2007.

49. Stampfil, HR. Clostridial diseases. In: The Merck Veterinary Manual, 10th ed. C. Kahn and S. Line, eds. Merck, Whitehouse Station, NJ. 2012.

50. Sterne, M and I Batty. Pathogenic *Clostridia*. Butterworths, London. 1975.

51. Sterne, M. Clostridial infections. British Veterinary Journal 137:443-454. 1981.

52. Borriello, SP and RJ Carman. Clostridial Diseases of the Gastrointestinal Tract in Animals. In: *Clostridia* in Gastrointestinal Disease. S. Borriello, ed. CRC Press, Inc, Boca Raton, FL. pp 195-221. 1985.

53. Songer, JG. Clostridial diseases in domestic animals. In: Handbook on *Clostridia*. P. Durre, ed. CRC Press: Taylor & Francis Group, Boca Raton, FL. pp 527-542. 2005.

54. Johnson, S and DN Gerding. Enterotoxemic infections. In: The *Clostridia*: Molecular Biology and Pathogenesis. J. Rood, B. McClane, J. Songer and R. Titball, eds. Academic Press, Inc, San Diego, CA. pp 117-140. 1997.

55. Timbermont, L, F Haesebrouck, R Ducatelle and F Van Immerseel. Necrotic enteritis in broilers: an updated review on the pathogenesis. Avian Pathology 40:341-347. 2011.

56. Opengart, K. Necrotic enteritis. In: Diseases of Poultry, 12th ed. Y. Saif, A. Fadly, J. Glisson, L. McDougald, L. Nolan and D. Swayne, eds. Blackwell Publishing, Ames, IA, USA. pp 872-879. 2008.

57. Hibberd, MC, AP Neumann, TG Rehberger and GR Siragusa. Multilocus sequence typing subtype of poultry *Clostridium perfringnes* isolates demonstrate disease niche partitioning. Journal of Clinical Microbiology 49:1556-1567. 2011.

58. Songer, JG. Clostridial diseases of animals. In: The *Clostridia*: Molecular Biology and Pathogenesis. J. Rood, B. McClane, J. Songer and R. Titball, eds. Academic Press, Inc, San Diego, CA. pp 153-182. 1997.

59. Yegani, M and DR Korver. Factors affecting intestinal health in poultry. Poultry Science 87:2052-2063. 2008.

60. Williams, RB. Intercurrent coccidiosis and necrotic enteritis of chickens: regional, integrated disease management by maintenance of gut integrity. Avian Pathology 34:159-180. 2005.

61. Finlay, BB and S Falkow. Common themes in microbial pathogenicity revisited. Microbiol Mol Biol Rev 61:136-169. 1997.

62. Wages, DP. Ulcerative enteritis (quail disease). In: Diseases of Poultry, 12th ed. Y. Saif, A. Fadly, J. Glisson, L. McDougald, L. Nolan and D. Swayne, eds. Blackwell Publishing, Ames, IA, USA. pp 867-871. 2008.

63. Feng, LJ and C Eaton. Soft-tissue infection in lower-extremity trauma. Clinics in Podiatric Medicine and Surgery 7:446-465. 1990.

64. Cainzos, M and FJ Gonzalez-Rodriguez. Necrotizing soft tissue infections. Current Opinions in Critical Care 13:433-439. 2007.

65. Camblin, JG and JG Kinley. Non-traumatic clostridial myonecrosis. The Ulster Medical Journal 39:150-153. 1970.

66. Smith, LDS and BL Williams. Clostridial wound infections. In: The Pathogenic Anaerobic Bacteria, 3rd ed. A. Balows, ed. Charles C Thomas Publisher, Springfield, IL, USA. pp 245-249. 1984.

67. Stevens, DL. Necrotizing clostridial soft tissue infections. In: The *Clostridia*: Molecular Biology and Pathogenesis. J. Rood, B. McClane, J. Songer and R. Titball, eds. Academic Press, Inc, San Diego, CA. pp 141-151. 1997.

68. Bryant, AE and DL Stevens. The Pathogenesis of Gas Gangrene. In: The *Clostridia*: Molecular Biology and Pathogenesis. J. Rood, B. McClane, J. Songer and R. Titball, eds. Academic Press, Inc, San Diego, CA. pp 185-196. 1997.

69. Stevens, DL, LL Laposky, P McDonald and I Harris. Spontaneous gas gangrene at a site of remote injury: localization due to circulating antitoxin. Western Journal of Medicine 148:204-205. 1988.

70. Stevens, DL, DM Musher, DA Watson, H Eddy, RJ Hamil, F Gyorkey, H Rosen and J Mader. Spontaneous, nontraumatic gangrene due to *Clostridium septicum*. Reviews of Infectious Disease 12:286-295. 1990.

71. Alpern, RJ and VR Dowell. *Clostridium septicum* infections and malignancy. The Journal of the American Medical Association 209:385-388. 1969.

72. Burell, MI, EA Hyson and GJ Walker Smith. Spontaneous clostridial infection and malignancy. American Journal of Roentgenology 134:1153-1159. 1980.

73. Odendaal, MW and NPJ Kriek. *Clostridium septicum* infections. In: Infectious Diseases of Livestock, 2nd ed. J. Coetzer and R. Tustin, eds. Oxford University Press South Africa, Cape Town. pp 1869-1873. 2004.

74. Hullard, TJ. Chapter 2: muscle and tendon. In: Pathology of Domestic Animals, 4th ed. K. Jubb, P. Kennedy and N. Palmer, eds. Academic Press, Inc, San Diego, CA. pp 183-265. 1993.

75. Kriek, NPJ and MW Odendaal. *Clostridium chauvoei* infections. In: Infectious Diseases of Livestock, 2nd edition ed. J. Coetzer and R. Tustin, eds. University Press South Africa, Cape Town. pp 1856-1862. 2004.

76. Feingold, DS. Gangrenous and crepitant cellulitis. Journal of the American Academy of Dermatology 6:289-299. 1982.

77. Opengart, K. Gangrenous dermatitis. In: Diseases of Poultry, 12th ed. Y. Saif, A. Fadly, J. Glisson, L. McDougald, L. Nolan and D. Swayne, eds. Blackwell Publishing, Ames, IA, USA. pp 885-889. 2008.

78. Li, G, HS Lillehoj, KW Lee, SI Jang, P Marc, CG Gay, GD Ritter, DA Bautista, K Phillips, AP Neumann, TG Rehberger and GR Siragusa. An outbreak of gangrenous dermatitis in commercial broiler chickens. Avian Pathology 39:247-253. 2010.

79. Charlton, BR, AJ Bermudez, M Boulianne, DA Halvorson, JS Scjrader, LJ Newman, JE Sander and PS Wakenell, eds. Avian Disease Manual, 6th ed. American Association of Avian Pathologists, Athens, GA, USA. 2006.

80. Swarbrick, O. Necrotic cellulitis in turkey breeders. Veterinary Record 129:555. 1991.

81. Dibner, Julia J. The role of gut barrier failure in gangrenous cellulitis of poultry. In: MTRPC Gold Medal Panel on [cellulitis] clostridial dermatitis Gobbles 651. 2009, Bloomington, MN. 2008.

82. Neumann, AP and TG Rehberger. MLST analysis reveals a highly conserved core genome among poultry isolates of *Clostridium septicum*. Anaerobe 15:99-106. 2009.

83. Davis, SW. Development of a successful model creating clostridium dermatitis in turkeys using an oral challenge model. In: American Association of Avian Pathologists, 147th American Veterinary Medical Association annual meetings (compact disc). Atlanta, Georgia. 2010.

84. Nagaraja, KV, AJ Thachil and DA Halvorson. Role of *Clostridium perfringens* and *septicum* in cellulitis in turkeys. In: 58th Western Poultry Disease Conference Madison, WI. p Page 10. 2009.

85. Shivaprasad, HL. Gangrenous dermatitis due to *Clostridium septicum* in turkeys. In: MTRPC Gold Medal Panel on [cellulitis] clostridial dermatitis Bloomington, MN. 2008.

86. Evans, AS. Causation and disease: the Henle-Koch postulates revisited. The Yale Journal of Biology and Medicine 49. 1976.

87. Thachil, AJ. Cellulitis in turkeys: characterization of causative agents and preventative measures. Doctor of Philosophy Dissertation in University of Minnesota. Minneapolis, MN. 2011.

88. Rivers, TM. Viruses and Koch's postulates. J Bacteriol 33:1. 1937.

89. Shapiro, SK and WB Sarles. Microorganisms in the intestinal tract of normal chickens. Journal of Bacteriology 58:531-544. 1949.

90. Timms, L. Observations on the bacterial flora of the alimentary tract in three age groups of normal chickens. British Veterinary Journal 124:470-477. 1968.

91. Neumann, AP, SM Dunham, TG Rehberger and GR Siragusa. Quantitative real-time PCR assay for *Clostridium septicum* in poultry gangrenous dermatitis associated samples. Molecular and Cellular Probes 24:211-218. 2010.

92. Alexander, CJ, DM Citron, JS Brazier and EJ Goldstein. Identification and antimicrobial resistance patterns of clinical isolates of *Clostridium clostridioforme, Clostridium innocuum,* and *Clostridium ramosen* compared with these of clinical isolates of *Clostridium perfringens*. Journal of Clinical Microbiology 33:3209-3215. 1995.

93. Brazier, JS, PN Levett, AL Stannard, KD Phillips and AT Willis. Antibiotic susceptibility of clinical isolates of *Clostridia*. Journal of Antimicrobial Chemotherapy 15:181-185. 1985.

94. Gabay, EL, RD Rolfe and SM Finegold. Susceptibility of *Clostridium septicum* to 23 antimicrobial agents. Antimicrobial Agents and Chemotherapy 20:852-853. 1981.

95. Marrie, TJ, EV Haldane, CA Swantee and EA Kerr. Sysceptibility of anaerobic bacteria to nine antimicrobial agents and demonstration of decreased susceptibility of *Clostridium perfringens* to penicillin. Antimicrobial Agents and Chemotherapy 19:51-55. 1981.

96. Musial, CE and JE Rosenblatt. Antimicrobial susceptibilities of anaerobic bacteria isolated at the Mayo Clinic during 1982 through 1987: comparison with results from 1977 through 1981. Mayo Clinic Proceedings 64:392-399. 1987.

97. Schwartzman, JD, LB Reller and WL Wang. Susceptibility of *Clostridium perfringens* isolated from human infections to twenty antibiotics. Antimicrobial Agents and Chemotherapy 11:695-697. 1977.

98. Traub, WH. Comparative in-vitro bactericidal activity of 24 antimicrobial drugs against *Clostridium perfringens*. Chemotherapy 36:127-135. 1990.

99. Selman, IE. Blackleg and malignant edema. Current Topics in Veterinary Medicine and Animal Science 6:247-254. 1981.

100. Claus, KD and DR Kolbe. Immunogenicity of *Clostridium septicum* in guinea pigs. Am J Vet Res 40:1752-1756. 1979.

101. Cortinas, TI, MA Mattar and AM Stefanini de Guzman. Alpha-toxin production by *Clostridium septicum* at different culture conditions. Anaerobe 3:199-202. 1997.

102. Hjerpe, CA. Clostridial disease vaccines. Veterinary Clinics of North America: Food Animal Practice 6:222-234. 1990.

103. Compendium of veterinary products electronic database. In. North American Compendiums, Inc. 2013.

104. USDA. Center for veterinary biologics notice no. 05-04. USDA-APHIS-VS-CBV. 2005.

105. Kulkarni, RR, VR Parreira, S Sharif and JF Prescott. *Clostridium perfringens* antigens recognized by broiler chickens immune to necrotic enteritis. Clinical and Vaccine Immunology 13:1358-1362. 2006.

106. Thompson, DR, VR Parreira, RR Kulkarni and JF Prescott. Live attenuated vaccine-based control of necrotic enteritis in broiler chickens. Vet Microbiol 113:25-34. 2006.

107. Robbins, K. Commercial turkey clostridial dermatitis vaccination and interventions. In: American Association of Avian Pathologists Scientific Program. Boston, MA. 2015.

108. Lighty, M. Chapter 5: Clostridial toxin production in turkeys with clostridial dermatitis. In: Epidemiology and Pathophysiology of Clostridial Dermatitis (Cellulitis) in Turkeys. Doctor of Philosophy Dissertation in Biomedical and Veterinary Sciences. Virginia Polytechnic Institute and State University. Blacksburg, VA. 2015.

109. Kohler, B. Blackleg, Blackquarter. In: Applied Veterinary Epidemiology. T. Blaha, ed. Elsevier, Amsterdam. pp 317-320. 1989.

Chapter 2 – Incidence of Clostridial Dermatitis (Cellulitis) and Factors for Development of the Disease in Turkeys

Megan E. Lighty,* François Elvinger,* Robert D. Evans,† Nammalwar Sriranganathan,‡ Tanya LeRoith,‡ and F. William Pierson*1

*Department of Population Health Sciences, Virginia-Maryland College of Veterinary Medicine, Blacksburg, Virginia 24061; †Elanco, Harrisonburg, Virginia 22801; and ‡Department of Biomedical Sciences and Pathobiology, Virginia-Maryland College of Veterinary Medicine, Blacksburg, Virginia 24061

A version of this chapter was submitted to the *Journal of Applied Poultry Research* and is currently under review.

2.0 Abstract

Clostridial dermatitis (CD), also referred to as cellulitis, is a disease of serious concern in turkeys in the United States whose incidence appears to have increased since its emergence in the early 1990s. The disease leads to increased mortality with the presence of fluid- and gas-filled lesions in the subcutaneous tissues of the breast, thigh, and tail-head. Management factors may contribute to the development of CD. The analysis of mortality and health records of turkey flocks placed over a one-year period for one vertically integrated turkey operation indicates that breed, flock type, weight at processing, and stocking density affected the incidence of CD. Season of placement, season of onset, prior health events, and prior vaccination and/or medication did not affect the incidence of CD. Development of CD, flock type, season of placement, and season of onset of CD affected livability. Breed did not affect livability. In a survey of eight vertically integrated and large commercial turkey companies, 639 of 3398 market turkey flocks (18.8%) had developed CD and 239 of 967 farms (24.7%) raising market turkeys had at least one flock develop CD over the course of a calendar year, with an estimated increase

in the cost of production for flocks that developed CD of 0.031 to 5.5 cents per kilogram of meat produced.

2.1 Introduction

Within the last twenty years the turkey industry has experienced an increase in the frequency and severity of subcutaneous clostridial infections, and poultry veterinarians have ranked CD as a top concern facing the turkey industry [1-4]. CD appears to be restricted to the vertically integrated and large-scale commercial turkey industry. Disease occurs in both conventional and organic production system; although, there have been no reports of this condition in wild, heritage breed, or range-reared turkeys.

CD, also referred to as cellulitis, is thought to be caused primarily by *Clostridium septicum* [5, 6]. *Clostridium perfringens* and *C. sordellii* may also be involved [5-7]. For an individual bird to be considered a case of CD based on the official definition developed by veterinarians and industry representatives, the bird must present with at least two of the following seven signs: i) subcutaneous emphysema; ii) subcutaneous serum and/or serosanguinous fluid; iii) vesicles on the skin, especially on the breast-inguinal area; iv) moist, dark, wrinkled skin, especially on the breast-inguinal area; v) cellular necrosis (microscopic); vi) organ involvement (spleen and/or liver); and vii) vesicles on the skin, moist, dark, wrinkled skin, or both on tail area [6]. A flock is diagnosed with CD if the mortality with lesions characteristic of the disease is greater than or equal to 0.5 dead birds per 1000 birds per day for two consecutive 24 hour periods [6]. Personal communications with flock supervisors and company veterinarians suggest that elevated mortality with characteristic necrotic lesions on the breast and

inguinal regions is the main criterion used in the field to identify CD-positive flocks. Histopathology and bacteriological isolation are generally not performed in routine diagnostics.

The pathogenesis of CD is not fully understood. It is hypothesized that the natural route of infection is via hematogenous spread of organisms invading or leaking from the gastrointestinal tract [6, 8]. While similarities exist between CD of turkeys and gangrenous dermatitis of broiler chickens, the subcutaneous lesions of CD are typically not accompanied by skin scratches and lesions seen in classic gangrenous dermatitis in broiler chickens. Some laboratories have reported success with experimental models to study CD in turkeys by subcutaneous and intravenous injection of *C. septicum* [9-11]. However, it is thought that an oral challenge model would be better suited to study this disease since a gastrointestinal source of *Clostridium* species may be implicated in natural infections [11]. The limited success of oral challenge models in eliciting the disease has led some researchers to believe that the natural route of infection is through breaks or scratches in the skin [6, 11-13].

The objectives of this study were to determine risk factors for occurrence of CD in one vertically integrated turkey operation and to evaluate incidence, disease management factors, and economic impact of CD in turkey operations across the United States.

2.2 Materials and Methods

2.2.1: Study 1 – Regional Incidence and Risk Factors

Production and health records were obtained from a vertically integrated turkey company in the Mid-Atlantic region for 1,057 flocks placed on 167 farms between January 1, 2007 and December 31, 2007 for a retrospective analysis of incidence and risk factors for the development of CD. Eight hundred eighteen flocks were light hen flocks which were processed at a median

age of 13.1 weeks of age (minimum 12.1; maximum 14.1) with an average weight of 7.1 ± 0.44 (mean ± standard deviation) kilograms at processing. One hundred eighty-one flocks were heavy hen flocks which were processed at a median age of 17.3 weeks of age (minimum 16.3; maximum 18.4) with an average weight of 10.4 ± 0.52 kilograms. Fifty eight flocks were identified as tom flocks which were processed at a median age of 20.1 weeks of age (minimum 15.1; maximum 21) with an average weight at processing of 18.5 ± 1.16 kilograms. Two hundred twenty-five flocks placed were Hybrid breed turkeys, 734 flocks were Nicholas (Aviagen Turkeys, Inc.) breed turkeys, and 96 flocks were composed of a mixture of Hybrid and Nicholas turkeys.

Identification of flocks positive for CD was based on visual confirmation of post-mortem lesions consistent with CD as determined by the flock supervisors and/or the company veterinarian. Health and production data were reviewed for each flock from the time of placement through the time of processing. Descriptive statistics were generated using JMP 8.0 software [14]. SAS 9.3 software was used to analyze risk factors for development of CD by either Proc LOGISTIC or Proc FREQ [15]. Proc LOGISTIC was used to evaluate the effect of flock type, breed, stocking density, final weight at processing, prior health events, and prior vaccination and/or medication on the development of CD. PROC FREQ with Fisher's exact was used to evaluate the effect of season of placement and season of onset on the development of CD. Proc GLM was used to determine the factors affecting livability in a model containing development of CD, flock type, breed, season of placement, and all 2-way interactions with development of CD. Effect of season of onset on livability was evaluated in a separate model that included flock type, breed, season of onset, and all 2- and 3-way interactions. Interactions that were not significant were removed from the final models. Livabilities are reported as least

square means ± standard error. The effect of a factor was determined to be significant at $p < 0.05$.

2.2.2: Study 2 – National Incidence and Economic Impact

A two part survey was e-mailed to the member companies of the National Turkey Federation in March 2009. A first questionnaire was directed to the flock supervisors or servicepersons in each company and included questions on the incidence of CD and aspects of disease management (Appendix A). The second questionnaire was directed to the live production and/or complex managers to obtain information on the economic impact of CD on their operation (Appendix B). Questions pertained to turkey flocks marketed during the 2008 calendar year. Completed company responses were collected by the National Turkey Federation's legal counsel. All identifying company information was removed and anonymized responses were sent to the authors for analysis.

2.3 Results

2.3.1: Study 1 – Regional Incidence and Risk Factors

Fifty-three of 167 farms (31.7%) had at least one flock placed in 2007 that developed CD which affected 120 of 1057 placed flocks (11.4%; Table 2.1). Flock type affected the incidence of CD ($p < 0.0001$). The odds of tom flocks to develop CD were 4.9 times the odds of light hen flocks to develop the disease (95% confidence interval (CI): [2.7; 9.2]). The odds of heavy hen flocks to develop cellulitis were 3.4 times the odds of light hen flocks to develop the disease (95% CI: [2.2; 5.3]). Breed affected the incidence of CD ($p = 0.0216$). Twenty-one of 225 (9.3%) Hybrid flocks, 95 of 734 (12.9%) Nicholas flocks, and 4 of 96 (4.2%) mixed flocks

developed CD. However, when flock type and breed were both included in a stepwise selection logistic regression model, only flock type remained significant ($p < 0.0001$). The age at time of onset of CD varied with flock type ($p = 0.0018$). For light hen flocks the minimum, maximum, and average (mean ± standard deviation) ages at time of onset were 8, 14, and 11.2 ± 1.12 weeks; for heavy hen flocks 4, 17, and 13.0 ± 2.97 weeks; for tom flocks 7, 19, and 13.1 ± 3.40 weeks.

In this study, season of placement was not associated with the occurrence of CD ($p = 0.2240$; Table 2.2). Onset of CD was associated with season ($p = 0.0003$; Table 2.3). No flocks paced in Winter 2007 developed CD; when data for Winter 2007 was omitted from the analysis, season was not associated with onset of disease ($p = 0.7141$).

Given that weight at processing is dependent on flock type, the effect of average weight at time of processing was analyzed for each flock type separately (Table 2.4). For each additional kilogram of weight at time of processing, heavy hens were 3.92 times more likely to develop CD ($p = 0.0003$). Weight at processing did not affect the odds of developing CD in light hens ($p = 0.6285$) and toms ($p = 0.8262$).

For light hen flocks the minimum, maximum, and average (mean ± standard deviation) bird densities at time of placement were 2.2, 16.1, and 4.4 ± 1.33 birds per square meter; for heavy hen flocks 1.3, 6.7, and 3.3 ± 0.49 birds per square meter; and for tom flocks 2.2, 4.2, and 2.7 ± 0.30 birds per square meter. Bird density had a limited affect on the incidence of CD. Given that the amount of floor space allotted per bird varies with flock type, the analysis was also conducted for flocks within each flock type. Bird density was not associated with CD in light hens ($p = 0. 7026$) or heavy hens ($p = 0.8071$); but there was a tendency in toms flocks that for every additional bird per square meter of floor space at time of placement tom flocks were 7.8 times more likely to develop CD ($p = 0.0772$). Stocking density is also commonly reported

in weight per unit area. When the analysis was conducted for weight in kilograms at time of processing per square meter of floor space, stocking density affected the incidence of CD ($p = 0.0032$). For each additional kilogram of weight per square meter of floor space flocks were 1.025 (95% CI: [1.008; 1.041]) times more likely to develop CD. However, stocking density by weight did not affect the incidence of CD for any of the individual flock types ($p > 0.10$).

No association was found between prior health events and development of CD ($p = 0.9595$); in particular, the presence of a prior enteric disease event had no impact on the incidence of CD in this study ($p = 0.9771$). Prior leg issues, including conformational problems and synovitis, were not associated with an increased incidence of CD ($p = 0.9192$). Administration of medications or vaccinations also had no effect on the incidence of CD ($p = 0.8306$).

Livability is defined as the percentage of birds placed that survive to the time of processing (percent livability = 100 – percent mortality). Livability was 88.8 ± 0.28% for all flocks without CD and 87.8 ± 0.44% for all flocks that developed CD ($p = 0.0144$). Livability was 92.3 ± 0.26% in light hen flocks, 90.4 ± 0.39% in heavy hen flocks, and 82.2 ± 0.60% in tom flocks ($p < 0.0001$). Birds placed in spring 2007 had a livability of 89.3 ± 0.37%, 89.0 ± 0.39% in winter 2007, 88.7 ± 0.36% in summer 2007, and 86.2 ± 0.40% in fall 2007 ($p < 0.0001$). There was no effect of breed on livability ($p = 0.3118$) and all 2-way interactions with CD were not significant and therefore not included in the final model. Livability was 92.0 ± 1.02% for light hen flocks with CD, 89.0 ± 1.14% for heavy hen flocks with CD, and 81.1 ± 1.50% for tom flocks with CD ($p < 0.0001$). Livability of flocks that developed CD in spring 2007 was 89.1 ± 1.27%, 88.4 ± 1.20% in summer 2007, 87.1 ± 1.28% in fall 2007, and 84.9 ±

1.37% in winter 2008 (p = 0.0264). There was no breed effect on livability of flocks with CD (p = 0.9093).

Table 2.1: Incidence of CD in flocks of one vertically integrated turkey company in the Mid-Atlantic region based on retrospective analysis of mortality and health reports (Study 1)

	Hybrid			Nicholas			Mixed			All Breeds[6]		
	N[1]	N_{CD}[2]	$\%_{CD}$[3]	N	N_{CD}	$\%_{CD}$	N	N_{CD}	$\%_{CD}$	N	N_{CD}	$\%_{CD}$
Light Hens	206	16	7.8	522	45	8.6	88	2	2.3	818[4]	63	7.7
Heavy Hens	8	2	25.0	165	36	21.8	8	2	25.0	181	40	22.1
Toms	11	3	27.3	47	14	29.8	0	0	n/a	58	17	29.3
All Flocks[5]	225	21	9.3	734	95	12.9	96	4	4.2	1057	120	11.4

[1]Number of flocks
[2]Number of flocks with CD
[3]Percent of flocks with CD
[4]The total number of light hen flocks includes 2 flocks for which breed was not identified
[5]Flock type associated with incidence of CD in univariate ($p < 0.0001$) and multivariate analysis ($p < 0.0001$)
[6]Breed associated with incidence of CD in univariate analysis ($p = 0.0216$)

Table 2.2: Incidence of CD in flocks placed for grow-out in a particular season for farms from one vertically integrated turkey company in the Mid-Atlantic region based on retrospective analysis of mortality and health reports (Study 1)

Season of Placement[1]	Total number of flocks placed	Number (percent) of flocks that developed CD
Winter 2007	195	28 (14.4)
Spring 2007	298	38 (12.6)
Summer 2007	314	32 (10.2)
Fall 2007	250	22 (8.8)

[1]Winter 2007 includes flocks placed in January, February, and March; Spring 2007 includes flocks placed in April, May, and June; Summer 2007 includes flocks placed in July, August, and September 2007; Fall 2007 includes flocks placed in October, November, and December 2007

Table 2.3: Season of onset of CD in turkey grow-out flocks placed in 2007 for farms of one vertically integrated turkey company in the Mid-Atlantic region based on retrospective analysis of mortality and health reports (Study 1)

Season of CD onset[1]	Number of flocks present in a given season	Number (percent) of flocks developing CD
Winter 2007	197	0 (0)
Spring 2007	493	30 (6.1)
Summer 2007	644	41 (6.4)
Fall 2007	588	30 (5.1)
Winter 2008	281	19 (6.8)

[1]Winter 2007 includes flocks present in January, February, or March 2007; Spring 2007 includes flocks present in April, May, or June 2007; Summer 2007 includes flocks present in July, August, or September 2007; Fall 2007 includes flocks present in October, November, or December 2007; Winter 2008 includes flocks present in January, February, or March 2008

Table 2.4: Factors affecting incidence of CD on farms of one vertically integrated turkey company in the Mid-Atlantic region based on retrospective evaluation of mortality and health reports and univariate analysis of individual risk categories (Study 1)

Factor	Category	Odds Ratio	95% Confidence Interval	p-Value
Weight at Processing[1]	Tom	0.948	[0.588; 1.529]	0.8262
	Heavy hen	3.921	[1.875; 8.199]	0.0003
	Light hen	1.155	[0.643; 2.075]	0.6285
Stocking Density (Birds)[2]	Tom	7.836	[0.799; 76.888]	0.0772
	Heavy hen	0.912	[0.437; 1.905]	0.8071
	Light hen	0.960	[0.779; 1.183]	0.7026

[1]Live weight, in kilograms
[2]Stocking density, in birds per square meter of floor space

2.3.2: Study 2 – National Incidence and Economic Impact

Incidence: Thirty nine flock supervisors/company veterinarians representing eight turkey companies completed the questionnaire on incidence and disease management of flocks marketed in 2008 (Table 2.5). CD was reported on close to 25% of turkey farms in this study. Livabilities for flocks with CD ranged from 87 to 96% for heavy hen flocks, 88 to 95% for light tom flocks, and 80 to 92% for heavy tom flocks.

Flock supervisors were also asked to identify the criteria of the official case definition for CD they actually use in identifying flocks with CD (Table 2.6). Nearly all respondents relied on the presence of subcutaneous emphysema (n = 37), serum/serosanguineous subcutaneous fluid (n = 38), and elevated flock mortality (n = 36) in identification of flocks with CD. Twenty seven respondents (69.2%) routinely relied on culture of *C. septicum*, *C. perfringens* type A, or *C. sordelli* from affected birds and only 22 (56.4%) relied on the presence of spleen and liver lesions. Only 5 respondents (12.8%) took samples for histopathology to identify the presence of cellular necrosis at the microscopic level.

Flock supervisors were asked to provide their thoughts on the causes and risk factors for the development of CD, management/treatment options and prevention strategies for the control of CD in turkey operations based on their own personal experiences. The most common responses regarding the cause and risk factors for development of CD included: infrequent mortality removal, wet litter conditions, presence of built-up litter in the house, and stress. Management and treatment options recommended by survey respondents include: increased mortality pick-up (at least 2-3 times per day), administration of penicillin and/or lincomycin via water, full clean out after every flock, and management to keep litter dry. Prevention strategies include: frequent mortality removal, full clean out after every flock, maintenance of dry litter conditions, increased down time between flocks, and the use of preventative antibiotics/iodine in the water.

Economic Impact: Seven companies returned the questionnaire on economic impact (Table 2.7). Two of the seven companies reported no cases of CD in turkey flocks marketed during the 2008 calendar year. Development of CD increased the cost of production for market

turkey flocks by 0.031 to 5.5 cents per kilogram for the five companies that reported cases of CD.

Table 2.5: Reports of CD for turkeys marketed during 2008 based on a national survey (Study 2)

	Total Number	Number with CD	Percent with CD
Companies	8	6	75
Farms	967	239[1]	24.7
Flocks	3398	639	18.8
Light hens	573	0	0
Heavy hens	211	10	4.7
Light toms	148	11	7.4
Heavy toms	2466	618	25.1

[1]Farms with at least one flock marketed during 2008 that developed CD

Table 2.6: Criteria used in identification of CD-positive flocks in 2008 based on a national survey of flock supervisors (Study 2); responses from 39 flock supervisors representing 8 companies

Criterion	Number (percent) of Respondents Using the Criterion
Subcutaneous emphysema (air bubbles under the skin)	37 (94.9)
Serum/serosanguineous subcutaneous fluid (fluid accumulation under the skin)	38 (97.4)
Vesicles (blisters) on the skin, especially in the breast/inguinal area	32 (82.0)
Moist, dark, wrinkled skin, especially in the breast/inguinal area	32 (82.0)
Cellular necrosis (microscopic)	5 (12.8)
Organ involvement (spleen/liver)	22 (56.4)
Vesicles on the skin, and/or moist, dark, wrinkled skin in the tail area	32 (82.0)
C. septicum, *C. perfringens* type A, or *C. sordelli* isolated from fluid or affected skin/tissue samples of affected/dead birds	27 (69.2)
Elevated mortality	36 (92.3)

Table 2.7: Increase in cost of production associated with development of CD in turkeys marketed in 2008 based on a national survey (Study 2)

Survey Code	Company Code	Increase in Cost of Production (cents/kilogram)
EI-1	3	N/A (no cases of clostridial dermatitis)
EI-2	4	1.1
EI-3	5	2.2
EI-4	6	5.5
EI-5	6a	4.6
EI-6	7	0.79
EI-7	8	0.031 (toms), 0.037 (hens)
EI-8	9	N/A (no cases of clostridial dermatitis)

2.4 Discussion

Flock type, breed, weight at time of processing, and stocking density affected the incidence of CD. 31.7% of farms in Study 1, 24.7% of farms in Study 2, and 42.3% of farms in a 2010 USDA study of fifteen turkey companies across the United States had at least one flock that developed CD during the study period [7]. The incidence of CD was highest in tom flocks and lowest in light hen flocks, which is consistent with industry reports [6]. In Study 1, 7.7% of light hen flocks developed CD while no light hen flocks were affected in Study 2. The incidence of CD in heavy hen flocks was much higher in the 2007 regional study (Study 1) than in the national survey (Study 2); 22.1% versus 4.7%, respectively. Incidences of CD in heavy tom flocks were similar in Study 1 (29.3%) and Study 2 (25.1%). No comparison can be made for light tom flocks as the company involved in the Study 1 does not raise that type of bird. Flock type was not evaluated in the 2010 USDA study [7].

Initial univariate analysis indicated that breed affected the incidence of CD. However, when flock type and breed were evaluated together in a single model, the effect of breed was not significant. Most of the heavy hen and tom flocks included in Study 1 were Nicholas flocks; therefore, Nicholas flocks appeared to have a higher incidence of CD than Hybrid or mixed

flocks. This corresponds to results from the 2010 USDA study evaluating risk factors for the development of CD in which effect of breed was also found not to be significant [7].

Bird density (birds per square meter of floor space) had a limited effect on the incidence of CD. Tom flocks were 7.8 times more likely to develop CD for each additional bird per square meter. Stocking density (kilograms at time of processing per square meter of floor space) had a larger impact on the incidence of CD. Flocks were 1.025 times more likely to develop CD for every additional kilogram per square meter. This is consistent with other reports that associate increased stocking density with an increased incidence of CD [6, 13].

Historically, CD lesions have typically been seen in older birds near the time of market. Onset of the disease generally occurs between 13 and 18 weeks of age, with the youngest age of onset reported to be 6 weeks of age [3, 6, 11, 16]. The earlier age of onset observed in Study 1 compared with earlier reports may reflect an increased awareness of CD on the part of flock supervisors/veterinarians and a better ability to detect early signs of the disease.

Season of placement, season of onset, prior health events, and prior vaccinations and/or medications did not affect the incidence of CD in Study 1. It has been reported that incidence and severity of cellulitis are worse in the summer and early fall [3, 7, 16]. No flocks placed in 2007 developed CD in January-April 2007; however, this does not necessarily imply that no flocks developed CD during those months since flocks placed in 2006 (which were not included in this study) may have developed CD during that time period. Few flocks were truly at risk for developing CD during Winter 2007 since many of these flocks were younger than the expected age range for onset of CD. Omitting results from Winter 2007 from the analysis negated the effect of season on the development of CD. Results from Study 1 do not show evidence for a seasonal effect on CD incidence.

As *C. septicum* and *C. perfringens* are normal inhabitants of the turkey's gastrointestinal tract, overgrowth of the organism and/or suppression of the bird's immune system are thought to play important roles in the development of CD. Maintenance of good intestinal health has been implicated as an important factor in preventing CD [6, 8]. Prior health events and prior administration of medications or vaccinations did not affect the incidence of CD in the regional study.

Livability was affected by development of CD, flock type, season of placement, and season of onset but not by breed. In the USDA 2010 study, average livability was reported to be between 89.3 and 89.9% for flocks without CD and 83 to 85.8 % for flocks with CD [7]. Mortality risk associated with CD has been reported as high as 1-2% per week [7, 11]. Decreased livability for flocks that developed CD in fall 2007 and winter 2008 is in contrast to the 2010 USDA study which reported an increased severity (increased mortality associated with CD) during the summer and fall months [7]. The livabilities obtained for heavy hens and toms in Study 1 fall within the ranges obtained in Study 2. While there was no seasonal pattern to the onset of CD, season of placement did affect the livability for flocks that developed CD in Study 1. The effect of season of placement on livability may reflect the impact of environmental factors on mortality during the crucial brooding period.

The results of the national survey in Study 2 suggest that flock supervisors rely most heavily on gross pathology findings and mortality when diagnosing flocks with CD. While it is commonly reported that increased frequency of mortality removal reduces the incidence and/or severity of CD as this practice removes a source of infection for other birds in the house [6], the frequency of mortality removal was not associated with the disease status of turkey farms in the 2010 USDA study [7]. In the United States, turkey houses are often not cleaned out between

flocks to keep costs down. The use of built-up litter in turkey houses has been implicated in the development of CD as this practice allows for the accumulation of clostridial spores in the environment [6, 17]. Wet litter, resulting from water spills in the turkey house or from turkeys experiencing diuresis or diarrhea, has been associated with an increased incidence of CD as it favors the proliferation of *Clostridium* species in the environment [6, 13]. Dexamethasone treatment, in the absence of *C. septicum* or *C. perfringens* challenge, results in the development of CD which suggests that stress may be a factor in the development of this disease [13]. These responses are in line with previously published recommendations [6, 7].

The average wholesale price for turkeys produced in the United States in 2008 was 124.6 cents per kilogram [18]. Development of CD increased the cost of production for market turkey flocks by 0.031 to 5.5 cents per kilogram. Statistical analysis and development of a predictive model for which flocks are likely to develop CD is constrained by the complex interactions between host, pathogen, and environmental factors which contribute to the development of this disease. When practical, producers should consider modifying the flock type, breed, stocking density, target body weight, and timing of placement in order to minimize the incidence and/or severity of CD outbreaks.

2.5 References

1. Rives, D., D. Mills and S. Clark. Current health and industry issues facing the turkey industry. Report of the Committee on Transmissible Diseases of Poultry and Other Avian Species. Minneapolis, MN. 2006.

2. Clark, S. R., B. Tilley and D. Mills. Current health and industry issues facing the turkey industry. In: Proc. 112th Annual Meeting of the USAHA, Greensboro, NC. Richardson Printing, Kansas City, MO.:530-535. 2009.

3. Carr, D, D Shaw, DA Halvorson, B Rings and D Roepke. Excessive mortality in market-age turkeys associated with cellulitis. Avian Diseases 40:736-741. 1996.

4. Fenstermacher, R and BS Pomeroy. *Clostridium* infection in turkeys. Cornell Veterinary Journal 29:25-28. 1939.

5. Tellez, G, NR Pumford, MJ Morgan, AD Wolfenden and BM Hargis. Evidence for *Clostridium septicum* as a primary cause of cellulitis in commercial turkeys. Journal of Veterinary Diagnostic Investigation 21:374-377. 2009.

6. Clark, S, R Porter, B McComb, R Lippert, S Olson, S Nohner and HL Shivaprasad. Clostridial dermatitis and cellulitis: an emerging disease of turkeys. Avian Diseases 54:788-794. 2010.

7. USDA. Poultry 2010: Clostridial dermatitis on US turkey-grower farms. USDA-APHIS-VS-CEAH-NAHMS. 2012.

8. Dibner, JJ. The role of gut barrier failure in gangrenous cellulitis of poultry. In: MTRPC Gold Medal Panel on [cellulitis] clostridial dermatitis. Bllomington, MN. p 20. 2008.

9. Tellez, G., N. R. Pumford, M. J. Morgan, A. D. Wolfenden and B. M. Hargis. Evidence for Clostridium septicum as a primary cause of cellulitis in commercial turkeys. J Vet. Diagn. Invest. 21:374-377. 2009.

10. Nagaraja, KV, AJ Thachil and DA Halvorson. Role of *Clostridium perfringens* and *septicum* in cellulitis in turkeys. In: 58th Western Poultry Disease Conference Madison, WI. p Page 10. 2009.

11. Thachil, AJ, B McComb, MM Anderson, DP Shaw, DA Halvorson and KV Nagaraja. Role of *Clostridium perfringens* and *Clostridium septicum* in causing turkey cellulitis. Avian Diseases 54:795-801. 2010.

12. Shivaprasad, H. L. Gangrenous dermatitis due to Clostridium septicum in turkeys. In: MTRPC Gold Medal Panel on [cellulitis] clostridial dermatitis Bloomington, MN. 2008.

13. Huff, G.R., W.E. Huff and N.C. Rath. Dexamethasone immunosuppression resulting in turkey clostridial dermatitis: a retrospective analysis of seven studies, 1998-2009. Avian Dis 57:730-736. 2013.

14. JMP, Version 8. SAS Institute Inc., Cary, NC. 2008.

15. SAS User's Guide, Version 9.3. SAS Inst. Inc., Cary, NC., 2010.

16. McComb, B. Upper midwest filed perspective of dermatitis in commercial turkeys. In: MTRPC Gold Medal Panel on [cellulitis] clostridial dermatitis. Bloomington, MN. pp 5-8. 2008.

17. Thachil, AJ, B McComb, M Kromm and KV Nagaraja. Vaccination of turkeys with *Clostridium septicum* bacterin-toxoid: evaluation of protection against clostridial dermatitis. Avian Dis 57:214-219. 2013.

18. USDA. Poultry - Production and value, 2009 summary. National Agricultural Statistic Service. 2010.

Chapter 3 – Presence of *Clostridium* spp. and Histopathologic Lesions in Asymptomatic Turkeys on Farms with a Chronic History of Clostridial Dermatitis

3.0 Abstract

Clostridial dermatitis (CD) is a disease of turkeys that presents with gangrenous lesions on inguinal breast and thigh. A sudden increase in mortality is typically the first sign of disease in affected flocks. *Clostridium septicum* has been identified as the primary causative agent for CD in turkeys; although other *Clostridium* species may also play a role in pathogenesis of the disease. For some clostridial diseases that result in soft tissue infections, including gangrenous dermatitis of poultry and malignant edema of ruminants, the route of entry for the organism is through breaks in the skin. However, this is not the case in turkeys with CD as lesions develop in the absence of preceding penetrating trauma. *C. septicum* is a Gram-positive, anaerobic, spore-forming, exotoxin-producing rod that is frequently isolated from the gastrointestinal tracts of healthy turkeys. We hypothesize that the vegetative form of the organism translocates from the gastrointestinal lumen into the intramural vasculature or lymphatics from where it can then enter peripheral circulation. The organism ultimately locates to the capillaries of skeletal muscle and/or subcutaneous tissues. At some point during this process the organism undergoes sporulation in an attempt to survive the oxygen rich environment of the blood and well-perfused tissues. Muscle, intestine, liver, and blood samples were obtained from asymptomatic turkeys on farms with a known history of CD as well as from farms with no history of CD. DNA was extracted from these samples and real time polymerase-chain reaction (qPCR) specific for the alpha toxin genes of *C. septicum* and *C. perfringens* was performed. Detection of *Clostridium* spp. in tissues from asymptomatic turkeys supports the hypothesis for hematogenous spread of the organism. Detection of these organisms in tissues from turkeys on farms with no history of

CD suggests that presence of the organism alone is not sufficient to cause disease. Histopathologic examination showed an increased incidence and severity of polyphasic myonecrosis in skeletal muscle sections from asymptomatic turkeys on farms with a chronic history of CD, suggesting an underlying predisposition for the development of CD.

3.1 Introduction

CD, previously known as cellulitis, is a disease of rapidly growing turkeys that initially presents as a sudden increase in flock mortality. Affected birds have gangrenous lesions of the subcutaneous tissues and muscle on the caudal breast, thigh, and inguinal region [1]. *Clostridium septicum* has been identified as the primary causative agent, with possible involvement of *C. perfringens* and/or *C. sordellii* [2, 3]. There are currently two theories as to how the organism(s) gain entry. The inside-out model suggests an exogenous (environmental) source of the organism which gains entry via scratches or penetrating trauma to the skin while the outside-in model suggests an endogenous (gastrointestinal) source of the organism with translocation and hematogenous spread to the muscle and/or subcutaneous tissue. The inside-out model is similar to the mechanism of pathogenesis for gangrenous dermatitis in chickens and malignant edema in ruminants while the outside-in model is similar to that of blackleg in ruminants and spontaneous gas gangrene in humans [4-8].

In turkeys with CD, gangrenous lesions typically develop in skeletal muscle and subcutaneous tissues without the presence of skin scratches or penetrating wounds [9, 10]. Given the absence of penetrating trauma in affected turkeys, we hypothesize that CD follows a similar pathogenesis to that of blackleg. With blackleg in cattle, spores of *C. chauvoei* have been shown to remain dormant in muscle until local conditions become favorable for germination and

proliferation [11, 12]. If the inside-out model of pathogenesis is true for CD in turkeys, we would expect to be able to identify genomic DNA from *C. septicum* and/or *C. perfringens* in muscle samples from asymptomatic turkey flocks in houses with a known history of CD. Histopathology of muscle should confirm that the spores of these organisms are present in the absence of lesions consistent with CD. Detection of these organisms in healthy turkeys from farms with no history of CD would imply that presence of the organism alone is not sufficient to cause disease.

3.2 Materials and Methods

3.2.1 Sample Collection:

Six turkey flocks between ten and nineteen weeks of age were divided into two groups: three with a chronic history of CD and three with no history of CD. Samples were collected from eight asymptomatic birds on each farm. Birds selected for inclusion in the study had no signs of lameness, muscle lesions, or evidence of cutaneous trauma. All samples were harvested from recently euthanized birds. The sample collection protocol was approved by the Virginia Tech Institutional Animal Care and Use Committee. Caudal breast muscle, thigh muscle, liver, ileal, and cecal samples were placed in 1.5mL microcentrifuge tubes (USA Scientific, Inc. Ocala, FL, USA) and flash frozen using dry ice and ethanol then stored at -80°C until DNA extraction could be performed. Blood was collected from the brachial vein in 10mL red-top collection tubes (Becton, Dickinson and Company, Fralin Lakes, NJ, USA). Blood samples were centrifuged for 5 minutes at 3000 x g, serum was removed from the clot, placed in a 2.0mL microcentrifuge tube, and stored at -20°C. Full thickness muscle and skin sections were

collected from the left caudal breast and inner thigh and stored in 10% buffered formalin (Fisher Thermo Scientific, Pittsburgh, PA, USA) for histopathology.

3.2.2 DNA Extraction and PCR for C. septicum and C. perfringens:

Total genomic DNA (bacterial and turkey) was extracted from the blood and tissue samples using a protocol modified from the QIAamp DNA Mini and Blood Mini Handbook (QIAGEN, Inc. Valencia, CA, USA). 25mg of tissue was placed in a 2.0mL microcentrifuge tube (USA Scientific) with 270 µL of tissue lysis Buffer ATL (QIAGEN). 30µL of proteinase K (QIAGEN) was added and the sample was incubated at 56°C, vortexing every 30 minutes, until the tissue was completely lysed (approximately 4-6 hours). 300µL of lysis Buffer AL (QIAGEN) was added and the sample was incubated at 70°C for 10 minutes. 300µL of ethanol (Acros Organics, Geel, Belgium) was added to the sample lysate to create conditions that favor the binding of DNA to the QIAamp Mini spin column. After the DNA was bound to the spin column membrane, several wash steps were used to remove contamination. DNA extracted from the tissue was eluted using 400µL of Buffer AE (QIAGEN).

DNA was extracted from serum samples using the QIAamp DNA Mini Kit (QIAGEN). 20µL of proteinase K, 200µL Buffer AL, and 200µL of serum were added to a 2.0mL microcentrifuge tube, vortexed to homogenize, and incubated at 56°C for 10 minutes. 200µL of ethanol was added to the sample lysate prior to binding, washing, and eluting DNA from the spin column following the same protocol use for the tissue samples.

Quantitative real-time PCR (qPCR) reactions were set up in a 96-well Hard Shell ® thin-walled PCR plate (Bio-Rad Life Science Research, Hercules, CA, USA) with 10µL iTaq

Universal SYBR Green Supermix (Bio-Rad), 7µL nuclease-free H2O, 1µL each of forward and reverse primers specific for the alpha toxins of *C. septicum* or *C. perfringens* (Life Technologies, Grand Island, NY, USA) (Table 1), and 1µL of template DNA. qPCR was performed using the CFX Connect System (Bio-Rad) using thermocycler conditions outlined by the primer developers [13, 14].

qPCR results were analyzed using Bio-Rad CFX Connect Manager software. Samples were determined to be positive for *C. septicum* if amplification of the alpha toxin gene (CsA) occurred below 30 cycles, suspect if amplification occurred between 30 and 35 cycles, and negative if amplification occurred after 35 cycles or if the product melting temperature was not consistent with the expected melting temperature for the CsA product. Samples were determined to be positive for *C. perfringens* if amplification of the alpha toxin gene (CpA) occurred below 28 cycles, suspect if amplification occurred between 28 and 35 cycles, and negative if amplification occurred after 35 cycles or if the product melting temperature was not consistent with the expected melting temperature for the CpA product. These thresholds were determined based on non-specific amplification of negative controls (*E. coli* field isolate, *C. septicum* ATCC 12464 for CpA assay, *C. perfringens* ATCC 13124 for CsA assay, and control tissue and serum obtained from 4-7 week old turkeys raised in research facilities at Virginia Tech). Tissue and blood samples were artificially-infected in the laboratory in order to verify the DNA extraction protocol and to determine the limit of detection for the qPCR assays. qPCR-positive samples contained at least 6.6×10^3 colony forming units (CFUs) of *C. septicum* or 2.1×10^4 CFUs of *C. perfringens.* qPCR-suspect samples contained between 6.6 and 6.6×10^2 CFUs of *C. septicum* or between 2.1 and 2.1×10^3 CFUs of *C. perfringens*. Statistical analysis was performed using the

Wilcoxon/Kruskal-Wallis test (nonparametric oneway ANOVA); significance was assigned based on $p < 0.05$ [15].

Table 3.1: Primer Sequences used for qPCR

Target Gene	Primer Sequence	Product Size (bp)	Product Melting Temp (°C)
C. septicum alpha toxin [14]	Forward: 5`-TAGGATTTGGATGGTGCGGTGGAA-3` Reverse: 5`-TGCACGATACCCACTTGCATAAGG-3`	149	77.0
C. perfringens alpha toxin [13]	Forward: 5`-AGAACTAGTAGCTTACATATCAACTAG TGGTG-3` Reverse: 5`-TTTCCTGGGTTGTCCATTTCC-3`	124	75.5

3.2.3 Histopathology

Skin and muscle samples from the inguinal breast and thigh were collected into 10% buffered formalin and fixed for a minimum of 24 hours prior to processing. The Histopathology Laboratory of Virginia Tech Animal Laboratory Services (ViTALS, Blacksburg, VA, USA) prepared the tissues for light microscopy by dehydration using ethanol and xylene as solvents. Dehydrated tissues were infiltrated with paraffin, sectioned, and stained with hematoxylin and eosin (H&E) stain. Tissue sections were examined for the presence of rod-shaped bacteria and cellular necrosis and scored using a Likert-type scale for the presence of rod-shaped bacteria consistent with *Clostridium* spp. and necrosis. Bacteria scores: 0 = no bacteria present, 1 = few isolated bacteria, 2 = mild bacteria, 3 = moderate bacteria, 4 = severe bacteria. Necrosis scores: 0 = within normal limits, 1 = few isolated necrotic cells, 2 = up to 25% necrotic cells, 3 = 25-50% necrotic cells, 4 = 50-75% necrotic cells, 5 = greater than 75% necrotic cells. Results were

compared to control breast and thigh muscle samples obtained from 6 ½ and 7 ½ week old turkey hens raised at a Virginia Tech research facility. Statistical analysis was performed using the Wilcoxon/Kruskal-Wallis test; significance was assigned based on $p \leq 0.05$ [15].

3.3 Results

3.2.1 Detection of Clostridium species in blood and tissues from asymptomatic birds

C. septicum was detected in breast muscle, thigh muscle, liver, ileal, and cecal samples in asymptomatic birds from farms with no history of CD (Table 3.2). Three of 24 (12.5%) birds were positive and 9 (37.5%) were suspect for the presence of *C. septicum.* Twelve of 120 (10%) tissue samples from these birds were positive and 24 (20%) were suspect (Table 3.3). No tissue samples from asymptomatic birds on farms with a chronic history of CD were positive for *C. septicum*; although, 14 of 24 (58.3%) birds and 28 of 120 (23%) tissue samples were suspect. Only two ileal samples from asymptomatic birds on farms with a chronic history of CD were positive for *C. perfringens* (Table 3.4). However, 13 of 120 (10.8%) of tissue samples from each type of farm were suspect for *C. perfringens* (Table. 3.5). The incidence of *C. septicum* and *C. perfringens* in tissue samples was not affected by farm history of CD ($p = 0.5586$ and $p = 0.5563$, respectively). Neither *C. septicum* nor *C. perfringens* were detected in blood samples from asymptomatic turkeys on any farm (Tables 3.2 and 3.4). One blood sample from turkeys on farms with no history of CD was suspicious for *C. septicum* while blood from another turkey was suspicious for the presence of *C. perfringens* (Table 3.3).

Table 3.2: Detection of *C. septicum* in tissue and blood samples from asymptomatic turkeys on farms with no history of CD and farms with a chronic history of CD

Farm	Breast			Thigh			Liver			Ileum			Cecum			Blood		
	+	+/-	-	+	+/-	-	+	+/-	-	+	+/-	-	+	+/-	-	+	+/-	-
No CD History	2	2	20	3	6	15	3	5	16	3	6	15	1	5	18	0	1	23
Chronic CD History	0	8	16	0	6	18	0	8	16	0	5	19	0	1	23	0	0	24

Positive (+): Cq < 30 cycles
Suspect (+/-): 30 cycles ≤ Cq < 35 cycles
Negative (-): Cq ≥ 35 cycles

Table 3.3: Cumulative values for detection of *C. septicum* in tissue and blood samples from asymptomatic turkeys

Farm	Muscle and Liver				Intestine				All Tissues				Blood			
	P[1]	P/S[2]	%P[3]	% P/S[4]	P	P/S	%P	% P/S	P	P/S	%P	% P/S	P	P/S	%P	% P/S
No CD history	8	21	11.1	29.2	4	15	3.1	31.3	12	36	10	30	0	1	0	4.2
Chronic CD history	0	22	0	30.6	0	6	0	12.5	0	28	0	23.3	0	0	0	0

[1]Number of samples positive for *C. septicum*
[2]Number of samples positive or suspect for *C. septicum*
[3]Percentage of total samples tested that were positive for *C. septicum*
[4]Percentage of total samples tested that were positive or suspect for *C. septicum*

Table 3.4: Detection of *C. perfringens* in tissue and blood samples from asymptomatic turkeys on farms with no history of CD and farms with a chronic history of CD

Farm	Breast			Thigh			Liver			Ileum			Cecum			Blood		
	+	+/-	-	+	+/-	-	+	+/-	-	+	+/-	-	+	+/-	-	+	+/-	-
No CD History	0	1	23	0	3	21	0	3	21	0	2	22	0	4	20	0	1	23
Chronic CD History	0	2	22	0	4	20	0	2	22	2	1	21	0	4	20	0	0	24

Positive (+): Cq < 28 cycles
Suspect (+/-): 28 cycles ≤ Cq < 35 cycles
Negative (-): Cq ≥ 35 cycles

Table 3.5: Cumulative values for detection of *C. perfringens* in tissue and blood samples from asymptomatic turkeys

Farm	Muscle and Liver				Intestine				All Tissues				Blood			
	P[1]	P/S[2]	%P[3]	% P/S[4]	P	P/S	%P	% P/S	P	P/S	%P	% P/S	P	P/S	%P	% P/S
No CD history	0	1	0	1.4	0	6	0	12.5	0	13	0	10.8	0	1	0	4.2
Chronic CD history	0	2	0	2.8	2	7	4.2	14.6	2	15	1.7	12.5	0	0	0	0

[1]Number of samples positive for *C. perfringens*
[2]Number of samples positive or suspect for *C. perfringens*
[3]Percentage of total samples tested that were positive for *C. perfringens*
[4]Percentage of total samples tested that were positive or suspect for *C. perfringens*

3.2.2 Histopathology of muscle and skin sections from asymptomatic birds

No rod-shaped bacteria were seen in any of the muscle or skin histopathology sections. Polyphasic myonecrosis, characterized by the presence of varying stages of degeneration, necrosis, and regeneration of individual myofibers within a tissue section, was seen in 75% of the muscle sections obtained from asymptomatic turkeys on farms (Figure 3.1). Both breast and thigh muscle sections were affected. Inflammatory cells (e.g. macrophages, heterophils) were present clearing necrotic debris in some of the tissue sections. Nerves in affected tissue sections were within normal limits. Subcutaneous tissues and connective tissue surrounding myofiber bundles were within normal limits for all tissue sections examined. No bacteria, inflammation, or necrosis were seen in any of the skin sections examined.

History of CD on the premises significantly influenced the average necrosis score for muscle tissue sections ($p = 0.0281$). The average necrosis score for muscle sections obtained from turkeys on farms with a chronic history of CD was 1.0 ± 0.12 (mean ± standard error) compared to 0.6 ± 0.15 for turkeys from a farm with no history of CD and 0.3 ± 0.21 for turkeys

from a research facility with no history of CD. Average necrosis score was also significantly influenced by age ($p = 0.0137$), with older flocks having higher average scores. Although not significant, there was a trend for feed conversion ratio (FCR) to be associated with average necrosis score ($p = 0.0509$); flocks with higher average necrosis scores tended to have higher feed conversion ratios (Figure 3.2). Average daily gain (ADG) and gender were not associated with average necrosis score ($p = 0.7372$ and $p = 0.8485$, respectively). There was no association between average necrosis score and detection of *C. septicum* or *C. perfringens* DNA on qPCR ($p = 0.0953$ and $p = 0.4873$, respectively).

Figure 3.1: Histomicrographs of muscle sections from asymptomatic turkeys

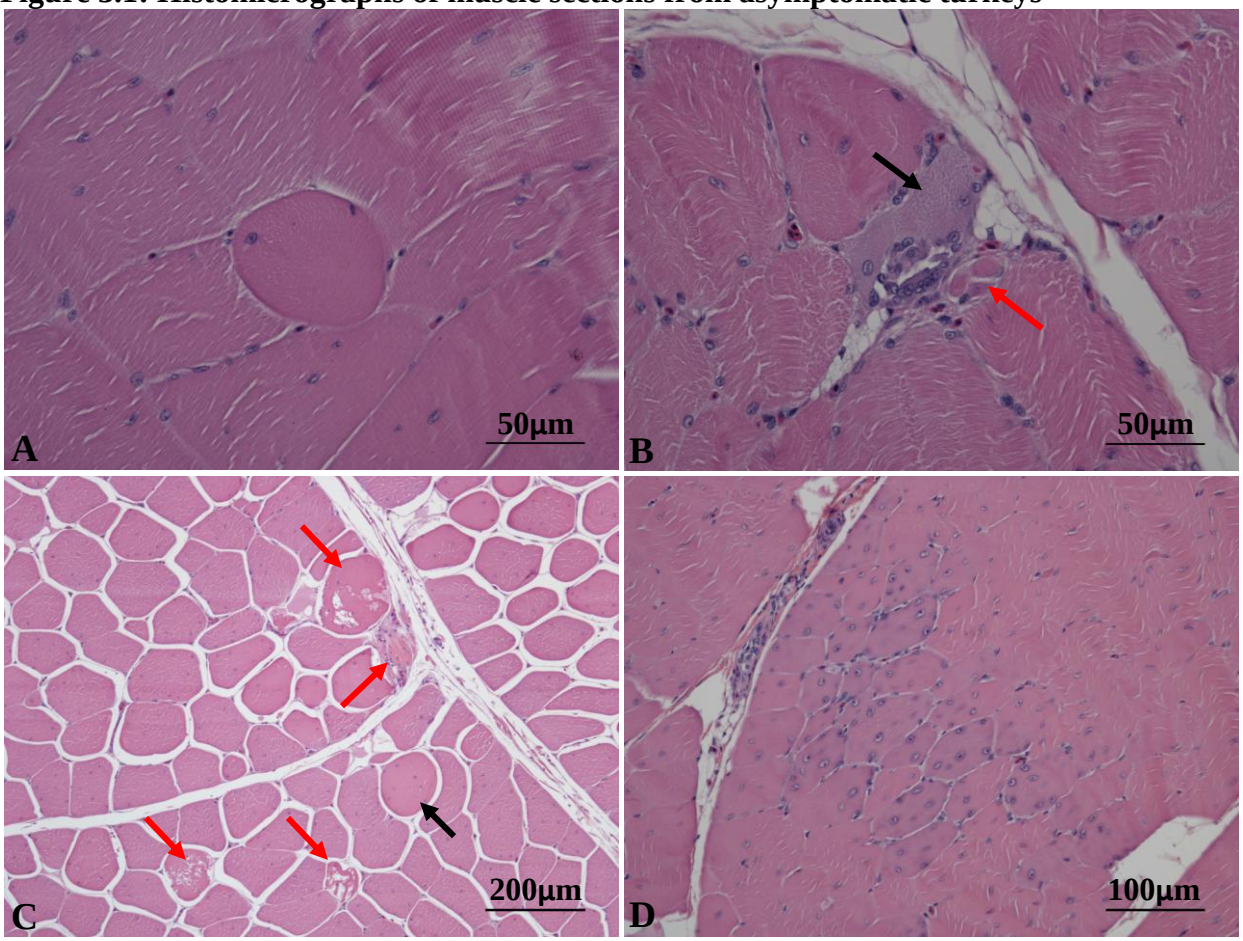

A: Degeneration of an individual myofiber; 400X magnification
B: Necrotic (red arrow) and regenerative (black arrow) myofibers; 400X magnification
C: Degenerate (black arrow) and necrotic (red arrows) myofibers; 100X magnification
D: Cluster of multiple regenerative myofibers; 200X magnification

Figure 3.2: Association of necrosis score with average daily gain (ADG) and feed conversion ratio (FCR)

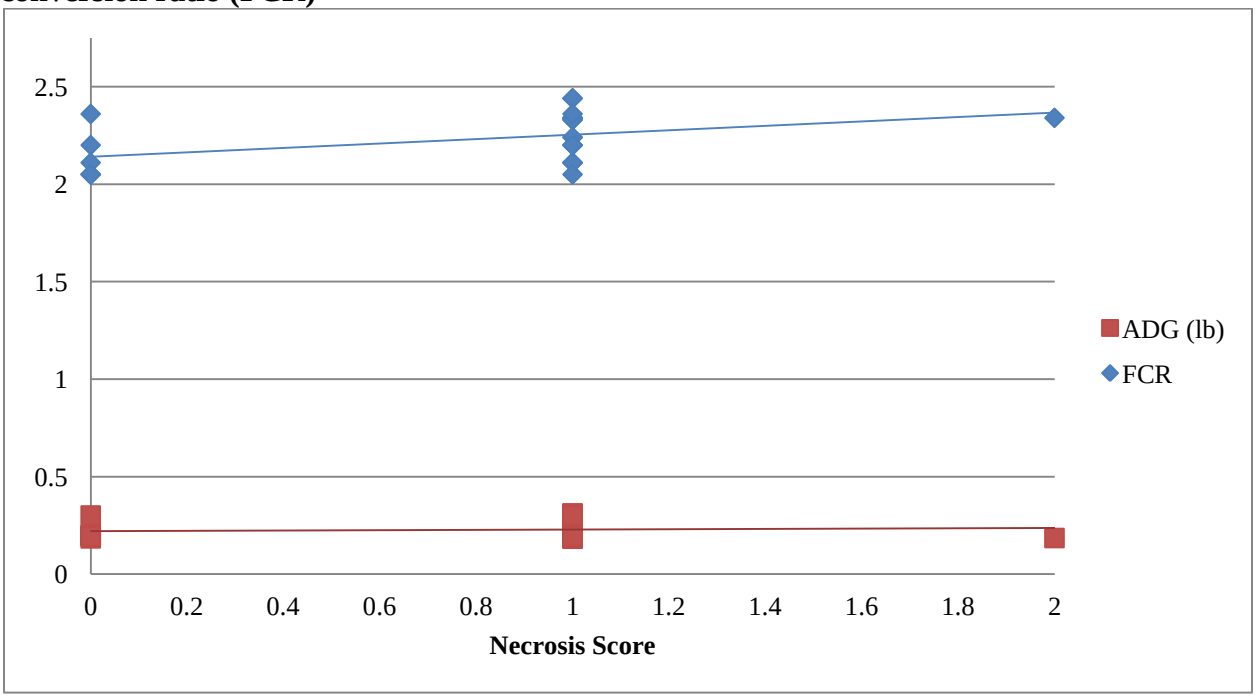

3.4 Discussion

The results of this study support the proposed mechanism for development of CD in turkeys. Although no rod-shaped bacteria consistent with *Clostridium* spp. were seen in histopathology sections of skeletal muscle from asymptomatic turkeys, *C. septicum* and *C. perfringens* were detected via qPCR in the gastrointestinal tract, liver, and skeletal muscle of asymptomatic turkeys. Focal polyphasic myonecrosis was present in breast and thigh skeletal muscle sections from asymptomatic turkeys. Incidence and severity of myonecrosis were associated with farm history of CD and flock age. Older birds on farms with a chronic history of CD were more likely to have focal myonecrosis which suggests that the presence of this myonecrosis may predispose birds to the development of CD.

Detection of *C. septicum* and *C. perfringens* in liver and skeletal muscle from turkeys with no external wounds supports the hypothesis for hematogenous spread of these organisms rather than direct inoculation via penetrating trauma. Thirty percent of tissue samples from farms with no history of CD and 23% of tissue samples from farms with a chronic history of CD were either positive or suspect for the presence of *C. septicum*. This implies that the presence of *C. septicum* in tissues alone is not sufficient to cause disease. Certain pathogen, host, and/or management factors which favor multiplication of this organism must also be present in order for birds to develop CD. Although *Clostridium* spp. were not detected in blood samples in this study, hematogenous spread remains the most likely explanation for the presence of these organisms in liver and skeletal muscle. This suggests that hematogenous spread of these organisms is transient and intermittent or that translocation requires an insult to the gastrointestinal tract.

The ability to detect *Clostridium* spp. in this study was limited by the sensitivity and specificity of the assays used. Although the primer sets used for the qPCR assays were previously validated and published as being specific for *C. septicum* and *C. perfringens*, the results from this study show cross-reactivity between *Clostridium* spp. These primer sets were originally developed for use in multiplex assays utilizing fluorogenic probes. In this study, all qPCR reactions were run as simplex assays without the use of probes which may have impacted the specificity of these assays. Some samples were classified as "suspect" for the presence of *C. septicum* and/or *C. perfringens* based on high Cq values. High Cq values could result from either low copy number (low number of organisms) in the sample or cross-reactivity between *Clostridium* spp. Administration of antibiotics to treat and/or prevent CD in flocks on farms with a chronic history of the disease may have reduced the number of organisms present in tissues to a

level below the limit of detection for these assays. The company veterinarian reported that five of the six houses sampled on farms with a chronic history of CD had received antibiotics via the drinking water at some point prior to sample collection for this study.

Focal skeletal myopathies characterized by degeneration and necrosis of individual myofibers in histopathology sections of breast and leg muscles from turkeys exhibiting no gross lesions or clinical signs of lameness have been reported since the 1960s [16-18]. The total number of myofibers present in a muscle is determined during embryonic development; postembryonic muscle growth is a factor of myofiber hypertrophy and elongation [19]. Since muscle fibers cannot be multiplied or replaced, necrosis of these fibers during growth may predispose birds to development of other conditions, such as CD, later in life. Myonecrosis may come first in the pathogenesis of CD with bacterial colonization of necrotic tissue by *Clostridium* spp. occurring as a sequella.

Higher incidences of focal skeletal myopathies in rapidly-growing lines of turkeys suggest that the pathogenesis of these conditions likely includes an underlying genetic predisposition; however, the inciting cause has not yet been identified [17, 20]. Several potential mechanisms have been proposed including ischemia, insufficient connective tissue support, nutritional deficiencies, and neuropathies [16-18, 20, 21]. Focal myopathy may be the result of micro-ischemia at the level of the terminal capillary beds surrounding individual muscle fibers [17, 18]. Prolonged, direct pressure on a particular muscle, as occurs in heavy hens and toms spending long periods of time sitting down in ventral recumbency, may result in a decrease in the arteriovenous pressure-gradient leading to decreased capillary blood flow [18]. Shortly after hatch, maturing myofibers may appear myotube-like with rounded and loosely-packed fibers in histologic sections [17]. Normal, mature myofibers are polygonal in shape and closely-packed

together. The presence of rounded, loosely-packed myofibers in older birds is thought to be due to the rate of connective tissue growth not keeping pace with myofiber growth ultimately resulting in disruption of normal cell-to-cell relationships [17]. In this study, muscle fibers in tissue sections with higher necrosis scores were typically more rounded and loosely packed than in unaffected tissue sections. Selenium deficiency typically results in gizzard and myocardial myopathies in chickens and turkeys, but it has also been shown to cause Zenker's degeneration of skeletal muscle [21]. A nutritional deficiency seems an unlikely cause for the skeletal myonecrosis seen in this study since histopathologic lesions were seen in both large-scale commercial and small-scale research flocks that were receiving feed from different sources. Monensin, an ionophore coccidiostat, has been shown to induce subclinical necrosis of skeletal muscle when used at therapeutic levels in poultry feed [22, 23]. While the commercial flocks included in this study had received monensin, focal polyphasic myonecrosis also occurred in asymptomatic turkeys from a research flock which had not received the coccidiostat. Monensin toxicity typically causes necrosis of Type I myofibers in the leg muscles of turkeys while the pectoral (breast) muscle primarily consists of Type II myofibers [22]. Since lesions were present in both the breast and thigh, monensin was likely not responsible for the focal polyphasic myonecrosis observed in this study. Neuropathic origin is thought to be unlikely since affected fibers are found scattered throughout a muscle; neuromuscular disorders typically present with a group of affected myofibers in close proximity to a nerve synapse [16, 18]. The normal appearance of the nerves present in the muscle sections included in this study and random distribution of affected myofibers throughout muscle sections supports the hypothesis that the focal myopathy observed in these birds is not the result of a neuromuscular disorder. Decreased capillary blood flow (micro-ischemia) to the caudal breast and thigh muscles secondary to

prolonged pressure from sitting and/or insufficient connective tissue support resulting from rapid growth rate likely contributed to the focal polyphasic myonecrosis seen in this study.

Turkeys from farms with a chronic history of CD had an increased incidence and severity of focal polyphasic myonecrosis. The polyphasic necrosis likely predisposes birds on these farms to the development of CD. Turkeys in eleven of the twelve turkey houses included in this study were of the same breed. Therefore, environmental and management conditions on individual farms rather than genetic differences probably have a greater impact on the incidence and severity of polyphasic myonecrosis.

The results from this study are consistent with previous reports of an increase in the incidence and severity of focal skeletal myopathies with increasing age [16, 17, 20]. Increased muscle size with insufficient vascular supply thought to contribute to the increased incidence of focal skeletal myopathies in older birds [16, 18]. As turkeys get older, and therefore larger, they have a tendency to develop a more sedentary lifestyle. Spending prolonged periods of time lying down on the breast muscle may result in relative-ischemia leading to development of focal skeletal myopathies [18]. Previous studies found that rapid growth rate was associated with an increased incidence of focal skeletal myopathies in turkeys [17, 20]. There was a tendency for increased FCR to be associated with an increased average necrosis score in this study. Statistical analysis was unable to determine the exact nature of this association; changes in FCR could be causing changes in necrosis scores or vice versa. FCR is associated with growth rate; improved FCR is typically accompanied by an increased rate of growth [24]. Based on the results of previous studies we would expect a decreased FCR, indicative of an increased rate of growth, to be associated with an increase in average necrosis score. However, the results of this study show the opposite; an increased FCR was associated with an increased necrosis score. Muscles

undergoing polyphasic necrosis would likely have an increased basal metabolic requirement due to an increased rate of myofiber regeneration which would lead to a higher FCR as more energy is being expended on maintenance rather than growth. Tom flocks typically have higher FCRs than heavy hen flocks so the apparent influence of FCR on average necrosis score could also be due to other factors that are dependent on flock type. In this study, there was no association between ADG and necrosis score. The previous studies involved comparisons between different genetic lines of turkeys. However, in this study, 44 of the 48 turkeys sampled were of the same breed. These data suggest that the minor differences in growth rate observed between different flocks of a particular genetic line are not large enough to affect the incidence or severity of focal skeletal myopathies. Previous studies noted a lack of regeneration associated with these focal myopathies, in contrast with the results of this study [16, 18]. Differences in the regenerative capacity of degenerate muscle fibers may contribute to individual susceptibility and breed differences in the incidence of CD [25].

The results of this study are consistent with the proposed "inside-out" mechanism for development of CD. *C. septicum*, the primary causative agent for CD, can be found in the liver and skeletal muscle from birds with no evidence of external/cutaneous trauma. This supports the hypothesis that *C. septicum* gains access to skeletal muscles via hematogenous spread from an endogenous source. The gastrointestinal tract is the most likely endogenous source for *Clostridium* spp. in turkeys [1, 25]. This study found that focal myonecrosis occurs more frequently and with increased severity in older birds and in birds on farms with a chronic history of CD. Large, heavily-muscled, rapidly-growing heavy hens and toms likely have insufficient connective tissue support for myofibers and may be prone to the development of micro-ischemia of the dependent skeletal muscles of the caudal breast, thigh, and inguinum which may

ultimately lead to the development of focal skeletal myonecrosis. The presence of polyphasic myonecrosis likely predisposes these birds to the development of CD. These patterns observed regarding the incidence and severity of focal myonecrosis are consistent with the fact that CD typically occurs in older birds and tends to recur in successive flocks raised on the same premises.

3.5 References

1. Clark, S, R Porter, B McComb, R Lippert, S Olson, S Nohner and HL Shivaprasad. Clostridial dermatitis and cellulitis: an emerging disease of turkeys. Avian Diseases 54:788-794. 2010.

2. Tellez, G, NR Pumford, MJ Morgan, AD Wolfenden and BM Hargis. Evidence for *Clostridium septicum* as a primary cause of cellulitis in commercial turkeys. Journal of Veterinary Diagnostic Investigation 21:374-377. 2009.

3. Thachil, AJ, B McComb, MM Anderson, DP Shaw, DA Halvorson and KV Nagaraja. Role of *Clostridium perfringens* and *Clostridium septicum* in causing turkey cellulitis. Avian Diseases 54:795-801. 2010.

4. Alpern, RJ and VR Dowell. *Clostridium septicum* infections and malignancy. The Journal of the American Medical Association 209:385-388. 1969.

5. Smith, LDS and BL Williams. *Clostridium chauvoei*. In: The Pathogenic Anaerobic Bacteria, 3rd ed. A. Balows, ed. Charles C Thomas Publisher, Springfield, IL, USA. pp 164-175. 1984.

6. Smith, LDS and BL Williams. *Clostridium septicum*. In: The Pathogenic Anaerobic Bacteria, 3rd ed. A. Balows, ed. Charles C Thomas Publisher, Springfield, IL, USA. pp 180-190. 1984.

7. Sterne, M and I Batty. Pathogenic *Clostridia*. Butterworths, London. 1975.

8. Charlton, BR, AJ Bermudez, M Boulianne, DA Halvorson, JS Scjrader, LJ Newman, JE Sander and PS Wakenell, eds. Avian Disease Manual, 6th ed. American Association of Avian Pathologists, Athens, GA, USA. 2006.

9. McComb, B. Upper midwest filed perspective of dermatitis in commercial turkeys. In: MTRPC Gold Medal Panel on [cellulitis] clostridial dermatitis. Bloomington, MN. pp 5-8. 2008.

10. Thachil, AJ and KV Nagaraja. Cellulitis in turkeys: An emerging threat to turkey industry. In: MTRPC Gold Medal Panel on [cellulitis] clostridial dermatitis. Bloomington, MN. p 16. 2008.

11. Kriek, NPJ and MW Odendaal. *Clostridium chauvoei* infections. In: Infectious Diseases of Livestock, 2nd edition ed. J. Coetzer and R. Tustin, eds. University Press South Africa, Cape Town. pp 1856-1862. 2004.

12. Songer, JG. Clostridial diseases of animals. In: The *Clostridia*: Molecular Biology and Pathogenesis. J. Rood, B. McClane, J. Songer and R. Titball, eds. Academic Press, Inc, San Diego, CA. pp 153-182. 1997.

13. Albini, S, I Brodard, A Jaussi, N Wollschlaeger, J Frey, R Mizerez and C Abril. Real-time multiplex PCR assays for reliable detection of *Clostridium perfringens* toxin genes in animal isolates. Vet Microbiol 127:179-185. 2008.

14. Neumann, AP, SM Dunham, TG Rehberger and GR Siragusa. Quantitative real-time PCR assay for *Clostridium septicum* in poultry gangrenous dermatitis associated samples. Molecular and Cellular Probes 24:211-218. 2010.

15. JMP Pro, Version 11. SAS Institute Inc., Cary, NC. 2013.

16. Sosnicki, A, RG Cassens, DR McIntyre, RJ Vimini and ML Greaser. Incidence of microscopically detectable degenerative characteristics in skeletal muscle of turkey. British Poultry Science 30:69-80. 1989.

17. Wilson, BW, PS Nieberg and RJ Buhr. Turkey muscle growth and focal myopathy. Poultry Science 69:1553-1562. 1990.

18. Sosnicki, AA, RG Cassens, RJ Vimini and ML Greaser. Histopathological and ultrastructural alterations of turkey skeletal muscle. Poultry Science 70:349-357. 1991.

19. Anthony, NB, DE Jones, EA Dunnington, DA Emmerson and PB Siegel. DNA, RNA, and total protein content of leg and breast muscles of white rock chickens selected for 56-day body weight. Growth, Development, & Aging 52:177-184. 1988.

20. Velleman, SG, JW Anderson, CS Coy and KE Nestor. Effect of selection for growth rate on muscle damage during turkey breast muscle development. Poultry Science 82. 2003.

21. Maronpot, RR, TJ Bucci and MA Stedham. Focal degenerative myopathy in turkeys. Avian Diseases 12:96-103. 1968.

22. Wages, DP and MD Ficken. Skeletal muscle lesions in turkeys associated with the feeding of monensin. Avian Diseases 32:583-586. 1988.

23. Cardona, CJ, FD Galey, AA Bickford, BR Charlton and GL Cooper. Skeletal myopathy produced with experimental dosing of turkeys with monensin. Avian Diseases 37:107-117. 1993.

24. Scott, TA. Varation in feed intake of broiler chickens. Recent Advances in Animal Nutrition in Australia 15:237-244. 2005.

25. Lighty, ME, F Elvinger, RD Evans, T LeRoith and FW Pierson. Chapter 2: Incidence of clostridial dermatitis (cellulitis) and factors for development of the disease in turkeys. In: Epidemiology and pathophysiology of clostridial dermatitis (cellulitis) of turkeys. Doctor of Philosophy in Biomedical and Veterinary Sciences. Virginia Polytechnic Institute and State University. Blacksburg, VA. 2015.

Chapter 4 – Decreased Tissue Blood Perfusion and Oxygen Saturation as a Proposed Mechanism for the Development of Clostridial Dermatitis in Turkeys

4.0 Abstract

Clostridium septicum has been identified as the primary causative agent for clostridial dermatitis (CD) in turkeys, yet the pathogenesis for this disease remains unclear. It is hypothesized that positional restriction of blood flow to the caudal breast and inner proximal thigh from spending prolonged periods of time in sternal recumbency with legs fully flexed, may predispose birds, particularly heavy hens and toms, to the development of CD. Decreased perfusion and subsequent reduction in oxygen tension within these tissues could allow previously trapped *C. septicum* spores or quiescent cells to become vegetative, proliferate locally, and produce toxins. A decrease in blood perfusion to tissues is generally associated with a corresponding decrease in surface temperature and oxygen saturation. Studies were conducted to determine whether thermal imaging and pulse oximetry could be used to detect changes in perfusion and oxygen saturation in areas prone to the development of CD. Since it is often difficult to identify individual birds in the early stages of CD, surface temperature and SpO_2 measurements were obtained from healthy breeder hens, pre-production breeder hens, and heavy toms while standing and recumbent. Recumbency with leg flexion was associated with decreased surface temperature over the medial proximal thigh ($p = 0.0009$) as well as decreased SpO_2 for the caudal breast ($p = 0.0384$) and medial proximal thigh ($p = 0.0183$) in pre-production breeder hens. These data suggest that prolonged sternal recumbency results in reduced blood flow to the caudal breast and medial thigh of turkeys.

4.1 Introduction

CD (cellulitis) is a disease of turkeys selected for rapid growth rate that results in gangrenous lesions of the subcutaneous tissues and muscles of the caudal breast and inner proximal thigh. *C. septicum* has been identified as the primary causative agent for this disease, yet the mechanism of pathogenesis is not well understood. *C. septicum* is a spore-forming, anaerobic organism commonly found in the gastrointestinal tract of turkeys and has been identified in the blood, liver, and muscle of asymptomatic birds [1, 2]. This organism should not proliferate in healthy tissues of immune-competent individuals. It is hypothesized that non-vegetative cells of *C. septicum* lodge in the capillary beds of the caudal breast and thigh muscles where they remain dormant until local conditions become favorable for germination and proliferation. *C. septicum* has a relatively low infectious dose; fewer than ten spores of *C. septicum* are capable of inducing a fatal infection when present in debilitated tissue [3, 4]. While *C. septicum* is classified as an anaerobic organism, it is considered to be moderately aerotolerant [3, 5]. Therefore, decreased tissue perfusion and the subsequent decrease in oxygen saturation in that tissue may be sufficient to allow for the germination of *C. septicum* spores or reactivation of organisms that are in a low metabolic state within otherwise healthy tissues.

Large, heavy turkeys, particularly heavy hens and toms, are more prone to the development of CD [2, 6]. Increased body weight and rapid rate of growth have been associated with a reduction in the number of capillaries supplying the pectoralis major muscle [7]. Fewer capillaries may result in decreased oxygen saturation of the breast muscle in larger birds. Selection for increased breast muscle yield and rapid rate of gain has resulted in turkeys and broiler chickens which lack the adequate skeletal conformation and strength to fully support their increased weight [8, 9]. Increased body mass, without a compensatory increase in skeletal

support, leads to compression, shearing, and torque on the coxofemoral joint which results in chronic inadequate blood flow to the growth plates of the proximal femoral head and tibiotarsus. Inadequate blood flow predisposes birds to the development of bacterial chondronecrosis with osteomyelitis [9, 10]. Similarly, it is hypothesized that large turkeys that spend more time in sternal recumbency with their legs in full flexion may experience partial disruption of blood flow to the caudal breast and inner thigh regions. This disruption may predispose them to development of CD.

Several techniques have been developed to measure peripheral tissue perfusion and oxygen saturation; however, these technologies are often expensive, invasive, and/or impractical for clinical use in turkeys destined for market. Two more practical techniques may be thermal imaging and pulse oximetry. Thermal imaging uses infrared radiation to detect changes in surface temperature which may be associated with a decrease in blood perfusion within underlying tissues [11]. Pulse oximetry provides an inexpensive, non-invasive method for estimating peripheral arterial oxygen saturation (SpO_2) by measuring the percentage of hemoglobin binding sites that are bound to oxygen [12, 13]. SpO_2 is typically used to assess the adequacy of respiratory function. However, since oxygen extraction occurs in the capillaries, SpO_2 on the arterial side of the capillary bed, and therefore available to be delivered to tissues, should be similar to arterial SpO_2 [12]. SpO_2 is affected by increased pressure and impaired peripheral circulation; increased pressure or decreased perfusion to a tissue results in a lower recorded SpO_2 [12, 14]. While thermal imaging and pulse oximetry may not be ideal technologies to measure oxygen delivery at the tissue level in the caudal breast and inner thigh muscles, they may serve as non-invasive and relatively inexpensive alternatives. Therefore, these technologies were evaluated to determine whether they could be used to detect changes in

tissue blood perfusion and oxygen saturation in the aforementioned areas while birds were in sternal recumbency.

4.2 Materials and Methods

A Nonin PalmSat 2500A Vet handheld pulse oximeter (Nonin Medical, Inc. Plymouth, MN, USA) was used to measure SpO_2. A Nonin 2000T transreflectance sensor with the light source and photodetector on a single point of contact was used to take measurements at three locations on each bird: the mucous membranes of the cloaca (as a within-bird control); the dependent portion of the caudal breast, off to the side of the keel; and the proximal medial surface of the thigh, as close to the junction of the thigh and abdomen as possible. The sensor was held in place on a non-feathered area of skin and allowed to equilibrate for several minutes before recording measurements. A FLIR T400 infrared thermal imaging camera (FLIR Systems, Inc. Boston, MA, USA) was used to record surface temperatures in the same areas of caudal breast and inner thigh. FLIR QuickReport software was used to calculate an average surface temperature for each image [15]. Since it is often difficult to identify birds with early signs of CD, asymptomatic heavy toms and hens on breeder farms were used to compare oxygen saturation between normal birds and birds that had spent a prolonged period of time in sternal recumbency with legs fully-flexed. All protocols were approved by the Virginia Tech Institutional Animal Care and Use Committee. Statistical analyses were performed using matched pairs analysis to compare means within a group and oneway ANOVA to compare means across treatment groups [16]. Nonparametric tests were used for non-normally distributed data. Significance was based on $p < 0.05$. SpO_2 and surface temperatures are reported as mean ± standard deviation.

4.2.1 Experiments 1 and 2: Breeder Hens

Broody hens in a breeder flock instinctively desire to sit on and incubate eggs. These birds were used to measure oxygen saturation in a population of birds that had spent prolonged periods of time in sternal recumbency. Broody hens had been previously identified by farm personnel and moved to a separate pen within the breeder house. SpO_2 measurements were taken on 20 in-production Hybrid breeder hens and 20 broody hens in each experiment. The same breeder flock was used for Experiments 1 and 2. For Experiment 1, hens were 46 week old and 15 weeks into the lay cycle. Birds were picked up by the legs and held upside down briefly while measurements were recorded. For Experiment 2, hens were 51 weeks old and 20 weeks into the lay cycle. Measurements were taken while birds were in normal anatomical positions: standing for normal hens and sitting (sternal recumbency) for broody hens.

4.2.3 Experiments 3 and 4: Pre-production Breeder Hens

For Experiment 3, measurements were taken on 21 week old pre-production Hybrid breeder hens during the dark-out period (6 hours light, 18 hours dark). Experiment 4 was conducted on the same farm with the same lighting schedule when the hens were 28 weeks old. SpO_2 and thermal images were recorded on 15 asymptomatic birds in each of two houses: one house with an ongoing outbreak of CD and one house with no disease. Measurements were taken on asymptomatic birds in both houses. Data collection was performed at two time-points. The first was under total dark-out conditions when the lights had been off for more than fifteen consecutive hours. The second time point was later that same day after the lights had been turned on for more than three consecutive hours. Birds were fairly inactive during the dark period, with most birds in the house in sternal recumbency; birds were fairly active during the

light period, with most birds in the house standing or walking around. SpO_2 measurements were taken while birds were in a normal anatomical position: hens were standing when the lights were on and recumbent in darkness. Oxygen saturation measurements were recorded then birds were briefly rolled onto their back and the right leg extended away from the body to capture thermal images.

4.2.4 Experiment 5: Heavy Toms

In Experiment 5, oxygen saturation was measured in 40 20-week old Hybrid heavy toms on transport trucks upon arrival at the processing plant. Birds had been in the transport crates for a minimum of five hours at the time of sampling. Control measurements were taken on a farm for 40 age-, breed-, and gender-matched controls. Measurements were taken with birds in a normal anatomical position: in sternal recumbency with legs fully flexed for birds on the transport trucks and standing for birds on the farm.

4.3 Results

4.3.1 Experiment 1: Breeder Hens

For the control (standing) hen group, cloacal SpO_2 was greater than breast and thigh SpO_2 ($p = 0.0029$ and $p = 0.0023$, respectively; Table 4.1). Breast SpO_2 was greater for the normal hens compared to the broody hens ($p = 0.0181$). No other significant differences were present within or between groups.

Table 4.1: Oxygen saturation (SpO_2) of cloaca, breast, and thigh for normal and broody hens in Experiment 1

Hen Type	Cloaca SpO_2 (%)[1]	Breast SpO_2 (%)[1]	Thigh SpO_2 (%)[1]
Normal	$89.2 \pm 3.3^{a,c}$	$88.8 \pm 2.8^{b,c}$	$88.5 \pm 3.8^{b,c}$
Broody	$86.9 \pm 5.7^{a,c}$	$85.5 \pm 5.0^{a,d}$	$85.7 \pm 4.9^{a,c}$

[1]Mean ± standard deviation
[a-b]Means within a row with different superscripts differ ($p < 0.05$)
[c-d]Means within a column with different superscripts differ ($p < 0.05$)

4.3.2 Experiment 2: Breeder Hens

No significant differences were present within or between groups in Experiment 2 (Table 4.2). There were no differences between the cloacal, breast, and thigh SpO_2 within either the normal ($p = 0.4574$, $p = 0.9966$, and $p = 0.4469$) or the broody groups ($p = 0.6953$, $p = 0.9512$, and $p = 0.8535$). There were no differences between the normal and broody groups for cloacal, breast, or thigh SpO_2 ($p = 0.0927$, $p = 0.5410$, and $p = 0.0971$).

Table 4.2: Oxygen saturation (SpO_2) of cloaca, breast, and thigh for normal and broody hens in Experiment 2

Hen Type	Cloaca SpO_2 (%)[1]	Breast SpO_2 (%)[1]	Thigh SpO_2 (%)[1]
Normal	$90 \pm 4.5^{a,c}$	$88.7 \pm 4.3^{a,c}$	$90.2 \pm 5.4^{a,c}$
Broody	$88 \pm 2.5^{a,c}$	$87.9 \pm 3.1^{a,c}$	$87.3 \pm 5.4^{a,c}$

[1]Mean ± standard deviation
[a-b]Means within a row with different superscripts differ ($p < 0.05$)
[c-d]Means within a column with different superscripts differ ($p < 0.05$)

4.3.3 Experiment 3: Pre-production Breeder Hens

Medial thigh SpO_2 was greater than cloacal SpO_2 in Group 4 and in the standing group ($p = 0.0387$ and $p = 0.0241$, respectively; Table 4.3). Thigh SpO_2 was greater than breast SpO_2 for birds in the house with an ongoing outbreak of CD ($p = 0.0194$). Cloacal, breast, and thigh SpO_2 were all greater in the standing hens compared to the recumbent hens ($p = 0.0189$, $p = 0.0384$,

and p = 0.0183, respectively; Figure 4.1). An ongoing outbreak of CD in the flock had no effect on the cloacal, breast, or thigh SpO_2 (p = 0.5895, p = 0.3998, and p = 1.000, respectively).

Medial thigh temperature was greater than breast temperature for all groups (p < 0.0059; Table 4.4). Medial thigh temperature was greater in standing birds compared to recumbent birds (p = 0.0009), but position had no effect on breast temperature (p = 0.0831; Figure 4.2). Breast and medial thigh temperatures were greater in the house with an ongoing outbreak of CD compared to the house with no disease (p = 0.0029 and p = 0.0250, respectively). There was no correlation between SpO_2 and surface temperature for either the breast or the medial thigh. Feathering appeared to affect surface temperature (Figure 4.3).

Table 4.3: Oxygen saturation (SpO_2) of cloaca, breast, and thigh by group in Experiment 3

Group	Lights	CD	Cloaca SpO_2 (%)[1]	Breast SpO_2 (%)[1]	Thigh SpO_2 (%)[1]
1	Off	No	82.3 ± 6.2[a; c]	83.3 ± 8.1[a; c]	83.2 ± 9.0[a; c]
2	Off	Yes	87.1 ± 6.3[a; d]	86.4 ± 8.9[a; c]	87.9 ± 8.5[a; c,d]
3	On	No	91.9 ± 3.8[a; e]	92.0 ± 3.7[a; d]	92.7 ± 4.9[a; d]
4	On	Yes	85.2 ± 5.7[a; c, d]	85.7 ± 5.7[a,b; c]	88.0 ± 6.4[b; c,d]

[1]Mean ± standard deviation
[a-b]Means within a row with different superscripts differ (p < 0.05)
[c-e]Means within a column with different superscripts differ (p < 0.05)

Figure 4.1: Effect of position on oxygen saturation (SpO_2) for pre-production breeder hens in Experiment 3

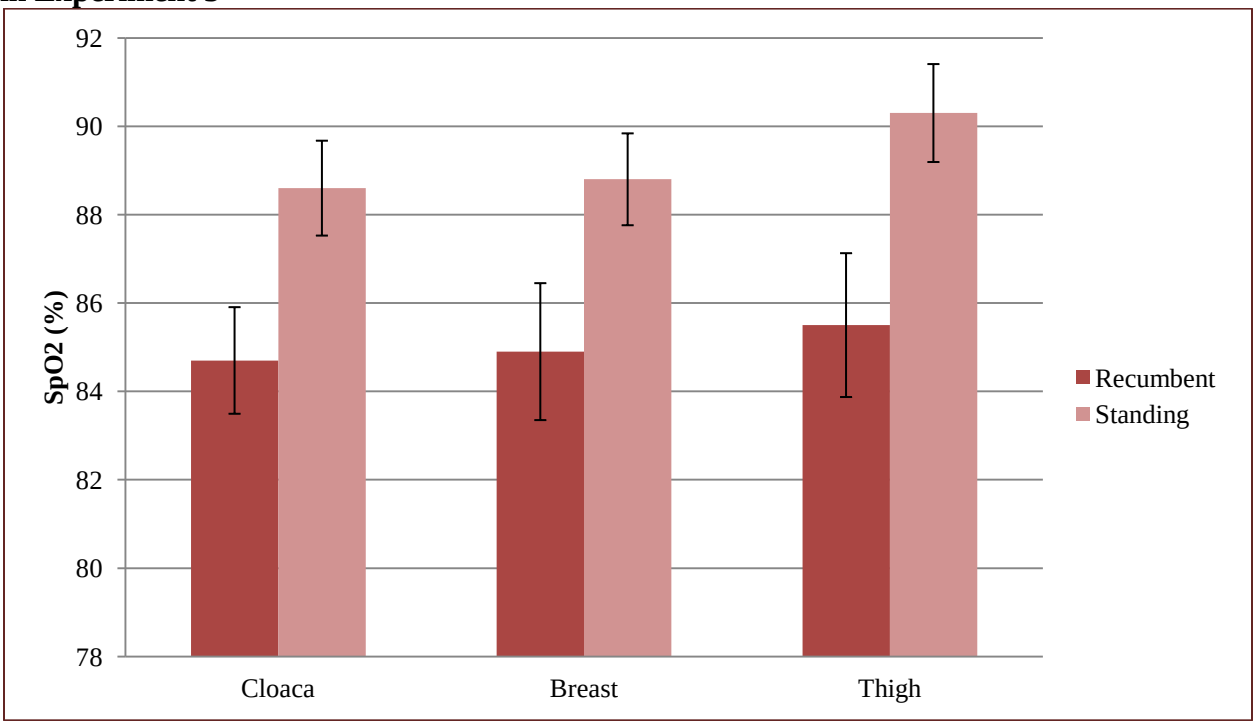

Table 4.4: Surface temperature of breast and thigh by group in Experiment 3

Group	Lights	CD	Breast Temp (°F)[1]	Thigh Temp (°F)[1]
1	Off	No	74.8 ± 5.0[a; c]	82.6 ± 6.8[b; c]
2	Off	Yes	77.2 ± 6.0[a; c]	85.1 ± 5.5[b; c]
3	On	No	75.7 ± 2.2[a; c]	86.8 ± 5.9[b; c]
4	On	Yes	80.9 ± 4.4[a; d]	92.0 ± 5.3[b; d]

[1]Mean ± standard deviation
[a-b]Means within a row with different superscripts differ ($p < 0.05$)
[c-d]Means within a column with different superscripts differ ($p < 0.05$)

Figure 4.2: Effect of position on surface temperature for pre-production breeder hens in Experiment 3

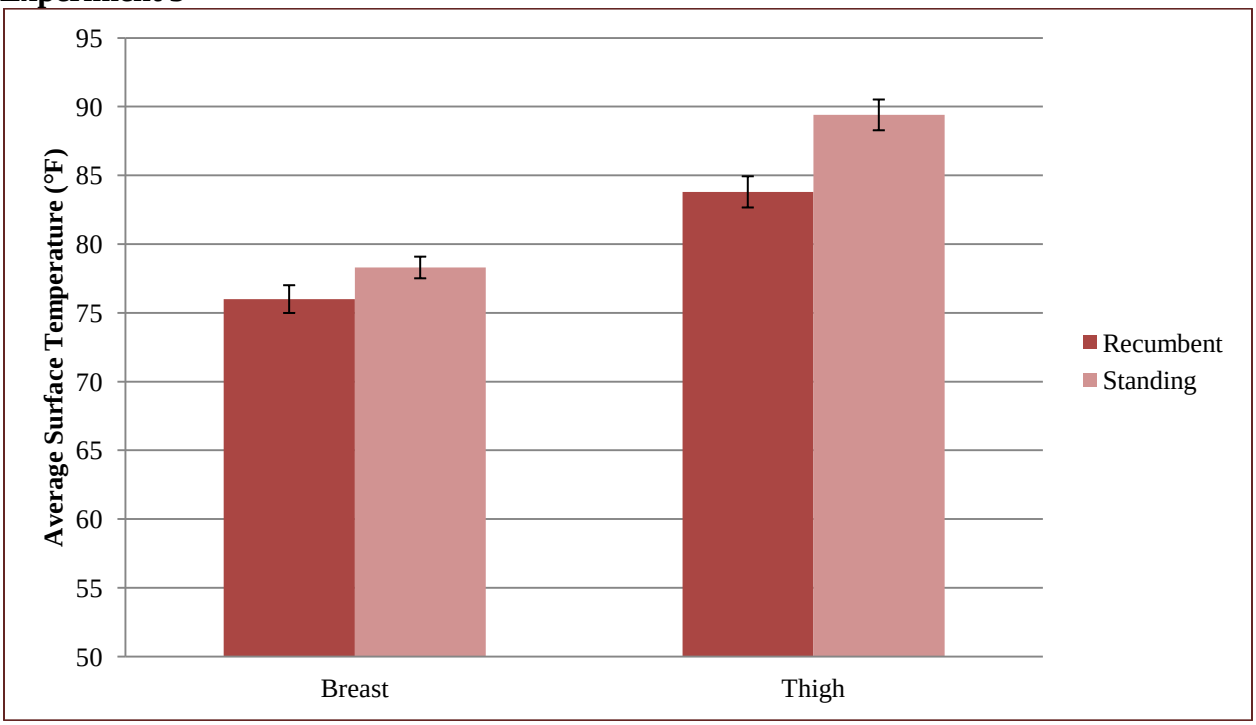

Figure 4.3: Thermal (infrared) images of turkeys in Experiment 3

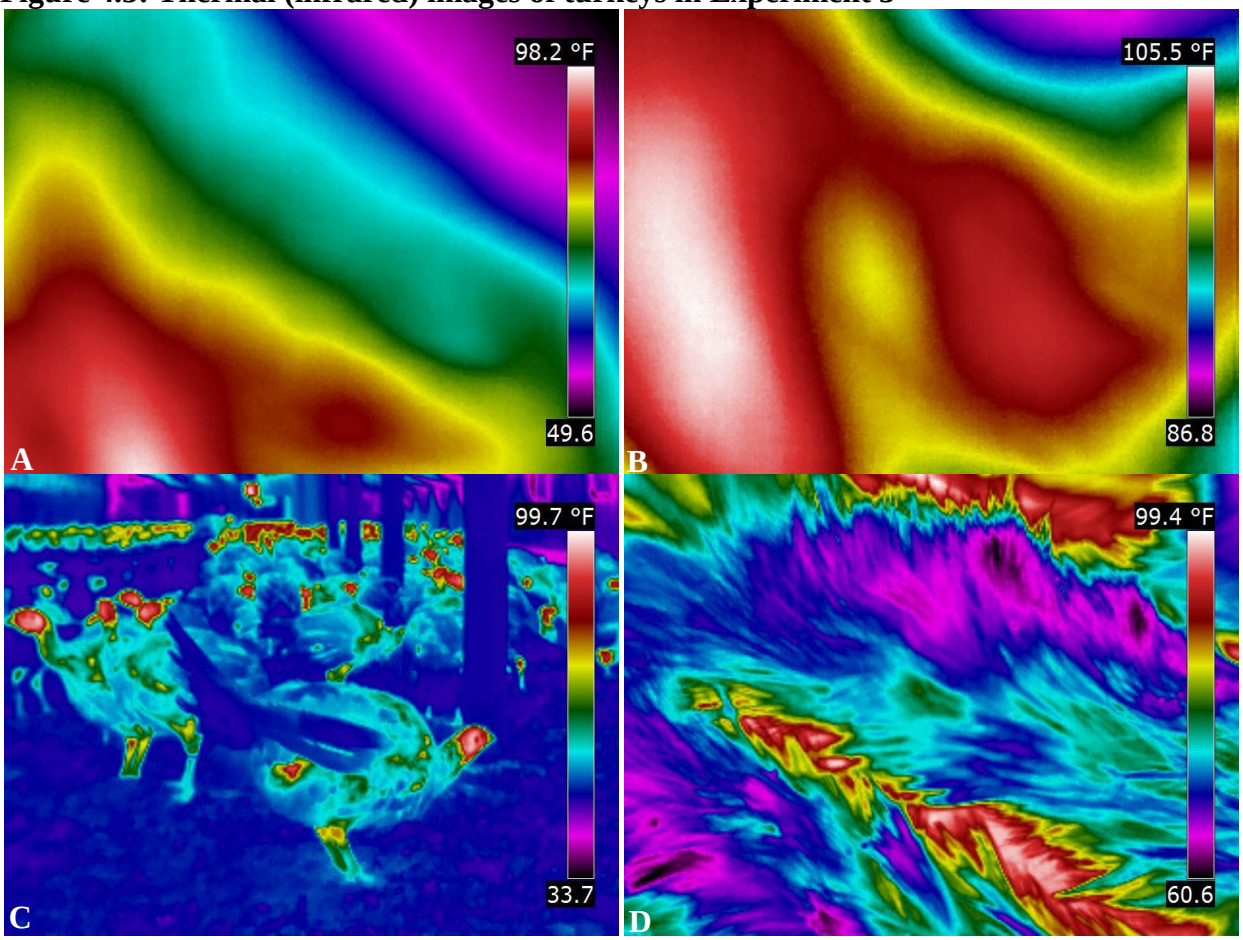

A: Thermal (infrared) image of proximal medial thigh region of recumbent hen
B: Thermal (infrared) image of proximal medial thigh region of standing hen
C: Thermal (infrared) image of turkey hens in a turkey house; unfeathered areas (heads) appear warmer than feathered areas (body)
D: Thermal (infrared) image showing the feather pattern over the caudal breast of a turkey hen; turkey positioned with head to the lower right, keel bone appears as the warmer (red) zone running diagonally from upper left to lower right

4.3.4 Experiment 4: Pre-production Breeder Hens

Breast SpO_2 was greater than thigh SpO_2 for Group 3 and for standing birds ($p = 0.0406$ and $p = 0.0205$, respectively; Table 4.5). Breast SpO_2 was also higher than thigh SpO_2 ($p = 0.0073$) for birds in the house with no disease. All other within-group comparisons were not significant. Position and an ongoing outbreak of clostridial dermatitis had no effect on cloacal, breast, or thigh SpO_2.

Medial thigh temperature was higher than breast temperature for Groups 2, 3, and 4 ($p = 0.0163$, $p = 0.0353$, and $p = 0.0121$, respectively; Table 4.6). Breast and thigh temperatures were higher for Group 3 compared to Groups 1, 2, and 4; breast and thigh temperatures were also higher for Group 4 compared to Groups 1 and 2 ($p < 0.0001$). Medial thigh temperature was higher than breast temperature in both the standing group and the recumbent group ($p = 0.0138$ and $p = 0.0010$, respectively). Position affected breast and thigh temperatures ($p < 0.0001$). An ongoing outbreak of CD did not affect breast ($p = 0.0502$) or thigh temperatures ($p = 0.3630$). There was no correlation between SpO_2 and temperature for either the breast or medial thigh.

Table 4.5: Oxygen saturation (SpO2) of cloaca, breast, and thigh by group in Experiment 4

Group	Lights	CD	Cloaca SpO_2 (%)[1]	Breast SpO_2 (%)[1]	Thigh SpO_2 (%)[1]
1	Off	No	$87.1 \pm 3.2^{a;\ c}$	$88.3 \pm 2.6^{a;\ c}$	$87.8 \pm 2.4^{a;\ c}$
2	Off	Yes	$88.6 \pm 5.3^{a;\ c}$	$89.3 \pm 4.5^{a;\ c}$	$89.3 \pm 4.2^{a;\ c}$
3	On	No	$86.8 \pm 3.5^{a,b;\ c}$	$87.3 \pm 5.0^{a;\ c}$	$86.3 \pm 3.8^{b;\ c}$
4	On	Yes	$89.0 \pm 4.6^{a;\ c}$	$89.3 \pm 4.8^{a;\ c}$	$88.9 \pm 5.7^{a;\ c}$

[1]Mean ± standard deviation
[a-b]Means within a row with different superscripts differ ($p < 0.05$)
[c-e]Means within a column with different superscripts differ ($p < 0.05$)

Table 4.6: Surface temperature of breast and thigh by group in Experiment 4

Group	Lights	CD	Breast Temp (°F)[1]	Thigh Temp (°F)[1]
1	Off	No	73.9 ± 5.5[a; e]	76.0 ± 6.4[a; e]
2	Off	Yes	72.0 ± 5.2[b; e]	77.9 ± 8.4[a; e]
3	On	No	86.2 ± 5.6[b; c]	90.6 ± 3.4[a; c]
4	On	Yes	80.5 ± 3.5[b; d]	84.8 ± 4.4[a; d]

[1]Mean ± standard deviation
[a-b]Means within a row with different superscripts differ ($p < 0.05$)
[c-e]Means within a column with different superscripts differ ($p < 0.05$)

4.3.3 Experiment 5: Heavy Toms

There were no within-group differences between cloacal, breast, and thigh SpO_2 for heavy toms on the farm ($p = 0.9310$, $p = 0.4937$, and $p = 0.5109$, respectively) or in transport crates ($p = 0.9352$, $p = 0.6022$, and $p = 0.7939$, respectively; Table 5.7). Position had no effect on cloacal, breast, or thigh SpO_2 ($p = 0.1541$, $p = 0.4366$, and $p = 0.7999$, respectively).

Table 4.7: Oxygen saturation (SpO_2) for heavy toms in transport crates and on-farm controls

Bird Location	Cloaca SpO_2 (%)[1]	Breast SpO_2 (%)[1]	Thigh SpO_2 (%)[1]
On Farm	81.9 ± 5.1[a,c]	82.6 ± 6.6[a, c]	83.3 ± 9.5[a, c]
On Transport Trucks	86.2 ± 11.2[a,c]	82.4 ± 16.0[a,c]	82.88 ± 13.3[a,c]

[1]Mean ± standard deviation
[a-b]Means within a row with different superscripts differ ($p < 0.05$)
[c-d]Means within a column with different superscripts differ ($p < 0.05$)

4.3.4 Combined Results for Experiments 2-5

Position did not affect cloacal, breast, or thigh SpO_2 ($p = 0.6530$, $p = 0.5878$, and $p = 0.9392$, respectively; Table 4.8). Cloacal, breast, and thigh SpO_2 values were all lower for heavy toms than for either in-production or pre-production breeder hens ($p < 0.0001$, $p = 0.0007$, and $p = 0.0368$, respectively; Table 4.9). Medial thigh SpO_2 was greater than cloacal SpO_2 within the

pre-production breeder hen group ($p = 0.0096$). There were no other significant differences in SpO_2 within or between groups. Generally, the lowest recorded SpO_2 value was lower for the recumbent birds compared to standing birds of the same type (Table 4.10).

Table 4.8: Effect of position on oxygen saturation (SpO_2), combined results for Experiments 2-5

Position	Cloaca SpO_2 (%)[1]	Breast SpO_2 (%)[1]	Thigh SpO_2 (%)[1]
Standing	$86.4 \pm 5.9^{a; c}$	$86.6 \pm 6.3^{a; c}$	$87.3 \pm 7.6^{a; c}$
Recumbent	$85.3 \pm 8.6^{a; c}$	$86.5 \pm 8.5^{a; c}$	$86.4 \pm 9.9^{a; c}$

[1]Mean ± standard deviation
[a-b]Means within a row with different superscripts differ ($p < 0.05$)
[c-d]Means within a column with different superscripts differ ($p < 0.05$)

Table 4.9: Oxygen saturation (SpO_2) by bird type; combined results for Experiments 2-5

Bird Type	Cloaca SpO_2 (%)[1]	Breast SpO_2 (%)[1]	Thigh SpO_2 (%)[1]
Breeder Hens[2]	$89.0 \pm 3.7^{b; c}$	$88.3 \pm 3.7^{b; c}$	$88.7 \pm 5.5^{b; c}$
Pre-production Breeder Hens[3]	$87.2 \pm 5.5^{b; d}$	$87.7 \pm 6.1^{b; c,d}$	$88.0 \pm 6.3^{b; c}$
Heavy Toms[4]	$82.2 \pm 9.5^{a; c}$	$84.0 \pm 9.6^{a; c}$	$84.2 \pm 12.2^{a; c}$

[1]Mean ± standard deviation
[2]Birds from Experiment 2
[3]Birds from Experiments 3 and 4
[4]Birds from Experiment 5
[a-b]Means within a row with different superscripts differ ($p < 0.05$)
[c-d]Means within a column with different superscripts differ ($p < 0.05$)

Table 4.10: Distribution of oxygen saturation (SpO_2) values by bird type; combined results for Experiments 2-5

Bird Type	Position	Cloaca SpO_2 (%)				Breast SpO_2 (%)				Thigh SpO_2 (%)			
		Min[1]	Med[2]	Mode[3]	Max[4]	Min	Med	Mode	Max	Min	Med	Mode	Max
Breeder Hens	Standing	84	89	89	99	84	88	84, 92	98	84	88.5	84, 85, 88	100
	Recumbent	83	89	89	91	84	88	84, 88, 89, 90	96	70	88	88	100
Pre-production Breeder Hens	Standing	77	89	89, 90	97	77	88	88	100	73	89	88	100
	Recumbent	74	87	88	99	69	87.5	84, 87, 91, 93	100	60	88	88, 92	100
Heavy Toms	Standing	69	83	83	93	72	81.5	80	100	54	83	79	100
	Recumbent	52	82.5	80, 95	100	42	85.5	80, 92, 100	100	52	98	100	100

[1]Minimum, [2]Median, [3]Mode(s), [4]Maximum

4.4 Discussion

It is hypothesized that prolonged sternal recumbency results in decreased perfusion to the caudal breast and medial thigh which may predispose birds to the development of CD. Pulse oximetry measures oxygen saturation within arterial circulation near the skin surface. It appeared to be a suitable means of assessing perfusion to the caudal breast and medial thigh muscles of turkeys. However, thermal imaging was only acceptable for assessing perfusion to the medial thigh. Since perfusion to avian skin occurs through branches of vessels supplying the underlying skeletal muscles, impairment of blood supply to the skeletal muscle should be accompanied by a similar impairment in blood supply to the overlying skin [17]. Experiments 1 and 3 showed that position (standing versus recumbent) affected SpO_2 for the caudal breast and medial thigh. Average surface temperature over the medial thigh was also affected by position in Experiment 3. Recumbency was associated with decreased SpO_2 and decreased surface temperature. This supports the hypothesis that prolonged sternal recumbency reduced blood flow to the caudal breast and medial thigh of turkeys.

For Experiment 1, birds were briefly restrained by the legs in order to measure oxygen saturation. This method of restraint was chosen in order to minimize bird movement which is known to interfere with pulse oximetry measurement and to ensure consistent placement of the sensor on each bird [18, 19]. However, there was concern that holding the birds in this manner may have altered the blood flow to the regions of interest (caudal breast and medial thigh) and thus affected the obtained SpO_2 values. Therefore, the methods were altered slightly for Experiment 2. In Experiment 2, measurements were taken while the birds were in a normal anatomical position. Control hens were measured while standing and broody hens were measured while in sternal recumbency. No differences were detected in SpO_2 measurements

between normal and broody hens in Experiment 2. However, it was noted that the hens in the broody pen on the day Experiment 2 was conducted were far more active than they had been on the day measurements were taken for Experiment 1. Nishihara et al. demonstrated that increased activity in chickens was correlated with increased blood flow to the breast [20]. Increased blood flow associated with activity likely offset any reduction in blood flow that resulted from being in sternal recumbency during data collection.

The cloacal SpO_2 measurement was intended as a within-bird control point since it was assumed that the mucous membranes of the cloaca would be well-perfused regardless of position. However, that was not the case. The combined data from Experiments 3 and 4 showed that cloacal SpO_2 was affected by position with cloacal SpO_2 being reduced in recumbent birds. Therefore, the cloacal mucous membrane was not an appropriate control.

SpO_2 values were low for many of the birds measured in this study. While SpO_2 values were expected to be low in recumbent birds due to decreased perfusion to the caudal breast and medial thigh, values were unexpectedly low in standing birds. SpO_2 in a healthy animal should be above 95%; however, average SpO_2 values were in the 80s for most groups. Pulse oximetry relies on the pulsatile nature of circulation to differentiate between arterial and venous oxygen saturation [11]. However, the pulse oximeter was unable to reliably register a pulse for all birds in this study. Ideally, the pulse oximeter sensor should be placed above a pulsatile arterial bed [18]. Generally speaking, turkey skin does not contain many large vessels; those that are present do not follow the feather tracts but rather travel across them [17]. Placement of the pulse oximeter sensor over an area of skin without an underlying artery may have resulted in an artificially lower SpO_2 value due to the inability of the sensor to accurately record a pulse. Additionally, SpO_2 tends to underestimate actual arterial oxygen saturation (SaO_2) in birds due to

differences in spectralphotometric characteristics between avian and mammalian hemoglobin [18]. However, the absolute SpO_2 values obtained in this study were not as important as the relative differences detected between standing and recumbent birds. Therefore, pulse oximetry may be a satisfactory technology for measuring positional restriction of blood flow in turkeys.

The reproducibility between Experiments 3 and 4 was poor in this study. Use of privately-owned turkey flocks as the study population limited the number of variables that were within researcher control. Most of the birds in the house were recumbent when the lights were off and standing when the lights were on; however, there was no way to know the exact position or activity level for individual birds during the minutes and hours prior to taking the measurements. Although the same farm was used for each experiment, the birds were seven weeks older at the time of Experiment 4. As older and therefore heavier birds, these hens likely spent a larger proportion of time sitting down even when the lights were on. This may have decreased the difference between oxygen saturation in 'standing' and recumbent birds in Experiment 4.

While there was a difference between the mean breast temperature and mean thigh temperature for all groups in Experiment 3, this difference is at least partially due to differences in feathering rather than actual differences in perfusion to these regions. Thermal imaging records the surface temperature of the skin for non-feathered regions; however, it records the temperature of the feathers up to a few millimeters below the feather surface for feathered regions [21]. The caudal breast area of the turkeys was heavily feathered while the medial thigh region was sparsely feathered. It is logical that the mean breast temperature was lower than the mean medial thigh temperature in this study as the temperature measured for well-feathered areas of skin tends to be closer to ambient temperature than the temperature measured for non-

feathered regions [21]. Studies with House Finches demonstrated that for birds exposed to the same convective conditions, there is no difference in surface temperature between resting and active birds [22]. This suggests that the medial thigh temperature differences observed between standing and recumbent birds in this study were due to differences in perfusion rather than differences in metabolic activity.

No differences were seen in cloacal, breast, or thigh SpO_2 between standing and recumbent heavy toms. Stress from transport may have caused a catecholamine response resulting in an increase in heart rate, blood pressure, respiratory rate, and skeletal muscle perfusion [23]. Many of the birds in transport crates were panting while the recumbent measurements were taken, either in response to stress or high ambient temperature. Increased respiratory rate is known to increase SpO_2. These responses may have masked any decrease in perfusion to the caudal breast and medial thigh that occurred as a result of spending a prolonged period of time in sternal recumbency.

There was no effect of position on mean oxygen saturation for the combined results from Experiments 2 though 5. However, differences in age, gender, and production type between the study populations may have offset any positional effect on SpO_2. Analysis of oxygen saturation by bird type showed that cloacal, breast, and thigh SpO_2 values were lower in heavy toms compared to in-production and pre-production breeder hens. Lower SpO_2 values appeared to be associated with risk for developing CD as incidence of the disease is highest in heavy toms [24]. Additionally, the minimum SpO_2 value recorded for a particular tissue was typically lower in recumbent birds than in standing birds of the same type. The range of SpO_2 values obtained for recumbent birds suggests that some yet undetermined factor makes some birds susceptible to the effect of prolonged recumbency on microcirculation. All of the flocks available to researchers

for inclusion in this study consisted of Hybrid birds. However, previous studies found that Nicholas flocks were more likely to develop CD [24]. The effect of position on tissue perfusion might have been more apparent in a breed more prone to development of CD.

Pulse oximetry appeared to be an acceptable means of accessing peripheral perfusion to the caudal breast and medial thigh of turkeys while thermal imaging was only acceptable for assessing perfusion to the non-feathered medial thigh. Recumbency was associated with decreased perfusion to these areas; however, reproducibility of results was limited due by the experimental design. Future studies should be conducted with birds in a controlled laboratory setting to allow for paired standing and recumbent measurements on the same bird. Likewise, crates could be used to encourage protracted recumbency without transport stress being a factor. Acclimation by repeatedly placing birds in the crates and gradually increasing the duration should reduce any stress/catecholamine response since novelty, duration, and severity as modifiers will make the treatment perceptually less stressful given the assurance of release. The hurdle to such studies is that prolonged physical restraint without analgesia and/or anesthesia is classified as Category E under the USDA Pain and Distress Category Assessment Guide [25]. However, these data and the potential for acclimation suggest the necessity and potential value of undertaking such studies. Oxygen saturation could also be compared between Hybrid and Nicholas birds to determine whether the apparent breed differences in susceptibility to development of CD are related to differences in microcirculation. Despite the difficulties, the results of this study support the hypothesis that recumbency is associated with decreased perfusion to tissues prone to the development of CD lesions. These findings provide justification for evaluation of other more reliable technologies for assessing tissue oxygen saturation.

4.5 References

1. Neumann, AP and TG Rehberger. MLST analysis reveals a highly conserved core genome among poultry isolates of *Clostridium septicum*. Anaerobe 15:99-106. 2009.

2. Lighty, M. Chapter 3: Detection of *Clostridium septicum* and *Clostridium perfringens* in tissues from asymptomatic turkeys. In: Epidemiology and pathophysiology of clostridial dermatitis (cellulitis) in turkeys. Doctor of Philosophy Dissertation in Biomedical and Veterinary Sciences. Virginia Polytechnich Institute and State Univeristy. Blacksburg, VA. 2015.

3. Smith, LDS and BL Williams. *Clostridium septicum*. In: The Pathogenic Anaerobic Bacteria, 3rd ed. A. Balows, ed. Charles C Thomas Publisher, Springfield, IL, USA. pp 180-190. 1984.

4. Stevens, DL, DM Musher, DA Watson, H Eddy, RJ Hamil, F Gyorkey, H Rosen and J Mader. Spontaneous, nontraumatic gangrene due to *Clostridium septicum*. Reviews of Infectious Disease 12:286-295. 1990.

5. Hill, GB and S Osterhout. Experimental Effects of Hyperbaric Oxygen on Selected Clostridial Species. I. In-Vitro Studies. The Journal of Infectious Disease 125:17-25. 1972.

6. Clark, S, R Porter, B McComb, R Lippert, S Olson, S Nohner and HL Shivaprasad. Clostridial dermatitis and cellulitis: an emerging disease of turkeys. Avian Diseases 54:788-794. 2010.

7. Velleman, SG, JW Anderson, CS Coy and KE Nestor. Effect of selection for growth rate on muscle damage during turkey breast muscle development. Poultry Science 82:1069-1074. 2003.

8. Nestor, KE, WL Bacon, YM Saif and PA Renner. The influence of genetic increases in shank width on body weight, walking ability, and reproduction of turkeys. Poultry Science 64:2248-2255. 1985.

9. Prisby, R, T Menezes, J Campbell, T Benson, E Samraj, I Pevzner and R F Wideman Jr. Kinetic examination of femoral bone modeling in broilers. Poultry Science 93:1122-1129. 2014.

10. Wideman Jr, R F. Multifactorial lameness: fast growth and bacterial infections. In: 86th Northeastern Conference on Avian Diseases. N. Evans, ed., State College, PA. 2014.

11. Lima, A and J Bakker. Noninvasive monitoring of peripheral perfusion. Intensive Care Med 31:1316-1326. 2005.

12. Nitzan, M, A Romem and R Koppel. Pulse oximetry: fundamentals and technology update. Medical Devices: Evidence and Research 7:231-239. 2014.

13. Soubani, AO. Noninvasive monitoring of oxygen and carbon dioxide. American Journal of Emergency Medicine 19:141-146. 2001.

14. Barker, SJ and KK Tremper. Pulse Oximetry: Applications and Limitations. Int Anesthesiol Clin 25:155-175. 1987.

15. FLIR QuickReport, Version 1.2 SP2. FLIR Systems, 2009.

16. JMP Pro, Version 11. SAS Institute Inc., Cary, NC. 2013.

17. Stettenheim, P. The integument of birds. In: Avian Biology. D. Farmer and J. King, eds. Academic Press, New York. pp 1-63. 1972.

18. Schmitt, PM, T Gobel and E Trautvetter. Evaluation of pulse oximetry as a monitoring method in avian anesthesia. Jounral of Avian Medicine and Surgery 12:91-99. 1998.

19. Sakr, Y. Techniques to assess tissue oxygenation in the clinical setting. Transfusion and Apheresis Science 43:79-94. 2010.

20. Nishihara, K, W Iwasaki, M Nakamura, E Higurashi, T Soh, T Itoh, H Okada, R Maeda and R Sawada. Development of a wireless sensor for the measurement of chicken blood flow using the laser doppler blood flow meter technique. IEE Transactions on Biomeical Engineering 60:1645-1653. 2013.

21. McCafferty, DJ. Applications of thermal imaging in avian science. IBIS: The International Journal of Avian Science 155:4-15. 2013.

22. Zerba, E, AN Dana and MA Lucia. The influence of wind and locomotor activity on surface temperature and energy expenditure of the Eastern House Finch (*Carpodacus mexicanus*) during cold stress. Physiol. Biochem. Zool. 72. 1999.

23. Siegel, HS. Stress, strains and resistance. British Poultry Science 36:3-22. 1995.

24. Lighty, ME, F Elvinger, RD Evans, T LeRoith and FW Pierson. Chapter 2: Incidence of clostridial dermatitis (cellulitis) and factors for development of the disease in turkeys. In: Epidemiology and pathophysiology of clostridial dermatitis (cellulitis) of turkeys. Doctor of Philosophy in Biomedical and Veterinary Sciences. Virginia Polytechnic Institute and State University. Blacksburg, VA. 2015.

25. USDA Animal Care Policy #11, Painful Procedures. In: AWA Section 2143. 9 CFR, Part 2, Sections 2.31(d)(1)(i,ii,iv), 2.31(e)(4), 2.33(b)(4), 2.36(b)(5,6,7). 1997.

Chapter 5 – Association between Clostridial Toxin Gene Expression and Development of Histopathological Lesions in Clostridial Dermatitis of Turkeys

5.0 Abstract

Lesions and mortality associated with clostridial diseases result from the action of exotoxins on host tissues and on biochemical processes. Toxin production by *Clostridium* spp. is highly dependent on nutrient availability and environmental conditions. *C. septicum* has been identified as the primary causative agent of clostridial dermatitis (CD) in turkeys; however, the exact mechanism of pathogenesis is not fully understood. Other *Clostridium* spp., including *C. perfringens*, are occasionally isolated from affected birds. Studies were undertaken to evaluate *C. septicum* and *C. perfringens* alpha toxin mRNA expression (CsA and CpA, respectively) in tissues from birds with varying stages of CD lesions. Presence of CsA was associated with CD ($p < 0.0001$) but presence of CpA did not appear to be associated with disease ($p = 0.7218$). *C. septicum* genomic DNA was detected in tissues from asymptomatic birds with no corresponding production of CsA mRNA suggesting that the organism was present in a quiescent form. Histopathological examination of skeletal muscle sections from affected birds revealed that lesions were primarily necrotic rather than inflammatory in nature and were present in the muscle and subcutaneous tissues rather than skin. This suggests that the name 'clostridial dermatitis' does not accurately describe the clinical presentation in turkeys.

5.1 Introduction

Fifteen of the 35 known pathogenic species of *Clostridium* produce potent exotoxins, antigenic proteins with bioactive properties that damage host tissues or interfere with biochemical processes in the host resulting in disease [1-3]. The toxins produced by a given

Clostridium spp. were named using Greek letters according to their order of discovery for that species; therefore, similarly named toxins produced by different species do not necessarily share similar structures or functions [2]. *Clostridium septicum* produces four major toxins: the alpha toxin is a lethal, necrotizing, pore-forming hemolysin; the beta toxin is a deoxyribonuclease (DNase) and leukocidin; the gamma toxin is a hyaluronidase; and the delta toxin is a necrotizing, oxygen-labile hemolysin [2, 4-6]. *C. septicum* also produces spreading factors and other potentially toxic proteins which may be involved in the pathogenesis of disease including neuraminidase (sialidase), hemagglutinin, fibrinolysin, and chitinase [4, 5, 7]. *C. perfringens* isolates are capable of producing at least seventeen distinct toxins depending on the strain [2, 4].

Clostridial toxin production is highly dependent on nutrient availability, environmental conditions, and stage of growth [3, 8]. Considerable variation has been demonstrated in the amount of a particular toxin produced by different cultures of the same strain of *C. septicum*, even when those cultures were grown in seemingly identical media [9]. Hemolysin production has been shown to be associated with the short rod form of *C. septicum* while production of DNase, hyaluronidase, and neuraminidase are associated with the presence of swarm cells [10]. Successful prevention and treatment of clostridial diseases typically involves developing immunity against or neutralization of specific toxins. Protection from *C. septicum* infection is primarily mediated by antibodies against toxins rather than antibodies against cell-surface proteins [8]. Hyperimmune serum can be used to provide passive protection for unvaccinated animals in the face of a disease outbreak [5]. While numerous studies have been conducted to evaluate toxin production by *C. septicum* (Cs) and *C. perfringens* (Cp) under various culture conditions, little is known regarding the specific toxins involved in the pathogenesis of CD in turkeys.

Traditional methods to analyze clostridial toxins in clinical samples involve the use of specific antibodies (antitoxins) to detect the toxin protein itself [3]. Commonly used methods include toxin neutralization assays and immunohistochemistry [11]. The mouse toxin neutralization assay is considered the gold standard method for toxin analysis. A purified toxin is injected into a mouse which creates a lesion and/or results in the death of the mouse. If the appropriate antibody (antitoxin) is injected along with the toxin, the detrimental effects of the toxin are neutralized. Immunohistochemistry techniques allow for rapid differentiation of *Clostridium* species and toxins through the use of fluorescent-labeled antibodies against specific toxins. A second immunohistochemistry method depends on knowing the molecular weight of the toxin of interest. Those determined to-date range from 22 to 600 kilodaltons (kD) [2]. Sodium dodecylsulfate polyacrylamide gel electrophoresis (SDS-PAGE) can be used to separate proteins based on size and can be followed by western blot. All of these methods for the identification of toxin proteins require the availability of specific antibodies (mono- or polyclonal) against the toxin(s) of interest.

Genomic analysis can give an idea of which toxins may be involved in the pathogenesis of diseases caused by that organism. PCR genotyping can aid in toxin expression analysis studies for *Clostridium* spp. where there is a strong correlation between genotype and phenotype as is seen with *C. perfringens* enterotoxemia [5]. However, the presence of a gene does not necessarily mean that that gene is expressed during infection. Therefore, demonstration of active transcription into messenger RNA (mRNA) is necessary to affirm toxin production in the absence of immunologic reagents [12]. RNA extraction and quantitative reverse transcriptase polymerase chain reaction (qRT-PCR) were used to analyze *in vivo* clostridial toxin gene expression in tissue samples from birds with varying stages of disease in flocks with an ongoing

outbreak of CD. Detection of mRNA sequences for the Cs and Cp alpha toxins in tissue samples from affected birds and not in unaffected controls will aid in determination as to whether these toxins are involved in the pathogenesis of CD.

There has been some debate regarding the nature and extent of lesions associated with this disease. While 'clostridial dermatitis' is the officially recognized name, we contend that lesions are restricted to skeletal muscle and subcutaneous tissues. Therefore, tissue sections from birds with lesions of varying severity were evaluated histopathologically. Statistical analyses were performed to determine the association between CsA and CpA mRNA expression and lesion development.

5.2 Materials and Methods

5.2.1 Sample Collection

As approved by the Virginia Tech Institutional Animal Care and Use Committee, turkey flocks with ongoing CD were identified by the flock supervisor or company veterinarian. Following euthanasia per company protocol by the grower or flock supervisor, samples were obtained from clinically ill birds with early/mild (ECD) or late/severe (LCD) gross lesions consistent with CD. Unaffected culls served as in-flock controls (CON). Skin and skeletal muscle from the caudal breast and medial thigh were obtained via a 6 mm disposable Keyes biopsy punch (Jorgensen Laboratories, Inc., Loveland, CO, USA). Sections of ileum and cecum ½-inch in length were also collected. Samples were placed in RNAlater (Life Technologies, Grand Island, NY, USA) and held at 4°C for 24 hours and then transferred to -80°C for long-term storage until they could be analyzed for clostridial alpha toxin mRNA. Samples of skin and

muscle were also placed in 10% neutral buffered formalin and allowed to fix at room temperature for a minimum of 24 hours prior to processing for histopathology.

5.2.2 RNA Extraction and qRT-PCR

Total RNA was extracted from up to 100 mg of thawed tissue following a protocol modified from the FastRNA Pro Green Kit (MP Biomedicals, LLC., Solon, OH, USA) (Appendix D). qRT-PCR was performed using the iTaq Universal SYBR Green One-Step Kit (Bio-Rad) and published primers specific for the Cs alpha toxin (CsA) and Cp alpha toxin (CpA) gene sequences [13, 14]. The presence of mRNA corresponding to the alpha toxin genes from Cs and Cp was compared between CON, ECD, and LCD birds to determine which toxins were being expressed during infection and might be responsible for the associated pathology. DNA extraction was performed on 32 tissue samples that were negative for CsA on qRT-PCR following a protocol modified from the QIAamp DNA Mini and Blood Mini Handbook (QIAGEN, Inc. Valencia, CA, USA) followed by qPCR for Cs genomic DNA. RNA extraction and qRT-PCR were also performed on 30 tissue samples obtained from asymptomatic turkeys on farms that were positive or suspect for the presence of Cs genomic DNA (see Chapter 3).

5.2.3 Histopathology

Paraffin embedded, formalin-fixed tissues were sectioned (4.0 μm) and stained with hematoxylin and eosin (H&E) by Virginia Tech Animal Laboratory Services (ViTALS, Blacksburg, VA, USA). Sections were examined for the presence of rod-shaped bacteria consistent with *Clostridium* spp. and histopathological evidence of disease. The dermis, subcutis, and muscle were examined to determine the nature and extent of pathology. Muscle

sections were scored on Likert-type scales for the presence of rod-shaped bacteria and histopathologic lesions. Bacterial scores were assigned as follows: 0 = no bacteria present, 1 = few isolated bacteria, 2 = mild bacteria, 3 = moderate bacteria, 4 = severe bacteria. The absence of inflammatory cells is characteristic of clostridial infections due to the rapid progression of lesions and the inhibitory and/or cytotoxic effects of some clostridial toxins on leukocytes [15]. Cellular necrosis was the only consistent lesion that could be staged. Therefore, histopathology scores were assigned as follows: 0 = within normal limits, 1 = few isolated necrotic cells, 2 = up to 25% necrotic cells, 3 = 25-50% necrotic cells, 4 = 50-75% necrotic cells, 5 = greater than 75% necrotic cells. Statistical analysis was performed using nonparametric oneway ANOVA (Wilcoxon/Kruskal-Wallis test) and nonparametric multivariate correlation (Spearman's p) [16]. Significance was assigned at $p < 0.05$.

5.3 Results

5.3.1 RNA Extraction and RT-qPCR

Of muscle samples from CON birds, 0/30 (0.0%) were positive for CsA mRNA; whereas 4/15 (26.7%) and 15/22 (68.2%) were positive from ECD and LCD birds, respectively (Table 5.1). CsA mRNA was also detected in breast skin, thigh skin, ileal, and cecal samples from ECD and LCD birds. No muscle or skin samples from any birds were positive for the presence of CpA mRNA (Table 5.2). One ileal sample from an ECD bird was positive for CpA mRNA while 3/6 (50.0%) of ileal and cecal samples from LCD birds were suspect for CpA mRNA. The presence of CsA mRNA was affected by disease status ($p < 0.0001$) but not by tissue type ($p = 0.0597$) while the presence of CpA mRNA was affected by tissue type ($p = 0.0001$) but not by disease status ($p = 0.7218$). Sixty-two tissue samples from asymptomatic turkeys were tested for

the presence of both Cs chromosomal DNA and CsA mRNA. Cs DNA was clearly found in 13/62 (21.0%), while 24/62 (38.7%) samples were suspect (Table 5.3). However, 0/62 (0.0%) were positive for CSA mRNA.

Table 5.1: Detection of CsA mRNA in tissues from turkeys in flocks with active CD

Disease Status	**Breast Muscle**			**Thigh Muscle**			**Breast Skin[1]**			**Thigh Skin[1]**			**Ileum**			**Cecum**		
	+[2]	+/-	-	+	+/-	-	+	+/-	-	+	+/-	-	+	+/-	-	+	+/-	-
CON	0	2	13	0	3	12	0	0	8	0	1	7	0	2	1	0	2	1
ECD	3	2	3	2	1	4	1	0	4	1	0	4	2	0	0	1	0	1
LCD	8	0	3	7	1	3	1	1	1	2	0	1	2	0	1	2	1	0

[1]Sample includes skin and underlying subcutaneous tissue
[2]Positive (+) if Cq value < 30; Suspect (+/-) if 30 ≤ Cq < 35; Negative (-) if Cq ≥ 35

Table 5.2: Detection of CpA mRNA in tissues from turkeys in flocks with active CD

Disease Status	**Breast Muscle**			**Thigh Muscle**			**Breast Skin[1]**			**Thigh Skin[1]**			**Ileum**			**Cecum**		
	+[2]	+/-	-	+	+/-	-	+	+/-	-	+	+/-	-	+	+/-	-	+	+/-	-
CON	0	2	13	0	0	15	0	0	8	0	0	8	0	1	2	0	1	2
ECD	0	0	7	0	0	7	0	0	5	0	0	5	1	0	1	0	0	2
LCD	0	0	11	0	0	11	0	0	3	0	0	3	0	2	1	0	1	2

[1]Sample may include underlying subcutaneous tissue
[2]Positive (+) if Cq value < 30; Suspect (+/-) if 30 ≤ Cq < 35; Negative (-) if Cq ≥ 35

Table 5.3: Detection of Cs chromosomal DNA and CsA mRNA in tissues from asymptomatic turkeys

Tissue	Cs chromosomal DNA			CsA mRNA		
	+[1]	+/-[2]	-[3]	+	+/-	-
Breast Muscle	2	6	10	0	0	18
Breast Skin	0	2	3	0	0	5
Thigh Muscle	4	3	9	0	0	16
Thigh Skin	0	3	2	0	0	5
Liver	3	3	0	0	0	6
Ileum	3	3	0	0	0	6
Cecum	1	4	1	0	0	6
All Tissues	13	24	25	0	0	62

[1]Positive (+) if Cq value < 30
[2]Suspect (+/-) if 30 ≤ Cq < 35
[3]Negative (-) if Cq ≥ 35

5.3.2 Histopathology

Mean bacterial score and mean histopathology score increased with increasing severity of CD (Table 5.3). No rod-shaped bacteria consistent with *Clostridium* spp. were seen in any of the muscle sections examined from CON or ECD birds. Rod-shaped bacteria were present in muscle sections from 10 of 15 (66.7%) of LCD birds. Muscle sections from 9/18 (50.0%) asymptomatic and 3/8 (37.5%) mildly affected birds were within normal limits. Sections from 7/18 (38.9%) asymptomatic birds had histopathology scores of 1 characterized by focal to multifocal polyphasic myonecrosis (Figure 5.1). One of 18 (5.6%) asymptomatic birds had a histopathology score of 2 while another asymptomatic bird had a necrosis score of 3. Of those with mild gross lesions 3/8 (37.5%) had a histopathology score of 2 and 2/8 (25.0%) had a histopathology score of 3. All muscle sections from severe cases of CD showed at least mild necrosis on histopathological examination. Affected tissue sections displayed varying degrees of necrosis, edema, dystrophic mineralization, and colonization with rod-shaped bacteria within skeletal muscle and subcutaneous tissues (Figure 5.2). Of those with severe gross lesions 5/15

(33.3%) had scores of 1, 1/15 (6.7%) had a score of 2, 2/15 (13.3%) had a scores of 3, 4/15 (26.7%) had a scores of 4, and 3/15 (20.0%) had a scores of 5. No or minimal inflammatory cells were present in affected tissue sections; fibrin was observed in some sections. Skin overlying affected subcutaneous tissue and skeletal muscle was within normal limits for all tissue sections examined.

Disease status affected the mean bacterial score ($p < 0.0001$) and mean histopathology score ($p = 0.0002$) for the muscle sections examined. The presence of CsA mRNA was significantly associated with both bacterial ($p < 0.0001$) and histopathology ($p = 0.0340$) scores. Increase in histopathology score was correlated with an increase in bacterial score ($R= 0.8358$; $p < 0.0001$).

Figure 5.1: Muscle sections from birds presenting with mild (early) CD

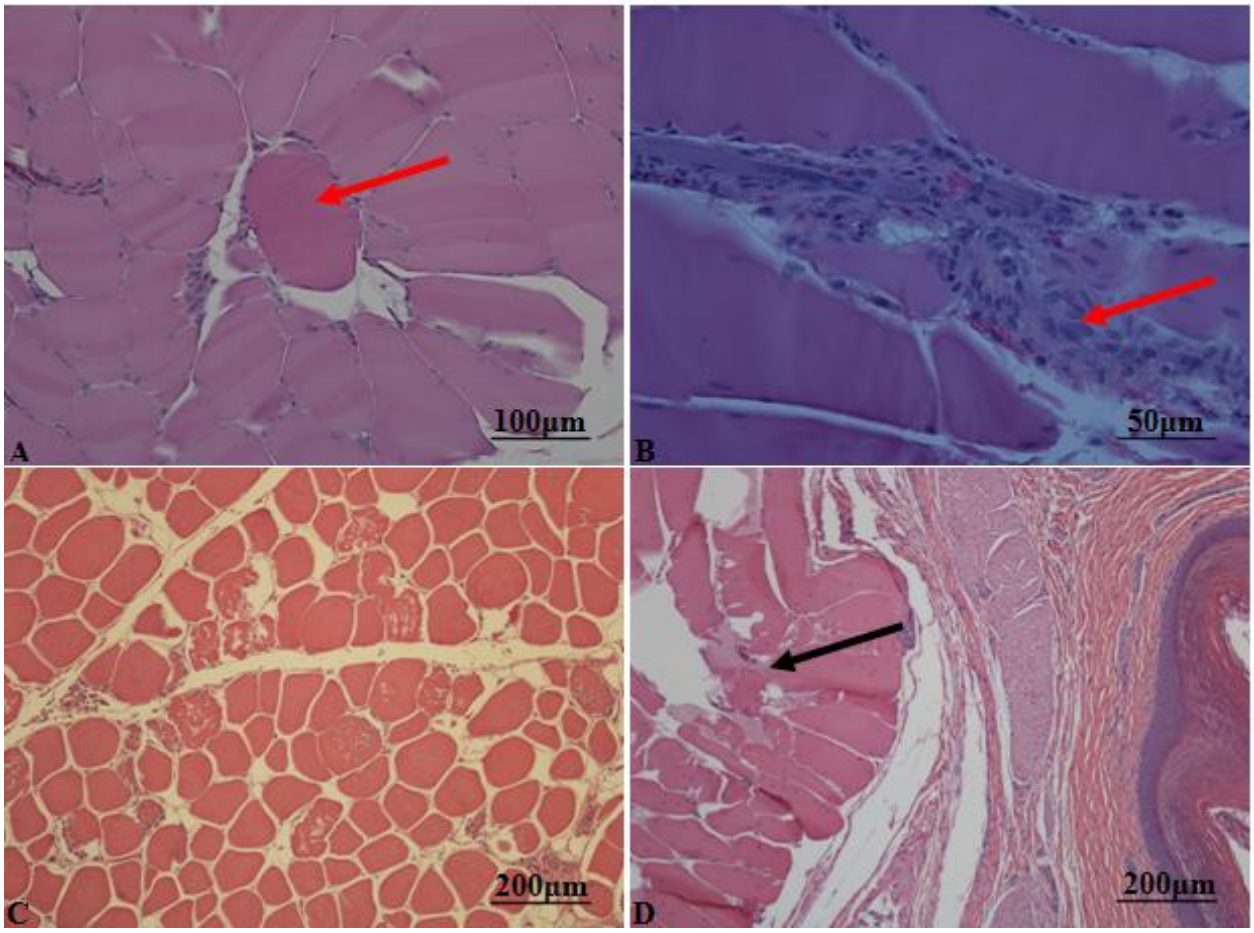

A: Degenerative myofiber (red arrow); 200X magnification
B: Regenerative myofiber (red arrow); 400X magnification
C: Myonecrosis; 100X magnification
D: Myonecrosis (black arrow) with normal overlying subcutis, dermis, and epidermis; 100X magnification

Figure 5.2: Muscle sections from birds presenting with severe (late) CD

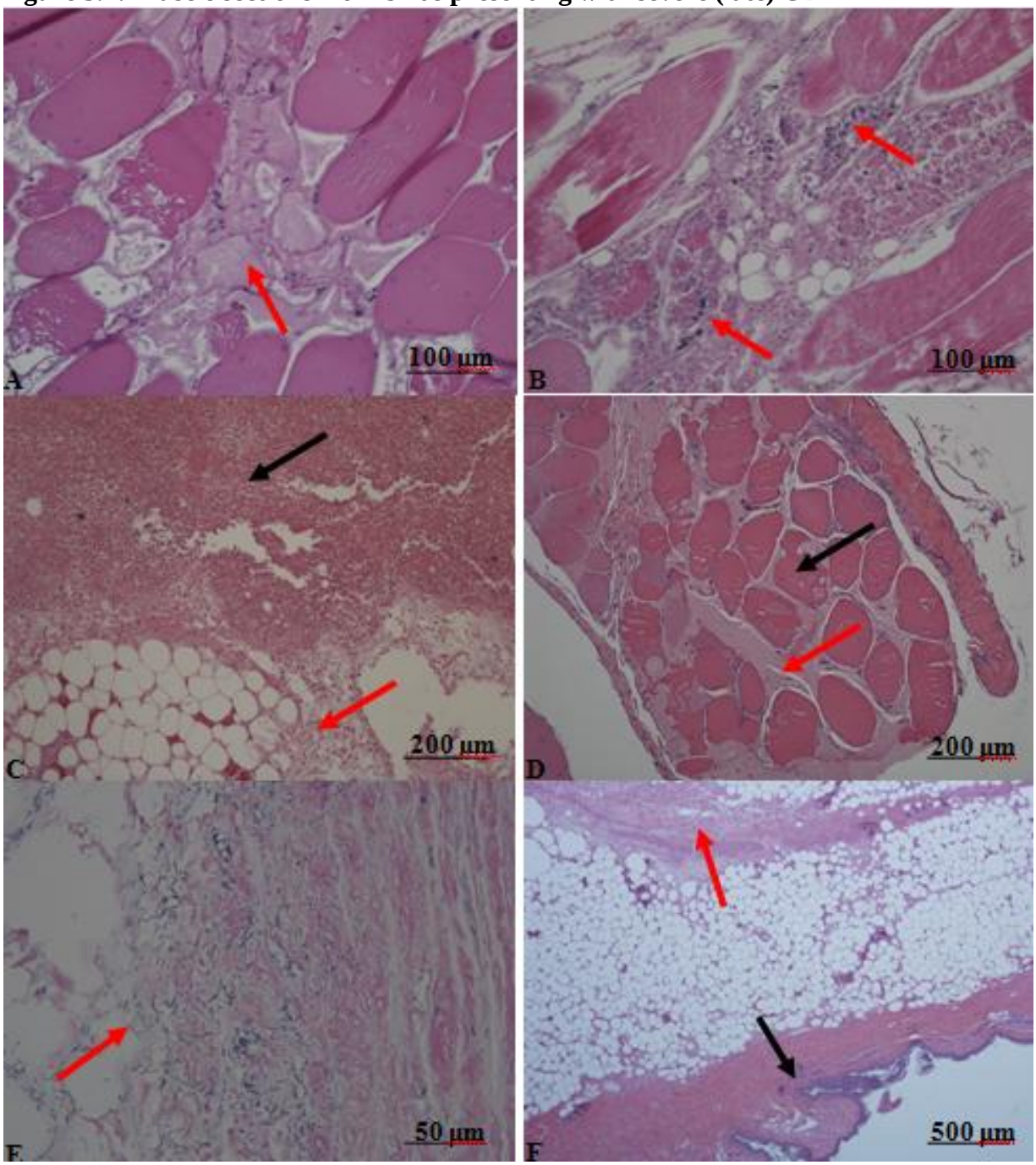

A: Degeneration, necrosis, edema, and rod-shaped bacteria (red arrows); 200X magnification
B: Necrosis, mineralization (red arrows), and rod-shaped bacteria; 200X magnification
C: Necrosis (black arrow) and edema (red arrow); 100X magnification
D: Cellulitis (black arrow) and steatitis (red arrow); 100X magnification
E: Cellulitis with rod-shaped bacteria (red arrow); 400X magnification
F: Cellulitis (red arrow) with normal overlying dermis and epidermis (black arrow); 40X magnification

Table 5.4: Average bacterial and histopathology scores for muscle sections from turkeys in flocks with CD

Disease Status	Bacterial Score (Mean ± Standard Error)	Histopathology Score (Mean ± Standard Error)
CON	0 ± 0.21^{b}	0.7 ± 0.28^{b}
ECD	0 ± 0.32^{b}	0.9 ± 0.42^{b}
LCD	1.9 ± 0.22^{a}	2.9 ± 0.31^{a}

[a,b]Means in same column with different superscripts are different ($p < 0.05$)

5.4 Discussion

The results of *in vivo* toxin gene expression analysis in samples from field cases of CD suggest that the alpha toxin of *C. septicum* was important in the pathogenesis of CD in turkeys. These findings are consistent with other studies that have demonstrated that the alpha toxin is essential for virulence [17]. However, the alpha toxin of *C. perfringens* did not appear to be involved in the pathogenesis of CD. Microscopic examination of tissue sections from affected birds showed necrosis of the skeletal muscle and subcutaneous tissues; however, all skin sections examined were normal. Few or no inflammatory cells were seen in affected tissue sections; although fibrin, an inflammatory product, was present in some sections. These findings indicate that the name 'clostridial dermatitis' was not an accurate descriptor for the condition seen in these birds.

The alpha toxin is generally recognized as the primary virulence factor of *C. septicum* [1, 4, 18]. The presence of CsA mRNA was associated with both disease status and mean histopathology score, suggesting that the alpha toxin played a role in the pathogenesis of CD by contributing to development of tissue necrosis. This observation is consistent with the known functions of CsA. This toxin is a lethal, necrotic, oxygen-stable hemolysin which induces cytotoxicity via formation of pores in lipid bilayers [1, 19]. Host cells respond to the resulting

disruption of cellular ion homeostasis and depletion of ATP through a process of necrosis-dependent cell death, ultimately manifesting as myonecrosis [1, 15]. Although CsA mRNA was not found in every affected tissue sample tested, this was an anticipated limitation of the methodology used in this study. Low numbers of *Clostridium* spp. are typically present in infected tissues resulting in relatively small amounts of bacterial RNA compared with host RNA [20]. Additionally, bacterial mRNA is inherently unstable, with a half-life of mere minutes [12]. Although every effort was made to reduce the time between euthanasia and sample collection, degradation of CsA mRNA may have occurred thus limiting detection by qRT-PCR.

While the activity of CsA is likely essential for the development of CD, it alone does not account for the entirety of the pathology seen. Cross-complementation studies have shown that CsA must act in concert with other Cs toxins for production of the full spectrum of pathology associated with gas gangrene caused by *C. septicum* [15]. Therefore, other toxins are likely involved in the pathogenesis of CD. The characteristic lack of inflammation associated with the necrotic lesions is better explained by the activity of the Cs beta toxin, a leukocidal deoxyribonuclease which has been demonstrated to induce rounding, degranulation, and karyolysis of polymorphonuclear leucocytes [21]. Activity of the hyaluronidase, neuraminidase, and fibrinolysin produced by *C. septicum* are also consistent with the pathology observed in cases of CD [2, 4].

The fact that the presence of CpA mRNA was affected by tissue type but not by disease status suggests that the alpha toxin of *C. perfringens* did not play a role in the pathogenesis of CD. This lack of effect implies either that *C. perfringens* is not involved in the pathogenesis of CD or that *C. perfringens* is involved but that the action of a toxin other than CpA contributes to the observed pathology. The alpha toxin of *C. perfringens* has been demonstrated to be the

primary toxin responsible for development of post-traumatic gas gangrene in humans [3]. Initial theories on the pathogenesis of necrotic enteritis in chickens suggested that the alpha toxin of *C. perfringens* was also primarily responsible for development of the disease. However, recent studies have demonstrated that CpA-negative mutants are still capable of causing disease [22]. The NetB toxin has been identified as essential for development of necrotic enteritis while the alpha toxin does not play a direct role in pathogenesis of the disease. Therefore, it is conceivable that another toxin produced by *C. perfringens* may be involved in the pathogenesis of CD. *C. perfringens* produced CpA *in vitro* in a culture system designed to simulate nutrient availability in skeletal muscle *in vivo* (see Appendix D). However, CpA mRNA was not detected in skeletal muscle samples from cases of CD. Therefore, we theorize that *C. perfringens* was probably not a major contributor to pathogenesis. While *C. perfringens* has been isolated from some cases of CD, this organism was likely present as a secondary invader or a post-mortem contaminant [11, 23]. Another recent study of field cases of CD has also concluded that *C. perfringens* was only present as a secondary contaminant [24].

The presence of CsA and CpA mRNA in intestinal samples suggests that toxin production occurred both in the skeletal muscle as well as in the intestinal tract of birds with CD. Perhaps there were other concurrent conditions in the gastrointestinal tract of some affected birds that favored Cs and Cp proliferation and toxin production. Sick birds often exhibit ileus which may have promoted a shift in the gastrointestinal microbiome. Intestinal production of CsA and CpA may contribute to the rapid mortality seen with CD as these toxins are presumably absorbed through the wall of the gastrointestinal tract. Circulating Cs and Cp toxins ultimately result in shock, cardiovascular collapse, and death [1, 7, 25].

Thirty seven tissue samples were either positive or suspicious for the presence of *C. septicum* genomic DNA but negative for CsA mRNA. These data suggest that *C. septicum* was present in a quiescent form, either as a spore or in a low metabolic state that was not producing alpha toxin. Although it is generally considered more difficult to extract DNA from spores, several commercially available DNA extraction kits have been shown to be able to detect DNA from both vegetative cells and spores of *Clostridium* spp. [26]. The methods used in this study were not able to differentiate between DNA from vegetative cells and spores.

Ideally, all controls should have been healthy birds. However, compromises were made in order to be able to collect samples from privately-owned turkey flocks. The average histopathology score obtained for the control group in this study may have been higher than it would have been if the control birds had been healthy. Histopathology scores for birds that were culled for leg reasons (e.g. synovitis, broken leg, conformational defects) may have been higher than those for healthy birds or birds culled for non-leg related issues (e.g. broken wing, pendulous crop) since birds with leg issues likely spent a larger proportion of the day sitting down in sternal recumbency. This may have resulted in micro-ischemia and focal myonecrosis in the caudal breast and inguinal regions which are hypothesized to predispose birds to the development of CD [27].

Although CD is the officially recognized name for this disease, the microscopic lesions observed in affected birds were not consistent with dermatitis. Necrosis was present in the skeletal muscle (myonecrosis) and subcutaneous tissues of affected birds, while the overlying dermis and epidermis were within normal limits on histopathologic examination. Additionally, dermatitis implies an inflammatory process, yet few to no inflammatory cells were present in affected tissue sections. Although fibrin, an inflammatory product, was present in some affected

tissue sections, lesions were primarily necrotic rather than inflammatory in nature. Lack of an inflammatory response is a hallmark of clostridial gas gangrene given the peracute nature of the disease and the fact that several clostridial toxins are known leukocyte inhibitors, either through direct cytotoxic effects or through the inhibition of leukocyte migration and activation [3, 5, 15, 28-30]. Absence of inflammatory cells in histopathology sections from cases of CD suggests that the Cs beta toxin may play an important role in pathogenesis [5, 21]. This toxin had been previously identified as a DNase with leukocidal activity based on the function of Cs culture filtrates; however, neither the protein nor gene sequence is currently known.

Data indicates that Cs is present in tissues of otherwise normal birds and that certain events and/or conditions that foster up-regulation of toxin genes, with the alpha toxin likely one of many, are ultimately responsible the development of the disease. Identification of other toxins that may also be involved in the pathogenesis of this disease was limited by the fact that gene sequences are not yet known for the other toxins produced by *C. septicum.* Whole-genome sequencing and identification of the toxin genes in *C. septicum* are necessary to facilitate further study of toxin expression in cases of CD. The presence of Cs DNA in the absence of CsA mRNA in skeletal muscle samples from asymptomatic birds supports the proposed mechanism of pathogenesis: the organism can remain in these tissues in a quiescent or spore form until local oxygen concentrations decrease to a level that allows for proliferation and elaboration of toxins. Histopathological examination of tissue sections from affected turkeys suggests that ‘clostridial myo- and subcuticular necrosis’ may be a more accurate descriptor for this disease than the officially recognized name ‘clostridial dermatitis’.

5.5 References

1. Popoff, MR and P Bouvet. Clostridial toxins. Future Microbiology 4:1021-1064. 2009.

2. Hatheway, CL. Toxigenic *Clostridia*. Clinical Microbiology Reviews 3:66-98. 1990.

3. Popoff, MR and BG Stiles. Clostridial toxins vs. other bacterial toxins. In: Handbook on *Clostridia*. P. Durre, ed. CRC Press: Taylor & Francis Group, Boca Raton, FL. pp 323-383. 2005.

4. MacLennan, JD. The histotoxic clostridial infections of man. Bacteriological Reviews 26:177-275. 1962.

5. Songer, JG and KW Post. The Genus *Clostridium*. In: Veterinary Microbiology: Bacterial and Fungal Agents of Animal Diseases. Elsevier Saunders, St. Louis, MO, USA. pp 261-282. 2005.

6. Timoney, JF, JA Gillespie, FW Scott and JE Barlough. The genus *Clostridium*. In: Hagan and Bruner's Microbiology and Infectious Diseases of Domestic Animals, 8th ed. Cornell University Press, Ithaca, New York. pp 214-240. 1988.

7. Smith, LDS and BL Williams. *Clostridium septicum*. In: The Pathogenic Anaerobic Bacteria, 3rd ed. A. Balows, ed. Charles C Thomas Publisher, Springfield, IL, USA. pp 180-190. 1984.

8. Cortinas, TI, MA Mattar and AM Stefanini de Guzman. Alpha-toxin production by *Clostridium septicum* at different culture conditions. Anaerobe 3:199-202. 1997.

9. Gadalla, MSA and JG Collee. The relationship of the neuraminidase of *Clostridium septicum* to the haemagglutinin and other soluble products of the organism. Journal of Pathology and Bacteriology 96:169-185. 1968.

10. Macfarlane, S, MJ Hopkins and GT Macfarlane. Toxin synthesis and mucin breakdown are related to swarming phenomenon in *Clostridium septicum*. Infection and Immunity 69:1120-1126. 2001.

11. Sterne, M and I Batty. Pathogenic *Clostridia*. Butterworths, London. 1975.

12. Rauhut, R and G Klug. mRNA degradation in bacteria. FEMS Microbiology Reviews 23:353-370. 1999.

13. Neumann, AP, SM Dunham, TG Rehberger and GR Siragusa. Quantitative real-time PCR assay for *Clostridium septicum* in poultry gangrenous dermatitis associated samples. Molecular and Cellular Probes 24:211-218. 2010.

14. Albini, S, I Brodard, A Jaussi, N Wollschlaeger, J Frey, R Mizerez and C Abril. Real-time multiplex PCR assays for reliable detection of *Clostridium perfringens* toxin genes in animal isolates. Vet Microbiol 127:179-185. 2008.

15. Bryant, AE and DL Stevens. Clostridial toxins in the pathogenesis of gas gangrene. In: The Comprehensive Sourcebook of Bacterial Protein Toxins, 4th ed. J. Alouf, D. Ladant and M. Popoff, eds. Elsevier Ltd, Amsterdam. pp 977-994. 2015.

16. JMP Pro, Version 11. SAS Institute Inc., Cary, NC. 2013.

17. Kennedy, CL, EO Krejany, LF Young, JR O'Connor, MM Awad, RL Boyd, JJ Emmins, D Lyras and JI Rood. The alpha-toxin of *Clostridium septicum* is essential for virulence. Molecular Microbiology 57:1357-1366. 2005.

18. Bernheimer, AW Parallelism in the lethal and hemolytic activity of the toxin of *Clostridium septicum*. Journal of Experimental Medicine 80:309-320. 1944.

19. Moussa, RS. Complexity of toxins from *Clostridium septicum* and *Clostridium chauvoei*. Journal of Bacteriology 76:538-545. 1958.

20. Gyles, CL and JF Prescott. Themes in bacterial pathogenic mechanisms. In: Pathogenesis of Bacterial Infections in Animals, 4th ed. C. Gyles, J. Prescott, J. Songer and C. Thoen, eds. Wiley-Blackwell, Ames, IA. pp 3-14. 2010.

21. Warrack, GH, E Bidwell and CL Oakley. The beta-toxin (deoxyribonuclease) of *Cl. septicum*. J Pathol Bacteriol 63:293-302. 1951.

22. Van Immerseel, F, JI Rood, RJ Moore and RW Titball. Rethinking our understanding of the pathogenesis of necrotic enteritis in chickens. Trends Microbiol 17:32-36. 2009.

23. Smith, LDS and BL Williams. The *Clostridia*. In: The Pathogenic Anaerobic Bacteria, 3rd ed. A. Balows, ed. Charles C Thomas Publisher, Springfield, IL, USA. pp 94-100. 1984.

24. Robbins, K. Commercial turkey clostridial dermatitis vaccination and interventions. In: American Association of Avian Pathologists Scientific Program. Boston, MA. 2015.

25. Bryant, AE and DL Stevens. The Pathogenesis of Gas Gangrene. In: The *Clostridia*: Molecular Biology and Pathogenesis. J. Rood, B. McClane, J. Songer and R. Titball, eds. Academic Press, Inc, San Diego, CA. pp 185-196. 1997.

26. Metcalf, D and JS Weese. Evaluation of commercial kits for extraction of DNA and RNA from *Clostridium difficile*. Anaerobe 18:608-613. 2012.

27. Lighty, M. Chapter 3: Detection of *Clostridium septicum* and *Clostridium perfringens* in tissues from asymptomatic turkeys. In: Epidemiology and pathophysiology of clostridial dermatitis (cellulitis) in turkeys. Doctor of Philosophy Dissertation in Biomedical and Veterinary Sciences. Virginia Polytechnich Institute and State Univeristy. Blacksburg, VA. 2015.

28. Stevens, DL and AE Bryant. The role of clostridial toxins in the pathogenesis of gas gangrene. Clinical Infectious Diseases 35:S93-S100. 2002.

29. Stevens, DL, J Mitten and C Henry. Effects of alpha and theta toxins from *Clostridium perfringens* on human polymorphonuclear leukocytes. J Infect Dis 156:324-333. 1987.

30. Hickey, MJ, RYQ Kwan, MM Awad, CL Kennedy, LF Young, P Hall, LM Cordner, D Lyras, JJ Emmins and JI Rood. Molecular and cellular basis of microvascular perfusion deficits induced by *Clostridium perfringnes* and *Clostridium septicum*. PLoS Pathogens 4:e1000045. 2008.

Chapter 6 – *De Novo* Whole-Genome Sequencing of *Clostridium septicum* Type Strain

6.0 Abstract

Clostridium septicum is an important pathogen in both human and veterinary medicine. To date, only the alpha toxin and a handful of housekeeping genes have been sequenced. Identification of the toxin and other virulence genes produced by this organism would aid researchers in understanding disease pathogenesis and may lead to the development of more effective prevention and treatment strategies. The *C. septicum* type strain ATCC 12464 was d*e novo* sequenced using the Illumina MiSeq platform. Whole genome (optical) mapping generated a high-resolution, ordered restriction map for use as a template during assembly. Multiple approaches were evaluated, ultimately resulting in a 3,361,374 bp draft genome with 27.7% GC content which was assembled into 12 scaffolds. A BLAST search revealed that *C. septicum* shares significant homology with other members of the genus *Clostridium.* The genome contained 3,073 coding sequences and 70 RNAs. A deoxyribonuclease was present which may account for the activity of the beta toxin. The genome contains multiple hyaluronoglucosaminidase proteins which are consistent with the function of the gamma toxin. Several hemolysins were identified which may correspond with the delta toxin. A gene consistent with a Panton-Valentine leukocidin chain S precursor, a toxin typically found in virulent strains of *Staphylococcus aureus*, was also present. Coding sequences for neuraminidase, a putative ADP-ribosylating toxin, several proteins in the beta-lactamase family, and numerous phage proteins may also contribute to the virulence of *C. septicum.* Multiple repetitive sequences were present which hindered alignment with the whole genome (optical) map. Additional analysis is underway to identify regions of misalignment, resolve gaps and low

quality sequences within scaffolds, close gaps between scaffolds, and validate chromosome assembly.

6.1 Introduction

C. septicum is a Gram positive, spore-forming, exotoxin-producing anaerobe commonly found in soil and in the gastrointestinal tracts of humans and animals [1]. It is an important pathogen in both human and veterinary medicine as the causative agent of clostridial myonecrosis (gas gangrene) in humans, malignant edema in ruminants, and clostridial dermatitis (CD) in turkeys [1-3]. Diseases caused by this organism are typically rapidly progressing and can be fatal if treatment is not started early in the course of disease. Despite being the first anaerobe discovered by Pasteur and Joubert in 1877, surprisingly little is known about the toxins produced by *C. septicum* (*Vibrion septique*), or about their role in the pathogenesis of disease [1, 4, 5]. Increased incidence of morbidity and mortality associated with *C. septicum* infection in humans the late 1980s renewed interest into this organism [5]. *C. septicum* is known to produce at least four toxins. The alpha-toxin is a lethal, necrotizing, pore-forming, oxygen-stable hemolysin with lecithinase activity [1, 6]. The beta-toxin is a deoxyribonuclease and leukocidin; the gamma-toxin is a hyaluronidase; and the delta-toxin is a necrotizing, oxygen-labile hemolysin [1, 6-9]. *C. septicum* is also known to produce at least two additional extracellular proteins which play a role in pathogenesis of disease: a neuraminidase (sialidase) and a fibrinolysin [5, 6].

Currently, only the alpha-toxin, neuraminidase (sialidase), and a small number of house-keeping genes have been sequenced [10-12]. The alpha-toxin exhibits more sequence similarity with the aerolysin of *Aeromonas hydrophila* than it does with known sequences for other

clostridial toxins [13]. *De novo* sequencing for the whole genome of the *C. septicum* type strain was performed in order to identify potential loci corresponding to other toxins and extracellular proteins important in pathogenesis. Knowing these would not only aid our understanding of the disease process but also be of benefit in the development of prevention and treatment strategies for diseases caused by this organism. Therefore, a project was undertaken to better understand the organization of the *C. septicum* genome using the Illumina MiSeq platform.

6.2 Materials and Methods

6.2.1 de novo Whole Genome Sequencing

C. septicum type strain ATCC 12464 was obtained from the American Type Culture Collection (ATCC, Manassas, VA, USA) as a frozen culture. The organism was thawed, inoculated in brain heart infusion (BHI) broth (Becton, Dickinson and Company, Fralin Lakes, NJ, USA) and incubated overnight at 37 °C in an anaerobic chamber (< 1 ppm dissolved oxygen). 1.5 mL of broth culture was placed in a 1.5 mL microcentrifuge tube (USA Scientific, Inc. Ocala, FL, USA) and centrifuged at 7500 x *g* for 10 minutes. The supernatant was removed and the cell pellet was resuspended in 300 µL Tissue and Cell Lysis Solution (Epicentre, Madison, WI, USA) containing 1.0 µL of 50 µg/µL Proteinase K (Epicentre). Samples were incubated at 65 °C for 15 minutes then cooled to 37 °C prior to addition of 1.0 µL of 5 mg/mL RNase A (Epicentre). They were then incubated at 37 °C for 30 minutes and frozen at -20 °C. Frozen samples were shipped on ice packs to ACGT, Inc. for DNA extraction and *de novo* whole genome sequencing (ACGT, Inc. Wheeling, IL, USA). DNA extraction was completed using the MasterPure Compete DNA and RNA Purification Kit (Epicentre). It was purified using the

Zymo genomic DNA Clean and Concentrator kit (Zymo Research Corporation, Irvine, CA, USA).

DNA was pooled for tagmentation, a modified transposition reaction, following the Nextera Mate Pair Gel-Plus protocol (Illumina, San Diego, CA, USA). DNA was sheared using dsDNA Fragmentase (New England BioLabs, Ipswich, MA, USA) per manufacturer's instructions and fragment size selection (2,000-10,000bp) was performed using the BluePippin platform (Sage Science, Inc. Beverly, MA, USA). The final library was loaded on Illumina MiSeq at 8pmol and a PE150 run was performed. Reads were filtered and de-multiplexed using MiSeq Reporter software. Adapter and low quality sequences (<Q20) were trimmed and short reads (< 35 bp) were filtered out using Trim Galore! software (Babraham Bioinformatics Group, Cambridge, UK). Trimmed reads were assembled *de novo* using Velvet (European Bioinformatics Institute, Cambridge, UK) and BLAST (National Center for Biotechnology Information, Bethesda, MD) was used to compare several large scaffolds of the assembly against other genome sequences in GenBank. The similarity of the *C. septicum* sequence to known genomes was deemed insufficient for annotation purposes and assembled scaffolds were annotated *de novo* with Rapid Annotation using Subsystem Technology (RAST) [14, 15]. NextClip software was used to orient the mate pair library [16].

6.2.2 Whole Genome Mapping

A pure culture of *C. septicum* was grown in BHI. One milliliter of culture was transferred to a 1.5 mL microcentrifuge tube (USA Scientific, Inc. Ocala, FL, USA) and centrifuged at 5000 x *g* for 5 minutes at room temperature. The cell pellet was resuspended in 500 µL of 200 mM NaCl (Thermo Fisher Scientific, Pittsburgh, PA, USA), 100 mM EDTA

(Sigma-Aldrich Corp. St. Louis, MO, USA), 10 mM Tris (Fisher Scientific) pH 7.2. Resuspended cells were mixed with an equal volume of a 1% low-melting point agarose (Cambrex Bio Science Rockland, Inc. Rockland, ME, USA) solution dissolved in DEPC-treated water (Life Technologies, Grand Island, NY, USA). One hundred microliters of the cell-agarose suspension was aliquoted into each well of a 10-well plug mold (Bio-Rad Laboratories, Hercules, CA, USA) and incubated at 4°C for 90 minutes. Plugs were removed from the mold and incubated for 2 hours at 37 °C with shaking at 40 rpm in 5 mL of a spheroplasting solution of 200 mM NaCl (Fisher Scientific), 100 mM EDTA (Sigma-Aldrich), 10 mM Tris (Fisher Scientific), pH 7.2 containing 20 mg/mL lysozyme (Sigma-Aldrich) and 50 μg/mL lysostaphin (Sigma-Aldrich). Plugs were then transferred into 5 mL of lysis buffer comprised of 1% N-lauroylsarcosine (Sigma-Aldrich) in 0.5 M EDTA pH 9.5 with 2 mg/mL proteinase K (Sigma-Aldrich) and incubated at 40 rpm overnight at 37 °C. The next morning, lysis plugs were stored in 0.5 M EDTA pH 9.5 and sent to OpGen, Inc. (OpGen, Inc. Gaithersburg, MD, USA) for whole genome mapping.

High molecular-weight genomic DNA was prepared using an agarose plug DNA isolation protocol. Enzyme Chooser software (OpGen, Inc.) was used to select an optimal restriction enzyme (SpeI) that would generate restriction fragments with an average size of 6-12 kb and with no single fragment greater than 80 kb. A whole genome map was prepared using the ARGUS Whole Genome Mapping System (OpGen, Inc.). Single DNA molecules were captured onto an ARGUS charged glass surface within a MapCard, digested with SpeI restriction enzyme, stained with JOJO-1 Iodide (OpGen, Inc.) on the ARGUS MapCard Processor, and analyzed by automated fluorescent microscopy using the ARGUS Whole Genome Mapper. The software recorded the size and order of restriction fragments for each DNA molecule and then assembled

collections of single molecule restriction maps according to overlapping fragment patterns. The resulting Whole Genome Map was then used as a scaffold to orient and order FASTA sequence scaffolds using Map Solver software (OpGen, Inc.).

6.3 Results

6.3.1 De novo *Whole Genome Sequencing*

Initial DNA extraction efforts for the *C. septicum* type strain yielded insufficient quality and quantity for generating a Nextera Mate Pair Library. Therefore, whole genome amplification was performed using the Illustra TempliPhi 100 Amplification Kit. The FASTA sequence obtained from ACGT, Inc. was 2,813,808 bp in length and was comprised of 506 scaffolds. The longest scaffold was 432,776 bp and the mean scaffold size was 5,561 bp. There appeared to be an issue with the orientation of some of the mate pairs and several additional analytic approaches failed to improve assembly. Multiple DNA extraction protocols were evaluated in order to identify a method that yielded sufficient quality and quantity for preparation of the mate-pair library. *De novo* whole genome sequencing was repeated using the higher quality DNA product.

The resulting FASTA sequence consisted of 12 scaffolds with a total length of 3,361,374 bp. The longest scaffold contained 855,904 bp while the mean scaffold size was 280,114.5 bp. There was insufficient homology with other *Clostridium* genome sequences in GenBank to identify the closest matching reference for annotation and assembly purposes; sequence similarity ranged from 75-85%. *De novo* annotation using RAST determined that the genome had a GC content of 27.7% and contained 3,073 coding sequences and 70 RNAs (see Appendix G). 1,387 of the 3,073 (45.1%) coding sequences were contained within 358 subsystems while

1,686 of 3,073 (54.9%) were not included within any subsystem (Figure 6.1). Of the coding sequences present within identified subsystems, 1,372 of 1,387 (95.7%) were non-hypothetical proteins while 60 of 1,387 (4.3%) were hypothetical proteins. Of the sequences not contained within identified subsystems, 876 of 1,686 (52.0%) coded for non-hypothetical and 810 of 1,686 (48.0%) for hypothetical proteins. The closest neighboring organisms to the *C. septicum* type strain were all within in the genus *Clostridium* (Table 6.1). Several gaps were present within and between scaffolds.

6.3.2 Whole Genome Mapping

Whole genome (optical) mapping generated a high-resolution, ordered restriction map spanning the entire *C. septicum* genome. Reads from multiple single-molecule restriction maps (Figure 6.2) were assembled to create a unique 'barcode' with each vertical line representing a SpeI restriction enzyme cut site (Figure 6.3). The *de novo* FASTA sequence arranged into 12 scaffolds was aligned with the SpeI optical map using MapSolver default settings (Figure 6.4). Nine of twelve (75.0%) scaffolds aligned with at least one region in the optical map, covering 12.8% of the total genome. Ten gaps were present; the average gap size was 240,362.3 bp. The scaffolds were then separated into 20 smaller scaffolds and a second map was generated which optimized the alignment between the sequence and the restriction map (Figure 6.5). Eighteen of twenty scaffolds (90.0%) aligned with at least one region in the optical map, covering 18.1% of the genome. Thirteen gaps were present; the average gap size was 173,638.2 bp.

Figure 6.1: Subsystem features of *C. septicum* ATCC 12464 as determined by *de novo* RAST annotation[1]

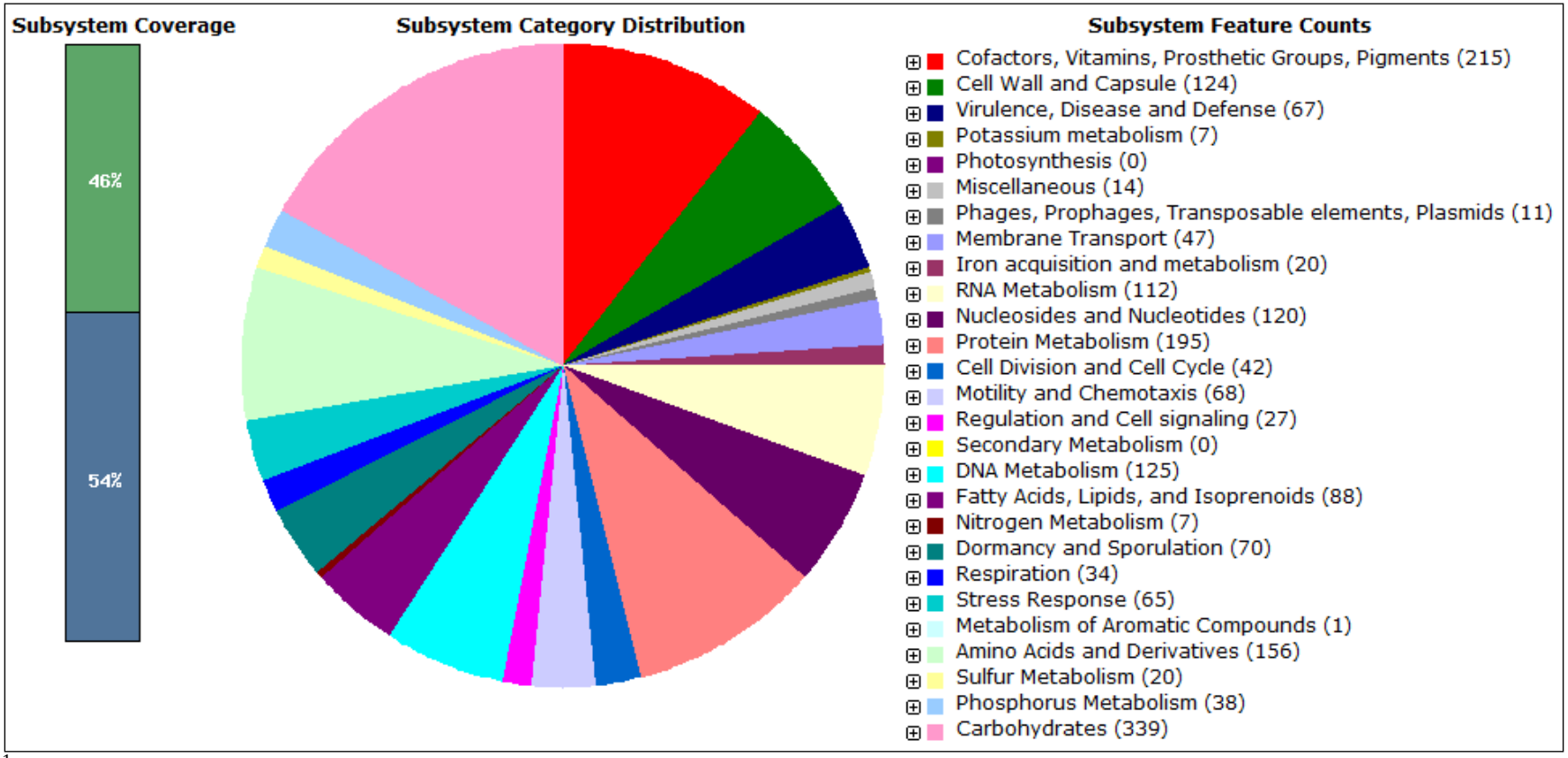

[1]Subsystem coverage of coding sequences (CDS) in the *C. septicum* type strain based on *de novo* annotation using RAST. The bar on the left shows the proportion of CDS included in the subsystems (green bar) versus those not in any subsystem (blue bar). The pie chart demonstrates the distribution of CDS within the subsystem. The number in parenthesis gives the number of *C. septicum* proteins identified within that subsystem.

Table 6.1: Closest neighbor organisms to *C. septicum* ATCC 12464 according to RAST

Genome ID	Score[1]	Genome Name
457396.3	539	*Clostridium sp.* 7_2_43FAA[2]
290402.34	479	*Clostridium beijerincki* beijerinckii NCIMB 8052
290402.41	468	*Clostridium beijerinckii* NCIMB 8052
447214.4	445	*Clostridium butyricum* 5521
632245.3	433	*Clostridium butyricum* E4 str. BoNT E BL5262
195102.1	394	*Clostridium perfringens* str. 13
508765.6	393	*Clostridium botulinum* B str. Eklund 17B
536233.3	389	*Clostridium botulinum* E1 str. 'BoNT E Beluga'
508767.4	385	*Clostridium botulinum* E3 str. Alaska E43
195102.6	381	*Clostridium perfringens* str. 13
508767.5	375	*Clostridium botulinum* E3 str. Alaska E43
289380.14	365	*Clostridium perfringens* SM101
195103.1	356	*Clostridium perfringens* ATCC 13124
451756.6	353	*Clostridium perfringens* CPE str. F4969
289380.15	352	*Clostridium perfringens* SM101
445334.5	352	*Clostridium perfringens* C str. JGS1495
451755.5	348	*Clostridium perfringens* E str. JGS1987
451754.5	345	*Clostridium perfringens* B str. ATCC 3626
195103.9	343	*Clostridium perfringens* ATCC 13124
488537.5	336	*Clostridium perfringens* D str. JGS1721
451757.5	331	*Clostridium perfringens* NCTC 8239
413999.4	262	*Clostridium botulinum* A str. ATCC 3502
471871.7	261	*Clostridium sporogenes* ATCC 15579
573061.3	255	*Clostridium cellulovorans* 743B
498214.7	250	*Clostridium botulinum* A3 str. Loch Maree
445335.4	250	*Clostridium botulinum* NCTC 2916
413999.7	245	*Clostridium botulinum* A str. ATCC 3502
445336.4	245	*Clostridium botulinum* Bf
441770.4	243	*Clostridium botulinum* A str. ATCC 19397
498213.7	243	*Clostridium botulinum* B1 str. Okra

[1]Score represents the number of times that a particular neighboring genome was the top BLAST hit against a candidate from the set of unique gene within the *C. septicum* genome; a higher number suggests that the two genomes are likely to be metabolically similar.
[2]Isolate from the gastrointestinal tract of a human patient with Chron's disease; sequenced as part of the Human Microbiome Project of NIH [17]

Figure 6.2: *C. septicum* ATCC 12464 SpeI Whole Genome Map[1]

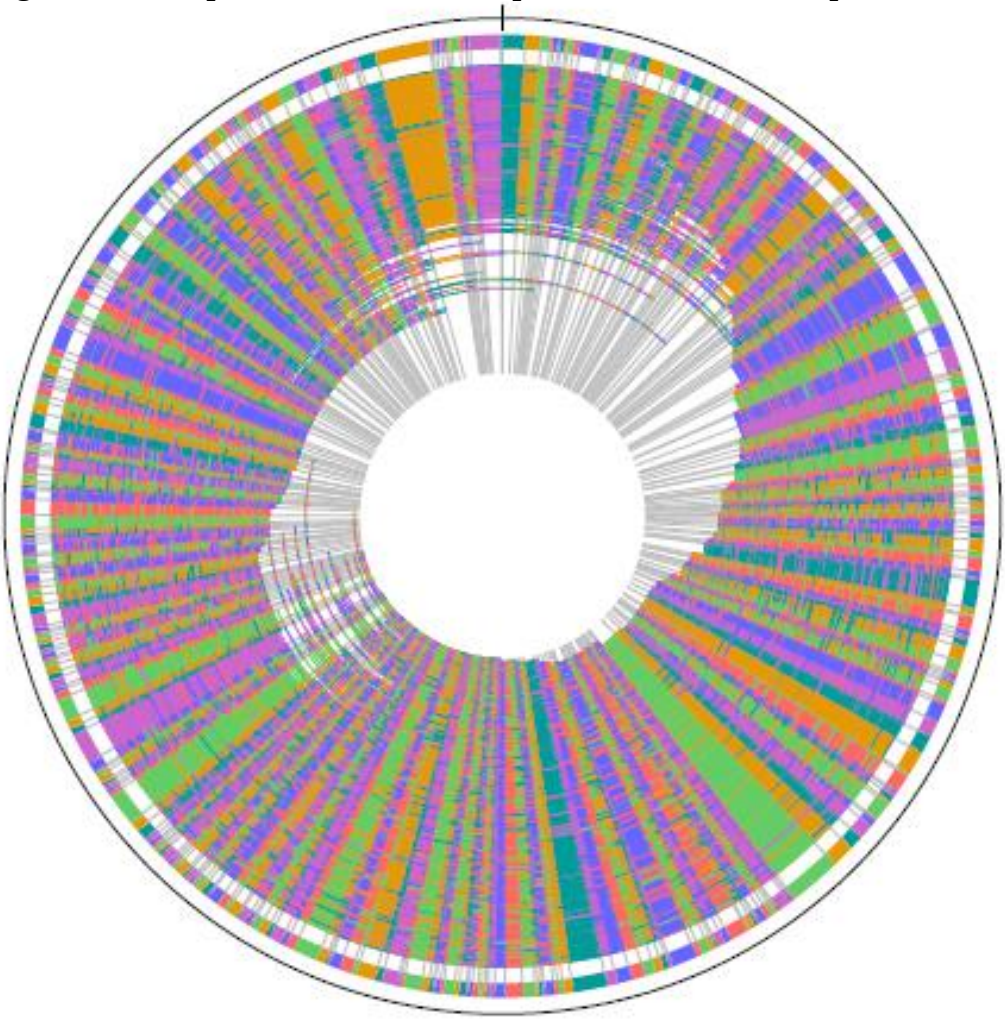

[1]The outermost multicolored ring depicts the consensus map for the *C. septicum* type strain generated by the ARGUS Whole Genome Mapping System. It was constructed from maps of individual DNA molecules cleaved with the SpeI restriction enzyme (depicted as individual arcs within the circle). Homologous restriction fragments in the consensus map are represented by a common color; the order of the color scheme is random, selected to provide visual contrast.

Figure 6.3: *C. septicum* ATCC 12464 SpeI restriction enzyme map[1]

[1]'Barcode' depicting the consensus Whole Genome Map Assembly where the dark blue vertical lines represent SpeI restriction enzyme cut sites and the white spaces between lines indicate the size of restriction fragments. Map was generated using MapSolver software.

Figure 6.4: Alignment of *C. septicum* ATCC 12464 *de novo* FASTA sequence with SpeI whole genome map[1]

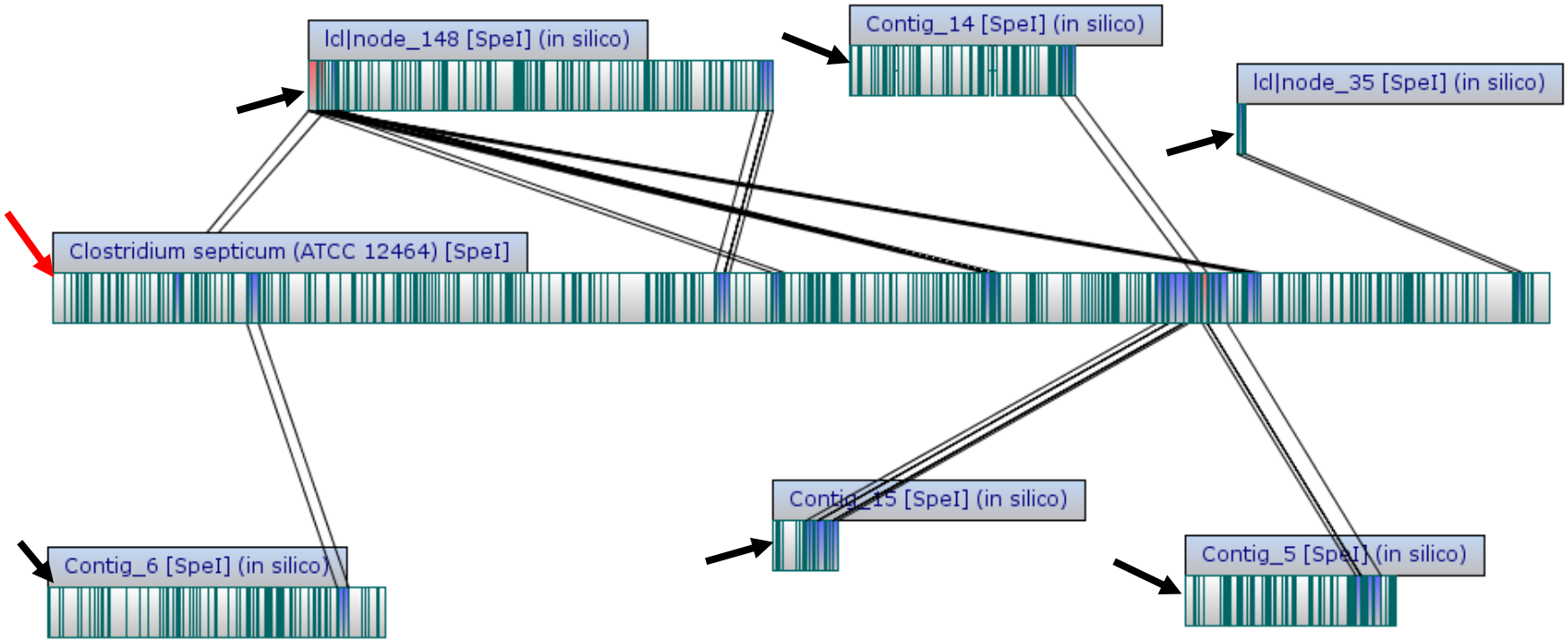

[1]Map generated using MapSolver software default settings. Whole-genome SpeI restriction enzyme map for the *C. septicum* type strain (red arrow) with the dark green vertical lines representing SpeI restriction enzyme cut sites. MapSolver software was used to predict locations for SpeI restriction sites in the individual scaffolds from the *de novo* FASTA sequence (black arrows). Black lines running between the scaffolds and the restriction map show regions of alignment. Fragments highlighted in light blue have aligned with one other segment; fragments highlighted in red have aligned with multiple other segments. Overall there was poor alignment between the scaffolds and the whole genome map. Only 50% of the scaffolds aligned, at least partially, covering 12.5% of the total genome.

Figure 6.5: Optimized alignment of *C. septicum* ATCC 12464 sequence with SpeI whole genome map[1]

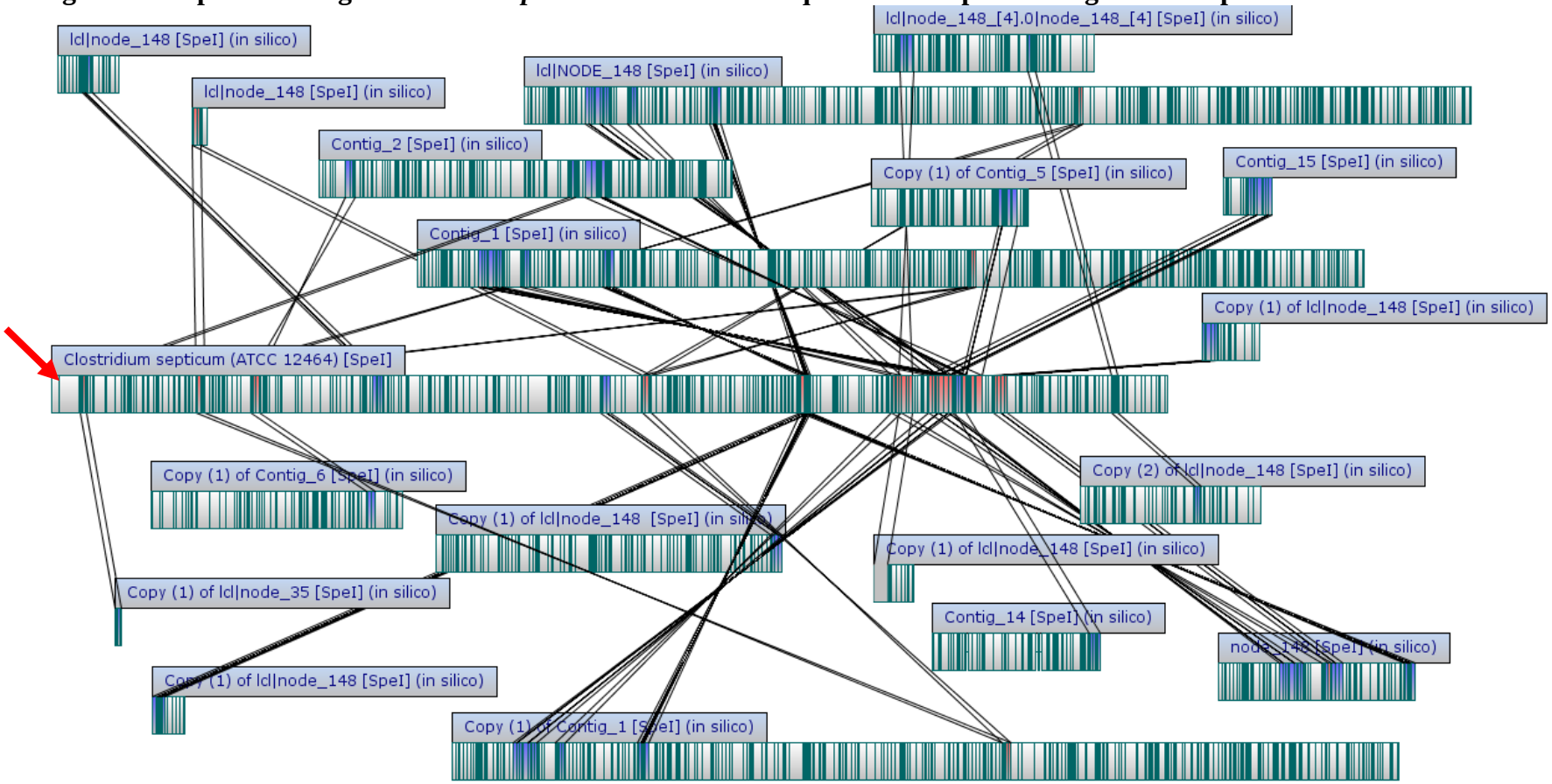

[1]Map generated using MapSolver software using partially-deconstructed scaffolds and settings selected to optimize alignment. Black lines which connect individual scaffolds to the whole-genome restriction map (indicated by red arrow) show regions of homology. The dark green vertical lines within each barcode represent SpeI restriction enzyme cut sites. Fragments highlighted in light blue have aligned with one other segment; fragments highlighted in red have aligned with multiple other segments. There was improved alignment compared to Figure 6.5; however, overall there was still poor alignment of scaffolds with the optical map. 90% of the deconstructed scaffolds aligned, at least partially, covering 18.1% of the total genome.

6.4 Discussion

The *de novo* sequence obtained for the *C. septicum* type strain ATCC 12464 was most similar to those for other members of the genus *Clostridium.* The low GC content of the *C. septicum* genome is consistent with other *Clostridium* spp. [18]. Several coding sequences have been identified which may correlate with known or potential toxins. However, there was poor alignment of the *de novo* FASTA sequence with the whole genome map and additional analysis is necessary to close gaps and correct misassemblies resulting from repetitions.

A 1,323 bp coding sequence (CDS) was present beginning at position 208,675 that is consistent with the *C. septicum* alpha toxin gene [10]. *C. septicum* also produces a second, oxygen-labile hemolysin (delta toxin) [1, 6]. Four CDS were identified which may correspond with this toxin. A 648 bp stretch starting at position 20,274 and a 666 bp sequence at position 26,289 were consistent with membrane hemolysin proteins. A 498 bp segment present at 29,068 and a 3,759 bp run at position 121,797 were predicted to be hemagglutinin- or hemolysin-related proteins. The putative deoxyribonuclease (YcfH), a 786 bp CDS at position 21,851, may correspond with the beta toxin which has been previously identified as a DNase with leukocidal activity [7]. A Panton-Valentine leukocidin chain S precursor was present as a 951 bp CDS at position 179,497. This prophage-encoded cytotoxin is typically found in virulent strains of *Staphylococcus aureus*; it causes leukocyte destruction and tissue necrosis associated with necrotizing skin infections and pneumonia [19]. The gamma toxin of *C. septicum* has been identified as a hyaluronidase. Three coding sequences were identified which may correspond with this toxin. A 3,909 bp segment which starts at position 192,129 and a 3,768 stretch beginning at position 197,693 code for putative hyaluronoglucosaminidase proteins while a 3,957 bp sequence starting at position 338,108 codes for a hyaluronoglucosaminidase precursor.

C. septicum produces a neuraminidase which, while not recognized as one of the major toxins, appears to play a role in pathogenesis of disease by inducing cell damage and allowing for spread of the organism through tissues [1, 20]. Neuraminidase is thought to render target sites susceptible to the activity of other clostridial toxins by altering glycoproteins on cell membranes and in mucoid secretions [6]. A 2,586 bp segment beginning at position 409,380 was consistent with neuraminidase NanP. Two additional coding sequences were identified as putative toxins which did not correspond with any of the known toxins produced by *C. septicum*: a 303 bp stretch starting at position 30,833 with unknown function and a 294 bp sequence at position 57,304 with similarity to ADP-ribosylating toxins. This family of toxin includes *C. perfringens* ι-toxin, *C. spiroforme* toxin, *C. difficile* ADP-ribosyltransferase (CD'1'), and the C2 toxin and C3 exoenzyme produced by C. botulinum types C and D. They cause depolymeraization of actin filaments which results in loss of cell morphology (rounding), alteration of cellular functions, inhibition of leukocyte migration and activation, inhibition of smooth muscle contraction, and interference with endocytosis, exocytosis, and cytokinesis [21, 22]. These toxins also cause disruption of intracellular tight junctions which leads to breakdown of vascular endothelium, ultimately resulting in edema and hypotonic shock [21]. Eight hundred seventy additional CDS were identified as hypothetical proteins; some of these proteins may correspond with toxins or other substances involved in the pathogenesis of disease.

Bacterial genomes with low GC content, such as *Clostridium* spp., commonly harbor bacteriophages which are known to play an important role in the virulence of many bacterial pathogens [23]. Phages can insert and integrate their genomes into a bacterial chromosome as prophages. Prophages are mobile DNA elements (transposons) and can move throughout the bacterial genome or mediate horizontal gene transfer between bacteria [23]. Numerous phage

proteins were present within the *C. septicum* genome. Several bacterial toxins, including some clostridial toxins (e.g. *C. botulinum* neurotoxins C1 and D, *C. botulinum* C3 exoenzyme, *C. novyi* alpha toxin, and C2 toxin), are encoded by prophages that have been incorporated into a bacterial genome [23-25]. Some of the phage proteins identified in the *C. septicum* genome may play a role in the pathogenesis of diseases caused by this organism. Several coding sequences were identified as corresponding to proteins in the Beta-lactamase family. As penicillin is commonly and effectively used in the treatment and prevention of field outbreaks of CD (cellulitis) in turkeys caused by *C. septicum*, this information is surprising and warrants further investigation [26].

There were gaps within and between scaffolds that must be addressed before the *C. septicum* genome can be fully assembled. There were also numerous repetitive sequences which is a known limitation of Next Generation Sequencing (NGS) technologies [27]. Large genomes typically contain numerous repetitive sequences, with up to 40% of some bacterial genomes comprised of repeat regions [28]. These regions are more likely to misassemble, especially when using NGS platforms with short read lengths. This can result in collapse (erroneous alignment of two distant chromosomal regions), expansion (insertion of extra copies of the repeat) or gaps (if the repeats are longer than the read length) [28, 29]. Sequencing is difficult at extremes of AT content, and the *C. septicum* genome had an AT content of 72.3%. AT-rich genomes can cause issues of this nature, especially when using short read NGS platforms like Illumina [30]. While Illumina *de novo* sequencing is 99.9% accurate at the base-pair level, there is no good quality metric for analyzing the entire sequence [31]. Traditionally, contig length has been used to assess assembly quality; however, larger contigs may simply indicate overly-aggressive joining [32].

There was poor alignment between the *de novo* FASTA sequence and the optical map. The SpeI restriction enzyme cuts genomic DNA sequences with an average fragment size of 6-12 kb. Contigs need to be ~40 kb or larger in order to have a 90+% chance of properly aligning to a restriction map generated using SpeI. Therefore, smaller contigs are unlikely to align with the optical map. Small contig size is a known limitation of the Illumina sequencing platform used in this study [27]. Misassembly of repetitive sequences may also be contributing to the poor alignment. Computer software, such as Lasergene GeneQuest (DNASTAR, Inc., Madison, WI, USA), can be used to strip away the repeats. The remaining contigs could then be aligned with the Whole Genome Map. However, this method would likely result in creation of addition gaps that would need to be closed using primer walking and Sanger sequencing. Additional optical maps could also be generated using other restriction enzymes, selected using Enzyme Chooser software (OpGen, Inc.) that may allow for better alignment. Another potential explanation for the failure of some of the scaffolds to align with the optical map is that they may have been comprised of extrachromosomal (e.g. plasmid) DNA. Although no plasmids have currently been identified in *C. septicum* isolates, nor were any seen in the type strain, many toxins genes for other *Clostridium* spp. are encoded on plasmids [24].

While the *C. septicum* type strain genome is not yet closed (i.e. fully assembled into a single chromosome), this draft genome moves us farther toward that goal. The next step is to determine whether the presence of repetitive sequences has resulted in misassembly. Computer software, such as Lasergene GeneQuest (DNASTAR, Inc., Madison, WI, USA), can be used to identify all of the repeat sequences within the genome, build a consensus for each family of repeats, and classify them. Primer walking can be used to help resolve small gaps, low-quality segments within scaffolds, and to close the gaps between the scaffolds. Primers can be designed

using Lasergene SeqManPro software (DNASTAR) to complement the last ~20 bases of the known sequence. The amplified PCR product can then be sequenced using the chain termination method (Sanger sequencing) with the end of the new sequence serving as the template for the next primer in an iterative manner until the gap is fully sequenced. Finally, the assembled genome will need to be validated. Unfortunately, this process is largely manual, expensive, and time-consuming as no automated validation tools currently exist [29]. Despite the difficulties, ensuring accuracy of the final genome is essential. The completed *C. septicum* genome will be important in identifying coding sequences for the toxin genes produced by this organism. Discovery of these genes will be crucial for the success of studies on the pathophysiology of diseases caused by *C. septicum* and in the development of antitoxins and vaccine targets to diagnose, treat and prevent such conditions.

6.5 References

1. Smith, LDS and BL Williams. *Clostridium septicum*. In: The Pathogenic Anaerobic Bacteria, 3rd ed. A. Balows, ed. Charles C Thomas Publisher, Springfield, IL, USA. pp 180-190. 1984.

2. Tellez, G, NR Pumford, MJ Morgan, AD Wolfenden and BM Hargis. Evidence for *Clostridium septicum* as a primary cause of cellulitis in commercial turkeys. Journal of Veterinary Diagnostic Investigation 21:374-377. 2009.

3. Thachil, AJ, B McComb, MM Anderson, DP Shaw, DA Halvorson and KV Nagaraja. Role of *Clostridium perfringens* and *Clostridium septicum* in causing turkey cellulitis. Avian Diseases 54:795-801. 2010.

4. *Clostridium septicum* and malignancy. JAMA 209:410-411. 1969.

5. Ballard, JD and RK Tweten. *Clostridium septicum* alphat-toxin. In: The Clostridia: Molecular Biology and Pathogenesis. J. Rood, B. McClane, J. Songer and R. Titball, eds. Academic Press, San Diego. 1997.

6. Hatheway, CL. Toxigenic *Clostridia*. Clinical Microbiology Reviews 3:66-98. 1990.

7. Songer, JG and KW Post. The Genus *Clostridium*. In: Veterinary Microbiology: Bacterial and Fungal Agents of Animal Diseases. Elsevier Saunders, St. Louis, MO, USA. pp 261-282. 2005.

8. MacLennan, JD. The histotoxic clostridial infections of man. Bacteriological Reviews 26:177-275. 1962.

9. Timoney, JF, JA Gillespie, FW Scott and JE Barlough. The genus *Clostridium*. In: Hagan and Bruner's Microbiology and Infectious Diseases of Domestic Animals, 8th ed. Cornell University Press, Ithaca, New York. pp 214-240. 1988.

10. Imagawa, T, Y Dohi and Y Higashi. Cloning, nucleotide sequence and expression of a hemolysin gene of *Clostridium septicum*. FEMS Microbiology Letters 117:287-292. 1994.

11. Neumann, AP and TG Rehberger. MLST analysis reveals a highly conserved core genome among poultry isolates of *Clostridium septicum*. Anaerobe 15:99-106. 2009.

12. Zenz, KI, P Roggentin and R Schauer. Isolation and properties of the natural and recombinant sialidase from *Clostridium septicum* NC 0054714. Glycocong J 10:50-56. 1993.

13. Ballard, J, J Crabtree, BA Roe and RK Tweten. The primary structure of *Clostridium septicum* alpha-toxin exhibits similarity with that of *Aeromonas hydrophila* aerolysin. Infection and Immunity 63:340-344. 1995.

14. Aziz, RK, D Bartels, AA Best, M DeJongh, T Disz, RA Edwards, K Formsma, S Gerdes, EM Glass, M Gubal, F Meyer, GJ Olsen, R Olson, AL Osterman, RA Overbeek, LK McNeil, D Paarmann, T Paczian, B Parrello, GD Pusch, C Reich, R Stevens, O Vassieva, V Vonstein, A Wilke and O Zagnitko. The RAST Server: Rapid Annotations using Subsystems Technology. BCM Genomics 9. 2008.

15. Overbeek, R, R Olson, GD Pusch, GJ Olsen, JJ Davis, T Disz, RA Edwards, S Gerdes, B Parrello, M Shukla, V Vonstein, AR Wattam, F Xia and R Stevens. The SEED and the Rapid Annotation of microbial genomes using Subsystems Technology (RAST). Nucleic Acids Research 42:D206-D214. 2014.

16. Leggett, RM, BJ Clavijo, L Clissold, MD Clark and M Caccamo. NextClip: an analysis and read preparation tool for Nextera Long Mate Pair libraries. Bioinformatics 30:566-568. 2014.

17. Tatusova, T, S Ciufo, B Fedorov, K O'Neill and I Tolstoy. RefSeq microbial genomes database: new representation and annotation strategy. Nucleic Acids Res 42:D553-559. 2014.

18. Smith, LDS and BL Williams. The *Clostridia*. In: The Pathogenic Anaerobic Bacteria, 3rd ed. A. Balows, ed. Charles C Thomas Publisher, Springfield, IL, USA. pp 94-100. 1984.

19. Lina, G, Y Piemont, F Godail-Gamot, M Bes, MO Peter, V Gauduchon, F Vandensch and J Etienne. Involvement of Panton-Valentine Leukocidin-producing *Staphylococcus aureus* in primary skin infections and pneumonia. Clinical Infectious Diseases 29:1128-1132. 1999.

20. Wilson, LM and GT Macfarlane. Cytotoxicity, adhesion and invasion of *Clostridium septicum* in cultured human epithelial cells (CACO-2, HEp-2): Pathological significance of swarm cell differentiation. Anaerobe 2:71-79. 1996.

21. Popoff, MR and P Bouvet. Clostridial toxins. Future Microbiology 4:1021-1064. 2009.

22. Boquet, P, P Munro, C Fiorentini and I Just. Toxins from anaerobic bacteria: specificity and molecular mechanisms of action. Current Opinion in Microbiology 1:66-74. 1998.

23. Brussow, H, C Canchaya and W-D Hardt. Phages and the evolution of bacterial pathogens: from genomic rearrangements to lysogenic conversion. Microbiol Mol Biol Rev 68:650-602. 2004.

24. Gyles, C and P Boerlin. Horizontally transferred genetic elements and their role in pathogenesis of bacterial disease. Veterinary Pathology 51:328-340. 2014.

25. Popoff, MR and BG Stiles. Clostridial toxins vs. other bacterial toxins. In: Handbook on *Clostridia*. P. Durre, ed. CRC Press: Taylor & Francis Group, Boca Raton, FL. pp 323-383. 2005.

26. Clark, S, R Porter, B McComb, R Lippert, S Olson, S Nohner and HL Shivaprasad. Clostridial dermatitis and cellulitis: an emerging disease of turkeys. Avian Diseases 54:788-794. 2010.

27. Zavodna, M, A Bagshaw, R Brauning and NJ Gemmell. The accuracy, feasibility and challenges of sequencing short tandem repeats using next-generation sequencing platforms. PLos ONE 9:e113862. 2014.

28. Treangen, TJ and SL Salzberg. Repetitive DNA and next-generation sequencing: computational challenges and solutions. Nature Reviews Genetics 13:36-46. 2012.

29. Phillippy, AM, MC Schatz and M Pop. Genome assembly forensics: finding the elusive mis-assembly. Genome Biology 9:R55. 2008.

30. Harismendy, O, PC Ng, RL Strausberg, X Wang, TB Stockwell, KY Beeson, NL Schork, SS Murray, EJ Topol, S Levy and KA Frazer. Evaluation of next generation sequencing platforms for population targeted sequencing studies. Genome Biology 10:R32. 2009.

31. Quail, MA, M Smith, P Coupland, TD Otto, SR Harris, TR Connor, A Bertoni, HP Swerdlow and Y Gu. A tale of three next generation sequencing platforms: comparison of Ion Torrent, Pacific Biosciences and Illumina MiSeq sequencers. BMC Genomics 13:341. 2012.

32. Salzberg, SL and JA Yorke. Beware of mis-assembled genomes. Bioinformatics 21:4320-4321. 2005.

Chapter 7 – Conclusions and Future Work

7.0 Introduction

Clostridial dermatitis (CD) is a disease of rapidly growing turkeys that presents with gangrenous lesions on the caudal breast and thigh. Despite the name, this condition is not a true dermatitis. Microscopic lesions consist of necrosis of skeletal muscle and subcutaneous tissues; the overlying skin is typically unaffected. Few if any inflammatory cells are present in affected tissues. Prior to 2008, the disease was commonly referred to as 'cellulitis.' The name 'clostridial dermatitis' was selected in 2008 by a committee of turkey industry representatives, veterinarians, and researchers during the Gold Medal Panel on Cellulitis. This name was chosen in order to differentiate this condition in turkeys from cellulitis (infectious process) in chickens caused by *E. coli* [1]. There also seems to be some confusion regarding the distinction between CD of turkeys and gangrenous dermatitis that occurs in both chickens and turkeys. While both conditions can be caused by *Clostridium* spp. they are two distinct pathologies with very different mechanisms of pathogenesis. Gangrenous dermatitis is a true dermatitis with infection of the skin occurring secondary to scratches or other penetrating trauma; whereas, CD affects subcutaneous tissues and skeletal muscle with an endogenous (gastrointestinal) source of the causative organism as opposed to exogenous (traumatic) [1, 2].

CD in turkeys is a multifactorial disease; the presence of *C. septicum* alone is not sufficient to cause illness. This organism can be found in the gastrointestinal tract, blood, liver, and skeletal muscle of asymptomatic birds. Certain host (genetic), pathogen (virulence), and/or environmental factors are required to allow *C. septicum* to proliferate in tissues. While lesions similar to CD have been described in turkeys since the 1930s, they were uncommon occurrences

[3]. Advancements in genetic selection of turkeys for increased weight and rapid growth rate as well as changes in management practices may have contributed to recent increases in incidence and severity of CD.

7.1 Causation of Multifactorial Diseases

Establishment of causation for conditions caused by obligate, as opposed to opportunistic, pathogens is fairly straightforward. The Henle-Koch Postulates can be fulfilled for such diseases: the causative organism can be isolated from cases of the disease, inoculated into a susceptible host to induce the same pathology, and be isolated anew from the new host [4]. These postulates further stipulate that the causative agent should be present in every case of the disease and not be found in other diseases as a fortuitous and nonpathogenic organism. Therefore, they are often inadequate for determining causation of multifactorial diseases involving opportunistic pathogens. Development of multifactorial diseases depends on complex interactions between multiple host, pathogen, and environmental factors. While the presence of certain individual factors may be necessary for disease to develop, various combinations can potentially lead to development of the same disease [5]. The presence of a single necessary factor alone may not be sufficient. Monocausal models also do not account for situations where a particular causative agent is present in the absence of disease. Many 'pathogens' are capable of establishing a relatively peaceful coexistence with their hosts, either as part of the host's normal microflora or after disease has occurred and an asymptomatic carrier state develops. Opportunistic pathogens cause disease when the host's immune system is compromised.

Inability to "reproduce the disease anew" is often the largest hurdle in establishing causation [6]. Evan's Unified Concept is a more appropriate guide for determining causation of

multifactorial diseases involving opportunistic pathogens (see Table 1.3) [4]. Incidence and prevalence of disease should be significantly higher in those individuals exposed to the putative cause(s). Additionally, diseased individuals should have higher rates of exposure than non-affected controls. Development of disease must occur following exposure to the putative cause(s). Within a population of exposed individuals, a spectrum host responses should occur along a biological gradient from mild to severe. This host response (e.g. lesions, antibodies, etc.) should regularly appear or increase in magnitude following exposure. Disease incidence should be higher following experimental exposure to the putative cause(s) compared to non-exposed controls. Elimination or modification of the putative cause(s) and prevention or modification of the host's response following exposure should reduce the incidence and/or severity of disease. Most importantly, the proposed pathogenesis should make sense from both a biological and epidemiological standpoint.

7.2 Evidence Supporting Proposed Mechanism for Pathogenesis of Clostridial Dermatitis

While the studies presented in this dissertation do not definitively prove the proposed mechanism of pathogenesis for CD, they provide strong evidence in support of that hypothesis. Results from these studies demonstrate that the proposed mechanism either satisfies or partially satisfies 8 of 10 criteria laid out in Evan's Unified Concept of Causality (Table 7.1) [4]. Low numbers of *C. septicum* were detected in intestinal, liver, and skeletal muscle samples from asymptomatic turkeys (Chapter 3). The distribution of organisms in various tissues apart from the gastrointestinal tract and the absence of skin scratches or penetrating trauma suggest that *C. septicum* spreads hematogenously from an endogenous source. Despite the organism being present in tissues, alpha toxin mRNA was not expressed in asymptomatic birds (Chapter 5).

Certain host factors must be present in order for *C. septicum* to proliferate and elaborate toxins leading to necrosis of skeletal muscle and subcutaneous tissues.

C. septicum is a spore-forming anaerobe that is ubiquitous in the environment and commonly isolated from the gastrointestinal tract of healthy turkeys [7, 8]. Studies have shown that *C. septicum* originates from the gastrointestinal tract in more than 50% of cases of nontraumatic gas gangrene [9]. Therefore, the intestines are the most likely endogenous source of *C. septicum* in cases of CD. The intestinal mucus layer and tight junctions between mucosal endothelial cells normally prevent bacteria from entering systemic circulation [10, 11]. However, numerous factors are known to alter intestinal mucosal integrity and increase 'leakiness' of these epithelial tight junctions leading to bacterial translocation. Subclinical damage to the intestinal epithelium allows bacteria to enter the intramural vasculature. From there, they can then spread through the bloodstream to other tissues where they may then cause disease. A similar mechanism has been proposed for development of spontaneous clostridial myonecrosis associated with malignancy in humans [12, 13]. Predisposing factors for development of this condition include any pathology which allows bacteria from the intestine to enter the bloodstream [14].

Table 7.1: Application of Evan's Criteria for Causation to Proposed Mechanism for Pathogenesis of Clostridial Dermatitis

Criteria for Causation	Applies to Proposed Mechanism for CD?
1. *Prevalence* of the disease should be significantly higher in those exposed to the putative cause than in cases controls not so exposed.	Yes: breed, flock type, weight at processing, and stocking density affect prevalence of CD (Ch. 2)
2. *Exposure* to the putative cause should be present more commonly in those with the disease than in controls without the disease when all risk factors are held constant.	Yes: increased incidence and severity of focal polyphasic myonecrosis on farms with a chronic history of CD (Ch. 3); positional reduction in oxygen saturation was associated with flock types at higher risk for CD (Ch. 4)
3. *Incidence* of the disease should be significantly higher in those exposed to the putative cause than in those not so exposed as shown in prospective studies.	Yes: breed, flock type, weight at processing, and stocking density affect incidence of CD (Ch. 2)
4. *Temporally*, the disease should *follow* exposure to the putative agent with a distribution of incubation periods on a bell shaped curve.	Probable: *C. septicum* present in muscle of asymptomatic birds without corresponding production of CsA mRNA; presence of CsA mRNA associated with CD (Ch. 3 and 5)
5. *A spectrum* of host responses should follow exposure to the putative agent along a logical biological gradient from mild to severe.	Yes: severity of gross and histopathologic lesions was associated with the presence of CsA mRNA (Ch. 5)
6. *A measureable host response* following exposure to the putative cause should *regularly appear* in those lacking this before exposure (i.e., antibody, cancer cells) or should *increase* in magnitude if present before exposure; this pattern should not occur in persons so exposed.	Yes: development of CD was associated with the presence of CsA mRNA (Ch. 5)
7. *Experimental reproduction of the disease* should occur in higher incidence in animals or man appropriately exposed to the putative cause than in those not so exposed; this exposure may be deliberate in volunteers, experimentally induced in the laboratory, or demonstrated in a controlled regulation of natural exposure.	Not evaluated
8. *Elimination or modification* of the putative cause or of the vector carrying it should decrease the incidence of the disease.	Not directly evaluated; however, anecdotal evidence suggests that management factors affect incidence of CD (Ch. 2)
9. *Prevention or modification* of the host's response on exposure to the putative cause should decrease or eliminate the disease.	Not evaluated; however, characterization of the causative agent (Ch. 6) is a first step towards identification of vaccine targets
10. The whole thing should make biological and epidemiological sense.	Yes

Diet can influence changes in gastrointestinal microflora. The use of growth-promoting antibiotics (e.g. bacitracin, virginiamycin, tylosin, spiramycin, salinomycin and avilamycin) in feed has been shown to reduce intestinal numbers of *C. perfringens* and reduce the incidence of necrotic enteritis in broilers [15, 16]. Diets high in wheat, barley, rye, oats, fish meal, methionine, or that increase intestinal production of mucus all favor proliferation of *Clostridium* spp. [17-19]. Damage to the intestinal mucosa caused by coccidia can lead to overgrowth of *Clostridium* spp. [17] due to an increase in mucus which serves as a nutrient source favoring rapid clostridial proliferation. Genetic selection for increased body weight in broilers has also been shown to result in microbiome changes [20]. The presence of factors that lead to increased numbers of *C. septicum* in the gastrointestinal tract place birds at an increased risk of developing CD.

Numerous factors influence the integrity of epithelial tight junctions. Various amino acids, including glutamine and tryptophan, peptides including casein, fatty acids, vitamins A and D, polyphenols, and probiotics have been shown to decrease intestinal tight junction permeability [11]. Dexamethasone, a corticosteroid that can be used to mimic the stress response, has been shown to increase permeability [21, 22]. Subclinical damage caused by other enteric pathogens, such as coccidia, also increases membrane general permeability through destruction of epithelial cells which results in increased bacterial translocation [17]. Once bacteria leave the gastrointestinal tract they are able to spread hematogenously to other tissues.

C. septicum was detected in skeletal muscle from birds on farms with a chronic history of CD as well as farms with no history of the disease (Chapter 3). Therefore, multiple host and/or environmental factors must be present in order for disease to occur. Heavier birds are more prone to develop CD, particularly heavy hens and toms during the finishing period (Chapter 2).

Genetic selection of meat-type birds for rapid growth rate and increased breast muscle yield has inadvertently selected for birds with insufficient cardiovascular, skeletal, and immune support [23, 24]. Skeletal muscle development in rapidly growing turkeys has been shown to outpace cardiovascular and connective tissue development [23, 25-27]. Myogenesis outpaces angiogenesis; therefore, some muscle fibers may lack adequate capillary networks for the delivery of oxygen and other nutrients. This resulting micro-ischemia is thought to contribute to the development of focal myonecrosis [26, 27]. Faster growing lines of turkeys have been shown to have a higher number of degenerating skeletal muscle fibers [25-28]. Although the incidence and severity of polyphasic necrosis, characterized by the presence of muscle fibers in varying stages of degeneration, necrosis, and regeneration, are increased in older birds, young turkeys raised under ideal laboratory conditions show similar myofiber pathology [26, 28]. This suggests that there may be a genetic predisposition for development of such lesions. Incidence and severity of multifocal polyphasic myonecrosis in the breast and thigh were associated with risk of developing CD (Chapter 3). Presence of focal polyphasic myonecrosis may be a predisposing factor for the development of CD (Figure 7.1). If the microischemia thought to lead to the development of focal polyphasic myonecrosis was alone sufficient to reduce oxygen levels to a point allowing for clostridial growth, CD lesions would be expected to occur throughout the entire breast and thigh. The caudoventral distribution of CD lesions in the breast muscle is consistent with the hypothesis of positional restriction of blood flow as a necessary step in the pathogenesis of CD.

Figure 7.1: Proposed Role of Focal Polyphasic Myonecrosis in Development of CD

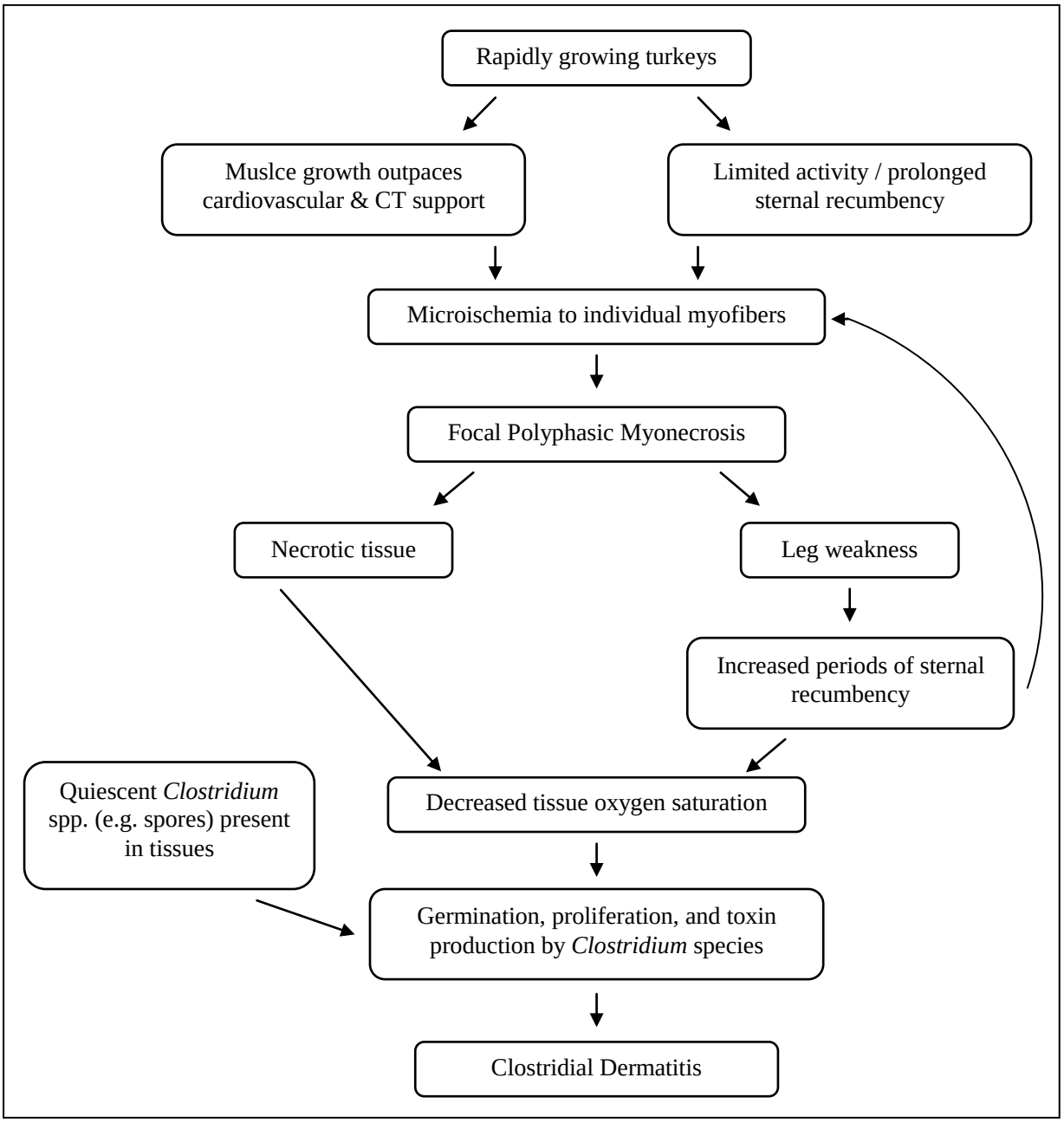

Prolonged sternal recumbency leads to decreased blood flow to tissues of the caudal breast and medial thigh (Chapter 4). It also results in venous pooling in these dependent tissues. Reductions in arterial supply and venous return can lead to decreased oxygen saturation within tissues. Genetic selection has resulted in rapidly growing birds with increased skeletal muscle

mass; however, there has been no corresponding increase in lung volume [23, 29]. Additionally, since avian lungs are fixed within the ribcage and do not expand, pulmonary capillaries have limited capacity to accommodate increased blood flow [29, 30]. Consequently, these birds may lack sufficient lung capacity to meet the increased oxygen demand of large, rapidly growing muscles. Fast-growing meat-type birds have been shown to have a lower oxygen hemoglobin saturation as a result of inadequate respiratory capacity and/or increased oxygen consumption [31, 32]. High feed consumption also results in large digestive tracts which compete for space with the abdominal air sacs reducing tidal volume [31]. Insufficient pulmonary function combined with inefficient oxygen transport intuitively result in decreased oxygen saturation within the skeletal muscle of rapidly growing turkeys. Therefore, it is plausible that myonecrosis in tandem with slight decreases in oxygen saturation contribute to the development of CD by allowing for the proliferation of the relatively aerotolerant *C. septicum* (albeit in a low/dormant metabolic state) within skeletal muscle and subcutaneous tissue.

Studies found that dexamethasone-treated birds were more likely to develop CD than untreated controls [33]. Researchers concluded that stress was contributing to pathogenesis of the disease via altered cutaneous permeability and immunosuppression. However, we propose an alternative explanation for success of the dexamethasone model in inducing development of CD. Dexamethasone causes increased permeability of intestinal epithelial tight junctions which may result in increased translocation of bacteria, including *C. septicum* [21, 22]. In one challenge model, turkeys were placed in crates on transport trucks to induce stress [34]. This methodology also forced birds to spend a prolonged period of time in sternal recumbency which has been suggested to reduce perfusion to the caudal breast and medial thigh (Chapter 4). Dexamethasone has also been shown to induce lameness associated with necrosis of the

proximal tibial and femoral heads which would likely lead to birds spending prolonged periods in sternal recumbency [35]. Decreased perfusion and the subsequent decrease in oxygen saturation in dependent skeletal muscles would foster proliferation of previously-trapped *C. septicum* and elaboration of toxins leading to development of CD.

One turkey producer reported a decrease in the incidence of CD after halting the use of penicillin in the face of outbreaks [36]. This may suggest that repeated use of penicillin induced selection pressure favoring proliferation of more virulent *C. septicum* isolates that were resistant to penicillin. *De novo* whole genome sequencing has identified the presence of multiple beta-lactamase coding sequences within the *C. septicum* genome (Chapter 6) which would suggest that at least some *C. septicum* isolates could be resistant to penicillins. However, another possible explanation for these results is that the use of penicillin masked poor management practices (e.g. infrequent dead bird pick-up, water spills, etc.). Once growers realized that the use of penicillin was no longer an option to treat outbreaks, they were forced to improve management factors in order to control CD.

The presence of the *C. septicum* alpha toxin mRNA (CsA) was associated with CD, whereas this was not the case with *C. perfringens* (Chapter 5). CsA has been identified as the main virulence factor in *C. septicum* due to its pore-forming, dermonecrotic, hemolytic, and lethal activities [37, 38]. These functions are consistent with the pathology seen with CD. However, the actions of this toxin alone do not explain the entirety of the pathology seen. Other toxins are likely also expressed during pathogenesis of CD. The lack of inflammatory cells associated with CD lesions suggests that beta toxin may also contribute to pathogenesis as it is a known leukocidin [39]. *In vitro* protein expression studies suggest that CpA should be produced during infection of turkey skeletal muscle (Appendix D), but the lack of association between

CpA mRNA expression and CD suggests that *C. perfringens* is probably not involved in development of the disease.

Data presented in Chapter 2 showed that leg issues were not associated with incidence of CD which is counterintuitive given the proposed mechanism for pathogenesis. However, there were several limitations to this study. Prior leg issues were recorded for 27 of the 120 (22.5%) flocks that developed CD. As this was a retrospective study, growers and flock supervisors were not specifically directed to monitor for the presence of leg issues in flocks. Production and/or health issues were only recorded if they were deemed significant by either the grower or the flock supervisor. Additionally, an unrelated disease outbreak occupied flock supervisors' time for a 6-week period during this study which likely affected the completeness of some flock health and production records. Therefore, the actual incidence of leg issues in flocks may have been higher than was recorded.

7.3 Recommendations for Control of Clostridial Dermatitis

There are a number of strategies that turkey producers could employ to reduce the incidence and/or severity of CD outbreaks. Decreasing stocking density, growth rate, final market weight, and implementing total cleanout after every flock would likely decrease the incidence of CD in turkey flocks (Chapter 2). However, these are impractical solutions due to the economics of commercial turkey production.

There are some management changes that turkey producers could implement that may reduce the incidence and/or severity of CD without drastically altering costs. One possible strategy is to increase bird activity by changing lighting schedules. Prolonged recumbency associated with decreased blood perfusion to the caudal breast and proximal medial thigh is

hypothesized to predispose birds to the development of CD (Chapter 4). Producers could reduce the duration of dark periods. The ratio of light to dark periods can remain unchanged, but reducing the length of individual dark periods will encourage increased activity. Reducing the time spent in sternal recumbency (i.e. increasing physical activity) would likely improve blood flow and tissue oxygenation which would likely lead to a decrease in the incidence of CD. Another strategy to increase activity would be to increase the number of times per day that the producer walks through the turkey house. Turkeys are typically more active when people are in the house. Most producers also indicate that increased frequency of dead bird pick-up reduces mortality in the face of a CD outbreak. Some conclude that this is associated with removal of carcasses that contain high numbers of the causative agent(s) and serve as sources of infection for other birds [1]. While reduction of the bacterial load in the house is likely a contributing factor in mortality reduction, increased frequency of carcass removal requires growers to walk through the turkey house more frequently. This action would therefore have a dual effect. Increased activity and subsequent increases in tissue oxygen saturation would likely inhibit *C. septicum* proliferation within muscle and subcutaneous tissues. Improved tissue perfusion may also reduce the incidence and severity of polyphasic myonecrosis, which may predispose birds to the development of CD.

The poultry industry has recognized problems associated with selection for rapid rate of gain since the 1970s [23, 24, 40]. Many of the adverse conditions associated with genetic selection for rapid growth and increased muscle yield are exacerbated by diets that are formulated to maximize average daily gain and feed conversion. One approach to control CD might be to formulate diets in a manner that would decrease the rate of growth early in development to allow time for sufficient skeletal development. Reduced growth rate would also

decrease the metabolic rate, thus allowing pulmonary function to keep pace with oxygen demand in skeletal muscle [30]. While this strategy would result in decreased weights during the brooding and early growing periods, compensatory growth following feeding at a higher plane of nutrition during the late growing and finishing periods would allow birds to reach final market weights close to current targets. Decreased rate of gain early followed by a period compensatory growth has been shown to reduce the incidence of skeletal abnormalities without significantly affecting final market weight [41]. A similar strategy could conceivably reduce the incidence of CD later during the finishing period. However, a non-peer reviewed Aviagen technical bulletin reports that this type of strategy may result in abnormalities in respiratory and skeletal development [42]. Additional studies are necessary to determine the optimal growth curve of turkeys for reducing development of CD.

While it is not practical to completely eliminate *C. septicum* from turkeys or turkey houses, there are strategies that producers could employ to reduce organism numbers. Elimination or reduction of dietary components that are mucogenic (e.g. nonstarch polysaccharides) or contain high levels of animal-derived protein (e.g. fishmeal, meat and bone meal) may reduce gastrointestinal numbers of *Clostridium* spp. as presence of these factors tend to favor clostridial proliferation [43, 44]. The use of prebiotics, probiotics and/or competitive exclusion products aids in the maintenance of a stable gut microbiome [17, 45]. Use of these products can effectively reduce *Clostridium* numbers in the gastrointestinal tract [1, 44, 46]. Prebiotics and probiotics have also been shown to enhance mucosal immunity leading to reduce bacterial translocation from the gastrointestinal tract [47]. Therefore, use of these products could potentially decrease the incidence of CD by reducing numbers of *C. septicum* within skeletal muscle. Evaluation of the effectiveness of these strategies at reducing the incidence and/or

severity of CD in turkey flocks will further add to our understanding of the mechanism of pathogenesis of this disease.

Ideally, a reproducible experimental model that mimics field challenge still needs to be developed to study the effectiveness of treatment and prevention strategies. However, this may not be possible due to the multifactorial nature of the disease. Turkey companies frequently conduct small-scale field trials to test new treatment and prevention strategies for controlling various diseases. However, maintaining a competitive edge often prevents companies from collaborating or sharing results from these trials. Additionally, small sample size, short duration, and inability to control confounding variables in these trials often results in data sets that lack sufficient power or uniformity in disease definition/criteria to detect differences between treatment groups. Turkey companies routinely collect data on numerous production parameters for flocks, yet health data is often far less extensive and consistent. Turkey companies may wish to incorporate additional health parameters into their routine flock records and make this data more widely available to researchers for epidemiological analysis. Companies could also consult with researchers and statisticians when designing field trials to maximize the power of the studies they conduct. Ideally, the poultry industry could also work towards establishing uniform nomenclature, specific criteria for diagnosis of particular diseases, and minimum standards for diagnostic sample collection. Such efforts would enable consistent interpretation and comparison of results between various studies.

7.4 Future Work

Flock type affects development of CD with the highest incidence occurring in toms (Chapter 2). Increased market weight and rapid growth rate of these birds likely accounts for

this difference. Although the disease occurs in both genders, current results cannot rule out the potential role of testosterone as a contributing factor for the development of CD. Additional work can be performed to determine if there is any association between the ratio of testosterone to estrogen and incidence of CD.

While the data presented in Chapter 3 supports the hypothesis of gastrointestinal translocation and hematogenous spread of *C. septicum*, further work is needed to definitively prove that this process occurs in asymptomatic turkeys. Previous work has shown that a characterized strain of *Campylobacter jejuni* can be detected in the liver and spleen of broiler chicks one hour after oral inoculation [48]. Immunohistochemistry and/or electron microscopy using gold colloid labeling can be used to demonstrate translocation of *Clostridium* spp. within epithelial tight junctions or in the subepithelial space. Studies could be designed to evaluate the effect of various factors (e.g. diet, stress, changes in gut microflora) on the permeability of epithelial tight junctions and frequency of clostridial translocation.

Results from the pulse oximetry and thermal imaging studies suggest that prolonged sternal recumbency causes reduced blood perfusion to and oxygen saturation of tissues in the caudal breast and thigh regions. However, there were several limitations with these studies. There was poor reproducibility of results between experimental replicates, the experimental design did not allow for paired standing and recumbent measurements to be taken on the same individual, and the technologies used did not directly assess perfusion or oxygen saturation of skeletal muscle and subcutaneous tissue. Additional studies should be conducted in a controlled laboratory setting to minimize confounding variables and to collect paired measurements on individual birds. These results justify exploration of other more expensive technologies to assess

perfusion and tissue oxygen saturation. Methods to consider include direct and indirect blood pressure monitoring, near-infrared spectroscopy (NIRS), and laser Doppler flowmetry.

Several autogenous vaccine products based on *C. septicum* or fluids from affected birds have been tested. Unfortunately, these products have been largely unsuccessful in preventing CD outbreaks [49]. Limited understanding of the toxins involved in the pathogenesis of CD has hindered vaccine development. Additionally, there is still some debate regarding whether induction of protective immunity against *C. septicum* requires production of antibodies against secreted toxin proteins or antibodies against cell-surface proteins [50, 51]. *C. septicum* isolates also demonstrate antigenic heterogenicity. Several H and O agglutination antigens have been identified and classification of isolates into six antigenic groups has been recommended based on the presence of two somatic and five flagellar antigens [52].

The *de novo s*equencing of *C. septicum* performed as a part of this dissertation was a first step in the identification of more specific, targeted immunogens. Additional work is necessary to completely assemble the draft *C. septicum* genome. Multiple repetitive sequences are present in the genome which creates problems for assembly software. Repeats may be erroneously combined, joining together two regions that do not belong near each other [53]. Lasergene GeneQuest software (DNASTAR, Inc., Madison, WI, USA) can be used to strip away these repeats and reassemble the contigs to align with the Whole Genome Map. Primer walking with Sanger sequencing can then be used to resolve gaps and low quality sequences within scaffolds and to close the gaps between scaffolds. Lasergene SeqManPro software (DNASTAR) allows for the development of primers to improve coverage and walk into gaps as well for assembly of the resulting sequences. Finally, validation is necessary to ensure proper chromosome assembly.

Several coding sequences have been identified which may correspond with the toxin genes of *C. septicum* (Chapter 6). Putative toxins can either be synthesized based on the predicted protein sequence or can be cloned into an *E. coli* expression vector. A battery of assays can be run on the resulting proteins to determine whether their functions are consistent with the known toxins produced by *C. septicum.* Methods for evaluating toxin function include: mouse lethality testing, hemolysin and necrotoxin assays, agar plate method for hyaluronidase activity, and activity on fixed rabbit leucocytes (DNase assay) [39, 54-56]. Once gene sequences have been identified for additional *C. septicum* toxins, gene expression analysis can be performed on tissue samples from cases of CD (Chapter 5). Finally, the toxin proteins themselves must be demonstrated in affected tissues. This will require preparation of specific antitoxins for use in immunohistochemistry assays.

Several coding sequences consistent with proteins in the beta-lactamase family were identified in the *C. septicum* genome (Chapter 6). This is surprising given that penicillin is widely and effectively used to control outbreaks of CD in turkeys [1]. The isolate used for *de novo* whole genome sequencing was the type strain obtained from ATCC. This is a laboratory-passaged strain derived from a culture originating at the Pasteur Institute and studied by Robertson in 1918-1920 [57, 58]. This strain was originally isolated prior to the discovery of penicillin. Therefore, the beta lactamase genes present in the *C. septicum* type strain reflect either resistance to naturally-occurring pencillins produced by molds in the environment or a laboratory-acquired resistance in response to propagation. The presence of a gene does not necessarily mean that the gene is actively transcribed. Additional studies are needed to determine if the type strain demonstrates *in vitro* resistant to penicillin and other beta-lactamase antibiotics. A century of environmental selection pressures have been exerted on the type strain

and field isolates of *C. septicum.* Comparative genomic studies can be performed on field isolates from turkeys with CD to determine whether these resistance genes are conserved.

CD is a disease of significant economic concern to the turkey industry with mortality in affected flocks reported as high as 1-2% per week. The studies presented in this dissertation made significant progress toward understanding the pathophysiology of this condition. However, further studies are necessary to elucidate details in the mechanism of pathogenesis and to validate the efficacy of purported prevention and treatment methods. Since CD is a multifactorial disease, successful control will likely require the integration of multiple strategies that reduce *C. septicum* numbers and enhance host immunity.

7.5 References

1. Clark, S, R Porter, B McComb, R Lippert, S Olson, S Nohner and HL Shivaprasad. Clostridial dermatitis and cellulitis: an emerging disease of turkeys. Avian Diseases 54:788-794. 2010.

2. Opengart, K. Gangrenous dermatitis. In: Diseases of Poultry, 12th ed. Y. Saif, A. Fadly, J. Glisson, L. McDougald, L. Nolan and D. Swayne, eds. Blackwell Publishing, Ames, IA, USA. pp 885-889. 2008.

3. Fenstermacher, R and BS Pomeroy. *Clostridium* infection in turkeys. Cornell Veterinary Journal 29:25-28. 1939.

4. Evans, AS. Causation and disease: the Henle-Koch postulates revisited. The Yale Journal of Biology and Medicine 49. 1976.

5. Gori, GB. Epidemiology and the concept of causation in multifactorial diseases. Regulatory Toxicology and Pharmacology 9:263-272. 1989.

6. Evans, AS. Limitations of the Henle-Koch postulates: Effect of new concepts and of technology. In: Causation and disease: a chronological journey
Plenum Medical Book Company, New York. pp 123-146. 1993.

7. Smith, LDS and BL Williams. *Clostridium septicum*. In: The Pathogenic Anaerobic Bacteria, 3rd ed. A. Balows, ed. Charles C Thomas Publisher, Springfield, IL, USA. pp 180-190. 1984.

8. USDA. Poultry 2010: Clostridial dermatitis on US turkey-grower farms. USDA-APHIS-VS-CEAH-NAHMS. 2012.

9. Songer, JG and KW Post. The Genus *Clostridium*. In: Veterinary Microbiology: Bacterial and Fungal Agents of Animal Diseases. Elsevier Saunders, St. Louis, MO, USA. pp 261-282. 2005.

10. Smirnov, A, R Perez, E Amit-Romach, D Sklan and Z Uni. Mucin dynamics and microbial populations in chicken small intestine are changed by dietary probiotic and antibiotic growth promoter supplementation. The Journal of Nutrition 135:187-192. 2005.

11. Suzuki, T. Regulation of intestinal epithelial permeability by tight junctions. Cell Mol Life Sci 70:631-659. 2013.

12. Stevens, DL, DM Musher, DA Watson, H Eddy, RJ Hamil, F Gyorkey, H Rosen and J Mader. Spontaneous, nontraumatic gangrene due to *Clostridium septicum*. Reviews of Infectious Disease 12:286-295. 1990.

13. Burell, MI, EA Hyson and GJ Walker Smith. Spontaneous clostridial infection and malignancy. American Journal of Roentgenology 134:1153-1159. 1980.

14. Bryant, AE and DL Stevens. Clostridial toxins in the pathogenesis of gas gangrene. In: The Comprehensive Sourcebook of Bacterial Protein Toxins, 4th ed. J. Alouf, D. Ladant and M. Popoff, eds. Elsevier Ltd, Amsterdam. pp 977-994. 2015.

15. Van Immerseel, F, JI Rood, RJ Moore and RW Titball. Rethinking our understanding of the pathogenesis of necrotic enteritis in chickens. Trends Microbiol 17:32-36. 2009.

16. Knarreborg, A, MA Simon, RM Engberg, BB jensen and GW Tannock. Effects of dietary fat source and subtherapeutic levels of antibiotic on the bacterial community in the ileum of broiler chickens at various ages. Applied and Environmental Microbiology 68:5918-5924. 2002.

17. Williams, RB. Intercurrent coccidiosis and necrotic enteritis of chickens: regional, integrated disease management by maintenance of gut integrity. Avian Pathology 34:159-180. 2005.

18. Timbermont, L, F Haesebrouck, R Ducatelle and F Van Immerseel. Necrotic enteritis in broilers: an updated review on the pathogenesis. Avian Pathology 40:341-347. 2011.

19. Yegani, M and DR Korver. Factors affecting intestinal health in poultry. Poultry Science 87:2052-2063. 2008.

20. Meng, H, Y Zhang, L Zhao, W Zhao, C He, CF Honaker, Z Zhai, Z Sun and PB Siegel. Body weight selection affects quantitative genetic correlated responses in gut microbiota. PLOS One 9. 2014.

21. Caso, JR, JC Leza and L Menchen. The effects of physical and physiological stress on the gastrointestinal tract: lessons from animal models. Curr Mol Med 8:299-312. 2008.

22. Gareau, MG, MA Silva and MH Perdue. Pathophysiological mechanisms of stress-induced intestinal damage. Curr Mol Med 8:274-281. 2008.

23. Julian, RJ. Rapid growth problems: ascites and skeletal deformities in broilers. Poultry Science 77:1773-1780. 1998.

24. Bayyari, GR, WE Huff, NC Rath, JM Balog, LA Newberry, JD Villines, JK Skeeles, NB Anthony and KE Nestor. Effect of the genetic selection of turkeys for increased body weight and egg production on immune and physiological responses. Poultry Science 76:289-296. 1997.

25. Sosnicki, AA, RG Cassens, RJ Vimini and ML Greaser. Histopathological and ultrastructural alterations of turkey skeletal muscle. Poultry Science 70:349-357. 1991.

26. Wilson, BW, PS Nieberg and RJ Buhr. Turkey muscle growth and focal myopathy. Poultry Science 69:1553-1562. 1990.

27. Velleman, SG, JW Anderson, CS Coy and KE Nestor. Effect of selection for growth rate on muscle damage during turkey breast muscle development. Poultry Science 82. 2003.

28. Sosnicki, A, RG Cassens, DR McIntyre, RJ Vimini and ML Greaser. Incidence of microscopically detectable degenerative characteristics in skeletal muscle of turkey. British Poultry Science 30:69-80. 1989.

29. Julian, RJ. Lung volume of meat-type chickens. Avian Diseases 33:174-176. 1989.

30. Julian, RJ. Production and growth related disorders and other metabolic diseases of poultry - a review. The Veterinary Journal 169:350-369. 2005.

31. Julian, RJ and SM Mirsalimi. Blood oxygen concentration of fast-growing and slow-growing broiler chickens with ascites from right ventricular failure. Avian Diseases 36:730-732. 1992.

32. Scheele, CW. Pathological changes in metabolism of poultry related to increasing production levels. Veterinary Quarterly 19:127-130. 1997.

33. Huff, GR, WE Huff and NC Rath. Dexamethasone immunosuppression resulting in turkey clostridial dermatitis: a retrospective analysis of seven studies, 1998-2009. Avian Diseases 57:730-736. 2013.

34. Davis, S. Use of a repeatable model creating significant clostridial dermatitis mortality in turkeys to determine management and other risk factors that affect severity of the disease. In: Annual Meeting of the American Association of Avian Pathologists. St Louis, MO. 2011.

35. Jr, RF Wideman and I Pevzner. Dexamethasone triggers lameness associated with necrosis of the proximal tibial head and proximal femoral head in broilers. Poultry Science 91:2464-2474. 2012.

36. Parker, R. General Manager, Circle S Ranch. 2015.

37. Popoff, MR and P Bouvet. Clostridial toxins. Future Microbiology 4:1021-1064. 2009.

38. Hatheway, CL. Toxigenic *Clostridia*. Clinical Microbiology Reviews 3:66-98. 1990.

39. Warrack, GH, E Bidwell and CL Oakley. The beta-toxin (deoxyribonuclease) of *Cl. septicum*. J Pathol Bacteriol 63:293-302. 1951.

40. Anthony, NB. A review of genetic practices in poultry: efforts to improve meat quality. Journal of Muscle Foods 9:25-33. 1998.

41. Hester, PY, KK Krueger and M Jackson. The effect of restrictive and compensatory growth on the incidence of leg abnormalities and performance of comercial male turkeys. Poultry Science 69:1731-1742. 1990.

42. Turkeys, Aviagen. Optimum growth pattern for commercial turkeys. Technical Bulletin Issue 10.

43. Langhout, DJ, JB Schutte, PV Leeuwen, J Wiebenga and S Tamminga. Effect of dietary high and low methylated citrus pectin on the activitity of the ileal microflora and morphology of the small intestinal wall of broiler chicks. British Poultry Science 40:340-347. 1999.

44. Van Immerseel, F, J De Buck, F Pasmans, G Huyghebaert, F Haesebrouck and R Ductalle. *Clostridium perfringens* in poultry: an emerging threat for animal and public health. Avian Pathology 33:537-549. 2004.

45. Cooper, KK and JG Songer. Necrotic enteritis in chickens: a paradigm of enteric infection by *Clostridium perfringens* Type A. Anaerobe 15:55-60. 2009.

46. Ragione, RM La and MJ Woodward. Competitive exclusion by *Bacillus subtillis* spores of *Salmonella enterica* serotype Enteritidis and *Clostridium perfringens* in young chickens. Vet Microbiol 94:245-256. 2003.

47. Choct, M. Managing gut health through nutrition. British Poultry Science 50:9-15. 2009.

48. Cox, NA, CL Hofacre, JS Bailey, RJ Buhr, JL Wilson, KL Hiett, LJ Richardson, MT Musgrove, DE Cosby, JD Tankson, YL Vizzier, PF Cray, LE Vaughn, PS Holt and DV Bourassaa. Presence of *Campylobacter jejuni* in various organs one hour, one day, and one week following oral or intracloacal inoculations of broiler chicks. Avian Diseases 49:155-158. 2005.

49. Robbins, K. Commercial turkey clostridial dermatitis vaccination and interventions. In: American Association of Avian Pathologists Scientific Program. Boston, MA. 2015.

50. Cortinas, TI, MA Mattar and AM Stefanini de Guzman. Alpha-toxin production by *Clostridium septicum* at different culture conditions. Anaerobe 3:199-202. 1997.

51. Songer, JG. Clostridial enteric diseases of domestic animals. Clinical Microbiology Reviews 9:216-234. 1996.

52. MacLennan, JD. The histotoxic clostridial infections of man. Bacteriological Reviews 26:177-275. 1962.

53. Treangen, TJ and SL Salzberg. Repetitive DNA and next-generation sequencing: computational challenges and solutions. Nature Reviews Genetics 13:36-46. 2012.

54. Sterne, M and I Batty. Pathogenic *Clostridia*. Butterworths, London. 1975.

55. Moussa, RS. Complexity of toxins from *Clostridium septicum* and *Clostridium chauvoei*. Journal of Bacteriology 76:538-545. 1958.

56. Princewill, TJ and CL Oakley. The deoxyribonucleases and hyaluronidases of *Clostridium septicum* and *Cl. chauvoei*. II. An agar plate method for testing for hyaluronidase. Journal of Medical Laboratory Technology 29:255-260. 1972.

57. Robertson, M. Notes on *Vibrion septique*. British Medical Journal 1:538. 1918.

58. Robertson, M. Serological groupings of *Vibrion septique* and their relation to the production of toxin. Journal of Pathology and Bacteriology 23:153-170. 1920.

Appendix A – **Questions included in survey distributed to flock supervisors/servicepersons within each member company of the National Turkey Federation.**

1. In 2007, the National Turkey Federation developed a definition of CD that included the signs and criteria listed below. What signs or criteria have you or would you have used in 2008 to determine that turkeys in flocks that you supervised had CD? (please check all that apply)

- Subcutaneous emphysema (air-bubbles under the skin)
- Serum/serosanguineous subcutaneous fluid (fluid accumulation under the skin)
- Vesicles (blisters) on the skin, especially in the breast/inguinal area
- Moist, dark, wrinkled skin, especially in the breast/inguinal area
- Cellular necrosis (microscopic)
- Organ involvement (spleen/liver)
- Vesicles on the skin, and/or moist, dark, wrinkled skin in the tail area
- *Clostridium septicum*, *C. perfringens* type A, or *C. sordelli* isolated from fluid or affected skin/tissue samples of affected/dead birds
- Elevated mortality
- Other

For the following questions, please consider only those flocks that you supervised and which were marketed during the 2008 calendar year (January 1, 2008 – December 31, 2008).

2. How many FARMS did you supervise that had flocks marketed during 2008?

2a. What was the sum total of houses on these farms?

3. What is the average flock size for those flock types which you supervise? If you do not supervise a particular flock type, please write N/A.

3a. Average flock size (# of birds) for light hens

3b. Average flock size (# of birds) for heavy hens

3c. Average flock size (# of birds) for light toms

3d. Average flock size (# of birds) for heavy toms

4. How many FLOCKS under your supervision were marketed during the 2008 calendar year?

4a. Number of light hen flocks

4b. Number of heavy hen flocks

4c. Number of light tom flocks

4d. Number of heavy tom flocks

5. How many FARMS supervised by you had at least one flock marketed in 2008 that at some point during production had signs which you considered compatible with CD?

6. How many FLOCKS supervised by you and marketed during the 2008 calendar year had signs that you considered compatible with CD?

6a. Number of light hen flocks that had CD

6b. Number of heavy hen flocks that had CD

6c. Number of light tom flocks that had CD

6d. Number of heavy tom flocks that had CD

7. What was the average % livability for FLOCKS that developed CD?

7a. Average % livability for light hen flocks with CD

7b. Average % livability for heavy hen flocks with CD

7c. Average % livability for light tom flocks with CD

7d. Average % livability for heavy tom flocks with CD

For the following questions, please provide YOUR own opinion or knowledge derived from YOUR experience as a turkey flock supervisor/serviceperson.

8. What are your thoughts concerning the causes of and risk factors for CD in turkeys? (Please rank in order of importance.)

9. What do you think are the best management/treatment options for flocks with CD? (Please rank in order of importance.)

10. What do you think are the best options to prevent flocks from developing CD? (Please rank in order of importance.)

Appendix B – Questionnaire distributed to each live production/complex manager within each member company of the National Turkey Federation.

1. For flocks marketed during the 2008 calendar year, was there a difference in the live production costs between flocks that had CD and flocks that did not have CD? (yes or no)
2. If you answered yes to the previous question, please calculate the difference in average live production costs between flocks that had CD and flocks that did not have CD? (cents/lb)

Appendix C – RNA Extraction Protocol

Tissue Lysis and RNA Extraction

1. Add 1mL RNApro Solution (MP Biomedicals, LLC., Solon, OH, USA) to green-cap tube containing Lysing Matrix D beads (MP Biomedicals)
2. Add up to 100mg animal tissue sample to tube
3. Securely close the cap to prevent leakage
    a. Must leave ~1/4 inch (5mm) airspace in matrix tube to allow for effective homogenization
4. Process sample tube in FastPrep-24 instrument (MP Biomedicals)
    a. 3 rounds of 6.0M/S for 40 seconds
        i. Place sample tubes on ice for 5 minutes between successive FastPrep homogenization rounds to prevent sample heating and possible RNA degradation
5. Centrifuge sample tube at a minimum of 12,000g for 5min at 4°C
6. Transfer the upper phase to a 2mL heavy Phase Lock Gel tube (5-Prime, Gaithersburg, MD, USA)
    a. immediately prior to use, Phase Lock Gel at 12-16,000g for 20-30 seconds
    b. avoid transferring the debris pellet and lysing matrix
7. Incubate transferred sample for 5min at room temperature to increase RNA yield
8. Add 300µL chloroform without isoamyl alcohol (Sigma-Aldrich)
    a. Shake tube vigorously by hand for 30sec.
9. Incubate 5min at room temperature to permit nucleoprotein dissociation and increase RNA purity.
10. Centrifuge sample tube at minimum of 12,000g for 5 min at 4°C
11. Transfer upper phase to a new microcentrifuge tube without disturbing the gel or interphase
12. Add 500µL cold absolute ethanol (Acros Organics, Geel, Belgium) to the sample
    a. Invert 5 times to mix
    b. Precipitate at -20°C for at least 30 minutes
13. Centrifuge at minimum of 12,000g for 15 min at 4°C and remove the supernatant
    a. RNA will appear as a white pellet in the tube; if pellet is floating the sample may be recentrifuged to place the pellet at the tube bottom
14. Wash the pellet with 500µL of cold 75% ethanol made with DEPC-H2O (MP Biomedicals)
    a. Remove the ethanol, air dry for 5 min at room temperature
    b. Re-suspend RNA in 87.5µL DEPC-H2O
    c. Incubate 5 min at room temperature to facilitate RNA resuspension
15. DNase treatment
    a. 87.5µL RNA solution from previous step
    b. Add 2.5µL DNase I stock solution(QIAGEN, Inc. Valencia, CA, USA)
    c. Add 10µL Buffer RDD (QIAGEN)
    d. Incubate at 37°C for 30 minutes
16. Inactivate DNase by phenol-chloroform extraction (see RNA Cleanup)

RNA Cleanup

1. Immediately prior to use, pellet Phase Lock Gel at 12-16,000g for 20-30 seconds
2. Transfer RNA product following DNase treatment to a 2mL heavy PLG tube and add 100µL of phenol-chloroform (Fluka BioChemika, St. Gallen, Switzerland)
    a. Cap the tube securely and shake tube vigorously by hand for 30 seconds
    b. Incubate for 5 minutes at room temperature
    c. Centrifuge sample at 14,000 rpm at 4°C for 2 min
3. Transfer RNA product from previous step to new 2mL PLG tube and add 500µL chloroform to the sample
    a. Cap the tube securely and shake tube vigorously by hand for 30 seconds
    b. Incubate for 5 minutes at room temperature
    c. Centrifuge sample at 14,000 rpm at 4°C for 2 min
4. Transfer RNA product from previous step to new 2mL PLG tube and add 500µL chloroform to the sample
    a. Cap the tube securely and shake tube vigorously by hand for 30 seconds
    b. Incubate for 5 minutes at room temperature
    c. Centrifuge sample at 14,000 rpm at 4°C for 2 min
5. Transfer the upper aqueous phase to a 1.5mL microcentrifuge tube
    a. Add 1mL cold 100% ethanol and precipitate at -80°C for at least 1 hour
6. Centrifuge the precipitating RNA at 14,000rpm at 4°C for 15 min
    a. remove and discard the supernatant
7. Wash the pellet with 500µL 75% ethanol
    a. Centrifuge the samples at 14,000rpm at 4°C for 10 min
    b. Remove and discard the supernatant; air-dry the pellet (make sure no residual ethanol remains)
8. Suspend the RNA pellet in 50µL DEPC-H_2O
    a. Store RNA product at -80°C

Appendix D – Analysis of *In Vitro* Toxin Protein Expression by *C. septicum* and *C. perfringens* in Chopped Turkey Meat (CTM) Broth

D.0 Abstract

Clostridium septicum has been identified as the primary causative agent for clostridial dermatitis (CD); although other *Clostridium* spp., such as *C. perfringens*, have also been implicated. Although exotoxins are thought to play an important role in pathogenesis, the specific toxins that contribute to development of disease have not yet been identified. *C. septicum* and *C. perfringens* were grown in a chopped turkey meat (CTM) broth to model the nutrient environment present *in vivo* in turkey skeletal muscle in cases of CD. *In vitro* protein expression was analyzed using sodium dodecylsulfate polyacrylamide gel electrophoresis (SDS-PAGE) and western blot. *C. septicum* alpha toxin was produced in both 6- and 24-hour CTM cultures; although, toxin production was greater at 24-hours. The *C. perfringens* alpha toxin was produced in a 4-hour CTM culture. Identification of other proteins produced by these cultures was limited by the unavailability of specific antitoxins against other known clostridial toxins thought to play a role in pathogenesis of CD.

D.1 Introduction

Clostridium septicum (Cs) has been identified as the primary causative agent for CD in turkeys [1, 2]. Other *Clostridium* spp., including *C. perfringens* (Cp), may also play a role in pathogenesis [3]. However, little is currently known about the clostridial toxins which contribute to the pathology associated with this disease. Clostridial toxin production is highly variable depending on the availability of nutrients and environmental conditions in a particular culture system [4, 5]. While numerous studies have been conducted evaluating toxin production by Cs

and Cp in minimal media, little is known about the toxins produced by these organisms during pathogenesis of CD in turkeys. Cs and Cp were grown *in vitro* in a chopped turkey meat (CTM) broth medium to simulate nutrient availability *in vivo.* Protein expression was analyzed by sodium dodecylsulfate polyacrylamide gel electrophoresis (SDS-PAGE) and western blot in order to identify proteins that might correspond with the toxins produced during pathogenesis of CD.

D.2 Materials and Methods

D.2.1 Bacterial Culture

C. septicum (Cs) type strain ATCC 12464 and *C. perfringens* (Cp) type strain ATCC 13124 (American Type Culture Collection, Manassas, VA, USA) were grown in a chopped turkey meat (CTM) broth media to better simulate the nutrient environment that might be found *in vivo*. CTM media was prepared using 500 g/L chopped turkey breast muscle (VMCVM research turkey flock, Blacksburg, VA, USA), 0.5 g/L cysteine (Alexis Biochemicals, Lausen, Switzerland), and 4 mL/L resazurin solution (MP Biomedicals, LLC., Solon, OH, USA) following a protocol modified from the Anaerobe Laboratory Manual [6]. Cultures were incubated under anaerobic conditions (< 1 ppm dissolved oxygen) at 37°C. Cs cultures were grown to mid-log phase (six-hours) and plateau phase (24 hours) while Cp cultures were grown to mid-log phase (four hours; see Appendix E).

D.2.2 Protein Concentration and Analysis

Following culture, cell-free supernatant was obtained by centrifugation at 1,000 x *g* for 15 minutes. Multiple methods for precipitation and concentration of proteins were evaluated

including: saturated ammonium sulfate precipitation with and without dialysis; trichloroacetic acid (TCA) precipitation; and hollow-fiber filtration (Appendix F). Proteins were analyzed using SDS-PAGE. Protein expression profiles were compared between uninoculated CTM and CTM samples inoculated with Cs or Cp. Protein concentrations were determined using the Pierce BCA Protein Assay Kit (Thermo Fisher Scientific, Inc., Waltham, MA, USA).

Known molecular weights of clostridial toxins were used to aid in identification of protein bands. Western blots were performed using antibodies against Cs and Cp and pooled turkey serum obtained from asymptomatic birds on farms with a chronic history of CD (Table 5.1). Horseradish peroxidase- (HRP) conjugated rabbit-anti-goat, HRP-conjugated goat-anti-horse, or HRP-conjugated goat-anti-turkey was used as the secondary antibody (KPL, Gaithersburg, MD, USA). Visualization was performed using TMB membrane peroxidase substrate (KPL).

Table D.1: Primary antibodies used for western blot analysis of proteins produced by *C. septicum* and *C. perfringens* in chopped turkey meat medium

Antibody	Target Antigen	Species[1]	Source
Clostridium septicum (whole cell)	whole cell	goat	TechLab, Inc. Blacksburg, VA, USA
Clostridium septicum IRP 600	alpha toxin	horse	USDA-APHIS-VS Center for Veterinary Biologics Ames, IA, USA
Clostridium perfringens Type A IRP 564	alpha toxin	goat	USDA-APHIS-VS Center for Veterinary Biologics Ames, IA, USA
Turkey Polyclonal	non-specific	turkey	Turkeys on farm with chronic history of CD North Carolina, USA

[1]Species used to produce the antitoxin

D.3 Results

Proteins prepared by hollow fiber filtration of the cell-free supernatant yielded the best separation on SDS-PAGE (results from ammonium sulfate and TCA precipitation not shown). All protein bands visible in either the 6- or 24-hour *C. septicum* cultures were also present in the uninoculated CTM control (Figure D.1). Western blot using the TechLab antibody against *C. septicum* (whole cell) did not identify any proteins present in the inoculated samples that were not also present in the uninoculated CTM control (Figure D.2). A ~20kD protein band was present in the uninoculated CTM control that was only present for the highest concentration of proteins from the 6-hour Cs sample. Western blot using antibody against USDA *C. septicum* IRP 600 alpha toxin revealed a faint ~40kD protein band present in both the 6-hour and 24-hour samples with no corresponding band present in the uninoculated CTM control (Figure D.3). This protein band was stronger for the 24-hour Cs sample compared to the 6-hour Cs samples. Western blot using polyclonal turkey serum revealed a ~20kD protein band in the uninoculated CTM control that was not present in inoculated samples (Figure D.4). A ~30 kD protein band was present in the 6-hour samples and two protein bands, ~10 and ~15 kD, respectively, were present in both the 6- and 24-hour samples.

SDS-PAGE performed on CTM cultures inoculated with *C. perfringens* revealed three protein bands with weights between 10 and 15 kD in the 4-hour *C. perfringens* sample that were not also present in the uninoculated CTM control (Figure D.5). Numerous proteins were present between 25 and 75kD for the two highest concentrations of the uninoculated CTM control that were not visible at lower concentrations or in the Cp samples. Western blot using antibody against antibody against USDA *C. perfringens* type A recombinant-alpha toxin revealed a ~35 kD protein band in the Cp samples (Figure D.6). Several faint protein bands were also present

between 50 and 150 kD in the Cp samples. Western blot using polyclonal turkey serum revealed a ~20 kD protein in the uninoculated CTM control that was not detectable in the Cp-inoculated samples (Figure D.7).

Figure D.1: SDS-PAGE of proteins from cell-free supernatant of 6- and 24-hour *C. septicum* culture versus uninoculated chopped turkey meat (CTM)

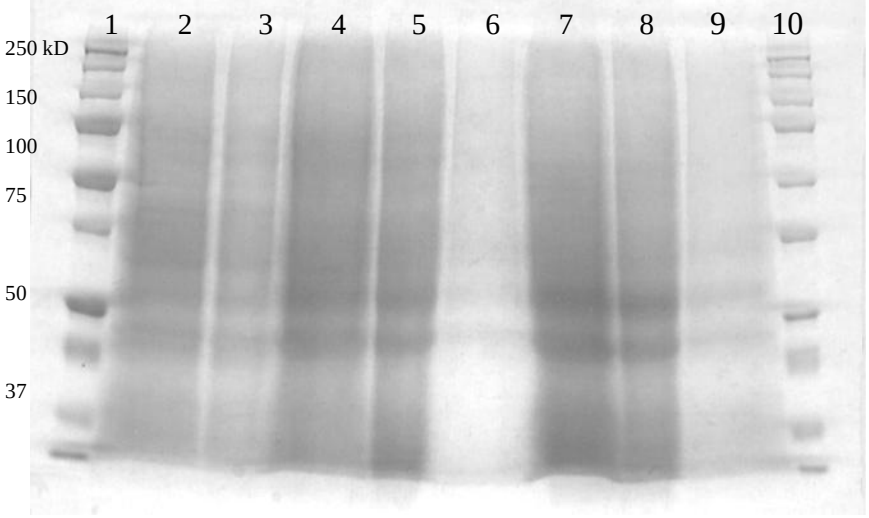

Lanes 1 and 10: protein standards
Lanes 2 and 3: uninoculated CTM
Lanes 4-6: 6-hour *C. septicum* culture in CTM
Lanes 7-9: 24-hour *C. septicum* culture in CTM

Figure D.2: Western blot of proteins from cell-free supernatant of 6- and 24-hour *C. septicum* culture versus uninoculated chopped turkey meat (CTM) using antibody against *C. septicum* (whole cell)

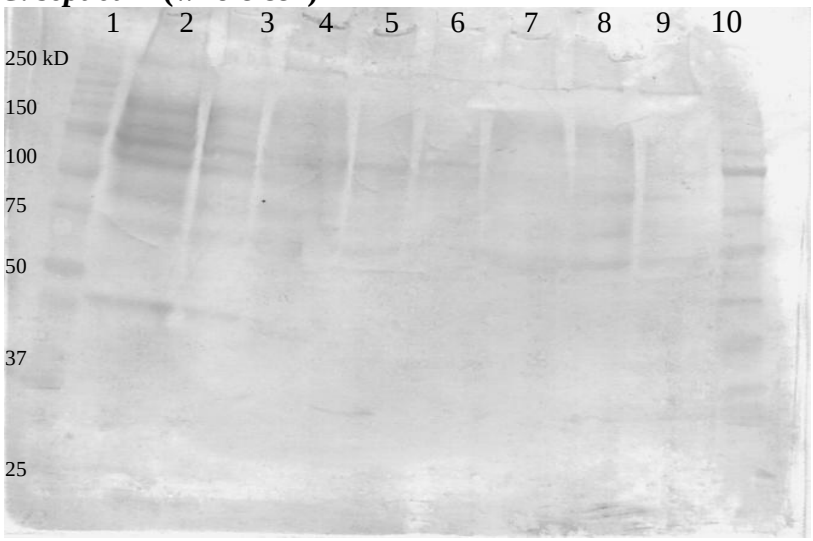

Lanes 1 and 10: protein standards
Lanes 2 and 3: uninoculated CTM
Lanes 4-6: 6-hour *C. septicum* culture in CTM
Lanes 7-9: 24-hour *C. septicum* culture in CTM
A ~20 kD protein band was present in the uninoculated CTM control (Lanes 2 and 3) A corresponding band was only present as a faint band at the highest concentration of proteins from the 6-hour Cs sample (Lane 4) and not detectable for all other samples (Lanes 6-9).

Figure D.3: Western blot of proteins from cell-free supernatant of 6- and 24-hour *C. septicum* culture versus uninoculated chopped turkey meat (CTM) using antibody against USDA *Clostridium septicum* IRP 600 alpha-toxin

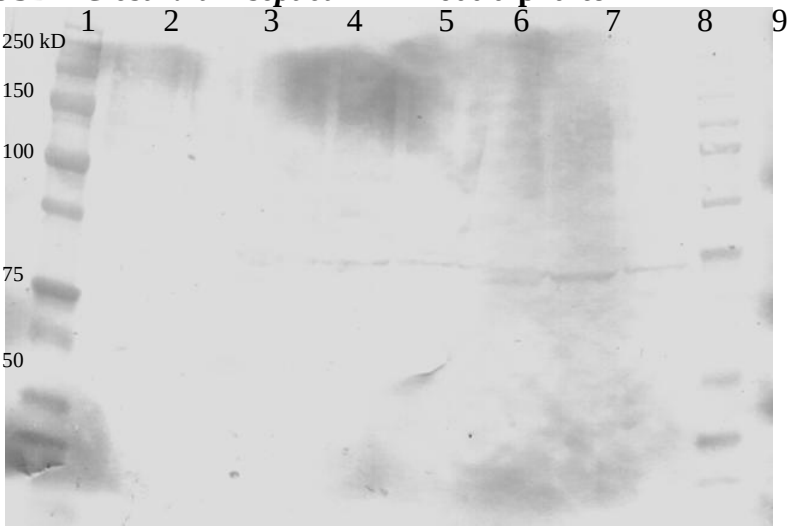

Lanes 1 and 10: protein standards
Lanes 2 and 3: uninoculated CTM
Lanes 4-6: 6-hour *C. septicum* culture in CTM
Lanes 7-9: 24-hour *C. septicum* culture in CTM
A ~40 kD protein band was present in the Cs samples (lanes 4-9) but not in the uninoculated CTM control. This protein band was stronger for the 24-hour Cs samples compared to the 6-hour samples.

Figure D.4: Western blot of proteins from cell-free supernatant of 6- and 24-hour *C. septicum* culture versus uninoculated chopped turkey meat (CTM) using polyclonal turkey serum

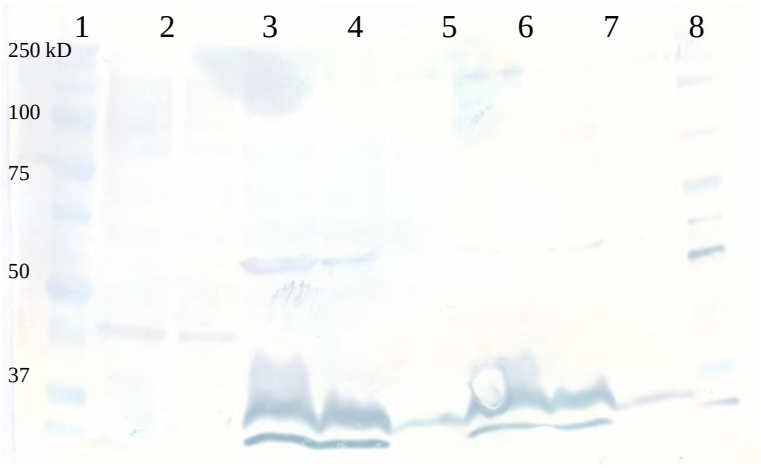

Lanes 1 and 10: protein standards
Lanes 2 and 3: uninoculated CTM
Lanes 4-6: 6-hour *C. septicum* culture in CTM
Lanes 7-9: 24-hour *C. septicum* culture in CTM

A ~30 kD protein was present in the samples inoculated with Cs and incubated for 6 hours (Lanes 4-6). A ~20 kD protein band was present in the uninoculated CTM control (Lanes 2 and 3) that was not present in any of the samples inoculated with Cs (lanes 4-9). Two protein bands, ~10 and ~15 kD, respectively, are present in the 6-hour and 24-hour Cs samples (Lanes 4-9).

Figure D.5: SDS-PAGE of proteins from cell-free supernatant of 4-hour *C. perfringens* culture versus uninoculated chopped turkey meat (CTM)

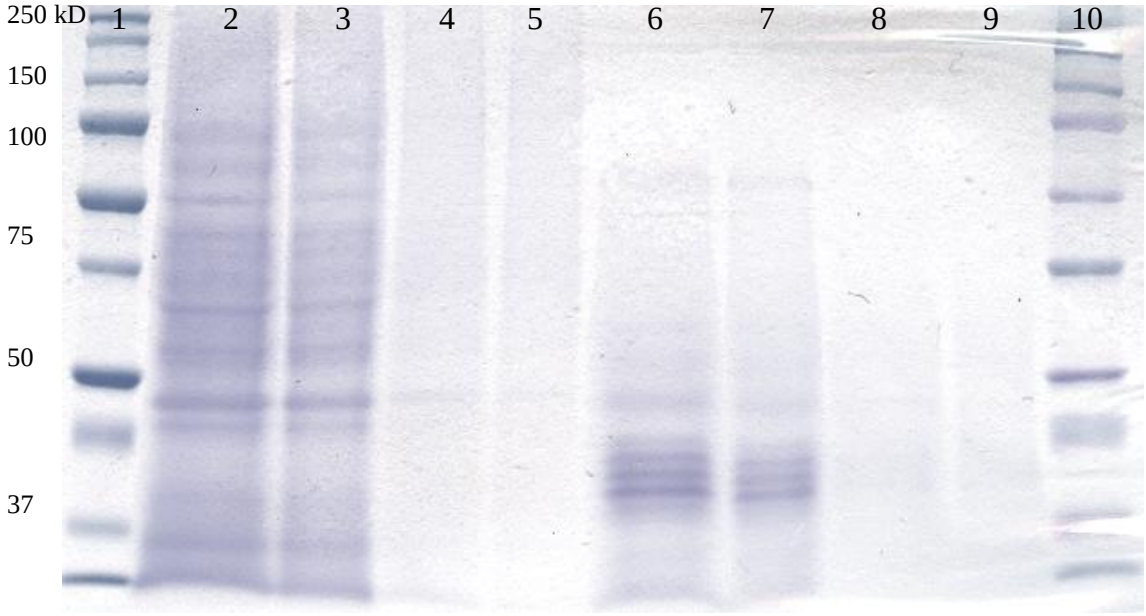

Lanes 1 and 10: protein standards
Lanes 2-5: uninoculated CTM
Lanes 6-9: *C. perfringens* in CTM
Three protein bands with weights between 10 and 15 kD were present in the Cp samples (Lanes 6-9) but not in the uninoculated CTM control (Lanes 2-5). Numerous proteins were present between 25 and 75kD for the two highest concentrations of the uninoculated CTM control (Lanes 2 and 3) that were not clearly visible at lower concentrations (Lanes 4 and 5) or in the Cp samples (Lanes 6-9).

Figure D.6: Western blot of proteins from cell-free supernatant of 4-hour *C. perfringens* culture versus uninoculated chopped turkey meat (CTM) using antibody against USDA *C. perfringens* type A recombinant-alpha toxin

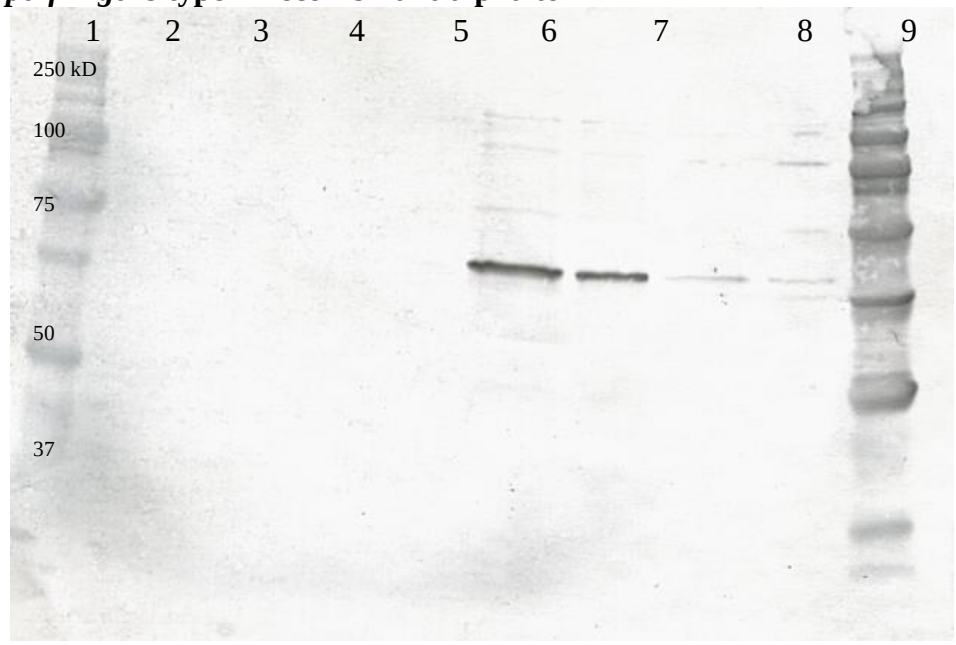

Lanes 1 and 10: protein standards
Lanes 2-5: uninoculated CTM
Lanes 6-9: *C. perfringens* in CTM
A ~35 kD protein band was present in the Cp samples (Lanes 6-9) that was not present in the uninoculated CTM control (Lanes 2-5). Several faint protein bands are present between 50 and 150 kD in the Cp samples (Lanes 6-9).

Figure D.7: Western blot of proteins from cell-free supernatant of 4-hour *C. perfringens* culture versus uninoculated chopped turkey meat (CTM) using polyclonal turkey serum

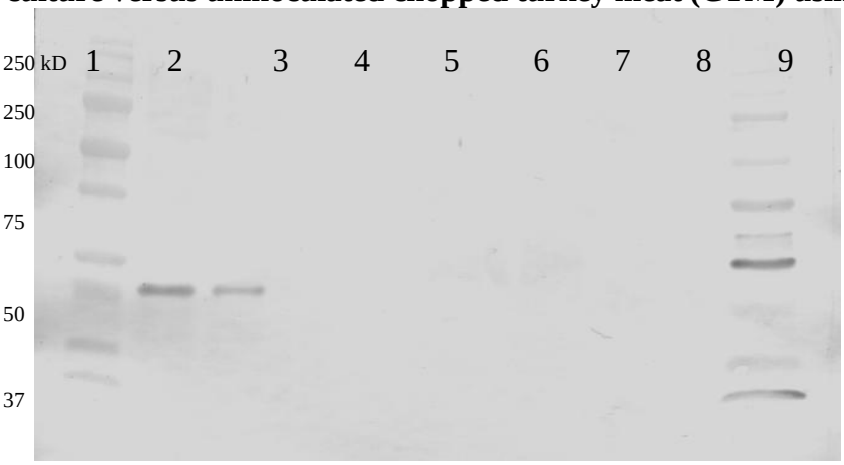

Lanes 1 and 10: protein standards
Lanes 2-5: uninoculated CTM
Lanes 6-9: *C. perfringens* in CTM
A ~20 kD protein band was present at the higher concentrations of the uninoculated CTM control (Lanes 2 and 3) that was not present in any of the Cp samples (Lanes 6-9).

D.4 Discussion

SDS-PAGE and western blot analysis of *in vitro* protein expression for *C. septicum* and *C. perfringens* cultures in CTM showed expression of CsA and CpA, respectively. These data suggest that CsA and CpA would likely be expressed in turkey skeletal muscle infected with these organisms. SDS-PAGE resulted in poor separation of proteins for Cs and Cp cultures in CTM. No protein bands were identified on SDS-PAGE for either the 6- or 24-hour *C. septicum* cultures that were not also present in the un-inoculated CTM control. SDS-PAGE analysis lacked the resolution to distinguish the large number of proteins present in the uninoculated media from proteins produced by *C. septicum.* Protein expression analysis is typically performed on cultures grown in minimal media to minimize the number of proteins present in uninoculated media. However, the goal of this study was to determine the protein expression

profile for these organisms in a culture system that mimicked *in vivo* infection of turkey skeletal muscle.

Over-exposure of membranes with horseradish peroxidase membrane substrate in an attempt to visualize faint protein bands resulted in high background color development due to non-specific binding. This non-specific binding likely contributed to the poor image quality obtained for many of the western blots presented in this study. Additionally, curvature was present in several of the western membranes (left and right protein ladders do not line up) which may have distorted interpretation of molecular weights for some of the observed protein bands.

Western blot using antibody against the USDA *C. septicum* alpha-toxin identified a protein band with a molecular weight of a ~40 kD protein that is consistent with the alpha toxin which is produced as a 46 kD pro-toxin and then cleaved to form a 42 kD active toxin [4, 7]. The results of this study showed greater alpha toxin production in the 24-hour *C. septicum* culture compared to the 6-hour culture. The type and amount of toxin produced by a particular *Clostridium* isolate have been shown to vary greatly depending on the length of incubation. Early studies with *C. septicum* demonstrated that production of DNase (beta toxin), hyaluronidase (gamma toxin), and oxygen-labile hemolysin (delta toxin) were greatest during the first 18 hours of incubation while maximal alpha toxin production occurred after prolonged incubation [8]. Conversely, other studies have shown that production of alpha toxin occurs during the first day of growth with maximum production occurring during the exponential (log) phase of growth [4, 9, 10]. The log phase of growth occurred between 5 and 9 hours of incubation for *C. septicum* in chopped turkey meat media (see Appendix E). Comparison between the 6- and 24-hour Cs cultures showed that CsA production was greater after 24 hours

of incubation in CTM. Additional studies with more time points would be necessary to determine the exact period during which CsA production is maximal in CTM.

The absence of the ~20 kD protein band in the Cs-inoculated samples which was present in the uninoculated CTM suggests that this protein was digested by proteolytic enzyme activity during incubation. Western blot with pooled polyclonal turkey serum from birds on a farm with a chronic history of CD revealed several protein bands present in *C. septicum*-inoculated CTM that were not present in the uninoculated control. The presence of these bands suggests that at least some turkeys on chronically affected farms are producing antibodies against *C. septicum* proteins; however, the exact identity of these proteins and their potential for providing protective immunity cannot be determined at this time. These proteins (10, 15, and 30 kD in size) were not consistent with the predicted size for the beta toxin of *C. septicum* (~45kD); however, molecular weights for the gamma and delta toxins have not yet been determined [11].

The three protein bands between 15 and 20 kD in size that were detected by SDS-PAGE for the *C. perfringens*-inoculated samples are all smaller than currently known clostridial toxins which vary in size from 22-600 kD [11]. The ~35 kD protein identified by western blot using antibody against the *C. perfringens* type A recombinant-alpha toxin was smaller than expected size for the *C. perfringens* alpha toxin (molecular mass 43 kD). However, the intensity of the protein-antibody reaction suggests that this band was likely the alpha toxin [11]. The identity of the multiple faint protein bands ranging in size from 50-150 kD cannot be determined based on the methods utilized in this study. The ~20 kD protein band present in the uninoculated CTM control on the western blot using polyclonal turkey serum (Figure D.7) is likely the same protein that was present in the *C. septicum* western blots (Figures D.2 and D.3). Its absence in the Cp

samples suggests that proteolytic digestion of this protein also occurred during incubation with Cp.

In vitro protein expression analysis showed that CsA and CpA were produced in CTM. Incubation in CTM presents a similar nutrient environment to that which would be available *in vivo* in cases of CD. This suggests that CsA and CpA would likely be produced *in vivo* if *C. septicum* and *C. perfringens* were present during infection. The actions of multiple toxins are involved in the pathogenesis of many clostridial diseases [11, 12]. SDS-PAGE analysis lacked the resolution to distinguish between the many proteins present in uninoculated CTM and proteins produced by *C. septicum* and *C. perfringens.* Immunohistochemistry techniques such as western blot are necessary to identify specific proteins. Unfortunately, specific antitoxins are unavailable for many of the other toxins thought to play a role in the pathogenesis of CD. Additionally, while the culture system used in this study was designed as a model of *in vivo* infection, an *in vitro* culture system cannot perfectly replicate *in vivo* conditions. Previous studies with *C. septicum* have shown that lipids present in cooked meat media inactivate CsA [10]. Therefore, *in vivo* studies on toxin expression in tissues from cases of CD are necessary in order to determine which clostridial toxins contribute to pathogenesis of the disease.

D.5 References:

1. Thachil, AJ, B McComb, MM Anderson, DP Shaw, DA Halvorson and KV Nagaraja. Role of *Clostridium perfringens* and *Clostridium septicum* in causing turkey cellulitis. Avian Diseases 54:795-801. 2010.

2. Tellez, G, NR Pumford, MJ Morgan, AD Wolfenden and BM Hargis. Evidence for *Clostridium septicum* as a primary cause of cellulitis in commercial turkeys. Journal of Veterinary Diagnostic Investigation 21:374-377. 2009.

3. Clark, S, R Porter, B McComb, R Lippert, S Olson, S Nohner and HL Shivaprasad. Clostridial dermatitis and cellulitis: an emerging disease of turkeys. Avian Diseases 54:788-794. 2010.

4. Cortinas, TI, MA Mattar and AM Stefanini de Guzman. Alpha-toxin production by *Clostridium septicum* at different culture conditions. Anaerobe 3:199-202. 1997.

5. Popoff, MR and BG Stiles. Clostridial toxins vs. other bacterial toxins. In: Handbook on *Clostridia*. P. Durre, ed. CRC Press: Taylor & Francis Group, Boca Raton, FL. pp 323-383. 2005.

6. Holdeman, LV, EP Cato and WEC Moore, eds. Anaerobe Laboratory Manual, 4th ed. VPI Anaerobe Laboratory, Blacksburg, VA. 1977.

7. Songer, JG and KW Post. The Genus *Clostridium*. In: Veterinary Microbiology: Bacterial and Fungal Agents of Animal Diseases. Elsevier Saunders, St. Louis, MO, USA. pp 261-282. 2005.

8. Moussa, RS. Complexity of toxins from *Clostridium septicum* and *Clostridium chauvoei*. Journal of Bacteriology 76:538-545. 1958.

9. Ballard, J, A Bryant, D Stevens and RK Tweten. Purification and characterization of the lethal toxin (alpha toxin) of *Clostridium septicum*. Infection and Immunity 60:784-790. 1992.

10. Smith, LDS and BL Williams. *Clostridium septicum*. In: The Pathogenic Anaerobic Bacteria, 3rd ed. A. Balows, ed. Charles C Thomas Publisher, Springfield, IL, USA. pp 180-190. 1984.

11. Hatheway, CL. Toxigenic *Clostridia*. Clinical Microbiology Reviews 3:66-98. 1990.

12. Sterne, M and I Batty. Pathogenic *Clostridia*. Butterworths, London. 1975.

Appendix E – Growth Curves for *C. septicum* and *C. perfringens* in CTM

Figure E.1: Growth curve for *C. septicum* in CTM with CFUs/mL determined by serial dilution plate count on phenylethyl alcohol (PEA) and Columbia blood agar

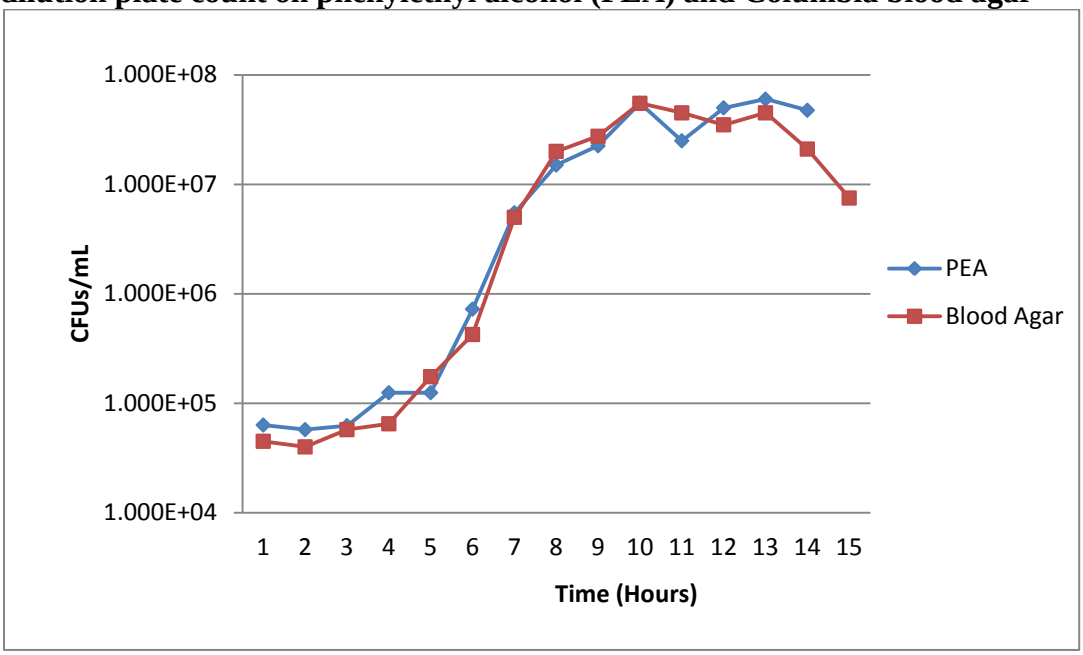

Figure E.2: Growth curve for *C. perfringens* in CTM with CFUs/mL determined by serial dilution plate count on Columbia blood agar

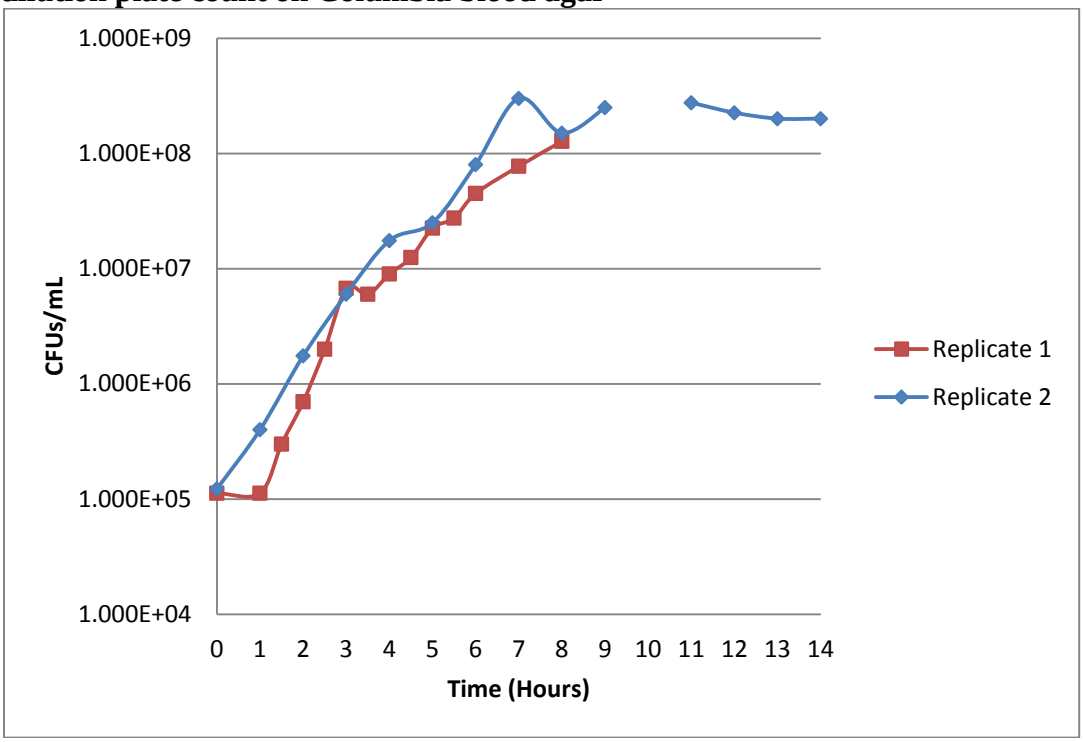

Replicate 1 was only incubated for 8 hours
Plates for Replicate 2 were uncountable at 10 hours

Appendix F – Protocols for *In Vitro* Protein Expression Analysis

Ammonium Sulfate Protein Precipitation

1. Grow the bacteria to the desired stage
2. Harvest by centrifugation and retain the supernatant (discard the pellet)
3. Prepare saturated ammonium sulfate
    a. Add 80g ammonium sulfate (Sigma-Aldrich Corp. St. Louis, MO, USA) to 100mL dH20
    b. heat gently while stirring until ammonium sulfate dissolves
    c. cool back to room temperature while stirring
    d. use the supernatant – the ammonium sulfate that the dH20 can't hold will fall out of solution; final concentration of ammonium sulfate in the supernatant is ~4M
4. Place the supernatant in a 50mL beaker with a stir bar, stir gently
5. While stirring, add saturated ammonium sulfate until a precipitate starts to form
6. Stir for about an hour
7. Divide into microcentrifuge tubes and centrifuge 15 min at 10,000g
8. Keep and combine pellets and re-suspend in PBS (Thermo Fisher Scientific, Inc., Waltham, MA, USA)
9. OPTIONAL: Dialyze overnight against PBS using 10,000 MWCO Slide-A-Lyzer Cassettes (Thermo Fisher Scientific)
    a. Hydrate membrane
        i. Place dialysis cassette into grove of buoy and immerse dialysis cassette in PBS
        ii. Hydrate for 1-2 minutes
        iii. Remove cassette from PBS and remove excess liquid by tapping the edge of the cassette gently on paper towels. DO NOT blot the membrane.
    b. Add sample
        i. Load sample into syringe with an 18g 1" needle
        ii. Penetrate gasket through one of the syringe ports at a corner of the cassette w/ needle and inject sample. Mark the cassette corner w/ permanent marker. Note: if sample contains ammonium sulfate, use a fill volume that is ≤ 80% of the cassette's total volume
        iii. With the needle still in the cassette cavity, draw up on the piston to remove air and to compress the membrane window
        iv. Remove syringe needle from the cassette while retaining the air in the syringe
        v. Place the cassette in the groove of a buoy and float the assembly in a beaker of PBS overnight
    c. Remove sample
        i. Fill syringe w/ volume of air at least equal to the sample size
        ii. Penetrate the gasket through a top unused syringe guide port. Discharge air into cassette cavity to separate membranes.
        iii. Turn the unit so that needle is on the bottom and allow sample to collect near the port. Withdraw the sample into the syringe.
10. Store at 4°C until ready to run SDS-PAGE

Trichloroacetic Acid (TCA) Protein Precipitation

1. Grow the bacteria to the desired stage
2. Harvest by centrifugation and retain the supernatant (discard the pellet)
3. Add 1 volume of 6.1 N Trichloroacetic acid solution (Thermo Fisher Scientific, Inc., Waltham, MA, USA) to 4 volumes of protein sample
    a. i.e. in 1.5mL microcentrifuge tube, add 250µL TCA to 1mL of cell-free supernatant
4. Incubate 10 min at 4°C
5. Centrifuge tube at max speed (13.2 rpm) for 5 min at 4°C
6. Remove supernatant, leaving protein pellet intact (pellet should be formed from whitish, fluffy precipitate)
7. Wash pellet with 200µL cold acetone (Thermo Fisher Scientific)
8. Centrifuge tube at max speed (13.2 rpm) for 5 min at 4°C
9. Repeat steps 4-6 for a total of 2 acetone washes
10. Dry pellet by leaving cap open at room temperature for ~10-20 minutes to drive off acetone
11. Re-suspend pellet in 400µL 1X Tris-Glycine Running Buffer with SDS (See SDS-PAGE Protocol)
    a. May be difficult to re-suspend, can heat sample in heat block at 56°C to aid in re-suspension of pellet
12. Store sample at 4°C until ready to run SDS-PAGE

Hollow Fiber Filtration of Cell-Free Supernatant

1. Grow the bacteria to the desired stage
2. Harvest by centrifugation and retain the supernatant (discard the pellet)
3. Prepare MicroKros modified polyethersulfone (mPES) 30kDa, 20cm^2, dry hollow fiber filter module (Spectrum Laboratories, Inc., Rancho Dominguez, CA, USA)
    a. Flush with 2mL water per cm^2 surface area (40mL) to remove trace levels of glycerin
    b. Connect syringes according to manufacturers' instructions
    c. Perform crossflow filtration by applying pressure to one syringe while allowing the other syringes to move freely; continue the process by applying pressure first the one syringe then the other, repeatedly
4. Store filtered sample at 4°C until ready to run SDS-PAGE

SDS-PAGE Protocol for Viewing Proteins

1. Prepare buffers:
    a. Running Buffer
        i. 3.03g Tris Base (Thermo Fisher Scientific, Inc., Waltham, MA, USA)
        ii. 14.4g Glycine (Thermo Fisher Scientific)
        iii. 1.0g Sodium dodecyl sulfate (SDS) (Thermo Fisher Scientific)
        iv. 1L dH_2O
    b. Coomassie Stain
        i. 1g Coomassie Brilliant Blue R-250 (Bio-Rad Laboratories, Hercules, CA, USA)
        ii. 450mL Methanol (Thermo Fisher Scientific)
        iii. 450mL dH_2O
        iv. 100mL Glacial Acetic Acid (Thermo Fisher Scientific)
    c. Coomassie Destain
        i. 450mL Methanol
        ii. 450mL dH_2O
        iii. 100mL Glacial Acetic Acid
    d. Gel Drying Solution
        i. 50mL Glycerin (Sigma-Aldrich)
        ii. 143mL 70% Ethanol (Decon Laboratories, Inc., King of Prussia, PA, USA)
        iii. 307mL dH_2O
2. Place beaker of water on hot plate and bring to a boil.
3. Prepare electrophoresis unit and gel.
    a. 12% MiniProtean TGXgel (Bio-Rad)
4. Pour running buffer in the center of the electrophoresis unit until the level is above the top of the gel. Wait a few minutes to make sure it isn't leaking, and then pour running buffer in the outer chamber of the electrophoresis unit until the level is above the bottom of the gel.
5. Add 2X Laemmli buffer (Sigma-Aldrich) to protein sample.
    a. 1 µL Laemmli buffer for every 1 µL of protein sample.
6. Boil samples for five minutes.
7. Remove sample tubes from boiling water and give a quick spin in the microcentrifuge.
8. Add the appropriate amount (10 µL of protein standards, 10-30 µL of sample) to each well.
9. Run gel at 100V for 70-80 minutes
10. To stain the gel, put it directly into Coomassie Brilliant Blue Stain for about 30-45 minutes. Add destain and swirl gently to remove bulk of stain. Discard destain, and add fresh. Leave until destain is fairly blue, and then discard. Repeat until gel is destained sufficiently.
11. When gel is sufficiently destained, replace destain solution with dH2O and let soak for about 30 minutes to rehydrate gel.
12. Discard dH2O and soak gel in Gel Drying Solution for 30 minutes.
13. Near the end of the 30 minutes, place two cellophane drying sheets (Sigma-Aldrich) in dH2O
14. Place one drying sheet onto solid half of drying frame (Sigma-Aldrich)
    a. Make sure to smooth out all bubbles.
15. Place gel onto drying sheet on drying frame, taking care to smooth out all bubbles.
16. Place second drying sheet on top of gel, smoothing out all bubbles, adding dH2O with a transfer pipette if necessary to remove bubbles.

17. Place non-solid half of drying frame on top of second drying sheet, and clamp together using large binder clips on two sides. Then place drying frame clamps on other two sides. Remove binder clips, and place drying frame clamps on those sides.
18. Allow to dry at least 24-48 hours before removing from frame. Dried gel can be scanned or photographed for a digital image.

Western Blot Protocol – Part 1:

1. Prepare Western Blot Transfer Buffer (at least one day before use)
    a. 5.82 g Tris base
    b. 2.93 g Glycine
    c. 200 ml Methanol
    d. 800 ml dH2O
    e. Store in refrigerator (buffer should be cold when used).
1. Run an SDS-PAGE gel according to protocol above.
2. Transfer gel to a container of Western Transfer buffer and leave at room temperature for 30 minutes.
3. Place Nitrocellulose Membrane 0.45µm (Bio-Rad) into a container of western transfer buffer by holding one end and slowly dipping the other end into the buffer until the entire membrane is submerged. DO NOT use the same container the gel is in! Sliding the membrane in allows the buffer to "wick" up through the membrane and will insure that there are no bubbles trapped in the pores of the membrane so that transfer will be more efficient. Leave membrane in western transfer buffer 10-15 minutes.
4. Just prior to use wet two pieces of thick blotting paper (Bio-Rad) in western transfer buffer. DO NOT use the same container the gel is in.
5. Prepare the western transfer unit: Trans-Blot SD Semi-Dry Transfer Cell (Bio-Rad)
    a. Remove both lids of the western transfer unit.
    b. On the base of the unit, place one piece of soaked blotting paper.
    c. Place the pre-soaked membrane on top of the blotting paper.
    d. Carefully place the gel on the membrane. It is important to place the gel properly the first time, as some proteins may transfer on contact with the membrane.
    e. Place the other pre-soaked piece of thick blotting paper on top of the gel.
    f. Replace the inner lid of the western transfer unit and lock into place, taking care not to disturb the gel/membrane "sandwich" inside.
    g. Replace the outer lid of the western transfer unit.
6. Run at 10V for 30 minutes.
7. While gel is blotting, prepare 2% milk in PBS in a 50 ml centrifuge tube. Mix well.
    a. 1 g powdered milk (Foodhold USA, LLC., Landover, MD, USA)
    b. 50 ml PBS (Thermo Fisher Scientific)
8. When transfer is complete, gently place membrane into 50 ml centrifuge tube containing 2% milk and store in refrigerator on its side until use.

Western Blot Protocol – Part 2:

1. Place membrane in a container and rinse the membrane with PBST
    a. 0.05% Tween-20 (Bio-Rad) in PBS
2. Dilute primary antibody 1:1000 in PBST
3. Add primary antibody to membrane, incubate for 1hr at room temperature on shaker plate
4. Rinse membrane 3 times with PBST
5. Dilute HRP Goat-anti-Turkey secondary antibody (KPL, Gaithersburg, MD, USA) according to package directions
6. Add secondary antibody to membrane, incubate for 1hr at room temperature on shaker plate
7. Rinse membrane 3 times with PBST
8. Add ~10mL TMB membrane peroxidase substrate (KPL) to membrane (stored at 4°C, bring to room temp before use) and swirl container while wait for color to develop
9. When color is sufficiently developed, pour off membrane substrate and add dH20 to stop the reaction
10. Allow membrane to dry and then use plain light to document (digital camera or scanner)

Appendix G – Coding Sequences (CDS) and RNAs present in *C. septicum* type strain ATCC 12464

Feature ID	Type	Contig	Start	Stop	Length (bp)	Function	Subsystems	Begin	End
fig|1504.6.peg.1	CDS	Contig_14	3291	67	3225	Carbamoyl-phosphate synthase large chain (EC 6.3.5.5)	De Novo Pyrimidine Synthesis, Macromolecular synthesis operon	67	3291
fig|1504.6.peg.2	CDS	Contig_14	4354	3305	1050	Carbamoyl-phosphate synthase small chain (EC 6.3.5.5)	De Novo Pyrimidine Synthesis, Macromolecular synthesis operon	3305	4354
fig|1504.6.peg.3	CDS	Contig_14	4850	5581	732	Na+ ABC transporter (ATP-binding protein), NATA	- none -	4850	5581
fig|1504.6.peg.4	CDS	Contig_14	5574	6761	1188	Na+ ABC transporter, NATB	- none -	5574	6761
fig|1504.6.peg.5	CDS	Contig_14	7417	7139	279	hypothetical protein	- none -	7139	7417
fig|1504.6.peg.6	CDS	Contig_14	8241	7420	822	HAD superfamily hydrolase	- none -	7420	8241
fig|1504.6.peg.7	CDS	Contig_14	9037	8252	786	3-oxoacyl-[acyl-carrier protein] reductase (EC 1.1.1.100)	Fatty Acid Biosynthesis FASII	8252	9037
fig|1504.6.peg.8	CDS	Contig_14	11306	9183	2124	Ferrous iron transport protein B	- none -	9183	11306
fig|1504.6.peg.9	CDS	Contig_14	11557	11306	252	Fe2+ transport system protein A	- none -	11306	11557
fig|1504.6.peg.10	CDS	Contig_14	12374	11679	696	SanA protein	- none -	11679	12374
fig|1504.6.peg.11	CDS	Contig_14	12869	12399	471	FIG01201438: hypothetical protein	- none -	12399	12869
fig|1504.6.peg.12	CDS	Contig_14	14267	13023	1245	Gamma-glutamyl phosphate reductase (EC 1.2.1.41)	Proline Synthesis	13023	14267
fig|1504.6.peg.13	CDS	Contig_14	15096	14293	804	Glutamate 5-kinase (EC 2.7.2.11)	Proline Synthesis	14293	15096
fig|1504.6.peg.14	CDS	Contig_14	15597	16958	1362	Predicted arginine uptake transporter	- none -	15597	16958
fig|1504.6.peg.15	CDS	Contig_14	17097	17573	477	PTS system, glucose-specific IIA component (EC 2.7.1.69)	Trehalose Uptake and Utilization	17097	17573
fig|1504.6.peg.16	CDS	Contig_14	19465	17765	1701	Isopentenyl-diphosphate delta-isomerase (EC 5.3.3.2)	Isoprenoid Biosynthesis, Isoprenoid Biosynthesis: Interconversions	17765	19465
fig|1504.6.peg.17	CDS	Contig_14	20059	19478	582	hypothetical protein	- none -	19478	20059
fig|1504.6.peg.18[1]	CDS	Contig_14	20274	20921	648	COG1272: Predicted membrane protein hemolysin III homolog	- none -	20274	20921

Feature ID	Type	Contig	Start	Stop	Length (bp)	Function	Subsystems	Begin	End
fig|1504.6.peg.19	CDS	Contig_14	22299	20986	1314	sodium:neurotransmitter symporter family protein	- none -	20986	22299
fig|1504.6.peg.20	CDS	Contig_14	22775	24382	1608	ABC transporter ATP-binding protein uup	CBSS-393121.3.peg.2760	22775	24382
fig|1504.6.peg.21	CDS	Contig_14	25226	24438	789	Hydrolase (HAD superfamily)	- none -	24438	25226
fig|1504.6.peg.22	CDS	Contig_14	27026	25302	1725	Periplasmic [Fe] hydrogenase large subunit (EC 1.12.7.2)	- none -	25302	27026
fig|1504.6.peg.23	CDS	Contig_14	27713	27390	324	hypothetical protein	- none -	27390	27713
fig|1504.6.peg.24	CDS	Contig_14	27864	28751	888	Phosphatidylserine decarboxylase (EC 4.1.1.65)	Glycerolipid and Glycerophospholipid Metabolism in Bacteria	27864	28751
fig|1504.6.peg.25	CDS	Contig_14	28771	29571	801	Sialic acid utilization regulator, RpiR family	Sialic Acid Metabolism	28771	29571
fig|1504.6.peg.26	CDS	Contig_14	31064	29700	1365	6-phospho-beta-glucosidase (EC 3.2.1.86)	Beta-Glucoside Metabolism	29700	31064
fig|1504.6.peg.27	CDS	Contig_14	32318	31179	1140	FIG00512997: hypothetical protein	- none -	31179	32318
fig|1504.6.peg.28	CDS	Contig_14	33909	32494	1416	NAD(FAD)-utilizing dehydrogenase	- none -	32494	33909
fig|1504.6.peg.29	CDS	Contig_14	34963	34193	771	ABC-type Fe3+-siderophore transport system, ATPase component	- none -	34193	34963
fig|1504.6.peg.30	CDS	Contig_14	35991	34966	1026	Iron(III) dicitrate transport system permease protein FecD (TC 3.A.1.14.1)	- none -	34966	35991
fig|1504.6.peg.31	CDS	Contig_14	36994	35984	1011	Iron(III) dicitrate transport system permease protein FecD (TC 3.A.1.14.1)	- none -	35984	36994
fig|1504.6.peg.32	CDS	Contig_14	37128	38069	942	Iron(III) dicitrate transport system, periplasmic iron-binding protein FecB (TC 3.A.1.14.1)	- none -	37128	38069
fig|1504.6.rna.1	RNA	Contig_14	38412	38339	74	tRNA-Arg-ACG	- none -	38339	38412
fig|1504.6.peg.33	CDS	Contig_14	39376	38531	846	periplasmic sensor signal transduction histidine kinase	- none -	38531	39376
fig|1504.6.peg.34	CDS	Contig_14	40432	39680	753	hypothetical protein	- none -	39680	40432
fig|1504.6.peg.35	CDS	Contig_14	40603	41829	1227	ErfK/YbiS/YcfS/YnhG family protein	- none -	40603	41829
fig|1504.6.peg.36	CDS	Contig_14	42023	43381	1359	tRNA nucleotidyltransferase (EC 2.7.7.21) (EC 2.7.7.25)	tRNA nucleotidyltransferase	42023	43381

Feature ID	Type	Contig	Start	Stop	Length (bp)	Function	Subsystems	Begin	End
fig|1504.6.peg.37	CDS	Contig_14	43617	44363	747	Phosphosugar-binding transcriptional regulator, RpiR family	- none -	43617	44363
fig|1504.6.peg.38	CDS	Contig_14	44730	46502	1773	Sialidase (EC 3.2.1.18)	Galactosylceramide and Sulfatide metabolism, Sialic Acid Metabolism	44730	46502
fig|1504.6.peg.39	CDS	Contig_14	47043	46720	324	hypothetical protein	- none -	46720	47043
fig|1504.6.peg.40	CDS	Contig_14	50804	47070	3735	ATP-dependent nuclease, subunit A	ATP-dependent Nuclease	47070	50804
fig|1504.6.peg.41	CDS	Contig_14	54250	50807	3444	ATP-dependent nuclease, subunit B	ATP-dependent Nuclease	50807	54250
fig|1504.6.peg.42	CDS	Contig_14	54880	54293	588	Acetyltransferase, GNAT family (EC 2.3.1.-)	- none -	54293	54880
fig|1504.6.peg.43	CDS	Contig_14	56131	55187	945	Mlc, transcriptional repressor of MalT (the transcriptional activator of maltose regulon) and manXYZ operon	Maltose and Maltodextrin Utilization	55187	56131
fig|1504.6.rna.2	RNA	Contig_14	56425	56338	88	tRNA-Ser-GCT	- none -	56338	56425
fig|1504.6.rna.3	RNA	Contig_14	56546	56459	88	tRNA-Ser-TGA	- none -	56459	56546
fig|1504.6.rna.4	RNA	Contig_14	56778	56691	88	tRNA-Ser-TGA	- none -	56691	56778
fig|1504.6.peg.44	CDS	Contig_14	57411	57025	387	Aspartate 1-decarboxylase (EC 4.1.1.11)	Coenzyme A Biosynthesis, Coenzyme A Biosynthesis cluster, Folate biosynthesis cluster	57025	57411
fig|1504.6.peg.45	CDS	Contig_14	58271	57426	846	Pantoate--beta-alanine ligase (EC 6.3.2.1)	Coenzyme A Biosynthesis, Coenzyme A Biosynthesis cluster, Folate biosynthesis cluster	57426	58271
fig|1504.6.peg.46	CDS	Contig_14	59115	58288	828	3-methyl-2-oxobutanoate hydroxymethyltransferase (EC 2.1.2.11)	Coenzyme A Biosynthesis, Coenzyme A Biosynthesis cluster	58288	59115
fig|1504.6.peg.47	CDS	Contig_14	59975	59112	864	Ketopantoate reductase PanG (EC 1.1.1.169)	Coenzyme A Biosynthesis, Coenzyme A Biosynthesis cluster, Folate biosynthesis cluster	59112	59975
fig|1504.6.peg.48	CDS	Contig_14	61651	60374	1278	Seryl-tRNA synthetase (EC 6.1.1.11)	Glycine and Serine Utilization, tRNA aminoacylation, Ser	60374	61651
fig|1504.6.peg.49	CDS	Contig_14	62255	62025	231	no significant homology.	- none -	62025	62255

Feature ID	Type	Contig	Start	Stop	Length (bp)	Function	Subsystems	Begin	End
fig|1504.6.peg.50	CDS	Contig_14	63686	62274	1413	Glycerol-3-phosphate dehydrogenase (EC 1.1.5.3)	Glycerol and Glycerol-3-phosphate Uptake and Utilization, Glycerolipid and Glycerophospholipid Metabolism in Bacteria, Respiratory dehydrogenases 1	62274	63686
fig|1504.6.peg.51	CDS	Contig_14	64217	63711	507	Transcriptional repressor for NAD biosynthesis in gram-positives	NAD and NADP cofactor biosynthesis global	63711	64217
fig|1504.6.peg.52	CDS	Contig_14	64733	64233	501	probable HD superfamily hydrolase	- none -	64233	64733
fig|1504.6.rna.5	RNA	Contig_14	67891	64988	2904	Large Subunit Ribosomal RNA; lsuRNA; LSU rRNA	- none -	64988	67891
fig|1504.6.rna.6	RNA	Contig_14	69710	68136	1575	Small Subunit Ribosomal RNA; ssuRNA; SSU rRNA	- none -	68136	69710
fig|1504.6.rna.7	RNA	Contig_14	70451	70335	117	5S RNA	- none -	70335	70451
fig|1504.6.rna.8	RNA	Contig_14	73557	70654	2904	Large Subunit Ribosomal RNA; lsuRNA; LSU rRNA	- none -	70654	73557
fig|1504.6.rna.9	RNA	Contig_14	75376	73802	1575	Small Subunit Ribosomal RNA; ssuRNA; SSU rRNA	- none -	73802	75376
fig|1504.6.peg.57	CDS	Contig_14	76386	75781	606	Alkanesulfonates ABC transporter ATP-binding protein / Sulfonate ABC transporter, ATP-binding subunit SsuB	Alkanesulfonates Utilization	75781	76386
fig|1504.6.peg.58	CDS	Contig_14	77116	76388	729	ABC-type nitrate/sulfonate/bicarbonate transport system, permease component	- none -	76388	77116
fig|1504.6.peg.59	CDS	Contig_14	78083	77124	960	ABC-type nitrate/sulfonate/bicarbonate transport systems, periplasmic components	- none -	77124	78083
fig|1504.6.rna.10	RNA	Contig_14	78378	78262	117	5S RNA	- none -	78262	78378
fig|1504.6.rna.11	RNA	Contig_14	81484	78581	2904	Large Subunit Ribosomal RNA; lsuRNA; LSU rRNA	- none -	78581	81484
fig|1504.6.rna.12	RNA	Contig_14	83303	81729	1575	Small Subunit Ribosomal RNA; ssuRNA; SSU rRNA	- none -	81729	83303
fig|1504.6.rna.13	RNA	Contig_14	84079	83994	86	5S RNA	- none -	83994	84079

Feature ID	Type	Contig	Start	Stop	Length (bp)	Function	Subsystems	Begin	End
fig|1504.6.peg.60	CDS	Contig_14	91988	89427	2562	DNA gyrase subunit A (EC 5.99.1.3)	Cell Division Subsystem including YidCD, DNA gyrase subunits, DNA replication cluster 1, DNA topoisomerases, Type II, ATP-dependent, Resistance to fluoroquinolones	89427	91988
fig|1504.6.peg.61	CDS	Contig_14	93923	92010	1914	DNA gyrase subunit B (EC 5.99.1.3)	Cell Division Subsystem including YidCD, DNA gyrase subunits, DNA replication cluster 1, DNA topoisomerases, Type II, ATP-dependent, Resistance to fluoroquinolones	92010	93923
fig|1504.6.peg.62	CDS	Contig_14	94246	93986	261	OrfX	DNA replication cluster 1	93986	94246
fig|1504.6.peg.63	CDS	Contig_14	95347	94262	1086	DNA recombination and repair protein RecF	Cell Division Subsystem including YidCD, DNA repair, bacterial RecFOR pathway, DNA replication cluster 1, Hypothetical Coupled to RecF	94262	95347
fig|1504.6.peg.64	CDS	Contig_14	95638	95432	207	FIG002958: hypothetical protein	DNA replication cluster 1, Hypothetical Coupled to RecF	95432	95638
fig|1504.6.peg.65	CDS	Contig_14	96797	95697	1101	DNA polymerase III beta subunit (EC 2.7.7.7)	Cell Division Subsystem including YidCD, DNA-replication, DNA replication cluster 1	95697	96797
fig|1504.6.peg.66	CDS	Contig_14	98413	97055	1359	Chromosomal replication initiator protein DnaA	Cell Division Subsystem including YidCD, DNA-replication, DNA replication cluster 1	97055	98413
fig|1504.6.peg.67	CDS	Contig_14	98951	99085	135	LSU ribosomal protein L34p	Cell Division Subsystem including YidCD, RNA modification cluster, Ribosome LSU bacterial	98951	99085

Feature ID	Type	Contig	Start	Stop	Length (bp)	Function	Subsystems	Begin	End
fig|1504.6.peg.68	CDS	Contig_14	99149	99499	351	Ribonuclease P protein component (EC 3.1.26.5)	Cell Division Subsystem including YidCD, RNA modification cluster, tRNA processing	99149	99499
fig|1504.6.peg.69	CDS	Contig_14	99499	99708	210	Protein YidD	Cell Division Subsystem including YidCD, Mycobacterium virulence operon involved in an unknown function with a Jag Protein and YidC and YidD, RNA modification cluster	99499	99708
fig|1504.6.peg.70	CDS	Contig_14	99728	100492	765	Inner membrane protein translocase component YidC, short form OxaI-like	Cell Division Subsystem including YidCD, Mycobacterium virulence operon involved in an unknown function with a Jag Protein and YidC and YidD, RNA modification cluster	99728	100492
fig|1504.6.peg.71	CDS	Contig_14	100533	101159	627	RNA-binding protein Jag	Cell Division Subsystem including YidCD, Mycobacterium virulence operon involved in an unknown function with a Jag Protein and YidC and YidD	100533	101159
fig|1504.6.peg.72	CDS	Contig_14	101291	102670	1380	GTPase and tRNA-U34 5-formylation enzyme TrmE	Cell Division Subsystem including YidCD, RNA modification and chromosome partitioning cluster, RNA modification cluster, Universal GTPases, mnm5U34 biosynthesis bacteria, tRNAmodification position 34	101291	102670

Feature ID	Type	Contig	Start	Stop	Length (bp)	Function	Subsystems	Begin	End
fig|1504.6.peg.73	CDS	Contig_14	102685	104565	1881	tRNA uridine 5-carboxymethylaminomethyl modification enzyme GidA	Cell Division Subsystem including YidCD, RNA modification and chromosome partitioning cluster, mnm5U34 biosynthesis bacteria, tRNAmodification position 34	102685	104565
fig|1504.6.peg.74	CDS	Contig_14	104583	105302	720	rRNA small subunit 7-methylguanosine (m7G) methyltransferase GidB	Cell Division Subsystem including YidCD, RNA methylation, RNA modification and chromosome partitioning cluster	104583	105302
fig|1504.6.peg.75	CDS	Contig_14	105506	106294	789	Chromosome (plasmid) partitioning protein ParB	Bacterial Cytoskeleton, Cell Division Subsystem including YidCD, RNA modification and chromosome partitioning cluster	105506	106294
fig|1504.6.peg.76	CDS	Contig_14	106511	107272	762	Chromosome (plasmid) partitioning protein ParA	Bacterial Cell Division, Bacterial Cytoskeleton, Cell Division Subsystem including YidCD, RNA modification and chromosome partitioning cluster, Ribosome post-transcriptional modification and chromosomal segregation cluster	106511	107272
fig|1504.6.peg.77	CDS	Contig_14	107287	108150	864	Chromosome (plasmid) partitioning protein ParB	Bacterial Cytoskeleton, Cell Division Subsystem including YidCD, RNA modification and chromosome partitioning cluster	107287	108150
fig|1504.6.peg.78	CDS	Contig_14	108227	108724	498	FIG072699: hypothetical protein	- none -	108227	108724
fig|1504.6.peg.79	CDS	Contig_14	109382	108786	597	Spore protease GPR related protein	- none -	108786	109382
fig|1504.6.peg.80	CDS	Contig_14	110539	109448	1092	protein of unknown function UPF0118	- none -	109448	110539
fig|1504.6.peg.81	CDS	Contig_14	111701	110532	1170	Cysteine desulfurase (EC 2.8.1.7)	Alanine biosynthesis, CBSS-84588.1.peg.1247, mnm5U34 biosynthesis bacteria	110532	111701

Feature ID	Type	Contig	Start	Stop	Length (bp)	Function	Subsystems	Begin	End
fig|1504.6.peg.82	CDS	Contig_14	111880	112119	240	no significant homology	- none -	111880	112119
fig|1504.6.peg.83	CDS	Contig_14	112141	113016	876	Potassium efflux system KefA protein / Small-conductance mechanosensitive channel	Potassium homeostasis	112141	113016
fig|1504.6.peg.84	CDS	Contig_14	113059	113244	186	FIG001891: protein involved in chromosome partitioning	- none -	113059	113244
fig|1504.6.peg.85	CDS	Contig_14	113350	113640	291	SSU ribosomal protein S6p	Ribosome SSU bacterial	113350	113640
fig|1504.6.peg.86	CDS	Contig_14	113655	114110	456	Single-stranded DNA-binding protein	DNA repair, bacterial, DNA repair, bacterial RecFOR pathway	113655	114110
fig|1504.6.peg.87	CDS	Contig_14	114141	114383	243	SSU ribosomal protein S18p @ SSU ribosomal protein S18p, zinc-dependent	Ribosome SSU bacterial, Ribosome SSU bacterial	114141	114383
fig|1504.6.peg.88	CDS	Contig_14	114610	114927	318	FIG00522193: hypothetical protein	- none -	114610	114927
fig|1504.6.peg.89	CDS	Contig_14	114951	116897	1947	Phosphoesterase, DHH family protein	CBSS-262719.3.peg.410	114951	116897
fig|1504.6.peg.90	CDS	Contig_14	116899	117345	447	LSU ribosomal protein L9p	CBSS-262719.3.peg.410, Ribosome LSU bacterial	116899	117345
fig|1504.6.peg.91	CDS	Contig_14	117358	119256	1899	ATP-dependent protease LonB-like Type I	- none -	117358	119256
fig|1504.6.peg.92	CDS	Contig_14	119427	120764	1338	Replicative DNA helicase (EC 3.6.1.-) [SA14-24]	CBSS-262719.3.peg.410, DNA-replication	119427	120764
fig|1504.6.peg.93	CDS	Contig_14	121149	120793	357	hypothetical protein	- none -	120793	121149
fig|1504.6.peg.94	CDS	Contig_14	121285	122085	801	Pyrroline-5-carboxylate reductase (EC 1.5.1.2)	A Hypothetical Protein Related to Proline Metabolism, Proline Synthesis	121285	122085
fig|1504.6.peg.95	CDS	Contig_14	123350	122175	1176	NADP-dependent malic enzyme (EC 1.1.1.40)	Pyruvate metabolism I: anaplerotic reactions, PEP	122175	123350
fig|1504.6.peg.96	CDS	Contig_14	123576	124865	1290	Adenylosuccinate synthetase (EC 6.3.4.4)	CBSS-262719.3.peg.410, Purine conversions	123576	124865
fig|1504.6.peg.97	CDS	Contig_14	124976	125170	195	hypothetical protein	- none -	124976	125170
fig|1504.6.peg.98	CDS	Contig_14	125321	125503	183	no significant homology	- none -	125321	125503
fig|1504.6.peg.99	CDS	Contig_14	125590	126339	750	Acyl-acyl carrier protein thioesterase (EC 3.1.2.14)	- none -	125590	126339

Feature ID	Type	Contig	Start	Stop	Length (bp)	Function	Subsystems	Begin	End
fig|1504.6.peg.100	CDS	Contig_14	127638	126391	1248	NAD(FAD)-utilizing dehydrogenases	- none -	126391	127638
fig|1504.6.peg.101	CDS	Contig_14	127733	128314	582	FIG00517830: hypothetical protein	- none -	127733	128314
fig|1504.6.rna.14	RNA	Contig_14	128455	128526	72	tRNA-Glu-TTC	- none -	128455	128526
fig|1504.6.rna.15	RNA	Contig_14	128538	128610	73	tRNA-Val-TAC	- none -	128538	128610
fig|1504.6.rna.16	RNA	Contig_14	128623	128696	74	tRNA-Asp-GTC	- none -	128623	128696
fig|1504.6.rna.17	RNA	Contig_14	128723	128794	72	tRNA-Thr-TGT	- none -	128723	128794
fig|1504.6.peg.102	CDS	Contig_14	129882	128908	975	DNA replication protein DnaC	DNA-replication	128908	129882
fig|1504.6.peg.103	CDS	Contig_14	130870	129875	996	DNA replication protein DnaD	- none -	129875	130870
fig|1504.6.peg.104	CDS	Contig_14	131039	132259	1221	Membrane proteins related to metalloendopeptidases	CBSS-393121.3.peg.2760	131039	132259
fig|1504.6.peg.105	CDS	Contig_14	133466	132270	1197	subtilase family protein	- none -	132270	133466
fig|1504.6.peg.106	CDS	Contig_14	133963	133532	432	Conserved membrane protein	- none -	133532	133963
fig|1504.6.peg.107	CDS	Contig_14	134500	134045	456	Dimeric dUTPase (EC 3.6.1.23)	Housecleaning nucleoside triphosphate pyrophosphatases	134045	134500
fig|1504.6.peg.108	CDS	Contig_14	135220	134684	537	no significant homology	- none -	134684	135220
fig|1504.6.peg.109	CDS	Contig_14	135640	136899	1260	UDP-N-acetylglucosamine 1-carboxyvinyltransferase (EC 2.5.1.7)	Sporulation-related Hypotheticals, UDP-N-acetylmuramate from Fructose-6-phosphate Biosynthesis	135640	136899
fig|1504.6.peg.110	CDS	Contig_14	136922	137713	792	Zn-dependent hydrolase (beta-lactamase superfamily)	- none -	136922	137713
fig|1504.6.peg.111	CDS	Contig_14	137851	138348	498	Protein export cytoplasm protein SecA ATPase RNA helicase (TC 3.A.5.1.1)	CBSS-393121.3.peg.2760	137851	138348
fig|1504.6.peg.112	CDS	Contig_14	138432	139073	642	Transcriptional regulators of sugar metabolism	- none -	138432	139073
fig|1504.6.peg.113	CDS	Contig_14	139186	139848	663	hypothetical protein	- none -	139186	139848
fig|1504.6.peg.114	CDS	Contig_14	139893	140372	480	LSU m3Psi1915 methyltransferase RlmH	RNA methylation, Ribosome biogenesis bacterial	139893	140372
fig|1504.6.peg.115	CDS	Contig_14	140517	141761	1245	DNA-cytosine methyltransferase (EC 2.1.1.37)	DNA repair, bacterial	140517	141761

Feature ID	Type	Contig	Start	Stop	Length (bp)	Function	Subsystems	Begin	End
fig|1504.6.peg.116	CDS	Contig_14	142298	141786	513	hypothetical protein	- none -	141786	142298
fig|1504.6.peg.117	CDS	Contig_14	143491	142310	1182	hypothetical protein	- none -	142310	143491
fig|1504.6.peg.118	CDS	Contig_14	143750	144058	309	conserved hypothetical protein	- none -	143750	144058
fig|1504.6.peg.119	CDS	Contig_14	144126	144464	339	hypothetical protein	- none -	144126	144464
fig|1504.6.peg.120	CDS	Contig_14	144484	144789	306	hypothetical protein	- none -	144484	144789
fig|1504.6.peg.121	CDS	Contig_14	144865	145197	333	cassette chromosome recombinase B	- none -	144865	145197
fig|1504.6.peg.122	CDS	Contig_14	146499	149858	3360	Exonuclease SbcC	DNA repair, bacterial, Rad50-Mre11 DNA repair cluster	146499	149858
fig|1504.6.peg.123	CDS	Contig_14	149862	151892	2031	DNA-repair protein	- none -	149862	151892
fig|1504.6.peg.124	CDS	Contig_14	151885	152073	189	hypothetical protein	- none -	151885	152073
fig|1504.6.peg.125	CDS	Contig_14	152074	154101	2028	hypothetical protein	- none -	152074	154101
fig|1504.6.peg.126	CDS	Contig_14	154108	154560	453	hypothetical protein	- none -	154108	154560
fig|1504.6.peg.127	CDS	Contig_14	154878	156767	1890	hypothetical protein	- none -	154878	156767
fig|1504.6.peg.128	CDS	Contig_14	157074	159041	1968	hypothetical protein	- none -	157074	159041
fig|1504.6.peg.129	CDS	Contig_14	159066	159800	735	hypothetical protein	- none -	159066	159800
fig|1504.6.peg.130	CDS	Contig_14	159821	160510	690	FIG01032596: hypothetical protein	- none -	159821	160510
fig|1504.6.peg.131	CDS	Contig_14	160708	161382	675	Phosphate regulon transcriptional regulatory protein PhoB (SphR)	High affinity phosphate transporter and control of PHO regulon, PhoR-PhoB two-component regulatory system, Phosphate metabolism	160708	161382
fig|1504.6.peg.132	CDS	Contig_14	161385	162788	1404	Osmosensitive K+ channel histidine kinase KdpD (EC 2.7.3.-)	Potassium homeostasis	161385	162788
fig|1504.6.peg.133	CDS	Contig_14	163063	162908	156	no significant homology.	- none -	162908	163063
fig|1504.6.peg.134	CDS	Contig_14	163349	168097	4749	Beta-galactosidase (EC 3.2.1.23)	Galactosylceramide and Sulfatide metabolism, Lactose and Galactose Uptake and Utilization, Lactose utilization	163349	168097

Feature ID	Type	Contig	Start	Stop	Length (bp)	Function	Subsystems	Begin	End
fig|1504.6.peg.135	CDS	Contig_14	168386	169798	1413	PTS system, trehalose-specific IIB component (EC 2.7.1.69) / PTS system, trehalose-specific IIC component (EC 2.7.1.69)	Trehalose Uptake and Utilization, Trehalose Uptake and Utilization	168386	169798
fig|1504.6.peg.136	CDS	Contig_14	169893	171551	1659	Trehalose-6-phosphate hydrolase (EC 3.2.1.93)	Trehalose Uptake and Utilization	169893	171551
fig|1504.6.peg.137	CDS	Contig_14	171586	172296	711	Trehalose operon transcriptional repressor	Trehalose Uptake and Utilization	171586	172296
fig|1504.6.peg.138	CDS	Contig_14	172675	173652	978	Mlc, transcriptional repressor of MalT (the transcriptional activator of maltose regulon) and manXYZ operon	Maltose and Maltodextrin Utilization	172675	173652
fig|1504.6.peg.139	CDS	Contig_14	173695	174318	624	Haloacid dehalogenase-like hydrolase	- none -	173695	174318
fig|1504.6.peg.140	CDS	Contig_14	174444	175265	822	FIG00526165: hypothetical protein	- none -	174444	175265
fig|1504.6.peg.141	CDS	Contig_14	175466	175618	153	hypothetical protein	- none -	175466	175618
fig|1504.6.peg.142	CDS	Contig_14	175880	176425	546	FIG00514020: hypothetical protein	- none -	175880	176425
fig|1504.6.peg.143	CDS	Contig_14	177226	176597	630	acetyltransferase, GNAT family family	- none -	176597	177226
fig|1504.6.peg.144	CDS	Contig_14	177357	178172	816	Transcriptional regulator, MerR family	Cobalt-zinc-cadmium resistance	177357	178172
fig|1504.6.peg.145	CDS	Contig_14	178221	179150	930	Probable DNA polymerase III epsilon chain	- none -	178221	179150
fig|1504.6.peg.146	CDS	Contig_14	179214	180701	1488	N-6 DNA methylase	- none -	179214	180701
fig|1504.6.peg.147	CDS	Contig_14	180814	181458	645	Quinolone resistance protein	- none -	180814	181458
fig|1504.6.peg.148	CDS	Contig_14	181814	182026	213	Anaerobic sulfite reductase subunit A	Anaerobic respiratory reductases	181814	182026
fig|1504.6.peg.149	CDS	Contig_14	182027	182821	795	Anaerobic sulfite reductase subunit B	Anaerobic respiratory reductases	182027	182821
fig|1504.6.peg.150	CDS	Contig_14	182835	183086	252	Anaerobic sulfite reductase subunit C (EC 1.8.1.-)	Anaerobic respiratory reductases	182835	183086
fig|1504.6.peg.151	CDS	Contig_14	183119	183889	771	Anaerobic sulfite reductase subunit C (EC 1.8.1.-)	Anaerobic respiratory reductases	183119	183889
fig|1504.6.peg.152	CDS	Contig_14	185269	183893	1377	Sigma-54-dependent transcriptional activator	- none -	183893	185269
fig|1504.6.peg.153	CDS	Contig_14	185671	186648	978	Choline permease LicB	- none -	185671	186648
fig|1504.6.peg.154	CDS	Contig_14	186671	189247	2577	putative glutamate synthase, small chain	- none -	186671	189247

Feature ID	Type	Contig	Start	Stop	Length (bp)	Function	Subsystems	Begin	End
fig|1504.6.peg.155	CDS	Contig_14	189312	190046	735	Phosphoglycerate mutase (EC 5.4.2.1)	Entner-Doudoroff Pathway, Glycolysis and Gluconeogenesis, Phosphoglycerate mutase protein family	189312	190046
fig|1504.6.peg.156	CDS	Contig_14	190240	191619	1380	Proton/sodium-glutamate symport protein	- none -	190240	191619
fig|1504.6.peg.157	CDS	Contig_14	191728	192156	429	Predicted transcriptional regulator of cysteine synthase, Rrf2 family	Rrf2 family transcriptional regulators	191728	192156
fig|1504.6.peg.158	CDS	Contig_14	192213	192515	303	no significant homology	- none -	192213	192515
fig|1504.6.peg.159	CDS	Contig_14	194334	192757	1578	DEAD-box ATP-dependent RNA helicase CshA (EC 3.6.4.13)	- none -	192757	194334
fig|1504.6.peg.160	CDS	Contig_14	194662	195171	510	Methylated-DNA--protein-cysteine methyltransferase (EC 2.1.1.63)	DNA repair, bacterial	194662	195171
fig|1504.6.peg.161	CDS	Contig_14	195446	196540	1095	hypothetical protein	- none -	195446	196540
fig|1504.6.peg.162	CDS	Contig_14	196797	198059	1263	Multidrug and toxin extrusion (MATE) family efflux pump YdhE/NorM, homolog	Multidrug Resistance Efflux Pumps	196797	198059
fig|1504.6.peg.163	CDS	Contig_14	198891	198214	678	1-acyl-sn-glycerol-3-phosphate acyltransferase (EC 2.3.1.51)	Glycerolipid and Glycerophospholipid Metabolism in Bacteria, Ribosome post-transcriptional modification and chromosomal segregation cluster	198214	198891
fig|1504.6.rna.18	RNA	Contig_14	199151	199222	72	tRNA-Arg-CCT	- none -	199151	199222
fig|1504.6.peg.164	CDS	Contig_14	199619	200794	1176	Magnesium and cobalt efflux protein CorC	CBSS-56780.10.peg.1536, Magnesium transport	199619	200794
fig|1504.6.peg.165	CDS	Contig_14	200861	201304	444	tRNA-specific adenosine-34 deaminase (EC 3.5.4.-)	tRNA processing, tRNAmodification position 34	200861	201304
fig|1504.6.peg.166	CDS	Contig_14	201325	202854	1530	Two-component sensor histidine kinase, malate (EC 2.7.3.-)	Pyruvate metabolism I: anaplerotic reactions, PEP	201325	202854
fig|1504.6.peg.167	CDS	Contig_14	202871	203569	699	Two-component response regulator, malate (EC 2.7.3.-)	Pyruvate metabolism I: anaplerotic reactions, PEP	202871	203569
fig|1504.6.peg.168	CDS	Contig_14	203707	205131	1425	Fumarate reductase flavoprotein subunit (EC 1.3.99.1)	Succinate dehydrogenase	203707	205131

Feature ID	Type	Contig	Start	Stop	Length (bp)	Function	Subsystems	Begin	End
fig|1504.6.peg.169	CDS	Contig_14	205158	205502	345	Fumarate reductase flavoprotein subunit (EC 1.3.99.1)	Succinate dehydrogenase	205158	205502
fig|1504.6.peg.170	CDS	Contig_14	205647	206414	768	Prolipoprotein diacylglyceryl transferase (EC 2.4.99.-)	- none -	205647	206414
fig|1504.6.rna.19	RNA	Contig_14	206599	206685	87	tRNA-Ser-GGA	- none -	206599	206685
fig|1504.6.peg.171	CDS	Contig_14	207630	207142	489	Dihydrofolate reductase (EC 1.5.1.3)	5-FCL-like protein, Folate Biosynthesis	207142	207630
fig|1504.6.peg.172	CDS	Contig_14	208421	207630	792	Thymidylate synthase (EC 2.1.1.45)	Folate Biosynthesis, pyrimidine conversions	207630	208421
fig|1504.6.peg.173	CDS	Contig_14	208639	210255	1617	DNA polymerase III subunits gamma and tau (EC 2.7.7.7)	DNA-replication, DNA processing cluster	208639	210255
fig|1504.6.peg.174	CDS	Contig_14	210358	210702	345	FIG000557: hypothetical protein co-occurring with RecR	DNA processing cluster	210358	210702
fig|1504.6.peg.175	CDS	Contig_14	210780	211376	597	Recombination protein RecR	DNA-replication, DNA processing cluster, DNA repair, bacterial RecFOR pathway	210780	211376
fig|1504.6.peg.176	CDS	Contig_14	211479	213014	1536	Cardiolipin synthetase (EC 2.7.8.-)	Cardiolipin synthesis, Glycerolipid and Glycerophospholipid Metabolism in Bacteria	211479	213014
fig|1504.6.peg.177	CDS	Contig_14	213285	214199	915	ABC transporter, ATP-binding protein	- none -	213285	214199
fig|1504.6.peg.178	CDS	Contig_14	214200	215444	1245	FIG00512710: hypothetical protein	- none -	214200	215444
fig|1504.6.peg.179	CDS	Contig_14	215593	215838	246	FIG015094: hypothetical protein	DNA processing cluster	215593	215838
fig|1504.6.peg.180	CDS	Contig_14	215884	216132	249	Inhibitor of pro-sigmaK processing BofA	DNA processing cluster	215884	216132
fig|1504.6.peg.181	CDS	Contig_14	216375	216563	189	no significant homology.	- none -	216375	216563
fig|1504.6.peg.182	CDS	Contig_14	216662	217114	453	Large-conductance mechanosensitive channel	Potassium homeostasis	216662	217114
fig|1504.6.peg.183	CDS	Contig_14	217433	217314	120	hypothetical protein	- none -	217314	217433
fig|1504.6.peg.184	CDS	Contig_14	217767	218843	1077	Serine--pyruvate aminotransferase (EC 2.6.1.51)	Serine-glyoxylate cycle	217767	218843

Feature ID	Type	Contig	Start	Stop	Length (bp)	Function	Subsystems	Begin	End
fig|1504.6.peg.185	CDS	Contig_14	218912	219826	915	D-3-phosphoglycerate dehydrogenase (EC 1.1.1.95)	Glycine and Serine Utilization, Pyridoxin (Vitamin B6) Biosynthesis, Serine Biosynthesis	218912	219826
fig|1504.6.peg.186	CDS	Contig_14	219851	220768	918	Related to HTH domain of SpoOJ/ParA/ParB/repB family, involved in chromosome partitioning	- none -	219851	220768
fig|1504.6.peg.187	CDS	Contig_14	220966	221097	132	Related to HTH domain of SpoOJ/ParA/ParB/repB family, involved in chromosome partitioning	- none -	220966	221097
fig|1504.6.peg.188	CDS	Contig_14	221150	221464	315	hypothetical protein	- none -	221150	221464
fig|1504.6.peg.189	CDS	Contig_14	221859	221722	138	Mobile element protein	- none -	221722	221859
fig|1504.6.peg.190	CDS	Contig_14	221951	222127	177	ABC transporter, ATP-binding/permease protein	- none -	221951	222127
fig|1504.6.peg.191	CDS	Contig_14	222527	222694	168	hypothetical protein	- none -	222527	222694
fig|1504.6.peg.192	CDS	Contig_14	223716	223021	696	5'-methylthioadenosine nucleosidase (EC 3.2.2.16) @ S-adenosylhomocysteine nucleosidase (EC 3.2.2.9)	Adenosyl nucleosidases, Adenosyl nucleosidases, Methionine Biosynthesis, Methionine Degradation, Polyamine Metabolism	223021	223716
fig|1504.6.peg.193	CDS	Contig_14	224638	223811	828	CAAX amino terminal protease family protein	- none -	223811	224638
fig|1504.6.peg.194	CDS	Contig_14	224771	225529	759	CsdL (EC-YgdL) protein of the HesA/MoeB/ThiF family, part of the CsdA-E-L sulfur transfer pathway	- none -	224771	225529
fig|1504.6.peg.195	CDS	Contig_14	226499	225630	870	DNA-binding response regulator, AraC family	- none -	225630	226499
fig|1504.6.peg.196	CDS	Contig_14	226675	227568	894	N-Acetyl-D-glucosamine ABC transport system, permease protein	- none -	226675	227568
fig|1504.6.peg.197	CDS	Contig_14	227583	228479	897	ABC-type sugar transport system, permease component	- none -	227583	228479
fig|1504.6.peg.198	CDS	Contig_14	228498	230654	2157	Lacto-N-biose phosphorylase (EC 2.4.1.211)	Lacto-N-Biose I and Galacto-N-Biose Metabolic Pathway	228498	230654
fig|1504.6.peg.199	CDS	Contig_14	230691	230846	156	hypothetical protein	- none -	230691	230846

Feature ID	Type	Contig	Start	Stop	Length (bp)	Function	Subsystems	Begin	End
fig|1504.6.peg.200	CDS	Contig_14	230971	232323	1353	Sugar ABC transporter sugar-binding protein	- none -	230971	232323
fig|1504.6.peg.201	CDS	Contig_14	232484	233041	558	Substrate-specific component BioY of biotin ECF transporter	Biotin biosynthesis, ECF class transporters	232484	233041
fig|1504.6.peg.202	CDS	Contig_14	233059	234018	960	Biotin synthase (EC 2.8.1.6)	Biotin biosynthesis, Biotin biosynthesis Experimental	233059	234018
fig|1504.6.peg.203	CDS	Contig_14	234018	234719	702	Dethiobiotin synthetase (EC 6.3.3.3)	Biotin biosynthesis, Biotin biosynthesis Experimental	234018	234719
fig|1504.6.peg.204	CDS	Contig_14	234733	236079	1347	Adenosylmethionine-8-amino-7-oxononanoate aminotransferase (EC 2.6.1.62)	Biotin biosynthesis, Biotin biosynthesis Experimental	234733	236079
fig|1504.6.peg.205	CDS	Contig_14	236762	236259	504	conserved protein	- none -	236259	236762
fig|1504.6.peg.206	CDS	Contig_14	236881	237000	120	hypothetical protein	- none -	236881	237000
fig|1504.6.peg.207	CDS	Contig_14	238505	237066	1440	Lysine-specific permease	- none -	237066	238505
fig|1504.6.peg.208	CDS	Contig_14	239046	239981	936	Ribosomal-protein-S5p-alanine acetyltransferase	Ribosomal protein S5p acylation, Ribosome biogenesis bacterial	239046	239981
fig|1504.6.peg.209	CDS	Contig_14	240586	240062	525	PTS system, glucose-specific IIA component (EC 2.7.1.69)	Trehalose Uptake and Utilization	240062	240586
fig|1504.6.peg.210	CDS	Contig_14	241057	242496	1440	PTS system, N-acetylglucosamine-specific IIB component (EC 2.7.1.69) / PTS system, N-acetylglucosamine-specific IIC component (EC 2.7.1.69)	Chitin and N-acetylglucosamine utilization, Chitin and N-acetylglucosamine utilization, Sialic Acid Metabolism, Sialic Acid Metabolism	241057	242496
fig|1504.6.rna.20	RNA	Contig_14	243155	244729	1575	Small Subunit Ribosomal RNA; ssuRNA; SSU rRNA	- none -	243155	244729
fig|1504.6.rna.21	RNA	Contig_14	244974	247877	2904	Large Subunit Ribosomal RNA; lsuRNA; LSU rRNA	- none -	244974	247877
fig|1504.6.rna.22	RNA	Contig_14	248080	248196	117	5S RNA	- none -	248080	248196
fig|1504.6.peg.211	CDS	Contig_14	248512	249945	1434	Glycogen synthase, ADP-glucose transglucosylase (EC 2.4.1.21)	Glycogen metabolism	248512	249945

Feature ID	Type	Contig	Start	Stop	Length (bp)	Function	Subsystems	Begin	End
fig|1504.6.peg.212	CDS	Contig_14	249978	252413	2436	Glycogen phosphorylase (EC 2.4.1.1)	Glycogen metabolism, Maltose and Maltodextrin Utilization	249978	252413
fig|1504.6.peg.213	CDS	Contig_14	252643	253779	1137	Glucose-1-phosphate adenylyltransferase (EC 2.7.7.27)	Glycogen metabolism	252643	253779
fig|1504.6.peg.214	CDS	Contig_14	253799	254908	1110	Glycogen biosynthesis protein GlgD, glucose-1-phosphate adenylyltransferase family	Glycogen metabolism	253799	254908
fig|1504.6.peg.215	CDS	Contig_14	255056	255778	723	Transcriptional activator tipA	- none -	255056	255778
fig|1504.6.rna.23	RNA	Contig_14	260484	260600	117	5S RNA	- none -	260484	260600
fig|1504.6.rna.24	RNA	Contig_14	260606	260678	73	tRNA-Lys-CTT	- none -	260606	260678
fig|1504.6.peg.216	CDS	Contig_14	260864	261814	951	L-lactate dehydrogenase (EC 1.1.1.27)	Fermentations: Lactate, Fermentations: Mixed acid	260864	261814
fig|1504.6.rna.25	RNA	Contig_14	262151	262267	117	5S RNA	- none -	262151	262267
fig|1504.6.rna.26	RNA	Contig_14	262273	262345	73	tRNA-Lys-TTT	- none -	262273	262345
fig|1504.6.peg.217	CDS	Contig_14	263189	262440	750	similar to sp:LSPA_STACA LIPOPROTEIN SIGNAL PEPTIDASE (EC 3.4.23.36) (PROLIPOPROTEIN SIGNAL PEPTIDASE) (SIGNAL PEPTIDASE II) (SPASE II) from Staphylococcus carnosus (159 aa); 23.4% identity in 145 aa overlap. Putative N-terminal signal sequence and 5 putative transmembrane regions were found by PSORT.	- none -	262440	263189
fig|1504.6.peg.218	CDS	Contig_14	263374	264180	807	ATP/GTP-binding protein, SA1392 homolog	CBSS-349161.4.peg.2427	263374	264180
fig|1504.6.peg.219	CDS	Contig_14	264331	265218	888	Patatin	- none -	264331	265218
fig|1504.6.rna.27	RNA	Contig_14	269924	270040	117	5S RNA	- none -	269924	270040
fig|1504.6.peg.220	CDS	Contig_14	270416	272437	2022	1,4-alpha-glucan (glycogen) branching enzyme, GH-13-type (EC 2.4.1.18)	Glycogen metabolism	270416	272437
fig|1504.6.peg.221	CDS	Contig_14	272438	273874	1437	Glycogen synthase, ADP-glucose transglucosylase (EC 2.4.1.21)	Glycogen metabolism	272438	273874

Feature ID	Type	Contig	Start	Stop	Length (bp)	Function	Subsystems	Begin	End
fig|1504.6.peg.222	CDS	Contig_14	273903	276335	2433	Glycogen phosphorylase (EC 2.4.1.1)	Glycogen metabolism, Maltose and Maltodextrin Utilization	273903	276335
fig|1504.6.peg.223	CDS	Contig_14	276351	278177	1827	Neopullulanase (EC 3.2.1.135)	Maltose and Maltodextrin Utilization	276351	278177
fig|1504.6.peg.224	CDS	Contig_14	278261	279460	1200	Glucose-1-phosphate adenylyltransferase (EC 2.7.7.27)	Glycogen metabolism	278261	279460
fig|1504.6.peg.225	CDS	Contig_14	279510	280616	1107	Glycogen biosynthesis protein GlgD, glucose-1-phosphate adenylyltransferase family	Glycogen metabolism	279510	280616
fig|1504.6.rna.28	RNA	Contig_14	281142	282716	1575	Small Subunit Ribosomal RNA; ssuRNA; SSU rRNA	- none -	281142	282716
fig|1504.6.rna.29	RNA	Contig_14	282961	285864	2904	Large Subunit Ribosomal RNA; lsuRNA; LSU rRNA	- none -	282961	285864
fig|1504.6.rna.30	RNA	Contig_14	286035	286107	73	tRNA-Ala-TGC	- none -	286035	286107
fig|1504.6.peg.226	CDS	Contig_14	286352	286504	153	hypothetical protein	- none -	286352	286504
fig|1504.6.peg.227	CDS	Contig_14	286661	287104	444	no significant homology.	- none -	286661	287104
fig|1504.6.peg.228	CDS	Contig_14	287184	287630	447	acetobutylicum phosphotransbutyrylase	- none -	287184	287630
fig|1504.6.peg.229	CDS	Contig_14	289188	287740	1449	Cardiolipin synthetase (EC 2.7.8.-)	Cardiolipin synthesis, Glycerolipid and Glycerophospholipid Metabolism in Bacteria	287740	289188
fig|1504.6.peg.230	CDS	Contig_14	289489	291036	1548	Aminobenzoyl-glutamate transport protein	- none -	289489	291036
fig|1504.6.peg.231	CDS	Contig_14	291283	292722	1440	membrane protein	- none -	291283	292722
fig|1504.6.peg.232	CDS	Contig_14	293122	293238	117	hypothetical protein	- none -	293122	293238
fig|1504.6.peg.233	CDS	Contig_14	293289	293654	366	GtrA family protein	- none -	293289	293654
fig|1504.6.peg.234	CDS	Contig_14	293975	294910	936	Glycosyltransferase	- none -	293975	294910
fig|1504.6.peg.235	CDS	Contig_14	295062	297137	2076	Translation elongation factor G-related protein	Translation elongation factor G family, Translation elongation factors bacterial	295062	297137
fig|1504.6.peg.236	CDS	Contig_14	297230	297466	237	hypothetical protein	- none -	297230	297466

Feature ID	Type	Contig	Start	Stop	Length (bp)	Function	Subsystems	Begin	End
fig|1504.6.peg.237	CDS	Contig_14	297590	298078	489	Molybdopterin binding motif, CinA N-terminal domain / C-terminal domain of CinA type S	NAD and NADP cofactor biosynthesis global, NAD and NADP cofactor biosynthesis global, Riboflavin, FMN and FAD metabolism in plants, Riboflavin, FMN and FAD metabolism in plants, Riboflavin synthesis cluster	297590	298078
fig|1504.6.peg.238	CDS	Contig_14	298268	299203	936	CAAX amino terminal protease family protein	- none -	298268	299203
fig|1504.6.peg.239	CDS	Contig_14	299711	299283	429	conserved protein	- none -	299283	299711
fig|1504.6.peg.240	CDS	Contig_14	299845	300054	210	hypothetical protein	- none -	299845	300054
fig|1504.6.rna.31	RNA	Contig_14	300154	300226	73	tRNA-Phe-GAA	- none -	300154	300226
fig|1504.6.peg.241	CDS	Contig_14	300546	300755	210	hypothetical protein	- none -	300546	300755
fig|1504.6.peg.242	CDS	Contig_14	301528	300851	678	Uracil-DNA glycosylase, family 1	DNA Repair Base Excision, Uracil-DNA glycosylase	300851	301528
fig|1504.6.rna.32	RNA	Contig_14	302063	303637	1575	Small Subunit Ribosomal RNA; ssuRNA; SSU rRNA	- none -	302063	303637
fig|1504.6.rna.33	RNA	Contig_14	303882	306785	2904	Large Subunit Ribosomal RNA; lsuRNA; LSU rRNA	- none -	303882	306785
fig|1504.6.rna.34	RNA	Contig_14	306988	307104	117	5S RNA	- none -	306988	307104
fig|1504.6.rna.35	RNA	Contig_14	307111	307183	73	tRNA-Phe-GAA	- none -	307111	307183
fig|1504.6.peg.243	CDS	Contig_14	311272	310814	459	Thiol peroxidase, Bcp-type (EC 1.11.1.15)	Thioredoxin-disulfide reductase	310814	311272
fig|1504.6.peg.244	CDS	Contig_14	311440	312186	747	Foldase protein PrsA precursor (EC 5.2.1.8)	Peptidyl-prolyl cis-trans isomerase	311440	312186
fig|1504.6.peg.245	CDS	Contig_14	312353	313591	1239	Mobile element protein	- none -	312353	313591
fig|1504.6.peg.246	CDS	Contig_14	314442	313801	642	HAD-superfamily hydrolase, subfamily IA, variant 3 protein family	- none -	313801	314442
fig|1504.6.peg.247	CDS	Contig_14	315923	314574	1350	Periplasmic [Fe] hydrogenase (EC 1.12.7.2)	- none -	314574	315923
fig|1504.6.peg.248	CDS	Contig_14	316037	316165	129	hypothetical protein	- none -	316037	316165

Feature ID	Type	Contig	Start	Stop	Length (bp)	Function	Subsystems	Begin	End
fig|1504.6.rna.36	RNA	Contig_14	316455	316383	73	tRNA-Pro-TGG	- none -	316383	316455
fig|1504.6.peg.249	CDS	Contig_14	316588	316893	306	hypothetical protein	- none -	316588	316893
fig|1504.6.peg.250	CDS	Contig_14	317270	318526	1257	Cell wall-associated hydrolase	- none -	317270	318526
fig|1504.6.peg.251	CDS	Contig_14	318649	319398	750	tRNA (adenine37-N(6))-methyltransferase TrmN6 (EC 2.1.1.223)	RNA methylation	318649	319398
fig|1504.6.peg.252	CDS	Contig_14	319401	320246	846	rRNA small subunit methyltransferase I	16S rRNA modification within P site of ribosome, Heat shock dnaK gene cluster extended	319401	320246
fig|1504.6.peg.253	CDS	Contig_14	320567	320328	240	Transition state regulatory protein AbrB	- none -	320328	320567
fig|1504.6.peg.254	CDS	Contig_14	321098	321688	591	FIG00515603: hypothetical protein	- none -	321098	321688
fig|1504.6.peg.255	CDS	Contig_14	321959	324253	2295	DinG family ATP-dependent helicase CPE1197	DNA repair, bacterial DinG and relatives	321959	324253
fig|1504.6.peg.256	CDS	Contig_14	325186	324308	879	Aldose 1-epimerase	- none -	324308	325186
fig|1504.6.peg.257	CDS	Contig_14	325423	326274	852	Ribonuclease BN (EC 3.1.-.-)	- none -	325423	326274
fig|1504.6.peg.258	CDS	Contig_14	327345	326359	987	UDP-glucose 4-epimerase (EC 5.1.3.2)	Lacto-N-Biose I and Galacto-N-Biose Metabolic Pathway, Lactose and Galactose Uptake and Utilization, N-linked Glycosylation in Bacteria, Rhamnose containing glycans	326359	327345
fig|1504.6.peg.259	CDS	Contig_14	327462	327821	360	Single-stranded DNA-binding protein	DNA repair, bacterial, DNA repair, bacterial RecFOR pathway	327462	327821
fig|1504.6.peg.260	CDS	Contig_14	330592	327950	2643	Probable flavoprotein	- none -	327950	330592
fig|1504.6.peg.261	CDS	Contig_14	330964	331281	318	Conserved protein	- none -	330964	331281
fig|1504.6.peg.262	CDS	Contig_14	331392	331763	372	Holo-[acyl-carrier protein] synthase (EC 2.7.8.7)	CBSS-176299.4.peg.1292, Fatty Acid Biosynthesis FASII	331392	331763
fig|1504.6.peg.263	CDS	Contig_14	331764	333266	1503	NAD(P)HX epimerase / NAD(P)HX dehydratase	YjeE, YjeE	331764	333266

Feature ID	Type	Contig	Start	Stop	Length (bp)	Function	Subsystems	Begin	End
fig|1504.6.peg.264	CDS	Contig_14	333337	333945	609	Uncharacterized secreted protein associated with spyDAC	Bacterial checkpoint-control-related cluster	333337	333945
fig|1504.6.peg.265	CDS	Contig_14	334276	334518	243	Programmed cell death antitoxin YdcD	MazEF toxin-antitoxing (programmed cell death) system, Phd-Doc, YdcE-YdcD toxin-antitoxin (programmed cell death) systems	334276	334518
fig|1504.6.peg.266	CDS	Contig_14	334528	334881	354	Programmed cell death toxin YdcE	MazEF toxin-antitoxing (programmed cell death) system, Phd-Doc, YdcE-YdcD toxin-antitoxin (programmed cell death) systems	334528	334881
fig|1504.6.peg.267	CDS	Contig_14	335329	336153	825	Transketolase, N-terminal section (EC 2.2.1.1)	Pentose phosphate pathway	335329	336153
fig|1504.6.peg.268	CDS	Contig_14	336153	337106	954	Transketolase, C-terminal section (EC 2.2.1.1)	Pentose phosphate pathway	336153	337106
fig|1504.6.peg.269	CDS	Contig_14	337330	338172	843	hypothetical protein BH3604	CBSS-393121.3.peg.2760	337330	338172
fig|1504.6.peg.270	CDS	Contig_14	338203	339039	837	hypothetical protein BH3604	CBSS-393121.3.peg.2760	338203	339039
fig|1504.6.peg.271	CDS	Contig_14	339194	339880	687	Cell division transporter, ATP-binding protein FtsE (TC 3.A.5.1.1)	Bacterial Cell Division, CBSS-393121.3.peg.2760	339194	339880
fig|1504.6.peg.272	CDS	Contig_14	339870	340760	891	Cell division protein FtsX	Bacterial Cell Division, CBSS-393121.3.peg.2760	339870	340760
fig|1504.6.peg.273	CDS	Contig_14	340837	342096	1260	Carboxyl-terminal protease (EC 3.4.21.102)	Phosphoglycerate mutase protein family	340837	342096
fig|1504.6.peg.274	CDS	Contig_14	342107	343378	1272	Cell division topological determinant MinJ	Bacillus subtilis scratch - gjo	342107	343378
fig|1504.6.peg.275	CDS	Contig_14	343504	345471	1968	Excinuclease ABC subunit B	DNA repair, UvrABC system	343504	345471
fig|1504.6.peg.276	CDS	Contig_14	345610	346365	756	hypothetical protein	- none -	345610	346365
fig|1504.6.peg.277	CDS	Contig_14	346531	347598	1068	Malate permease	Pyruvate metabolism I: anaplerotic reactions, PEP	346531	347598
fig|1504.6.peg.278	CDS	Contig_14	347614	348612	999	D-lactate dehydrogenase (EC 1.1.1.28)	Fermentations: Lactate, Fermentations: Mixed acid	347614	348612

Feature ID	Type	Contig	Start	Stop	Length (bp)	Function	Subsystems	Begin	End
fig|1504.6.peg.279	CDS	Contig_14	348716	350293	1578	Two-component sensor histidine kinase, malate (EC 2.7.3.-)	Pyruvate metabolism I: anaplerotic reactions, PEP	348716	350293
fig|1504.6.peg.280	CDS	Contig_14	350271	350945	675	Two-component response regulator, malate (EC 2.7.3.-)	Pyruvate metabolism I: anaplerotic reactions, PEP	350271	350945
fig|1504.6.peg.281	CDS	Contig_14	351400	354225	2826	Excinuclease ABC subunit A	DNA repair, UvrABC system	351400	354225
fig|1504.6.peg.282	CDS	Contig_14	354302	354754	453	FHA-domain containing secreted protein	- none -	354302	354754
fig|1504.6.peg.283	CDS	Contig_14	354765	355988	1224	Cell division protein FtsW	Bacterial Cell Division, Bacterial Cytoskeleton, cell division cluster containing FtsQ	354765	355988
fig|1504.6.peg.284	CDS	Contig_14	355992	357467	1476	Cell division protein FtsI [Peptidoglycan synthetase] (EC 2.4.1.129)	16S rRNA modification within P site of ribosome, Bacterial Cell Division, Bacterial Cytoskeleton, CBSS-83331.1.peg.3039, Flagellum in Campylobacter	355992	357467
fig|1504.6.peg.285	CDS	Contig_14	357633	358178	546	dTDP-4-dehydrorhamnose 3,5-epimerase (EC 5.1.3.13)	Rhamnose containing glycans, dTDP-rhamnose synthesis	357633	358178
fig|1504.6.peg.286	CDS	Contig_14	358308	360167	1860	Excinuclease ABC subunit C	DNA repair, UvrABC system	358308	360167
fig|1504.6.peg.287	CDS	Contig_14	360275	361189	915	UDP-N-acetylenolpyruvoylglucosamine reductase (EC 1.1.1.158)	UDP-N-acetylmuramate from Fructose-6-phosphate Biosynthesis	360275	361189
fig|1504.6.peg.288	CDS	Contig_14	361474	362580	1107	Biosynthetic Aromatic amino acid aminotransferase beta (EC 2.6.1.57) @ Histidinol-phosphate aminotransferase (EC 2.6.1.9)	Phenylalanine and Tyrosine Branches from Chorismate	361474	362580
fig|1504.6.peg.289	CDS	Contig_14	362625	363509	885	Hypothetical ATP-binding protein UPF0042, contains P-loop	- none -	362625	363509
fig|1504.6.peg.290	CDS	Contig_14	363506	364855	1350	FIG002813: LPPG:FO 2-phospho-L-lactate transferase like, CofD-like	- none -	363506	364855
fig|1504.6.peg.291	CDS	Contig_14	365220	366113	894	hypothetical protein	- none -	365220	366113

Feature ID	Type	Contig	Start	Stop	Length (bp)	Function	Subsystems	Begin	End
fig|1504.6.peg.292	CDS	Contig_14	367030	366404	627	no significant homology. 6 putative transmembrane regions were found by PSORT.	- none -	366404	367030
fig|1504.6.peg.293	CDS	Contig_14	367573	368292	720	Autolysis response regulater LytR	Murein hydrolase regulation and cell death	367573	368292
fig|1504.6.peg.294	CDS	Contig_14	368621	369220	600	Accessory gene regulator protein C	- none -	368621	369220
fig|1504.6.peg.295	CDS	Contig_14	369348	369770	423	no significant homology Putative N-terminal signal sequence and 3 putative transmembrane regions were found by PSORT.	- none -	369348	369770
fig|1504.6.peg.296	CDS	Contig_14	369871	371025	1155	periplasmic component of efflux system	- none -	369871	371025
fig|1504.6.peg.297	CDS	Contig_14	371028	371702	675	ABC transporter, ATP-binding protein	- none -	371028	371702
fig|1504.6.peg.298	CDS	Contig_14	371702	372910	1209	ABC transporter, permease protein	- none -	371702	372910
fig|1504.6.peg.299	CDS	Contig_14	373094	374044	951	FIG001886: Cytoplasmic hypothetical protein	- none -	373094	374044
fig|1504.6.peg.300	CDS	Contig_14	374065	377625	3561	DNA polymerase III alpha subunit (EC 2.7.7.7)	CBSS-350688.3.peg.1509, DNA-replication	374065	377625
fig|1504.6.peg.301	CDS	Contig_14	378080	379039	960	6-phosphofructokinase (EC 2.7.1.11)	Glycolysis and Gluconeogenesis, N-Acetyl-Galactosamine and Galactosamine Utilization	378080	379039
fig|1504.6.peg.302	CDS	Contig_14	379141	380559	1419	Pyruvate kinase (EC 2.7.1.40)	Entner-Doudoroff Pathway, Glycerate metabolism, Glycolysis and Gluconeogenesis, Pyruvate metabolism I: anaplerotic reactions, PEP	379141	380559
fig|1504.6.peg.303	CDS	Contig_14	381123	381485	363	no significant homology.	- none -	381123	381485
fig|1504.6.peg.304	CDS	Contig_14	381640	383010	1371	RNA methyltransferase, TrmA family	- none -	381640	383010
fig|1504.6.peg.305	CDS	Contig_14	384749	383340	1410	Mobile element protein	- none -	383340	384749
fig|1504.6.peg.306	CDS	Contig_14	385230	389900	4671	cell wall-associated serine proteinase(EC:3.4.21.96)	- none -	385230	389900
fig|1504.6.peg.307	CDS	Contig_14	390357	390875	519	hypothetical protein	- none -	390357	390875

Feature ID	Type	Contig	Start	Stop	Length (bp)	Function	Subsystems	Begin	End
fig|1504.6.peg.308	CDS	Contig_14	390927	391070	144	hypothetical protein	- none -	390927	391070
fig|1504.6.peg.309	CDS	Contig_14	391097	391249	153	hypothetical protein	- none -	391097	391249
fig|1504.6.peg.310	CDS	Contig_14	391300	391920	621	Probable poly(beta-D-mannuronate) O-acetylase (EC 2.3.1.-)	- none -	391300	391920
fig|1504.6.peg.311	CDS	Contig_14	392034	392360	327	Probable poly(beta-D-mannuronate) O-acetylase (EC 2.3.1.-)	- none -	392034	392360
fig|1504.6.peg.312	CDS	Contig_14	392909	393076	168	hypothetical protein	- none -	392909	393076
fig|1504.6.peg.313	CDS	Contig_14	393365	394066	702	Phosphate regulon transcriptional regulatory protein PhoB (SphR)	High affinity phosphate transporter and control of PHO regulon, PhoR-PhoB two-component regulatory system, Phosphate metabolism	393365	394066
fig|1504.6.peg.314	CDS	Contig_14	394209	395648	1440	two-component sensor histidine kinase	- none -	394209	395648
fig|1504.6.peg.315	CDS	Contig_14	395925	397436	1512	Putative amino acid activating enzyme (EC 6.3.2.-)	- none -	395925	397436
fig|1504.6.peg.316	CDS	Contig_14	397440	398627	1188	Diaminopimelate decarboxylase (EC 4.1.1.20)	Lysine Biosynthesis DAP Pathway, Lysine Biosynthesis DAP Pathway, GJO scratch	397440	398627
fig|1504.6.peg.317	CDS	Contig_14	398646	398876	231	hypothetical protein	- none -	398646	398876
fig|1504.6.peg.318	CDS	Contig_14	399162	400463	1302	Probable poly(beta-D-mannuronate) O-acetylase (EC 2.3.1.-)	- none -	399162	400463
fig|1504.6.peg.319	CDS	Contig_14	400476	401426	951	hypothetical protein	- none -	400476	401426
fig|1504.6.peg.320	CDS	Contig_14	402217	403302	1086	diglucosyldiacylglycerol synthase (LTA membrane anchor synthesis)	Teichoic and lipoteichoic acids biosynthesis	402217	403302
fig|1504.6.peg.321	CDS	Contig_14	403400	404002	603	polysaccharide deacetylase	- none -	403400	404002
fig|1504.6.peg.322	CDS	Contig_14	403983	405017	1035	Integral membrane protein	- none -	403983	405017
fig|1504.6.peg.323	CDS	Contig_14	405796	406458	663	ABC transporter ATP-binding protein	- none -	405796	406458
fig|1504.6.peg.324	CDS	Contig_14	406458	407675	1218	ABC-type antimicrobial peptide transport system, permease component	- none -	406458	407675
fig|1504.6.peg.325	CDS	Contig_14	407675	408478	804	hypothetical protein	- none -	407675	408478
fig|1504.6.peg.53	CDS	Contig_14	410663	411868	1206	FIG00516388: hypothetical protein	- none -	410663	411868

Feature ID	Type	Contig	Start	Stop	Length (bp)	Function	Subsystems	Begin	End
fig|1504.6.peg.54	CDS	Contig_14	412067	413626	1560	Glycine betaine transport system permease protein / Glycine betaine-binding protein	- none -	412067	413626
fig|1504.6.peg.55	CDS	Contig_14	413645	414607	963	L-proline glycine betaine ABC transport system permease protein ProV (TC 3.A.1.12.1)	Choline and Betaine Uptake and Betaine Biosynthesis	413645	414607
fig|1504.6.peg.56	CDS	Contig_14	414844	414719	126	hypothetical protein	- none -	414719	414844
fig|1504.6.peg.326	CDS	Contig_15	2248	1970	279	hypothetical protein	- none -	1970	2248
fig|1504.6.peg.327	CDS	Contig_15	3659	2250	1410	Tail length tape measure protein	- none -	2250	3659
fig|1504.6.peg.328	CDS	Contig_15	4360	3662	699	Prophage Lp1 protein 51	- none -	3662	4360
fig|1504.6.peg.329	CDS	Contig_15	6516	4360	2157	Phage tail length tape-measure protein	Phage tail proteins, Phage tail proteins 2	4360	6516
fig|1504.6.peg.330	CDS	Contig_15	7207	6878	330	Phage tail length tape-measure protein	Phage tail proteins, Phage tail proteins 2	6878	7207
fig|1504.6.peg.331	CDS	Contig_15	7415	7278	138	hypothetical protein	- none -	7278	7415
fig|1504.6.peg.332	CDS	Contig_15	7990	7460	531	hypothetical protein	- none -	7460	7990
fig|1504.6.peg.333	CDS	Contig_15	8645	8043	603	FIG00524463: hypothetical protein	- none -	8043	8645
fig|1504.6.peg.334	CDS	Contig_15	9001	8648	354	hypothetical protein	- none -	8648	9001
fig|1504.6.peg.335	CDS	Contig_15	9496	9014	483	FIG00516490: hypothetical protein	- none -	9014	9496
fig|1504.6.peg.336	CDS	Contig_15	9936	9502	435	FIG00514492: hypothetical protein	- none -	9502	9936
fig|1504.6.peg.337	CDS	Contig_15	10292	9933	360	FIG00523471: hypothetical protein	- none -	9933	10292
fig|1504.6.peg.338	CDS	Contig_15	10704	10294	411	FIG00517443: hypothetical protein	- none -	10294	10704
fig|1504.6.peg.339	CDS	Contig_15	10981	10709	273	hypothetical protein	- none -	10709	10981
fig|1504.6.peg.340	CDS	Contig_15	12056	11031	1026	Phage major capsid protein #Fam0021	Phage capsid proteins	11031	12056
fig|1504.6.peg.341	CDS	Contig_15	12446	12075	372	hypothetical protein	- none -	12075	12446
fig|1504.6.peg.342	CDS	Contig_15	13096	12461	636	FIG00515289: hypothetical protein	- none -	12461	13096
fig|1504.6.peg.343	CDS	Contig_15	14372	13638	735	FIG00517164: hypothetical protein	- none -	13638	14372
fig|1504.6.peg.344	CDS	Contig_15	15622	14534	1089	Ribose-phosphate pyrophosphokinase (EC 2.7.6.1)	De Novo Purine Biosynthesis, Pentose phosphate pathway, Transcription repair cluster	14534	15622

Feature ID	Type	Contig	Start	Stop	Length (bp)	Function	Subsystems	Begin	End
fig|1504.6.peg.345	CDS	Contig_15	16536	15847	690	FIG00519969: hypothetical protein	- none -	15847	16536
fig|1504.6.peg.346	CDS	Contig_15	17112	16546	567	Substrate-specific component STY3230 of queuosine-regulated ECF transporter	ECF class transporters, Queuosine-Archaeosine Biosynthesis	16546	17112
fig|1504.6.peg.347	CDS	Contig_15	18110	17133	978	preQ1-regulated inosine-uridine nucleoside hydrolase (EC 3.2.2.1)	Purine conversions, Queuosine-Archaeosine Biosynthesis	17133	18110
fig|1504.6.peg.348	CDS	Contig_15	18721	18491	231	hypothetical protein	- none -	18491	18721
fig|1504.6.peg.349	CDS	Contig_15	20101	19007	1095	TPR repeats containing protein	- none -	19007	20101
fig|1504.6.peg.350	CDS	Contig_15	21934	20207	1728	Phosphoglucosamine mutase (EC 5.4.2.10)	Bacterial checkpoint-control-related cluster, Sialic Acid Metabolism, UDP-N-acetylmuramate from Fructose-6-phosphate Biosynthesis	20207	21934
fig|1504.6.peg.351	CDS	Contig_15	22647	22063	585	LSU ribosomal protein L25p	Ribosome LSU bacterial, Transcription repair cluster	22063	22647
fig|1504.6.peg.352	CDS	Contig_15	24066	22897	1170	D-alanyl-D-alanine carboxypeptidase (EC 3.4.16.4)	CBSS-84588.1.peg.1247, Metallocarboxypeptidases (EC 3.4.17.-), Murein Hydrolases	22897	24066
fig|1504.6.peg.353	CDS	Contig_15	25205	24162	1044	hypothetical protein	- none -	24162	25205
fig|1504.6.peg.354	CDS	Contig_15	25635	25183	453	Purine nucleoside phosphorylase (EC 2.4.2.1)	Adenosyl nucleosidases, Deoxyribose and Deoxynucleoside Catabolism, Purine conversions, pyrimidine conversions	25183	25635
fig|1504.6.peg.355	CDS	Contig_15	28087	25730	2358	Recombination inhibitory protein MutS2	DNA repair, bacterial MutL-MutS system	25730	28087
fig|1504.6.peg.356	CDS	Contig_15	28469	28110	360	hypothetical protein	- none -	28110	28469
fig|1504.6.peg.357	CDS	Contig_15	30831	28483	2349	Protease (EC 3.4.-.-)	- none -	28483	30831
fig|1504.6.peg.358	CDS	Contig_15	32984	31746	1239	Mobile element protein	- none -	31746	32984
fig|1504.6.peg.359	CDS	Contig_15	33758	33114	645	no significant homology	- none -	33114	33758

Feature ID	Type	Contig	Start	Stop	Length (bp)	Function	Subsystems	Begin	End
fig|1504.6.peg.360	CDS	Contig_15	34705	33899	807	FIG028593: membrane protein	- none -	33899	34705
fig|1504.6.peg.361	CDS	Contig_15	37268	34890	2379	Phenylalanyl-tRNA synthetase beta chain (EC 6.1.1.20)	tRNA aminoacylation, Phe	34890	37268
fig|1504.6.peg.362	CDS	Contig_15	38303	37284	1020	Phenylalanyl-tRNA synthetase alpha chain (EC 6.1.1.20)	tRNA aminoacylation, Phe	37284	38303
fig|1504.6.peg.363	CDS	Contig_15	39467	38685	783	FIG011178: rRNA methylase	RNA methylation	38685	39467
fig|1504.6.peg.364	CDS	Contig_15	40147	39479	669	Trk system potassium uptake protein TrkA	Bacterial RNA-metabolizing Zn-dependent hydrolases, Conserved gene cluster associated with Met-tRNA formyltransferase, Potassium homeostasis, Potassium homeostasis	39479	40147
fig|1504.6.peg.365	CDS	Contig_15	41499	40159	1341	Potassium uptake protein, integral membrane component, KtrB	- none -	40159	41499
fig|1504.6.peg.366	CDS	Contig_15	41994	41635	360	LSU ribosomal protein L20p	Mycobacterium virulence operon involved in protein synthesis (LSU ribosomal proteins), Ribosome LSU bacterial	41635	41994
fig|1504.6.peg.367	CDS	Contig_15	42217	42020	198	LSU ribosomal protein L35p	Mycobacterium virulence operon involved in protein synthesis (LSU ribosomal proteins), Ribosome LSU bacterial	42020	42217
fig|1504.6.peg.368	CDS	Contig_15	42760	42239	522	Translation initiation factor 3	Mycobacterium virulence operon involved in protein synthesis (LSU ribosomal proteins), Translation initiation factors bacterial	42239	42760
fig|1504.6.peg.369	CDS	Contig_15	43858	42968	891	FIG01165827: hypothetical protein	- none -	42968	43858
fig|1504.6.peg.370	CDS	Contig_15	43991	44692	702	hypothetical protein	- none -	43991	44692
fig|1504.6.peg.371	CDS	Contig_15	45439	44744	696	tRNA nucleotidyltransferase (EC 2.7.7.21) (EC 2.7.7.25)	tRNA nucleotidyltransferase	44744	45439
fig|1504.6.rna.37	RNA	Contig_15	45564	45635	72	tRNA-Cys-GCA	- none -	45564	45635

Feature ID	Type	Contig	Start	Stop	Length (bp)	Function	Subsystems	Begin	End
fig|1504.6.peg.372	CDS	Contig_15	46247	45756	492	hypothetical protein	- none -	45756	46247
fig|1504.6.peg.373	CDS	Contig_15	47591	46707	885	Chaperonin (heat shock protein 33)	Streptococcus pyogenes recombinatorial zone	46707	47591
fig|1504.6.peg.374	CDS	Contig_15	48443	47619	825	Methyltransferase (EC 2.1.1.-)	- none -	47619	48443
fig|1504.6.peg.375	CDS	Contig_15	48699	48448	252	Small acid-soluble spore protein beta	- none -	48448	48699
fig|1504.6.peg.376	CDS	Contig_15	48924	49913	990	Aspartate-semialdehyde dehydrogenase (EC 1.2.1.11)	Lysine Biosynthesis DAP Pathway, Lysine Biosynthesis DAP Pathway, GJO scratch, Threonine and Homoserine Biosynthesis	48924	49913
fig|1504.6.peg.377	CDS	Contig_15	49944	50825	882	4-hydroxy-tetrahydrodipicolinate synthase (EC 4.3.3.7)	Lysine Biosynthesis DAP Pathway, Lysine Biosynthesis DAP Pathway, GJO scratch	49944	50825
fig|1504.6.peg.378	CDS	Contig_15	50835	51587	753	4-hydroxy-tetrahydrodipicolinate reductase (EC 1.17.1.8)	Lysine Biosynthesis DAP Pathway, Lysine Biosynthesis DAP Pathway, GJO scratch	50835	51587
fig|1504.6.peg.379	CDS	Contig_15	52271	51621	651	Mobile element protein	- none -	51621	52271
fig|1504.6.peg.380	CDS	Contig_15	52868	52431	438	Mobile element protein	- none -	52431	52868
fig|1504.6.peg.381	CDS	Contig_15	53254	53406	153	conserved hypothetical protein	- none -	53254	53406
fig|1504.6.peg.382	CDS	Contig_15	54408	53617	792	Mobile element protein	- none -	53617	54408
fig|1504.6.peg.383	CDS	Contig_15	56189	54546	1644	Oligopeptide ABC transporter, periplasmic oligopeptide-binding protein OppA (TC 3.A.1.5.1)	ABC transporter oligopeptide (TC 3.A.1.5.1), Sex pheromones in Enterococcus faecalis and other Firmicutes	54546	56189
fig|1504.6.peg.384	CDS	Contig_15	57227	56250	978	Oligopeptide transport ATP-binding protein OppF (TC 3.A.1.5.1)	ABC transporter oligopeptide (TC 3.A.1.5.1)	56250	57227
fig|1504.6.peg.385	CDS	Contig_15	58234	57227	1008	Oligopeptide transport ATP-binding protein OppD (TC 3.A.1.5.1)	ABC transporter oligopeptide (TC 3.A.1.5.1)	57227	58234
fig|1504.6.peg.386	CDS	Contig_15	59192	58248	945	Oligopeptide transport system permease protein OppC (TC 3.A.1.5.1)	ABC transporter oligopeptide (TC 3.A.1.5.1)	58248	59192
fig|1504.6.peg.387	CDS	Contig_15	60125	59208	918	Oligopeptide transport system permease protein OppB (TC 3.A.1.5.1)	ABC transporter oligopeptide (TC 3.A.1.5.1)	59208	60125

Feature ID	Type	Contig	Start	Stop	Length (bp)	Function	Subsystems	Begin	End
fig|1504.6.peg.388	CDS	Contig_15	61356	60685	672	Single-stranded DNA-binding protein	DNA repair, bacterial, DNA repair, bacterial RecFOR pathway	60685	61356
fig|1504.6.peg.389	CDS	Contig_15	62229	61471	759	Polysaccharide deacetylase	Polysaccharide deacetylases	61471	62229
fig|1504.6.peg.390	CDS	Contig_15	62361	62894	534	no significant homology	- none -	62361	62894
fig|1504.6.peg.391	CDS	Contig_15	63769	62891	879	Surface antigen	- none -	62891	63769
fig|1504.6.peg.392	CDS	Contig_15	63969	64214	246	no significant homology.	- none -	63969	64214
fig|1504.6.peg.393	CDS	Contig_15	65399	64257	1143	ATP-dependent RNA helicase YfmL	ATP-dependent RNA helicases, bacterial	64257	65399
fig|1504.6.peg.394	CDS	Contig_15	66180	65491	690	N-acetylmuramoyl-L-alanine amidase (EC 3.5.1.28)	Murein Hydrolases, Recycling of Peptidoglycan Amino Acids	65491	66180
fig|1504.6.peg.395	CDS	Contig_15	67257	66322	936	Ribonuclease Z (EC 3.1.26.11)	tRNA processing	66322	67257
fig|1504.6.peg.396	CDS	Contig_15	68067	67360	708	Purine nucleoside phosphorylase (EC 2.4.2.1)	Adenosyl nucleosidases, Deoxyribose and Deoxynucleoside Catabolism, Purine conversions, pyrimidine conversions	67360	68067
fig|1504.6.peg.397	CDS	Contig_15	69531	68218	1314	Dihydrofolate synthase (EC 6.3.2.12) / Folylpolyglutamate synthase (EC 6.3.2.17)	Folate Biosynthesis, Folate Biosynthesis	68218	69531
fig|1504.6.peg.398	CDS	Contig_15	69721	70152	432	no significant homology	- none -	69721	70152
fig|1504.6.peg.399	CDS	Contig_15	73057	70415	2643	Valyl-tRNA synthetase (EC 6.1.1.9)	tRNA aminoacylation, Val	70415	73057
fig|1504.6.peg.400	CDS	Contig_15	73688	73521	168	conserved hypothetical protein	- none -	73521	73688
fig|1504.6.peg.401	CDS	Contig_15	73829	73704	126	hypothetical protein	- none -	73704	73829
fig|1504.6.peg.402	CDS	Contig_15	74911	73964	948	Hypothetical sugar kinase in cluster with indigoidine synthase indA , PfkB family of kinases	- none -	73964	74911
fig|1504.6.peg.403	CDS	Contig_15	75176	75532	357	TPR repeats containing protein	- none -	75176	75532
fig|1504.6.peg.404	CDS	Contig_15	76614	75544	1071	Transglutaminase-like enzyme, putative cysteine protease	- none -	75544	76614

Feature ID	Type	Contig	Start	Stop	Length (bp)	Function	Subsystems	Begin	End
fig|1504.6.peg.405	CDS	Contig_15	77264	76626	639	regulatory protein RecX	- none -	76626	77264
fig|1504.6.peg.406	CDS	Contig_15	78519	77281	1239	probable zinc protease	- none -	77281	78519
fig|1504.6.peg.407	CDS	Contig_15	78907	79584	678	Phosphate regulon transcriptional regulatory protein PhoB (SphR)	High affinity phosphate transporter and control of PHO regulon, PhoR-PhoB two-component regulatory system, Phosphate metabolism	78907	79584
fig|1504.6.peg.408	CDS	Contig_15	79565	81085	1521	sensor histidine kinase	- none -	79565	81085
fig|1504.6.peg.409	CDS	Contig_15	81261	81124	138	hypothetical protein	- none -	81124	81261
fig|1504.6.peg.410	CDS	Contig_15	82595	81390	1206	Na+/H+-exchanging protein	- none -	81390	82595
fig|1504.6.peg.411	CDS	Contig_15	84111	82768	1344	Mg/Co/Ni transporter MgtE / CBS domain	Magnesium transport	82768	84111
fig|1504.6.peg.412	CDS	Contig_15	86678	84495	2184	DNA topoisomerase III (EC 5.99.1.2)	DNA processing cluster, DNA topoisomerases, Type I, ATP-independent	84495	86678
fig|1504.6.peg.413	CDS	Contig_15	87377	86826	552	hypothetical protein	- none -	86826	87377
fig|1504.6.peg.414	CDS	Contig_15	87677	87528	150	hypothetical protein	- none -	87528	87677
fig|1504.6.peg.415	CDS	Contig_15	88129	87779	351	hypothetical protein	- none -	87779	88129
fig|1504.6.peg.416	CDS	Contig_15	89164	88295	870	hypothetical protein	- none -	88295	89164
fig|1504.6.peg.417	CDS	Contig_15	89844	89176	669	RNA polymerase sigma-54 factor RpoN	Flagellar motility, Flagellum, Transcription initiation, bacterial sigma factors	89176	89844
fig|1504.6.peg.418	CDS	Contig_15	90698	89955	744	3-oxoacyl-[acyl-carrier protein] reductase (EC 1.1.1.100)	Fatty Acid Biosynthesis FASII	89955	90698
fig|1504.6.peg.419	CDS	Contig_15	91647	90715	933	Microsomal dipeptidase (EC 3.4.13.19)	- none -	90715	91647
fig|1504.6.peg.420	CDS	Contig_15	92622	91660	963	Conserved protein	- none -	91660	92622
fig|1504.6.peg.421	CDS	Contig_15	92772	93929	1158	probable secreted protein homolog of yjcM/yhbB B. subtilis	- none -	92772	93929
fig|1504.6.peg.422	CDS	Contig_15	94930	93968	963	Ribosomal RNA small subunit methyltransferase B (EC 2.1.1.-)	- none -	93968	94930

Feature ID	Type	Contig	Start	Stop	Length (bp)	Function	Subsystems	Begin	End
fig|1504.6.peg.423	CDS	Contig_15	95790	94984	807	Cobalt-zinc-cadmium resistance protein	Cobalt-zinc-cadmium resistance	94984	95790
fig|1504.6.peg.424	CDS	Contig_15	96864	96112	753	Exodeoxyribonuclease III (EC 3.1.11.2)	DNA repair, bacterial	96112	96864
fig|1504.6.peg.425	CDS	Contig_15	98416	96947	1470	Methyl-accepting chemotaxis protein	- none -	96947	98416
fig|1504.6.peg.426	CDS	Contig_15	98573	99478	906	radical activating enzyme	- none -	98573	99478
fig|1504.6.peg.427	CDS	Contig_15	100986	99529	1458	Catalase (EC 1.11.1.6)	Oxidative stress, Protection from Reactive Oxygen Species	99529	100986
fig|1504.6.peg.428	CDS	Contig_15	102348	101116	1233	Serine hydroxymethyltransferase (EC 2.1.2.1)	5-FCL-like protein, Glycine Biosynthesis, Glycine and Serine Utilization, Serine-glyoxylate cycle, Serine Biosynthesis	101116	102348
fig|1504.6.peg.429	CDS	Contig_15	103245	103481	237	Mobile element protein	- none -	103245	103481
fig|1504.6.peg.430	CDS	Contig_15	103927	104691	765	Integral membrane protein	- none -	103927	104691
fig|1504.6.peg.431	CDS	Contig_15	104694	105155	462	Membrane spanning protein	- none -	104694	105155
fig|1504.6.peg.432	CDS	Contig_15	106548	105193	1356	Putative sodium-dependent transporter	- none -	105193	106548
fig|1504.6.peg.433	CDS	Contig_15	110577	106933	3645	Cell wall-associated murein hydrolase LytC	- none -	106933	110577
fig|1504.6.peg.434	CDS	Contig_15	111094	110822	273	FIG00513547: hypothetical protein	- none -	110822	111094
fig|1504.6.peg.435	CDS	Contig_15	111266	112432	1167	NADH-dependent butanol dehydrogenase A (EC 1.1.1.-)	Butanol Biosynthesis	111266	112432
fig|1504.6.peg.436	CDS	Contig_15	115041	112606	2436	ATP-dependent DNA helicase RecQ	DNA-replication, DNA repair, bacterial RecFOR pathway	112606	115041
fig|1504.6.peg.437	CDS	Contig_15	115541	116275	735	putative histidinol phosphatase and related hydrolases of the PHP family	- none -	115541	116275
fig|1504.6.peg.438	CDS	Contig_15	118116	116329	1788	Aspartyl-tRNA synthetase (EC 6.1.1.12)	tRNA aminoacylation, Asp and Asn	116329	118116
fig|1504.6.peg.439	CDS	Contig_15	119380	118133	1248	Histidyl-tRNA synthetase (EC 6.1.1.21)	tRNA aminoacylation, His	118133	119380
fig|1504.6.peg.440	CDS	Contig_15	120250	119393	858	Hypothetical radical SAM family enzyme, NOT coproporphyrinogen III oxidase, oxygen-independent	Heat shock dnaK gene cluster extended, Heme and Siroheme Biosynthesis	119393	120250

Feature ID	Type	Contig	Start	Stop	Length (bp)	Function	Subsystems	Begin	End
fig|1504.6.peg.441	CDS	Contig_5	1173	1589	417	Transcriptional regulator, MarR family	- none -	1173	1589
fig|1504.6.peg.442	CDS	Contig_5	1607	2962	1356	Multi antimicrobial extrusion protein (Na(+)/drug antiporter), MATE family of MDR efflux pumps	Multidrug Resistance Efflux Pumps, Riboflavin, FMN and FAD metabolism in plants	1607	2962
fig|1504.6.peg.443	CDS	Contig_5	3248	3063	186	FIG00513841: hypothetical protein	- none -	3063	3248
fig|1504.6.peg.444	CDS	Contig_5	3371	3946	576	Spore maturation protein A	Spore Core Dehydration	3371	3946
fig|1504.6.peg.445	CDS	Contig_5	3964	4488	525	Spore maturation protein B	Spore Core Dehydration	3964	4488
fig|1504.6.peg.446	CDS	Contig_5	4638	4856	219	hypothetical protein	- none -	4638	4856
fig|1504.6.peg.447	CDS	Contig_5	4861	5541	681	Hcp transcriptional regulator HcpR (Crp/Fnr family)	Nitrosative stress	4861	5541
fig|1504.6.peg.448	CDS	Contig_5	5647	7287	1641	Hydroxylamine reductase (EC 1.7.-.-)	Nitrosative stress	5647	7287
fig|1504.6.peg.449	CDS	Contig_5	8565	7354	1212	Proton/glutamate symport protein @ Sodium/glutamate symport protein	- none -	7354	8565
fig|1504.6.peg.450	CDS	Contig_5	8834	9274	441	ACT domain-containing protein	- none -	8834	9274
fig|1504.6.peg.451	CDS	Contig_5	9296	10564	1269	Xaa-Pro aminopeptidase (EC 3.4.11.9)	Aminopeptidases (EC 3.4.11.-)	9296	10564
fig|1504.6.peg.452	CDS	Contig_5	10991	12733	1743	Na+/H+ antiporter	- none -	10991	12733
fig|1504.6.peg.453	CDS	Contig_5	12868	14634	1767	Xaa-Pro aminopeptidase (EC 3.4.11.9)	Aminopeptidases (EC 3.4.11.-)	12868	14634
fig|1504.6.peg.454	CDS	Contig_5	15210	14689	522	hypothetical protein	- none -	14689	15210
fig|1504.6.peg.455	CDS	Contig_5	15789	15256	534	hypothetical protein	- none -	15256	15789
fig|1504.6.peg.456	CDS	Contig_5	15956	16315	360	hypothetical protein	- none -	15956	16315
fig|1504.6.peg.457	CDS	Contig_5	16687	18630	1944	Methionyl-tRNA synthetase (EC 6.1.1.10)	tRNA aminoacylation, Met	16687	18630
fig|1504.6.peg.458	CDS	Contig_5	19962	18856	1107	Mobile element protein	- none -	18856	19962
fig|1504.6.peg.459	CDS	Contig_5	20002	21630	1629	Methionyl-tRNA synthetase, clostridial paralog	tRNA aminoacylation, Met	20002	21630
fig|1504.6.peg.460[2]	CDS	Contig_5	21851	22636	786	Putative deoxyribonuclease YcfH	YcfH	21851	22636
fig|1504.6.peg.461	CDS	Contig_5	22907	23956	1050	Cell wall-binding protein	- none -	22907	23956
fig|1504.6.peg.462	CDS	Contig_5	24084	24638	555	Ribonuclease M5 (EC 3.1.26.8)	Ribosome biogenesis bacterial	24084	24638

Feature ID	Type	Contig	Start	Stop	Length (bp)	Function	Subsystems	Begin	End
fig|1504.6.peg.463	CDS	Contig_5	24640	25482	843	SSU rRNA (adenine(1518)-N(6)/adenine(1519)-N(6))-dimethyltransferase (EC 2.1.1.182)	RNA methylation, Ribosome biogenesis bacterial	24640	25482
fig|1504.6.peg.464	CDS	Contig_5	25646	27019	1374	FIG00513411: hypothetical protein	- none -	25646	27019
fig|1504.6.peg.465	CDS	Contig_5	27126	27602	477	Conserved membrane-associated protein	- none -	27126	27602
fig|1504.6.peg.466	CDS	Contig_5	27737	28573	837	Conserved protein	- none -	27737	28573
fig|1504.6.peg.467	CDS	Contig_5	28588	29427	840	Mrp protein	- none -	28588	29427
fig|1504.6.peg.468	CDS	Contig_5	29492	29680	189	Ferredoxin	Soluble cytochromes and functionally related electron carriers	29492	29680
fig|1504.6.peg.469	CDS	Contig_5	30376	29735	642	Substrate-specific component ThiT of thiamin ECF transporter	ECF class transporters, Thiamin biosynthesis	29735	30376
fig|1504.6.peg.470	CDS	Contig_5	30776	30570	207	hypothetical protein	- none -	30570	30776
fig|1504.6.peg.471	CDS	Contig_5	31727	30885	843	DegV family protein	- none -	30885	31727
fig|1504.6.peg.472	CDS	Contig_5	32363	31908	456	Transcriptional regulator PadR-like	- none -	31908	32363
fig|1504.6.peg.473	CDS	Contig_5	33210	32365	846	DegV family protein	- none -	32365	33210
fig|1504.6.peg.474	CDS	Contig_5	34375	33377	999	BH0638 unknown conserved protein	- none -	33377	34375
fig|1504.6.peg.475	CDS	Contig_5	34633	36750	2118	Ribonucleotide reductase of class III (anaerobic), large subunit (EC 1.17.4.2)	Ribonucleotide reduction	34633	36750
fig|1504.6.peg.476	CDS	Contig_5	37219	38382	1164	Homocitrate synthase (EC 2.3.3.14)	- none -	37219	38382
fig|1504.6.peg.477	CDS	Contig_5	38419	40338	1920	Aconitate hydratase (EC 4.2.1.3)	Serine-glyoxylate cycle	38419	40338
fig|1504.6.peg.478	CDS	Contig_5	40565	41074	510	Ribonucleotide reductase of class III (anaerobic), activating protein (EC 1.97.1.4)	Ribonucleotide reduction	40565	41074
fig|1504.6.peg.479	CDS	Contig_5	41311	41883	573	Xanthine phosphoribosyltransferase (EC 2.4.2.22)	Purine conversions, Xanthine Metabolism in Bacteria	41311	41883
fig|1504.6.peg.480	CDS	Contig_5	42169	43647	1479	Cytosol aminopeptidase PepA (EC 3.4.11.1)	Aminopeptidases (EC 3.4.11.-)	42169	43647
fig|1504.6.peg.481	CDS	Contig_5	44797	43793	1005	Transcriptional regulator, AraC family	- none -	43793	44797
fig|1504.6.peg.482	CDS	Contig_5	45081	46034	954	Ferrichrome-binding periplasmic protein precursor (TC 3.A.1.14.3)	- none -	45081	46034

Feature ID	Type	Contig	Start	Stop	Length (bp)	Function	Subsystems	Begin	End
fig|1504.6.peg.483	CDS	Contig_5	46018	47010	993	ABC-type Fe3+-siderophore transport system, permease component	- none -	46018	47010
fig|1504.6.peg.484	CDS	Contig_5	47010	48017	1008	ABC-type Fe3+-siderophore transport system, permease 2 component	- none -	47010	48017
fig|1504.6.peg.485	CDS	Contig_5	48020	48814	795	Ferrichrome transport ATP-binding protein FhuC (TC 3.A.1.14.3)	- none -	48020	48814
fig|1504.6.peg.486	CDS	Contig_5	48811	50073	1263	ABC transporter, permease protein, putative	- none -	48811	50073
fig|1504.6.peg.487	CDS	Contig_5	50714	51538	825	membrane protein	- none -	50714	51538
fig|1504.6.peg.488	CDS	Contig_5	51528	52397	870	hypothetical protein	- none -	51528	52397
fig|1504.6.peg.489	CDS	Contig_5	52390	53202	813	hypothetical protein	- none -	52390	53202
fig|1504.6.peg.490	CDS	Contig_5	53225	53878	654	ABC transporter, ATP-binding protein	- none -	53225	53878
fig|1504.6.peg.491	CDS	Contig_5	55437	54043	1395	Asparaginyl-tRNA synthetase (EC 6.1.1.22)	tRNA aminoacylation, Asp and Asn	54043	55437
fig|1504.6.peg.492	CDS	Contig_5	55833	56522	690	Cytochrome b5	- none -	55833	56522
fig|1504.6.peg.493	CDS	Contig_5	57265	56570	696	FIG00515497: hypothetical protein	- none -	56570	57265
fig|1504.6.peg.494	CDS	Contig_5	57417	58493	1077	probable proline dipeptidase	- none -	57417	58493
fig|1504.6.peg.495	CDS	Contig_5	59798	58575	1224	Nucleoside permease NupC	- none -	58575	59798
fig|1504.6.peg.496	CDS	Contig_5	60753	59935	819	Purine nucleoside phosphorylase (EC 2.4.2.1)	Adenosyl nucleosidases, Deoxyribose and Deoxynucleoside Catabolism, Purine conversions, pyrimidine conversions	59935	60753
fig|1504.6.peg.497	CDS	Contig_5	62554	61181	1374	UDP-N-acetylmuramate--alanine ligase (EC 6.3.2.8)	Peptidoglycan biosynthesis--gjo, cell division cluster containing FtsQ	61181	62554
fig|1504.6.peg.498	CDS	Contig_5	62875	63318	444	PurR: transcription regulator associated with purine metabolism	De Novo Purine Biosynthesis	62875	63318
fig|1504.6.peg.499	CDS	Contig_5	63433	63690	258	PurR: transcription regulator associated with purine metabolism	De Novo Purine Biosynthesis	63433	63690

Feature ID	Type	Contig	Start	Stop	Length (bp)	Function	Subsystems	Begin	End
fig|1504.6.peg.500	CDS	Contig_5	63826	64110	285	Protein of unknown function identified by role in sporulation (SpoVG)	Sporulation-associated proteins with broader functions	63826	64110
fig|1504.6.peg.501	CDS	Contig_5	64320	65690	1371	N-acetylglucosamine-1-phosphate uridyltransferase (EC 2.7.7.23) / Glucosamine-1-phosphate N-acetyltransferase (EC 2.3.1.157)	Sialic Acid Metabolism, Sialic Acid Metabolism, Transcription repair cluster, Transcription repair cluster, UDP-N-acetylmuramate from Fructose-6-phosphate Biosynthesis, UDP-N-acetylmuramate from Fructose-6-phosphate Biosynthesis	64320	65690
fig|1504.6.peg.502	CDS	Contig_5	65745	66704	960	Ribose-phosphate pyrophosphokinase (EC 2.7.6.1)	De Novo Purine Biosynthesis, Pentose phosphate pathway, Transcription repair cluster	65745	66704
fig|1504.6.peg.503	CDS	Contig_5	66886	67572	687	Response regulator (CheY-like receiver domain and HTH-type DNA-binding domain)	- none -	66886	67572
fig|1504.6.peg.504	CDS	Contig_5	67572	68990	1419	Phosphate regulon sensor protein PhoR (SphS) (EC 2.7.13.3)	High affinity phosphate transporter and control of PHO regulon, PhoR-PhoB two-component regulatory system, Phosphate metabolism	67572	68990
fig|1504.6.peg.505	CDS	Contig_5	69011	70138	1128	Serine protease, DegP/HtrA, do-like (EC 3.4.21.-)	- none -	69011	70138
fig|1504.6.peg.506	CDS	Contig_5	70282	70857	576	Peptidyl-tRNA hydrolase (EC 3.1.1.29)	Cell division-ribosomal stress proteins cluster, Sporulation-associated proteins with broader functions, Transcription repair cluster, Translation termination factors bacterial	70282	70857

Feature ID	Type	Contig	Start	Stop	Length (bp)	Function	Subsystems	Begin	End
fig|1504.6.peg.507	CDS	Contig_5	70878	74390	3513	Transcription-repair coupling factor	Cell division-ribosomal stress proteins cluster, DNA-replication, Sporulation Cluster, Transcription factors bacterial, Transcription repair cluster	70878	74390
fig|1504.6.peg.508	CDS	Contig_5	74489	75466	978	Foldase protein PrsA precursor (EC 5.2.1.8)	Peptidyl-prolyl cis-trans isomerase	74489	75466
fig|1504.6.peg.509	CDS	Contig_5	75606	76154	549	Stage V sporulation protein T, AbrB family transcriptional regulator (SpoVT)	Sporulation Cluster, Sporulation gene orphans	75606	76154
fig|1504.6.peg.510	CDS	Contig_5	76262	77797	1536	Stage V sporulation protein B	Sporulation gene orphans	76262	77797
fig|1504.6.peg.511	CDS	Contig_5	77817	79277	1461	possible tetrapyrrole methyltransferase domain / Nucleoside triphosphate pyrophosphohydrolase MazG (EC 3.6.1.8)	Nucleoside triphosphate pyrophosphohydrolase MazG, Sporulation Cluster, Sporulation Cluster	77817	79277
fig|1504.6.peg.512	CDS	Contig_5	79496	79771	276	DNA-binding protein HBsu	DNA structural proteins, bacterial	79496	79771
fig|1504.6.peg.513	CDS	Contig_5	79832	80092	261	Ribosome-associated heat shock protein implicated in the recycling of the 50S subunit (S4 paralog)	Cell division-ribosomal stress proteins cluster, DNA replication cluster 1, Heat shock dnaK gene cluster extended, Sporulation Cluster	79832	80092
fig|1504.6.peg.514	CDS	Contig_5	80145	80438	294	FIG007421: forespore shell protein	Sporulation Cluster	80145	80438
fig|1504.6.peg.515	CDS	Contig_5	80444	80833	390	Spore cortex biosynthesis protein	Cell division-ribosomal stress proteins cluster, Sporulation Cluster	80444	80833
fig|1504.6.peg.516	CDS	Contig_5	81010	81201	192	Cell division protein DivIC (FtsB), stabilizes FtsL against RasP cleavage	Bacterial Cell Division, Bacterial Cytoskeleton, Cell division-ribosomal stress proteins cluster, Sporulation Cluster, Stationary phase repair cluster	81010	81201
fig|1504.6.peg.517	CDS	Contig_5	81283	81696	414	RNA binding protein, contains ribosomal protein S1 domain	Cell division-ribosomal stress proteins cluster, Sporulation Cluster	81283	81696

Feature ID	Type	Contig	Start	Stop	Length (bp)	Function	Subsystems	Begin	End
fig|1504.6.rna.38	RNA	Contig_5	81966	82049	84	tRNA-Leu-TAA	- none -	81966	82049
fig|1504.6.rna.39	RNA	Contig_5	82076	82148	73	tRNA-Met-CAT	- none -	82076	82148
fig|1504.6.rna.40	RNA	Contig_5	82159	82232	74	tRNA-Met-CAT	- none -	82159	82232
fig|1504.6.peg.518	CDS	Contig_5	83047	85434	2388	Stage II sporulation serine phosphatase for sigma-F activation (SpoIIE)	Sporulation Cluster, Sporulation gene orphans	83047	85434
fig|1504.6.peg.519	CDS	Contig_5	85585	86976	1392	tRNA(Ile)-lysidine synthetase (EC 6.3.4.19)	Cell division-ribosomal stress proteins cluster, Folate biosynthesis cluster, tRNA processing, tRNAmodification position 34	85585	86976
fig|1504.6.peg.520	CDS	Contig_5	86981	87517	537	Hypoxanthine-guanine phosphoribosyltransferase (EC 2.4.2.8)	Cell division-ribosomal stress proteins cluster, Folate biosynthesis cluster, Purine conversions	86981	87517
fig|1504.6.peg.521	CDS	Contig_5	87570	89372	1803	Cell division protein FtsH (EC 3.4.24.-)	Bacterial Cell Division, Cell division-ribosomal stress proteins cluster, Folate biosynthesis cluster	87570	89372
fig|1504.6.peg.522	CDS	Contig_5	89673	91343	1671	Formate--tetrahydrofolate ligase (EC 6.3.4.3)	5-FCL-like protein, One-carbon metabolism by tetrahydropterines, Serine-glyoxylate cycle	89673	91343
fig|1504.6.peg.523	CDS	Contig_5	91478	92257	780	Pantothenate kinase type III, CoaX-like (EC 2.7.1.33)	Coenzyme A Biosynthesis, Coenzyme A Biosynthesis cluster	91478	92257
fig|1504.6.peg.524	CDS	Contig_5	92264	93235	972	tRNA dihydrouridine synthase B (EC 1.-.-.-)	- none -	92264	93235
fig|1504.6.peg.525	CDS	Contig_5	93449	93931	483	Transcription elongation factor GreA	Transcription factors bacterial	93449	93931
fig|1504.6.peg.526	CDS	Contig_5	93945	95456	1512	Lysyl-tRNA synthetase (class II) (EC 6.1.1.6)	tRNA aminoacylation, Lys	93945	95456
fig|1504.6.rna.41	RNA	Contig_5	95726	95797	72	tRNA-Asn-GTT	- none -	95726	95797
fig|1504.6.rna.42	RNA	Contig_5	95833	95904	72	tRNA-Asn-GTT	- none -	95833	95904
fig|1504.6.peg.527	CDS	Contig_5	96276	97667	1392	Glycyl-tRNA synthetase (EC 6.1.1.14)	CBSS-349161.4.peg.2427, tRNA aminoacylation, Gly	96276	97667

Feature ID	Type	Contig	Start	Stop	Length (bp)	Function	Subsystems	Begin	End
fig|1504.6.peg.528	CDS	Contig_5	97923	99302	1380	UDP-N-acetylmuramoylalanine--D-glutamate ligase (EC 6.3.2.9)	Peptidoglycan biosynthesis--gjo	97923	99302
fig|1504.6.peg.529	CDS	Contig_5	100341	99349	993	Basic protein	- none -	99349	100341
fig|1504.6.rna.43	RNA	Contig_5	100821	102395	1575	Small Subunit Ribosomal RNA; ssuRNA; SSU rRNA	- none -	100821	102395
fig|1504.6.rna.44	RNA	Contig_5	102438	102510	73	tRNA-Ala-TGC	- none -	102438	102510
fig|1504.6.rna.45	RNA	Contig_5	102517	102590	74	tRNA-Ile-GAT	- none -	102517	102590
fig|1504.6.rna.46	RNA	Contig_5	105197	105313	117	5S RNA	- none -	105197	105313
fig|1504.6.rna.47	RNA	Contig_5	105319	105391	73	tRNA-Phe-GAA	- none -	105319	105391
fig|1504.6.rna.48	RNA	Contig_5	105400	105470	71	tRNA-Cys-GCA	- none -	105400	105470
fig|1504.6.peg.530	CDS	Contig_5	106443	105508	936	Muramoyltetrapeptide carboxypeptidase (EC 3.4.17.13)	Metallocarboxypeptidases (EC 3.4.17.-), Murein Hydrolases, Recycling of Peptidoglycan Amino Acids	105508	106443
fig|1504.6.peg.531	CDS	Contig_5	107485	106538	948	Zinc transport protein ZntB	- none -	106538	107485
fig|1504.6.peg.532	CDS	Contig_5	107763	108266	504	hypothetical protein	- none -	107763	108266
fig|1504.6.peg.533	CDS	Contig_5	109447	108296	1152	Catalyzes the cleavage of p-aminobenzoyl-glutamate to p-aminobenzoate and glutamate, subunit A	- none -	108296	109447
fig|1504.6.peg.534	CDS	Contig_5	109586	109804	219	hypothetical protein	- none -	109586	109804
fig|1504.6.peg.535	CDS	Contig_5	109821	110453	633	Thymidylate kinase (EC 2.7.4.9)	CBSS-393133.3.peg.2787, pyrimidine conversions	109821	110453
fig|1504.6.peg.536	CDS	Contig_5	110537	110866	330	protein from nitrogen regulatory protein P-II (GLNB) family, ortholog YAAQ B. subtilis	CBSS-393133.3.peg.2787	110537	110866
fig|1504.6.peg.537	CDS	Contig_5	110884	111816	933	DNA polymerase III delta prime subunit (EC 2.7.7.7)	DNA-replication	110884	111816
fig|1504.6.peg.538	CDS	Contig_5	111819	112724	906	Signal peptidase-like protein	Heat shock dnaK gene cluster extended	111819	112724
fig|1504.6.peg.539	CDS	Contig_5	112736	112939	204	Predicted metal-binding protein of ferredoxin fold	- none -	112736	112939
fig|1504.6.peg.540	CDS	Contig_5	113050	113220	171	Ferredoxin	Soluble cytochromes and functionally related electron carriers	113050	113220

Feature ID	Type	Contig	Start	Stop	Length (bp)	Function	Subsystems	Begin	End
fig|1504.6.peg.541	CDS	Contig_5	113925	113293	633	Zn-dependent hydrolases of the metallo-beta-lactamase superfamily	- none -	113293	113925
fig|1504.6.peg.542	CDS	Contig_5	114137	114592	456	Transcriptional regulator CtsR	Proteolysis in bacteria, ATP-dependent	114137	114592
fig|1504.6.peg.543	CDS	Contig_5	114661	117114	2454	ATP-dependent Clp protease, ATP-binding subunit ClpC / Negative regulator of genetic competence clcC/mecB	Proteolysis in bacteria, ATP-dependent	114661	117114
fig|1504.6.peg.544	CDS	Contig_5	117448	118389	942	Thioredoxin reductase (EC 1.8.1.9)	Thioredoxin-disulfide reductase, pyrimidine conversions	117448	118389
fig|1504.6.peg.545	CDS	Contig_5	118391	118618	228	conserved hypothetical protein	- none -	118391	118618
fig|1504.6.peg.546	CDS	Contig_5	118656	120119	1464	Non-phosphorylating glyceraldehyde-3-phosphate dehydrogenase (NADP) (EC 1.2.1.9)	Entner-Doudoroff Pathway, Glycolysis and Gluconeogenesis	118656	120119
fig|1504.6.peg.547	CDS	Contig_5	120386	120159	228	Glutaredoxin	Glutaredoxins, Glutathione: Redox cycle, Phage DNA synthesis	120159	120386
fig|1504.6.peg.548	CDS	Contig_5	120693	120532	162	hypothetical protein	- none -	120532	120693
fig|1504.6.peg.549	CDS	Contig_5	120822	121544	723	Predicted transcriptional regulator of N-Acetylglucosamine utilization, GntR family	Chitin and N-acetylglucosamine utilization	120822	121544
fig|1504.6.peg.550	CDS	Contig_5	121541	122272	732	Glucosamine-6-phosphate deaminase (EC 3.5.99.6)	Chitin and N-acetylglucosamine utilization, Sialic Acid Metabolism	121541	122272
fig|1504.6.peg.551	CDS	Contig_5	122439	123806	1368	DNA repair protein RadA	DNA repair, bacterial, Proteolysis in bacteria, ATP-dependent	122439	123806
fig|1504.6.peg.552	CDS	Contig_5	123823	124887	1065	DNA integrity scanning protein disA	- none -	123823	124887
fig|1504.6.peg.553	CDS	Contig_5	125366	124968	399	FIG00895125: hypothetical protein	- none -	124968	125366
fig|1504.6.peg.554	CDS	Contig_5	125667	126752	1086	Membrane-associated protein containing RNA-binding TRAM domain and ribonuclease PIN-domain, YacL B.subtilis ortholog	Proteolysis in bacteria, ATP-dependent	125667	126752

Feature ID	Type	Contig	Start	Stop	Length (bp)	Function	Subsystems	Begin	End
fig|1504.6.peg.555	CDS	Contig_5	126769	127443	675	2-C-methyl-D-erythritol 4-phosphate cytidylyltransferase (EC 2.7.7.60)	Isoprenoid Biosynthesis, Nonmevalonate Branch of Isoprenoid Biosynthesis, Stationary phase repair cluster, Teichoic and lipoteichoic acids biosynthesis	126769	127443
fig|1504.6.peg.556	CDS	Contig_5	127786	129498	1713	Prolyl-tRNA synthetase (EC 6.1.1.15), bacterial type	tRNA aminoacylation, Pro	127786	129498
fig|1504.6.peg.557	CDS	Contig_5	129510	130910	1401	Cysteinyl-tRNA synthetase (EC 6.1.1.16)	Conserved gene cluster possibly involved in RNA metabolism, tRNA aminoacylation, Cys	129510	130910
fig|1504.6.peg.558	CDS	Contig_5	130958	131374	417	COG1939: Ribonuclease III family protein	Conserved gene cluster possibly involved in RNA metabolism	130958	131374
fig|1504.6.peg.559	CDS	Contig_5	131402	132325	924	23S rRNA (guanosine-2'-O-) - methyltransferase rlmB (EC 2.1.1.-)	RNA methylation	131402	132325
fig|1504.6.peg.560	CDS	Contig_5	132351	132863	513	Hypothetical protein DUF901, similar to C-terminal domain of ribosome protection-type Tc-resistance proteins	Conserved gene cluster possibly involved in RNA metabolism	132351	132863
fig|1504.6.peg.561	CDS	Contig_5	132934	133578	645	RNA polymerase sporulation specific sigma factor SigH	Conserved gene cluster possibly involved in RNA metabolism, Sporulation-associated proteins with broader functions, Transcription initiation, bacterial sigma factors	132934	133578
fig|1504.6.rna.49	RNA	Contig_5	133661	133733	73	tRNA-Thr-GGT	- none -	133661	133733
fig|1504.6.peg.562	CDS	Contig_5	133833	135026	1194	Translation elongation factor Tu	Mycobacterium virulence operon involved in protein synthesis (SSU ribosomal proteins), Translation elongation factors bacterial, Universal GTPases	133833	135026

Feature ID	Type	Contig	Start	Stop	Length (bp)	Function	Subsystems	Begin	End
fig|1504.6.peg.563	CDS	Contig_5	135404	135637	234	Preprotein translocase subunit SecE (TC 3.A.5.1.1)	LSU ribosomal proteins cluster	135404	135637
fig|1504.6.peg.564	CDS	Contig_5	135671	136192	522	Transcription antitermination protein NusG	LSU ribosomal proteins cluster, Transcription factors bacterial	135671	136192
fig|1504.6.peg.565	CDS	Contig_5	136268	136693	426	LSU ribosomal protein L11p (L12e)	LSU ribosomal proteins cluster, Ribosome LSU bacterial	136268	136693
fig|1504.6.peg.566	CDS	Contig_5	136746	137435	690	LSU ribosomal protein L1p (L10Ae)	LSU ribosomal proteins cluster, Ribosome LSU bacterial	136746	137435
fig|1504.6.peg.567	CDS	Contig_5	137644	138147	504	LSU ribosomal protein L10p (P0)	LSU ribosomal proteins cluster, Ribosome LSU bacterial	137644	138147
fig|1504.6.peg.568	CDS	Contig_5	138181	138549	369	LSU ribosomal protein L7/L12 (P1/P2)	LSU ribosomal proteins cluster, Ribosome LSU bacterial	138181	138549
fig|1504.6.peg.569	CDS	Contig_5	138910	142620	3711	DNA-directed RNA polymerase beta subunit (EC 2.7.7.6)	Mycobacterium virulence operon involved in DNA transcription, RNA polymerase bacterial	138910	142620
fig|1504.6.peg.570	CDS	Contig_5	142642	146172	3531	DNA-directed RNA polymerase beta' subunit (EC 2.7.7.6)	Mycobacterium virulence operon involved in DNA transcription, RNA polymerase bacterial	142642	146172
fig|1504.6.peg.571	CDS	Contig_5	146472	146852	381	SSU ribosomal protein S12p (S23e)	Mycobacterium virulence operon involved in protein synthesis (SSU ribosomal proteins), Ribosomal protein S12p Asp methylthiotransferase, Ribosome SSU bacterial	146472	146852

Feature ID	Type	Contig	Start	Stop	Length (bp)	Function	Subsystems	Begin	End
fig|1504.6.peg.572	CDS	Contig_5	146995	147465	471	SSU ribosomal protein S7p (S5e)	Mycobacterium virulence operon involved in protein synthesis (SSU ribosomal proteins), Ribosome SSU bacterial	146995	147465
fig|1504.6.peg.573	CDS	Contig_5	147540	149600	2061	Translation elongation factor G	Mycobacterium virulence operon involved in protein synthesis (SSU ribosomal proteins), Tetracycline resistance, ribosome protection type, Tetracycline resistance, ribosome protection type, too, Translation elongation factor G family, Translation elongation factors bacterial, Universal GTPases	147540	149600
fig|1504.6.peg.574	CDS	Contig_5	149787	150980	1194	Translation elongation factor Tu	Mycobacterium virulence operon involved in protein synthesis (SSU ribosomal proteins), Translation elongation factors bacterial, Universal GTPases	149787	150980
fig|1504.6.peg.575	CDS	Contig_5	152954	153262	309	SSU ribosomal protein S10p (S20e)	Ribosome SSU bacterial	152954	153262
fig|1504.6.peg.576	CDS	Contig_5	153340	153969	630	LSU ribosomal protein L3p (L3e)	Ribosome LSU bacterial	153340	153969
fig|1504.6.peg.577	CDS	Contig_5	153993	154613	621	LSU ribosomal protein L4p (L1e)	Ribosome LSU bacterial	153993	154613
fig|1504.6.peg.578	CDS	Contig_5	154613	154909	297	LSU ribosomal protein L23p (L23Ae)	Ribosome LSU bacterial	154613	154909
fig|1504.6.peg.579	CDS	Contig_5	154973	155806	834	LSU ribosomal protein L2p (L8e)	Ribosome LSU bacterial	154973	155806
fig|1504.6.peg.580	CDS	Contig_5	155875	156159	285	SSU ribosomal protein S19p (S15e)	Ribosome SSU bacterial	155875	156159
fig|1504.6.peg.581	CDS	Contig_5	156181	156516	336	LSU ribosomal protein L22p (L17e)	Ribosome LSU bacterial	156181	156516
fig|1504.6.peg.582	CDS	Contig_5	156536	157204	669	SSU ribosomal protein S3p (S3e)	Ribosome SSU bacterial	156536	157204
fig|1504.6.peg.583	CDS	Contig_5	157222	157656	435	LSU ribosomal protein L16p (L10e)	Ribosome LSU bacterial	157222	157656
fig|1504.6.peg.584	CDS	Contig_5	157656	157868	213	LSU ribosomal protein L29p (L35e)	Ribosome LSU bacterial	157656	157868
fig|1504.6.peg.585	CDS	Contig_5	157891	158145	255	SSU ribosomal protein S17p (S11e)	Ribosome SSU bacterial	157891	158145

Feature ID	Type	Contig	Start	Stop	Length (bp)	Function	Subsystems	Begin	End
fig|1504.6.peg.586	CDS	Contig_5	158231	158542	312	LSU ribosomal protein L14p (L23e)	Ribosome LSU bacterial	158231	158542
fig|1504.6.peg.587	CDS	Contig_5	158560	158874	315	LSU ribosomal protein L24p (L26e)	Ribosome LSU bacterial	158560	158874
fig|1504.6.peg.588	CDS	Contig_5	158897	159439	543	LSU ribosomal protein L5p (L11e)	Ribosome LSU bacterial	158897	159439
fig|1504.6.peg.589	CDS	Contig_5	159455	159640	186	SSU ribosomal protein S14p (S29e) @ SSU ribosomal protein S14p (S29e), zinc-dependent	Ribosome SSU bacterial, Ribosome SSU bacterial	159455	159640
fig|1504.6.peg.590	CDS	Contig_5	159670	160068	399	SSU ribosomal protein S8p (S15Ae)	Ribosome SSU bacterial	159670	160068
fig|1504.6.peg.591	CDS	Contig_5	160135	160677	543	LSU ribosomal protein L6p (L9e)	Ribosome LSU bacterial	160135	160677
fig|1504.6.peg.592	CDS	Contig_5	160698	161060	363	LSU ribosomal protein L18p (L5e)	Ribosome LSU bacterial	160698	161060
fig|1504.6.peg.593	CDS	Contig_5	161080	161577	498	SSU ribosomal protein S5p (S2e)	Ribosomal protein S5p acylation, Ribosome SSU bacterial	161080	161577
fig|1504.6.peg.594	CDS	Contig_5	161590	161769	180	LSU ribosomal protein L30p (L7e)	Ribosome LSU bacterial	161590	161769
fig|1504.6.peg.595	CDS	Contig_5	161792	162232	441	LSU ribosomal protein L15p (L27Ae)	Ribosome LSU bacterial	161792	162232
fig|1504.6.peg.596	CDS	Contig_5	162234	163508	1275	Preprotein translocase secY subunit (TC 3.A.5.1.1)	- none -	162234	163508
fig|1504.6.peg.597	CDS	Contig_5	163531	164181	651	Adenylate kinase (EC 2.7.4.3)	Purine conversions	163531	164181
fig|1504.6.peg.598	CDS	Contig_5	164181	164930	750	Methionine aminopeptidase (EC 3.4.11.18)	CBSS-312309.3.peg.1965, Translation termination factors bacterial	164181	164930
fig|1504.6.peg.599	CDS	Contig_5	164982	165293	312	FIG00513560: hypothetical protein	- none -	164982	165293
fig|1504.6.peg.600	CDS	Contig_5	165301	165519	219	Translation initiation factor 1	Translation initiation factors bacterial	165301	165519
fig|1504.6.peg.601	CDS	Contig_5	165565	165678	114	LSU ribosomal protein L36p	Ribosome LSU bacterial	165565	165678
fig|1504.6.peg.602	CDS	Contig_5	165896	166261	366	SSU ribosomal protein S13p (S18e)	Ribosome SSU bacterial	165896	166261
fig|1504.6.peg.603	CDS	Contig_5	166277	166672	396	SSU ribosomal protein S11p (S14e)	Ribosome SSU bacterial	166277	166672
fig|1504.6.peg.604	CDS	Contig_5	166696	167316	621	SSU ribosomal protein S4p (S9e)	Ribosome SSU bacterial	166696	167316
fig|1504.6.peg.605	CDS	Contig_5	167419	168366	948	DNA-directed RNA polymerase alpha subunit (EC 2.7.7.6)	RNA polymerase bacterial	167419	168366
fig|1504.6.peg.606	CDS	Contig_5	168382	168723	342	LSU ribosomal protein L17p	Ribosome LSU bacterial	168382	168723

Feature ID	Type	Contig	Start	Stop	Length (bp)	Function	Subsystems	Begin	End
fig|1504.6.peg.607	CDS	Contig_5	169041	169886	846	ATPase component of general energizing module of ECF transporters	ECF class transporters	169041	169886
fig|1504.6.peg.608	CDS	Contig_5	169871	170731	861	ATPase component of general energizing module of ECF transporters	ECF class transporters	169871	170731
fig|1504.6.peg.609	CDS	Contig_5	170747	171550	804	Transmembrane component of general energizing module of ECF transporters	ECF class transporters	170747	171550
fig|1504.6.peg.610	CDS	Contig_5	171579	172319	741	tRNA pseudouridine synthase A (EC 4.2.1.70)	RNA pseudouridine syntheses, tRNA processing	171579	172319
fig|1504.6.peg.611	CDS	Contig_5	172482	172916	435	LSU ribosomal protein L13p (L13Ae)	Ribosome LSU bacterial	172482	172916
fig|1504.6.peg.612	CDS	Contig_5	172942	173334	393	SSU ribosomal protein S9p (S16e)	Ribosome SSU bacterial	172942	173334
fig|1504.6.peg.613	CDS	Contig_5	173534	175150	1617	Sodium-dependent phosphate transporter	NhaA, NhaD and Sodium-dependent phosphate transporters, Phosphate metabolism	173534	175150
fig|1504.6.peg.614	CDS	Contig_5	175299	176528	1230	hypothetical protein	- none -	175299	176528
fig|1504.6.peg.615	CDS	Contig_5	176543	176734	192	hypothetical protein	- none -	176543	176734
fig|1504.6.peg.616	CDS	Contig_5	176913	177602	690	N-acetylmuramoyl-L-alanine amidase (EC 3.5.1.28)	Murein Hydrolases, Recycling of Peptidoglycan Amino Acids	176913	177602
fig|1504.6.peg.617	CDS	Contig_5	177783	178625	843	Fumarate hydratase class I, aerobic (EC 4.2.1.2); L(+)-tartrate dehydratase alpha subunit (EC 4.2.1.32)	Muconate lactonizing enzyme family, Serine-glyoxylate cycle	177783	178625
fig|1504.6.peg.618	CDS	Contig_5	178644	179201	558	Fumarate hydratase class I, aerobic (EC 4.2.1.2); L(+)-tartrate dehydratase beta subunit (EC 4.2.1.32)	Muconate lactonizing enzyme family, Serine-glyoxylate cycle	178644	179201
fig|1504.6.peg.619	CDS	Contig_5	180226	179366	861	protein of unknown function DUF161	- none -	179366	180226
fig|1504.6.peg.620	CDS	Contig_5	180419	181114	696	DNA-binding response regulator	- none -	180419	181114
fig|1504.6.peg.621	CDS	Contig_5	181098	182873	1776	two-component sensor histidine kinase	- none -	181098	182873
fig|1504.6.peg.622	CDS	Contig_5	182931	183281	351	Arsenate reductase (EC 1.20.4.1)	Anaerobic respiratory reductases, Transcription repair cluster	182931	183281
fig|1504.6.peg.623	CDS	Contig_5	183492	185723	2232	Ribonucleotide reductase of class Ia (aerobic), alpha subunit (EC 1.17.4.1)	Ribonucleotide reduction	183492	185723

Feature ID	Type	Contig	Start	Stop	Length (bp)	Function	Subsystems	Begin	End
fig|1504.6.peg.624	CDS	Contig_5	185759	186793	1035	Ribonucleotide reductase of class Ia (aerobic), beta subunit (EC 1.17.4.1)	Ribonucleotide reduction	185759	186793
fig|1504.6.peg.625	CDS	Contig_5	187161	186862	300	conserved hypothetical protein	- none -	186862	187161
fig|1504.6.peg.626	CDS	Contig_5	187517	189136	1620	Phosphoenolpyruvate-protein phosphotransferase of PTS system (EC 2.7.3.9)	Fructose utilization	187517	189136
fig|1504.6.peg.627	CDS	Contig_5	189267	189803	537	Chromate transport protein	- none -	189267	189803
fig|1504.6.peg.628	CDS	Contig_5	189804	190328	525	Chromate transport protein	- none -	189804	190328
fig|1504.6.peg.629	CDS	Contig_5	190349	191512	1164	TPR-repeat-containing protein	- none -	190349	191512
fig|1504.6.peg.630	CDS	Contig_5	191530	192705	1176	Isoaspartyl dipeptidase (EC 3.4.19.5) @ Asp-X dipeptidase	Cyanophycin Metabolism, Protein degradation, Protein degradation	191530	192705
fig|1504.6.peg.631	CDS	Contig_5	193333	192746	588	Spore cortex-lytic enzyme precursor	- none -	192746	193333
fig|1504.6.peg.632	CDS	Contig_5	194400	193411	990	hypothetical protein	- none -	193411	194400
fig|1504.6.peg.633	CDS	Contig_5	194565	195422	858	Diadenylate cyclase spyDAC; Bacterial checkpoint controller DisA with nucleotide-binding domain	Bacterial checkpoint-control-related cluster, Bacterial checkpoint-control-related cluster	194565	195422
fig|1504.6.peg.634	CDS	Contig_5	195503	196639	1137	Uncharacterized secreted protein associated with spyDAC	Bacterial checkpoint-control-related cluster	195503	196639
fig|1504.6.peg.635	CDS	Contig_5	196812	198410	1599	NAD(FAD)-utilizing dehydrogenase, sll0175 homolog	- none -	196812	198410
fig|1504.6.peg.636	CDS	Contig_5	198631	199536	906	phosphotransbutyrylase (EC 2.3.1.19)	- none -	198631	199536
fig|1504.6.peg.637	CDS	Contig_5	199560	200630	1071	Butyrate kinase (EC 2.7.2.7)	- none -	199560	200630
fig|1504.6.peg.638	CDS	Contig_5	200801	201634	834	HTH DNA-binding protein	- none -	200801	201634
fig|1504.6.peg.639	CDS	Contig_5	201728	202024	297	His repressor	CBSS-393121.3.peg.1913	201728	202024
fig|1504.6.peg.640	CDS	Contig_5	202164	203507	1344	Phosphoglucosamine mutase (EC 5.4.2.10)	Bacterial checkpoint-control-related cluster, Sialic Acid Metabolism, UDP-N-acetylmuramate from Fructose-6-phosphate Biosynthesis	202164	203507
fig|1504.6.peg.641	CDS	Contig_5	204990	205556	567	Adenosine deaminase (EC 3.5.4.4)	Purine conversions	204990	205556

Feature ID	Type	Contig	Start	Stop	Length (bp)	Function	Subsystems	Begin	End
fig|1504.6.peg.642	CDS	Contig_5	206436	205606	831	MSM (multiple sugar metabolism) operon regulatory protein	Fructooligosaccharides(FOS) and Raffinose Utilization	205606	206436
fig|1504.6.peg.643	CDS	Contig_5	206808	208283	1476	Agmatine/putrescine antiporter, associated with agmatine catabolism	Polyamine Metabolism	206808	208283
fig|1504.6.peg.644	CDS	Contig_5	208310	211393	3084	Evolved beta-D-galactosidase, alpha subunit	Lactose utilization	208310	211393
fig|1504.6.peg.645	CDS	Contig_5	211798	211977	180	hypothetical protein	- none -	211798	211977
fig|1504.6.peg.646	CDS	Contig_5	212205	212624	420	no significant homology	- none -	212205	212624
fig|1504.6.peg.647	CDS	Contig_5	212833	213507	675	ABC transporter ATP-binding protein MJ0796	- none -	212833	213507
fig|1504.6.peg.648	CDS	Contig_5	213520	214455	936	hypothetical protein	- none -	213520	214455
fig|1504.6.peg.649	CDS	Contig_5	214458	215753	1296	FIG00525744: hypothetical protein	- none -	214458	215753
fig|1504.6.peg.650	CDS	Contig_5	215889	216353	465	hypothetical protein	- none -	215889	216353
fig|1504.6.peg.651	CDS	Contig_5	216456	216701	246	COG2827: putative endonuclease containing a URI domain	- none -	216456	216701
fig|1504.6.peg.652	CDS	Contig_5	216770	217315	546	hypothetical protein	- none -	216770	217315
fig|1504.6.peg.653	CDS	Contig_5	218041	219867	1827	Glucosamine--fructose-6-phosphate aminotransferase [isomerizing] (EC 2.6.1.16)	Sialic Acid Metabolism, UDP-N-acetylmuramate from Fructose-6-phosphate Biosynthesis	218041	219867
fig|1504.6.peg.654	CDS	Contig_5	219903	220064	162	hypothetical protein	- none -	219903	220064
fig|1504.6.peg.655	CDS	Contig_5	220290	222665	2376	Two-component sensor histidine kinase	- none -	220290	222665
fig|1504.6.peg.656	CDS	Contig_5	222777	223433	657	membrane protein	- none -	222777	223433
fig|1504.6.peg.657	CDS	Contig_5	224250	223513	738	NAD-dependent protein deacetylase of SIR2 family	Pyruvate metabolism II: acetyl-CoA, acetogenesis from pyruvate, Redox-dependent regulation of nucleus processes	223513	224250
fig|1504.6.peg.658	CDS	Contig_5	224398	224757	360	hypothetical protein	- none -	224398	224757
fig|1504.6.peg.659	CDS	Contig_5	224960	225073	114	hypothetical protein	- none -	224960	225073
fig|1504.6.peg.660	CDS	Contig_5	225213	226736	1524	hypothetical protein	- none -	225213	226736

Feature ID	Type	Contig	Start	Stop	Length (bp)	Function	Subsystems	Begin	End
fig|1504.6.peg.661	CDS	Contig_5	227262	226777	486	FIG018171: hypothetical protein of Cupin superfamily	- none -	226777	227262
fig|1504.6.peg.662	CDS	Contig_5	227441	228274	834	HAD hydrolase, IIB family	- none -	227441	228274
fig|1504.6.peg.663	CDS	Contig_5	228705	228301	405	Protein erfK/srfK precursor	- none -	228301	228705
fig|1504.6.peg.664	CDS	Contig_5	228740	228871	132	hypothetical protein	- none -	228740	228871
fig|1504.6.peg.665	CDS	Contig_5	229165	229803	639	Transcriptional regulators of sugar metabolism	- none -	229165	229803
fig|1504.6.peg.666	CDS	Contig_5	229930	231339	1410	Mobile element protein	- none -	229930	231339
fig|1504.6.rna.50	RNA	Contig_5	231493	231421	73	tRNA-Met-CAT	- none -	231421	231493
fig|1504.6.rna.51	RNA	Contig_5	231584	231512	73	tRNA-Met-CAT	- none -	231512	231584
fig|1504.6.peg.667	CDS	Contig_5	231919	232482	564	5-formyltetrahydrofolate cyclo-ligase (EC 6.3.3.2)	5-FCL-like protein, Folate Biosynthesis, One-carbon metabolism by tetrahydropterines, Serine-glyoxylate cycle	231919	232482
fig|1504.6.peg.668	CDS	Contig_5	232857	235304	2448	Putative isomerase	- none -	232857	235304
fig|1504.6.peg.669	CDS	Contig_5	235432	235809	378	transcriptional regulator, ArsR family/dinitrogenase iron-molybdenum cofactor family protein	- none -	235432	235809
fig|1504.6.peg.670	CDS	Contig_5	235812	236183	372	transcriptional regulator, ArsR family/dinitrogenase iron-molybdenum cofactor family protein	- none -	235812	236183
fig|1504.6.peg.671	CDS	Contig_5	238213	236276	1938	Threonyl-tRNA synthetase (EC 6.1.1.3)	tRNA aminoacylation, Thr	236276	238213
fig|1504.6.rna.52	RNA	Contig_5	238653	238733	81	tRNA-Leu-TAG	- none -	238653	238733
fig|1504.6.rna.53	RNA	Contig_5	238752	238823	72	tRNA-Gly-GCC	- none -	238752	238823
fig|1504.6.peg.672	CDS	Contig_5	239342	238932	411	Conserved protein	- none -	238932	239342
fig|1504.6.peg.673	CDS	Contig_5	239615	240217	603	no significant homology	- none -	239615	240217
fig|1504.6.rna.54	RNA	Contig_5	240283	240353	71	tRNA-Gly-TCC	- none -	240283	240353
fig|1504.6.rna.55	RNA	Contig_5	240360	240432	73	tRNA-Lys-CTT	- none -	240360	240432
fig|1504.6.peg.674	CDS	Contig_5	240818	242095	1278	Methionine transporter MetT	Methionine Biosynthesis, Methionine Degradation	240818	242095

Feature ID	Type	Contig	Start	Stop	Length (bp)	Function	Subsystems	Begin	End
fig|1504.6.peg.675	CDS	Contig_5	242593	242111	483	2-C-methyl-D-erythritol 2,4-cyclodiphosphate synthase (EC 4.6.1.12)	Isoprenoid Biosynthesis, Nonmevalonate Branch of Isoprenoid Biosynthesis, Stationary phase repair cluster	242111	242593
fig|1504.6.peg.676	CDS	Contig_5	242953	243540	588	Sortase A, LPXTG specific	Heme, hemin uptake and utilization systems in GramPositives, Sortase	242953	243540
fig|1504.6.peg.677	CDS	Contig_5	243559	244608	1050	FIG00513300: hypothetical protein	- none -	243559	244608
fig|1504.6.peg.678	CDS	Contig_5	244592	245371	780	Ribosomal large subunit pseudouridine synthase F (EC 4.2.1.70)	RNA pseudouridine syntheses	244592	245371
fig|1504.6.peg.679	CDS	Contig_5	246000	246488	489	Conserved protein	- none -	246000	246488
fig|1504.6.peg.680	CDS	Contig_5	246511	247887	1377	Aldehyde dehydrogenase (EC 1.2.1.3)	Glycerolipid and Glycerophospholipid Metabolism in Bacteria, Methylglyoxal Metabolism, Methylglyoxal Metabolism, Pyruvate metabolism II: acetyl-CoA, acetogenesis from pyruvate	246511	247887
fig|1504.6.peg.681	CDS	Contig_5	250580	247914	2667	Probable cation-transporting ATPase	- none -	247914	250580
fig|1504.6.peg.682	CDS	Contig_5	250929	251996	1068	Mannose-1-phosphate guanylyltransferase (GDP) (EC 2.7.7.22)	Mannose Metabolism	250929	251996
fig|1504.6.peg.683	CDS	Contig_5	252224	252817	594	FIG00516726: hypothetical protein	- none -	252224	252817
fig|1504.6.peg.684	CDS	Contig_5	253021	253380	360	Cadmium efflux system accessory protein	Cadmium resistance	253021	253380
fig|1504.6.peg.685	CDS	Contig_5	253396	255630	2235	Lead, cadmium, zinc and mercury transporting ATPase (EC 3.6.3.3) (EC 3.6.3.5); Copper-translocating P-type ATPase (EC 3.6.3.4)	Copper Transport System, Copper homeostasis	253396	255630
fig|1504.6.peg.686	CDS	Contig_5	256162	256821	660	Redox-sensitive transcriptional regulator (AT-rich DNA-binding protein)	Oxidative stress	256162	256821
fig|1504.6.peg.687	CDS	Contig_5	257088	257870	783	3-hydroxybutyryl-CoA dehydratase (EC 4.2.1.55)	Polyhydroxybutyrate metabolism	257088	257870
fig|1504.6.peg.688	CDS	Contig_5	257955	259094	1140	Butyryl-CoA dehydrogenase (EC 1.3.99.2)	- none -	257955	259094
fig|1504.6.peg.689	CDS	Contig_5	259114	259893	780	Electron transfer flavoprotein, beta subunit	- none -	259114	259893

Feature ID	Type	Contig	Start	Stop	Length (bp)	Function	Subsystems	Begin	End
fig|1504.6.peg.690	CDS	Contig_5	259915	260922	1008	Electron transfer flavoprotein, alpha subunit	- none -	259915	260922
fig|1504.6.peg.691	CDS	Contig_5	261037	261885	849	3-hydroxybutyryl-CoA dehydrogenase (EC 1.1.1.157)	Butanol Biosynthesis, Polyhydroxybutyrate metabolism	261037	261885
fig|1504.6.peg.692	CDS	Contig_5	262006	262437	432	conserved hypothetical protein	- none -	262006	262437
fig|1504.6.peg.693	CDS	Contig_5	262527	263471	945	8-oxoguanine-DNA-glycosylase	- none -	262527	263471
fig|1504.6.peg.694	CDS	Contig_5	263669	264625	957	Kinase similar to eukaryotic-like N-acetylglucosamine kinase	- none -	263669	264625
fig|1504.6.peg.695	CDS	Contig_5	264911	265648	738	Predicted transcriptional regulator of N-Acetylglucosamine utilization, GntR family	Chitin and N-acetylglucosamine utilization	264911	265648
fig|1504.6.peg.696	CDS	Contig_5	265726	266889	1164	Galactosamine-6-phosphate isomerase (EC 5.3.1.-)	N-Acetyl-Galactosamine and Galactosamine Utilization	265726	266889
fig|1504.6.peg.697	CDS	Contig_5	266934	267365	432	PTS system, hyaluronate-oligosaccharide-specific IIA component (EC 2.7.1.69)	- none -	266934	267365
fig|1504.6.peg.698	CDS	Contig_5	267392	268249	858	Tagatose 1,6-bisphosphate aldolase (EC 4.1.2.40)	N-Acetyl-Galactosamine and Galactosamine Utilization	267392	268249
fig|1504.6.peg.699	CDS	Contig_5	268274	269611	1338	Tagatose-6-phosphate kinase AgaZ (EC 2.7.1.144)	N-Acetyl-Galactosamine and Galactosamine Utilization	268274	269611
fig|1504.6.peg.700	CDS	Contig_5	269830	271323	1494	Periplasmic [Fe] hydrogenase (EC 1.12.7.2)	- none -	269830	271323
fig|1504.6.peg.701	CDS	Contig_5	271434	272135	702	Alkaline phosphatase like protein	Phosphate metabolism	271434	272135
fig|1504.6.peg.702	CDS	Contig_5	272451	272735	285	Heat shock protein 60 family co-chaperone GroES	GroEL GroES	272451	272735
fig|1504.6.peg.703	CDS	Contig_5	272752	274377	1626	Heat shock protein 60 family chaperone GroEL	GroEL GroES	272752	274377
fig|1504.6.peg.704	CDS	Contig_5	274554	274970	417	prokaryotic N- methylation motif domain protein	- none -	274554	274970
fig|1504.6.peg.705	CDS	Contig_5	275059	275814	756	Leader peptidase (Prepilin peptidase) (EC 3.4.23.43) / N-methyltransferase (EC 2.1.1.-)	- none -	275059	275814
fig|1504.6.peg.706	CDS	Contig_5	276128	277579	1452	Inosine-5'-monophosphate dehydrogenase (EC 1.1.1.205)	Purine conversions, Purine salvage cluster	276128	277579
fig|1504.6.peg.707	CDS	Contig_5	277752	279284	1533	GMP synthase [glutamine-hydrolyzing] (EC 6.3.5.2)	Purine conversions	277752	279284
fig|1504.6.peg.708	CDS	Contig_5	279511	280863	1353	Glucose-6-phosphate isomerase (EC 5.3.1.9)	Glycolysis and Gluconeogenesis	279511	280863
fig|1504.6.peg.709	CDS	Contig_5	280863	281306	444	UPF0178 protein CA_C2825	- none -	280863	281306

Feature ID	Type	Contig	Start	Stop	Length (bp)	Function	Subsystems	Begin	End
fig|1504.6.peg.710	CDS	Contig_5	281462	283474	2013	spoIID-like domain containing protein, peptidoglycan-binding domain	- none -	281462	283474
fig|1504.6.peg.711	CDS	Contig_5	283529	284275	747	Membrane-bound lytic murein transglycosylase D precursor (EC 3.2.1.-)	CBSS-228410.1.peg.134, CBSS-342610.3.peg.1536, Murein Hydrolases	283529	284275
fig|1504.6.peg.712	CDS	Contig_5	284456	285172	717	Ribosomal small subunit pseudouridine synthase A (EC 4.2.1.70)	RNA pseudouridine syntheses	284456	285172
fig|1504.6.peg.713	CDS	Contig_5	285537	286124	588	Transcriptional regulator, TetR family	- none -	285537	286124
fig|1504.6.peg.714	CDS	Contig_5	286377	287204	828	hypothetical protein	- none -	286377	287204
fig|1504.6.peg.715	CDS	Contig_5	287522	287893	372	hypothetical protein	- none -	287522	287893
fig|1504.6.peg.716	CDS	Contig_5	287953	289002	1050	Macrolide export ATP-binding/permease protein MacB (EC 3.6.3.-)	Multidrug Resistance Efflux Pumps	287953	289002
fig|1504.6.peg.717	CDS	Contig_5	289014	290276	1263	ABC transporter, permease protein	- none -	289014	290276
fig|1504.6.peg.718	CDS	Contig_5	290276	290938	663	ABC transporter, ATP-binding protein	- none -	290276	290938
fig|1504.6.peg.719	CDS	Contig_5	291192	293426	2235	ATP-dependent DNA helicase UvrD/PcrA	CBSS-393121.3.peg.1913, DNA repair, bacterial UvrD and related helicases	291192	293426
fig|1504.6.peg.720	CDS	Contig_5	293523	295514	1992	DNA ligase (EC 6.5.1.2)	CBSS-393121.3.peg.1913, DNA Repair Base Excision	293523	295514
fig|1504.6.peg.721	CDS	Contig_5	295521	295808	288	hypothetical protein	- none -	295521	295808
fig|1504.6.peg.722	CDS	Contig_5	296174	295875	300	hypothetical protein	- none -	295875	296174
fig|1504.6.peg.723	CDS	Contig_5	296330	297829	1500	Oligopeptide ABC transporter, periplasmic oligopeptide-binding protein OppA (TC 3.A.1.5.1)	ABC transporter oligopeptide (TC 3.A.1.5.1), Sex pheromones in Enterococcus faecalis and other Firmicutes	296330	297829
fig|1504.6.peg.724	CDS	Contig_5	299532	297874	1659	Conserved protein	- none -	297874	299532
fig|1504.6.peg.725	CDS	Contig_5	299628	300377	750	Ribonuclease PH (EC 2.7.7.56)	Heat shock dnaK gene cluster extended, tRNA processing	299628	300377
fig|1504.6.peg.726	CDS	Contig_5	300380	300991	612	Nucleoside 5-triphosphatase RdgB (dHAPTP, dITP, XTP-specific) (EC 3.6.1.15)	Heat shock dnaK gene cluster extended, Housecleaning nucleoside triphosphate pyrophosphatases	300380	300991
fig|1504.6.peg.727	CDS	Contig_5	301001	301483	483	FIG009886: phosphoesterase	Heat shock dnaK gene cluster extended	301001	301483

Feature ID	Type	Contig	Start	Stop	Length (bp)	Function	Subsystems	Begin	End
fig|1504.6.rna.56	RNA	Contig_5	301653	301725	73	tRNA-Pro-TGG	- none -	301653	301725
fig|1504.6.rna.57	RNA	Contig_5	301744	301814	71	tRNA-Gly-TCC	- none -	301744	301814
fig|1504.6.peg.728	CDS	Contig_5	303594	304220	627	Cytoplasmic copper homeostasis protein cutC	- none -	303594	304220
fig|1504.6.peg.729	CDS	Contig_5	304351	304473	123	hypothetical protein	- none -	304351	304473
fig|1504.6.peg.730	CDS	Contig_5	304487	305599	1113	Pullulanase (EC 3.2.1.41)	Maltose and Maltodextrin Utilization	304487	305599
fig|1504.6.peg.731	CDS	Contig_5	305699	305995	297	pullulanase, type I	- none -	305699	305995
fig|1504.6.rna.58	RNA	Contig_5	306142	306069	74	tRNA-Arg-TCG	- none -	306069	306142
fig|1504.6.rna.59	RNA	Contig_5	307898	310802	2905	Large Subunit Ribosomal RNA; lsuRNA; LSU rRNA	- none -	307898	310802
fig|1504.6.rna.60	RNA	Contig_5	310909	310980	72	tRNA-Asn-GTT	- none -	310909	310980
fig|1504.6.peg.732	CDS	Contig_5	311275	312213	939	Peptidoglycan N-acetylglucosamine deacetylase (EC 3.5.1.-)	Polysaccharide deacetylases	311275	312213
fig|1504.6.peg.733	CDS	Contig_5	312319	312999	681	Two-component response regulator	- none -	312319	312999
fig|1504.6.peg.734	CDS	Contig_5	312987	314393	1407	Osmosensitive K+ channel histidine kinase KdpD (EC 2.7.3.-)	Potassium homeostasis	312987	314393
fig|1504.6.peg.735	CDS	Contig_5	314399	315886	1488	Conserved protein	- none -	314399	315886
fig|1504.6.peg.736	CDS	Contig_5	315888	317267	1380	TldD protein, part of TldE/TldD proteolytic complex	CBSS-354.1.peg.2917, Putative TldE-TldD proteolytic complex	315888	317267
fig|1504.6.peg.737	CDS	Contig_5	317279	318622	1344	TldE protein, part of TldE/TldD proteolytic complex	Putative TldE-TldD proteolytic complex	317279	318622
fig|1504.6.peg.738	CDS	Contig_5	320675	318810	1866	Lipoteichoic acid synthase LtaS Type IVb	Polyglycerolphosphate lipoteichoic acid biosynthesis	318810	320675
fig|1504.6.peg.739	CDS	Contig_5	320895	321845	951	Sarcosine oxidase alpha subunit (EC 1.5.3.1)	Choline and Betaine Uptake and Betaine Biosynthesis	320895	321845
fig|1504.6.peg.740	CDS	Contig_5	322453	321881	573	Arylesterase precursor (EC 3.1.1.2)	- none -	321881	322453
fig|1504.6.peg.741	CDS	Contig_5	323095	322469	627	Possible Zn-finger containing protein	- none -	322469	323095

Feature ID	Type	Contig	Start	Stop	Length (bp)	Function	Subsystems	Begin	End
fig|1504.6.peg.742	CDS	Contig_5	323327	324337	1011	TsaD/Kae1/Qri7 protein, required for threonylcarbamoyladenosine t(6)A37 formation in tRNA	Bacterial RNA-metabolizing Zn-dependent hydrolases, Conserved gene cluster associated with Met-tRNA formyltransferase, Macromolecular synthesis operon, YgjD and YeaZ	323327	324337
fig|1504.6.peg.743	CDS	Contig_5	324369	325391	1023	hydrolase, alpha/beta fold family	- none -	324369	325391
fig|1504.6.peg.744	CDS	Contig_5	325551	326798	1248	Serine protease, DegP/HtrA, do-like (EC 3.4.21.-)	- none -	325551	326798
fig|1504.6.peg.745	CDS	Contig_5	326987	327286	300	PTS system, cellobiose-specific IIB component (EC 2.7.1.69)	Beta-Glucoside Metabolism	326987	327286
fig|1504.6.peg.746	CDS	Contig_5	327390	327806	417	FIG00522025: hypothetical protein	- none -	327390	327806
fig|1504.6.peg.747	CDS	Contig_5	327925	329004	1080	Ethanolamine permease	Ethanolamine utilization	327925	329004
fig|1504.6.peg.748	CDS	Contig_5	330108	329071	1038	Hypothetical similar to thiamin biosynthesis lipoprotein ApbE	Sex pheromones in Enterococcus faecalis and other Firmicutes	329071	330108
fig|1504.6.peg.749	CDS	Contig_5	330624	330208	417	Putative pheromone precursor lipoprotein	Sex pheromones in Enterococcus faecalis and other Firmicutes	330208	330624
fig|1504.6.peg.750	CDS	Contig_5	330960	331343	384	hypothetical protein	- none -	330960	331343
fig|1504.6.peg.751	CDS	Contig_5	331354	331866	513	Heptaprenyl diphosphate synthase component I (EC 2.5.1.30)	Isoprenoinds for Quinones, Polyprenyl Diphosphate Biosynthesis, Sex pheromones in Enterococcus faecalis and other Firmicutes	331354	331866
fig|1504.6.peg.752	CDS	Contig_5	332759	331881	879	Transcriptional regulator, LysR family	- none -	331881	332759
fig|1504.6.peg.753	CDS	Contig_5	332864	333991	1128	extracellular solute-binding protein	- none -	332864	333991
fig|1504.6.peg.754	CDS	Contig_5	335112	333988	1125	Glycosyltransferase	- none -	333988	335112
fig|1504.6.peg.755	CDS	Contig_5	335264	336259	996	Spore coat protein S	- none -	335264	336259
fig|1504.6.peg.756	CDS	Contig_5	336303	337061	759	Spore coat protein cotS related	- none -	336303	337061
fig|1504.6.peg.757	CDS	Contig_5	337051	338100	1050	Spore coat protein S	- none -	337051	338100
fig|1504.6.peg.758	CDS	Contig_5	339270	338149	1122	Glycosyltransferase	- none -	338149	339270

Feature ID	Type	Contig	Start	Stop	Length (bp)	Function	Subsystems	Begin	End
fig|1504.6.peg.759	CDS	Contig_5	339376	340377	1002	Spore coat protein S	- none -	339376	340377
fig|1504.6.peg.760	CDS	Contig_5	340462	341346	885	Sporulation-specific protease YabG	- none -	340462	341346
fig|1504.6.peg.761	CDS	Contig_5	341564	341800	237	Veg protein	- none -	341564	341800
fig|1504.6.peg.762	CDS	Contig_5	342275	343855	1581	FIG01032327: hypothetical protein	- none -	342275	343855
fig|1504.6.peg.763	CDS	Contig_5	344008	344844	837	Cyanophycinase (EC 3.4.15.6)	Cyanophycin Metabolism	344008	344844
fig|1504.6.peg.764	CDS	Contig_5	344825	347443	2619	Cyanophycin synthase (EC 6.3.2.29)(EC 6.3.2.30)	Cyanophycin Metabolism	344825	347443
fig|1504.6.peg.765	CDS	Contig_5	347559	348425	867	4-diphosphocytidyl-2-C-methyl-D-erythritol kinase (EC 2.7.1.148)	Isoprenoid Biosynthesis, Nonmevalonate Branch of Isoprenoid Biosynthesis	347559	348425
fig|1504.6.peg.766	CDS	Contig_5	348487	349134	648	Stage II sporulation protein required for processing of pro-sigma-E (SpoIIR)	Sporulation gene orphans	348487	349134
fig|1504.6.peg.767	CDS	Contig_5	349231	350220	990	tRNA (5-methylaminomethyl-2-thiouridylate)-methyltransferase (EC 2.1.1.61)	RNA methylation, Riboflavin, FMN and FAD metabolism in plants, mnm5U34 biosynthesis bacteria, tRNAmodification position 34	349231	350220
fig|1504.6.peg.768	CDS	Contig_5	350233	350649	417	hypothetical fig|282458.1.peg.583 homolog	- none -	350233	350649
fig|1504.6.peg.769	CDS	Contig_5	350765	351070	306	FIG00513362: hypothetical protein	- none -	350765	351070
fig|1504.6.peg.770	CDS	Contig_5	351240	352847	1608	CTP synthase (EC 6.3.4.2)	Ribosome post-transcriptional modification and chromosomal segregation cluster, pyrimidine conversions	351240	352847
fig|1504.6.peg.771	CDS	Contig_5	353205	354599	1395	Transcription termination factor Rho	Transcription factors bacterial	353205	354599
fig|1504.6.peg.772	CDS	Contig_5	355730	354630	1101	Monogalactosyldiacylglycerol synthase precursor	Teichoic and lipoteichoic acids biosynthesis	354630	355730
fig|1504.6.peg.773	CDS	Contig_5	356073	355867	207	LSU ribosomal protein L31p @ LSU ribosomal protein L31p, zinc-dependent	Ribosome LSU bacterial, Ribosome LSU bacterial	355867	356073
fig|1504.6.peg.774	CDS	Contig_5	356360	356947	588	Thymidine kinase (EC 2.7.1.21)	pyrimidine conversions	356360	356947
fig|1504.6.peg.775	CDS	Contig_5	356971	358728	1758	FIG069887: hypothetical protein	- none -	356971	358728

Feature ID	Type	Contig	Start	Stop	Length (bp)	Function	Subsystems	Begin	End
fig|1504.6.peg.776	CDS	Contig_5	358792	359877	1086	Peptide chain release factor 1	Translation termination factors bacterial	358792	359877
fig|1504.6.peg.777	CDS	Contig_5	359936	360526	591	hypothetical membrane protein	- none -	359936	360526
fig|1504.6.peg.778	CDS	Contig_5	360544	361593	1050	TsaC protein (YrdC-Sua5 domains) required for threonylcarbamoyladenosine t(6)A37 modification in tRNA	- none -	360544	361593
fig|1504.6.peg.779	CDS	Contig_5	361671	362120	450	Ribose 5-phosphate isomerase B (EC 5.3.1.6)	D-ribose utilization, Pentose phosphate pathway	361671	362120
fig|1504.6.peg.780	CDS	Contig_5	362172	362801	630	Uracil phosphoribosyltransferase (EC 2.4.2.9)	De Novo Pyrimidine Synthesis, pyrimidine conversions	362172	362801
fig|1504.6.peg.781	CDS	Contig_5	363080	363574	495	dCMP deaminase (EC 3.5.4.12); Late competence protein ComEB	- none -	363080	363574
fig|1504.6.peg.782	CDS	Contig_5	363592	364743	1152	UDP-N-acetylglucosamine 2-epimerase (EC 5.1.3.14)	CMP-N-acetylneuraminate Biosynthesis, Sialic Acid Metabolism	363592	364743
fig|1504.6.peg.783	CDS	Contig_5	364862	366043	1182	3-ketoacyl-CoA thiolase (EC 2.3.1.16) @ Acetyl-CoA acetyltransferase (EC 2.3.1.9)	Biotin biosynthesis, Butanol Biosynthesis, Fatty acid metabolism cluster, Isoprenoid Biosynthesis, Polyhydroxybutyrate metabolism, Polyhydroxybutyrate metabolism, Serine-glyoxylate cycle, Serine-glyoxylate cycle	364862	366043
fig|1504.6.peg.784	CDS	Contig_5	366746	367108	363	hypothetical protein	- none -	366746	367108
fig|1504.6.peg.785	CDS	Contig_5	367118	367789	672	ATP synthase F0 sector subunit a	- none -	367118	367789
fig|1504.6.peg.786	CDS	Contig_5	367809	368042	234	ATP synthase F0 sector subunit c	- none -	367809	368042
fig|1504.6.peg.787	CDS	Contig_5	368083	368562	480	ATP synthase F0 sector subunit b	- none -	368083	368562
fig|1504.6.peg.788	CDS	Contig_5	368565	369104	540	ATP synthase delta chain (EC 3.6.3.14)	- none -	368565	369104
fig|1504.6.peg.789	CDS	Contig_5	369115	370629	1515	ATP synthase alpha chain (EC 3.6.3.14)	- none -	369115	370629
fig|1504.6.peg.790	CDS	Contig_5	370666	371517	852	ATP synthase gamma chain (EC 3.6.3.14)	- none -	370666	371517
fig|1504.6.peg.791	CDS	Contig_5	371533	372924	1392	ATP synthase beta chain (EC 3.6.3.14)	- none -	371533	372924

Feature ID	Type	Contig	Start	Stop	Length (bp)	Function	Subsystems	Begin	End
fig|1504.6.peg.792	CDS	Contig_5	372939	373346	408	ATP synthase epsilon chain (EC 3.6.3.14)	- none -	372939	373346
fig|1504.6.peg.793	CDS	Contig_5	373478	374707	1230	hypothetical protein	- none -	373478	374707
fig|1504.6.peg.794	CDS	Contig_5	374722	374913	192	hypothetical protein	- none -	374722	374913
fig|1504.6.peg.795	CDS	Contig_5	375195	375842	648	FIG013354: hypothetical protein	Sporulation-related Hypotheticals	375195	375842
fig|1504.6.peg.796	CDS	Contig_5	375864	377123	1260	UDP-N-acetylglucosamine 1-carboxyvinyltransferase (EC 2.5.1.7)	Sporulation-related Hypotheticals, UDP-N-acetylmuramate from Fructose-6-phosphate Biosynthesis	375864	377123
fig|1504.6.peg.797	CDS	Contig_5	377310	378356	1047	Stage II sporulation protein D (SpoIID)	Sporulation-related Hypotheticals, Sporulation Cluster, Sporulation gene orphans	377310	378356
fig|1504.6.peg.798	CDS	Contig_5	378534	379283	750	Stage II sporulation protein related to metaloproteases (SpoIIQ)	Sporulation-related Hypotheticals, Sporulation gene orphans	378534	379283
fig|1504.6.peg.799	CDS	Contig_5	379363	379614	252	Stage III sporulation protein D	Sporulation-related Hypotheticals, Sporulation gene orphans	379363	379614
fig|1504.6.peg.800	CDS	Contig_5	379742	380776	1035	MreB-like protein (Mbl protein)	Bacterial Cytoskeleton, Sporulation-related Hypotheticals	379742	380776
fig|1504.6.peg.801	CDS	Contig_5	381358	380828	531	Spore protease GPR related protein	- none -	380828	381358
fig|1504.6.rna.61	RNA	Contig_5	381682	381763	82	tRNA-Tyr-GTA	- none -	381682	381763
fig|1504.6.peg.802	CDS	Contig_5	382588	383763	1176	S-adenosylmethionine synthetase (EC 2.5.1.6)	Methionine Biosynthesis, Methionine Degradation	382588	383763
fig|1504.6.peg.803	CDS	Contig_5	384955	383819	1137	N-acetylglucosamine-6-phosphate deacetylase (EC 3.5.1.25)	Chitin and N-acetylglucosamine utilization, Sialic Acid Metabolism	383819	384955
fig|1504.6.peg.804	CDS	Contig_5	385086	387317	2232	RecD-like DNA helicase YrrC	DNA repair, bacterial RecBCD pathway	385086	387317
fig|1504.6.peg.805	CDS	Contig_6	87	998	912	hypothetical protein	- none -	87	998
fig|1504.6.peg.806	CDS	Contig_6	982	1644	663	ABC transporter, ATP-binding protein	- none -	982	1644

Feature ID	Type	Contig	Start	Stop	Length (bp)	Function	Subsystems	Begin	End
fig|1504.6.peg.807	CDS	Contig_6	2126	2004	123	Mobile element protein	- none -	2004	2126
fig|1504.6.peg.808	CDS	Contig_6	4024	4137	114	hypothetical protein	- none -	4024	4137
fig|1504.6.peg.809	CDS	Contig_6	4211	5503	1293	Mobile element protein	- none -	4211	5503
fig|1504.6.peg.810	CDS	Contig_6	5493	6251	759	Mobile element protein	- none -	5493	6251
fig|1504.6.peg.811	CDS	Contig_6	6662	7183	522	Mobile element protein	- none -	6662	7183
fig|1504.6.peg.812	CDS	Contig_6	8635	7289	1347	Aminopeptidase	- none -	7289	8635
fig|1504.6.peg.813	CDS	Contig_6	8804	8980	177	hypothetical protein	- none -	8804	8980
fig|1504.6.peg.814	CDS	Contig_6	9256	11427	2172	Transcription accessory protein (S1 RNA-binding domain)	Cell division-ribosomal stress proteins cluster, Transcription factors bacterial	9256	11427
fig|1504.6.peg.815	CDS	Contig_6	11759	12355	597	Substrate-specific component RibU of riboflavin ECF transporter	ECF class transporters, Riboflavin, FMN and FAD metabolism, Riboflavin, FMN and FAD metabolism in plants	11759	12355
fig|1504.6.peg.816	CDS	Contig_6	12857	12408	450	Ribosomal-protein-S18p-alanine acetyltransferase (EC 2.3.1.-)	Bacterial RNA-metabolizing Zn-dependent hydrolases, Conserved gene cluster associated with Met-tRNA formyltransferase, Ribosome biogenesis bacterial	12408	12857
fig|1504.6.peg.817	CDS	Contig_6	13557	12841	717	TsaB protein, required for threonylcarbamoyladenosine (t(6)A) formation in tRNA	Bacterial RNA-metabolizing Zn-dependent hydrolases, Conserved gene cluster associated with Met-tRNA formyltransferase, Ribosome biogenesis bacterial, YgjD and YeaZ, YjeE	12841	13557
fig|1504.6.peg.818	CDS	Contig_6	14015	13554	462	TsaE protein, required for threonylcarbamoyladenosine t(6)A37 formation in tRNA	YjeE	13554	14015
fig|1504.6.peg.819	CDS	Contig_6	14277	15191	915	Zinc ABC transporter, periplasmic-binding protein ZnuA	- none -	14277	15191
fig|1504.6.rna.62	RNA	Contig_6	15248	15319	72	tRNA-Trp-CCA	- none -	15248	15319

Feature ID	Type	Contig	Start	Stop	Length (bp)	Function	Subsystems	Begin	End
fig|1504.6.peg.820	CDS	Contig_6	16491	15424	1068	Enoyl-[acyl-carrier-protein] reductase [FMN] (EC 1.3.1.9)	Fatty Acid Biosynthesis FASII	15424	16491
fig|1504.6.rna.63	RNA	Contig_6	16694	16765	72	tRNA-Trp-CCA	- none -	16694	16765
fig|1504.6.peg.821	CDS	Contig_6	16871	20113	3243	two-component sensor histidine kinase	- none -	16871	20113
fig|1504.6.peg.822	CDS	Contig_6	20236	20517	282	hypothetical protein	- none -	20236	20517
fig|1504.6.peg.823	CDS	Contig_6	20555	21031	477	Cys-tRNA(Pro) deacylase YbaK	tRNA aminoacylation, Pro	20555	21031
fig|1504.6.peg.824	CDS	Contig_6	21236	22084	849	Beta-glucoside bgl operon antiterminator, BglG family	Beta-Glucoside Metabolism	21236	22084
fig|1504.6.peg.825	CDS	Contig_6	22259	23947	1689	PTS system, glucose-specific IIC component / PTS system, glucose-specific IIB component (EC 2.7.1.69) / PTS system, glucose-specific IIA component	Trehalose Uptake and Utilization	22259	23947
fig|1504.6.peg.826	CDS	Contig_6	24025	26067	2043	PTS system, glucose-specific IIC component / PTS system, glucose-specific IIB component (EC 2.7.1.69) / PTS system, glucose-specific IIA component	Trehalose Uptake and Utilization	24025	26067
fig|1504.6.peg.827[3]	CDS	Contig_6	26289	26954	666	COG1272: Predicted membrane protein hemolysin III homolog	- none -	26289	26954
fig|1504.6.peg.828	CDS	Contig_6	26972	27220	249	FIG00521076: hypothetical protein	- none -	26972	27220
fig|1504.6.peg.829	CDS	Contig_6	27797	30103	2307	Putative isomerase	- none -	27797	30103
fig|1504.6.peg.830	CDS	Contig_6	30201	31112	912	Permease of the drug/metabolite transporter (DMT) superfamily	Queuosine-Archaeosine Biosynthesis	30201	31112
fig|1504.6.peg.831	CDS	Contig_6	32084	31158	927	Protein tyrosine phosphatase II superfamily protein	- none -	31158	32084
fig|1504.6.peg.832	CDS	Contig_6	32276	32458	183	Small acid-soluble spore protein, beta-type SASP	Small acid-soluble spore proteins	32276	32458
fig|1504.6.peg.833	CDS	Contig_6	32643	33773	1131	Exonuclease SbcD	DNA repair, bacterial, Rad50-Mre11 DNA repair cluster	32643	33773
fig|1504.6.peg.834	CDS	Contig_6	33763	36516	2754	Exonuclease SbcC	DNA repair, bacterial, Rad50-Mre11 DNA repair cluster	33763	36516
fig|1504.6.peg.835	CDS	Contig_6	36594	37472	879	Zinc ABC transporter, periplasmic-binding protein ZnuA	- none -	36594	37472
fig|1504.6.peg.836	CDS	Contig_6	37509	39308	1800	MutS-related protein, family 1	DNA repair, bacterial MutL-MutS system	37509	39308
fig|1504.6.peg.837	CDS	Contig_6	39460	40344	885	Beta-lactamase (EC 3.5.2.6)	Beta-lactamase	39460	40344

Feature ID	Type	Contig	Start	Stop	Length (bp)	Function	Subsystems	Begin	End
fig|1504.6.peg.838	CDS	Contig_6	40409	41302	894	exonuclease family protein	- none -	40409	41302
fig|1504.6.peg.839	CDS	Contig_6	41420	41830	411	Inosine-5'-monophosphate dehydrogenase (EC 1.1.1.205)	Purine conversions, Purine salvage cluster	41420	41830
fig|1504.6.peg.840	CDS	Contig_6	41960	42727	768	UPF0246 protein YaaA	- none -	41960	42727
fig|1504.6.peg.841	CDS	Contig_6	43439	42783	657	FIG00513465: hypothetical protein	- none -	42783	43439
fig|1504.6.peg.842	CDS	Contig_6	44101	43451	651	Phage shock protein A	- none -	43451	44101
fig|1504.6.peg.843	CDS	Contig_6	44143	45249	1107	Mobile element protein	- none -	44143	45249
fig|1504.6.peg.844	CDS	Contig_6	45785	45489	297	hypothetical protein	- none -	45489	45785
fig|1504.6.peg.845	CDS	Contig_6	45755	46165	411	hypothetical protein	- none -	45755	46165
fig|1504.6.peg.846	CDS	Contig_6	46457	47605	1149	SSU ribosomal protein S1p	Cell division-ribosomal stress proteins cluster, Ribosome SSU bacterial	46457	47605
fig|1504.6.peg.847	CDS	Contig_6	49112	47694	1419	Pyruvate kinase (EC 2.7.1.40)	Entner-Doudoroff Pathway, Glycerate metabolism, Glycolysis and Gluconeogenesis, Pyruvate metabolism I: anaplerotic reactions, PEP	47694	49112
fig|1504.6.peg.848	CDS	Contig_6	49275	50726	1452	Aminoacyl-histidine dipeptidase (Peptidase D) (EC 3.4.13.3)	Dipeptidases (EC 3.4.13.-), Recycling of Peptidoglycan Amino Acids	49275	50726
fig|1504.6.peg.849	CDS	Contig_6	50944	51639	696	no significant homology 1 putative transmembrane region was found by PSORT	- none -	50944	51639
fig|1504.6.peg.850	CDS	Contig_6	51883	52452	570	Septum formation protein Maf	Bacterial Cell Division, Bacterial Cytoskeleton, Bacterial cell division cluster, CBSS-354.1.peg.2917	51883	52452
fig|1504.6.peg.851	CDS	Contig_6	52490	53179	690	DNA repair protein RadC	Bacterial cell division cluster, DNA repair, bacterial	52490	53179
fig|1504.6.peg.852	CDS	Contig_6	53197	54216	1020	Rod shape-determining protein MreB	Bacterial Cell Division, Bacterial Cytoskeleton, Bacterial cell division cluster	53197	54216

Feature ID	Type	Contig	Start	Stop	Length (bp)	Function	Subsystems	Begin	End
fig|1504.6.peg.853	CDS	Contig_6	54216	55067	852	Rod shape-determining protein MreC	Bacterial Cell Division, Bacterial Cytoskeleton, Bacterial cell division cluster, CBSS-354.1.peg.2917	54216	55067
fig|1504.6.peg.854	CDS	Contig_6	55079	55573	495	Rod shape-determining protein MreD	Bacterial Cell Division, Bacterial Cytoskeleton, Bacterial cell division cluster, CBSS-354.1.peg.2917	55079	55573
fig|1504.6.peg.855	CDS	Contig_6	55967	56608	642	Septum site-determining protein MinC	Bacterial Cell Division, Bacterial Cytoskeleton, Bacterial cell division cluster, Septum site-determining cluster Min	55967	56608
fig|1504.6.peg.856	CDS	Contig_6	56626	57423	798	Septum site-determining protein MinD	Bacterial Cell Division, Bacterial Cytoskeleton, Bacterial cell division cluster, Septum site-determining cluster Min	56626	57423
fig|1504.6.peg.857	CDS	Contig_6	57439	57705	267	Cell division topological specificity factor MinE	Bacterial Cell Division, Bacterial Cytoskeleton, Bacterial cell division cluster, Septum site-determining cluster Min	57439	57705
fig|1504.6.peg.858	CDS	Contig_6	57850	58977	1128	Rod shape-determining protein RodA	Bacterial Cytoskeleton, Bacterial cell division cluster	57850	58977
fig|1504.6.peg.859	CDS	Contig_6	60482	61012	531	hypothetical protein	- none -	60482	61012
fig|1504.6.peg.860	CDS	Contig_6	61174	62034	861	Stage IV sporulation pro-sigma-K processing enzyme (SpoIVFB)	Sporulation gene orphans	61174	62034
fig|1504.6.peg.861	CDS	Contig_6	62202	64055	1854	FIG092679: Fe-S oxidoreductase	CBSS-335543.6.peg.1659	62202	64055
fig|1504.6.peg.862	CDS	Contig_6	64039	64740	702	FIG017108: hypothetical protein	CBSS-335543.6.peg.1659	64039	64740
fig|1504.6.peg.863	CDS	Contig_6	64753	66201	1449	Cytoplasmic axial filament protein CafA and Ribonuclease G (EC 3.1.4.-)	Bacterial Cell Division, CBSS-335543.6.peg.1659, CBSS-354.1.peg.2917, RNA processing and degradation, bacterial	64753	66201

Feature ID	Type	Contig	Start	Stop	Length (bp)	Function	Subsystems	Begin	End
fig|1504.6.peg.864	CDS	Contig_6	66331	66642	312	LSU ribosomal protein L21p	CBSS-176279.3.peg.868, Ribosome LSU bacterial	66331	66642
fig|1504.6.peg.865	CDS	Contig_6	66647	67033	387	FIG139598: Potential ribosomal protein	CBSS-176279.3.peg.868	66647	67033
fig|1504.6.peg.866	CDS	Contig_6	67027	67326	300	LSU ribosomal protein L27p	CBSS-176279.3.peg.868, Ribosome LSU bacterial	67027	67326
fig|1504.6.peg.867	CDS	Contig_6	67634	68923	1290	GTP-binding protein Obg	CBSS-176279.3.peg.868, Universal GTPases	67634	68923
fig|1504.6.peg.868	CDS	Contig_6	68935	69237	303	FIG004454: RNA binding protein	- none -	68935	69237
fig|1504.6.peg.869	CDS	Contig_6	69242	69841	600	Nicotinate-nucleotide adenylyltransferase (EC 2.7.7.18)	NAD and NADP cofactor biosynthesis global	69242	69841
fig|1504.6.peg.870	CDS	Contig_6	69846	70412	567	Hydrolase (HAD superfamily), YqeK	- none -	69846	70412
fig|1504.6.peg.871	CDS	Contig_6	70434	71786	1353	Cell envelope-associated transcriptional attenuator LytR-CpsA-Psr, subfamily M (as in PMID19099556)	Cell envelope-associated LytR-CpsA-Psr transcriptional attenuators	70434	71786
fig|1504.6.peg.872	CDS	Contig_6	71852	72736	885	Similar to ribosomal large subunit pseudouridine synthase D, CAC1266-type	- none -	71852	72736
fig|1504.6.peg.873	CDS	Contig_6	74031	72781	1251	D-alanyl-D-alanine carboxypeptidase (EC 3.4.16.4)	CBSS-84588.1.peg.1247, Metallocarboxypeptidases (EC 3.4.17.-), Murein Hydrolases	72781	74031
fig|1504.6.peg.874	CDS	Contig_6	74189	74896	708	Late competence protein ComEA, DNA receptor	- none -	74189	74896
fig|1504.6.peg.875	CDS	Contig_6	75021	75680	660	FIG00517544: hypothetical protein	- none -	75021	75680
fig|1504.6.peg.876	CDS	Contig_6	75748	76098	351	hypothetical protein	- none -	75748	76098
fig|1504.6.peg.877	CDS	Contig_6	76122	77477	1356	RNA methyltransferase, TrmA family	- none -	76122	77477
fig|1504.6.peg.878	CDS	Contig_6	77809	78648	840	Sialic acid utilization regulator, RpiR family	Sialic Acid Metabolism	77809	78648
fig|1504.6.peg.879	CDS	Contig_6	78995	80632	1638	Oligopeptide ABC transporter, periplasmic oligopeptide-binding protein OppA (TC 3.A.1.5.1)	ABC transporter oligopeptide (TC 3.A.1.5.1), Sex pheromones in Enterococcus faecalis and other Firmicutes	78995	80632
fig|1504.6.peg.880	CDS	Contig_6	80703	81662	960	Dipeptide transport system permease protein DppB (TC 3.A.1.5.2)	ABC transporter dipeptide (TC 3.A.1.5.2)	80703	81662
fig|1504.6.peg.881	CDS	Contig_6	81672	82601	930	Oligopeptide transport system permease protein OppC (TC 3.A.1.5.1)	ABC transporter oligopeptide (TC 3.A.1.5.1)	81672	82601

Feature ID	Type	Contig	Start	Stop	Length (bp)	Function	Subsystems	Begin	End
fig|1504.6.peg.882	CDS	Contig_6	82614	83654	1041	Oligopeptide transport ATP-binding protein OppD (TC 3.A.1.5.1)	ABC transporter oligopeptide (TC 3.A.1.5.1)	82614	83654
fig|1504.6.peg.883	CDS	Contig_6	83644	84663	1020	Oligopeptide transport ATP-binding protein OppF (TC 3.A.1.5.1)	ABC transporter oligopeptide (TC 3.A.1.5.1)	83644	84663
fig|1504.6.peg.884	CDS	Contig_6	84667	85596	930	N-acetylneuraminate lyase (EC 4.1.3.3)	Sialic Acid Metabolism	84667	85596
fig|1504.6.peg.885	CDS	Contig_6	85718	86683	966	FIG00522956: hypothetical protein	- none -	85718	86683
fig|1504.6.peg.886	CDS	Contig_6	86685	87644	960	xylan esterase 1	- none -	86685	87644
fig|1504.6.peg.887	CDS	Contig_6	87702	88400	699	N-acetylmannosamine-6-phosphate 2-epimerase (EC 5.1.3.9)	Sialic Acid Metabolism	87702	88400
fig|1504.6.peg.888	CDS	Contig_6	88405	89343	939	Glucokinase (EC 2.7.1.2)	Entner-Doudoroff Pathway, Glycolysis and Gluconeogenesis	88405	89343
fig|1504.6.peg.889	CDS	Contig_6	89547	90758	1212	Cys-tRNA(Pro) deacylase YbaK	tRNA aminoacylation, Pro	89547	90758
fig|1504.6.peg.890	CDS	Contig_6	91692	90769	924	Permease of the drug/metabolite transporter (DMT) superfamily	Queuosine-Archaeosine Biosynthesis	90769	91692
fig|1504.6.peg.891	CDS	Contig_6	92475	91720	756	Creatinine amidohydrolase (EC 3.5.2.10)	Creatine and Creatinine Degradation	91720	92475
fig|1504.6.peg.892	CDS	Contig_6	92745	94007	1263	Cytosine deaminase (EC 3.5.4.1)	Creatine and Creatinine Degradation, pyrimidine conversions	92745	94007
fig|1504.6.peg.893	CDS	Contig_6	95560	94454	1107	Mobile element protein	- none -	94454	95560
fig|1504.6.peg.894	CDS	Contig_6	95600	97606	2007	methyl-accepting chemotaxis protein	- none -	95600	97606
fig|1504.6.peg.895	CDS	Contig_6	97845	100622	2778	Alpha-L-fucosidase (EC 3.2.1.51)	- none -	97845	100622
fig|1504.6.peg.896	CDS	Contig_6	101338	100694	645	hypothetical protein	- none -	100694	101338
fig|1504.6.peg.897	CDS	Contig_6	101863	101483	381	FIG00519710: hypothetical protein	- none -	101483	101863
fig|1504.6.peg.898	CDS	Contig_6	102633	101860	774	Conserved protein	- none -	101860	102633
fig|1504.6.peg.899	CDS	Contig_6	102829	104484	1656	Uridine kinase (EC 2.7.1.48)	pyrimidine conversions	102829	104484
fig|1504.6.peg.900	CDS	Contig_6	104615	105295	681	L-serine dehydratase, beta subunit (EC 4.3.1.17)	Glycine and Serine Utilization, Pyruvate Alanine Serine Interconversions	104615	105295

Feature ID	Type	Contig	Start	Stop	Length (bp)	Function	Subsystems	Begin	End
fig|1504.6.peg.901	CDS	Contig_6	105297	106175	879	L-serine dehydratase, alpha subunit (EC 4.3.1.17)	Glycine and Serine Utilization, Pyruvate Alanine Serine Interconversions	105297	106175
fig|1504.6.peg.902	CDS	Contig_6	106378	106875	498	Substrate-specific component ThiW of predicted thiazole ECF transporter	5-FCL-like protein, ECF class transporters, Thiamin biosynthesis	106378	106875
fig|1504.6.peg.903	CDS	Contig_6	106966	107811	846	Hydroxyethylthiazole kinase (EC 2.7.1.50)	5-FCL-like protein, Thiamin biosynthesis	106966	107811
fig|1504.6.peg.904	CDS	Contig_6	108096	108995	900	Collagen adhesion protein	- none -	108096	108995
fig|1504.6.peg.905	CDS	Contig_6	109400	110749	1350	Cell wall surface anchor family protein	Sortase	109400	110749
fig|1504.6.peg.906	CDS	Contig_6	110961	112154	1194	collagen adhesion protein	- none -	110961	112154
fig|1504.6.peg.907	CDS	Contig_6	113585	112314	1272	Branched-chain amino acid transport system carrier protein	- none -	112314	113585
fig|1504.6.peg.908	CDS	Contig_6	114824	113874	951	Cell envelope-associated transcriptional attenuator LytR-CpsA-Psr, subfamily F1 (as in PMID19099556)	Cell envelope-associated LytR-CpsA-Psr transcriptional attenuators	113874	114824
fig|1504.6.peg.909	CDS	Contig_6	115825	114839	987	Cell envelope-associated transcriptional attenuator LytR-CpsA-Psr, subfamily F1 (as in PMID19099556)	Cell envelope-associated LytR-CpsA-Psr transcriptional attenuators	114839	115825
fig|1504.6.peg.910	CDS	Contig_6	116368	117120	753	Glycosyltransferase involved in cell wall biogenesis (EC 2.4.-.-)	- none -	116368	117120
fig|1504.6.peg.911	CDS	Contig_6	117121	117489	369	hypothetical protein	- none -	117121	117489
fig|1504.6.peg.912	CDS	Contig_6	117526	118554	1029	UDP-N-acetylglucosamine 4,6-dehydratase (EC 4.2.1.-)	N-linked Glycosylation in Bacteria	117526	118554
fig|1504.6.peg.913	CDS	Contig_6	118574	119764	1191	Bacillosamine/Legionaminic acid biosynthesis aminotransferase PglE; 4-keto-6-deoxy-N-Acetyl-D-hexosaminyl-(Lipid carrier) aminotransferase	N-linked Glycosylation in Bacteria	118574	119764
fig|1504.6.peg.914	CDS	Contig_6	119776	120972	1197	Phosphoribosylglycinamide synthetase, ATP-grasp (A) domain protein	- none -	119776	120972
fig|1504.6.peg.915	CDS	Contig_6	120986	122038	1053	N-acetylneuraminate synthase (EC 2.5.1.56)	CMP-N-acetylneuraminate Biosynthesis, Sialic Acid Metabolism	120986	122038

Feature ID	Type	Contig	Start	Stop	Length (bp)	Function	Subsystems	Begin	End
fig|1504.6.peg.916	CDS	Contig_6	122035	123048	1014	N-Acetylneuraminate cytidylyltransferase (EC 2.7.7.43)	CMP-N-acetylneuraminate Biosynthesis, Sialic Acid Metabolism	122035	123048
fig|1504.6.peg.917	CDS	Contig_6	123050	123781	732	Spore coat polysaccharide biosynthesis protein spsF	- none -	123050	123781
fig|1504.6.peg.918	CDS	Contig_6	123850	125274	1425	Membrane protein involved in the export of O-antigen, teichoic acid lipoteichoic acids	- none -	123850	125274
fig|1504.6.peg.919	CDS	Contig_6	125290	126345	1056	hypothetical protein	- none -	125290	126345
fig|1504.6.peg.920	CDS	Contig_6	126380	127312	933	Glycosyltransferase	- none -	126380	127312
fig|1504.6.peg.921	CDS	Contig_6	127407	128927	1521	membrane protein, related to Actinobacillus protein (1944168)	- none -	127407	128927
fig|1504.6.peg.922	CDS	Contig_6	129248	130126	879	dTDP-rhamnosyl transferase RfbF (EC 2.-.-.-)	dTDP-rhamnose synthesis	129248	130126
fig|1504.6.peg.923	CDS	Contig_6	130154	130972	819	Glycosyltransferase (EC 2.4.1.-)	- none -	130154	130972
fig|1504.6.peg.924	CDS	Contig_6	131005	132069	1065	Glycosyltransferase	- none -	131005	132069
fig|1504.6.peg.925	CDS	Contig_6	132073	133515	1443	Membrane protein involved in the export of O-antigen, teichoic acid lipoteichoic acids	- none -	132073	133515
fig|1504.6.peg.926	CDS	Contig_6	133657	134715	1059	Mannose-1-phosphate guanylyltransferase (GDP) (EC 2.7.7.22)	Mannose Metabolism	133657	134715
fig|1504.6.peg.927	CDS	Contig_6	134744	135868	1125	Glycosyltransferase	- none -	134744	135868
fig|1504.6.peg.928	CDS	Contig_6	135893	137002	1110	Glycosyltransferase	- none -	135893	137002
fig|1504.6.peg.929	CDS	Contig_6	137021	137935	915	Glycosyltransferase (EC 2.4.1.-)	- none -	137021	137935
fig|1504.6.peg.930	CDS	Contig_6	138130	137945	186	hypothetical protein	- none -	137945	138130
fig|1504.6.peg.931	CDS	Contig_6	138150	138566	417	Undecaprenyl-phosphate galactosephosphotransferase (EC 2.7.8.6)	Exopolysaccharide Biosynthesis	138150	138566
fig|1504.6.peg.932	CDS	Contig_6	138590	139480	891	dTDP-4-dehydrorhamnose reductase (EC 1.1.1.133)	Rhamnose containing glycans, dTDP-rhamnose synthesis	138590	139480
fig|1504.6.peg.933	CDS	Contig_6	139500	140366	867	Glucose-1-phosphate thymidylyltransferase (EC 2.7.7.24)	Rhamnose containing glycans, dTDP-rhamnose synthesis	139500	140366
fig|1504.6.peg.934	CDS	Contig_6	140372	140935	564	dTDP-4-dehydrorhamnose 3,5-epimerase (EC 5.1.3.13)	Rhamnose containing glycans, dTDP-rhamnose synthesis	140372	140935
fig|1504.6.peg.935	CDS	Contig_6	140969	142021	1053	dTDP-glucose 4,6-dehydratase (EC 4.2.1.46)	Rhamnose containing glycans, dTDP-rhamnose synthesis	140969	142021
fig|1504.6.peg.936	CDS	Contig_6	143522	142050	1473	hypothetical protein	- none -	142050	143522

Feature ID	Type	Contig	Start	Stop	Length (bp)	Function	Subsystems	Begin	End
fig|1504.6.peg.937	CDS	Contig_6	143697	147356	3660	N-acetylmuramoyl-L-alanine amidase	- none -	143697	147356
fig|1504.6.peg.938	CDS	Contig_6	148723	147476	1248	hypothetical protein	- none -	147476	148723
fig|1504.6.peg.939	CDS	Contig_6	148913	149782	870	UTP--glucose-1-phosphate uridylyltransferase (EC 2.7.7.9)	Ribosome post-transcriptional modification and chromosomal segregation cluster	148913	149782
fig|1504.6.peg.940	CDS	Contig_6	149965	151074	1110	Multiple sugar ABC transporter, ATP-binding protein	Fructooligosaccharides(FOS) and Raffinose Utilization, Maltose and Maltodextrin Utilization	149965	151074
fig|1504.6.peg.941	CDS	Contig_6	152272	151334	939	Acid phosphatase (EC 3.1.3.2)	- none -	151334	152272
fig|1504.6.peg.942	CDS	Contig_6	152313	153419	1107	Mobile element protein	- none -	152313	153419
fig|1504.6.peg.943	CDS	Contig_6	155014	154004	1011	Tryptophanyl-tRNA synthetase (EC 6.1.1.2)	tRNA aminoacylation, Trp	154004	155014
fig|1504.6.peg.944	CDS	Contig_6	155338	155159	180	hypothetical protein	- none -	155159	155338
fig|1504.6.peg.945	CDS	Contig_6	155620	155465	156	Zinc finger domain	- none -	155465	155620
fig|1504.6.peg.946	CDS	Contig_6	156923	155826	1098	Putative spore germination protein, GerB family	Spore germination	155826	156923
fig|1504.6.peg.947	CDS	Contig_6	157033	158466	1434	Spore germination protein GerKA	Spore germination	157033	158466
fig|1504.6.peg.948	CDS	Contig_6	158444	159562	1119	Spore germination protein GerKC	Spore germination	158444	159562
fig|1504.6.peg.949	CDS	Contig_6	159717	160859	1143	ATP-dependent DNA helicase	- none -	159717	160859
fig|1504.6.peg.950	CDS	Contig_6	160877	161290	414	hypothetical protein	- none -	160877	161290
fig|1504.6.peg.951	CDS	Contig_6	161489	162709	1221	Tyrosyl-tRNA synthetase (EC 6.1.1.1)	tRNA aminoacylation, Tyr	161489	162709
fig|1504.6.peg.952	CDS	Contig_6	162949	163812	864	Beta-glucoside bgl operon antiterminator, BglG family	Beta-Glucoside Metabolism	162949	163812
fig|1504.6.peg.953	CDS	Contig_6	164907	163852	1056	putative lipoprotein	- none -	163852	164907
fig|1504.6.peg.954	CDS	Contig_6	166414	164990	1425	Two-component sensor kinase precursor	- none -	164990	166414
fig|1504.6.peg.955	CDS	Contig_6	167102	166398	705	Phosphate regulon transcriptional regulatory protein PhoB (SphR)	High affinity phosphate transporter and control of PHO regulon, PhoR-PhoB two-component regulatory system, Phosphate metabolism	166398	167102

Feature ID	Type	Contig	Start	Stop	Length (bp)	Function	Subsystems	Begin	End
fig|1504.6.peg.956	CDS	Contig_6	167281	169260	1980	conserved hypothetical protein	- none -	167281	169260
fig|1504.6.peg.957	CDS	Contig_6	169301	169564	264	Flagellar biosynthesis related protein	- none -	169301	169564
fig|1504.6.peg.958	CDS	Contig_6	169573	170262	690	Ser/Thr protein phosphatase family protein	- none -	169573	170262
fig|1504.6.peg.959	CDS	Contig_6	170381	171175	795	Histidinol-phosphatase (EC 3.1.3.15)	- none -	170381	171175
fig|1504.6.peg.960	CDS	Contig_6	171302	171580	279	Transcriptional regulator, ArsR family	- none -	171302	171580
fig|1504.6.peg.961	CDS	Contig_6	171731	174181	2451	CoA-disulfide reductase (EC 1.8.1.14) / Disulfide bond regulator	CoA disulfide thiol-disulfide redox system	171731	174181
fig|1504.6.peg.962	CDS	Contig_6	174340	175035	696	two-component response regulator	- none -	174340	175035
fig|1504.6.peg.963	CDS	Contig_6	175125	176048	924	ABC-type multidrug transport system, ATPase component	- none -	175125	176048
fig|1504.6.peg.964	CDS	Contig_6	176041	176790	750	no significant homology. Putative N-terminal signal sequence and 5 putative transmembrane regions were found by PSORT.	- none -	176041	176790
fig|1504.6.peg.965	CDS	Contig_6	176812	177711	900	sensory transduction protein kinase	- none -	176812	177711
fig|1504.6.peg.966	CDS	Contig_6	177973	178167	195	hypothetical protein	- none -	177973	178167
fig|1504.6.peg.967[4]	CDS	Contig_6	178497	179447	951	Panton-Valentine leukocidin chain S precursor	- none -	178497	179447
fig|1504.6.peg.968	CDS	Contig_6	179647	180327	681	hypothetical protein	- none -	179647	180327
fig|1504.6.peg.969	CDS	Contig_6	180347	180544	198	Transcriptional regulator, Cro/CI family	- none -	180347	180544
fig|1504.6.peg.970	CDS	Contig_6	181552	180581	972	Methyl-accepting chemotaxis protein	- none -	180581	181552
fig|1504.6.peg.971	CDS	Contig_6	182319	181549	771	Conserved protein	- none -	181549	182319
fig|1504.6.peg.972	CDS	Contig_6	182504	183298	795	GTP pyrophosphokinase (EC 2.7.6.5)	- none -	182504	183298
fig|1504.6.peg.973	CDS	Contig_6	184812	183322	1491	membrane protein	- none -	183322	184812
fig|1504.6.peg.974	CDS	Contig_6	185078	185854	777	no significant homology.	- none -	185078	185854
fig|1504.6.peg.975	CDS	Contig_6	185872	186957	1086	MoxR-like ATPases	- none -	185872	186957
fig|1504.6.peg.976	CDS	Contig_6	186993	188327	1335	FIG00588672: hypothetical protein	- none -	186993	188327
fig|1504.6.peg.977	CDS	Contig_6	188421	189080	660	hypothetical protein	- none -	188421	189080

Feature ID	Type	Contig	Start	Stop	Length (bp)	Function	Subsystems	Begin	End
fig|1504.6.peg.978	CDS	Contig_6	189356	190846	1491	PTS system, N-acetylglucosamine-specific IIA component / PTS system, N-acetylglucosamine-specific IIB component (EC 2.7.1.69) / PTS system, N-acetylglucosamine-specific IIC component	Chitin and N-acetylglucosamine utilization, Sialic Acid Metabolism	189356	190846
fig|1504.6.peg.979	CDS	Contig_6	190916	191560	645	N-acetylmannosamine-6-phosphate 2-epimerase (EC 5.1.3.9)	Sialic Acid Metabolism	190916	191560
fig|1504.6.peg.980	CDS	Contig_6	191708	192505	798	Sialic acid utilization regulator, RpiR family	Sialic Acid Metabolism	191708	192505
fig|1504.6.peg.981	CDS	Contig_6	192767	193219	453	probable beta-D-galactosidase	Galactosylceramide and Sulfatide metabolism	192767	193219
fig|1504.6.peg.982	CDS	Contig_6	193424	193624	201	Sialic acid utilization regulator, RpiR family	Sialic Acid Metabolism	193424	193624
fig|1504.6.peg.983	CDS	Contig_6	194039	194908	870	Methionine aminopeptidase (EC 3.4.11.18)	CBSS-312309.3.peg.1965, Translation termination factors bacterial	194039	194908
fig|1504.6.peg.984	CDS	Contig_6	196342	195104	1239	Mobile element protein	- none -	195104	196342
fig|1504.6.peg.985	CDS	Contig_6	196806	196474	333	AsmA protein	- none -	196474	196806
fig|1504.6.peg.986	CDS	Contig_6	197081	197821	741	FIG00527171: hypothetical protein	- none -	197081	197821
fig|1504.6.peg.987	CDS	Contig_6	197864	198565	702	COG4478, integral membrane protein	- none -	197864	198565
fig|1504.6.peg.988	CDS	Contig_6	201081	198631	2451	Leucyl-tRNA synthetase (EC 6.1.1.4)	tRNA aminoacylation, Leu	198631	201081
fig|1504.6.peg.989	CDS	Contig_6	201548	201682	135	hypothetical protein	- none -	201548	201682
fig|1504.6.peg.990	CDS	Contig_6	202021	201854	168	hypothetical protein	- none -	201854	202021
fig|1504.6.peg.991	CDS	Contig_6	202746	203426	681	Mobile element protein	- none -	202746	203426
fig|1504.6.peg.992	CDS	Contig_6	203713	204078	366	Succinyl-CoA synthetase, alpha subunit-related enzymes	- none -	203713	204078
fig|1504.6.peg.993	CDS	Contig_6	204183	204944	762	Membrane protein, putative	- none -	204183	204944
fig|1504.6.peg.994	CDS	Contig_6	205019	205381	363	conserved hypothetical protein	- none -	205019	205381
fig|1504.6.peg.995	CDS	Contig_6	205713	206546	834	Endonuclease IV (EC 3.1.21.2)	DNA repair, bacterial	205713	206546
fig|1504.6.peg.996	CDS	Contig_6	207325	206654	672	Transcriptional regulator, AraC family	- none -	206654	207325
fig|1504.6.peg.997	CDS	Contig_6	207650	208168	519	Flavodoxin	Flavodoxin	207650	208168
fig|1504.6.peg.998	CDS	Contig_6	208177	208935	759	Nitrogenase subunit NifH paralog, type 2	- none -	208177	208935

Feature ID	Type	Contig	Start	Stop	Length (bp)	Function	Subsystems	Begin	End
fig|1504.6.peg.999	CDS	Contig_6	208965	209960	996	Heme transporter IsdDEF, lipoprotein IsdE	Heme, hemin uptake and utilization systems in GramPositives	208965	209960
fig|1504.6.peg.1000	CDS	Contig_6	209984	210991	1008	Heme transporter IsdDEF, permease component IsdF	Heme, hemin uptake and utilization systems in GramPositives	209984	210991
fig|1504.6.peg.1001	CDS	Contig_6	210981	211766	786	Heme transporter analogous to IsdDEF, ATP-binding protein	Heme, hemin uptake and utilization systems in GramPositives	210981	211766
fig|1504.6.peg.1002	CDS	Contig_6	211777	213087	1311	Similar to nitrogenase cofactor scaffold and assembly proteins	- none -	211777	213087
fig|1504.6.peg.1003	CDS	Contig_6	213074	214300	1227	Nitrogenase FeMo-cofactor scaffold and assembly protein NifE	- none -	213074	214300
fig|1504.6.peg.1004	CDS	Contig_6	215032	214766	267	Transposase	- none -	214766	215032
fig|1504.6.peg.1005	CDS	Contig_6	216021	216563	543	Rubrerythrin	Oxidative stress, Rubrerythrin	216021	216563
fig|1504.6.peg.1006	CDS	Contig_6	217060	217602	543	Rubrerythrin	Oxidative stress, Rubrerythrin	217060	217602
fig|1504.6.peg.1007	CDS	Contig_6	218366	219808	1443	Cardiolipin synthetase (EC 2.7.8.-)	Cardiolipin synthesis, Glycerolipid and Glycerophospholipid Metabolism in Bacteria	218366	219808
fig|1504.6.peg.1008	CDS	Contig_6	220221	221234	1014	2-keto-3-deoxy-D-arabino-heptulosonate-7-phosphate synthase I beta (EC 2.5.1.54)	Chorismate Synthesis, Common Pathway For Synthesis of Aromatic Compounds (DAHP synthase to chorismate)	220221	221234
fig|1504.6.peg.1009	CDS	Contig_6	221250	222308	1059	3-dehydroquinate synthase (EC 4.2.3.4)	Chorismate Synthesis, Common Pathway For Synthesis of Aromatic Compounds (DAHP synthase to chorismate)	221250	222308
fig|1504.6.peg.1010	CDS	Contig_6	222327	223622	1296	5-Enolpyruvylshikimate-3-phosphate synthase (EC 2.5.1.19)	Chorismate Synthesis, Common Pathway For Synthesis of Aromatic Compounds (DAHP synthase to chorismate)	222327	223622

Feature ID	Type	Contig	Start	Stop	Length (bp)	Function	Subsystems	Begin	End
fig|1504.6.peg.1011	CDS	Contig_6	223600	224682	1083	Chorismate synthase (EC 4.2.3.5)	Chorismate Synthesis, Common Pathway For Synthesis of Aromatic Compounds (DAHP synthase to chorismate)	223600	224682
fig|1504.6.peg.1012	CDS	Contig_6	224685	225812	1128	Chorismate mutase I (EC 5.4.99.5) / Prephenate dehydratase (EC 4.2.1.51)	Chorismate Synthesis, Chorismate Synthesis, Phenylalanine and Tyrosine Branches from Chorismate, Phenylalanine and Tyrosine Branches from Chorismate	224685	225812
fig|1504.6.peg.1013	CDS	Contig_6	225806	225928	123	hypothetical protein	- none -	225806	225928
fig|1504.6.peg.1014	CDS	Contig_6	225956	226759	804	Shikimate 5-dehydrogenase I alpha (EC 1.1.1.25)	Chorismate Synthesis, Cluster containing Alanyl-tRNA synthetase, Common Pathway For Synthesis of Aromatic Compounds (DAHP synthase to chorismate)	225956	226759
fig|1504.6.peg.1015	CDS	Contig_6	226778	227278	501	Shikimate kinase I (EC 2.7.1.71)	Chorismate Synthesis, Common Pathway For Synthesis of Aromatic Compounds (DAHP synthase to chorismate)	226778	227278
fig|1504.6.peg.1016	CDS	Contig_6	227297	227725	429	3-dehydroquinate dehydratase II (EC 4.2.1.10)	Chorismate Synthesis, Common Pathway For Synthesis of Aromatic Compounds (DAHP synthase to chorismate), Quinate degradation	227297	227725
fig|1504.6.peg.1017	CDS	Contig_6	227741	228754	1014	2-keto-3-deoxy-D-arabino-heptulosonate-7-phosphate synthase I beta (EC 2.5.1.54)	Chorismate Synthesis, Common Pathway For Synthesis of Aromatic Compounds (DAHP synthase to chorismate)	227741	228754
fig|1504.6.peg.1018	CDS	Contig_6	228822	229655	834	Prephenate and/or arogenate dehydrogenase (unknown specificity) (EC 1.3.1.12)(EC 1.3.1.43)	Chorismate Synthesis, Phenylalanine and Tyrosine Branches from Chorismate	228822	229655
fig|1504.6.peg.1019	CDS	Contig_6	229766	231181	1416	Stage V sporulation protein AF (SpoVAF)	Sporulation gene orphans	229766	231181

Feature ID	Type	Contig	Start	Stop	Length (bp)	Function	Subsystems	Begin	End
fig|1504.6.peg.1020	CDS	Contig_6	231312	232703	1392	membrane protein, putative	- none -	231312	232703
fig|1504.6.peg.1021	CDS	Contig_6	232864	234741	1878	FIG00518012: hypothetical protein	- none -	232864	234741
fig|1504.6.peg.1022	CDS	Contig_6	234754	235056	303	Ascorbate-specific PTS system, EIIA component (EC 2.7.1.-)	L-ascorbate utilization (and related gene clusters)	234754	235056
fig|1504.6.peg.1023	CDS	Contig_6	235014	235154	141	Ascorbate-specific PTS system, EIIA component (EC 2.7.1.-)	L-ascorbate utilization (and related gene clusters)	235014	235154
fig|1504.6.peg.1024	CDS	Contig_6	235156	235431	276	PTS system, IIB component, putative	- none -	235156	235431
fig|1504.6.peg.1025	CDS	Contig_6	235473	236828	1356	FIG00732228: membrane protein	- none -	235473	236828
fig|1504.6.peg.1026	CDS	Contig_6	237438	236878	561	Adenylate cyclase (EC 4.6.1.1)	cAMP signaling in bacteria	236878	237438
fig|1504.6.peg.1027	CDS	Contig_6	237773	238465	693	hypothetical protein	- none -	237773	238465
fig|1504.6.peg.1028	CDS	Contig_6	238522	239580	1059	Tail protein	- none -	238522	239580
fig|1504.6.peg.1029	CDS	Contig_6	239779	241497	1719	antigen, putative	- none -	239779	241497
fig|1504.6.peg.1030	CDS	Contig_6	242090	241530	561	Transcriptional regulator, TetR family	- none -	241530	242090
fig|1504.6.peg.1031	CDS	Contig_6	242573	242427	147	hypothetical protein	- none -	242427	242573
fig|1504.6.peg.1032	CDS	Contig_6	242746	242928	183	FIG00522459: hypothetical protein	- none -	242746	242928
fig|1504.6.peg.1033	CDS	Contig_6	243423	244736	1314	sodium:neurotransmitter symporter family protein	- none -	243423	244736
fig|1504.6.peg.1034	CDS	Contig_6	245011	245733	723	hypothetical protein	- none -	245011	245733
fig|1504.6.peg.1035	CDS	Contig_6	246019	246141	123	hypothetical protein	- none -	246019	246141
fig|1504.6.peg.1036	CDS	Contig_6	246208	246504	297	hypothetical protein	- none -	246208	246504
fig|1504.6.peg.1037	CDS	Contig_6	246489	247109	621	hypothetical protein	- none -	246489	247109
fig|1504.6.peg.1038	CDS	Contig_6	247274	247540	267	hypothetical protein	- none -	247274	247540
fig|1504.6.peg.1039	CDS	Contig_6	247581	250019	2439	Lead, cadmium, zinc and mercury transporting ATPase (EC 3.6.3.3) (EC 3.6.3.5); Copper-translocating P-type ATPase (EC 3.6.3.4)	Copper Transport System, Copper homeostasis	247581	250019
fig|1504.6.peg.1040	CDS	Contig_6	250062	250268	207	Copper chaperone	Copper homeostasis	250062	250268
fig|1504.6.peg.1041	CDS	Contig_6	250791	250312	480	hypothetical protein	- none -	250312	250791
fig|1504.6.peg.1042	CDS	Contig_6	250927	251367	441	hypothetical protein	- none -	250927	251367

Feature ID	Type	Contig	Start	Stop	Length (bp)	Function	Subsystems	Begin	End
fig|1504.6.peg.1043	CDS	Contig_6	251369	251509	141	hypothetical protein	- none -	251369	251509
fig|1504.6.peg.1044	CDS	Contig_6	252658	251795	864	Fructose-bisphosphate aldolase class II (EC 4.1.2.13)	Glycolysis and Gluconeogenesis	251795	252658
fig|1504.6.peg.1045	CDS	Contig_6	253137	252961	177	hypothetical protein	- none -	252961	253137
fig|1504.6.peg.1046	CDS	Contig_6	253285	254328	1044	conserved hypothetical protein	- none -	253285	254328
fig|1504.6.peg.1047	CDS	Contig_6	255567	254377	1191	Cell wall-binding protein	- none -	254377	255567
fig|1504.6.peg.1048	CDS	Contig_6	257306	255906	1401	Argininosuccinate lyase (EC 4.3.2.1)	- none -	255906	257306
fig|1504.6.peg.1049	CDS	Contig_6	258532	257309	1224	Argininosuccinate synthase (EC 6.3.4.5)	- none -	257309	258532
fig|1504.6.peg.1050	CDS	Contig_6	258919	260631	1713	Methyl-accepting chemotaxis protein	- none -	258919	260631
fig|1504.6.peg.1051	CDS	Contig_6	260914	261552	639	Collagen adhesion protein	- none -	260914	261552
fig|1504.6.peg.1052	CDS	Contig_6	261603	262133	531	Membrane-associated phospholipid phosphatase	- none -	261603	262133
fig|1504.6.peg.1053	CDS	Contig_6	262210	262578	369	hypothetical protein	- none -	262210	262578
fig|1504.6.peg.1054	CDS	Contig_6	262663	262857	195	hypothetical protein	- none -	262663	262857
fig|1504.6.peg.1055	CDS	Contig_6	263165	264637	1473	4-alpha-glucanotransferase (amylomaltase) (EC 2.4.1.25)	Glycogen metabolism, Maltose and Maltodextrin Utilization	263165	264637
fig|1504.6.peg.1056	CDS	Contig_6	264767	265570	804	Transcriptional regulator, MerR family	Cobalt-zinc-cadmium resistance	264767	265570
fig|1504.6.peg.1057	CDS	Contig_6	265621	266955	1335	Multi antimicrobial extrusion protein (Na(+)/drug antiporter), MATE family of MDR efflux pumps	Multidrug Resistance Efflux Pumps, Riboflavin, FMN and FAD metabolism in plants	265621	266955
fig|1504.6.peg.1058	CDS	Contig_6	266986	267273	288	YlxP-like protein	CBSS-350688.3.peg.1509, NusA-TFII Cluster	266986	267273
fig|1504.6.peg.1059	CDS	Contig_6	267342	267788	447	hypothetical protein	- none -	267342	267788
fig|1504.6.peg.1060	CDS	Contig_6	267976	268470	495	Histone acetyltransferase HPA2 and related acetyltransferases	CBSS-216591.1.peg.168	267976	268470
fig|1504.6.peg.1061	CDS	Contig_6	268795	269760	966	Methionine ABC transporter ATP-binding protein	Methionine Biosynthesis, Methionine Degradation	268795	269760
fig|1504.6.peg.1062	CDS	Contig_6	269760	270395	636	Methionine ABC transporter permease protein	Methionine Biosynthesis, Methionine Degradation	269760	270395
fig|1504.6.peg.1063	CDS	Contig_6	270434	271246	813	Methionine ABC transporter substrate-binding protein	Methionine Biosynthesis, Methionine Degradation	270434	271246

Feature ID	Type	Contig	Start	Stop	Length (bp)	Function	Subsystems	Begin	End
fig|1504.6.peg.1064	CDS	Contig_6	271571	272254	684	N-acetylmuramoyl-L-alanine amidase (EC 3.5.1.28)	Murein Hydrolases, Recycling of Peptidoglycan Amino Acids	271571	272254
fig|1504.6.peg.1065	CDS	Contig_6	274057	272312	1746	Cell division protein FtsH (EC 3.4.24.-)	Bacterial Cell Division, Cell division-ribosomal stress proteins cluster, Folate biosynthesis cluster	272312	274057
fig|1504.6.peg.1066	CDS	Contig_6	274443	274886	444	hypothetical protein	- none -	274443	274886
fig|1504.6.peg.1067	CDS	Contig_6	274965	275921	957	Conserved protein	- none -	274965	275921
fig|1504.6.peg.1068	CDS	Contig_6	275964	276596	633	Ribonuclease HI-related protein	Ribonuclease H	275964	276596
fig|1504.6.peg.1069	CDS	Contig_6	276678	276851	174	hypothetical protein	- none -	276678	276851
fig|1504.6.peg.1070	CDS	Contig_6	277266	278648	1383	Xre family DNA-binding domain and TPR-repeat-containing protein	- none -	277266	278648
fig|1504.6.peg.1071	CDS	Contig_6	278669	279931	1263	Xre family DNA-binding domain and TPR-repeat-containing protein	- none -	278669	279931
fig|1504.6.peg.1072	CDS	Contig_6	281571	280162	1410	Multi antimicrobial extrusion protein (Na(+)/drug antiporter), MATE family of MDR efflux pumps	Multidrug Resistance Efflux Pumps, Riboflavin, FMN and FAD metabolism in plants	280162	281571
fig|1504.6.peg.1073	CDS	Contig_6	282715	281909	807	Transcriptional repressor of the myo-inositol catabolic operon DeoR family	Inositol catabolism	281909	282715
fig|1504.6.peg.1074	CDS	Contig_6	282914	284068	1155	Fe-containing alcohol dehydrogenase	Inositol catabolism	282914	284068
fig|1504.6.peg.1075	CDS	Contig_6	284074	284919	846	5-keto-2-deoxy-D-gluconate-6 phosphate aldolase (EC 4.1.2.29)	Inositol catabolism	284074	284919
fig|1504.6.peg.1076	CDS	Contig_6	284933	285949	1017	5-keto-2-deoxygluconokinase (EC 2.7.1.92)	Inositol catabolism	284933	285949
fig|1504.6.peg.1077	CDS	Contig_6	285963	286730	768	5-deoxy-glucuronate isomerase (EC 5.3.1.-)	Inositol catabolism	285963	286730
fig|1504.6.peg.1078	CDS	Contig_6	286747	288666	1920	Epi-inositol hydrolase (EC 3.7.1.-)	Inositol catabolism	286747	288666
fig|1504.6.peg.1079	CDS	Contig_6	288708	289709	1002	Myo-inositol 2-dehydrogenase 1 (EC 1.1.1.18)	Inositol catabolism	288708	289709
fig|1504.6.peg.1080	CDS	Contig_6	289785	290678	894	Inosose dehydratase (EC 4.2.1.44)	Inositol catabolism	289785	290678
fig|1504.6.peg.1081	CDS	Contig_6	290769	292358	1590	Sodium/myo-inositol cotransporter	Inositol catabolism	290769	292358
fig|1504.6.peg.1082	CDS	Contig_6	292400	293446	1047	Myo-inositol 2-dehydrogenase 1 (EC 1.1.1.18)	Inositol catabolism	292400	293446

Feature ID	Type	Contig	Start	Stop	Length (bp)	Function	Subsystems	Begin	End
fig|1504.6.peg.1083	CDS	Contig_6	295682	293604	2079	Transcriptional regulator of various polyols utilization, AraC family	- none -	293604	295682
fig|1504.6.peg.1084	CDS	Contig_6	295924	298524	2601	ClpB protein	Protein chaperones, Proteolysis in bacteria, ATP-dependent	295924	298524
fig|1504.6.peg.1085	CDS	Contig_6	298622	299659	1038	unknown	- none -	298622	299659
fig|1504.6.rna.64	RNA	Contig_6	299783	299856	74	tRNA-Arg-TCT	- none -	299783	299856
fig|1504.6.rna.65	RNA	Contig_6	299900	299973	74	tRNA-Arg-TCT	- none -	299900	299973
fig|1504.6.rna.66	RNA	Contig_6	299982	300053	72	tRNA-Gln-TTG	- none -	299982	300053
fig|1504.6.rna.67	RNA	Contig_6	300060	300132	73	tRNA-Lys-TTT	- none -	300060	300132
fig|1504.6.rna.68	RNA	Contig_6	300186	300257	72	tRNA-Gly-GCC	- none -	300186	300257
fig|1504.6.peg.1086	CDS	Contig_6	300503	300321	183	Small acid-soluble spore protein, beta-type SASP	Small acid-soluble spore proteins	300321	300503
fig|1504.6.peg.1087	CDS	Contig_6	300761	300579	183	Small acid-soluble spore protein, beta-type SASP	Small acid-soluble spore proteins	300579	300761
fig|1504.6.peg.1088	CDS	Contig_6	301014	300832	183	Small acid-soluble spore protein, beta-type SASP	Small acid-soluble spore proteins	300832	301014
fig|1504.6.peg.1089	CDS	Contig_6	301867	301268	600	Substrate-specific component PanT of predicted pantothenate ECF transporter	Coenzyme A Biosynthesis, ECF class transporters	301268	301867
fig|1504.6.peg.1090	CDS	Contig_6	302128	302841	714	ABC transporter, ATP-binding protein	- none -	302128	302841
fig|1504.6.peg.1091	CDS	Contig_6	302834	303433	600	ABC transporter permease protein	- none -	302834	303433
fig|1504.6.peg.1092	CDS	Contig_6	303439	304431	993	ABC transporter permease protein	- none -	303439	304431
fig|1504.6.peg.1093	CDS	Contig_6	304667	304470	198	hypothetical protein	- none -	304470	304667
fig|1504.6.peg.1094	CDS	Contig_6	304950	304660	291	hypothetical protein	- none -	304660	304950
fig|1504.6.peg.1095	CDS	Contig_6	305181	305564	384	Transcriptional regulator, GntR family	- none -	305181	305564
fig|1504.6.peg.1096	CDS	Contig_6	305569	306699	1131	hypothetical protein	- none -	305569	306699
fig|1504.6.peg.1097	CDS	Contig_6	306828	307328	501	Histone acetyltransferase HPA2 and related acetyltransferases	CBSS-216591.1.peg.168	306828	307328
fig|1504.6.peg.1098	CDS	Contig_6	307496	308515	1020	Histidinol-phosphate aminotransferase (EC 2.6.1.9)	- none -	307496	308515
fig|1504.6.peg.1099	CDS	Contig_6	308813	308592	222	hypothetical protein	- none -	308592	308813

Feature ID	Type	Contig	Start	Stop	Length (bp)	Function	Subsystems	Begin	End
fig|1504.6.peg.1100	CDS	Contig_6	310060	309284	777	Histidinol-phosphatase (EC 3.1.3.15)	- none -	309284	310060
fig|1504.6.peg.1101	CDS	Contig_6	310215	310556	342	FIG00518547: hypothetical protein	- none -	310215	310556
fig|1504.6.peg.1102	CDS	Contig_6	310676	311821	1146	hypothetical protein	- none -	310676	311821
fig|1504.6.peg.1103	CDS	Contig_6	311835	313211	1377	Membrane proteins related to metalloendopeptidases	CBSS-393121.3.peg.2760	311835	313211
fig|1504.6.peg.1104	CDS	Contig_6	313629	313841	213	hypothetical protein	- none -	313629	313841
fig|1504.6.peg.1105	CDS	Contig_6	313964	314770	807	hypothetical protein	- none -	313964	314770
fig|1504.6.peg.1106	CDS	Contig_6	314881	316161	1281	Cell division trigger factor (EC 5.2.1.8)	Bacterial Cell Division	314881	316161
fig|1504.6.peg.1107	CDS	Contig_6	316462	317064	603	ATP-dependent Clp protease proteolytic subunit (EC 3.4.21.92)	Proteolysis in bacteria, ATP-dependent, cAMP signaling in bacteria	316462	317064
fig|1504.6.peg.1108	CDS	Contig_6	317094	318389	1296	ATP-dependent Clp protease ATP-binding subunit ClpX	Proteolysis in bacteria, ATP-dependent	317094	318389
fig|1504.6.peg.1109	CDS	Contig_6	318578	320239	1662	ATP-dependent protease La (EC 3.4.21.53) LonB Type I	- none -	318578	320239
fig|1504.6.peg.1110	CDS	Contig_6	320419	322752	2334	ATP-dependent protease La (EC 3.4.21.53) Type I	Proteolysis in bacteria, ATP-dependent	320419	322752
fig|1504.6.peg.1111	CDS	Contig_6	322742	323362	621	GTP-binding protein EngB	Universal GTPases	322742	323362
fig|1504.6.peg.1112	CDS	Contig_6	323365	323478	114	hypothetical protein	- none -	323365	323478
fig|1504.6.peg.1113	CDS	Contig_6	323525	323908	384	Keratin-associated protein 5-5 (Keratin-associated protein 5.5) (Ultrahigh sulfur keratin-associated protein 5.5) (Keratin-associated protein 5-11) (Keratin-associated protein 5.11)	- none -	323525	323908
fig|1504.6.peg.1114	CDS	Contig_6	323954	324193	240	no significant homology	- none -	323954	324193
fig|1504.6.peg.1115	CDS	Contig_6	324304	324852	549	FIG01270652: hypothetical protein	- none -	324304	324852
fig|1504.6.peg.1116	CDS	Contig_6	325959	325015	945	hypothetical protein	- none -	325015	325959
fig|1504.6.peg.1117	CDS	Contig_6	326489	326082	408	Zinc uptake regulation protein ZUR	Oxidative stress	326082	326489
fig|1504.6.peg.1118	CDS	Contig_6	326826	327158	333	hypothetical protein	- none -	326826	327158
fig|1504.6.peg.1119	CDS	Contig_6	327291	328514	1224	Predicted signal transduction protein	Flagellar motility	327291	328514
fig|1504.6.peg.1120	CDS	Contig_6	328628	328843	216	hypothetical protein	- none -	328628	328843

Feature ID	Type	Contig	Start	Stop	Length (bp)	Function	Subsystems	Begin	End
fig|1504.6.peg.1121	CDS	Contig_6	328971	330962	1992	ATP-dependent DNA helicase pcrA (EC 3.6.1.-)	CBSS-393121.3.peg.1913, DNA repair, bacterial UvrD and related helicases	328971	330962
fig|1504.6.peg.1122	CDS	Contig_6	331003	332991	1989	Cell division protein FtsA	Bacterial Cell Division, Bacterial Cytoskeleton, cell division cluster containing FtsQ, cell division core of larger cluster	331003	332991
fig|1504.6.peg.1123	CDS	Contig_6	333022	334227	1206	N-acetyl-L,L-diaminopimelate deacetylase (EC 3.5.1.47)	Lysine Biosynthesis DAP Pathway, Lysine Biosynthesis DAP Pathway, GJO scratch	333022	334227
fig|1504.6.peg.1124	CDS	Contig_6	334279	335247	969	Ribosomal large subunit pseudouridine synthase C (EC 4.2.1.70)	RNA pseudouridine syntheses, Ribosome biogenesis bacterial	334279	335247
fig|1504.6.peg.1125	CDS	Contig_6	335267	336886	1620	Stage V sporulation protein B	Sporulation gene orphans	335267	336886
fig|1504.6.peg.1126	CDS	Contig_6	338420	336921	1500	Stage V sporulation protein B	Sporulation gene orphans	336921	338420
fig|1504.6.peg.1127	CDS	Contig_6	338610	340349	1740	diguanylate cyclase/phosphodiesterase (GGDEF & EAL domains) with PAS/PAC sensor(s)	- none -	338610	340349
fig|1504.6.peg.1128	CDS	Contig_6	340839	342128	1290	Probable lipoprotein	- none -	340839	342128
fig|1504.6.peg.1129	CDS	Contig_6	342266	342802	537	Conserved protein	- none -	342266	342802
fig|1504.6.peg.1130	CDS	Contig_6	342951	344621	1671	Fe-S oxidoreductase	- none -	342951	344621
fig|1504.6.peg.1131	CDS	Contig_6	344901	345227	327	V-type ATP synthase subunit G (EC 3.6.3.14)	V-Type ATP synthase	344901	345227
fig|1504.6.peg.1132	CDS	Contig_6	345214	347169	1956	V-type ATP synthase subunit I (EC 3.6.3.14)	V-Type ATP synthase	345214	347169
fig|1504.6.peg.1133	CDS	Contig_6	347182	347667	486	V-type ATP synthase subunit K (EC 3.6.3.14)	V-Type ATP synthase	347182	347667
fig|1504.6.peg.1134	CDS	Contig_6	347686	348276	591	V-type ATP synthase subunit E (EC 3.6.3.14)	V-Type ATP synthase	347686	348276
fig|1504.6.peg.1135	CDS	Contig_6	348289	349290	1002	V-type ATP synthase subunit C (EC 3.6.3.14)	V-Type ATP synthase	348289	349290
fig|1504.6.peg.1136	CDS	Contig_6	349283	349594	312	V-type ATP synthase subunit F (EC 3.6.3.14)	V-Type ATP synthase	349283	349594
fig|1504.6.peg.1137	CDS	Contig_6	349614	351392	1779	V-type ATP synthase subunit A (EC 3.6.3.14)	V-Type ATP synthase	349614	351392

Feature ID	Type	Contig	Start	Stop	Length (bp)	Function	Subsystems	Begin	End
fig|1504.6.peg.1138	CDS	Contig_6	351385	352767	1383	V-type ATP synthase subunit B (EC 3.6.3.14)	V-Type ATP synthase	351385	352767
fig|1504.6.peg.1139	CDS	Contig_6	352771	353412	642	V-type ATP synthase subunit D (EC 3.6.3.14)	V-Type ATP synthase	352771	353412
fig|1504.6.peg.1140	CDS	Contig_6	353587	354540	954	Undecaprenyl-phosphate N-acetylglucosaminyl 1-phosphate transferase (EC 2.7.8.-)	Teichoic and lipoteichoic acids biosynthesis	353587	354540
fig|1504.6.peg.1141	CDS	Contig_6	354645	355187	543	5,10-methylenetetrahydrofolate reductase (EC 1.5.1.20)	5-FCL-like protein, Methionine Biosynthesis, One-carbon metabolism by tetrahydropterines, Serine-glyoxylate cycle	354645	355187
fig|1504.6.peg.1142	CDS	Contig_6	355258	355608	351	5,10-methylenetetrahydrofolate reductase (EC 1.5.1.20)	5-FCL-like protein, Methionine Biosynthesis, One-carbon metabolism by tetrahydropterines, Serine-glyoxylate cycle	355258	355608
fig|1504.6.peg.1143	CDS	Contig_6	355649	356350	702	Methionine synthase activation domain (EC 2.1.1.13)	Methionine Biosynthesis	355649	356350
fig|1504.6.peg.1144	CDS	Contig_6	356340	358727	2388	5-methyltetrahydrofolate--homocysteine methyltransferase (EC 2.1.1.13)	Methionine Biosynthesis	356340	358727
fig|1504.6.peg.1145	CDS	Contig_6	358777	358935	159	hypothetical protein	- none -	358777	358935
fig|1504.6.peg.1146	CDS	Contig_6	359845	358976	870	Transcriptional regulator, LysR family	- none -	358976	359845
fig|1504.6.peg.1147	CDS	Contig_6	360050	361849	1800	Putative ABC transporter (ATP-binding protein), spy1791 homolog	Heme, hemin uptake and utilization systems in GramPositives	360050	361849
fig|1504.6.peg.1148	CDS	Contig_6	361852	363525	1674	Putative ABC transporter ATP-binding protein, spy1790 homolog	Heme, hemin uptake and utilization systems in GramPositives	361852	363525
fig|1504.6.peg.1149	CDS	Contig_6	363594	363983	390	Hypothetical protein DUF454	- none -	363594	363983
fig|1504.6.peg.1150	CDS	Contig_6	363995	364288	294	conserved hypothetical protein	- none -	363995	364288
fig|1504.6.peg.1151	CDS	Contig_6	364532	365077	546	no significant homology Putative N-terminal signal sequence and 2 putative transmembrane regions were found by PSORT.	- none -	364532	365077

Feature ID	Type	Contig	Start	Stop	Length (bp)	Function	Subsystems	Begin	End
fig|1504.6.peg.1152	CDS	Contig_6	365135	365602	468	no significant homology 4 putative transmembrane regions were found by PSORT.	- none -	365135	365602
fig|1504.6.peg.1153	CDS	Contig_6	365595	366236	642	hypothetical protein	- none -	365595	366236
fig|1504.6.peg.1154	CDS	Contig_6	366249	366383	135	hypothetical protein	- none -	366249	366383
fig|1504.6.peg.1155	CDS	Contig_6	366448	368151	1704	Two-component response regulator	- none -	366448	368151
fig|1504.6.peg.1156	CDS	Contig_6	368297	369007	711	putative histidinol phosphatase and related hydrolases of the PHP family	- none -	368297	369007
fig|1504.6.peg.1157	CDS	Contig_6	369056	370252	1197	Alanyl-tRNA synthetase family protein	tRNA aminoacylation, Ala	369056	370252
fig|1504.6.peg.1158	CDS	Contig_6	370323	370913	591	ADP-ribose pyrophosphatase (EC 3.6.1.13)	CBSS-216591.1.peg.168, NAD and NADP cofactor biosynthesis global, Nudix proteins (nucleoside triphosphate hydrolases), Ribosome post-transcriptional modification and chromosomal segregation cluster	370323	370913
fig|1504.6.peg.1159	CDS	Contig_6	372104	370947	1158	Membrane-bound lytic murein transglycosylase D precursor (EC 3.2.1.-)	CBSS-228410.1.peg.134, CBSS-342610.3.peg.1536, Murein Hydrolases	370947	372104
fig|1504.6.peg.1160	CDS	Contig_6	372418	373551	1134	two-component sensor histidine kinase	- none -	372418	373551
fig|1504.6.peg.1161	CDS	Contig_6	373909	376293	2385	Two-component sensor histidine kinase	- none -	373909	376293
fig|1504.6.peg.1162	CDS	Contig_6	376496	377143	648	Membrane protein	- none -	376496	377143
fig|1504.6.peg.1163	CDS	Contig_6	377225	377461	237	no significant homology.	- none -	377225	377461
fig|1504.6.peg.1164	CDS	Contig_6	378854	377634	1221	Transposase, mutator type	- none -	377634	378854
fig|1504.6.peg.1165	CDS	Contig_6	379866	379024	843	Patatin-like phospholipase	- none -	379024	379866
fig|1504.6.peg.1166	CDS	Contig_6	380087	380638	552	CDS_ID OB0571	- none -	380087	380638
fig|1504.6.peg.1167	CDS	Contig_6	380751	381989	1239	Mobile element protein	- none -	380751	381989
fig|1504.6.peg.1168	CDS	Contig_6	383742	382291	1452	hypothetical protein	- none -	382291	383742
fig|1504.6.peg.1169	CDS	Contig_6	383795	383953	159	hypothetical protein	- none -	383795	383953
fig|1504.6.peg.1170	CDS	Contig_6	384203	385843	1641	hypothetical protein	- none -	384203	385843

Feature ID	Type	Contig	Start	Stop	Length (bp)	Function	Subsystems	Begin	End
fig|1504.6.peg.1171	CDS	Contig_6	386919	385903	1017	Aspartate--ammonia ligase (EC 6.3.1.1)	Glutamine, Glutamate, Aspartate and Asparagine Biosynthesis	385903	386919
fig|1504.6.peg.1172	CDS	Contig_6	387704	388225	522	FIG00522397: hypothetical protein	- none -	387704	388225
fig|1504.6.peg.1173	CDS	Contig_6	389592	388279	1314	Vancomycin B-type resistance protein VanW	Resistance to Vancomycin	388279	389592
fig|1504.6.peg.1174	CDS	Contig_6	389885	390091	207	no significant homology.	- none -	389885	390091
fig|1504.6.peg.1175	CDS	Contig_6	390194	391015	822	Metal transporter, ZIP family	- none -	390194	391015
fig|1504.6.peg.1176	CDS	Contig_6	391034	391363	330	hypothetical protein	- none -	391034	391363
fig|1504.6.peg.1177	CDS	Contig_6	391502	391684	183	Ferredoxin	Soluble cytochromes and functionally related electron carriers	391502	391684
fig|1504.6.peg.1178	CDS	Contig_6	391749	391922	174	no significant homology	- none -	391749	391922
fig|1504.6.peg.1179	CDS	Contig_6	392044	392466	423	hypothetical protein	- none -	392044	392466
fig|1504.6.peg.1180	CDS	Contig_6	392902	392693	210	Cold shock protein CspA	Cold shock, CspA family of proteins	392693	392902
fig|1504.6.peg.1181	CDS	Contig_6	393168	393596	429	5-carboxymethyl-2-oxo-hex-3- ene-1,7-dioate decarboxylase (EC 4.1.1.68)	- none -	393168	393596
fig|1504.6.peg.1182	CDS	Contig_6	393709	394101	393	no significant homology. Putative N-terminal signal sequence and 2 putative transmembrane regions were found by PSORT.	- none -	393709	394101
fig|1504.6.peg.1183	CDS	Contig_6	394624	395973	1350	Branched-chain amino acid transport system carrier protein	- none -	394624	395973
fig|1504.6.peg.1184	CDS	Contig_6	396039	396887	849	oxidoreductase, FAD-binding	- none -	396039	396887
fig|1504.6.peg.1185	CDS	Contig_6	397104	399794	2691	NtrC family Transcriptional regulator, ATPase domain	- none -	397104	399794
fig|1504.6.peg.1186	CDS	Contig_6	399988	400299	312	PTS system, cellobiose-specific IIB component (EC 2.7.1.69)	Beta-Glucoside Metabolism	399988	400299
fig|1504.6.peg.1187	CDS	Contig_6	400306	401643	1338	PTS system, cellobiose-specific IIC component (EC 2.7.1.69)	Beta-Glucoside Metabolism	400306	401643
fig|1504.6.peg.1188	CDS	Contig_6	401682	401996	315	PTS system, cellobiose-specific IIA component (EC 2.7.1.69)	Beta-Glucoside Metabolism	401682	401996
fig|1504.6.peg.1189	CDS	Contig_6	401999	403315	1317	6-phospho-beta-glucosidase (EC 3.2.1.86)	Beta-Glucoside Metabolism	401999	403315

Feature ID	Type	Contig	Start	Stop	Length (bp)	Function	Subsystems	Begin	End
fig|1504.6.peg.1190	CDS	Contig_6	403329	404066	738	Cellobiose phosphotransferase system YdjC-like protein	Beta-Glucoside Metabolism	403329	404066
fig|1504.6.peg.1191	CDS	Contig_6	404331	404188	144	hypothetical protein	- none -	404188	404331
fig|1504.6.peg.1192	CDS	Contig_6	404484	405248	765	Hypothetical membrane-spanning protein	- none -	404484	405248
fig|1504.6.peg.1193	CDS	Contig_6	405545	406156	612	UPF0059 membrane protein BF1149	- none -	405545	406156
fig|1504.6.peg.1194	CDS	Contig_6	406252	406593	342	Alkylphosphonate utilization operon protein PhnA	- none -	406252	406593
fig|1504.6.peg.1195	CDS	Contig_6	406747	407583	837	NADH pyrophosphatase (EC 3.6.1.22)	Nudix proteins (nucleoside triphosphate hydrolases)	406747	407583
fig|1504.6.peg.1196	CDS	Contig_6	407617	408768	1152	Histidine kinase-like ATPase	- none -	407617	408768
fig|1504.6.peg.1197	CDS	Contig_6	408770	409408	639	Two-component response regulator	- none -	408770	409408
fig|1504.6.peg.1198	CDS	Contig_6	409495	410430	936	ABC-type multidrug transport system, ATPase component	- none -	409495	410430
fig|1504.6.peg.1199	CDS	Contig_6	410446	411540	1095	Putative permease, ortholog yfkN B.subtilis	- none -	410446	411540
fig|1504.6.peg.1200	CDS	Contig_6	411531	412595	1065	membrane protein, putative	- none -	411531	412595
fig|1504.6.peg.1201	CDS	Contig_6	412617	413723	1107	Mobile element protein	- none -	412617	413723
fig|1504.6.peg.1202	CDS	Contig_6	414029	414154	126	hypothetical protein	- none -	414029	414154
fig|1504.6.peg.1203	CDS	Contig_6	414967	414119	849	Protein tyrosine phosphatase II superfamily protein	- none -	414119	414967
fig|1504.6.peg.1204	CDS	Contig_6	415160	416062	903	Transcriptional regulator, DeoR family	- none -	415160	416062
fig|1504.6.peg.1205	CDS	Contig_6	416129	416569	441	Transcriptional regulator, AraC family	- none -	416129	416569
fig|1504.6.peg.1206	CDS	Contig_6	416610	417482	873	Radical SAM domain protein	- none -	416610	417482
fig|1504.6.peg.1207	CDS	Contig_6	418010	417588	423	Cytidine deaminase (EC 3.5.4.5)	Murein hydrolase regulation and cell death, pyrimidine conversions	417588	418010
fig|1504.6.peg.1208	CDS	Contig_6	418685	418032	654	Predicted N-ribosylNicotinamide CRP-like regulator	NAD and NADP cofactor biosynthesis global	418032	418685
fig|1504.6.peg.1209	CDS	Contig_6	419138	423166	4029	Sialidase (EC 3.2.1.18)	Galactosylceramide and Sulfatide metabolism, Sialic Acid Metabolism	419138	423166

Feature ID	Type	Contig	Start	Stop	Length (bp)	Function	Subsystems	Begin	End
fig|1504.6.peg.1210	CDS	Contig_6	424558	427518	2961	Beta-hexosaminidase (EC 3.2.1.52)	Chitin and N-acetylglucosamine utilization, N-Acetyl-Galactosamine and Galactosamine Utilization	424558	427518
fig|1504.6.peg.1211	CDS	Contig_6	430030	427658	2373	Streptococcal cell surface hemoprotein receptor Shr	Heme, hemin uptake and utilization systems in GramPositives	427658	430030
fig|1504.6.peg.1212	CDS	Contig_6	431255	430509	747	Predicted regulator for deoxynucleoside utilization, GntR family	- none -	430509	431255
fig|1504.6.peg.1213	CDS	Contig_6	431605	432996	1392	Similar to tetracycline resistance protein	- none -	431605	432996
fig|1504.6.peg.1214	CDS	Contig_6	433579	433400	180	hypothetical protein	- none -	433400	433579
fig|1504.6.peg.1215	CDS	Contig_6	433626	435410	1785	Stage V sporulation protein K	- none -	433626	435410
fig|1504.6.peg.1216	CDS	Contig_6	435425	435913	489	hypothetical protein	- none -	435425	435913
fig|1504.6.peg.1217	CDS	Contig_6	435925	436635	711	hypothetical protein	- none -	435925	436635
fig|1504.6.peg.1218	CDS	Contig_6	436950	441533	4584	Beta-hexosaminidase (EC 3.2.1.52)	Chitin and N-acetylglucosamine utilization, N-Acetyl-Galactosamine and Galactosamine Utilization	436950	441533
fig|1504.6.peg.1219	CDS	Contig_6	441995	443137	1143	Alcohol dehydrogenase (EC 1.1.1.1)	5-FCL-like protein, Butanol Biosynthesis, Fermentations: Mixed acid, Glycerolipid and Glycerophospholipid Metabolism in Bacteria	441995	443137
fig|1504.6.peg.1220	CDS	Contig_6	443637	444467	831	Transcriptional regulator, MerR family	Cobalt-zinc-cadmium resistance	443637	444467
fig|1504.6.peg.1221	CDS	Contig_6	444981	446075	1095	Choline permease LicB	- none -	444981	446075
fig|1504.6.peg.1222	CDS	Contig_6	446080	446346	267	FIG00515214: hypothetical protein	- none -	446080	446346
fig|1504.6.peg.1223	CDS	Contig_6	446591	446887	297	PduJ-like protein clustered with pyruvate formate-lyase	- none -	446591	446887
fig|1504.6.peg.1224	CDS	Contig_6	446917	447225	309	EutM/PduA/PduJ-like protein 3 clustered with pyruvate formate-lyase	- none -	446917	447225
fig|1504.6.peg.1225	CDS	Contig_6	447260	448753	1494	Acetaldehyde dehydrogenase, ethanolamine utilization cluster (EC 1.2.1.10)	Ethanolamine utilization	447260	448753

Feature ID	Type	Contig	Start	Stop	Length (bp)	Function	Subsystems	Begin	End
fig|1504.6.peg.1226	CDS	Contig_6	448798	451338	2541	Pyruvate formate-lyase (EC 2.3.1.54)	Butanol Biosynthesis, Fermentations: Mixed acid	448798	451338
fig|1504.6.peg.1227	CDS	Contig_6	451471	452424	954	Pyruvate formate-lyase activating enzyme (EC 1.97.1.4)	Fermentations: Mixed acid	451471	452424
fig|1504.6.peg.1228	CDS	Contig_6	452463	452816	354	Propanediol utilization polyhedral body protein PduU	- none -	452463	452816
fig|1504.6.peg.1229	CDS	Contig_6	452831	453259	429	Ethanolamine utilization protein similar to PduV	Ethanolamine utilization	452831	453259
fig|1504.6.peg.1230	CDS	Contig_6	453266	453985	720	ATP:Cob(I)alamin adenosyltransferase (EC 2.5.1.17) @ ATP:Cob(I)alamin adenosyltransferase (EC 2.5.1.17), ethanolamine utilization	Ethanolamine utilization	453266	453985
fig|1504.6.peg.1231	CDS	Contig_6	453967	454815	849	Ethanolamine utilization protein EutJ	Ethanolamine utilization	453967	454815
fig|1504.6.peg.1232	CDS	Contig_6	454891	455136	246	FIG00515841: hypothetical protein	- none -	454891	455136
fig|1504.6.peg.1233	CDS	Contig_6	455130	455393	264	Ethanolamine utilization polyhedral-body-like protein EutN	Ethanolamine utilization	455130	455393
fig|1504.6.peg.1234	CDS	Contig_6	455469	456140	672	Ethanolamine utilization protein EutQ	Ethanolamine utilization	455469	456140
fig|1504.6.peg.1235	CDS	Contig_6	456162	456830	669	Ethanolamine utilization protein similar to PduA/PduJ	Ethanolamine utilization	456162	456830
fig|1504.6.peg.1236	CDS	Contig_6	456894	458486	1593	Acetaldehyde dehydrogenase, ethanolamine utilization cluster (EC 1.2.1.10)	Ethanolamine utilization	456894	458486
fig|1504.6.peg.1237	CDS	Contig_6	458486	459136	651	Ethanolamine utilization protein similar to PduL	Ethanolamine utilization	458486	459136
fig|1504.6.peg.1238	CDS	Contig_6	459207	459497	291	Ethanolamine utilization protein similar to PduA/PduJ	Ethanolamine utilization	459207	459497
fig|1504.6.peg.1239	CDS	Contig_6	459872	460834	963	Nitrogen regulation protein NIFR3	- none -	459872	460834
fig|1504.6.peg.1240	CDS	Contig_6	461061	465125	4065	Beta-galactosidase (EC 3.2.1.23)	Galactosylceramide and Sulfatide metabolism, Lactose and Galactose Uptake and Utilization, Lactose utilization	461061	465125
fig|1504.6.peg.1241	CDS	Contig_6	465342	466472	1131	FIG00525257: hypothetical protein	- none -	465342	466472
fig|1504.6.peg.1242	CDS	Contig_6	467077	466613	465	Transcription elongation factor GreA	Transcription factors bacterial	466613	467077
fig|1504.6.peg.1243	CDS	Contig_6	467773	467156	618	Unknown	- none -	467156	467773
fig|1504.6.peg.1244	CDS	Contig_6	468102	467791	312	Transcriptional regulator, PadR family	CBSS-1352.1.peg.856	467791	468102

Feature ID	Type	Contig	Start	Stop	Length (bp)	Function	Subsystems	Begin	End
fig|1504.6.peg.1245	CDS	Contig_6	469232	468489	744	conserved membrane-spanning protein	- none -	468489	469232
fig|1504.6.peg.1246	CDS	Contig_6	469466	469849	384	FIG01280259: hypothetical protein	- none -	469466	469849
fig|1504.6.peg.1247	CDS	Contig_6	469839	470225	387	hypothetical protein	- none -	469839	470225
fig|1504.6.peg.1248	CDS	Contig_6	470511	471239	729	hypothetical protein	- none -	470511	471239
fig|1504.6.peg.1249	CDS	Contig_6	471251	472153	903	Replicative DNA helicase (DnaB) (EC 3.6.4.12)	DNA-replication	471251	472153
fig|1504.6.peg.1250	CDS	Contig_6	472250	472771	522	hypothetical protein	- none -	472250	472771
fig|1504.6.peg.1251	CDS	Contig_6	472901	473668	768	Peptidoglycan N-acetylglucosamine deacetylase (EC 3.5.1.-)	Polysaccharide deacetylases	472901	473668
fig|1504.6.peg.1252	CDS	Contig_6	473910	475481	1572	MutS-related protein, family 1	DNA repair, bacterial MutL-MutS system	473910	475481
fig|1504.6.peg.1253	CDS	Contig_6	475671	475793	123	hypothetical protein	- none -	475671	475793
fig|1504.6.peg.1254	CDS	Contig_6	475935	476333	399	hypothetical protein	- none -	475935	476333
fig|1504.6.peg.1255	CDS	Contig_6	476833	481029	4197	hypothetical protein	- none -	476833	481029
fig|1504.6.peg.1256	CDS	Contig_6	481712	482845	1134	TPR domain protein in aerotolerance operon	- none -	481712	482845
fig|1504.6.peg.1257	CDS	Contig_6	483089	483628	540	hypothetical protein	- none -	483089	483628
fig|1504.6.peg.1258	CDS	Contig_6	483809	485113	1305	Alkaline phosphodiesterase I (EC 3.1.4.1) / Nucleotide pyrophosphatase (EC 3.6.1.9)	Purine conversions	483809	485113
fig|1504.6.peg.1259	CDS	Contig_6	485123	485590	468	membrane protein, putative	- none -	485123	485590
fig|1504.6.peg.1260	CDS	Contig_6	485635	486114	480	membrane protein, putative	- none -	485635	486114
fig|1504.6.peg.1261	CDS	Contig_6	486256	488154	1899	membrane spanning protein	- none -	486256	488154
fig|1504.6.peg.1262	CDS	Contig_6	488326	488880	555	hypothetical protein	- none -	488326	488880
fig|1504.6.peg.1263	CDS	Contig_6	490936	488996	1941	two-component sensor histidine kinase	- none -	488996	490936
fig|1504.6.peg.1264	CDS	Contig_6	491297	493348	2052	Fe-S OXIDOREDUCTASE (1.8.-.-)	- none -	491297	493348
fig|1504.6.peg.1265	CDS	Contig_6	493776	494585	810	Endo-beta-N-acetylglucosaminidase (EC 3.2.1.96)	- none -	493776	494585
fig|1504.6.peg.1266	CDS	Contig_6	495055	497070	2016	Anaerobic dehydrogenases, typically selenocysteine-containing	Anaerobic respiratory reductases	495055	497070
fig|1504.6.peg.1267	CDS	Contig_6	497152	497589	438	Nucleotidyltransferase (EC 2.7.7.-)	- none -	497152	497589

Feature ID	Type	Contig	Start	Stop	Length (bp)	Function	Subsystems	Begin	End
fig|1504.6.peg.1268	CDS	Contig_6	497589	497876	288	DNA polymerase beta domain protein region	- none -	497589	497876
fig|1504.6.peg.1269	CDS	Contig_6	498005	499042	1038	Deblocking aminopeptidase (EC 3.4.11.-)	Protein degradation	498005	499042
fig|1504.6.peg.1270	CDS	Contig_6	499307	500896	1590	two-component sensor histidine kinase	- none -	499307	500896
fig|1504.6.peg.1271	CDS	Contig_6	501146	501487	342	hypothetical protein	- none -	501146	501487
fig|1504.6.peg.1272	CDS	Contig_6	502162	501548	615	hypothetical protein	- none -	501548	502162
fig|1504.6.peg.1273	CDS	Contig_6	502931	502653	279	hypothetical protein	- none -	502653	502931
fig|1504.6.peg.1274	CDS	Contig_6	503616	502882	735	ABC transporter ATP-binding protein	- none -	502882	503616
fig|1504.6.peg.1275	CDS	Contig_6	504856	503738	1119	ABC transporter, permease protein	- none -	503738	504856
fig|1504.6.peg.1276	CDS	Contig_6	505908	504859	1050	Macrolide export ATP-binding/permease protein MacB (EC 3.6.3.-)	Multidrug Resistance Efflux Pumps	504859	505908
fig|1504.6.peg.1277	CDS	Contig_6	507351	507536	186	Guanine deaminase (EC 3.5.4.3)	Purine Utilization, Purine conversions	507351	507536
fig|1504.6.peg.1278	CDS	Contig_6	507621	508148	528	Guanine deaminase (EC 3.5.4.3)	Purine Utilization, Purine conversions	507621	508148
fig|1504.6.peg.1279	CDS	Contig_6	508135	508257	123	hypothetical protein	- none -	508135	508257
fig|1504.6.peg.1280	CDS	Contig_6	508487	509584	1098	FIG00515077: hypothetical protein	- none -	508487	509584
fig|1504.6.peg.1281	CDS	Contig_6	509934	509800	135	hypothetical protein	- none -	509800	509934
fig|1504.6.peg.1282	CDS	Contig_6	510118	512907	2790	Probable ATP-dependent RNA helicase	- none -	510118	512907
fig|1504.6.peg.1283	CDS	Contig_6	513044	513613	570	hypothetical protein	- none -	513044	513613
fig|1504.6.peg.1284	CDS	Contig_6	514035	514709	675	Two-component response regulator	- none -	514035	514709
fig|1504.6.peg.1285	CDS	Contig_6	514828	515727	900	Histidine kinase	- none -	514828	515727
fig|1504.6.peg.1286	CDS	Contig_6	515903	517132	1230	hypothetical protein	- none -	515903	517132
fig|1504.6.peg.1287	CDS	Contig_6	517147	517338	192	hypothetical protein	- none -	517147	517338
fig|1504.6.peg.1288	CDS	Contig_6	517503	518285	783	ABC transporter ATP-binding protein	- none -	517503	518285
fig|1504.6.peg.1289	CDS	Contig_6	518263	520245	1983	ABC transporter permease protein	- none -	518263	520245
fig|1504.6.peg.1290	CDS	Contig_6	521247	520489	759	hypothetical protein	- none -	520489	521247

Feature ID	Type	Contig	Start	Stop	Length (bp)	Function	Subsystems	Begin	End
fig|1504.6.peg.1291	CDS	Contig_6	522740	521583	1158	Alanine racemase (EC 5.1.1.1)	Alanine biosynthesis, Pyruvate Alanine Serine Interconversions	521583	522740
fig|1504.6.peg.1292	CDS	Contig_6	522866	524266	1401	Predicted transcriptional regulator of pyridoxine metabolism	Pyridoxin (Vitamin B6) Biosynthesis	522866	524266
fig|1504.6.peg.1293	CDS	Contig_6	524747	529858	5112	Beta-galactosidase (EC 3.2.1.23)	Galactosylceramide and Sulfatide metabolism, Lactose and Galactose Uptake and Utilization, Lactose utilization	524747	529858
fig|1504.6.peg.1294	CDS	Contig_6	530264	530758	495	hypothetical protein	- none -	530264	530758
fig|1504.6.peg.1295	CDS	Contig_6	530774	530977	204	Transcriptional regulator, Cro/CI family	- none -	530774	530977
fig|1504.6.peg.1296	CDS	Contig_6	530992	532848	1857	hypothetical protein	- none -	530992	532848
fig|1504.6.peg.1297	CDS	Contig_6	532985	533305	321	hypothetical protein	- none -	532985	533305
fig|1504.6.peg.1298	CDS	Contig_6	533567	534619	1053	Sugar diacid utilization regulator SdaR	D-galactarate, D-glucarate and D-glycerate catabolism, D-galactarate, D-glucarate and D-glycerate catabolism - gjo	533567	534619
fig|1504.6.peg.1299	CDS	Contig_6	534755	536014	1260	D-glycerate transporter (predicted)	D-galactarate, D-glucarate and D-glycerate catabolism, D-galactarate, D-glucarate and D-glycerate catabolism - gjo, Glycerate metabolism	534755	536014
fig|1504.6.peg.1300	CDS	Contig_6	536055	537185	1131	Glycerate kinase (EC 2.7.1.31)	D-galactarate, D-glucarate and D-glycerate catabolism, D-galactarate, D-glucarate and D-glycerate catabolism - gjo, Glycerate metabolism, Glycerolipid and Glycerophospholipid Metabolism in Bacteria, Glycine and Serine Utilization, Serine-glyoxylate cycle	536055	537185

Feature ID	Type	Contig	Start	Stop	Length (bp)	Function	Subsystems	Begin	End
fig|1504.6.peg.1301	CDS	Contig_6	537611	539344	1734	Glutamyl-tRNA synthetase (EC 6.1.1.17) @ Glutamyl-tRNA(Gln) synthetase (EC 6.1.1.24)	Heme and Siroheme Biosynthesis, tRNA aminoacylation, Glu and Gln, tRNA aminoacylation, Glu and Gln	537611	539344
fig|1504.6.peg.1302	CDS	Contig_6	539755	540708	954	FIG00514005: hypothetical protein	- none -	539755	540708
fig|1504.6.peg.1303	CDS	Contig_6	542412	540748	1665	Glutaminyl-tRNA synthetase (EC 6.1.1.18)	tRNA aminoacylation, Glu and Gln	540748	542412
fig|1504.6.peg.1304	CDS	Contig_6	542748	543620	873	metallo-beta-lactamase family protein	- none -	542748	543620
fig|1504.6.peg.1305	CDS	Contig_6	543694	544251	558	Substrate-specific component MtsA of methionine-regulated ECF transporter	ECF class transporters, Methionine Biosynthesis	543694	544251
fig|1504.6.peg.1306	CDS	Contig_6	544322	546025	1704	Duplicated ATPase component MtsB of energizing module of methionine-regulated ECF transporter	ECF class transporters, Methionine Biosynthesis	544322	546025
fig|1504.6.peg.1307	CDS	Contig_6	546025	546855	831	Transmembrane component MtsC of energizing module of methionine-regulated ECF transporter	ECF class transporters, Methionine Biosynthesis	546025	546855
fig|1504.6.peg.1308	CDS	Contig_6	547048	547902	855	CAAX amino terminal protease family	- none -	547048	547902
fig|1504.6.peg.1309	CDS	Contig_6	549550	548312	1239	Mobile element protein	- none -	548312	549550
fig|1504.6.peg.1310	CDS	Contig_6	549886	549647	240	Glycerol-3-phosphate regulon repressor GlpR	Glycerol and Glycerol-3-phosphate Uptake and Utilization	549647	549886
fig|1504.6.peg.1311	CDS	Contig_6	549861	550010	150	hypothetical protein	- none -	549861	550010
fig|1504.6.peg.1312	CDS	Contig_6	550257	550126	132	Lactose phosphotransferase system repressor	Lactose and Galactose Uptake and Utilization	550126	550257
fig|1504.6.peg.1313	CDS	Contig_6	550317	550595	279	Transaldolase (EC 2.2.1.2)	Fructose utilization, Pentose phosphate pathway	550317	550595
fig|1504.6.peg.1314	CDS	Contig_6	550821	551606	786	Predicted hydrolase	- none -	550821	551606
fig|1504.6.peg.1315	CDS	Contig_6	552083	551640	444	Transcriptional regulator, MarR family	- none -	551640	552083
fig|1504.6.peg.1316	CDS	Contig_6	552322	554574	2253	Lipid A export ATP-binding/permease protein MsbA	- none -	552322	554574
fig|1504.6.peg.1317	CDS	Contig_6	554567	556426	1860	ABC-type multidrug/protein/lipid transport system, ATPase component	- none -	554567	556426

Feature ID	Type	Contig	Start	Stop	Length (bp)	Function	Subsystems	Begin	End
fig|1504.6.peg.1318	CDS	Contig_6	556915	557715	801	Hydroxymethylpyrimidine phosphate kinase ThiD (EC 2.7.4.7)	- none -	556915	557715
fig|1504.6.peg.1319	CDS	Contig_6	557743	558522	780	Hydroxyethylthiazole kinase (EC 2.7.1.50)	5-FCL-like protein, Thiamin biosynthesis	557743	558522
fig|1504.6.peg.1320	CDS	Contig_6	558524	559183	660	Thiaminase II (EC 3.5.99.2) involved in salvage of thiamin pyrimidine moiety	- none -	558524	559183
fig|1504.6.peg.1321	CDS	Contig_6	559208	559819	612	Thiamin-phosphate pyrophosphorylase (EC 2.5.1.3)	5-FCL-like protein, Thiamin biosynthesis	559208	559819
fig|1504.6.peg.1322	CDS	Contig_6	559933	560184	252	Sucrose-6-phosphate hydrolase (EC 3.2.1.B3)	- none -	559933	560184
fig|1504.6.peg.1323	CDS	Contig_6	560579	561040	462	Transcriptional regulator of fatty acid biosynthesis FabT	Fatty Acid Biosynthesis FASII	560579	561040
fig|1504.6.peg.1324	CDS	Contig_6	561033	562400	1368	Multi antimicrobial extrusion protein (Na(+)/drug antiporter), MATE family of MDR efflux pumps	Multidrug Resistance Efflux Pumps, Riboflavin, FMN and FAD metabolism in plants	561033	562400
fig|1504.6.peg.1325	CDS	Contig_6	562508	564463	1956	Ribosome protection-type tetracycline resistance related proteins, group 2	Tetracycline resistance, ribosome protection type, Tetracycline resistance, ribosome protection type, too, Translation elongation factor G family	562508	564463
fig|1504.6.peg.1326	CDS	Contig_6	564551	565477	927	hypothetical protein	- none -	564551	565477
fig|1504.6.peg.1327	CDS	Contig_6	565490	565624	135	hypothetical protein	- none -	565490	565624
fig|1504.6.peg.1328	CDS	Contig_6	565694	566389	696	COG0613, Predicted metal-dependent phosphoesterases (PHP family)	CBSS-314276.3.peg.1499	565694	566389
fig|1504.6.peg.1329	CDS	Contig_6	566576	567952	1377	Multi antimicrobial extrusion protein (Na(+)/drug antiporter), MATE family of MDR efflux pumps	Multidrug Resistance Efflux Pumps, Riboflavin, FMN and FAD metabolism in plants	566576	567952
fig|1504.6.peg.1330	CDS	Contig_6	568473	570698	2226	Beta-galactosidase (EC 3.2.1.23)	Galactosylceramide and Sulfatide metabolism, Lactose and Galactose Uptake and Utilization, Lactose utilization	568473	570698
fig|1504.6.peg.1331	CDS	Contig_6	571182	572285	1104	Nicotinate-nucleotide--dimethylbenzimidazole phosphoribosyltransferase (EC 2.4.2.21)	Cobalamin synthesis, Coenzyme B12 biosynthesis	571182	572285
fig|1504.6.peg.1332	CDS	Contig_6	572296	572829	534	Cob(I)alamin adenosyltransferase (EC 2.5.1.17)	Cobalamin synthesis, Coenzyme B12 biosynthesis	572296	572829

Feature ID	Type	Contig	Start	Stop	Length (bp)	Function	Subsystems	Begin	End
fig|1504.6.peg.1333	CDS	Contig_6	572826	573377	552	Adenosylcobinamide-phosphate guanylyltransferase (EC 2.7.7.62)	Cobalamin synthesis, Coenzyme B12 biosynthesis	572826	573377
fig|1504.6.peg.1334	CDS	Contig_6	573374	574129	756	Cobalamin synthase (EC 2.7.8.26)	Cobalamin synthesis, Coenzyme B12 biosynthesis	573374	574129
fig|1504.6.peg.1335	CDS	Contig_6	574142	574522	381	conserved hypothetical protein	- none -	574142	574522
fig|1504.6.peg.1336	CDS	Contig_6	574515	575117	603	Alpha-ribazole-5'-phosphate phosphatase (EC 3.1.3.73)	CBSS-216591.1.peg.168, Cobalamin synthesis, Coenzyme B12 biosynthesis, Phosphoglycerate mutase protein family	574515	575117
fig|1504.6.peg.1337	CDS	Contig_6	575128	576072	945	Adenosylcobinamide-phosphate synthase (EC 6.3.1.10)	Cobalamin synthesis, Coenzyme B12 biosynthesis	575128	576072
fig|1504.6.peg.1338	CDS	Contig_6	576072	577142	1071	L-threonine 3-O-phosphate decarboxylase (EC 4.1.1.81)	Cobalamin synthesis, Coenzyme B12 biosynthesis	576072	577142
fig|1504.6.peg.1339	CDS	Contig_6	577250	578659	1410	Mobile element protein	- none -	577250	578659
fig|1504.6.peg.1340	CDS	Contig_6	578871	582347	3477	2',3'-cyclic-nucleotide 2'-phosphodiesterase (EC 3.1.4.16) / 5'-nucleotidase (EC 3.1.3.5)	Purine conversions, Purine conversions, pyrimidine conversions, pyrimidine conversions	578871	582347
fig|1504.6.peg.1341	CDS	Contig_6	582874	583791	918	Vitamin B12 ABC transporter, B12-binding component BtuF	Coenzyme B12 biosynthesis	582874	583791
fig|1504.6.peg.1342	CDS	Contig_6	583778	584806	1029	Vitamin B12 ABC transporter, permease component BtuC	Coenzyme B12 biosynthesis	583778	584806
fig|1504.6.peg.1343	CDS	Contig_6	584816	585571	756	Vitamin B12 ABC transporter, ATPase component BtuD	Coenzyme B12 biosynthesis	584816	585571
fig|1504.6.peg.1344	CDS	Contig_6	585583	586239	657	conserved hypothetical protein [Pyrococcus horikoshii] COG2102: Predicted ATPases of PP-loop superfamily IPR002761: Domain of unknown function DUF71: B12 cluster	- none -	585583	586239
fig|1504.6.peg.1345	CDS	Contig_6	586241	587728	1488	Cobyric acid synthase (EC 6.3.5.10)	Cobalamin synthesis, Coenzyme B12 biosynthesis	586241	587728
fig|1504.6.peg.1346	CDS	Contig_6	587863	588780	918	phospholipase, patatin family	- none -	587863	588780
fig|1504.6.peg.1347	CDS	Contig_6	588922	589293	372	hypothetical protein	- none -	588922	589293
fig|1504.6.peg.1348	CDS	Contig_6	589520	591580	2061	Methyl-accepting chemotaxis protein	- none -	589520	591580
fig|1504.6.peg.1349	CDS	Contig_6	591673	592728	1056	membrane protein, putative	- none -	591673	592728

Feature ID	Type	Contig	Start	Stop	Length (bp)	Function	Subsystems	Begin	End
fig|1504.6.peg.1350	CDS	Contig_6	592756	593745	990	D-lactate dehydrogenase (EC 1.1.1.28)	Fermentations: Lactate, Fermentations: Mixed acid	592756	593745
fig|1504.6.peg.1351	CDS	Contig_6	593751	594746	996	Biosynthetic Aromatic amino acid aminotransferase beta (EC 2.6.1.57) @ Histidinol-phosphate aminotransferase (EC 2.6.1.9)	Phenylalanine and Tyrosine Branches from Chorismate	593751	594746
fig|1504.6.peg.1352	CDS	Contig_6	594761	595414	654	DUF124 domain-containing protein	- none -	594761	595414
fig|1504.6.peg.1353	CDS	Contig_6	596538	595459	1080	site-specific recombinase, phage integrase family	- none -	595459	596538
fig|1504.6.peg.1354	CDS	Contig_6	597043	596585	459	Phage protein	- none -	596585	597043
fig|1504.6.peg.1355	CDS	Contig_6	597561	597064	498	Transcriptional regulator	- none -	597064	597561
fig|1504.6.peg.1356	CDS	Contig_6	597757	597957	201	hypothetical protein	- none -	597757	597957
fig|1504.6.peg.1357	CDS	Contig_6	598239	598526	288	hypothetical protein	- none -	598239	598526
fig|1504.6.peg.1358	CDS	Contig_6	598588	598785	198	hypothetical protein	- none -	598588	598785
fig|1504.6.peg.1359	CDS	Contig_6	598821	598997	177	hypothetical protein	- none -	598821	598997
fig|1504.6.peg.1360	CDS	Contig_6	599020	599274	255	hypothetical protein	- none -	599020	599274
fig|1504.6.peg.1361	CDS	Contig_6	599310	599435	126	hypothetical protein	- none -	599310	599435
fig|1504.6.peg.1362	CDS	Contig_6	599425	601347	1923	ATPase involved in DNA repair, phage associated	- none -	599425	601347
fig|1504.6.peg.1363	CDS	Contig_6	601349	601816	468	hypothetical protein	- none -	601349	601816
fig|1504.6.peg.1364	CDS	Contig_6	601828	602100	273	hypothetical protein	- none -	601828	602100
fig|1504.6.peg.1365	CDS	Contig_6	602118	603011	894	Recombinational DNA repair protein RecT (prophage associated)	DNA repair, bacterial	602118	603011
fig|1504.6.peg.1366	CDS	Contig_6	603053	603709	657	Metallo-beta-lactamase superfamily domain protein in prophage	Heme, hemin uptake and utilization systems in GramPositives	603053	603709
fig|1504.6.peg.1367	CDS	Contig_6	603735	604313	579	Predicted HD superfamily hydrolase	- none -	603735	604313
fig|1504.6.peg.1368	CDS	Contig_6	604315	604719	405	Single-stranded DNA-binding protein	DNA repair, bacterial, DNA repair, bacterial RecFOR pathway	604315	604719
fig|1504.6.peg.1369	CDS	Contig_6	604769	605413	645	Phage protein	- none -	604769	605413

Feature ID	Type	Contig	Start	Stop	Length (bp)	Function	Subsystems	Begin	End
fig|1504.6.peg.1370	CDS	Contig_6	605416	605640	225	hypothetical protein	- none -	605416	605640
fig|1504.6.peg.1371	CDS	Contig_6	605654	608248	2595	DNA primase (EC 2.7.7.-)	CBSS-349161.4.peg.2417, DNA-replication, Macromolecular synthesis operon	605654	608248
fig|1504.6.peg.1372	CDS	Contig_6	608262	608447	186	hypothetical protein	- none -	608262	608447
fig|1504.6.peg.1373	CDS	Contig_6	608440	608634	195	hypothetical protein	- none -	608440	608634
fig|1504.6.peg.1374	CDS	Contig_6	608666	608812	147	hypothetical protein	- none -	608666	608812
fig|1504.6.peg.1375	CDS	Contig_6	608814	609611	798	Phosphoadenylyl-sulfate reductase [thioredoxin] (EC 1.8.4.8)	Cysteine Biosynthesis	608814	609611
fig|1504.6.peg.1376	CDS	Contig_6	609760	610200	441	hypothetical protein	- none -	609760	610200
fig|1504.6.peg.1377	CDS	Contig_6	610321	610695	375	hypothetical protein	- none -	610321	610695
fig|1504.6.peg.1378	CDS	Contig_6	610788	611216	429	hypothetical protein	- none -	610788	611216
fig|1504.6.peg.1379	CDS	Contig_6	611429	611596	168	hypothetical protein	- none -	611429	611596
fig|1504.6.peg.1380	CDS	Contig_6	611617	612075	459	Dimeric dUTPase (EC 3.6.1.23)	Housecleaning nucleoside triphosphate pyrophosphatases	611617	612075
fig|1504.6.peg.1381	CDS	Contig_6	612075	612332	258	hypothetical protein	- none -	612075	612332
fig|1504.6.peg.1382	CDS	Contig_6	612653	612802	150	hypothetical protein	- none -	612653	612802
fig|1504.6.peg.1383	CDS	Contig_6	612854	613288	435	hypothetical protein	- none -	612854	613288
fig|1504.6.peg.1384	CDS	Contig_6	613444	613893	450	FIG00519857: hypothetical protein	- none -	613444	613893
fig|1504.6.peg.1385	CDS	Contig_6	614134	615900	1767	FIG00515055: hypothetical protein	- none -	614134	615900
fig|1504.6.peg.1386	CDS	Contig_6	615912	617243	1332	phage portal protein	- none -	615912	617243
fig|1504.6.peg.1387	CDS	Contig_6	617246	618679	1434	putative phage protein	- none -	617246	618679
fig|1504.6.peg.1388	CDS	Contig_6	618679	618879	201	hypothetical protein	- none -	618679	618879
fig|1504.6.peg.1389	CDS	Contig_6	618945	619253	309	hypothetical protein	- none -	618945	619253
fig|1504.6.peg.1390	CDS	Contig_6	619268	619531	264	FIG00630947: hypothetical protein	- none -	619268	619531
fig|1504.6.peg.1391	CDS	node_148_[2]	64	777	714	Nitrite reductase probable [NAD(P)H] subunit (EC 1.7.1.4)	Nitrate and nitrite ammonification	64	777
fig|1504.6.peg.1392	CDS	node_148_[2]	1806	847	960	Tellurite resistance protein	- none -	847	1806

Feature ID	Type	Contig	Start	Stop	Length (bp)	Function	Subsystems	Begin	End
fig|1504.6.peg.1393	CDS	node_148_[2]	2013	2516	504	Molybdopterin-guanine dinucleotide biosynthesis protein MobB	Molybdenum cofactor biosynthesis, ar-431-EC Molybdopterin-guanine dinucleotide biosynthesis	2013	2516
fig|1504.6.peg.1394	CDS	node_148_[2]	2761	3963	1203	Molybdopterin biosynthesis protein MoeA	Molybdenum cofactor biosynthesis	2761	3963
fig|1504.6.peg.1395	CDS	node_148_[2]	3982	4542	561	Molybdopterin-guanine dinucleotide biosynthesis protein MobA	Molybdenum cofactor biosynthesis, ar-431-EC Molybdopterin-guanine dinucleotide biosynthesis	3982	4542
fig|1504.6.peg.1396	CDS	node_148_[2]	4542	5033	492	Molybdenum cofactor biosynthesis protein MoaB	Molybdenum cofactor biosynthesis, ar-104-EC Molybdenum cofactor biosynthesis moaABCDE	4542	5033
fig|1504.6.peg.1397	CDS	node_148_[2]	5018	5791	774	Molybdenum ABC transporter, periplasmic molybdenum-binding protein ModA (TC 3.A.1.8.1)	Molybdenum cofactor biosynthesis	5018	5791
fig|1504.6.peg.1398	CDS	node_148_[2]	5801	6460	660	Molybdenum transport system permease protein ModB (TC 3.A.1.8.1)	Molybdenum cofactor biosynthesis	5801	6460
fig|1504.6.peg.1399	CDS	node_148_[2]	6478	7494	1017	Molybdopterin biosynthesis protein MoeA	Molybdenum cofactor biosynthesis	6478	7494
fig|1504.6.peg.1400	CDS	node_148_[2]	7506	7982	477	Molybdenum cofactor biosynthesis protein MoaC	Molybdenum cofactor biosynthesis, ar-104-EC Molybdenum cofactor biosynthesis moaABCDE	7506	7982
fig|1504.6.peg.1401	CDS	node_148_[2]	8105	8995	891	Molybdenum cofactor biosynthesis protein MoaA	Molybdenum cofactor biosynthesis, ar-104-EC Molybdenum cofactor biosynthesis moaABCDE	8105	8995
fig|1504.6.peg.1402	CDS	node_148_[2]	8999	9445	447	FIG060329: MOSC domain protein	Molybdenum cofactor biosynthesis	8999	9445
fig|1504.6.peg.1403	CDS	node_148_[2]	9934	9530	405	hypothetical protein	- none -	9530	9934
fig|1504.6.peg.1404	CDS	node_148_[2]	10066	10776	711	gliding motility protein	- none -	10066	10776
fig|1504.6.peg.1405	CDS	node_148_[2]	10769	12361	1593	hypothetical protein	- none -	10769	12361
fig|1504.6.peg.1406	CDS	node_148_[2]	12377	13105	729	serine/threonine protein phosphatase	- none -	12377	13105
fig|1504.6.peg.1407	CDS	node_148_[2]	13176	13943	768	Conserved protein	- none -	13176	13943

Feature ID	Type	Contig	Start	Stop	Length (bp)	Function	Subsystems	Begin	End
fig|1504.6.peg.1408	CDS	node_148_[2]	15510	14338	1173	Extracellular protein	- none -	14338	15510
fig|1504.6.peg.1409	CDS	node_148_[2]	15551	16657	1107	Mobile element protein	- none -	15551	16657
fig|1504.6.peg.1410	CDS	node_148_[2]	16969	17211	243	hypothetical protein	- none -	16969	17211
fig|1504.6.peg.1411	CDS	node_148_[2]	17316	18218	903	Malate permease	Pyruvate metabolism I: anaplerotic reactions, PEP	17316	18218
fig|1504.6.peg.1412	CDS	node_148_[2]	18304	19725	1422	SOS-response repressor and protease LexA (EC 3.4.21.88)	DNA repair, bacterial	18304	19725
fig|1504.6.peg.1413	CDS	node_148_[2]	19738	20298	561	FIG00515018: hypothetical protein	- none -	19738	20298
fig|1504.6.peg.1414	CDS	node_148_[2]	20341	20676	336	no significant homology.	- none -	20341	20676
fig|1504.6.peg.1415	CDS	node_148_[2]	21304	22638	1335	Permease of the drug/metabolite transporter (DMT) superfamily	Queuosine-Archaeosine Biosynthesis	21304	22638
fig|1504.6.peg.1416	CDS	node_148_[2]	22927	23142	216	hypothetical protein	- none -	22927	23142
fig|1504.6.peg.1417	CDS	node_148_[2]	23323	24831	1509	Cell division protein FtsH (EC 3.4.24.-)	Bacterial Cell Division, Cell division-ribosomal stress proteins cluster, Folate biosynthesis cluster	23323	24831
fig|1504.6.peg.1418	CDS	node_148_[2]	24928	25197	270	no significant homology	- none -	24928	25197
fig|1504.6.peg.1419	CDS	node_148_[2]	25743	25228	516	hypothetical protein	- none -	25228	25743
fig|1504.6.peg.1420	CDS	node_148_[2]	25911	26696	786	hypothetical protein	- none -	25911	26696
fig|1504.6.peg.1421	CDS	node_148_[2]	26770	28434	1665	Ribonuclease J2 (endoribonuclease in RNA processing)	Bacterial RNA-metabolizing Zn-dependent hydrolases, Ribonucleases in Bacillus	26770	28434
fig|1504.6.peg.1422	CDS	node_148_[2]	29169	29897	729	Phosphoserine phosphatase (EC 3.1.3.3)	Glycine and Serine Utilization, Serine Biosynthesis, Serine Biosynthesis	29169	29897
fig|1504.6.peg.1423	CDS	node_148_[2]	30050	30415	366	hypothetical protein	- none -	30050	30415
fig|1504.6.peg.1424	CDS	node_148_[2]	30568	31734	1167	multidrug resistance protein	- none -	30568	31734
fig|1504.6.peg.1630	CDS	node_148_[2]	34602	33496	1107	Mobile element protein	- none -	33496	34602
fig|1504.6.peg.1631	CDS	node_148_[2]	34642	35175	534	hypothetical protein	- none -	34642	35175
fig|1504.6.peg.1632	CDS	node_148_[2]	35240	35944	705	Zinc metalloprotease (EC 3.4.24.-)	- none -	35240	35944
fig|1504.6.peg.1633	CDS	node_148_[2]	36025	37329	1305	hypothetical protein	- none -	36025	37329

Feature ID	Type	Contig	Start	Stop	Length (bp)	Function	Subsystems	Begin	End
fig|1504.6.peg.1634	CDS	node_148_[2]	37442	38680	1239	Mobile element protein	- none -	37442	38680
fig|1504.6.peg.1635	CDS	node_148_[2]	40081	38882	1200	Threonine dehydratase (EC 4.3.1.19)	Threonine degradation	38882	40081
fig|1504.6.peg.1636	CDS	node_148_[2]	40242	40385	144	hypothetical protein	- none -	40242	40385
fig|1504.6.peg.1637	CDS	node_148_[2]	40387	41259	873	3-oxoacyl-[acyl-carrier protein] reductase (EC 1.1.1.100)	Fatty Acid Biosynthesis FASII	40387	41259
fig|1504.6.peg.1638	CDS	node_148_[2]	42145	41333	813	Endonuclease IV (EC 3.1.21.2)	DNA repair, bacterial	41333	42145
fig|1504.6.peg.1639	CDS	node_148_[2]	42503	43225	723	Ribosomal large subunit pseudouridine synthase B (EC 4.2.1.70)	CBSS-314276.3.peg.1499, RNA pseudouridine syntheses, Ribosome post-transcriptional modification and chromosomal segregation cluster	42503	43225
fig|1504.6.peg.1640	CDS	node_148_[2]	43236	43778	543	SAM-dependent methyltransferase, MraW methylase family (EC 2.1.1.-)	- none -	43236	43778
fig|1504.6.peg.1641	CDS	node_148_[2]	43918	44814	897	Transcriptional regulator, RpiR family	- none -	43918	44814
fig|1504.6.peg.1642	CDS	node_148_[2]	44995	46215	1221	NAD(FAD)-utilizing dehydrogenases	- none -	44995	46215
fig|1504.6.peg.1643	CDS	node_148_[2]	46315	46959	645	Cytidylate kinase (EC 2.7.4.25)	Ribosome post-transcriptional modification and chromosomal segregation cluster, pyrimidine conversions	46315	46959
fig|1504.6.peg.1644	CDS	node_148_[2]	47044	48951	1908	4-hydroxy-3-methylbut-2-enyl diphosphate reductase (EC 1.17.1.2) / SSU ribosomal protein S1p	Cell division-ribosomal stress proteins cluster, Isoprenoid Biosynthesis, Nonmevalonate Branch of Isoprenoid Biosynthesis, Ribosome SSU bacterial	47044	48951
fig|1504.6.peg.1645	CDS	node_148_[2]	49109	50062	954	Acetyltransferase Iojap substitute?	- none -	49109	50062
fig|1504.6.peg.1646	CDS	node_148_[2]	50082	50369	288	hypothetical protein	- none -	50082	50369
fig|1504.6.peg.1647	CDS	node_148_[2]	50598	51611	1014	N-acetylmuramoyl-L-alanine amidase (EC 3.5.1.28)	Murein Hydrolases, Recycling of Peptidoglycan Amino Acids	50598	51611
fig|1504.6.peg.1648	CDS	node_148_[2]	51850	52047	198	FIG00518168: hypothetical protein	- none -	51850	52047
fig|1504.6.peg.1649	CDS	node_148_[2]	53488	53237	252	Spore coat protein F	- none -	53237	53488
fig|1504.6.peg.1650	CDS	node_148_[2]	53686	53501	186	hypothetical protein	- none -	53501	53686

Feature ID	Type	Contig	Start	Stop	Length (bp)	Function	Subsystems	Begin	End
fig|1504.6.peg.1651	CDS	node_148_[2]	54144	55475	1332	tRNA-i(6)A37 methylthiotransferase	Methylthiotransferases, tRNA processing	54144	55475
fig|1504.6.peg.1652	CDS	node_148_[2]	55563	56066	504	hypothetical protein	- none -	55563	56066
fig|1504.6.peg.1653	CDS	node_148_[2]	56138	59392	3255	COG0553: Superfamily II DNA/RNA helicases, SNF2 family	- none -	56138	59392
fig|1504.6.peg.1654	CDS	node_148_[2]	59453	60253	801	Methyltransferase (EC 2.1.1.-)	- none -	59453	60253
fig|1504.6.peg.1655	CDS	node_148_[2]	60358	63000	2643	DNA mismatch repair protein MutS	DNA repair, bacterial MutL-MutS system, DNA repair system including RecA, MutS and a hypothetical protein	60358	63000
fig|1504.6.peg.1656	CDS	node_148_[2]	63014	64960	1947	DNA mismatch repair protein MutL	DNA repair, bacterial MutL-MutS system	63014	64960
fig|1504.6.peg.1657	CDS	node_148_[2]	64990	65916	927	tRNA dimethylallyltransferase (EC 2.5.1.75)	tRNA processing	64990	65916
fig|1504.6.peg.1658	CDS	node_148_[2]	65960	66190	231	RNA-binding protein Hfq	Hfl operon	65960	66190
fig|1504.6.peg.1659	CDS	node_148_[2]	66356	67633	1278	Aluminum resistance protein	- none -	66356	67633
fig|1504.6.peg.1660	CDS	node_148_[2]	68239	67649	591	hypothetical protein	- none -	67649	68239
fig|1504.6.peg.1661	CDS	node_148_[2]	68923	68309	615	SOS-response repressor and protease LexA (EC 3.4.21.88)	DNA repair, bacterial	68309	68923
fig|1504.6.peg.1662	CDS	node_148_[2]	69091	69474	384	Protein containing Zn-finger domain	- none -	69091	69474
fig|1504.6.peg.1663	CDS	node_148_[2]	70908	69541	1368	Probable integrase/recombinase	- none -	69541	70908
fig|1504.6.peg.1664	CDS	node_148_[2]	72875	71406	1470	Phage protein	- none -	71406	72875
fig|1504.6.peg.1665	CDS	node_148_[2]	73247	73062	186	conserved domain protein	- none -	73062	73247
fig|1504.6.peg.1666	CDS	node_148_[2]	74403	73273	1131	conserved protein	- none -	73273	74403
fig|1504.6.peg.1667	CDS	node_148_[2]	75793	74417	1377	Probable poly(beta-D-mannuronate) O-acetylase (EC 2.3.1.-)	- none -	74417	75793
fig|1504.6.peg.1668	CDS	node_148_[2]	76345	75866	480	hypothetical protein	- none -	75866	76345
fig|1504.6.peg.1669	CDS	node_148_[2]	78397	76475	1923	COG0488: ATPase components of ABC transporters with duplicated ATPase domains	- none -	76475	78397
fig|1504.6.peg.1670	CDS	node_148_[2]	78372	78497	126	hypothetical protein	- none -	78372	78497

Feature ID	Type	Contig	Start	Stop	Length (bp)	Function	Subsystems	Begin	End
fig|1504.6.peg.1671	CDS	node_148_[2]	79000	78500	501	Substrate-specific component QueT (COG4708) of predicted queuosine-regulated ECF transporter	ECF class transporters, Queuosine-Archaeosine Biosynthesis	78500	79000
fig|1504.6.peg.1672	CDS	node_148_[2]	83486	79254	4233	Activator of (R)-2-hydroxyglutaryl-CoA dehydratase	- none -	79254	83486
fig|1504.6.peg.1673	CDS	node_148_[2]	85062	83596	1467	Nicotinate phosphoribosyltransferase (EC 2.4.2.11)	NAD and NADP cofactor biosynthesis global, Redox-dependent regulation of nucleus processes	83596	85062
fig|1504.6.peg.1674	CDS	node_148_[2]	85738	85106	633	Nicotinamidase (EC 3.5.1.19)	NAD and NADP cofactor biosynthesis global, Redox-dependent regulation of nucleus processes	85106	85738
fig|1504.6.peg.1675	CDS	node_148_[2]	86649	85972	678	Transaldolase (EC 2.2.1.2)	Fructose utilization, Pentose phosphate pathway	85972	86649
fig|1504.6.peg.1676	CDS	node_148_[2]	87692	86937	756	Transcriptional regulator, DeoR family	- none -	86937	87692
fig|1504.6.peg.1677	CDS	node_148_[2]	90344	87936	2409	Pyruvate formate-lyase (EC 2.3.1.54)	Butanol Biosynthesis, Fermentations: Mixed acid	87936	90344
fig|1504.6.peg.1678	CDS	node_148_[2]	90588	91508	921	Pyruvate formate-lyase activating enzyme (EC 1.97.1.4)	Fermentations: Mixed acid	90588	91508
fig|1504.6.peg.1679	CDS	node_148_[2]	92696	91593	1104	Glycerol dehydrogenase (EC 1.1.1.6)	Respiratory dehydrogenases 1	91593	92696
fig|1504.6.peg.1680	CDS	node_148_[2]	94924	92849	2076	DNA double-strand break repair Rad50 ATPase	Rad50-Mre11 DNA repair cluster	92849	94924
fig|1504.6.peg.1681	CDS	node_148_[2]	95117	96100	984	Probable lipase	- none -	95117	96100
fig|1504.6.peg.1682	CDS	node_148_[2]	96663	96145	519	Arginine/ornithine antiporter ArcD	Arginine and Ornithine Degradation, Polyamine Metabolism	96145	96663
fig|1504.6.peg.1683	CDS	node_148_[2]	97491	96805	687	Orotate phosphoribosyltransferase (EC 2.4.2.10)	De Novo Pyrimidine Synthesis	96805	97491
fig|1504.6.peg.1684	CDS	node_148_[2]	97676	98323	648	putative lipoprotein	- none -	97676	98323
fig|1504.6.peg.1685	CDS	node_148_[2]	98795	98370	426	hypothetical protein	- none -	98370	98795
fig|1504.6.peg.1686	CDS	node_148_[2]	101822	99021	2802	putative large secreted protein	- none -	99021	101822
fig|1504.6.peg.1687	CDS	node_148_[2]	103256	101847	1410	putative large secreted protein	- none -	101847	103256

Feature ID	Type	Contig	Start	Stop	Length (bp)	Function	Subsystems	Begin	End
fig|1504.6.peg.1688	CDS	node_148_[2]	103628	104404	777	Mobile element protein	- none -	103628	104404
fig|1504.6.peg.1689	CDS	node_148_[2]	105630	104461	1170	Predicted sucrose permease, MFS family, FucP subfamily	- none -	104461	105630
fig|1504.6.peg.1690	CDS	node_148_[2]	106898	105729	1170	Aspartate aminotransferase (EC 2.6.1.1)	CBSS-216591.1.peg.168, Glutamine, Glutamate, Aspartate and Asparagine Biosynthesis, Threonine and Homoserine Biosynthesis	105729	106898
fig|1504.6.peg.1691	CDS	node_148_[2]	107377	106895	483	Transcriptional regulator, AsnC family	- none -	106895	107377
fig|1504.6.peg.1692	CDS	node_148_[2]	108673	107825	849	Integral membrane protein TerC	- none -	107825	108673
fig|1504.6.peg.1693	CDS	node_148_[2]	108907	109062	156	hypothetical protein	- none -	108907	109062
fig|1504.6.peg.1694	CDS	node_148_[2]	109083	109331	249	Polypeptide composition of the spore coat protein CotJB	- none -	109083	109331
fig|1504.6.peg.1695	CDS	node_148_[2]	109347	109616	270	Polypeptide composition of the spore coat protein CotJC	- none -	109347	109616
fig|1504.6.peg.1696	CDS	node_148_[2]	110273	109896	378	hypothetical protein	- none -	109896	110273
fig|1504.6.peg.1697	CDS	node_148_[2]	113505	110347	3159	SWF/SNF family helicase	- none -	110347	113505
fig|1504.6.peg.1698	CDS	node_148_[2]	114556	113729	828	Pyridoxal kinase (EC 2.7.1.35)	Pyridoxin (Vitamin B6) Biosynthesis	113729	114556
fig|1504.6.peg.1699	CDS	node_148_[2]	118025	114771	3255	ABC transporter permease protein	- none -	114771	118025
fig|1504.6.peg.1700	CDS	node_148_[2]	118729	118025	705	ABC transporter ATP-binding protein YvcR	- none -	118025	118729
fig|1504.6.peg.1701	CDS	node_148_[2]	120825	119107	1719	Oligoendopeptidase F (EC 3.4.24.-)	- none -	119107	120825
fig|1504.6.peg.1702	CDS	node_148_[2]	121141	120815	327	Thioredoxin	- none -	120815	121141
fig|1504.6.peg.1703	CDS	node_148_[2]	121703	121236	468	Membrane spanning protein	- none -	121236	121703
fig|1504.6.peg.1704	CDS	node_148_[2]	122468	121704	765	Membrane spanning protein	- none -	121704	122468
fig|1504.6.peg.1705	CDS	node_148_[2]	124011	122599	1413	Arginine decarboxylase (EC 4.1.1.19) / Lysine decarboxylase (EC 4.1.1.18)	Arginine and Ornithine Degradation, Lysine degradation, Polyamine Metabolism	122599	124011
fig|1504.6.peg.1706	CDS	node_148_[2]	125297	124080	1218	zinc protease	- none -	124080	125297

Feature ID	Type	Contig	Start	Stop	Length (bp)	Function	Subsystems	Begin	End
fig|1504.6.peg.1707	CDS	node_148_[2]	126674	125319	1356	FIG000557: hypothetical protein co-occurring with RecR	DNA processing cluster	125319	126674
fig|1504.6.peg.1708	CDS	node_148_[2]	126883	126746	138	hypothetical protein	- none -	126746	126883
fig|1504.6.peg.1709	CDS	node_148_[2]	127817	126963	855	Permease	- none -	126963	127817
fig|1504.6.peg.1710	CDS	node_148_[2]	128345	128767	423	Conserved domain protein	- none -	128345	128767
fig|1504.6.peg.1711	CDS	node_148_[2]	129442	128810	633	Ferric iron ABC transporter, ATP-binding protein	Iron acquisition in Streptococcus	128810	129442
fig|1504.6.peg.1712	CDS	node_148_[2]	131096	129432	1665	Ferric iron ABC transporter, permease protein	Iron acquisition in Streptococcus	129432	131096
fig|1504.6.peg.1713	CDS	node_148_[2]	132121	131099	1023	Ferric iron ABC transporter, iron-binding protein	Iron acquisition in Streptococcus	131099	132121
fig|1504.6.peg.1714	CDS	node_148_[2]	132234	132118	117	hypothetical protein	- none -	132118	132234
fig|1504.6.peg.1715	CDS	node_148_[2]	133487	132315	1173	Sucrose permease, major facilitator superfamily	- none -	132315	133487
fig|1504.6.peg.1716	CDS	node_148_[2]	135382	133598	1785	Lipoteichoic acid synthase LtaS Type IVb	Polyglycerolphosphate lipoteichoic acid biosynthesis	133598	135382
fig|1504.6.peg.1717	CDS	node_148_[2]	135533	136279	747	Probable DNA polymerase III epsilon chain	- none -	135533	136279
fig|1504.6.peg.1718	CDS	node_148_[2]	136937	136311	627	Hypothetical nudix hydrolase YeaB	Nudix proteins (nucleoside triphosphate hydrolases)	136311	136937
fig|1504.6.peg.1719	CDS	node_148_[2]	137348	137674	327	Proton/glutamate symport protein @ Sodium/glutamate symport protein	- none -	137348	137674
fig|1504.6.peg.1720	CDS	node_148_[2]	137740	138162	423	Proton/glutamate symport protein @ Sodium/glutamate symport protein	- none -	137740	138162
fig|1504.6.peg.1721	CDS	node_148_[2]	138444	138211	234	hypothetical protein	- none -	138211	138444
fig|1504.6.peg.1722	CDS	node_148_[2]	140656	138557	2100	Pyrophosphate-energized proton pump (EC 3.6.1.1)	Phosphate metabolism	138557	140656
fig|1504.6.peg.1723	CDS	node_148_[2]	141856	140927	930	Pyruvate formate-lyase activating enzyme (EC 1.97.1.4)	Fermentations: Mixed acid	140927	141856
fig|1504.6.peg.1724	CDS	node_148_[2]	144376	141965	2412	Pyruvate formate-lyase (EC 2.3.1.54)	Butanol Biosynthesis, Fermentations: Mixed acid	141965	144376
fig|1504.6.peg.1725	CDS	node_148_[2]	145313	144606	708	DNA-binding response regulator, AraC family	- none -	144606	145313
fig|1504.6.peg.1726	CDS	node_148_[2]	146544	145324	1221	two-component sensor histidine kinase	- none -	145324	146544
fig|1504.6.peg.1727	CDS	node_148_[2]	148878	147004	1875	Chaperone protein HtpG	Protein chaperones	147004	148878

Feature ID	Type	Contig	Start	Stop	Length (bp)	Function	Subsystems	Begin	End
fig|1504.6.peg.1728	CDS	node_148_[2]	149212	149826	615	Manganese superoxide dismutase (EC 1.15.1.1)	Oxidative stress, Protection from Reactive Oxygen Species	149212	149826
fig|1504.6.peg.1729	CDS	node_148_[2]	151577	149874	1704	subtilase family protein(EC:3.4.21.-)	- none -	149874	151577
fig|1504.6.peg.1730	CDS	node_148_[2]	153320	151596	1725	Ser-type protease	- none -	151596	153320
fig|1504.6.peg.1731	CDS	node_148_[2]	153499	153801	303	CDS_ID OB2939	- none -	153499	153801
fig|1504.6.peg.1732	CDS	node_148_[2]	154468	155760	1293	Guanine-hypoxanthine permease	Purine Utilization	154468	155760
fig|1504.6.peg.1733	CDS	node_148_[2]	157193	155835	1359	Methyl-accepting chemotaxis protein	- none -	155835	157193
fig|1504.6.peg.1734	CDS	node_148_[2]	158108	157419	690	hypothetical protein	- none -	157419	158108
fig|1504.6.peg.1735	CDS	node_148_[2]	158526	158128	399	conserved hypothetical protein	- none -	158128	158526
fig|1504.6.peg.1736	CDS	node_148_[2]	158729	159739	1011	hypothetical protein	- none -	158729	159739
fig|1504.6.peg.1737	CDS	node_148_[2]	161004	159802	1203	hypothetical protein	- none -	159802	161004
fig|1504.6.peg.1738	CDS	node_148_[2]	161242	161880	639	hypothetical protein	- none -	161242	161880
fig|1504.6.peg.1739	CDS	node_148_[2]	163183	161915	1269	Conserved protein	- none -	161915	163183
fig|1504.6.peg.1740	CDS	node_148_[2]	163486	163331	156	hypothetical protein	- none -	163331	163486
fig|1504.6.peg.1741	CDS	node_148_[2]	163656	164405	750	Transcriptional repressor of the fructose operon, DeoR family	Fructose utilization	163656	164405
fig|1504.6.peg.1742	CDS	node_148_[2]	164402	165319	918	1-phosphofructokinase (EC 2.7.1.56)	Fructose utilization	164402	165319
fig|1504.6.peg.1743	CDS	node_148_[2]	165323	167188	1866	PTS system, fructose-specific IIA component (EC 2.7.1.69) / PTS system, fructose-specific IIB component (EC 2.7.1.69) / PTS system, fructose-specific IIC component (EC 2.7.1.69)	Fructose utilization, Fructose utilization, Fructose utilization	165323	167188
fig|1504.6.peg.1744	CDS	node_148_[2]	167392	167252	141	hypothetical protein	- none -	167252	167392
fig|1504.6.peg.1745	CDS	node_148_[2]	170889	167641	3249	two-component sensor histidine kinase	- none -	167641	170889
fig|1504.6.peg.1746	CDS	node_148_[2]	172497	171067	1431	Adenylosuccinate lyase (EC 4.3.2.2)	De Novo Purine Biosynthesis, Purine conversions	171067	172497
fig|1504.6.peg.1747	CDS	node_148_[2]	172637	172855	219	hypothetical protein	- none -	172637	172855
fig|1504.6.peg.1748	CDS	node_148_[2]	173195	172935	261	Phosphocarrier protein of PTS system	- none -	172935	173195

Feature ID	Type	Contig	Start	Stop	Length (bp)	Function	Subsystems	Begin	End
fig|1504.6.peg.1749	CDS	node_148_[2]	173631	173371	261	Stage V sporulation protein required for dehydratation of the spore core and assembly of the coat (SpoVS)	SpoVS protein family, Sporulation gene orphans	173371	173631
fig|1504.6.peg.1750	CDS	node_148_[2]	175375	173834	1542	FIG002344: Hydrolase (HAD superfamily)	CBSS-469378.4.peg.430	173834	175375
fig|1504.6.peg.1751	CDS	node_148_[2]	176742	175696	1047	RecA protein	CBSS-469378.4.peg.430, DNA-replication, DNA repair, bacterial, DNA repair, bacterial RecFOR pathway, DNA repair system including RecA, MutS and a hypothetical protein	175696	176742
fig|1504.6.peg.1752	CDS	node_148_[2]	177494	176904	591	CDP-diacylglycerol--glycerol-3-phosphate 3-phosphatidyltransferase (EC 2.7.8.5)	Glycerolipid and Glycerophospholipid Metabolism in Bacteria	176904	177494
fig|1504.6.peg.1753	CDS	node_148_[2]	178815	177478	1338	Ribosomal protein S12p Asp88 (E. coli) methylthiotransferase	Methylthiotransferases, Ribosomal protein S12p Asp methylthiotransferase	177478	178815
fig|1504.6.peg.1754	CDS	node_148_[2]	181306	178904	2403	Cell division protein FtsK	Bacterial Cell Division, Bacterial Cytoskeleton, Bacterial RNA-metabolizing Zn-dependent hydrolases	178904	181306
fig|1504.6.peg.1755	CDS	node_148_[2]	182231	181503	729	Translocation-enhancing protein TepA	- none -	181503	182231
fig|1504.6.peg.1756	CDS	node_148_[2]	183480	182278	1203	Aspartokinase (EC 2.7.2.4)	CBSS-216591.1.peg.168, Lysine Biosynthesis DAP Pathway, Lysine Biosynthesis DAP Pathway, GJO scratch, Threonine and Homoserine Biosynthesis	182278	183480
fig|1504.6.peg.1757	CDS	node_148_[2]	183828	183502	327	hypothetical protein	- none -	183502	183828
fig|1504.6.peg.1758	CDS	node_148_[2]	185201	183894	1308	FIG007959: peptidase, M16 family	CBSS-1806.1.peg.3045, CBSS-350688.3.peg.1509	183894	185201
fig|1504.6.peg.1759	CDS	node_148_[2]	187432	185321	2112	Polyribonucleotide nucleotidyltransferase (EC 2.7.7.8)	Bacterial RNA-metabolizing Zn-dependent hydrolases, CBSS-1806.1.peg.3045, CBSS-350688.3.peg.1509	185321	187432
fig|1504.6.peg.1760	CDS	node_148_[2]	187857	187594	264	SSU ribosomal protein S15p (S13e)	CBSS-350688.3.peg.1509, Ribosome SSU bacterial	187594	187857

Feature ID	Type	Contig	Start	Stop	Length (bp)	Function	Subsystems	Begin	End
fig|1504.6.peg.1761	CDS	node_148_[2]	188912	187989	924	Riboflavin kinase (EC 2.7.1.26) / FMN adenylyltransferase (EC 2.7.7.2)	CBSS-350688.3.peg.1509, CBSS-350688.3.peg.1509, Riboflavin, FMN and FAD metabolism, Riboflavin, FMN and FAD metabolism, Riboflavin, FMN and FAD metabolism in plants, Riboflavin, FMN and FAD metabolism in plants, riboflavin to FAD, riboflavin to FAD	187989	188912
fig|1504.6.peg.1762	CDS	node_148_[2]	189802	188924	879	tRNA pseudouridine synthase B (EC 4.2.1.70)	CBSS-138119.3.peg.2719, CBSS-350688.3.peg.1509, RNA pseudouridine syntheses, Riboflavin, FMN and FAD metabolism in plants, tRNA processing	188924	189802
fig|1504.6.peg.1763	CDS	node_148_[2]	190776	189802	975	FIG146085: 3'-to-5' oligoribonuclease A, Bacillus type	CBSS-138119.3.peg.2719, RNA processing and degradation, bacterial	189802	190776
fig|1504.6.peg.1764	CDS	node_148_[2]	191128	190778	351	Ribosome-binding factor A	CBSS-138119.3.peg.2719, CBSS-350688.3.peg.1509, NusA-TFII Cluster, Translation initiation factors bacterial	190778	191128
fig|1504.6.peg.1765	CDS	node_148_[2]	193197	191146	2052	Translation initiation factor 2	CBSS-138119.3.peg.2719, CBSS-350688.3.peg.1509, NusA-TFII Cluster, Translation initiation factors bacterial, Universal GTPases	191146	193197
fig|1504.6.peg.1766	CDS	node_148_[2]	193527	193213	315	ribosomal protein L7Ae family protein	CBSS-350688.3.peg.1509, NusA-TFII Cluster, Transcription factors bacterial	193213	193527
fig|1504.6.peg.1767	CDS	node_148_[2]	193786	193520	267	COG2740: Predicted nucleic-acid-binding protein implicated in transcription termination	CBSS-350688.3.peg.1509, NusA-TFII Cluster, Transcription factors bacterial	193520	193786
fig|1504.6.peg.1768	CDS	node_148_[2]	194904	193801	1104	Transcription termination protein NusA	CBSS-350688.3.peg.1509, NusA-TFII Cluster, Transcription factors bacterial	193801	194904

Feature ID	Type	Contig	Start	Stop	Length (bp)	Function	Subsystems	Begin	End
fig|1504.6.peg.1769	CDS	node_148_[2]	195379	194921	459	FIG000325: clustered with transcription termination protein NusA	CBSS-350688.3.peg.1509, NusA-TFII Cluster, Transcription factors bacterial	194921	195379
fig|1504.6.peg.1770	CDS	node_148_[2]	197643	195658	1986	DNA polymerase III alpha subunit (EC 2.7.7.7)	CBSS-350688.3.peg.1509, DNA-replication	195658	197643
fig|1504.6.peg.1771	CDS	node_148_[2]	201325	200276	1050	1-hydroxy-2-methyl-2-(E)-butenyl 4-diphosphate synthase (EC 1.17.7.1)	CBSS-83331.1.peg.3039, Isoprenoid Biosynthesis, Nonmevalonate Branch of Isoprenoid Biosynthesis	200276	201325
fig|1504.6.peg.1772	CDS	node_148_[2]	202357	201338	1020	Membrane-associated zinc metalloprotease	- none -	201338	202357
fig|1504.6.peg.1773	CDS	node_148_[2]	203530	202370	1161	1-deoxy-D-xylulose 5-phosphate reductoisomerase (EC 1.1.1.267)	CBSS-83331.1.peg.3039, Isoprenoid Biosynthesis, Nonmevalonate Branch of Isoprenoid Biosynthesis	202370	203530
fig|1504.6.peg.1774	CDS	node_148_[2]	204511	203534	978	membrane protein, putative	- none -	203534	204511
fig|1504.6.peg.1775	CDS	node_148_[2]	205374	204613	762	Phosphatidate cytidylyltransferase (EC 2.7.7.41)	Glycerolipid and Glycerophospholipid Metabolism in Bacteria	204613	205374
fig|1504.6.peg.1776	CDS	node_148_[2]	206180	205425	756	Undecaprenyl diphosphate synthase (EC 2.5.1.31)	CBSS-83331.1.peg.3039, Isoprenoid Biosynthesis, Isoprenoinds for Quinones, Polyprenyl Diphosphate Biosynthesis	205425	206180
fig|1504.6.peg.1777	CDS	node_148_[2]	206789	206232	558	Ribosome recycling factor	Ribosome recycling related cluster, Translation termination factors bacterial	206232	206789
fig|1504.6.peg.1778	CDS	node_148_[2]	207517	206801	717	Uridine monophosphate kinase (EC 2.7.4.22)	CBSS-312309.3.peg.1965, Ribosome recycling related cluster	206801	207517
fig|1504.6.peg.1779	CDS	node_148_[2]	208499	207591	909	Translation elongation factor Ts	CBSS-312309.3.peg.1965, Ribosome recycling related cluster, Translation elongation factors bacterial	207591	208499

Feature ID	Type	Contig	Start	Stop	Length (bp)	Function	Subsystems	Begin	End
fig|1504.6.peg.1780	CDS	node_148_[2]	209284	208583	702	SSU ribosomal protein S2p (SAe)	CBSS-312309.3.peg.1965, Ribosome SSU bacterial, Ribosome recycling related cluster	208583	209284
fig|1504.6.peg.1781	CDS	node_148_[2]	210283	209507	777	GTP-sensing transcriptional pleiotropic repressor codY	Conserved gene cluster associated with Met-tRNA formyltransferase	209507	210283
fig|1504.6.peg.1782	CDS	node_148_[2]	212604	210505	2100	DNA topoisomerase I (EC 5.99.1.2)	CBSS-272943.3.peg.1367, Conserved gene cluster associated with Met-tRNA formyltransferase, DNA topoisomerases, Type I, ATP-independent	210505	212604
fig|1504.6.peg.1783	CDS	node_148_[2]	213719	212649	1071	Rossmann fold nucleotide-binding protein Smf possibly involved in DNA uptake	CBSS-272943.3.peg.1367, Conserved gene cluster associated with Met-tRNA formyltransferase	212649	213719
fig|1504.6.peg.1784	CDS	node_148_[2]	215233	213716	1518	MG(2+) CHELATASE FAMILY PROTEIN / ComM-related protein	- none -	213716	215233
fig|1504.6.peg.1785	CDS	node_148_[2]	215360	215731	372	Endonuclease (EC 3.1.-.-)	- none -	215360	215731
fig|1504.6.peg.1786	CDS	node_148_[2]	216546	215728	819	Ribonuclease HII (EC 3.1.26.4)	Conserved gene cluster associated with Met-tRNA formyltransferase, Ribonuclease H, Ribonucleases in Bacillus	215728	216546
fig|1504.6.peg.1787	CDS	node_148_[2]	217434	216547	888	50S ribosomal subunit maturation GTPase RbgA (B. subtilis YlqF)	Conserved gene cluster associated with Met-tRNA formyltransferase, Universal GTPases	216547	217434
fig|1504.6.peg.1788	CDS	node_148_[2]	217902	217552	351	LSU ribosomal protein L19p	Ribosome LSU bacterial	217552	217902
fig|1504.6.peg.1789	CDS	node_148_[2]	218731	218018	714	tRNA (Guanine37-N1) -methyltransferase (EC 2.1.1.31)	RNA methylation, Ribosome biogenesis bacterial	218018	218731
fig|1504.6.peg.1790	CDS	node_148_[2]	219218	218721	498	16S rRNA processing protein RimM	KH domain RNA binding protein YlqC, Ribosome biogenesis bacterial	218721	219218
fig|1504.6.peg.1791	CDS	node_148_[2]	219566	219321	246	KH domain RNA binding protein YlqC	KH domain RNA binding protein YlqC	219321	219566

Feature ID	Type	Contig	Start	Stop	Length (bp)	Function	Subsystems	Begin	End
fig|1504.6.peg.1792	CDS	node_148_[2]	219854	219609	246	SSU ribosomal protein S16p	KH domain RNA binding protein YlqC, Ribosome SSU bacterial	219609	219854
fig|1504.6.peg.1793	CDS	node_148_[2]	221245	219893	1353	Signal recognition particle, subunit Ffh SRP54 (TC 3.A.5.1.1)	Bacterial signal recognition particle (SRP), Universal GTPases	219893	221245
fig|1504.6.peg.1794	CDS	node_148_[2]	221591	221262	330	Signal recognition particle associated protein	Bacterial signal recognition particle (SRP)	221262	221591
fig|1504.6.peg.1795	CDS	node_148_[2]	222583	221672	912	Signal recognition particle receptor protein FtsY (=alpha subunit) (TC 3.A.5.1.1)	Bacterial Cell Division, Bacterial signal recognition particle (SRP), Universal GTPases	221672	222583
fig|1504.6.peg.1796	CDS	node_148_[2]	226159	222596	3564	Chromosome partition protein smc	DNA structural proteins, bacterial	222596	226159
fig|1504.6.peg.1797	CDS	node_148_[2]	227380	226346	1035	Oxygen-independent coproporphyrinogen III oxidase (EC 1.-.-.-)	- none -	226346	227380
fig|1504.6.peg.1798	CDS	node_148_[2]	228071	227373	699	Ribonuclease III (EC 3.1.26.3)	CBSS-176299.4.peg.1292, RNA processing and degradation, bacterial	227373	228071
fig|1504.6.peg.1799	CDS	node_148_[2]	228405	228175	231	Acyl carrier protein	Fatty Acid Biosynthesis FASII, Glycerolipid and Glycerophospholipid Metabolism in Bacteria	228175	228405
fig|1504.6.peg.1800	CDS	node_148_[2]	229484	228483	1002	Phosphate:acyl-ACP acyltransferase PlsX	Glycerolipid and Glycerophospholipid Metabolism in Bacteria	228483	229484
fig|1504.6.peg.1801	CDS	node_148_[2]	229726	229541	186	LSU ribosomal protein L32p	Ribosome LSU bacterial	229541	229726
fig|1504.6.peg.1802	CDS	node_148_[2]	230241	229729	513	COG1399 protein, clustered with ribosomal protein L32p	- none -	229729	230241
fig|1504.6.peg.1803	CDS	node_148_[2]	231747	230545	1203	Acetate kinase (EC 2.7.2.1)	Ethanolamine utilization, Fermentations: Lactate, Fermentations: Mixed acid, Pyruvate metabolism II: acetyl-CoA, acetogenesis from pyruvate	230545	231747

Feature ID	Type	Contig	Start	Stop	Length (bp)	Function	Subsystems	Begin	End
fig|1504.6.peg.1804	CDS	node_148_[2]	232768	231773	996	Phosphate acetyltransferase (EC 2.3.1.8)	Ethanolamine utilization, Fermentations: Lactate, Fermentations: Mixed acid, Pyruvate metabolism II: acetyl-CoA, acetogenesis from pyruvate	231773	232768
fig|1504.6.peg.1805	CDS	node_148_[2]	233003	234208	1206	FIG007079: UPF0348 protein family	- none -	233003	234208
fig|1504.6.peg.1806	CDS	node_148_[2]	234402	235445	1044	FIGfam003972: membrane protein	- none -	234402	235445
fig|1504.6.peg.1807	CDS	node_148_[2]	235967	235431	537	Cell division initiation protein	- none -	235431	235967
fig|1504.6.peg.1808	CDS	node_148_[2]	236463	235987	477	Phosphopantetheine adenylyltransferase (EC 2.7.7.3)	CBSS-266117.6.peg.1260, Coenzyme A Biosynthesis	235987	236463
fig|1504.6.peg.1809	CDS	node_148_[2]	237038	236487	552	Ribosomal RNA small subunit methyltransferase D (EC 2.1.1.-)	- none -	236487	237038
fig|1504.6.peg.1810	CDS	node_148_[2]	239133	237103	2031	ATP-dependent DNA helicase RecG (EC 3.6.1.-)	A Gram-positive cluster that relates ribosomal protein L28P to a set of uncharacterized proteins, DNA-replication	237103	239133
fig|1504.6.peg.1811	CDS	node_148_[2]	240866	239232	1635	Dihydroxyacetone kinase family protein	A Gram-positive cluster that relates ribosomal protein L28P to a set of uncharacterized proteins, Glycerolipid and Glycerophospholipid Metabolism in Bacteria	239232	240866
fig|1504.6.peg.1812	CDS	node_148_[2]	241225	240875	351	FIG001802: Putative alkaline-shock protein	A Gram-positive cluster that relates ribosomal protein L28P to a set of uncharacterized proteins	240875	241225
fig|1504.6.peg.1813	CDS	node_148_[2]	241469	241660	192	LSU ribosomal protein L28p @ LSU ribosomal protein L28p, zinc-dependent	A Gram-positive cluster that relates ribosomal protein L28P to a set of uncharacterized proteins, Ribosome LSU bacterial	241469	241660
fig|1504.6.peg.1814	CDS	node_148_[2]	242572	241937	636	Thiamin pyrophosphokinase (EC 2.7.6.2)	A Gram-positive cluster that relates ribosomal protein L28P to a set of uncharacterized proteins, Thiamin biosynthesis	241937	242572

Feature ID	Type	Contig	Start	Stop	Length (bp)	Function	Subsystems	Begin	End
fig|1504.6.peg.1815	CDS	node_148_[2]	243220	242576	645	Ribulose-phosphate 3-epimerase (EC 5.1.3.1)	A Gram-positive cluster that relates ribosomal protein L28P to a set of uncharacterized proteins, Conserved gene cluster associated with Met-tRNA formyltransferase, Pentose phosphate pathway, Riboflavin synthesis cluster	242576	243220
fig|1504.6.peg.1816	CDS	node_148_[2]	244083	243214	870	Ribosome small subunit-stimulated GTPase EngC	A Gram-positive cluster that relates ribosomal protein L28P to a set of uncharacterized proteins, Universal GTPases	243214	244083
fig|1504.6.peg.1817	CDS	node_148_[2]	246223	244220	2004	Serine/threonine protein kinase PrkC, regulator of stationary phase	A Gram-positive cluster that relates ribosomal protein L28P to a set of uncharacterized proteins, Conserved gene cluster associated with Met-tRNA formyltransferase	244220	246223
fig|1504.6.peg.1818	CDS	node_148_[2]	246944	246225	720	Protein serine/threonine phosphatase PrpC, regulation of stationary phase	Conserved gene cluster associated with Met-tRNA formyltransferase	246225	246944
fig|1504.6.peg.1819	CDS	node_148_[2]	247989	246958	1032	Ribosomal RNA large subunit methyltransferase N (EC 2.1.1.-)	Conserved gene cluster associated with Met-tRNA formyltransferase, RNA methylation	246958	247989
fig|1504.6.peg.1820	CDS	node_148_[2]	249317	247998	1320	Ribosomal RNA small subunit methyltransferase B (EC 2.1.1.-)	- none -	247998	249317
fig|1504.6.peg.1821	CDS	node_148_[2]	250028	249330	699	probable metal-dependent peptidase	- none -	249330	250028
fig|1504.6.peg.1822	CDS	node_148_[2]	250976	250050	927	Methionyl-tRNA formyltransferase (EC 2.1.2.9)	Conserved gene cluster associated with Met-tRNA formyltransferase, Translation initiation factors bacterial	250050	250976

Feature ID	Type	Contig	Start	Stop	Length (bp)	Function	Subsystems	Begin	End
fig|1504.6.peg.1823	CDS	node_148_[2]	251437	250994	444	Peptide deformylase (EC 3.5.1.88)	Bacterial RNA-metabolizing Zn-dependent hydrolases, Conserved gene cluster associated with Met-tRNA formyltransferase, Translation termination factors bacterial	250994	251437
fig|1504.6.peg.1824	CDS	node_148_[2]	253650	251449	2202	Helicase PriA essential for oriC/DnaA-independent DNA replication	Conserved gene cluster associated with Met-tRNA formyltransferase, DNA-replication	251449	253650
fig|1504.6.peg.1825	CDS	node_148_[2]	254909	253713	1197	Phosphopantothenoylcysteine decarboxylase (EC 4.1.1.36) / Phosphopantothenoylcysteine synthetase (EC 6.3.2.5)	Coenzyme A Biosynthesis, Coenzyme A Biosynthesis	253713	254909
fig|1504.6.peg.1826	CDS	node_148_[2]	255130	254912	219	DNA-directed RNA polymerase omega subunit (EC 2.7.7.6)	CBSS-176299.4.peg.1292, RNA polymerase bacterial	254912	255130
fig|1504.6.peg.1827	CDS	node_148_[2]	255752	255111	642	Guanylate kinase (EC 2.7.4.8)	CBSS-323097.3.peg.2594, Purine conversions	255111	255752
fig|1504.6.peg.1828	CDS	node_148_[2]	256021	255752	270	FIG003307: hypothetical protein	CBSS-323097.3.peg.2594	255752	256021
fig|1504.6.peg.1829	CDS	node_148_[2]	256917	256036	882	Protein YicC	CBSS-323097.3.peg.2594	256036	256917
fig|1504.6.peg.1830	CDS	node_148_[2]	258508	257138	1371	Xanthine/uracil/thiamine/ascorbate permease family protein	Purine Utilization	257138	258508
fig|1504.6.peg.1831	CDS	node_148_[2]	259783	258812	972	L-asparaginase (EC 3.5.1.1)	Glutamine, Glutamate, Aspartate and Asparagine Biosynthesis	258812	259783
fig|1504.6.peg.1832	CDS	node_148_[2]	260383	259979	405	spbA protein	- none -	259979	260383
fig|1504.6.peg.1833	CDS	node_148_[2]	262036	260558	1479	Stage IV sporulation protein A	Sporulation gene orphans	260558	262036
fig|1504.6.peg.1834	CDS	node_148_[2]	263236	262238	999	Glycerol-3-phosphate dehydrogenase [NAD(P)+] (EC 1.1.1.94)	Glycerol and Glycerol-3-phosphate Uptake and Utilization, Glycerolipid and Glycerophospholipid Metabolism in Bacteria	262238	263236
fig|1504.6.peg.1835	CDS	node_148_[2]	264555	263239	1317	GTP-binding protein EngA	Ribosome post-transcriptional modification and chromosomal segregation cluster, Universal GTPases	263239	264555

Feature ID	Type	Contig	Start	Stop	Length (bp)	Function	Subsystems	Begin	End
fig|1504.6.peg.1836	CDS	node_148_[2]	265894	264557	1338	Fe-S oxidoreductase, related to NifB/MoaA family with PDZ N-terminal domain	- none -	264557	265894
fig|1504.6.peg.1837	CDS	node_148_[2]	266693	266037	657	Phosphate transport system regulatory protein PhoU	High affinity phosphate transporter and control of PHO regulon, Phosphate metabolism	266037	266693
fig|1504.6.peg.1838	CDS	node_148_[2]	267492	266728	765	Phosphate transport ATP-binding protein PstB (TC 3.A.1.7.1)	High affinity phosphate transporter and control of PHO regulon, Phosphate metabolism	266728	267492
fig|1504.6.peg.1839	CDS	node_148_[2]	268343	267519	825	Phosphate transport system permease protein PstA (TC 3.A.1.7.1)	High affinity phosphate transporter and control of PHO regulon, Phosphate metabolism	267519	268343
fig|1504.6.peg.1840	CDS	node_148_[2]	269235	268345	891	Phosphate transport system permease protein PstC (TC 3.A.1.7.1)	High affinity phosphate transporter and control of PHO regulon, Phosphate metabolism	268345	269235
fig|1504.6.peg.1841	CDS	node_148_[2]	270164	269319	846	Phosphate ABC transporter, periplasmic phosphate-binding protein PstS (TC 3.A.1.7.1)	High affinity phosphate transporter and control of PHO regulon, PhoR-PhoB two-component regulatory system, Phosphate metabolism	269319	270164
fig|1504.6.peg.1842	CDS	node_148_[2]	272034	270343	1692	Phosphate regulon sensor protein PhoR (SphS) (EC 2.7.13.3)	High affinity phosphate transporter and control of PHO regulon, PhoR-PhoB two-component regulatory system, Phosphate metabolism	270343	272034
fig|1504.6.peg.1843	CDS	node_148_[2]	272736	272038	699	Phosphate regulon transcriptional regulatory protein PhoB (SphR)	High affinity phosphate transporter and control of PHO regulon, PhoR-PhoB two-component regulatory system, Phosphate metabolism	272038	272736
fig|1504.6.peg.1844	CDS	node_148_[2]	273488	272754	735	COG1496: Uncharacterized conserved protein	- none -	272754	273488
fig|1504.6.peg.1845	CDS	node_148_[2]	274262	273807	456	Ribonucleotide reductase transcriptional regulator NrdR	Ribonucleotide reduction	273807	274262
fig|1504.6.peg.1846	CDS	node_148_[2]	274666	274340	327	PRC-barrel domain protein	- none -	274340	274666
fig|1504.6.peg.1847	CDS	node_148_[2]	275635	274862	774	RNA polymerase sporulation specific sigma factor SigG	Sporulation gene orphans, Transcription initiation, bacterial sigma factors	274862	275635

Feature ID	Type	Contig	Start	Stop	Length (bp)	Function	Subsystems	Begin	End
fig|1504.6.peg.1848	CDS	node_148_[2]	276424	275717	708	RNA polymerase sporulation specific sigma factor SigE	Sporulation gene orphans, Transcription initiation, bacterial sigma factors	275717	276424
fig|1504.6.peg.1849	CDS	node_148_[2]	277234	276434	801	Sporulation sigma-E factor processing peptidase (SpoIIGA)	Sporulation gene orphans	276434	277234
fig|1504.6.peg.1850	CDS	node_148_[2]	278579	277455	1125	Cell division protein FtsZ (EC 3.4.24.-)	Bacterial Cell Division, Bacterial Cytoskeleton, cell division cluster containing FtsQ, cell division core of larger cluster	277455	278579
fig|1504.6.peg.1851	CDS	node_148_[2]	280564	279509	1056	Twitching motility protein PilT	- none -	279509	280564
fig|1504.6.peg.1852	CDS	node_148_[2]	281365	280670	696	RNA polymerase sporulation specific sigma factor SigK	Sporulation gene orphans, Transcription initiation, bacterial sigma factors	280670	281365
fig|1504.6.peg.1853	CDS	node_148_[2]	283272	281659	1614	Cell division protein FtsI [Peptidoglycan synthetase] (EC 2.4.1.129)	16S rRNA modification within P site of ribosome, Bacterial Cell Division, Bacterial Cytoskeleton, CBSS-83331.1.peg.3039, Flagellum in Campylobacter	281659	283272
fig|1504.6.peg.1854	CDS	node_148_[2]	283947	283330	618	Uridine kinase (EC 2.7.1.48) [C1]	pyrimidine conversions	283330	283947
fig|1504.6.peg.1855	CDS	node_148_[2]	285204	283969	1236	peptidase, U32 family large subunit [C1]	- none -	283969	285204
fig|1504.6.peg.1856	CDS	node_148_[2]	285855	285211	645	FIG011945: O-methyltransferase family protein	- none -	285211	285855
fig|1504.6.peg.1857	CDS	node_148_[2]	286879	285857	1023	FIG004453: protein YceG like	CBSS-323097.3.peg.2594, Cluster containing Alanyl-tRNA synthetase	285857	286879
fig|1504.6.peg.1858	CDS	node_148_[2]	288806	286980	1827	GTP-binding protein TypA/BipA	Universal GTPases	286980	288806
fig|1504.6.peg.1859	CDS	node_148_[2]	290635	288968	1668	Ribonuclease J2 (endoribonuclease in RNA processing)	Bacterial RNA-metabolizing Zn-dependent hydrolases, Ribonucleases in Bacillus	288968	290635
fig|1504.6.peg.1860	CDS	node_148_[2]	291170	290712	459	Ferric uptake regulation protein FUR	Bacterial RNA-metabolizing Zn-dependent hydrolases, Oxidative stress	290712	291170
fig|1504.6.peg.1861	CDS	node_148_[2]	291478	291203	276	FIG00513284: hypothetical protein	- none -	291203	291478

Feature ID	Type	Contig	Start	Stop	Length (bp)	Function	Subsystems	Begin	End
fig|1504.6.peg.1862	CDS	node_148_[2]	291974	291558	417	Putative Holliday junction resolvase YqgF	- none -	291558	291974
fig|1504.6.peg.1863	CDS	node_148_[2]	292277	292020	258	FIG01055109: hypothetical protein	- none -	292020	292277
fig|1504.6.peg.1864	CDS	node_148_[2]	295046	292407	2640	Alanyl-tRNA synthetase (EC 6.1.1.7)	Cluster containing Alanyl-tRNA synthetase, tRNA aminoacylation, Ala	292407	295046
fig|1504.6.peg.1865	CDS	node_148_[2]	296441	295410	1032	Permease	- none -	295410	296441
fig|1504.6.peg.1866	CDS	node_148_[2]	296916	296428	489	Conserved protein	- none -	296428	296916
fig|1504.6.peg.1867	CDS	node_148_[2]	298090	297011	1080	tRNA-specific 2-thiouridylase MnmA	RNA methylation	297011	298090
fig|1504.6.peg.1868	CDS	node_148_[2]	298535	298101	435	Iron-sulfur cluster assembly scaffold protein IscU/NifU-like	- none -	298101	298535
fig|1504.6.peg.1869	CDS	node_148_[2]	299718	298537	1182	Cysteine desulfurase (EC 2.8.1.7)	Alanine biosynthesis, CBSS-84588.1.peg.1247, mnm5U34 biosynthesis bacteria	298537	299718
fig|1504.6.peg.1870	CDS	node_148_[2]	300173	299721	453	Iron-sulfur cluster regulator IscR	Alanine biosynthesis, Rrf2 family transcriptional regulators	299721	300173
fig|1504.6.peg.1871	CDS	node_148_[2]	301533	300289	1245	ATPase, AAA family	- none -	300289	301533
fig|1504.6.peg.1872	CDS	node_148_[2]	302043	301558	486	hypothetical protein	- none -	301558	302043
fig|1504.6.peg.1873	CDS	node_148_[2]	304815	302191	2625	Alcohol dehydrogenase (EC 1.1.1.1); Acetaldehyde dehydrogenase (EC 1.2.1.10)	5-FCL-like protein, Butanol Biosynthesis, Butanol Biosynthesis, Fermentations: Lactate, Fermentations: Mixed acid, Fermentations: Mixed acid, Glycerolipid and Glycerophospholipid Metabolism in Bacteria, Pyruvate metabolism II: acetyl-CoA, acetogenesis from pyruvate	302191	304815
fig|1504.6.peg.1874	CDS	node_148_[2]	305715	305302	414	L-lactate dehydrogenase (FMN-dependent) and related alpha-hydroxy acid dehydrogenases	- none -	305302	305715
fig|1504.6.peg.1875	CDS	node_148_[2]	306624	305809	816	Acetyl-coenzyme A carboxyl transferase alpha chain (EC 6.4.1.2)	Fatty Acid Biosynthesis FASII	305809	306624

Feature ID	Type	Contig	Start	Stop	Length (bp)	Function	Subsystems	Begin	End
fig|1504.6.peg.1876	CDS	node_148_[2]	307492	306617	876	Acetyl-coenzyme A carboxyl transferase beta chain (EC 6.4.1.2)	Fatty Acid Biosynthesis FASII	306617	307492
fig|1504.6.peg.1877	CDS	node_148_[2]	308837	307485	1353	Biotin carboxylase of acetyl-CoA carboxylase (EC 6.3.4.14)	Fatty Acid Biosynthesis FASII	307485	308837
fig|1504.6.peg.1878	CDS	node_148_[2]	309269	308847	423	3-hydroxyacyl-[acyl-carrier-protein] dehydratase, FabZ form (EC 4.2.1.59)	Fatty Acid Biosynthesis FASII	308847	309269
fig|1504.6.peg.1879	CDS	node_148_[2]	309766	309272	495	Biotin carboxyl carrier protein of acetyl-CoA carboxylase	Fatty Acid Biosynthesis FASII	309272	309766
fig|1504.6.peg.1880	CDS	node_148_[2]	311019	309784	1236	3-oxoacyl-[acyl-carrier-protein] synthase, KASII (EC 2.3.1.179)	- none -	309784	311019
fig|1504.6.peg.1881	CDS	node_148_[2]	311775	311035	741	3-oxoacyl-[acyl-carrier protein] reductase (EC 1.1.1.100)	Fatty Acid Biosynthesis FASII	311035	311775
fig|1504.6.peg.1882	CDS	node_148_[2]	312714	311785	930	Malonyl CoA-acyl carrier protein transacylase (EC 2.3.1.39)	Fatty Acid Biosynthesis FASII	311785	312714
fig|1504.6.peg.1883	CDS	node_148_[2]	313645	312707	939	Enoyl-[acyl-carrier-protein] reductase [FMN] (EC 1.3.1.9)	Fatty Acid Biosynthesis FASII	312707	313645
fig|1504.6.peg.1884	CDS	node_148_[2]	313924	313703	222	Acyl carrier protein	Fatty Acid Biosynthesis FASII, Glycerolipid and Glycerophospholipid Metabolism in Bacteria	313703	313924
fig|1504.6.peg.1885	CDS	node_148_[2]	314949	313972	978	3-oxoacyl-[acyl-carrier-protein] synthase, KASIII (EC 2.3.1.180)	- none -	313972	314949
fig|1504.6.peg.1886	CDS	node_148_[2]	315411	314962	450	Transcriptional regulator of fatty acid biosynthesis FabT	Fatty Acid Biosynthesis FASII	314962	315411
fig|1504.6.peg.1887	CDS	node_148_[2]	316020	315607	414	hypothetical protein	- none -	315607	316020
fig|1504.6.peg.1888	CDS	node_148_[2]	316638	316132	507	conserved hypothetical protein	- none -	316132	316638
fig|1504.6.peg.1889	CDS	node_148_[2]	317556	316762	795	Electron transport complex protein RnfB	Na(+)-translocating NADH-quinone oxidoreductase and rnf-like group of electron transport complexes	316762	317556
fig|1504.6.peg.1890	CDS	node_148_[2]	318147	317569	579	Electron transport complex protein RnfA	Na(+)-translocating NADH-quinone oxidoreductase and rnf-like group of electron transport complexes	317569	318147

Feature ID	Type	Contig	Start	Stop	Length (bp)	Function	Subsystems	Begin	End
fig|1504.6.peg.1891	CDS	node_148_[2]	318864	318163	702	Electron transport complex protein RnfE	Na(+)-translocating NADH-quinone oxidoreductase and rnf-like group of electron transport complexes	318163	318864
fig|1504.6.peg.1892	CDS	node_148_[2]	319668	318889	780	Electron transport complex protein RnfG	Na(+)-translocating NADH-quinone oxidoreductase and rnf-like group of electron transport complexes	318889	319668
fig|1504.6.peg.1893	CDS	node_148_[2]	320563	319670	894	Electron transport complex protein RnfD	Na(+)-translocating NADH-quinone oxidoreductase and rnf-like group of electron transport complexes	319670	320563
fig|1504.6.peg.1894	CDS	node_148_[2]	321556	320615	942	Electron transport complex protein RnfC	Na(+)-translocating NADH-quinone oxidoreductase and rnf-like group of electron transport complexes	320615	321556
fig|1504.6.peg.1895	CDS	node_148_[2]	322904	321981	924	TPR-repeat-containing protein	- none -	321981	322904
fig|1504.6.peg.1896	CDS	node_148_[2]	323253	322921	333	hypothetical protein	- none -	322921	323253
fig|1504.6.peg.1897	CDS	node_148_[2]	324414	323281	1134	Protein export cytoplasm protein SecA ATPase RNA helicase (TC 3.A.5.1.1)	CBSS-393121.3.peg.2760	323281	324414
fig|1504.6.peg.1898	CDS	node_148_[2]	326707	324494	2214	ATP-dependent Clp protease ATP-binding subunit ClpA	ClpAS cluster, Proteolysis in bacteria, ATP-dependent, Ribosome recycling related cluster	324494	326707
fig|1504.6.peg.1899	CDS	node_148_[2]	327008	326709	300	ATP-dependent Clp protease adaptor protein ClpS	ClpAS cluster, Proteolysis in bacteria, ATP-dependent	326709	327008
fig|1504.6.peg.1900	CDS	node_148_[2]	327352	327155	198	hypothetical protein	- none -	327155	327352
fig|1504.6.peg.1901	CDS	node_148_[2]	330420	327535	2886	Penicillin-binding protein 2 (PBP-2)	16S rRNA modification within P site of ribosome, Bacterial cell division cluster, CBSS-83331.1.peg.3039	327535	330420
fig|1504.6.peg.1902	CDS	node_148_[2]	330879	330637	243	hypothetical protein	- none -	330637	330879
fig|1504.6.peg.1903	CDS	node_148_[2]	331669	330962	708	Fibronectin type III domain protein	- none -	330962	331669
fig|1504.6.peg.1904	CDS	node_148_[2]	334520	334768	249	hypothetical protein	- none -	334520	334768

Feature ID	Type	Contig	Start	Stop	Length (bp)	Function	Subsystems	Begin	End
fig|1504.6.peg.1905	CDS	node_148_[2]	336915	334930	1986	2',3'-cyclic-nucleotide 2'-phosphodiesterase (EC 3.1.4.16)	Purine conversions, pyrimidine conversions	334930	336915
fig|1504.6.peg.1906	CDS	node_148_[2]	339573	337252	2322	Glutathione biosynthesis bifunctional protein gshF (EC 6.3.2.2)(EC 6.3.2.3)	Glutathione: Biosynthesis and gamma-glutamyl cycle	337252	339573
fig|1504.6.peg.1907	CDS	node_148_[2]	340885	339557	1329	Multi antimicrobial extrusion protein (Na(+)/drug antiporter), MATE family of MDR efflux pumps	Multidrug Resistance Efflux Pumps, Riboflavin, FMN and FAD metabolism in plants	339557	340885
fig|1504.6.peg.1908	CDS	node_148_[2]	341074	342582	1509	Putative amino acid permease	- none -	341074	342582
fig|1504.6.peg.1909	CDS	node_148_[2]	343991	342621	1371	FIG00520102: hypothetical protein	- none -	342621	343991
fig|1504.6.peg.1910	CDS	node_148_[2]	344631	344086	546	hypothetical protein	- none -	344086	344631
fig|1504.6.peg.1911	CDS	node_148_[2]	345275	344754	522	Substrate-specific component PdxU2 of predicted pyridoxin-related ECF transporter	ECF class transporters	344754	345275
fig|1504.6.peg.1912	CDS	node_148_[2]	345442	345774	333	hypothetical protein	- none -	345442	345774
fig|1504.6.peg.1913	CDS	node_148_[2]	345848	347878	2031	Methyl-accepting chemotaxis protein	- none -	345848	347878
fig|1504.6.peg.1914	CDS	node_148_[2]	348107	347925	183	no significant homology	- none -	347925	348107
fig|1504.6.peg.1915	CDS	node_148_[2]	348670	348119	552	Uncharacterized conserved protein, YTFE family, possibly metal-binding	- none -	348119	348670
fig|1504.6.peg.1916	CDS	node_148_[2]	349317	348682	636	no significant homology	- none -	348682	349317
fig|1504.6.peg.1917	CDS	node_148_[2]	349530	349862	333	Transcriptional regulator, PadR family	CBSS-1352.1.peg.856	349530	349862
fig|1504.6.peg.1918	CDS	node_148_[2]	349864	350544	681	hypothetical protein	- none -	349864	350544
fig|1504.6.peg.1919	CDS	node_148_[2]	351095	350661	435	Transmembrane component CbiQ of energizing module of cobalt ECF transporter	Coenzyme B12 biosynthesis, ECF class transporters, Transport of Nickel and Cobalt	350661	351095
fig|1504.6.peg.1920	CDS	node_148_[2]	351612	351331	282	Additional substrate-specific component CbiN of cobalt ECF transporter	Coenzyme B12 biosynthesis, ECF class transporters, Transport of Nickel and Cobalt	351331	351612
fig|1504.6.peg.1921	CDS	node_148_[2]	352337	351612	726	Substrate-specific component CbiM of cobalt ECF transporter	Coenzyme B12 biosynthesis, ECF class transporters, Transport of Nickel and Cobalt	351612	352337
fig|1504.6.peg.1922	CDS	node_148_[2]	353119	352349	771	Cobalt-precorrin-6x reductase (EC 1.3.1.54)	Cobalamin synthesis, Coenzyme B12 biosynthesis	352349	353119
fig|1504.6.peg.1923	CDS	node_148_[2]	353832	353116	717	Cobalt-precorrin-3b C17-methyltransferase	Cobalamin synthesis, Coenzyme B12 biosynthesis	353116	353832

Feature ID	Type	Contig	Start	Stop	Length (bp)	Function	Subsystems	Begin	End
fig|1504.6.peg.1924	CDS	node_148_[2]	354816	353851	966	Cobalamin biosynthesis protein CbiG	Cobalamin synthesis, Coenzyme B12 biosynthesis	353851	354816
fig|1504.6.peg.1925	CDS	node_148_[2]	355565	354819	747	Cobalt-precorrin-4 C11-methyltransferase (EC 2.1.1.133)	Cobalamin synthesis, Coenzyme B12 biosynthesis	354819	355565
fig|1504.6.peg.1926	CDS	node_148_[2]	356240	355575	666	Cobalt-precorrin-2 C20-methyltransferase (EC 2.1.1.130)	Cobalamin synthesis, Coenzyme B12 biosynthesis	355575	356240
fig|1504.6.peg.1927	CDS	node_148_[2]	356821	356243	579	Cobalt-precorrin-6y C15-methyltransferase [decarboxylating] (EC 2.1.1.-)	Coenzyme B12 biosynthesis	356243	356821
fig|1504.6.peg.1928	CDS	node_148_[2]	357445	356843	603	Cobalt-precorrin-6y C5-methyltransferase (EC 2.1.1.-)	Coenzyme B12 biosynthesis	356843	357445
fig|1504.6.peg.1929	CDS	node_148_[2]	358535	357450	1086	Cobalt-precorrin-6 synthase, anaerobic	Cobalamin synthesis, Coenzyme B12 biosynthesis	357450	358535
fig|1504.6.peg.1930	CDS	node_148_[2]	359166	358543	624	Cobalt-precorrin-8x methylmutase (EC 5.4.1.2)	Cobalamin synthesis, Coenzyme B12 biosynthesis	358543	359166
fig|1504.6.peg.1931	CDS	node_148_[2]	360465	359179	1287	Cobyrinic acid A,C-diamide synthase	Cobalamin synthesis, Coenzyme B12 biosynthesis	359179	360465
fig|1504.6.peg.1932	CDS	node_148_[2]	361291	360440	852	Sirohydrochlorin cobaltochelatase CbiK (EC 4.99.1.3)	Cobalamin synthesis, Coenzyme B12 biosynthesis	360440	361291
fig|1504.6.peg.1933	CDS	node_148_[2]	362233	361730	504	acetyltransferase, GNAT family	- none -	361730	362233
fig|1504.6.peg.1934	CDS	node_148_[2]	362969	362640	330	PTS system, cellobiose-specific IIA component (EC 2.7.1.69)	Beta-Glucoside Metabolism	362640	362969
fig|1504.6.peg.1935	CDS	node_148_[2]	365245	363236	2010	Ferrous iron transport protein B	- none -	363236	365245
fig|1504.6.peg.1936	CDS	node_148_[2]	365503	365285	219	hypothetical protein	- none -	365285	365503
fig|1504.6.peg.1937	CDS	node_148_[2]	365743	365522	222	ferrous iron transport protein A	- none -	365522	365743
fig|1504.6.peg.1938	CDS	node_148_[2]	366021	365743	279	hypothetical protein	- none -	365743	366021
fig|1504.6.peg.1939	CDS	node_148_[2]	366286	367086	801	DUF124 domain-containing protein	- none -	366286	367086
fig|1504.6.peg.1940	CDS	node_148_[2]	367889	367116	774	endonuclease/exonuclease/phosphatase family protein	- none -	367116	367889
fig|1504.6.peg.1941	CDS	node_148_[2]	368093	370324	2232	Pyruvate formate-lyase (EC 2.3.1.54)	Butanol Biosynthesis, Fermentations: Mixed acid	368093	370324
fig|1504.6.peg.1942	CDS	node_148_[2]	370496	370642	147	hypothetical protein	- none -	370496	370642
fig|1504.6.peg.1943	CDS	node_148_[2]	370915	370718	198	hypothetical protein	- none -	370718	370915
fig|1504.6.peg.1944	CDS	node_148_[2]	372688	370946	1743	hypothetical protein	- none -	370946	372688

Feature ID	Type	Contig	Start	Stop	Length (bp)	Function	Subsystems	Begin	End
fig|1504.6.peg.1945	CDS	node_148_[2]	372821	373681	861	Muramoyltetrapeptide carboxypeptidase (EC 3.4.17.13)	Metallocarboxypeptidases (EC 3.4.17.-), Murein Hydrolases, Recycling of Peptidoglycan Amino Acids	372821	373681
fig|1504.6.peg.1946	CDS	node_148_[2]	373759	374706	948	hypothetical protein	- none -	373759	374706
fig|1504.6.peg.1947	CDS	node_148_[2]	375413	374838	576	hypothetical protein	- none -	374838	375413
fig|1504.6.peg.1948	CDS	node_148_[2]	375642	376184	543	hypothetical protein	- none -	375642	376184
fig|1504.6.peg.1949	CDS	node_148_[2]	376643	378271	1629	L-aspartate beta-decarboxylase (EC 4.1.1.12)	- none -	376643	378271
fig|1504.6.peg.1950	CDS	node_148_[2]	378395	380071	1677	Integral membrane protein	- none -	378395	380071
fig|1504.6.peg.1951	CDS	node_148_[2]	381051	380116	936	Lipoate-protein ligase A	Lipoic acid metabolism	380116	381051
fig|1504.6.peg.1952	CDS	node_148_[2]	382736	381045	1692	Dihydrolipoamide dehydrogenase (EC 1.8.1.4)	5-FCL-like protein	381045	382736
fig|1504.6.peg.1953	CDS	node_148_[2]	383172	382819	354	4-carboxymuconolactone decarboxylase (EC 4.1.1.44)	- none -	382819	383172
fig|1504.6.peg.1954	CDS	node_148_[2]	383687	383244	444	Transcriptional regulator, MarR family	- none -	383244	383687
fig|1504.6.rna.69	RNA	node_148_[2]	383983	384054	72	tRNA-Glu-CTC	- none -	383983	384054
fig|1504.6.peg.1955	CDS	node_148_[2]	384537	384127	411	hypothetical protein	- none -	384127	384537
fig|1504.6.peg.1956	CDS	node_148_[2]	384852	385982	1131	hypothetical protein	- none -	384852	385982
fig|1504.6.peg.1957	CDS	node_148_[2]	391176	389956	1221	Transposase, mutator type	- none -	389956	391176
fig|1504.6.peg.1958	CDS	node_148_[2]	399003	399137	135	hypothetical protein	- none -	399003	399137
fig|1504.6.peg.1959	CDS	node_148_[2]	400033	399770	264	CRISPR-associated protein Cas2	CRISPRs	399770	400033
fig|1504.6.peg.1960	CDS	node_148_[2]	401018	400035	984	CRISPR-associated protein Cas1	CRISPRs	400035	401018
fig|1504.6.peg.1961	CDS	node_148_[2]	401536	401021	516	CRISPR-associated RecB family exonuclease Cas4a	CRISPRs	401021	401536
fig|1504.6.peg.1962	CDS	node_148_[2]	403810	401546	2265	CRISPR-associated helicase Cas3	CRISPRs	401546	403810
fig|1504.6.peg.1963	CDS	node_148_[2]	404583	403849	735	CRISPR-associated protein Cas5	- none -	403849	404583
fig|1504.6.peg.1964	CDS	node_148_[2]	405468	404593	876	CRISPR-associated negative autoregulator	CRISPRs	404593	405468
fig|1504.6.peg.1965	CDS	node_148_[2]	407159	405468	1692	FIG00774117: hypothetical protein	- none -	405468	407159

Feature ID	Type	Contig	Start	Stop	Length (bp)	Function	Subsystems	Begin	End
fig|1504.6.peg.1966	CDS	node_148_[2]	407905	407171	735	CRISPR-associated protein, TM1814 family	- none -	407171	407905
fig|1504.6.peg.1967	CDS	node_148_[2]	408968	408030	939	FIG00521064: hypothetical protein	- none -	408030	408968
fig|1504.6.peg.1968	CDS	node_148_[2]	411965	409380	2586	Neuraminidase NanP	Galactosylceramide and Sulfatide metabolism	409380	411965
fig|1504.6.peg.1969	CDS	node_148_[2]	413547	412327	1221	Tripeptide aminopeptidase (EC 3.4.11.4)	- none -	412327	413547
fig|1504.6.peg.1970	CDS	node_148_[2]	414706	413642	1065	Peptidoglycan N-acetylglucosamine deacetylase (EC 3.5.1.-)	Polysaccharide deacetylases	413642	414706
fig|1504.6.peg.1971	CDS	node_148_[2]	414746	415852	1107	Mobile element protein	- none -	414746	415852
fig|1504.6.peg.1972	CDS	node_148_[2]	416165	416830	666	Phosphate regulon transcriptional regulatory protein PhoB (SphR)	High affinity phosphate transporter and control of PHO regulon, PhoR-PhoB two-component regulatory system, Phosphate metabolism	416165	416830
fig|1504.6.peg.1973	CDS	node_148_[2]	416835	418250	1416	Phosphate regulon sensor protein PhoR (SphS) (EC 2.7.13.3)	High affinity phosphate transporter and control of PHO regulon, PhoR-PhoB two-component regulatory system, Phosphate metabolism	416835	418250
fig|1504.6.peg.1974	CDS	node_148_[2]	418247	418849	603	hypothetical protein	- none -	418247	418849
fig|1504.6.peg.1975	CDS	node_148_[2]	420333	419092	1242	Radical SAM family enzyme, similar to coproporphyrinogen III oxidase, oxygen-independent, clustered with nucleoside-triphosphatase RdgB	Heat shock dnaK gene cluster extended, Heme and Siroheme Biosynthesis, Queuosine-Archaeosine Biosynthesis	419092	420333
fig|1504.6.peg.1976	CDS	node_148_[2]	421063	420656	408	COG1180: Radical SAM, Pyruvate-formate lyase-activating enzyme like	- none -	420656	421063
fig|1504.6.peg.1977	CDS	node_148_[2]	421774	421139	636	Arylesterase	- none -	421139	421774
fig|1504.6.peg.1978	CDS	node_148_[2]	422006	422548	543	Flagellar hook-length control protein FliK	Flagellum	422006	422548
fig|1504.6.peg.1979	CDS	node_148_[2]	422970	422560	411	Spermidine N1-acetyltransferase (EC 2.3.1.57)	Polyamine Metabolism	422560	422970
fig|1504.6.peg.1980	CDS	node_148_[2]	426172	423269	2904	Microbial collagenase (EC 3.4.24.3)	Metalloendopeptidases (EC 3.4.24.-)	423269	426172

Feature ID	Type	Contig	Start	Stop	Length (bp)	Function	Subsystems	Begin	End
fig|1504.6.peg.1981	CDS	node_148_[2]	430368	426478	3891	Sialidase (EC 3.2.1.18)	Galactosylceramide and Sulfatide metabolism, Sialic Acid Metabolism	426478	430368
fig|1504.6.peg.1982	CDS	node_148_[2]	437439	430795	6645	Alpha-N-acetylglucosaminidase (EC 3.2.1.50)	Chitin and N-acetylglucosamine utilization	430795	437439
fig|1504.6.peg.1983	CDS	node_148_[2]	439069	437822	1248	Phosphoribosylamine--glycine ligase (EC 6.3.4.13)	De Novo Purine Biosynthesis	437822	439069
fig|1504.6.peg.1984	CDS	node_148_[2]	440608	439106	1503	IMP cyclohydrolase (EC 3.5.4.10) / Phosphoribosylaminoimidazolecarboxamide formyltransferase (EC 2.1.2.3)	5-FCL-like protein, CBSS-366602.3.peg.5141, CBSS-366602.3.peg.5141, De Novo Purine Biosynthesis, De Novo Purine Biosynthesis	439106	440608
fig|1504.6.peg.1985	CDS	node_148_[2]	441237	440626	612	Phosphoribosylglycinamide formyltransferase (EC 2.1.2.2)	5-FCL-like protein, De Novo Purine Biosynthesis	440626	441237
fig|1504.6.peg.1986	CDS	node_148_[2]	442226	441225	1002	Phosphoribosylformylglycinamidine cyclo-ligase (EC 6.3.3.1)	De Novo Purine Biosynthesis	441225	442226
fig|1504.6.peg.1987	CDS	node_148_[2]	443663	442236	1428	Amidophosphoribosyltransferase (EC 2.4.2.14)	De Novo Purine Biosynthesis	442236	443663
fig|1504.6.peg.1988	CDS	node_148_[2]	444419	443715	705	Phosphoribosylaminoimidazole-succinocarboxamide synthase (EC 6.3.2.6)	De Novo Purine Biosynthesis	443715	444419
fig|1504.6.peg.1989	CDS	node_148_[2]	444898	444419	480	Phosphoribosylaminoimidazole carboxylase catalytic subunit (EC 4.1.1.21)	De Novo Purine Biosynthesis	444419	444898
fig|1504.6.peg.1990	CDS	node_148_[2]	448657	444911	3747	Phosphoribosylformylglycinamidine synthase, synthetase subunit (EC 6.3.5.3) / Phosphoribosylformylglycinamidine synthase, glutamine amidotransferase subunit (EC 6.3.5.3)	De Novo Purine Biosynthesis, De Novo Purine Biosynthesis	444911	448657
fig|1504.6.peg.1991	CDS	node_148_[2]	449663	449154	510	alkaline phosphatase-like protein	- none -	449154	449663
fig|1504.6.peg.1992	CDS	node_148_[2]	450075	449920	156	Zinc finger domain	- none -	449920	450075
fig|1504.6.peg.1993	CDS	node_148_[2]	450519	450364	156	Zinc finger domain	- none -	450364	450519
fig|1504.6.peg.1994	CDS	node_148_[2]	451223	450819	405	hypothetical protein	- none -	450819	451223
fig|1504.6.peg.1995	CDS	node_148_[2]	452219	451281	939	Putative stomatin/prohibitin-family membrane protease subunit YbbK	- none -	451281	452219
fig|1504.6.peg.1996	CDS	node_148_[2]	452652	452221	432	Putative activity regulator of membrane protease YbbK	- none -	452221	452652

Feature ID	Type	Contig	Start	Stop	Length (bp)	Function	Subsystems	Begin	End
fig|1504.6.peg.1997	CDS	node_148_[2]	452979	454883	1905	NAD synthetase (EC 6.3.1.5) / Glutamine amidotransferase chain of NAD synthetase	NAD and NADP cofactor biosynthesis global, NAD and NADP cofactor biosynthesis global	452979	454883
fig|1504.6.peg.1998	CDS	node_148_[2]	455582	454932	651	Deoxyadenosine kinase (EC 2.7.1.76) / Deoxyguanosine kinase (EC 2.7.1.113)	Purine conversions, Purine conversions	454932	455582
fig|1504.6.peg.1999	CDS	node_148_[2]	456289	455792	498	dCMP deaminase (EC 3.5.4.12)	- none -	455792	456289
fig|1504.6.peg.2000	CDS	node_148_[2]	457344	456364	981	Meso-diaminopimelate D-dehydrogenase (EC 1.4.1.16)	Lysine Biosynthesis DAP Pathway, Lysine Biosynthesis DAP Pathway, GJO scratch	456364	457344
fig|1504.6.peg.2001	CDS	node_148_[2]	459385	457454	1932	Conserved protein	- none -	457454	459385
fig|1504.6.peg.2002	CDS	node_148_[2]	460439	459504	936	hypothetical protein	- none -	459504	460439
fig|1504.6.peg.2003	CDS	node_148_[2]	465871	460745	5127	Fibronectin type III domain protein	- none -	460745	465871
fig|1504.6.peg.2004	CDS	node_148_[2]	466451	466260	192	hypothetical protein	- none -	466260	466451
fig|1504.6.peg.2005	CDS	node_148_[2]	467695	466466	1230	hypothetical protein	- none -	466466	467695
fig|1504.6.peg.2006	CDS	node_148_[2]	469291	467882	1410	Mobile element protein	- none -	467882	469291
fig|1504.6.peg.2007	CDS	node_148_[2]	470278	469418	861	Thioredoxin reductase (EC 1.8.1.9)	Thioredoxin-disulfide reductase, pyrimidine conversions	469418	470278
fig|1504.6.peg.2008	CDS	node_148_[2]	470609	470295	315	Thioredoxin	- none -	470295	470609
fig|1504.6.peg.2009	CDS	node_148_[2]	472508	470787	1722	Lipid A export ATP-binding/permease protein MsbA	- none -	470787	472508
fig|1504.6.peg.2010	CDS	node_148_[2]	472960	472538	423	DUF327 domain-containing protein	- none -	472538	472960
fig|1504.6.peg.2011	CDS	node_148_[2]	473135	475762	2628	Calcium-transporting ATPase (EC 3.6.3.8)	- none -	473135	475762
fig|1504.6.peg.2012	CDS	node_148_[2]	476494	475805	690	Glutamine transport ATP-binding protein GlnQ (TC 3.A.1.3.2)	- none -	475805	476494
fig|1504.6.peg.2013	CDS	node_148_[2]	477156	476506	651	amino acid ABC transporter, permease protein	- none -	476506	477156
fig|1504.6.peg.2014	CDS	node_148_[2]	477986	477177	810	amino acid ABC transporter, amino acid-binding protein	- none -	477177	477986
fig|1504.6.peg.2015	CDS	node_148_[2]	478960	478118	843	FIG00514536: hypothetical protein	- none -	478118	478960
fig|1504.6.peg.2016	CDS	node_148_[2]	479473	478973	501	carbonic anhydrase, family 3	- none -	478973	479473

Feature ID	Type	Contig	Start	Stop	Length (bp)	Function	Subsystems	Begin	End
fig|1504.6.peg.2017	CDS	node_148_[2]	479590	480624	1035	FIG00515906: hypothetical protein	- none -	479590	480624
fig|1504.6.peg.2018	CDS	node_148_[2]	481021	480683	339	hypothetical protein	- none -	480683	481021
fig|1504.6.peg.2019	CDS	node_148_[2]	481295	481762	468	Transcriptional regulator AsnC	- none -	481295	481762
fig|1504.6.peg.2020	CDS	node_148_[2]	481834	482040	207	DUF378 domain-containing protein	- none -	481834	482040
fig|1504.6.peg.2021	CDS	node_148_[2]	483841	482096	1746	Phosphoenolpyruvate carboxykinase [ATP] (EC 4.1.1.49)	Pyruvate metabolism I: anaplerotic reactions, PEP, Serine-glyoxylate cycle	482096	483841
fig|1504.6.peg.2022	CDS	node_148_[2]	484915	484205	711	1-acyl-sn-glycerol-3-phosphate acyltransferase (EC 2.3.1.51)	Glycerolipid and Glycerophospholipid Metabolism in Bacteria, Ribosome post-transcriptional modification and chromosomal segregation cluster	484205	484915
fig|1504.6.peg.2023	CDS	node_148_[2]	485171	485923	753	metallo-beta-lactamase family protein	- none -	485171	485923
fig|1504.6.peg.2024	CDS	node_148_[2]	486863	486015	849	FIG00516201: hypothetical protein	- none -	486015	486863
fig|1504.6.peg.2025	CDS	node_148_[2]	487156	487377	222	Ferrous iron transport protein A	- none -	487156	487377
fig|1504.6.peg.2026	CDS	node_148_[2]	487393	489153	1761	Ferrous iron transport protein B	- none -	487393	489153
fig|1504.6.peg.2027	CDS	node_148_[2]	489200	489349	150	hypothetical protein	- none -	489200	489349
fig|1504.6.peg.2028	CDS	node_148_[2]	490484	489369	1116	Permease	- none -	489369	490484
fig|1504.6.peg.2029	CDS	node_148_[2]	492290	490599	1692	Arginyl-tRNA synthetase (EC 6.1.1.19)	tRNA aminoacylation, Arg	490599	492290
fig|1504.6.peg.2030	CDS	node_148_[2]	492743	494251	1509	Exopolyphosphatase (EC 3.6.1.11)	Phosphate metabolism, Polyphosphate	492743	494251
fig|1504.6.peg.2031	CDS	node_148_[2]	495099	494458	642	Membrane metalloprotease	- none -	494458	495099
fig|1504.6.peg.2032	CDS	node_148_[2]	496657	495221	1437	Cell envelope-associated transcriptional attenuator LytR-CpsA-Psr, subfamily F1 (as in PMID19099556)	Cell envelope-associated LytR-CpsA-Psr transcriptional attenuators	495221	496657
fig|1504.6.peg.2033	CDS	node_148_[2]	496908	497888	981	Biotin operon repressor / Biotin-protein ligase (EC 6.3.4.15)	Biotin biosynthesis, Biotin biosynthesis	496908	497888
fig|1504.6.peg.2034	CDS	node_148_[2]	498139	499044	906	Arginase (EC 3.5.3.1)	Arginine and Ornithine Degradation	498139	499044

Feature ID	Type	Contig	Start	Stop	Length (bp)	Function	Subsystems	Begin	End
fig|1504.6.peg.2035	CDS	node_148_[2]	499117	499746	630	DNA polymerase III epsilon subunit (EC 2.7.7.7)	CBSS-228410.1.peg.134, CBSS-342610.3.peg.1536, DNA-replication	499117	499746
fig|1504.6.peg.2036	CDS	node_148_[2]	500513	499809	705	Pyruvate formate-lyase activating enzyme (EC 1.97.1.4)	Fermentations: Mixed acid	499809	500513
fig|1504.6.peg.2037	CDS	node_148_[2]	502883	500655	2229	Pyruvate formate-lyase (EC 2.3.1.54)	Butanol Biosynthesis, Fermentations: Mixed acid	500655	502883
fig|1504.6.peg.2038	CDS	node_148_[2]	504150	503053	1098	acetyltransferase, GNAT family	- none -	503053	504150
fig|1504.6.peg.2039	CDS	node_148_[2]	504607	505146	540	Transcriptional regulator, MerR family, near polyamine transporter	Polyamine Metabolism	504607	505146
fig|1504.6.peg.2040	CDS	node_148_[2]	505169	506218	1050	Putrescine transport ATP-binding protein PotA (TC 3.A.1.11.1)	Polyamine Metabolism	505169	506218
fig|1504.6.peg.2041	CDS	node_148_[2]	506208	507062	855	Spermidine Putrescine ABC transporter permease component PotB (TC 3.A.1.11.1)	Polyamine Metabolism	506208	507062
fig|1504.6.peg.2042	CDS	node_148_[2]	507056	507868	813	Spermidine Putrescine ABC transporter permease component potC (TC_3.A.1.11.1)	Polyamine Metabolism	507056	507868
fig|1504.6.peg.2043	CDS	node_148_[2]	507855	508925	1071	ABC transporter, periplasmic spermidine putrescine-binding protein PotD (TC 3.A.1.11.1)	Polyamine Metabolism	507855	508925
fig|1504.6.peg.2044	CDS	node_148_[2]	509384	508974	411	Nucleoside diphosphate kinase (EC 2.7.4.6)	Purine conversions, pyrimidine conversions	508974	509384
fig|1504.6.peg.2045	CDS	node_148_[2]	509517	509786	270	Acylphosphate phosphohydrolase (EC 3.6.1.7), putative	Pyruvate metabolism II: acetyl-CoA, acetogenesis from pyruvate	509517	509786
fig|1504.6.peg.2046	CDS	node_148_[2]	511217	509844	1374	Sodium/glycine symporter GlyP	- none -	509844	511217
fig|1504.6.peg.2047	CDS	node_148_[2]	511618	511830	213	hypothetical protein	- none -	511618	511830
fig|1504.6.peg.2048	CDS	node_148_[2]	511987	512787	801	Predicted hydrolase	- none -	511987	512787
fig|1504.6.peg.2049	CDS	node_148_[2]	513763	512804	960	D-3-phosphoglycerate dehydrogenase (EC 1.1.1.95)	Glycine and Serine Utilization, Pyridoxin (Vitamin B6) Biosynthesis, Serine Biosynthesis	512804	513763
fig|1504.6.peg.2050	CDS	node_148_[2]	516080	513927	2154	phage infection protein	- none -	513927	516080
fig|1504.6.peg.2051	CDS	node_148_[2]	517467	516346	1122	FIG00523152: hypothetical protein	- none -	516346	517467

Feature ID	Type	Contig	Start	Stop	Length (bp)	Function	Subsystems	Begin	End
fig|1504.6.peg.2052	CDS	node_148_[2]	518325	517561	765	Potassium voltage-gated channel subfamily KQT; possible potassium channel, VIC family	Potassium homeostasis	517561	518325
fig|1504.6.peg.2053	CDS	node_148_[2]	519573	518524	1050	Aldose 1-epimerase (EC 5.1.3.3)	Lactose and Galactose Uptake and Utilization, Maltose and Maltodextrin Utilization	518524	519573
fig|1504.6.peg.2054	CDS	node_148_[2]	521096	519582	1515	Galactose-1-phosphate uridylyltransferase (EC 2.7.7.10)	Lactose and Galactose Uptake and Utilization	519582	521096
fig|1504.6.peg.2055	CDS	node_148_[2]	522282	521119	1164	Galactokinase (EC 2.7.1.6)	Lactose and Galactose Uptake and Utilization	521119	522282
fig|1504.6.peg.2056	CDS	node_148_[2]	523491	522496	996	Evolved beta-D-galactosidase transcriptional repressor	Lactose utilization	522496	523491
fig|1504.6.peg.2057	CDS	node_148_[2]	524289	524041	249	hypothetical protein	- none -	524041	524289
fig|1504.6.peg.2058	CDS	node_148_[2]	525157	524372	786	UPF0135 protein Bsu YqfO	- none -	524372	525157
fig|1504.6.peg.2059	CDS	node_148_[2]	525862	525170	693	Putative tRNA-m1A22 methylase	CBSS-349161.4.peg.2417	525170	525862
fig|1504.6.peg.2060	CDS	node_148_[2]	527016	525907	1110	RNA polymerase sigma factor RpoD	CBSS-349161.4.peg.2417, Flagellum, Macromolecular synthesis operon, Transcription initiation, bacterial sigma factors	525907	527016
fig|1504.6.peg.2061	CDS	node_148_[2]	528825	527044	1782	DNA primase (EC 2.7.7.-)	CBSS-349161.4.peg.2417, DNA-replication, Macromolecular synthesis operon	527044	528825
fig|1504.6.peg.2062	CDS	node_148_[2]	530052	529024	1029	Deoxyguanosinetriphosphate triphosphohydrolase (EC 3.1.5.1)	- none -	529024	530052
fig|1504.6.peg.2063	CDS	node_148_[2]	530204	531271	1068	Spore coat protein S	- none -	530204	531271
fig|1504.6.peg.2064	CDS	node_148_[2]	533941	531311	2631	Pyruvate,phosphate dikinase (EC 2.7.9.1)	CBSS-349161.4.peg.2427, Glycolysis and Gluconeogenesis, Pyruvate metabolism I: anaplerotic reactions, PEP	531311	533941
fig|1504.6.peg.2065	CDS	node_148_[2]	534665	534027	639	CBS domain protein, lmo1865 homolog	CBSS-349161.4.peg.2427	534027	534665
fig|1504.6.peg.2066	CDS	node_148_[2]	535474	534860	615	N-terminal of elongation factor Ts	- none -	534860	535474

Feature ID	Type	Contig	Start	Stop	Length (bp)	Function	Subsystems	Begin	End
fig|1504.6.peg.2067	CDS	node_148_[2]	536231	535482	750	DNA recombination and repair protein RecO	CBSS-176299.4.peg.1292, DNA repair, bacterial RecFOR pathway	535482	536231
fig|1504.6.peg.2068	CDS	node_148_[2]	537130	536240	891	GTP-binding protein Era	Bacterial Cell Division, CBSS-176299.4.peg.1292, Universal GTPases	536240	537130
fig|1504.6.peg.2069	CDS	node_148_[2]	537540	537139	402	Cytidine deaminase (EC 3.5.4.5)	Murein hydrolase regulation and cell death, pyrimidine conversions	537139	537540
fig|1504.6.peg.2070	CDS	node_148_[2]	538357	537656	702	Diacylglycerol kinase (EC 2.7.1.107)	Glycerolipid and Glycerophospholipid Metabolism in Bacteria, Riboflavin synthesis cluster	537656	538357
fig|1504.6.peg.2071	CDS	node_148_[2]	538881	538378	504	Metal-dependent hydrolase YbeY, involved in rRNA and/or ribosome maturation and assembly	CBSS-56780.10.peg.1536	538378	538881
fig|1504.6.peg.2072	CDS	node_148_[2]	540993	538945	2049	Membrane protein containing HD superfamily hydrolase domain, YQFF ortholog	CBSS-56780.10.peg.1536	538945	540993
fig|1504.6.peg.2073	CDS	node_148_[2]	542161	541025	1137	Stage IV sporulation protein	- none -	541025	542161
fig|1504.6.peg.2074	CDS	node_148_[2]	542445	542167	279	FIG00512905: hypothetical protein	- none -	542167	542445
fig|1504.6.peg.2075	CDS	node_148_[2]	543003	542554	450	Transamidase GatB domain protein	Macromolecular synthesis operon	542554	543003
fig|1504.6.peg.2076	CDS	node_148_[2]	543212	543036	177	SSU ribosomal protein S21p	Macromolecular synthesis operon, Ribosome SSU bacterial	543036	543212
fig|1504.6.peg.2077	CDS	node_148_[2]	543674	543333	342	HIT family hydrolase	- none -	543333	543674
fig|1504.6.peg.2078	CDS	node_148_[2]	545066	543762	1305	tRNA-t(6)A37 methylthiotransferase	Heat shock dnaK gene cluster extended, Methylthiotransferases	543762	545066
fig|1504.6.peg.2079	CDS	node_148_[2]	545830	545066	765	Ribosomal RNA small subunit methyltransferase E (EC 2.1.1.-)	Heat shock dnaK gene cluster extended, RNA methylation	545066	545830
fig|1504.6.peg.2080	CDS	node_148_[2]	546795	545854	942	Ribosomal protein L11 methyltransferase (EC 2.1.1.-)	Heat shock dnaK gene cluster extended, Ribosome biogenesis bacterial	545854	546795
fig|1504.6.peg.2081	CDS	node_148_[2]	547445	546948	498	Thiol peroxidase, Tpx-type (EC 1.11.1.15)	Thioredoxin-disulfide reductase	546948	547445

Feature ID	Type	Contig	Start	Stop	Length (bp)	Function	Subsystems	Begin	End
fig|1504.6.peg.2082	CDS	node_148_[2]	547747	547595	153	hypothetical protein	- none -	547595	547747
fig|1504.6.peg.2083	CDS	node_148_[2]	549559	548006	1554	Ferredoxin--sulfite reductase (EC 1.8.7.1)	- none -	548006	549559
fig|1504.6.peg.2084	CDS	node_148_[2]	550841	549711	1131	Chaperone protein DnaJ	GroEL GroES, Heat shock dnaK gene cluster extended, Protein chaperones	549711	550841
fig|1504.6.peg.2085	CDS	node_148_[2]	552787	550934	1854	Chaperone protein DnaK	GroEL GroES, Heat shock dnaK gene cluster extended, Protein chaperones	550934	552787
fig|1504.6.peg.2086	CDS	node_148_[2]	553449	552835	615	Heat shock protein GrpE	GroEL GroES, Heat shock dnaK gene cluster extended, Protein chaperones	552835	553449
fig|1504.6.peg.2087	CDS	node_148_[2]	554501	553470	1032	Heat-inducible transcription repressor HrcA	GroEL GroES, Heat shock dnaK gene cluster extended	553470	554501
fig|1504.6.peg.2088	CDS	node_148_[2]	555803	554670	1134	Hypothetical radical SAM family enzyme in heat shock gene cluster, similarity with CPO of BS HemN-type	Heat shock dnaK gene cluster extended, Heme and Siroheme Biosynthesis	554670	555803
fig|1504.6.peg.2089	CDS	node_148_[2]	556201	555932	270	no significant homology	- none -	555932	556201
fig|1504.6.peg.2090	CDS	node_148_[2]	556367	557275	909	Patatin-like protein	- none -	556367	557275
fig|1504.6.peg.2091	CDS	node_148_[2]	559145	557340	1806	Translation elongation factor LepA	Heat shock dnaK gene cluster extended, Translation elongation factors bacterial, Universal GTPases	557340	559145
fig|1504.6.peg.2092	CDS	node_148_[2]	559823	559260	564	hypothetical protein	- none -	559260	559823
fig|1504.6.peg.2093	CDS	node_148_[2]	560981	559887	1095	Stage II sporulation protein P	Sporulation gene orphans	559887	560981
fig|1504.6.peg.2094	CDS	node_148_[2]	562121	561147	975	Endopeptidase spore protease Gpr (EC 3.4.24.78)	Small acid-soluble spore proteins	561147	562121
fig|1504.6.peg.2095	CDS	node_148_[2]	562297	562560	264	SSU ribosomal protein S20p	Ribosome SSU bacterial	562297	562560
fig|1504.6.peg.2096	CDS	node_148_[2]	563638	562607	1032	DNA polymerase III delta subunit (EC 2.7.7.7)	DNA-replication	562607	563638
fig|1504.6.peg.2097	CDS	node_148_[2]	565351	563654	1698	Late competence protein ComEC, DNA transport	- none -	563654	565351
fig|1504.6.peg.2098	CDS	node_148_[2]	567870	565366	2505	Probable calcium-transporting ATPase	- none -	565366	567870
fig|1504.6.peg.2099	CDS	node_148_[2]	568375	568019	357	Stage V sporulation protein AE (SpoVAE)	Sporulation gene orphans	568019	568375
fig|1504.6.peg.2100	CDS	node_148_[2]	569424	568396	1029	Stage V sporulation protein AD (SpoVAD)	Sporulation gene orphans	568396	569424

Feature ID	Type	Contig	Start	Stop	Length (bp)	Function	Subsystems	Begin	End
fig|1504.6.peg.2101	CDS	node_148_[2]	569933	569463	471	Stage V sporulation protein AC (SpoVAC)	Sporulation gene orphans	569463	569933
fig|1504.6.peg.2102	CDS	node_148_[2]	570878	570123	756	RNA polymerase sporulation specific sigma factor SigF	Sporulation gene orphans, Transcription initiation, bacterial sigma factors	570123	570878
fig|1504.6.peg.2103	CDS	node_148_[2]	571325	570888	438	Anti-sigma F factor (EC 2.7.11.1)	- none -	570888	571325
fig|1504.6.peg.2104	CDS	node_148_[2]	571676	571341	336	Anti-sigma F factor antagonist (spoIIAA-2); Anti-sigma B factor antagonist RsbV	SigmaB stress responce regulation	571341	571676
fig|1504.6.peg.2105	CDS	node_148_[2]	574141	571844	2298	ATP-dependent protease La (EC 3.4.21.53) Type II	Proteolysis in bacteria, ATP-dependent	571844	574141
fig|1504.6.peg.2106	CDS	node_148_[2]	574986	574312	675	Deoxyribose-phosphate aldolase (EC 4.1.2.4)	Deoxyribose and Deoxynucleoside Catabolism	574312	574986
fig|1504.6.peg.2107	CDS	node_148_[2]	576168	575119	1050	DNA polymerase IV (EC 2.7.7.7)	DNA repair, bacterial	575119	576168
fig|1504.6.peg.2108	CDS	node_148_[2]	577132	576182	951	hypothetical protein	- none -	576182	577132
fig|1504.6.peg.2109	CDS	node_148_[2]	577350	578258	909	Quinolinate synthetase (EC 2.5.1.72)	Mycobacterium virulence operon possibly involved in quinolinate biosynthesis, NAD and NADP cofactor biosynthesis global	577350	578258
fig|1504.6.peg.2110	CDS	node_148_[2]	578652	579551	900	L-aspartate oxidase (EC 1.4.3.16)	Mycobacterium virulence operon possibly involved in quinolinate biosynthesis, NAD and NADP cofactor biosynthesis global	578652	579551
fig|1504.6.peg.2111	CDS	node_148_[2]	579532	579981	450	Quinolinate phosphoribosyltransferase [decarboxylating] (EC 2.4.2.19)	Mycobacterium virulence operon possibly involved in quinolinate biosynthesis, NAD and NADP cofactor biosynthesis global	579532	579981
fig|1504.6.peg.2112	CDS	node_148_[2]	580177	580368	192	Quinolinate phosphoribosyltransferase [decarboxylating] (EC 2.4.2.19)	Mycobacterium virulence operon possibly involved in quinolinate biosynthesis, NAD and NADP cofactor biosynthesis global	580177	580368
fig|1504.6.peg.2113	CDS	node_148_[2]	580822	580409	414	hypothetical protein	- none -	580409	580822
fig|1504.6.peg.2114	CDS	node_148_[2]	581578	580988	591	Rubrerythrin	Oxidative stress, Rubrerythrin	580988	581578

Feature ID	Type	Contig	Start	Stop	Length (bp)	Function	Subsystems	Begin	End
fig|1504.6.peg.2115	CDS	node_148_[2]	582718	582056	663	hypothetical protein	- none -	582056	582718
fig|1504.6.peg.2116	CDS	node_148_[2]	582909	583583	675	hypothetical protein	- none -	582909	583583
fig|1504.6.peg.2117	CDS	node_148_[2]	584894	583632	1263	Lysine 2,3-aminomutase (EC 5.4.3.2)	Lysine degradation	583632	584894
fig|1504.6.peg.2118	CDS	node_148_[2]	585411	585070	342	FIG00516679: hypothetical protein	- none -	585070	585411
fig|1504.6.peg.2119	CDS	node_148_[2]	585782	585657	126	hypothetical protein	- none -	585657	585782
fig|1504.6.peg.2120	CDS	node_148_[2]	586306	586031	276	hypothetical protein	- none -	586031	586306
fig|1504.6.peg.2121	CDS	node_148_[2]	586472	587005	534	protein from bacterioferritin family	- none -	586472	587005
fig|1504.6.peg.2122	CDS	node_148_[2]	587629	587063	567	Methyltransferase type 11	- none -	587063	587629
fig|1504.6.peg.2123	CDS	node_148_[2]	587844	588260	417	FIG00512748: hypothetical protein	- none -	587844	588260
fig|1504.6.peg.2124	CDS	node_148_[2]	589458	588304	1155	tRNA S(4)U 4-thiouridine synthase (former ThiI)	Thiamin biosynthesis	588304	589458
fig|1504.6.peg.2125	CDS	node_148_[2]	590600	589455	1146	Cysteine desulfurase (EC 2.8.1.7)	Alanine biosynthesis, CBSS-84588.1.peg.1247, mnm5U34 biosynthesis bacteria	589455	590600
fig|1504.6.peg.2126	CDS	node_148_[2]	590837	591229	393	hypothetical protein	- none -	590837	591229
fig|1504.6.peg.2127	CDS	node_148_[2]	591862	591425	438	ACT domain-containing protein	- none -	591425	591862
fig|1504.6.peg.2128	CDS	node_148_[2]	591956	591837	120	hypothetical protein	- none -	591837	591956
fig|1504.6.peg.2129	CDS	node_148_[2]	594812	592263	2550	Cation-transporting ATPase	- none -	592263	594812
fig|1504.6.peg.2130	CDS	node_148_[2]	594953	595267	315	PlcB, ORFX, ORFP, ORFB, ORFA, ldh gene	- none -	594953	595267
fig|1504.6.peg.2131	CDS	node_148_[2]	595521	597161	1641	Manganese-dependent inorganic pyrophosphatase (EC 3.6.1.1)	Phosphate metabolism	595521	597161
fig|1504.6.peg.2132	CDS	node_148_[2]	597971	597198	774	Flagellar basal-body rod protein FlgG	Flagellum	597198	597971
fig|1504.6.peg.2133	CDS	node_148_[2]	598756	597986	771	Flagellar basal-body rod protein FlgF	Flagellum	597986	598756
fig|1504.6.peg.2134	CDS	node_148_[2]	598956	598753	204	hypothetical protein	- none -	598753	598956
fig|1504.6.peg.2135	CDS	node_148_[2]	599399	598959	441	hypothetical protein	- none -	598959	599399
fig|1504.6.peg.2136	CDS	node_148_[2]	600137	599412	726	RNA polymerase sigma factor for flagellar operon	Flagellar motility, Flagellum, Transcription initiation, bacterial sigma factors	599412	600137
fig|1504.6.peg.2137	CDS	node_148_[2]	600789	600151	639	Flagellar protein	- none -	600151	600789

Feature ID	Type	Contig	Start	Stop	Length (bp)	Function	Subsystems	Begin	End
fig|1504.6.peg.2138	CDS	node_148_[2]	601660	600800	861	Flagellar synthesis regulator FleN	Flagellar motility, Flagellum	600800	601660
fig|1504.6.peg.2139	CDS	node_148_[2]	602817	601654	1164	Flagellar biosynthesis protein FlhF	Flagellar motility, Flagellum	601654	602817
fig|1504.6.peg.2140	CDS	node_148_[2]	604880	602814	2067	Flagellar biosynthesis protein FlhA	Flagellar motility, Flagellum	602814	604880
fig|1504.6.peg.2141	CDS	node_148_[2]	606745	604895	1851	Flagellar biosynthesis protein FliR / Flagellar biosynthesis protein FlhB	Flagellar motility, Flagellar motility, Flagellum, Flagellum	604895	606745
fig|1504.6.peg.2142	CDS	node_148_[2]	607026	606757	270	Flagellar biosynthesis protein FliQ	Flagellum	606757	607026
fig|1504.6.peg.2143	CDS	node_148_[2]	607812	607036	777	Flagellar biosynthesis protein FliP	Flagellum	607036	607812
fig|1504.6.peg.2144	CDS	node_148_[2]	608196	607825	372	Flagellar biosynthesis protein FliZ	Flagellum	607825	608196
fig|1504.6.peg.2145	CDS	node_148_[2]	608659	608210	450	Flagellar biosynthesis protein FliL	Flagellum	608210	608659
fig|1504.6.peg.2146	CDS	node_148_[2]	609407	608664	744	Flagellar motor rotation protein MotB	Flagellar motility, Flagellum	608664	609407
fig|1504.6.peg.2147	CDS	node_148_[2]	610213	609407	807	Flagellar motor rotation protein MotA	Flagellar motility, Flagellum	609407	610213
fig|1504.6.peg.2148	CDS	node_148_[2]	610416	610225	192	Flagellar protein FlbD	Flagellum	610225	610416
fig|1504.6.peg.2149	CDS	node_148_[2]	613154	610503	2652	Flagellar hook protein FlgE	Flagellum	610503	613154
fig|1504.6.peg.2150	CDS	node_148_[2]	613620	613234	387	Putative flagellar hook associated protein	- none -	613234	613620
fig|1504.6.peg.2151	CDS	node_148_[2]	614347	613685	663	Flagellar basal-body rod modification protein FlgD	Flagellar motility, Flagellum	613685	614347
fig|1504.6.peg.2152	CDS	node_148_[2]	615777	614359	1419	Flagellar hook-length control protein FliK	Flagellum	614359	615777
fig|1504.6.peg.2153	CDS	node_148_[2]	616227	615778	450	Flagellar protein FliJ	Flagellum	615778	616227
fig|1504.6.peg.2154	CDS	node_148_[2]	617552	616242	1311	Flagellum-specific ATP synthase FliI	Flagellar motility, Flagellum	616242	617552
fig|1504.6.peg.2155	CDS	node_148_[2]	618329	617571	759	Flagellar assembly protein FliH	Flagellum	617571	618329
fig|1504.6.peg.2156	CDS	node_148_[2]	619329	618313	1017	Flagellar motor switch protein FliG	Flagellum	618313	619329
fig|1504.6.peg.2157	CDS	node_148_[2]	620902	619334	1569	Flagellar M-ring protein FliF	Flagellum	619334	620902
fig|1504.6.peg.2158	CDS	node_148_[2]	621212	620922	291	Flagellar hook-basal body complex protein FliE	Flagellum, Flagellum in Campylobacter	620922	621212
fig|1504.6.peg.2159	CDS	node_148_[2]	621652	621248	405	Flagellar basal-body rod protein FlgC	Flagellum, Flagellum in Campylobacter	621248	621652
fig|1504.6.peg.2160	CDS	node_148_[2]	622050	621655	396	Flagellar basal-body rod protein FlgB	Flagellum, Flagellum in Campylobacter	621655	622050

Feature ID	Type	Contig	Start	Stop	Length (bp)	Function	Subsystems	Begin	End
fig|1504.6.peg.2161	CDS	node_148_[2]	623410	622550	861	Flagellin protein FlaA	Flagellum, Flagellum in Campylobacter	622550	623410
fig|1504.6.peg.2162	CDS	node_148_[2]	624702	623491	1212	Lysine-N-methylase (EC 2.1.1.-)	- none -	623491	624702
fig|1504.6.peg.1425	CDS	node_148_[2]	627199	626117	1083	Flagellin protein FlaA	Flagellum, Flagellum in Campylobacter	626117	627199
fig|1504.6.peg.1426	CDS	node_148_[2]	628160	627393	768	Flagellin protein FlaA	Flagellum, Flagellum in Campylobacter	627393	628160
fig|1504.6.peg.1427	CDS	node_148_[2]	630080	629757	324	hypothetical protein	- none -	629757	630080
fig|1504.6.peg.1428	CDS	node_148_[2]	631563	630082	1482	Flagellar hook-associated protein FliD	Flagellum	630082	631563
fig|1504.6.peg.1429	CDS	node_148_[2]	631962	631582	381	Flagellar biosynthesis protein FliS	Flagellum	631582	631962
fig|1504.6.peg.1430	CDS	node_148_[2]	632257	631973	285	FIG00515802: hypothetical protein	- none -	631973	632257
fig|1504.6.peg.1431	CDS	node_148_[2]	632614	632273	342	Flagellin	Flagellar motility	632273	632614
fig|1504.6.peg.1432	CDS	node_148_[2]	632839	632624	216	Carbon storage regulator	Carbon Starvation, Carbon storage regulator	632624	632839
fig|1504.6.peg.1433	CDS	node_148_[2]	633353	632934	420	Flagellar assembly factor FliW	Carbon storage regulator	632934	633353
fig|1504.6.peg.1434	CDS	node_148_[2]	634360	633368	993	Flagellar hook-associated protein FlgL	Flagellum	633368	634360
fig|1504.6.peg.1435	CDS	node_148_[2]	636212	634377	1836	Flagellar hook-associated protein FlgK	Flagellum	634377	636212
fig|1504.6.peg.1436	CDS	node_148_[2]	636680	636258	423	FIG00513492: hypothetical protein	- none -	636258	636680
fig|1504.6.peg.1437	CDS	node_148_[2]	636958	636683	276	Negative regulator of flagellin synthesis	Flagellum	636683	636958
fig|1504.6.peg.1438	CDS	node_148_[2]	638199	637066	1134	Flagellar motor switch protein FliN	Flagellar motility, Flagellum	637066	638199
fig|1504.6.peg.1439	CDS	node_148_[2]	639187	638192	996	Flagellar motor switch protein FliM	Flagellar motility, Flagellum	638192	639187
fig|1504.6.peg.1440	CDS	node_148_[2]	639602	639204	399	Positive regulator of CheA protein activity (CheW)	- none -	639204	639602
fig|1504.6.peg.1441	CDS	node_148_[2]	639986	639627	360	Chemotaxis regulator - transmits chemoreceptor signals to flagelllar motor components CheY	Flagellar motility	639627	639986
fig|1504.6.peg.1442	CDS	node_148_[2]	640596	640000	597	Chemotaxis protein CheC -- inhibitor of MCP methylation	- none -	640000	640596
fig|1504.6.peg.1443	CDS	node_148_[2]	642627	640612	2016	Signal transduction histidine kinase CheA (EC 2.7.3.-)	Flagellar motility	640612	642627
fig|1504.6.peg.1444	CDS	node_148_[2]	643409	642642	768	Chemotaxis protein methyltransferase CheR (EC 2.1.1.80)	- none -	642642	643409

Feature ID	Type	Contig	Start	Stop	Length (bp)	Function	Subsystems	Begin	End
fig|1504.6.peg.1445	CDS	node_148_[2]	644005	643418	588	Chemotaxis response regulator protein-glutamate methylesterase CheB (EC 3.1.1.61)	- none -	643418	644005
fig|1504.6.peg.1446	CDS	node_148_[2]	644512	644021	492	Chemotaxis protein CheD	- none -	644021	644512
fig|1504.6.peg.1447	CDS	node_148_[2]	644973	644518	456	Positive regulator of CheA protein activity (CheW)	- none -	644518	644973
fig|1504.6.peg.1448	CDS	node_148_[2]	646756	644984	1773	Serine phosphatase RsbU, regulator of sigma subunit	SigmaB stress responce regulation	644984	646756
fig|1504.6.peg.1449	CDS	node_148_[2]	647641	646823	819	Branched-chain amino acid aminotransferase (EC 2.6.1.42)	Alanine biosynthesis, Pyruvate Alanine Serine Interconversions	646823	647641
fig|1504.6.peg.1450	CDS	node_148_[2]	648295	647657	639	Phosphoserine phosphatase (EC 3.1.3.3)	Glycine and Serine Utilization, Serine Biosynthesis, Serine Biosynthesis	647657	648295
fig|1504.6.peg.1451	CDS	node_148_[2]	649696	648503	1194	Aspartate aminotransferase (EC 2.6.1.1)	CBSS-216591.1.peg.168, Glutamine, Glutamate, Aspartate and Asparagine Biosynthesis, Threonine and Homoserine Biosynthesis	648503	649696
fig|1504.6.peg.1452	CDS	node_148_[2]	650536	649712	825	COG0613, Predicted metal-dependent phosphoesterases (PHP family)	CBSS-314276.3.peg.1499	649712	650536
fig|1504.6.peg.1453	CDS	node_148_[2]	651061	650708	354	FIG00513315: hypothetical protein	- none -	650708	651061
fig|1504.6.peg.1454	CDS	node_148_[2]	654718	651212	3507	Pyruvate-flavodoxin oxidoreductase (EC 1.2.7.-)	Methionine Degradation, Pyruvate:ferredoxin oxidoreductase	651212	654718
fig|1504.6.peg.1455	CDS	node_148_[2]	655334	654909	426	Flavodoxin	Flavodoxin	654909	655334
fig|1504.6.peg.1456	CDS	node_148_[2]	656583	655501	1083	UDP-N-acetylglucosamine--N-acetylmuramyl-(pentapeptide) pyrophosphoryl-undecaprenol N-acetylglucosamine transferase (EC 2.4.1.227)	cell division core of larger cluster	655501	656583
fig|1504.6.peg.1457	CDS	node_148_[2]	656834	657016	183	Small acid-soluble spore protein, beta-type SASP	Small acid-soluble spore proteins	656834	657016
fig|1504.6.peg.1458	CDS	node_148_[2]	658956	657181	1776	Single-stranded-DNA-specific exonuclease RecJ (EC 3.1.-.-)	DNA-replication, DNA Repair Base Excision, DNA repair, bacterial RecFOR pathway	657181	658956

Feature ID	Type	Contig	Start	Stop	Length (bp)	Function	Subsystems	Begin	End
fig|1504.6.peg.1459	CDS	node_148_[2]	659523	658981	543	DJ-1/YajL/PfpI superfamily, includes chaperone protein YajL (former ThiJ), parkinsonism-associated protein DJ-1, peptidases PfpI, Hsp31	- none -	658981	659523
fig|1504.6.peg.1460	CDS	node_148_[2]	662457	659545	2913	Topoisomerase IV subunit A (EC 5.99.1.-)	DNA topoisomerases, Type II, ATP-dependent, Resistance to fluoroquinolones	659545	662457
fig|1504.6.peg.1461	CDS	node_148_[2]	664424	662475	1950	Topoisomerase IV subunit B (EC 5.99.1.-)	DNA topoisomerases, Type II, ATP-dependent, Resistance to fluoroquinolones	662475	664424
fig|1504.6.peg.1462	CDS	node_148_[2]	666018	664627	1392	N-acetylglucosaminyltransferase (EC 2.4.1.-)	- none -	664627	666018
fig|1504.6.peg.1463	CDS	node_148_[2]	667689	666343	1347	NADP-specific glutamate dehydrogenase (EC 1.4.1.4)	Arginine and Ornithine Degradation, Glutamate dehydrogenases, Glutamine, Glutamate, Aspartate and Asparagine Biosynthesis, Proline Synthesis	666343	667689
fig|1504.6.peg.1464	CDS	node_148_[2]	667928	669169	1242	probable UV endonuclease	- none -	667928	669169
fig|1504.6.peg.1465	CDS	node_148_[2]	669830	669216	615	Arginine/ornithine antiporter ArcD	Arginine and Ornithine Degradation, Polyamine Metabolism	669216	669830
fig|1504.6.peg.1466	CDS	node_148_[2]	670803	669835	969	Conserved membrane protein	- none -	669835	670803
fig|1504.6.peg.1467	CDS	node_148_[2]	672613	670814	1800	oligoendopeptidase F	- none -	670814	672613
fig|1504.6.peg.1468	CDS	node_148_[2]	673044	672646	399	conserved hypothetical protein	- none -	672646	673044
fig|1504.6.peg.1469	CDS	node_148_[2]	673196	673591	396	hypothetical protein	- none -	673196	673591
fig|1504.6.peg.1470	CDS	node_148_[2]	673581	674327	747	Zinc ABC transporter, ATP-binding protein ZnuC	- none -	673581	674327
fig|1504.6.peg.1471	CDS	node_148_[2]	674374	675165	792	Zinc ABC transporter, inner membrane permease protein ZnuB	- none -	674374	675165
fig|1504.6.peg.1472	CDS	node_148_[2]	675603	675187	417	transcriptional regulator, Fur family	Oxidative stress	675187	675603
fig|1504.6.peg.1473	CDS	node_148_[2]	676222	675665	558	Conjugative transfer protein PilR in PFGI-1-like cluster	- none -	675665	676222

Feature ID	Type	Contig	Start	Stop	Length (bp)	Function	Subsystems	Begin	End
fig|1504.6.peg.1474	CDS	node_148_[2]	676410	677627	1218	6-phosphofructokinase (EC 2.7.1.11)	Glycolysis and Gluconeogenesis, N-Acetyl-Galactosamine and Galactosamine Utilization	676410	677627
fig|1504.6.peg.1475	CDS	node_148_[2]	678953	677661	1293	Cysteine desulfurase (EC 2.8.1.7)	Alanine biosynthesis, CBSS-84588.1.peg.1247, mnm5U34 biosynthesis bacteria	677661	678953
fig|1504.6.peg.1476	CDS	node_148_[2]	679088	679795	708	hypothetical protein	- none -	679088	679795
fig|1504.6.peg.1477	CDS	node_148_[2]	679803	680420	618	hypothetical protein	- none -	679803	680420
fig|1504.6.peg.1478	CDS	node_148_[2]	681669	680470	1200	ABC transporter permease protein	- none -	680470	681669
fig|1504.6.peg.1479	CDS	node_148_[2]	682268	681687	582	ABC transporter, ATP-binding protein	- none -	681687	682268
fig|1504.6.peg.1480	CDS	node_148_[2]	683227	682379	849	Probable Co/Zn/Cd efflux system membrane fusion protein	Cobalt-zinc-cadmium resistance	682379	683227
fig|1504.6.peg.1481	CDS	node_148_[2]	683394	685310	1917	COG0488: ATPase components of ABC transporters with duplicated ATPase domains	- none -	683394	685310
fig|1504.6.peg.1482	CDS	node_148_[2]	686701	685481	1221	Transposase, mutator type	- none -	685481	686701
fig|1504.6.peg.1483	CDS	node_148_[2]	688197	686959	1239	Mobile element protein	- none -	686959	688197
fig|1504.6.peg.1484	CDS	node_148_[2]	688784	688344	441	Deoxyuridine 5'-triphosphate nucleotidohydrolase (EC 3.6.1.23)	Housecleaning nucleoside triphosphate pyrophosphatases, Nudix proteins (nucleoside triphosphate hydrolases)	688344	688784
fig|1504.6.peg.1485	CDS	node_148_[2]	689607	688885	723	no significant homology	- none -	688885	689607
fig|1504.6.peg.1486	CDS	node_148_[2]	691168	689693	1476	diguanylate cyclase/phosphodiesterase (GGDEF & EAL domains) with PAS/PAC sensor(s)	- none -	689693	691168
fig|1504.6.peg.1487	CDS	node_148_[2]	692663	691374	1290	Uracil permease	De Novo Pyrimidine Synthesis, Pyrimidine utilization	691374	692663
fig|1504.6.peg.1488	CDS	node_148_[2]	693016	693753	738	Peptidoglycan N-acetylglucosamine deacetylase (EC 3.5.1.-)	Polysaccharide deacetylases	693016	693753
fig|1504.6.peg.1489	CDS	node_148_[2]	694317	693784	534	Substrate-specific component TrpP of tryptophan ECF transporter	ECF class transporters	693784	694317
fig|1504.6.peg.1490	CDS	node_148_[2]	696082	694721	1362	Multi antimicrobial extrusion protein (Na(+)/drug antiporter), MATE family of MDR efflux pumps	Multidrug Resistance Efflux Pumps, Riboflavin, FMN and FAD metabolism in plants	694721	696082

Feature ID	Type	Contig	Start	Stop	Length (bp)	Function	Subsystems	Begin	End
fig|1504.6.peg.1491	CDS	node_148_[2]	696122	697228	1107	Mobile element protein	- none -	696122	697228
fig|1504.6.peg.1492	CDS	node_148_[2]	699075	698947	129	hypothetical protein	- none -	698947	699075
fig|1504.6.peg.1493	CDS	node_148_[2]	700474	700286	189	hypothetical protein	- none -	700286	700474
fig|1504.6.peg.1494	CDS	node_148_[2]	700740	700618	123	hypothetical protein	- none -	700618	700740
fig|1504.6.peg.1495	CDS	node_148_[2]	700860	701720	861	Hydrolase (HAD superfamily)	- none -	700860	701720
fig|1504.6.peg.1496	CDS	node_148_[2]	702663	701797	867	tRNA(Cytosine32)-2-thiocytidine synthetase	- none -	701797	702663
fig|1504.6.peg.1497	CDS	node_148_[2]	702826	703854	1029	Conserved protein	- none -	702826	703854
fig|1504.6.peg.1498	CDS	node_148_[2]	704195	703893	303	Stress responsive alpha-beta barrel domain protein Dabb	- none -	703893	704195
fig|1504.6.peg.1499	CDS	node_148_[2]	704709	704248	462	hypothetical protein	- none -	704248	704709
fig|1504.6.peg.1500	CDS	node_148_[2]	706100	704739	1362	FAD-linked oxidoreductase family	- none -	704739	706100
fig|1504.6.peg.1501	CDS	node_148_[2]	707634	706234	1401	Carbon starvation protein A	Carbon Starvation	706234	707634
fig|1504.6.peg.1502	CDS	node_148_[2]	708487	707774	714	Hypothetical response regulatory protein ypdB	- none -	707774	708487
fig|1504.6.peg.1503	CDS	node_148_[2]	710158	708503	1656	Autolysis histidine kinase LytS	Murein hydrolase regulation and cell death	708503	710158
fig|1504.6.peg.1504	CDS	node_148_[2]	710718	710281	438	hypothetical protein	- none -	710281	710718
fig|1504.6.peg.1505	CDS	node_148_[2]	711353	710712	642	Pyrrolidone-carboxylate peptidase (EC 3.4.19.3)	Omega peptidases (EC 3.4.19.-)	710712	711353
fig|1504.6.peg.1506	CDS	node_148_[2]	712313	711384	930	FIG001614: Membrane protein	CBSS-521098.4.peg.1460	711384	712313
fig|1504.6.peg.1507	CDS	node_148_[2]	713015	712314	702	FIG015373: Membrane protein	CBSS-521098.4.peg.1460	712314	713015
fig|1504.6.peg.1508	CDS	node_148_[2]	714237	713302	936	membrane protein, putative	- none -	713302	714237
fig|1504.6.peg.1509	CDS	node_148_[2]	714370	714927	558	Transcriptional regulator	- none -	714370	714927
fig|1504.6.peg.1510	CDS	node_148_[2]	716282	715086	1197	hypothetical protein	- none -	715086	716282
fig|1504.6.peg.1511	CDS	node_148_[2]	716939	716403	537	Phage protein	- none -	716403	716939
fig|1504.6.peg.1512	CDS	node_148_[2]	719101	717788	1314	Beta-galactosidase (EC 3.2.1.23)	Galactosylceramide and Sulfatide metabolism, Lactose and Galactose Uptake and Utilization, Lactose utilization	717788	719101

Feature ID	Type	Contig	Start	Stop	Length (bp)	Function	Subsystems	Begin	End
fig|1504.6.peg.1513	CDS	node_148_[2]	721449	719194	2256	Alpha-N-arabinofuranosidase (EC 3.2.1.55)	- none -	719194	721449
fig|1504.6.peg.1514	CDS	node_148_[2]	721771	721592	180	hypothetical protein	- none -	721592	721771
fig|1504.6.peg.1515	CDS	node_148_[2]	722966	722124	843	Non-heme chloroperoxidase (EC 1.11.1.10)	- none -	722124	722966
fig|1504.6.peg.1516	CDS	node_148_[2]	723327	723136	192	hypothetical protein	- none -	723136	723327
fig|1504.6.peg.1517	CDS	node_148_[2]	724571	723342	1230	hypothetical protein	- none -	723342	724571
fig|1504.6.peg.1518	CDS	node_148_[2]	726281	724725	1557	ABC transporter ATP-binding protein	- none -	724725	726281
fig|1504.6.peg.1519	CDS	node_148_[2]	726984	726427	558	no significant homology	- none -	726427	726984
fig|1504.6.peg.1520	CDS	node_148_[2]	728221	727154	1068	ABC transporter, periplasmic spermidine putrescine-binding protein PotD (TC 3.A.1.11.1)	Polyamine Metabolism	727154	728221
fig|1504.6.peg.1521	CDS	node_148_[2]	728598	728350	249	hypothetical protein	- none -	728350	728598
fig|1504.6.peg.1522	CDS	node_148_[2]	728744	730081	1338	Biotin synthase related domain containing protein	- none -	728744	730081
fig|1504.6.peg.1523	CDS	node_148_[2]	730099	730836	738	Domain often clustered or fused with uracil-DNA glycosylase	Uracil-DNA glycosylase	730099	730836
fig|1504.6.peg.1524	CDS	node_148_[2]	731259	730879	381	Bona fide RidA/YjgF/TdcF/RutC subgroup	- none -	730879	731259
fig|1504.6.peg.1525	CDS	node_148_[2]	731346	731513	168	hypothetical protein	- none -	731346	731513
fig|1504.6.peg.1526	CDS	node_148_[2]	731811	732833	1023	Branched-chain amino acid aminotransferase (EC 2.6.1.42)	Alanine biosynthesis, Pyruvate Alanine Serine Interconversions	731811	732833
fig|1504.6.peg.1527	CDS	node_148_[2]	732989	733882	894	FIG028593: membrane protein	- none -	732989	733882
fig|1504.6.peg.1528	CDS	node_148_[2]	734449	733904	546	Nitroreductase family protein	- none -	733904	734449
fig|1504.6.peg.1529	CDS	node_148_[2]	735333	734557	777	Formate efflux transporter (TC 2.A.44 family)	Fermentations: Mixed acid	734557	735333
fig|1504.6.peg.1530	CDS	node_148_[2]	736302	735526	777	Sirohydrochlorin cobaltochelatase CbiK (EC 4.99.1.3)	Cobalamin synthesis, Coenzyme B12 biosynthesis	735526	736302
fig|1504.6.peg.1531	CDS	node_148_[2]	737596	736322	1275	Glutamate-1-semialdehyde aminotransferase (EC 5.4.3.8)	CBSS-196164.1.peg.461, Heme and Siroheme Biosynthesis	736322	737596
fig|1504.6.peg.1532	CDS	node_148_[2]	738566	737598	969	Porphobilinogen synthase (EC 4.2.1.24)	Heme and Siroheme Biosynthesis	737598	738566

Feature ID	Type	Contig	Start	Stop	Length (bp)	Function	Subsystems	Begin	End
fig|1504.6.peg.1533	CDS	node_148_[2]	740055	738586	1470	Uroporphyrinogen-III methyltransferase (EC 2.1.1.107) / Uroporphyrinogen-III synthase (EC 4.2.1.75)	Coenzyme B12 biosynthesis, Heme and Siroheme Biosynthesis, Heme and Siroheme Biosynthesis	738586	740055
fig|1504.6.peg.1534	CDS	node_148_[2]	740938	740066	873	Porphobilinogen deaminase (EC 2.5.1.61)	Heme and Siroheme Biosynthesis	740066	740938
fig|1504.6.peg.1535	CDS	node_148_[2]	741621	740953	669	Siroheme synthase / Precorrin-2 oxidase (EC 1.3.1.76) / Sirohydrochlorin ferrochelatase (EC 4.99.1.4)	Heme and Siroheme Biosynthesis, Heme and Siroheme Biosynthesis	740953	741621
fig|1504.6.peg.1536	CDS	node_148_[2]	742784	741585	1200	Glutamyl-tRNA reductase (EC 1.2.1.70)	Heme and Siroheme Biosynthesis	741585	742784
fig|1504.6.peg.1537	CDS	node_148_[2]	744014	743052	963	Anaerobic sulfite reductase subunit C (EC 1.8.1.-)	Anaerobic respiratory reductases	743052	744014
fig|1504.6.peg.1538	CDS	node_148_[2]	744821	744027	795	Anaerobic sulfite reductase subunit B	Anaerobic respiratory reductases	744027	744821
fig|1504.6.peg.1539	CDS	node_148_[2]	745829	744822	1008	Anaerobic sulfite reductase subunit A	Anaerobic respiratory reductases	744822	745829
fig|1504.6.peg.1540	CDS	node_148_[2]	746809	746120	690	transcriptional regulator, Crp/Fnr family	Oxidative stress	746120	746809
fig|1504.6.peg.1541	CDS	node_148_[2]	747335	746934	402	hypothetical protein	- none -	746934	747335
fig|1504.6.peg.1542	CDS	node_148_[2]	747507	747914	408	UPF0047 protein Bsu YugU	- none -	747507	747914
fig|1504.6.peg.1543	CDS	node_148_[2]	748012	748653	642	Undecaprenyl diphosphate synthase (EC 2.5.1.31)	CBSS-83331.1.peg.3039, Isoprenoid Biosynthesis, Isoprenoinds for Quinones, Polyprenyl Diphosphate Biosynthesis	748012	748653
fig|1504.6.peg.1544	CDS	node_148_[2]	749233	748712	522	hypothetical protein	- none -	748712	749233
fig|1504.6.peg.1545	CDS	node_148_[2]	749450	749325	126	Homoserine O-succinyltransferase (EC 2.3.1.46)	Methionine Biosynthesis	749325	749450
fig|1504.6.peg.1546	CDS	node_148_[2]	749876	751612	1737	Adenine deaminase (EC 3.5.4.2)	Purine conversions	749876	751612
fig|1504.6.peg.1547	CDS	node_148_[2]	753012	751804	1209	[FeFe]-hydrogenase maturation GTPase HydF	- none -	751804	753012
fig|1504.6.peg.1548	CDS	node_148_[2]	754399	753026	1374	[FeFe]-hydrogenase maturation protein HydG	- none -	753026	754399
fig|1504.6.peg.1549	CDS	node_148_[2]	755558	754428	1131	[FeFe]-hydrogenase maturation protein HydE	- none -	754428	755558

Feature ID	Type	Contig	Start	Stop	Length (bp)	Function	Subsystems	Begin	End
fig|1504.6.peg.1550	CDS	node_148_[2]	755704	755561	144	hypothetical protein	- none -	755561	755704
fig|1504.6.peg.1551	CDS	node_148_[2]	761993	756213	5781	Fibronectin type III domain protein	- none -	756213	761993
fig|1504.6.peg.1552	CDS	node_148_[2]	763087	762176	912	Regulator of polyketide synthase expression	- none -	762176	763087
fig|1504.6.peg.1553	CDS	node_148_[2]	763571	763191	381	no significant homology.	- none -	763191	763571
fig|1504.6.peg.1554	CDS	node_148_[2]	764486	763734	753	Integral membrane protein	- none -	763734	764486
fig|1504.6.peg.1555	CDS	node_148_[2]	766098	764611	1488	Chemotaxis regulator - transmits chemoreceptor signals to flagelllar motor components CheY	Flagellar motility	764611	766098
fig|1504.6.peg.1556	CDS	node_148_[2]	767833	766091	1743	two-component sensor histidine kinase	- none -	766091	767833
fig|1504.6.peg.1557	CDS	node_148_[2]	768653	767946	708	Mg(2+) transport ATPase protein C	Magnesium transport	767946	768653
fig|1504.6.peg.1558	CDS	node_148_[2]	769748	768675	1074	Putrescine transport ATP-binding protein PotA (TC 3.A.1.11.1)	Polyamine Metabolism	768675	769748
fig|1504.6.peg.1559	CDS	node_148_[2]	771458	769761	1698	Ferric iron ABC transporter, permease protein	Iron acquisition in Streptococcus	769761	771458
fig|1504.6.peg.1560	CDS	node_148_[2]	772541	771519	1023	Ferric iron ABC transporter, iron-binding protein	Iron acquisition in Streptococcus	771519	772541
fig|1504.6.peg.1561	CDS	node_148_[2]	773355	772690	666	Sulfite reductase, assimilatory-type (EC 1.8.-.-)	- none -	772690	773355
fig|1504.6.peg.1562	CDS	node_148_[2]	774289	773486	804	Predicted hydrolase	- none -	773486	774289
fig|1504.6.peg.1563	CDS	node_148_[2]	774653	774384	270	no significant homology	- none -	774384	774653
fig|1504.6.peg.1564	CDS	node_148_[2]	774918	774748	171	hypothetical protein	- none -	774748	774918
fig|1504.6.peg.1565	CDS	node_148_[2]	776558	775113	1446	ATP-dependent RNA helicase YxiN	ATP-dependent RNA helicases, bacterial	775113	776558
fig|1504.6.peg.1566	CDS	node_148_[2]	777280	776783	498	hypothetical protein	- none -	776783	777280
fig|1504.6.peg.1567	CDS	node_148_[2]	778011	777376	636	Peptidyl-prolyl cis-trans isomerase (EC 5.2.1.8)	Queuosine-Archaeosine Biosynthesis	777376	778011
fig|1504.6.peg.1568	CDS	node_148_[2]	778274	778155	120	Mobile element protein	- none -	778155	778274
fig|1504.6.peg.1569	CDS	node_148_[2]	779189	779052	138	hypothetical protein	- none -	779052	779189
fig|1504.6.peg.1570	CDS	node_148_[2]	779690	779274	417	hypothetical protein	- none -	779274	779690
fig|1504.6.peg.1571	CDS	node_148_[2]	780617	779811	807	Cu(I)-responsive transcriptional regulator	Copper homeostasis	779811	780617

Feature ID	Type	Contig	Start	Stop	Length (bp)	Function	Subsystems	Begin	End
fig|1504.6.peg.1572	CDS	node_148_[2]	780719	782053	1335	Multi antimicrobial extrusion protein (Na(+)/drug antiporter), MATE family of MDR efflux pumps	Multidrug Resistance Efflux Pumps, Riboflavin, FMN and FAD metabolism in plants	780719	782053
fig|1504.6.peg.1573	CDS	node_148_[2]	782865	782149	717	Glycerophosphoryl diester phosphodiesterase (EC 3.1.4.46)	Glycerol and Glycerol-3-phosphate Uptake and Utilization	782149	782865
fig|1504.6.peg.1574	CDS	node_148_[2]	783494	782892	603	Mg(2+) transport ATPase, P-type (EC 3.6.3.2)	Magnesium transport	782892	783494
fig|1504.6.peg.1575	CDS	node_148_[2]	785474	784032	1443	Probable ATP-dependent RNA helicase	- none -	784032	785474
fig|1504.6.peg.1576	CDS	node_148_[2]	785873	785499	375	Probable ATP-dependent RNA helicase	- none -	785499	785873
fig|1504.6.peg.1577	CDS	node_148_[2]	786061	786771	711	Carboxysome protein CcmM	- none -	786061	786771
fig|1504.6.peg.1578	CDS	node_148_[2]	787464	786829	636	Metal-dependent hydrolase	- none -	786829	787464
fig|1504.6.peg.1579	CDS	node_148_[2]	788433	787489	945	phospholipase, patatin family	- none -	787489	788433
fig|1504.6.peg.1580	CDS	node_148_[2]	789211	788609	603	Integral membrane protein	- none -	788609	789211
fig|1504.6.peg.1581	CDS	node_148_[2]	789654	789337	318	FIG136845: Rhodanese-related sulfurtransferase	- none -	789337	789654
fig|1504.6.peg.1582	CDS	node_148_[2]	791241	789766	1476	Inner membrane protein YqiK	- none -	789766	791241
fig|1504.6.peg.1583	CDS	node_148_[2]	792620	791508	1113	Streptolysin S export transmembrane permease (SagI)	- none -	791508	792620
fig|1504.6.peg.1584	CDS	node_148_[2]	793752	792613	1140	Streptolysin S export transmembrane permease (SagH)	- none -	792613	793752
fig|1504.6.peg.1585	CDS	node_148_[2]	794691	793762	930	ABC transporter, ATP-binding protein	- none -	793762	794691
fig|1504.6.peg.1586	CDS	node_148_[2]	795974	795021	954	ABC transporter, permease protein	- none -	795021	795974
fig|1504.6.peg.1587	CDS	node_148_[2]	797088	795976	1113	ABC transporter, permease protein	- none -	795976	797088
fig|1504.6.peg.1588	CDS	node_148_[2]	798607	797078	1530	Predicted nucleoside ABC transporter, ATP-binding component	D-ribose utilization, Deoxyribose and Deoxynucleoside Catabolism	797078	798607
fig|1504.6.peg.1589	CDS	node_148_[2]	799861	798779	1083	Unspecified monosaccharide ABC transport system, substrate-binding component / CD4+ T cell-stimulating antigen, lipoprotein	- none -	798779	799861
fig|1504.6.peg.1590	CDS	node_148_[2]	800617	801498	882	hypothetical protein	- none -	800617	801498

Feature ID	Type	Contig	Start	Stop	Length (bp)	Function	Subsystems	Begin	End
fig|1504.6.peg.1591	CDS	node_148_[2]	802493	801621	873	ABC transporter, predicted N-acetylneuraminate transport system permease protein 2	Sialic Acid Metabolism	801621	802493
fig|1504.6.peg.1592	CDS	node_148_[2]	803439	802513	927	ABC transporter, predicted N-acetylneuraminate transport system permease protein 1	Sialic Acid Metabolism	802513	803439
fig|1504.6.peg.1593	CDS	node_148_[2]	804829	803507	1323	ABC transporter, predicted N-acetylneuraminate-binding protein	Sialic Acid Metabolism	803507	804829
fig|1504.6.peg.1594	CDS	node_148_[2]	805974	804973	1002	LACI-family transcription regulator	- none -	804973	805974
fig|1504.6.peg.1595	CDS	node_148_[2]	806574	806344	231	hypothetical protein	- none -	806344	806574
fig|1504.6.peg.1596	CDS	node_148_[2]	807645	806662	984	Ribose operon repressor	D-ribose utilization	806662	807645
fig|1504.6.peg.1597	CDS	node_148_[2]	808679	807762	918	Ribose ABC transport system, periplasmic ribose-binding protein RbsB (TC 3.A.1.2.1)	D-ribose utilization	807762	808679
fig|1504.6.peg.1598	CDS	node_148_[2]	809643	808708	936	Ribose ABC transport system, permease protein RbsC (TC 3.A.1.2.1)	D-ribose utilization	808708	809643
fig|1504.6.peg.1599	CDS	node_148_[2]	811165	809663	1503	Ribose ABC transport system, ATP-binding protein RbsA (TC 3.A.1.2.1)	D-ribose utilization	809663	811165
fig|1504.6.peg.1600	CDS	node_148_[2]	811574	811179	396	Ribose ABC transport system, high affinity permease RbsD (TC 3.A.1.2.1)	D-ribose utilization	811179	811574
fig|1504.6.peg.1601	CDS	node_148_[2]	812505	811576	930	Ribokinase (EC 2.7.1.15)	D-ribose utilization, Deoxyribose and Deoxynucleoside Catabolism	811576	812505
fig|1504.6.peg.1602	CDS	node_148_[2]	813269	812853	417	Transcriptional regulator, MarR family	- none -	812853	813269
fig|1504.6.peg.1603	CDS	node_148_[2]	813846	813286	561	no significant homology.	- none -	813286	813846
fig|1504.6.peg.1604	CDS	node_148_[2]	814693	813980	714	hypothetical protein	- none -	813980	814693
fig|1504.6.peg.1605	CDS	node_148_[2]	816005	814926	1080	DNA-binding response regulator, AraC family	- none -	814926	816005
fig|1504.6.peg.1606	CDS	node_148_[2]	818342	816030	2313	Signal transduction histidine kinase	- none -	816030	818342
fig|1504.6.peg.1607	CDS	node_148_[2]	819486	818806	681	Ribosomal large subunit pseudouridine synthase F (EC 4.2.1.70)	RNA pseudouridine syntheses	818806	819486
fig|1504.6.peg.1608	CDS	node_148_[2]	825160	819698	5463	Cobalt-zinc-cadmium resistance protein CzcA; Cation efflux system protein CusA	Cobalt-zinc-cadmium resistance, Cobalt-zinc-cadmium resistance	819698	825160
fig|1504.6.peg.1609	CDS	node_148_[2]	827773	825785	1989	probable ABC transporter	- none -	825785	827773

Feature ID	Type	Contig	Start	Stop	Length (bp)	Function	Subsystems	Begin	End
fig|1504.6.peg.1610	CDS	node_148_[2]	828533	827763	771	ABC transporter, ATP-binding protein	- none -	827763	828533
fig|1504.6.peg.1611	CDS	node_148_[2]	829650	828637	1014	two-component sensor histidine kinase	- none -	828637	829650
fig|1504.6.peg.1612	CDS	node_148_[2]	830318	829641	678	Two-component response regulator BceR	- none -	829641	830318
fig|1504.6.peg.1613	CDS	node_148_[2]	833887	830393	3495	Exonuclease SbcC	DNA repair, bacterial, Rad50-Mre11 DNA repair cluster	830393	833887
fig|1504.6.peg.1614	CDS	node_148_[2]	835091	833874	1218	Exonuclease SbcD	DNA repair, bacterial, Rad50-Mre11 DNA repair cluster	833874	835091
fig|1504.6.peg.1615	CDS	node_148_[2]	835309	836793	1485	FAD flavoprotein oxidase	- none -	835309	836793
fig|1504.6.peg.1616	CDS	node_148_[2]	837657	836989	669	Ethanolamine utilization protein similar to PduL	Ethanolamine utilization	836989	837657
fig|1504.6.peg.1617	CDS	node_148_[2]	839831	837777	2055	Methyl-accepting chemotaxis protein	- none -	837777	839831
fig|1504.6.peg.1618	CDS	node_148_[2]	840221	840619	399	Mutator mutT protein (7,8-dihydro-8-oxoguanine-triphosphatase) (EC 3.6.1.-)	Nudix proteins (nucleoside triphosphate hydrolases)	840221	840619
fig|1504.6.peg.1619	CDS	node_148_[2]	843665	840771	2895	DNA repair helicase rad25	- none -	840771	843665
fig|1504.6.peg.1620	CDS	node_148_[2]	844639	843845	795	hypothetical protein	- none -	843845	844639
fig|1504.6.peg.1621	CDS	node_148_[2]	844749	845441	693	transcriptional regulator, Crp/Fnr family	Oxidative stress	844749	845441
fig|1504.6.peg.1622	CDS	node_148_[2]	845529	847340	1812	Ser-type protease	- none -	845529	847340
fig|1504.6.peg.1623	CDS	node_148_[2]	847333	849057	1725	Ser-type protease	- none -	847333	849057
fig|1504.6.peg.1624	CDS	node_148_[2]	849996	849208	789	5'-methylthioadenosine nucleosidase (EC 3.2.2.16) @ S-adenosylhomocysteine nucleosidase (EC 3.2.2.9)	Adenosyl nucleosidases, Adenosyl nucleosidases, Methionine Biosynthesis, Methionine Degradation, Polyamine Metabolism	849208	849996
fig|1504.6.peg.1625	CDS	node_148_[2]	851444	850278	1167	conserved hypothetical protein	- none -	850278	851444
fig|1504.6.peg.1626	CDS	node_148_[2]	851842	852150	309	FIG00518134: hypothetical protein	- none -	851842	852150
fig|1504.6.peg.1627	CDS	node_148_[2]	853489	852197	1293	Enolase (EC 4.2.1.11)	Entner-Doudoroff Pathway, Glycolysis and Gluconeogenesis, Serine-glyoxylate cycle	852197	853489
fig|1504.6.peg.1628	CDS	node_148_[2]	854655	853867	789	Exodeoxyribonuclease III (EC 3.1.11.2)	DNA repair, bacterial	853867	854655

Feature ID	Type	Contig	Start	Stop	Length (bp)	Function	Subsystems	Begin	End
fig|1504.6.peg.1629	CDS	node_148_[2]	855879	854659	1221	PTS system, maltose and glucose-specific IIC component (EC 2.7.1.69) / PTS system, maltose and glucose-specific IIB component (EC 2.7.1.69)	Maltose and Maltodextrin Utilization, Maltose and Maltodextrin Utilization	854659	855879
fig|1504.6.peg.2163	CDS	node_148_[3]	9	221	213	Glycerophosphoryl diester phosphodiesterase (EC 3.1.4.46)	Glycerol and Glycerol-3-phosphate Uptake and Utilization	9	221
fig|1504.6.peg.2164	CDS	node_148_[3]	1532	258	1275	probable secreted protein homolog of yjcM/yhbB B. subtilis	- none -	258	1532
fig|1504.6.peg.2165	CDS	node_148_[3]	1782	1928	147	hypothetical protein	- none -	1782	1928
fig|1504.6.peg.2166	CDS	node_148_[3]	2760	3035	276	hypothetical protein	- none -	2760	3035
fig|1504.6.peg.2167	CDS	node_148_[3]	3060	3314	255	hypothetical protein	- none -	3060	3314
fig|1504.6.peg.2168	CDS	node_148_[3]	3351	5183	1833	DNA double-strand break repair Rad50 ATPase	Rad50-Mre11 DNA repair cluster	3351	5183
fig|1504.6.peg.2169	CDS	node_148_[3]	6073	5282	792	Methyl-directed repair DNA adenine methylase (EC 2.1.1.72)	DNA repair, bacterial	5282	6073
fig|1504.6.peg.2170	CDS	node_148_[3]	6180	7025	846	hypothetical protein	- none -	6180	7025
fig|1504.6.peg.2171	CDS	node_148_[3]	7156	7860	705	Mobile element protein	- none -	7156	7860
fig|1504.6.peg.2172	CDS	node_148_[3]	7868	8389	522	Mobile element protein	- none -	7868	8389
fig|1504.6.peg.2173	CDS	node_148_[3]	8949	8596	354	hypothetical protein	- none -	8596	8949
fig|1504.6.peg.2174	CDS	node_148_[3]	9370	9495	126	hypothetical protein	- none -	9370	9495
fig|1504.6.peg.2175	CDS	node_148_[3]	9773	10954	1182	Nucleoside permease NupC	- none -	9773	10954
fig|1504.6.peg.2176	CDS	node_148_[3]	11286	11405	120	hypothetical protein	- none -	11286	11405
fig|1504.6.peg.2177	CDS	node_148_[3]	11787	12971	1185	putative amidohydrolase	- none -	11787	12971
fig|1504.6.peg.2178	CDS	node_148_[3]	13385	15493	2109	Membrane-associated methyl-accepting chemotaxis protein with HAMP domain	- none -	13385	15493
fig|1504.6.peg.2179	CDS	node_148_[3]	15912	16853	942	2-dehydropantoate 2-reductase (EC 1.1.1.169)	Coenzyme A Biosynthesis	15912	16853
fig|1504.6.peg.2180	CDS	node_148_[3]	16875	17942	1068	membrane protein, putative	- none -	16875	17942
fig|1504.6.peg.2181	CDS	node_148_[3]	18153	19265	1113	ATP-dependent RNA helicase BA2475	ATP-dependent RNA helicases, bacterial	18153	19265
fig|1504.6.peg.2182	CDS	node_148_[3]	19819	20964	1146	Regulator of polyketide synthase expression	- none -	19819	20964

Feature ID	Type	Contig	Start	Stop	Length (bp)	Function	Subsystems	Begin	End
fig|1504.6.peg.2183	CDS	node_148_[3]	21158	23359	2202	Ornithine decarboxylase (EC 4.1.1.17)	Arginine and Ornithine Degradation, Polyamine Metabolism	21158	23359
fig|1504.6.peg.2184	CDS	node_148_[3]	23453	24811	1359	Putrescine/proton symporter, putrescine/ornithine antiporter PotE	Polyamine Metabolism	23453	24811
fig|1504.6.peg.2185	CDS	node_148_[3]	25822	24872	951	LacI family transcriptional regulator	- none -	24872	25822
fig|1504.6.peg.2186	CDS	node_148_[3]	25952	26845	894	4-hydroxy-tetrahydrodipicolinate synthase (EC 4.3.3.7)	Lysine Biosynthesis DAP Pathway, Lysine Biosynthesis DAP Pathway, GJO scratch	25952	26845
fig|1504.6.peg.2187	CDS	node_148_[3]	27011	27388	378	hypothetical protein	- none -	27011	27388
fig|1504.6.peg.2188	CDS	node_148_[3]	27446	28543	1098	Macrolide export ATP-binding/permease protein MacB (EC 3.6.3.-)	Multidrug Resistance Efflux Pumps	27446	28543
fig|1504.6.peg.2189	CDS	node_148_[3]	28540	29784	1245	permease, putative domain protein	- none -	28540	29784
fig|1504.6.peg.2190	CDS	node_148_[3]	29787	30455	669	ABC transporter ATP-binding protein	- none -	29787	30455
fig|1504.6.peg.2191	CDS	node_148_[3]	30591	30917	327	hypothetical protein	- none -	30591	30917
fig|1504.6.peg.2192	CDS	node_148_[3]	31284	32978	1695	Methyl-accepting chemotaxis protein	- none -	31284	32978
fig|1504.6.peg.2193	CDS	node_148_[3]	33480	34514	1035	Maltose operon transcriptional repressor MalR, LacI family	Maltose and Maltodextrin Utilization	33480	34514
fig|1504.6.peg.2194	CDS	node_148_[3]	34660	36324	1665	Alpha-glucosidase (EC 3.2.1.20)	Maltose and Maltodextrin Utilization	34660	36324
fig|1504.6.peg.2195	CDS	node_148_[3]	36699	36286	414	hypothetical protein	- none -	36286	36699
fig|1504.6.peg.2196	CDS	node_148_[4]	17	139	123	hypothetical protein	- none -	17	139
fig|1504.6.peg.2197	CDS	node_148_[4]	1514	228	1287	hypothetical protein	- none -	228	1514
fig|1504.6.peg.2198	CDS	node_148_[4]	2218	1544	675	hypothetical protein	- none -	1544	2218
fig|1504.6.peg.2199	CDS	node_148_[4]	2422	4188	1767	sensor histidine kinase	- none -	2422	4188
fig|1504.6.peg.2200	CDS	node_148_[4]	4190	5704	1515	DNA-binding response regulator, AraC family	- none -	4190	5704
fig|1504.6.peg.2201	CDS	node_148_[4]	5999	7753	1755	Choline binding protein A	Choline and Betaine Uptake and Betaine Biosynthesis	5999	7753
fig|1504.6.peg.2202	CDS	node_148_[4]	7975	13452	5478	probable hemagglutinin-related protein	- none -	7975	13452
fig|1504.6.peg.2203	CDS	node_148_[4]	13470	13682	213	hypothetical protein	- none -	13470	13682

Feature ID	Type	Contig	Start	Stop	Length (bp)	Function	Subsystems	Begin	End
fig|1504.6.peg.2204	CDS	node_148_[4]	14060	14761	702	Guanosine polyphosphate pyrophosphohydrolases/synthetases	- none -	14060	14761
fig|1504.6.peg.2205	CDS	node_148_[4]	14774	15121	348	hypothetical protein	- none -	14774	15121
fig|1504.6.peg.2206	CDS	node_148_[4]	15890	15657	234	hypothetical protein	- none -	15657	15890
fig|1504.6.peg.2207	CDS	node_148_[4]	16048	16566	519	Rhs-family protein	- none -	16048	16566
fig|1504.6.peg.2208	CDS	node_148_[4]	16584	16886	303	Lmo0143 protein	- none -	16584	16886
fig|1504.6.peg.2209	CDS	node_148_[4]	17373	17798	426	CDS_ID OB3369	- none -	17373	17798
fig|1504.6.peg.2210	CDS	node_148_[4]	17785	18132	348	CDS_ID OB3368	- none -	17785	18132
fig|1504.6.peg.2211	CDS	node_148_[4]	19286	20161	876	recombinase	- none -	19286	20161
fig|1504.6.peg.2212	CDS	node_148_[4]	20175	20561	387	hypothetical protein	- none -	20175	20561
fig|1504.6.peg.2213	CDS	node_148_[4]	20576	20719	144	hypothetical protein	- none -	20576	20719
fig|1504.6.peg.2214	CDS	node_148_[4]	21236	21355	120	hypothetical protein	- none -	21236	21355
fig|1504.6.peg.2215	CDS	node_148_[4]	21620	22849	1230	Mobile element protein	- none -	21620	22849
fig|1504.6.peg.2216	CDS	node_148_[4]	23093	23374	282	hypothetical protein	- none -	23093	23374
fig|1504.6.peg.2217	CDS	node_148_[4]	23385	23711	327	hypothetical protein	- none -	23385	23711
fig|1504.6.peg.2218	CDS	node_148_[4]	25198	25497	300	hypothetical protein	- none -	25198	25497
fig|1504.6.peg.2219	CDS	node_148_[4]	25457	26332	876	Integrase, site-specific recombinase	- none -	25457	26332
fig|1504.6.peg.2220	CDS	node_148_[4]	26347	26733	387	hypothetical protein	- none -	26347	26733
fig|1504.6.peg.2221	CDS	node_148_[4]	26730	26891	162	hypothetical protein	- none -	26730	26891
fig|1504.6.peg.2222	CDS	node_148_[4]	27194	27316	123	hypothetical protein	- none -	27194	27316
fig|1504.6.peg.2223	CDS	node_148_[4]	27675	28904	1230	Mobile element protein	- none -	27675	28904
fig|1504.6.peg.2224[5]	CDS	node_148_[4]	29068	29565	498	hemagglutinin/hemolysin-related protein	- none -	29068	29565
fig|1504.6.peg.2225	CDS	node_148_[4]	29593	29997	405	hypothetical protein	- none -	29593	29997
fig|1504.6.peg.2226[6]	CDS	node_148_[4]	30833	31135	303	Putative toxin component near putative ESAT-related proteins, repetitive / Repetitive hypothetical protein near ESAT cluster, SA0282 homolog	- none -	30833	31135
fig|1504.6.peg.2227	CDS	node_148_[4]	31160	31663	504	hypothetical protein	- none -	31160	31663

Feature ID	Type	Contig	Start	Stop	Length (bp)	Function	Subsystems	Begin	End
fig|1504.6.peg.2228	CDS	node_148_[4]	32110	32475	366	hypothetical protein	- none -	32110	32475
fig|1504.6.peg.2229	CDS	node_148_[4]	32749	32862	114	hypothetical protein	- none -	32749	32862
fig|1504.6.peg.2230	CDS	node_148_[4]	32865	33224	360	hypothetical protein	- none -	32865	33224
fig|1504.6.peg.2231	CDS	node_148_[4]	33232	33759	528	RNA:NAD 2'-phosphotransferase	- none -	33232	33759
fig|1504.6.peg.2232	CDS	node_148_[4]	33886	34038	153	hypothetical protein	- none -	33886	34038
fig|1504.6.peg.2233	CDS	node_148_[4]	34073	34783	711	hypothetical protein	- none -	34073	34783
fig|1504.6.peg.2234	CDS	node_148_[4]	35542	36084	543	Rhs-family protein	- none -	35542	36084
fig|1504.6.peg.2235	CDS	node_148_[4]	36086	36316	231	hypothetical protein	- none -	36086	36316
fig|1504.6.peg.2236	CDS	node_148_[4]	37220	37633	414	Rhs-family protein	- none -	37220	37633
fig|1504.6.peg.2237	CDS	node_148_[4]	37662	37922	261	hypothetical protein	- none -	37662	37922
fig|1504.6.peg.2238	CDS	node_148_[4]	38427	38819	393	Putative DNA-binding prophage protein	- none -	38427	38819
fig|1504.6.peg.2239	CDS	node_148_[4]	38886	39326	441	Phage integrase	- none -	38886	39326
fig|1504.6.peg.2240	CDS	node_148_[4]	39580	39729	150	hypothetical protein	- none -	39580	39729
fig|1504.6.peg.2241	CDS	node_148_[4]	39840	40814	975	Mobile element protein	- none -	39840	40814
fig|1504.6.peg.2242	CDS	node_148_[4]	40859	41251	393	Ribosomal protein S1	- none -	40859	41251
fig|1504.6.peg.2243	CDS	node_148_[4]	41262	41570	309	integral membrane protein	- none -	41262	41570
fig|1504.6.peg.2244	CDS	node_148_[4]	43427	43981	555	hypothetical protein	- none -	43427	43981
fig|1504.6.peg.2245	CDS	node_148_[4]	44969	45283	315	FIG00525257: hypothetical protein	- none -	44969	45283
fig|1504.6.peg.2246	CDS	node_148_[4]	45283	45630	348	hypothetical protein	- none -	45283	45630
fig|1504.6.peg.2247	CDS	node_148_[4]	46452	46219	234	hypothetical protein	- none -	46219	46452
fig|1504.6.peg.2248	CDS	node_148_[4]	46610	47413	804	Rhs-family protein	- none -	46610	47413
fig|1504.6.peg.2249	CDS	node_148_[4]	47425	47991	567	hypothetical protein	- none -	47425	47991
fig|1504.6.peg.2250	CDS	node_148_[4]	48203	48340	138	hypothetical protein	- none -	48203	48340
fig|1504.6.peg.2251	CDS	node_148_[4]	48814	49563	750	Rhs-family protein	- none -	48814	49563
fig|1504.6.peg.2252	CDS	node_148_[4]	49579	50133	555	hypothetical protein	- none -	49579	50133
fig|1504.6.peg.2253	CDS	node_148_[4]	51137	51589	453	Tyrosine recombinase XerD	- none -	51137	51589

Feature ID	Type	Contig	Start	Stop	Length (bp)	Function	Subsystems	Begin	End
fig|1504.6.peg.2254	CDS	node_148_[4]	51950	52228	279	hypothetical protein	- none -	51950	52228
fig|1504.6.peg.2255	CDS	node_148_[4]	52638	53195	558	Rhs-family protein	- none -	52638	53195
fig|1504.6.peg.2256	CDS	node_148_[4]	53213	53734	522	hypothetical protein	- none -	53213	53734
fig|1504.6.peg.2257	CDS	node_148_[4]	54925	55266	342	Rhs-family protein	- none -	54925	55266
fig|1504.6.peg.2258	CDS	node_148_[4]	55471	55773	303	hypothetical protein	- none -	55471	55773
fig|1504.6.peg.2259	CDS	node_148_[4]	56366	56875	510	Choline binding protein A	Choline and Betaine Uptake and Betaine Biosynthesis	56366	56875
fig|1504.6.peg.2260	CDS	node_148_[4]	56889	57236	348	hypothetical protein	- none -	56889	57236
fig|1504.6.peg.2261[7]	CDS	node_148_[4]	57304	57597	294	Lmo0066 homolog within ESAT-6 gene cluster, similarity to ADP-ribosylating toxins	- none -	57304	57597
fig|1504.6.peg.2262	CDS	node_148_[4]	57610	57945	336	hypothetical protein	- none -	57610	57945
fig|1504.6.peg.2263	CDS	node_148_[4]	58769	59527	759	hypothetical protein	- none -	58769	59527
fig|1504.6.peg.2264	CDS	node_148_[4]	59542	59928	387	hypothetical protein	- none -	59542	59928
fig|1504.6.peg.2265	CDS	node_148_[4]	60370	60972	603	Ribonuclease (EC 3.1.27.-)	- none -	60370	60972
fig|1504.6.peg.2266	CDS	node_148_[4]	61029	61607	579	hypothetical protein	- none -	61029	61607
fig|1504.6.peg.2267	CDS	node_148_[4]	61750	61971	222	hypothetical protein	- none -	61750	61971
fig|1504.6.peg.2268	CDS	node_148_[4]	61992	62225	234	Hypothetical protein, CF-7 family. Related to CAC1969	- none -	61992	62225
fig|1504.6.peg.2269	CDS	node_148_[4]	62257	62526	270	Hypothetical protein, CF-38 family	- none -	62257	62526
fig|1504.6.peg.2270	CDS	node_148_[4]	62505	62711	207	Hypothetical protein, CF-38 family	- none -	62505	62711
fig|1504.6.peg.2271	CDS	node_148_[4]	62949	63908	960	Multiple sugar ABC transporter, membrane-spanning permease protein MsmF	Fructooligosaccharides(FOS) and Raffinose Utilization	62949	63908
fig|1504.6.peg.2272	CDS	node_148_[4]	63929	64894	966	Multiple sugar ABC transporter, membrane-spanning permease protein MsmG	Fructooligosaccharides(FOS) and Raffinose Utilization	63929	64894
fig|1504.6.peg.2273	CDS	node_148_[4]	65021	68152	3132	Alpha-mannosidase (EC 3.2.1.24)	Fructooligosaccharides(FOS) and Raffinose Utilization, Mannose Metabolism	65021	68152
fig|1504.6.peg.2274	CDS	node_148_[4]	68426	69874	1449	Multiple sugar ABC transporter, substrate-binding protein	Fructooligosaccharides(FOS) and Raffinose Utilization	68426	69874
fig|1504.6.peg.2275	CDS	node_148_[4]	69963	72350	2388	FIG00520824: hypothetical protein	- none -	69963	72350

Feature ID	Type	Contig	Start	Stop	Length (bp)	Function	Subsystems	Begin	End
fig|1504.6.peg.2276	CDS	node_148_[4]	72691	73167	477	no significant homology 2 putative transmembrane regions were found by PSORT.	- none -	72691	73167
fig|1504.6.peg.2277	CDS	node_148_[4]	73174	75024	1851	glycosyl hydrolase, family 20	- none -	73174	75024
fig|1504.6.peg.2278	CDS	node_148_[4]	75177	76622	1446	Multiple sugar ABC transporter, substrate-binding protein	Fructooligosaccharides(FOS) and Raffinose Utilization	75177	76622
fig|1504.6.peg.2279	CDS	node_148_[4]	76772	78166	1395	Beta-glucosidase (EC 3.2.1.21)	Beta-Glucoside Metabolism, Fructooligosaccharides(FOS) and Raffinose Utilization	76772	78166
fig|1504.6.peg.2280	CDS	node_148_[4]	78185	79087	903	N-acetylmannosamine kinase (EC 2.7.1.60)	Sialic Acid Metabolism	78185	79087
fig|1504.6.peg.2281	CDS	node_148_[4]	79127	80083	957	Mlc, transcriptional repressor of MalT (the transcriptional activator of maltose regulon) and manXYZ operon	Maltose and Maltodextrin Utilization	79127	80083
fig|1504.6.peg.2282	CDS	node_148_[4]	80221	81159	939	Mannose-6-phosphate isomerase (EC 5.3.1.8)	Mannose Metabolism	80221	81159
fig|1504.6.peg.2283	CDS	node_148_[4]	81469	81732	264	hypothetical protein	- none -	81469	81732
fig|1504.6.peg.2284	CDS	node_148_[4]	81719	81991	273	ABC transporter, ATP-binding/permease protein	- none -	81719	81991
fig|1504.6.peg.2285	CDS	node_148_[4]	82753	82118	636	hypothetical protein	- none -	82118	82753
fig|1504.6.peg.2286	CDS	node_148_[4]	82913	83347	435	hypothetical protein	- none -	82913	83347
fig|1504.6.peg.2287	CDS	node_148_[4]	83588	83881	294	hypothetical protein	- none -	83588	83881
fig|1504.6.peg.2288	CDS	node_148_[4]	84197	86443	2247	COG0503: Adenine/guanine phosphoribosyltransferases and related PRPP-binding proteins	- none -	84197	86443
fig|1504.6.peg.2289	CDS	node_148_[4]	86485	87558	1074	putative ATP/GTP-binding protein protein	- none -	86485	87558
fig|1504.6.peg.2290	CDS	node_148_[4]	87578	88372	795	conserved protein	- none -	87578	88372
fig|1504.6.peg.2291	CDS	node_148_[4]	88457	90001	1545	FIG013452: putative tellurium resistance protein	- none -	88457	90001
fig|1504.6.peg.2292	CDS	node_148_[4]	90026	91360	1335	toxic anion resistance protein	- none -	90026	91360
fig|1504.6.peg.2293	CDS	node_148_[4]	91516	92145	630	Tellurium resistance protein TerD	- none -	91516	92145
fig|1504.6.peg.2294	CDS	node_148_[4]	92174	92755	582	Tellurium resistance protein TerD	- none -	92174	92755
fig|1504.6.peg.2295	CDS	node_148_[4]	92773	93408	636	Tellurium resistance protein TerD	- none -	92773	93408

Feature ID	Type	Contig	Start	Stop	Length (bp)	Function	Subsystems	Begin	End
fig|1504.6.peg.2296	CDS	node_148_[4]	93506	96178	2673	Lead, cadmium, zinc and mercury transporting ATPase (EC 3.6.3.3) (EC 3.6.3.5); Copper-translocating P-type ATPase (EC 3.6.3.4)	Copper Transport System, Copper homeostasis	93506	96178
fig|1504.6.peg.2297	CDS	node_148_[4]	96293	97132	840	hypothetical protein	- none -	96293	97132
fig|1504.6.peg.2298	CDS	node_148_[4]	97906	97172	735	hypothetical protein	- none -	97172	97906
fig|1504.6.peg.2299	CDS	node_148_[4]	98339	103423	5085	hypothetical protein	- none -	98339	103423
fig|1504.6.peg.2300	CDS	node_148_[4]	103449	104285	837	pneumococcal surface protein A	- none -	103449	104285
fig|1504.6.peg.2301	CDS	node_148_[4]	104269	105051	783	NPQTN specific sortase B	Heme, hemin uptake and utilization systems in GramPositives, Sortase	104269	105051
fig|1504.6.peg.2302	CDS	node_148_[4]	105840	105115	726	CAAX amino terminal protease family protein	- none -	105115	105840
fig|1504.6.peg.2303	CDS	node_148_[4]	106279	105863	417	hypothetical protein	- none -	105863	106279
fig|1504.6.peg.2304	CDS	node_148_[4]	106451	107254	804	Hydrolase (HAD superfamily) in cluster with DUF1447	Bacterial RNA-metabolizing Zn-dependent hydrolases, Conserved gene cluster associated with Met-tRNA formyltransferase, Queuosine-Archaeosine Biosynthesis	106451	107254
fig|1504.6.peg.2305	CDS	node_148_[4]	107563	108147	585	FIG00513816: hypothetical protein	- none -	107563	108147
fig|1504.6.peg.2306	CDS	node_148_[4]	108314	108955	642	Phosphoglycerate mutase family	Phosphoglycerate mutase protein family	108314	108955
fig|1504.6.peg.2307	CDS	node_148_[4]	109855	109070	786	Transcriptional repressor of the fructose operon, DeoR family	Fructose utilization	109070	109855
fig|1504.6.peg.2308	CDS	node_148_[4]	110671	109874	798	hypothetical protein	- none -	109874	110671
fig|1504.6.peg.2309	CDS	node_148_[4]	111123	112187	1065	Probable L-ascorbate-6-phosphate lactonase UlaG (EC 3.1.1.-) (L-ascorbate utilization protein G)	L-ascorbate utilization (and related gene clusters)	111123	112187
fig|1504.6.peg.2310	CDS	node_148_[4]	112279	112722	444	Ascorbate-specific PTS system, EIIA component (EC 2.7.1.-)	L-ascorbate utilization (and related gene clusters)	112279	112722
fig|1504.6.peg.2311	CDS	node_148_[4]	112818	114272	1455	Ascorbate-specific PTS system, EIIC component	L-ascorbate utilization (and related gene clusters)	112818	114272

Feature ID	Type	Contig	Start	Stop	Length (bp)	Function	Subsystems	Begin	End
fig|1504.6.peg.2312	CDS	node_148_[4]	114486	114776	291	Ascorbate-specific PTS system, EIIB component (EC 2.7.1.69)	L-ascorbate utilization (and related gene clusters)	114486	114776
fig|1504.6.peg.2313	CDS	node_148_[4]	114884	115921	1038	FIG00518753: hypothetical protein	- none -	114884	115921
fig|1504.6.peg.2314	CDS	node_148_[4]	115958	116650	693	L-ribulose-5-phosphate 4-epimerase (EC 5.1.3.4)	L-ascorbate utilization (and related gene clusters)	115958	116650
fig|1504.6.peg.2315	CDS	node_148_[4]	116672	117523	852	L-xylulose 5-phosphate 3-epimerase (EC 5.1.3.-)	L-ascorbate utilization (and related gene clusters)	116672	117523
fig|1504.6.peg.2316	CDS	node_148_[4]	117915	118721	807	Transketolase, N-terminal section (EC 2.2.1.1)	Pentose phosphate pathway	117915	118721
fig|1504.6.peg.2317	CDS	node_148_[4]	118735	119661	927	Transketolase, C-terminal section (EC 2.2.1.1)	Pentose phosphate pathway	118735	119661
fig|1504.6.peg.2318	CDS	node_148_[4]	119816	120466	651	Transaldolase (EC 2.2.1.2)	Fructose utilization, Pentose phosphate pathway	119816	120466
fig|1504.6.peg.2319	CDS	node_148_[4]	120783	121226	444	hypothetical protein	- none -	120783	121226
fig|1504.6.peg.2320	CDS	node_148_[4]	123203	121533	1671	Alkyl hydroperoxide reductase protein F (EC 1.6.4.-)	Thioredoxin-disulfide reductase	121533	123203
fig|1504.6.peg.2321	CDS	node_148_[4]	123886	123323	564	Alkyl hydroperoxide reductase protein C (EC 1.6.4.-)	Thioredoxin-disulfide reductase	123323	123886
fig|1504.6.peg.2322	CDS	node_148_[4]	124221	125816	1596	Peptide chain release factor 3	Translation termination factors bacterial	124221	125816
fig|1504.6.peg.2323	CDS	node_148_[4]	126137	126448	312	no significant homology. 2 putative transmembrane regions were found by PSORT.	- none -	126137	126448
fig|1504.6.peg.2324	CDS	node_148_[4]	126454	126663	210	Transcriptional regulator, Cro/CI family	- none -	126454	126663
fig|1504.6.peg.2325	CDS	node_148_[4]	126905	127321	417	3-hydroxybutyryl-CoA dehydratase (EC 4.2.1.55)	Polyhydroxybutyrate metabolism	126905	127321
fig|1504.6.peg.2326	CDS	node_148_[4]	127541	127993	453	Transcriptional regulator	- none -	127541	127993
fig|1504.6.peg.2327	CDS	node_148_[4]	128090	128938	849	Transcriptional regulator	- none -	128090	128938
fig|1504.6.peg.2328	CDS	node_148_[4]	130952	129141	1812	FIG00520746: hypothetical protein	- none -	129141	130952
fig|1504.6.peg.2329	CDS	node_148_[4]	131632	130949	684	ABC transporter ATP-binding protein	- none -	130949	131632
fig|1504.6.peg.2330	CDS	node_148_[4]	132769	131705	1065	sensor histidine kinase	- none -	131705	132769
fig|1504.6.peg.2331	CDS	node_148_[4]	133437	132751	687	Two-component response regulator	- none -	132751	133437
fig|1504.6.peg.2332	CDS	node_148_[4]	133892	135439	1548	Acetyl-CoA:acetoacetyl-CoA transferase, alpha subunit (EC 2.8.3.8)	- none -	133892	135439

Feature ID	Type	Contig	Start	Stop	Length (bp)	Function	Subsystems	Begin	End
fig|1504.6.peg.2333	CDS	node_148_[4]	135538	136713	1176	Oxalate/formate antiporter	- none -	135538	136713
fig|1504.6.peg.2334	CDS	node_148_[4]	137263	142926	5664	Sialidase (EC 3.2.1.18)	Galactosylceramide and Sulfatide metabolism, Sialic Acid Metabolism	137263	142926
fig|1504.6.peg.2335	CDS	node_148_[4]	144110	143277	834	HMP-PP hydrolase (pyridoxal phosphatase) Cof, detected in genetic screen for thiamin metabolic genes (PMID:15292217)	- none -	143277	144110
fig|1504.6.peg.2336	CDS	node_148_[4]	144836	144252	585	putative RNA polymerase sigma factor	- none -	144252	144836
fig|1504.6.peg.2337	CDS	node_148_[4]	145013	145219	207	hypothetical protein	- none -	145013	145219
fig|1504.6.peg.2338	CDS	node_148_[4]	145241	145459	219	hypothetical protein	- none -	145241	145459
fig|1504.6.peg.2339	CDS	node_148_[4]	145820	146359	540	putative RNA polymerase sigma factor	- none -	145820	146359
fig|1504.6.peg.2340	CDS	node_148_[4]	146759	147436	678	Tyrosine-protein kinase transmembrane modulator EpsC	Exopolysaccharide Biosynthesis	146759	147436
fig|1504.6.peg.2341	CDS	node_148_[4]	147449	148099	651	Tyrosine-protein kinase EpsD (EC 2.7.10.2)	Exopolysaccharide Biosynthesis	147449	148099
fig|1504.6.peg.2342	CDS	node_148_[4]	148100	148873	774	Manganese-dependent protein-tyrosine phosphatase (EC 3.1.3.48)	Exopolysaccharide Biosynthesis	148100	148873
fig|1504.6.peg.2343	CDS	node_148_[4]	148972	149634	663	Undecaprenyl-phosphate galactosephosphotransferase (EC 2.7.8.6)	Exopolysaccharide Biosynthesis	148972	149634
fig|1504.6.peg.2344	CDS	node_148_[4]	149662	150822	1161	UDP-N-acetylglucosamine 2-epimerase (EC 5.1.3.14)	CMP-N-acetylneuraminate Biosynthesis, Sialic Acid Metabolism	149662	150822
fig|1504.6.peg.2345	CDS	node_148_[4]	150852	152081	1230	UDP-glucose dehydrogenase (EC 1.1.1.22)	- none -	150852	152081
fig|1504.6.peg.2346	CDS	node_148_[4]	152125	152862	738	N-acetylmannosaminyltransferase (EC 2.4.1.187)	Teichoic and lipoteichoic acids biosynthesis	152125	152862
fig|1504.6.peg.2347	CDS	node_148_[4]	152864	153913	1050	Glycosyltransferase (EC 2.4.1.-)	- none -	152864	153913
fig|1504.6.peg.2348	CDS	node_148_[4]	153925	155484	1560	Proposed peptidoglycan lipid II flippase MurJ	Peptidoglycan lipid II flippase	153925	155484
fig|1504.6.peg.2349	CDS	node_148_[4]	155486	156421	936	hypothetical protein	- none -	155486	156421
fig|1504.6.peg.2350	CDS	node_148_[4]	156435	156875	441	Serine acetyltransferase (EC 2.3.1.30)	Conserved gene cluster possibly involved in RNA metabolism, Cysteine Biosynthesis, Methionine Biosynthesis	156435	156875

Feature ID	Type	Contig	Start	Stop	Length (bp)	Function	Subsystems	Begin	End
fig|1504.6.peg.2351	CDS	node_148_[4]	156896	158740	1845	hypothetical protein	- none -	156896	158740
fig|1504.6.peg.2352	CDS	node_148_[4]	158813	160135	1323	CapK protein, putative	- none -	158813	160135
fig|1504.6.peg.2353	CDS	node_148_[4]	160169	161296	1128	hypothetical protein	- none -	160169	161296
fig|1504.6.peg.2354	CDS	node_148_[4]	161617	161823	207	Mobile element protein	- none -	161617	161823
fig|1504.6.peg.2355	CDS	node_148_[4]	162243	163199	957	Mobile element protein	- none -	162243	163199
fig|1504.6.peg.2356	CDS	node_148_[4]	163435	163683	249	Mobile element protein	- none -	163435	163683
fig|1504.6.peg.2357	CDS	node_148_[4]	163787	164098	312	Mobile element protein	- none -	163787	164098
fig|1504.6.peg.2358	CDS	node_148_[4]	166575	164842	1734	spoIID-like domain containing protein, peptidoglycan-binding domain	- none -	164842	166575
fig|1504.6.peg.2359	CDS	node_148_[4]	166829	169360	2532	hypothetical protein	- none -	166829	169360
fig|1504.6.peg.2360	CDS	node_148_[4]	169546	172056	2511	Possible surface protein, responsible for cell interaction; contains cell adhesion domain and ChW-repeats	- none -	169546	172056
fig|1504.6.peg.2361	CDS	node_148_[4]	172120	172242	123	hypothetical protein	- none -	172120	172242
fig|1504.6.peg.2362	CDS	node_148_[4]	172260	173633	1374	Internalin G (LPXTG motif)	Listeria surface proteins: Internalin-like proteins	172260	173633
fig|1504.6.peg.2363	CDS	node_148_[4]	175460	173988	1473	protease, putative	- none -	173988	175460
fig|1504.6.peg.2364	CDS	node_148_[4]	175648	176574	927	hypothetical protein	- none -	175648	176574
fig|1504.6.peg.2365	CDS	node_148_[4]	176598	178523	1926	Choline binding protein A	Choline and Betaine Uptake and Betaine Biosynthesis	176598	178523
fig|1504.6.peg.2366	CDS	node_148_[4]	178708	179706	999	UDP-glucose 4-epimerase (EC 5.1.3.2)	Lacto-N-Biose I and Galacto-N-Biose Metabolic Pathway, Lactose and Galactose Uptake and Utilization, N-linked Glycosylation in Bacteria, Rhamnose containing glycans	178708	179706
fig|1504.6.peg.2367	CDS	node_148_[4]	180124	180801	678	Tyrosine-protein kinase transmembrane modulator EpsC	Exopolysaccharide Biosynthesis	180124	180801
fig|1504.6.peg.2368	CDS	node_148_[4]	180829	181479	651	Tyrosine-protein kinase EpsD (EC 2.7.10.2)	Exopolysaccharide Biosynthesis	180829	181479
fig|1504.6.peg.2369	CDS	node_148_[4]	181776	182333	558	Phosphotransbutyrylase	- none -	181776	182333

Feature ID	Type	Contig	Start	Stop	Length (bp)	Function	Subsystems	Begin	End
fig|1504.6.peg.2370	CDS	node_148_[4]	182932	185067	2136	internalin, putative	Listeria surface proteins: Internalin-like proteins	182932	185067
fig|1504.6.peg.2371	CDS	node_148_[4]	185569	189084	3516	Cobalt-zinc-cadmium resistance protein CzcA; Cation efflux system protein CusA	Cobalt-zinc-cadmium resistance, Cobalt-zinc-cadmium resistance	185569	189084
fig|1504.6.peg.2372	CDS	node_148_[4]	189230	189643	414	hypothetical protein	- none -	189230	189643
fig|1504.6.peg.2373	CDS	node_148_[4]	190179	191021	843	hypothetical protein	- none -	190179	191021
fig|1504.6.peg.2374	CDS	node_148_[4]	191196	191735	540	hypothetical protein	- none -	191196	191735
fig|1504.6.peg.2375[8]	CDS	node_148_[4]	192129	196037	3909	putative hyaluronoglucosaminidase	- none -	192129	196037
fig|1504.6.peg.2376	CDS	node_148_[4]	197071	197430	360	hypothetical protein	- none -	197071	197430
fig|1504.6.peg.2377[9]	CDS	node_148_[4]	197693	201460	3768	putative hyaluronoglucosaminidase	- none -	197693	201460
fig|1504.6.peg.2378	CDS	node_148_[4]	203093	203509	417	hypothetical protein	- none -	203093	203509
fig|1504.6.peg.2379	CDS	node_148_[4]	203729	206167	2439	SOS-response repressor and protease LexA (EC 3.4.21.88)	DNA repair, bacterial	203729	206167
fig|1504.6.peg.2380	CDS	node_148_[4]	206893	206441	453	hypothetical protein	- none -	206441	206893
fig|1504.6.peg.2381	CDS	node_148_[4]	206933	208039	1107	Mobile element protein	- none -	206933	208039
fig|1504.6.peg.2382[10]	CDS	node_148_[4]	208675	209997	1323	Alpha-toxin	- none -	208675	209997
fig|1504.6.peg.2383	CDS	node_148_[4]	210589	210756	168	hypothetical protein	- none -	210589	210756
fig|1504.6.peg.2384	CDS	node_148_[4]	211224	210943	282	hypothetical protein	- none -	210943	211224
fig|1504.6.peg.2385	CDS	node_148_[4]	211473	212840	1368	PTS system, N-acetylmuramic acid-specific IIB component (EC 2.7.1.69) / PTS system, N-acetylmuramic acid-specific IIC component	Sialic Acid Metabolism	211473	212840
fig|1504.6.peg.2386	CDS	node_148_[4]	212920	213990	1071	Outer surface protein of unknown function, cellobiose operon	Beta-Glucoside Metabolism	212920	213990
fig|1504.6.peg.2387	CDS	node_148_[4]	214914	215393	480	hypothetical protein	- none -	214914	215393
fig|1504.6.peg.2388	CDS	node_148_[4]	216117	215479	639	hypothetical protein	- none -	215479	216117
fig|1504.6.peg.2389	CDS	node_148_[4]	216420	216875	456	hypothetical protein	- none -	216420	216875
fig|1504.6.peg.2390	CDS	node_148_[4]	217154	217750	597	SSU ribosomal protein S4p (S9e)	Ribosome SSU bacterial	217154	217750
fig|1504.6.peg.2391	CDS	node_148_[4]	218085	218627	543	hypothetical protein	- none -	218085	218627

Feature ID	Type	Contig	Start	Stop	Length (bp)	Function	Subsystems	Begin	End
fig|1504.6.peg.2392	CDS	node_148_[4]	218631	220826	2196	hypothetical protein	- none -	218631	220826
fig|1504.6.peg.2393	CDS	node_148_[4]	220988	221116	129	hypothetical protein	- none -	220988	221116
fig|1504.6.peg.2394	CDS	node_148_[4]	221285	221557	273	hypothetical protein	- none -	221285	221557
fig|1504.6.peg.2395	CDS	node_148_[4]	221573	222544	972	hypothetical protein	- none -	221573	222544
fig|1504.6.peg.2396	CDS	node_148_[4]	222567	223898	1332	Replicative DNA helicase (DnaB) (EC 3.6.4.12)	DNA-replication	222567	223898
fig|1504.6.peg.2397	CDS	node_148_[4]	224602	224925	324	hypothetical protein	- none -	224602	224925
fig|1504.6.peg.2398	CDS	node_148_[4]	225056	225688	633	hypothetical protein	- none -	225056	225688
fig|1504.6.peg.2399	CDS	node_148_[4]	226461	225955	507	hypothetical protein	- none -	225955	226461
fig|1504.6.peg.2400	CDS	node_148_[4]	226785	228017	1233	hypothetical protein	- none -	226785	228017
fig|1504.6.peg.2401	CDS	node_148_[4]	228023	228688	666	Teicoplanin resistance protein vanZ	- none -	228023	228688
fig|1504.6.peg.2402	CDS	node_148_[4]	230056	228980	1077	membrane protein	- none -	228980	230056
fig|1504.6.peg.2403	CDS	node_148_[4]	230569	230832	264	Signal transduction histidine kinase	- none -	230569	230832
fig|1504.6.peg.2404	CDS	node_148_[4]	231317	232093	777	ABC transporter ATP-binding protein	- none -	231317	232093
fig|1504.6.peg.2405	CDS	node_148_[4]	232083	234116	2034	ABC-type antimicrobial peptide transport system, permease component	- none -	232083	234116
fig|1504.6.peg.2406	CDS	node_148_[4]	234128	234814	687	Phosphate regulon transcriptional regulatory protein PhoB (SphR)	High affinity phosphate transporter and control of PHO regulon, PhoR-PhoB two-component regulatory system, Phosphate metabolism	234128	234814
fig|1504.6.peg.2407	CDS	node_148_[4]	234807	235832	1026	sensor histidine kinase	- none -	234807	235832
fig|1504.6.peg.2408	CDS	node_148_[4]	235855	235974	120	FIG00512917: hypothetical protein	- none -	235855	235974
fig|1504.6.peg.2409	CDS	node_148_[4]	236400	236720	321	Transcriptional regulator, PadR family	CBSS-1352.1.peg.856	236400	236720
fig|1504.6.peg.2410	CDS	node_148_[4]	236736	237464	729	FIG00516591: hypothetical protein	- none -	236736	237464
fig|1504.6.peg.2411	CDS	node_148_[4]	237586	237960	375	Cytidine deaminase (EC 3.5.4.5)	Murein hydrolase regulation and cell death, pyrimidine conversions	237586	237960
fig|1504.6.peg.2412	CDS	node_148_[4]	238477	239766	1290	putative cytoplasmic protein	- none -	238477	239766
fig|1504.6.peg.2413	CDS	node_148_[4]	241554	239926	1629	cassette chromosome recombinase B	- none -	239926	241554

Feature ID	Type	Contig	Start	Stop	Length (bp)	Function	Subsystems	Begin	End
fig|1504.6.peg.2414	CDS	node_148_[4]	241733	241557	177	hypothetical protein	- none -	241557	241733
fig|1504.6.peg.2415	CDS	node_148_[4]	241893	242519	627	hypothetical protein	- none -	241893	242519
fig|1504.6.peg.2416	CDS	node_148_[4]	242781	243713	933	hypothetical protein	- none -	242781	243713
fig|1504.6.peg.2417	CDS	node_148_[4]	244223	244804	582	hypothetical protein	- none -	244223	244804
fig|1504.6.peg.2418	CDS	node_148_[4]	244823	245854	1032	hypothetical protein	- none -	244823	245854
fig|1504.6.peg.2419	CDS	node_148_[4]	246035	246589	555	hypothetical protein	- none -	246035	246589
fig|1504.6.peg.2420	CDS	node_148_[4]	246634	247182	549	hypothetical protein	- none -	246634	247182
fig|1504.6.peg.2421	CDS	node_148_[4]	247661	247335	327	hypothetical protein	- none -	247335	247661
fig|1504.6.peg.2422	CDS	node_148_[4]	247838	248038	201	hypothetical protein	- none -	247838	248038
fig|1504.6.peg.2423	CDS	node_148_[4]	248040	248468	429	hypothetical protein	- none -	248040	248468
fig|1504.6.peg.2424	CDS	node_148_[4]	248518	249138	621	hypothetical protein	- none -	248518	249138
fig|1504.6.peg.2425	CDS	node_148_[4]	249628	251490	1863	Type III restriction-modification system methylation subunit (EC 2.1.1.72)	Restriction-Modification System	249628	251490
fig|1504.6.peg.2426	CDS	node_148_[4]	251506	254205	2700	Type III restriction-modification system DNA endonuclease res (EC 3.1.21.5)	Restriction-Modification System	251506	254205
fig|1504.6.peg.2427	CDS	node_148_[4]	254275	255813	1539	Serine/threonine protein kinase PrkC, regulator of stationary phase	A Gram-positive cluster that relates ribosomal protein L28P to a set of uncharacterized proteins, Conserved gene cluster associated with Met-tRNA formyltransferase	254275	255813
fig|1504.6.peg.2428	CDS	node_148_[4]	256086	256424	339	hypothetical protein	- none -	256086	256424
fig|1504.6.peg.2429	CDS	node_148_[4]	256453	257355	903	hypothetical protein	- none -	256453	257355
fig|1504.6.peg.2430	CDS	node_148_[4]	257519	257893	375	hypothetical protein	- none -	257519	257893
fig|1504.6.peg.2431	CDS	node_148_[4]	257954	258454	501	hypothetical protein	- none -	257954	258454
fig|1504.6.peg.2432	CDS	node_148_[4]	258835	259293	459	Transcriptional regulator, XRE family	- none -	258835	259293
fig|1504.6.peg.2433	CDS	node_148_[4]	259440	261548	2109	Methyl-accepting chemotaxis protein	- none -	259440	261548
fig|1504.6.peg.2434	CDS	node_148_[4]	262367	261699	669	hypothetical protein	- none -	261699	262367
fig|1504.6.peg.2435	CDS	node_148_[4]	262690	262364	327	hypothetical protein	- none -	262364	262690

Feature ID	Type	Contig	Start	Stop	Length (bp)	Function	Subsystems	Begin	End
fig|1504.6.peg.2436	CDS	node_148_[4]	263223	262705	519	RNA polymerase sigma-70 factor, ECF subfamily	- none -	262705	263223
fig|1504.6.peg.2437	CDS	node_148_[4]	263444	263782	339	FIG00529811: hypothetical protein	- none -	263444	263782
fig|1504.6.peg.2438	CDS	node_148_[4]	264001	265464	1464	Type I restriction-modification system, DNA-methyltransferase subunit M (EC 2.1.1.72)	Restriction-Modification System, Type I Restriction-Modification	264001	265464
fig|1504.6.peg.2439	CDS	node_148_[4]	265468	266655	1188	Type I restriction-modification system, specificity subunit S (EC 3.1.21.3)	Restriction-Modification System, Type I Restriction-Modification	265468	266655
fig|1504.6.peg.2440	CDS	node_148_[4]	266685	266801	117	hypothetical protein	- none -	266685	266801
fig|1504.6.peg.2441	CDS	node_148_[4]	266918	270262	3345	Type I restriction-modification system, restriction subunit R (EC 3.1.21.3)	Restriction-Modification System, Type I Restriction-Modification	266918	270262
fig|1504.6.peg.2442	CDS	node_148_[4]	271603	272589	987	hypothetical protein	- none -	271603	272589
fig|1504.6.peg.2443	CDS	node_148_[4]	272745	272870	126	hypothetical protein	- none -	272745	272870
fig|1504.6.peg.2444	CDS	node_148_[4]	273431	273760	330	FIG00518518: hypothetical protein	- none -	273431	273760
fig|1504.6.peg.2445	CDS	node_148_[4]	274255	273857	399	hypothetical protein	- none -	273857	274255
fig|1504.6.peg.2446	CDS	node_148_[4]	274830	274967	138	hypothetical protein	- none -	274830	274967
fig|1504.6.peg.2447	CDS	node_148_[4]	275357	275022	336	hypothetical protein	- none -	275022	275357
fig|1504.6.peg.2448	CDS	node_148_[4]	275481	275969	489	Mobile element protein	- none -	275481	275969
fig|1504.6.peg.2449	CDS	node_148_[4]	276147	276503	357	Mobile element protein	- none -	276147	276503
fig|1504.6.peg.2450	CDS	node_148_[4]	277146	278192	1047	Macrolide export ATP-binding/permease protein MacB (EC 3.6.3.-)	Multidrug Resistance Efflux Pumps	277146	278192
fig|1504.6.peg.2451	CDS	node_148_[4]	278197	279420	1224	Cell division protein FtsX	Bacterial Cell Division, CBSS-393121.3.peg.2760	278197	279420
fig|1504.6.peg.2452	CDS	node_148_[4]	279417	280100	684	ABC transporter, ATP-binding protein	- none -	279417	280100
fig|1504.6.peg.2453	CDS	node_148_[4]	280700	280197	504	hypothetical protein	- none -	280197	280700
fig|1504.6.peg.2454	CDS	node_148_[4]	280903	281079	177	hypothetical protein	- none -	280903	281079
fig|1504.6.peg.2455	CDS	node_148_[4]	282482	281100	1383	FIG00512724: hypothetical protein	- none -	281100	282482
fig|1504.6.peg.2456	CDS	node_148_[4]	283573	282881	693	ABC transporter ATP-binding protein	- none -	282881	283573

Feature ID	Type	Contig	Start	Stop	Length (bp)	Function	Subsystems	Begin	End
fig|1504.6.peg.2457	CDS	node_148_[4]	284797	283574	1224	ABC transporter, permease protein	- none -	283574	284797
fig|1504.6.peg.2458	CDS	node_148_[4]	285892	284801	1092	Macrolide export ATP-binding/permease protein MacB (EC 3.6.3.-)	Multidrug Resistance Efflux Pumps	284801	285892
fig|1504.6.peg.2459	CDS	node_148_[4]	286331	288163	1833	hypothetical protein	- none -	286331	288163
fig|1504.6.peg.2460	CDS	node_148_[4]	288558	288674	117	hypothetical protein	- none -	288558	288674
fig|1504.6.peg.2461	CDS	node_148_[4]	288797	288952	156	hypothetical protein	- none -	288797	288952
fig|1504.6.peg.2462	CDS	node_148_[4]	289210	290442	1233	Sodium/dicarboxylate symporter	- none -	289210	290442
fig|1504.6.peg.2463	CDS	node_148_[4]	290489	291253	765	hypothetical protein	- none -	290489	291253
fig|1504.6.peg.2464	CDS	node_148_[4]	291511	292074	564	RNA polymerase sigma-70 factor, ECF family	- none -	291511	292074
fig|1504.6.peg.2465	CDS	node_148_[4]	292064	292864	801	hypothetical protein	- none -	292064	292864
fig|1504.6.peg.2466	CDS	node_148_[4]	292866	293729	864	ABC transporter ATP-binding protein	- none -	292866	293729
fig|1504.6.peg.2467	CDS	node_148_[4]	293730	294098	369	putative membrane protein	- none -	293730	294098
fig|1504.6.peg.2468	CDS	node_148_[4]	294125	294493	369	putative membrane protein	- none -	294125	294493
fig|1504.6.peg.2469	CDS	node_148_[4]	294503	295681	1179	putative membrane protein	- none -	294503	295681
fig|1504.6.peg.2470	CDS	node_148_[4]	296366	295728	639	Teicoplanin resistance protein vanZ	- none -	295728	296366
fig|1504.6.peg.2471	CDS	node_148_[4]	297060	297518	459	hypothetical protein	- none -	297060	297518
fig|1504.6.peg.2472	CDS	node_148_[4]	297750	298712	963	Internalin G (LPXTG motif)	Listeria surface proteins: Internalin-like proteins	297750	298712
fig|1504.6.peg.2473	CDS	node_148_[4]	299227	299538	312	hypothetical protein	- none -	299227	299538
fig|1504.6.peg.2474	CDS	node_148_[4]	299596	299847	252	hypothetical protein	- none -	299596	299847
fig|1504.6.peg.2475	CDS	node_148_[4]	301968	299950	2019	Sensory box/GGDEF family protein	- none -	299950	301968
fig|1504.6.peg.2476	CDS	node_148_[4]	302237	302899	663	Transcriptional regulator, DeoR family	- none -	302237	302899
fig|1504.6.peg.2477	CDS	node_148_[4]	303134	303640	507	Signal peptidase I (EC 3.4.21.89)	CBSS-176299.4.peg.1292, Signal peptidase	303134	303640
fig|1504.6.peg.2478	CDS	node_148_[4]	303670	304335	666	hypothetical protein	- none -	303670	304335
fig|1504.6.peg.2479	CDS	node_148_[4]	304346	304993	648	no significant homology. Putative N-terminal signal sequence was found by PSORT	- none -	304346	304993
fig|1504.6.peg.2480	CDS	node_148_[4]	305097	305669	573	hypothetical protein	- none -	305097	305669

Feature ID	Type	Contig	Start	Stop	Length (bp)	Function	Subsystems	Begin	End
fig|1504.6.peg.2481	CDS	node_148_[4]	305716	306384	669	hypothetical protein	- none -	305716	306384
fig|1504.6.peg.2482	CDS	node_148_[4]	306473	308197	1725	cell wall surface anchor family protein	- none -	306473	308197
fig|1504.6.peg.2483	CDS	node_148_[4]	308325	308861	537	RNA polymerase sigma factor SigV	Transcription initiation, bacterial sigma factors	308325	308861
fig|1504.6.peg.2484	CDS	node_148_[4]	308886	309572	687	NPQTN specific sortase B	Heme, hemin uptake and utilization systems in GramPositives, Sortase	308886	309572
fig|1504.6.peg.2485	CDS	node_148_[4]	311050	309680	1371	Sensory transduction protein kinase (EC 2.7.3.-)	- none -	309680	311050
fig|1504.6.peg.2486	CDS	node_148_[4]	311714	311037	678	DNA-binding response regulator	- none -	311037	311714
fig|1504.6.peg.2487	CDS	node_148_[4]	311880	312560	681	hypothetical protein	- none -	311880	312560
fig|1504.6.peg.2488	CDS	node_148_[4]	312759	315290	2532	membrane protein, putative	- none -	312759	315290
fig|1504.6.peg.2489	CDS	node_148_[4]	315484	316200	717	Two-component response regulator	- none -	315484	316200
fig|1504.6.peg.2490	CDS	node_148_[4]	316214	317518	1305	sensor histidine kinase, putative virS	- none -	316214	317518
fig|1504.6.peg.2491	CDS	node_148_[4]	317651	318589	939	Hydrolase, alpha/beta fold family	- none -	317651	318589
fig|1504.6.peg.2492	CDS	node_148_[4]	319977	318673	1305	Cell division protein FtsW	Bacterial Cell Division, Bacterial Cytoskeleton, cell division cluster containing FtsQ	318673	319977
fig|1504.6.peg.2493	CDS	node_148_[4]	320309	319968	342	Transcriptional regulator, PadR family	CBSS-1352.1.peg.856	319968	320309
fig|1504.6.peg.2494	CDS	node_148_[4]	321134	320814	321	FIG00518518: hypothetical protein	- none -	320814	321134
fig|1504.6.peg.2495	CDS	node_148_[4]	321377	321562	186	hypothetical protein	- none -	321377	321562
fig|1504.6.peg.2496	CDS	node_148_[4]	321847	322509	663	hypothetical protein	- none -	321847	322509
fig|1504.6.peg.2497	CDS	node_148_[4]	323104	323382	279	hypothetical protein	- none -	323104	323382
fig|1504.6.peg.2498	CDS	node_148_[4]	324152	323505	648	FIG00527569: hypothetical protein	- none -	323505	324152
fig|1504.6.peg.2499	CDS	node_148_[4]	324318	324776	459	FIG00519197: hypothetical protein	- none -	324318	324776
fig|1504.6.peg.2500	CDS	node_148_[4]	325117	326556	1440	iron-sulfur cluster-binding protein, rieske family	- none -	325117	326556
fig|1504.6.peg.2501	CDS	node_148_[4]	326894	327457	564	6-phospho-beta-glucosidase (EC 3.2.1.86)	Beta-Glucoside Metabolism	326894	327457

Feature ID	Type	Contig	Start	Stop	Length (bp)	Function	Subsystems	Begin	End
fig|1504.6.peg.2502	CDS	node_148_[4]	328208	327582	627	Heme oxygenase (EC 1.14.99.3)	Heme, hemin uptake and utilization systems in GramPositives	327582	328208
fig|1504.6.peg.2503	CDS	node_148_[4]	329191	331101	1911	Threonyl-tRNA synthetase (EC 6.1.1.3)	tRNA aminoacylation, Thr	329191	331101
fig|1504.6.peg.2504	CDS	node_148_[4]	331160	331480	321	Inorganic pyrophosphatase	- none -	331160	331480
fig|1504.6.peg.2505	CDS	node_148_[4]	331619	332050	432	hypothetical protein	- none -	331619	332050
fig|1504.6.peg.2506	CDS	node_148_[4]	332289	332783	495	Conserved domain protein	- none -	332289	332783
fig|1504.6.peg.2507	CDS	node_148_[4]	334387	332897	1491	CDS_ID OB0252	- none -	332897	334387
fig|1504.6.peg.2508	CDS	node_148_[4]	335193	334633	561	Adenosylhomocysteinase (EC 3.3.1.1)	Methionine Biosynthesis, Methionine Degradation	334633	335193
fig|1504.6.peg.2509	CDS	node_148_[4]	335695	335321	375	no significant homology. Putative N-terminal signal sequence and 1 putative transmembrane region were found by PSORT	- none -	335321	335695
fig|1504.6.peg.2510	CDS	node_148_[4]	336597	335860	738	FIG00513275: hypothetical protein	- none -	335860	336597
fig|1504.6.peg.2511	CDS	node_148_[4]	337470	336598	873	ABC transporter ATP-binding protein	- none -	336598	337470
fig|1504.6.peg.2512	CDS	node_148_[4]	337834	337463	372	Transcriptional regulator, GntR family	- none -	337463	337834
fig|1504.6.peg.2513[11]	CDS	node_148_[4]	338108	342064	3957	Hyaluronoglucosaminidase precursor (EC 3.2.1.35)	- none -	338108	342064
fig|1504.6.peg.2514	CDS	node_148_[4]	342199	342831	633	pentapeptide repeat protein	- none -	342199	342831
fig|1504.6.peg.2515	CDS	node_148_[4]	343012	343686	675	Trypanothione synthetase domain protein	- none -	343012	343686
fig|1504.6.peg.2516	CDS	node_148_[4]	343859	345658	1800	Methyl-accepting chemotaxis protein	- none -	343859	345658
fig|1504.6.peg.2517	CDS	node_148_[4]	346485	346075	411	Mobile element protein	- none -	346075	346485
fig|1504.6.peg.2518	CDS	node_148_[4]	347018	346725	294	hypothetical protein	- none -	346725	347018
fig|1504.6.peg.2519	CDS	node_148_[4]	347281	348726	1446	amino acid ABC transporter, amino acid-binding protein/permease protein, His/Glu/Gln/Arg/opine family	- none -	347281	348726
fig|1504.6.peg.2520	CDS	node_148_[4]	348739	349476	738	amino acid ABC transporter, ATP-binding protein	- none -	348739	349476
fig|1504.6.peg.2521	CDS	node_148_[4]	349573	349887	315	Thioredoxin	- none -	349573	349887

Feature ID	Type	Contig	Start	Stop	Length (bp)	Function	Subsystems	Begin	End
fig|1504.6.peg.2522	CDS	node_148_[4]	351539	349998	1542	Periplasmic [Fe] hydrogenase large subunit (EC 1.12.7.2)	- none -	349998	351539
fig|1504.6.peg.2523	CDS	node_148_[4]	351651	352001	351	Putative Dihydrolipoamide dehydrogenase (EC 1.8.1.4); Mercuric ion reductase (EC 1.16.1.1); PF00070 family, FAD-dependent NAD(P)-disulphide oxidoreductase	Mercuric reductase, Mercuric reductase, Mercury resistance operon	351651	352001
fig|1504.6.peg.2524	CDS	node_148_[4]	352018	352503	486	hypothetical protein	- none -	352018	352503
fig|1504.6.peg.2525	CDS	node_148_[4]	352536	352880	345	Transcriptional regulator, HxlR family	- none -	352536	352880
fig|1504.6.peg.2526	CDS	node_148_[4]	353187	354284	1098	Cytochrome c-type biogenesis protein CcdA (DsbD analog) / Cytochrome c-type biogenesis protein ResA	Biogenesis of c-type cytochromes, Biogenesis of c-type cytochromes, CBSS-196164.1.peg.461, Periplasmic disulfide interchange	353187	354284
fig|1504.6.peg.2527	CDS	node_148_[4]	354377	355000	624	Haloacid dehalogenase-like hydrolase	- none -	354377	355000
fig|1504.6.peg.2528	CDS	node_148_[4]	355688	357691	2004	GAF domain/GGDEF domain protein	- none -	355688	357691
fig|1504.6.peg.2529	CDS	node_148_[4]	357722	359488	1767	ATP-dependent DNA helicase RecQ	DNA-replication, DNA repair, bacterial RecFOR pathway	357722	359488
fig|1504.6.peg.2530	CDS	node_148_[4]	359826	365069	5244	Beta-hexosaminidase (EC 3.2.1.52)	Chitin and N-acetylglucosamine utilization, N-Acetyl-Galactosamine and Galactosamine Utilization	359826	365069
fig|1504.6.peg.2531	CDS	node_148_[4]	366017	372241	6225	Beta-galactosidase (EC 3.2.1.23)	Galactosylceramide and Sulfatide metabolism, Lactose and Galactose Uptake and Utilization, Lactose utilization	366017	372241
fig|1504.6.peg.2532	CDS	node_148_[4]	372411	374333	1923	Serine protein kinase (prkA protein), P-loop containing	- none -	372411	374333
fig|1504.6.peg.2533	CDS	node_148_[4]	374340	375512	1173	FIG002076: hypothetical protein	- none -	374340	375512
fig|1504.6.peg.2534	CDS	node_148_[4]	375516	376883	1368	FIG004684: SpoVR-like protein	- none -	375516	376883
fig|1504.6.peg.2535	CDS	node_148_[4]	377020	377562	543	Rubrerythrin	Oxidative stress, Rubrerythrin	377020	377562
fig|1504.6.peg.2536	CDS	node_148_[4]	377574	378440	867	hypothetical protein	- none -	377574	378440
fig|1504.6.peg.2537	CDS	node_148_[4]	378504	378848	345	hypothetical protein	- none -	378504	378848

Feature ID	Type	Contig	Start	Stop	Length (bp)	Function	Subsystems	Begin	End
fig|1504.6.peg.2538	CDS	node_148_[4]	379415	378894	522	CDP-diacylglycerol--serine O-phosphatidyltransferase (EC 2.7.8.8)	Glycerolipid and Glycerophospholipid Metabolism in Bacteria	378894	379415
fig|1504.6.peg.2539	CDS	node_148_[4]	379701	380588	888	Transcription regulator [contains diacylglycerol kinase catalytic domain]	- none -	379701	380588
fig|1504.6.peg.2540	CDS	node_148_[4]	380659	381300	642	no significant homology. Putative N-terminal signal sequence and 6 putative transmembrane regions were found by PSORT.	- none -	380659	381300
fig|1504.6.peg.2541	CDS	node_148_[4]	381686	382942	1257	Magnesium transporter	- none -	381686	382942
fig|1504.6.peg.2542	CDS	node_148_[4]	383351	384256	906	Cysteine synthase (EC 2.5.1.47)	Cysteine Biosynthesis, Methionine Biosynthesis	383351	384256
fig|1504.6.peg.2543	CDS	node_148_[4]	384299	384883	585	Serine acetyltransferase (EC 2.3.1.30)	Conserved gene cluster possibly involved in RNA metabolism, Cysteine Biosynthesis, Methionine Biosynthesis	384299	384883
fig|1504.6.peg.2544	CDS	node_148_[4]	384894	385886	993	Epoxyqueuosine (oQ) reductase QueG	Queuosine-Archaeosine Biosynthesis	384894	385886
fig|1504.6.peg.2545	CDS	node_148_[4]	385927	386631	705	1-acyl-sn-glycerol-3-phosphate acyltransferase (EC 2.3.1.51)	Glycerolipid and Glycerophospholipid Metabolism in Bacteria, Ribosome post-transcriptional modification and chromosomal segregation cluster	385927	386631
fig|1504.6.peg.2546	CDS	node_148_[4]	386640	387287	648	Endonuclease III (EC 4.2.99.18)	DNA Repair Base Excision	386640	387287
fig|1504.6.peg.2547	CDS	node_148_[4]	388175	387303	873	Permease of the drug/metabolite transporter (DMT) superfamily	Queuosine-Archaeosine Biosynthesis	387303	388175
fig|1504.6.peg.2548	CDS	node_148_[4]	388383	389288	906	D-alanine--D-alanine ligase (EC 6.3.2.4)	Peptidoglycan biosynthesis--gjo, cell division cluster containing FtsQ	388383	389288
fig|1504.6.peg.2549	CDS	node_148_[4]	389462	390178	717	Phosphate regulon transcriptional regulatory protein PhoB (SphR)	High affinity phosphate transporter and control of PHO regulon, PhoR-PhoB two-component regulatory system, Phosphate metabolism	389462	390178
fig|1504.6.peg.2550	CDS	node_148_[4]	390168	391727	1560	sensor histidine kinase	- none -	390168	391727

Feature ID	Type	Contig	Start	Stop	Length (bp)	Function	Subsystems	Begin	End
fig|1504.6.peg.2551	CDS	node_148_[4]	391807	392748	942	Lyzozyme M1 (1,4-beta-N-acetylmuramidase) (EC 3.2.1.17)	- none -	391807	392748
fig|1504.6.peg.2552	CDS	node_148_[4]	392966	394375	1410	Vancomycin B-type resistance protein VanW	Resistance to Vancomycin	392966	394375
fig|1504.6.peg.2553	CDS	node_148_[4]	394553	395392	840	FIG00515414: hypothetical protein	- none -	394553	395392
fig|1504.6.peg.2554	CDS	node_148_[4]	395444	396451	1008	Spore photoproduct lyase (EC 4.1.99.-)	- none -	395444	396451
fig|1504.6.peg.2555	CDS	node_148_[4]	396577	397038	462	tRNA (cytidine(34)-2'-O)-methyltransferase (EC 2.1.1.207)	RNA methylation	396577	397038
fig|1504.6.peg.2556	CDS	node_148_[4]	397059	397895	837	DegV family protein	- none -	397059	397895
fig|1504.6.peg.2557	CDS	node_148_[4]	398136	403139	5004	Beta-galactosidase (EC 3.2.1.23)	Galactosylceramide and Sulfatide metabolism, Lactose and Galactose Uptake and Utilization, Lactose utilization	398136	403139
fig|1504.6.peg.2558	CDS	node_148_[4]	403360	404736	1377	RNA polymerase sigma-54 factor RpoN	Flagellar motility, Flagellum, Transcription initiation, bacterial sigma factors	403360	404736
fig|1504.6.peg.2559	CDS	node_148_[4]	404931	405971	1041	Central glycolytic genes regulator	- none -	404931	405971
fig|1504.6.peg.2560	CDS	node_148_[4]	406023	407021	999	NAD-dependent glyceraldehyde-3-phosphate dehydrogenase (EC 1.2.1.12)	Entner-Doudoroff Pathway, Glycolysis and Gluconeogenesis, Pyridoxin (Vitamin B6) Biosynthesis, Redox-dependent regulation of nucleus processes	406023	407021
fig|1504.6.peg.2561	CDS	node_148_[4]	407236	408411	1176	Phosphoglycerate kinase (EC 2.7.2.3)	Entner-Doudoroff Pathway, Glycolysis and Gluconeogenesis	407236	408411
fig|1504.6.peg.2562	CDS	node_148_[4]	408493	409239	747	Triosephosphate isomerase (EC 5.3.1.1)	CBSS-331978.3.peg.2915, Glycolysis and Gluconeogenesis	408493	409239
fig|1504.6.peg.2563	CDS	node_148_[4]	409414	410643	1230	hypothetical protein	- none -	409414	410643
fig|1504.6.peg.2564	CDS	node_148_[4]	410658	410849	192	hypothetical protein	- none -	410658	410849

Feature ID	Type	Contig	Start	Stop	Length (bp)	Function	Subsystems	Begin	End
fig|1504.6.peg.2565	CDS	node_148_[4]	411131	412669	1539	2,3-bisphosphoglycerate-independent phosphoglycerate mutase (EC 5.4.2.1)	Entner-Doudoroff Pathway, Glycolysis and Gluconeogenesis, Phosphoglycerate mutase protein family	411131	412669
fig|1504.6.peg.2566	CDS	node_148_[4]	412815	413681	867	DegV family protein	- none -	412815	413681
fig|1504.6.peg.2567	CDS	node_148_[4]	413978	414808	831	4-deoxy-L-threo-5-hexosulose-uronate ketol-isomerase (EC 5.3.1.17)	- none -	413978	414808
fig|1504.6.peg.2568	CDS	node_148_[4]	414822	416012	1191	Unsaturated glucuronyl hydrolase (EC 3.2.1.-)	- none -	414822	416012
fig|1504.6.peg.2569	CDS	node_148_[4]	416028	416522	495	PTS system, hyaluronate-oligosaccharide-specific IIB component (EC 2.7.1.69)	- none -	416028	416522
fig|1504.6.peg.2570	CDS	node_148_[4]	416609	417406	798	PTS system, hyaluronate-oligosaccharide-specific IIC component (EC 2.7.1.69)	- none -	416609	417406
fig|1504.6.peg.2571	CDS	node_148_[4]	417396	418208	813	PTS system, hyaluronate-oligosaccharide-specific IID component (EC 2.7.1.69)	- none -	417396	418208
fig|1504.6.peg.2572	CDS	node_148_[4]	418326	418739	414	PTS system, N-acetylgalactosamine- and galactosamine-specific IIA component (EC 2.7.1.69)	N-Acetyl-Galactosamine and Galactosamine Utilization	418326	418739
fig|1504.6.peg.2573	CDS	node_148_[4]	418744	419019	276	Preprotein translocase subunit YajC (TC 3.A.5.1.1)	CBSS-211586.1.peg.2832	418744	419019
fig|1504.6.peg.2574	CDS	node_148_[4]	419037	419816	780	2-deoxy-D-gluconate 3-dehydrogenase (EC 1.1.1.125)	- none -	419037	419816
fig|1504.6.peg.2575	CDS	node_148_[4]	419813	420445	633	4-Hydroxy-2-oxoglutarate aldolase (EC 4.1.3.16) @ 2-dehydro-3-deoxyphosphogluconate aldolase (EC 4.1.2.14)	Entner-Doudoroff Pathway	419813	420445
fig|1504.6.peg.2576	CDS	node_148_[4]	420457	421473	1017	2-dehydro-3-deoxygluconate kinase (EC 2.7.1.45)	Entner-Doudoroff Pathway	420457	421473
fig|1504.6.peg.2577	CDS	node_148_[4]	421547	423568	2022	Heparinase II/III-like	CBSS-366602.3.peg.5141	421547	423568
fig|1504.6.peg.2578	CDS	node_148_[4]	423608	424654	1047	Transcriptional regulator RegR, rpressor of hyaluronate and KDG utilization	- none -	423608	424654
fig|1504.6.peg.2579	CDS	node_148_[4]	424783	425373	591	Serine/threonine kinase	- none -	424783	425373
fig|1504.6.peg.2580	CDS	node_148_[4]	425504	426733	1230	hypothetical protein	- none -	425504	426733
fig|1504.6.peg.2581	CDS	node_148_[4]	426748	426939	192	hypothetical protein	- none -	426748	426939

Feature ID	Type	Contig	Start	Stop	Length (bp)	Function	Subsystems	Begin	End
fig|1504.6.peg.2582	CDS	node_148_[4]	427550	428626	1077	ABC transporter, permease protein	- none -	427550	428626
fig|1504.6.peg.2583	CDS	node_148_[4]	428631	429944	1314	Cell division protein FtsX	Bacterial Cell Division, CBSS-393121.3.peg.2760	428631	429944
fig|1504.6.peg.2584	CDS	node_148_[4]	429941	430606	666	ABC transporter, ATP-binding protein	- none -	429941	430606
fig|1504.6.peg.2585	CDS	node_148_[4]	430790	432085	1296	Enolase (EC 4.2.1.11)	Entner-Doudoroff Pathway, Glycolysis and Gluconeogenesis, Serine-glyoxylate cycle	430790	432085
fig|1504.6.peg.2586	CDS	node_148_[4]	432386	432616	231	Preprotein translocase subunit SecG (TC 3.A.5.1.1)	CBSS-331978.3.peg.2915, Murein hydrolase regulation and cell death	432386	432616
fig|1504.6.peg.2587	CDS	node_148_[4]	432691	433068	378	DUF1696 domain-containing protein	- none -	432691	433068
fig|1504.6.peg.2588	CDS	node_148_[4]	433243	435516	2274	3'-to-5' exoribonuclease RNase R	RNA processing and degradation, bacterial	433243	435516
fig|1504.6.peg.2589	CDS	node_148_[4]	435595	436065	471	tmRNA-binding protein SmpB	Heat shock dnaK gene cluster extended, Translation termination factors bacterial	435595	436065
fig|1504.6.peg.2590	CDS	node_148_[4]	436187	438097	1911	GAF modulated sigma54 specific transcriptional regulator, Fis family	- none -	436187	438097
fig|1504.6.peg.2591	CDS	node_148_[4]	438316	439482	1167	Alcohol dehydrogenase (EC 1.1.1.1); Acetaldehyde dehydrogenase (EC 1.2.1.10)	5-FCL-like protein, Butanol Biosynthesis, Butanol Biosynthesis, Fermentations: Lactate, Fermentations: Mixed acid, Fermentations: Mixed acid, Glycerolipid and Glycerophospholipid Metabolism in Bacteria, Pyruvate metabolism II: acetyl-CoA, acetogenesis from pyruvate	438316	439482
fig|1504.6.peg.2592	CDS	node_148_[4]	439719	440606	888	2-polyprenylphenol hydroxylase and related flavodoxin oxidoreductases	- none -	439719	440606
fig|1504.6.peg.2593	CDS	node_148_[4]	440606	441997	1392	Glutamate synthase [NADPH] large chain (EC 1.4.1.13)	Ammonia assimilation, Glutamine, Glutamate, Aspartate and Asparagine Biosynthesis	440606	441997

Feature ID	Type	Contig	Start	Stop	Length (bp)	Function	Subsystems	Begin	End
fig|1504.6.peg.2594	CDS	node_148_[4]	442250	444778	2529	Beta-hexosaminidase (EC 3.2.1.52)	Chitin and N-acetylglucosamine utilization, N-Acetyl-Galactosamine and Galactosamine Utilization	442250	444778
fig|1504.6.peg.2595	CDS	node_148_[4]	444924	445319	396	Nitrite-sensitive transcriptional repressor NsrR	Nitrosative stress, Oxidative stress, Rrf2 family transcriptional regulators	444924	445319
fig|1504.6.peg.2596	CDS	node_148_[5]	863	450	414	Nitrite reductase probable electron transfer 4Fe-S subunit (EC 1.7.1.4)	Nitrate and nitrite ammonification	450	863
fig|1504.6.peg.2597	CDS	node_148_[5]	2954	876	2079	Assimilatory nitrate reductase large subunit (EC:1.7.99.4)	Nitrate and nitrite ammonification	876	2954
fig|1504.6.peg.2598	CDS	node_148_[5]	3575	3348	228	hypothetical protein	- none -	3348	3575
fig|1504.6.peg.2599	CDS	node_148_[5]	3823	3662	162	hypothetical protein	- none -	3662	3823
fig|1504.6.peg.2600	CDS	node_148_[5]	4081	5640	1560	Mobile element protein	- none -	4081	5640
fig|1504.6.peg.2601	CDS	node_148_[5]	6047	5856	192	hypothetical protein	- none -	5856	6047
fig|1504.6.peg.2602	CDS	node_148_[5]	7291	6062	1230	Repeated DNA sequence	- none -	6062	7291
fig|1504.6.peg.2603	CDS	node_148_[5]	8027	7479	549	hypothetical protein	- none -	7479	8027
fig|1504.6.peg.2604	CDS	node_148_[5]	9057	8116	942	Conserved protein	- none -	8116	9057
fig|1504.6.peg.2605	CDS	node_148_[5]	9504	9175	330	hypothetical protein	- none -	9175	9504
fig|1504.6.peg.2606	CDS	node_148_[5]	9701	10651	951	L-lactate dehydrogenase (EC 1.1.1.27)	Fermentations: Lactate, Fermentations: Mixed acid	9701	10651
fig|1504.6.peg.2607	CDS	node_148_[5]	13271	10677	2595	ATP-dependent DNA helicase UvrD/PcrA, clostridial paralog	DNA repair, bacterial UvrD and related helicases	10677	13271
fig|1504.6.peg.2608	CDS	node_148_[5]	14401	13502	900	3'->5' exoribonuclease Bsu YhaM	Rad50-Mre11 DNA repair cluster, Ribonucleases in Bacillus	13502	14401
fig|1504.6.peg.2609	CDS	node_148_[5]	15303	14470	834	Pyridoxal kinase (EC 2.7.1.35)	Pyridoxin (Vitamin B6) Biosynthesis	14470	15303
fig|1504.6.peg.2610	CDS	node_148_[5]	15840	15322	519	Substrate-specific component PdxU2 of predicted pyridoxin-related ECF transporter	ECF class transporters	15322	15840
fig|1504.6.peg.2611	CDS	node_148_[5]	16540	16929	390	Transcriptional regulator, PadR family	CBSS-1352.1.peg.856	16540	16929
fig|1504.6.peg.2612	CDS	node_148_[5]	17941	16922	1020	Phosphate ABC transporter, permease protein PstC	- none -	16922	17941

Feature ID	Type	Contig	Start	Stop	Length (bp)	Function	Subsystems	Begin	End
fig|1504.6.peg.2613	CDS	node_148_[5]	18818	17922	897	ABC transporter, ATP-binding protein	- none -	17922	18818
fig|1504.6.peg.2614	CDS	node_148_[5]	19202	18819	384	Transcriptional regulator, GntR family	- none -	18819	19202
fig|1504.6.peg.2615	CDS	node_148_[5]	19834	19199	636	hypothetical protein	- none -	19199	19834
fig|1504.6.peg.2616	CDS	node_148_[5]	20643	19999	645	putative lipoprotein	- none -	19999	20643
fig|1504.6.peg.2617	CDS	node_148_[5]	20832	21290	459	hypothetical protein	- none -	20832	21290
fig|1504.6.peg.2618	CDS	node_148_[5]	21881	21333	549	no significant homology	- none -	21333	21881
fig|1504.6.peg.2619	CDS	node_148_[5]	22086	21901	186	hypothetical protein	- none -	21901	22086
fig|1504.6.peg.2620	CDS	node_148_[5]	22782	22198	585	hypothetical protein	- none -	22198	22782
fig|1504.6.peg.2621	CDS	node_148_[5]	24409	22847	1563	Voltage-gated chloride channel family protein	- none -	22847	24409
fig|1504.6.peg.2622	CDS	node_148_[5]	25110	24559	552	Transcriptional regulator, TetR family	- none -	24559	25110
fig|1504.6.peg.2623	CDS	node_148_[5]	25293	25652	360	hypothetical protein	- none -	25293	25652
fig|1504.6.peg.2624	CDS	node_148_[5]	26372	26923	552	Maltose O-acetyltransferase (EC 2.3.1.79)	Maltose and Maltodextrin Utilization	26372	26923
fig|1504.6.peg.2625	CDS	node_148_[5]	27394	27056	339	hypothetical protein	- none -	27056	27394
fig|1504.6.peg.2626	CDS	node_148_[5]	28076	29296	1221	Transposase, mutator type	- none -	28076	29296
fig|1504.6.peg.2627	CDS	node_148_[5]	29909	29742	168	hypothetical protein	- none -	29742	29909
fig|1504.6.peg.2628	CDS	node_148_[5]	30112	29954	159	hypothetical protein	- none -	29954	30112
fig|1504.6.peg.2629	CDS	node_148_[5]	30687	30514	174	hypothetical protein	- none -	30514	30687
fig|1504.6.peg.2630	CDS	node_148_[5]	31453	31157	297	N-acetylmuramoyl-L-alanine amidase (EC 3.5.1.28)	Murein Hydrolases, Recycling of Peptidoglycan Amino Acids	31157	31453
fig|1504.6.peg.2631	CDS	node_148_[5]	31849	31580	270	N-acetylmuramoyl-L-alanine amidase (EC 3.5.1.28)	Murein Hydrolases, Recycling of Peptidoglycan Amino Acids	31580	31849
fig|1504.6.peg.2632	CDS	node_148_[5]	32152	32036	117	hypothetical protein	- none -	32036	32152
fig|1504.6.peg.2633	CDS	node_148_[5]	32896	32405	492	Fragment flavodoxin oxidoreductase	- none -	32405	32896
fig|1504.6.peg.2634	CDS	node_148_[5]	32906	33181	276	Transcriptional regulator (phage-related) (Xre family)	- none -	32906	33181
fig|1504.6.peg.2635	CDS	node_148_[5]	33632	33258	375	Phage protein	- none -	33258	33632
fig|1504.6.peg.2636	CDS	node_148_[5]	34656	33583	1074	hypothetical protein	- none -	33583	34656

Feature ID	Type	Contig	Start	Stop	Length (bp)	Function	Subsystems	Begin	End
fig|1504.6.peg.2637	CDS	node_148_[5]	35018	34677	342	hypothetical protein	- none -	34677	35018
fig|1504.6.peg.2638	CDS	node_148_[5]	37024	36353	672	Polypeptide composition of the spore coat protein CotJC	- none -	36353	37024
fig|1504.6.peg.2639	CDS	node_148_[5]	37210	37395	186	hypothetical protein	- none -	37210	37395
fig|1504.6.peg.2640	CDS	node_148_[5]	37408	37659	252	Spore coat protein F	- none -	37408	37659
fig|1504.6.peg.2641	CDS	node_148_[5]	38120	37821	300	Spore coat protein F (CotF) family protein	- none -	37821	38120
fig|1504.6.peg.2642	CDS	node_148_[5]	38339	38142	198	FIG00518168: hypothetical protein	- none -	38142	38339
fig|1504.6.peg.2643	CDS	node_148_[5]	38707	38573	135	hypothetical protein	- none -	38573	38707
fig|1504.6.peg.2644	CDS	node_148_[5]	39088	38879	210	Small acid-soluble spore protein, alpha-type SASP	Small acid-soluble spore proteins	38879	39088
fig|1504.6.peg.2645	CDS	node_148_[5]	40671	39694	978	N-acetylmuramoyl-L-alanine amidase (EC 3.5.1.28)	Murein Hydrolases, Recycling of Peptidoglycan Amino Acids	39694	40671
fig|1504.6.peg.2646	CDS	node_148_[5]	41146	40721	426	toxin secretion/phage lysis holin	- none -	40721	41146
fig|1504.6.peg.2647	CDS	node_148_[5]	44647	41318	3330	hypothetical protein	- none -	41318	44647
fig|1504.6.peg.2648	CDS	node_148_[5]	45209	44832	378	Hypothetical protein, CF-35 family	- none -	44832	45209
fig|1504.6.peg.2649	CDS	node_148_[5]	45444	45196	249	hypothetical protein	- none -	45196	45444
fig|1504.6.peg.2650	CDS	node_148_[5]	45801	45457	345	hypothetical protein	- none -	45457	45801
fig|1504.6.peg.2651	CDS	node_148_[5]	49908	45817	4092	Phage tail length tape-measure protein	Phage tail proteins, Phage tail proteins 2	45817	49908
fig|1504.6.peg.2652	CDS	node_148_[5]	50207	49905	303	hypothetical protein	- none -	49905	50207
fig|1504.6.peg.2653	CDS	node_148_[5]	50734	50339	396	hypothetical protein	- none -	50339	50734
fig|1504.6.peg.2654	CDS	node_148_[5]	51219	50812	408	putative major tail protein	- none -	50812	51219
fig|1504.6.peg.2655	CDS	node_148_[5]	51593	51237	357	hypothetical protein	- none -	51237	51593
fig|1504.6.peg.2656	CDS	node_148_[5]	52063	51590	474	hypothetical protein	- none -	51590	52063
fig|1504.6.peg.2657	CDS	node_148_[5]	52380	52066	315	hypothetical protein	- none -	52066	52380
fig|1504.6.peg.2658	CDS	node_148_[5]	52699	52364	336	hypothetical protein	- none -	52364	52699
fig|1504.6.peg.2659	CDS	node_148_[5]	53616	52711	906	Phage tail fiber protein	Phage tail fiber proteins	52711	53616
fig|1504.6.peg.2660	CDS	node_148_[5]	54288	53641	648	Phage capsid and scaffold	Phage capsid proteins	53641	54288

Feature ID	Type	Contig	Start	Stop	Length (bp)	Function	Subsystems	Begin	End
fig|1504.6.peg.2661	CDS	node_148_[5]	54660	54397	264	FIG00630947: hypothetical protein	- none -	54397	54660
fig|1504.6.peg.2662	CDS	node_148_[5]	55253	54906	348	hypothetical protein	- none -	54906	55253
fig|1504.6.peg.2663	CDS	node_148_[5]	56935	55259	1677	Phage protein	- none -	55259	56935
fig|1504.6.peg.2664	CDS	node_148_[5]	58364	56973	1392	Phage portal protein	Phage packaging machinery	56973	58364
fig|1504.6.peg.2665	CDS	node_148_[5]	59809	58526	1284	Terminase large subunit [Bacteriophage A118]	- none -	58526	59809
fig|1504.6.peg.2666	CDS	node_148_[5]	60524	59802	723	FIG00523812: hypothetical protein	- none -	59802	60524
fig|1504.6.peg.2667	CDS	node_148_[5]	61169	60555	615	Site-specific recombinase, DNA invertase Pin related protein	- none -	60555	61169
fig|1504.6.peg.2668	CDS	node_148_[5]	62292	61648	645	site-specific recombinase, phage integrase family	- none -	61648	62292
fig|1504.6.peg.2669	CDS	node_148_[5]	62777	62421	357	hypothetical protein	- none -	62421	62777
fig|1504.6.peg.2670	CDS	node_148_[5]	63261	63028	234	FIG003307: hypothetical protein	CBSS-323097.3.peg.2594	63028	63261
fig|1504.6.peg.2671	CDS	node_148_[5]	63906	63313	594	Phage protein	- none -	63313	63906
fig|1504.6.peg.2672	CDS	node_148_[5]	64144	63911	234	Phage protein	- none -	63911	64144
fig|1504.6.peg.2673	CDS	node_148_[5]	64333	64166	168	hypothetical protein	- none -	64166	64333
fig|1504.6.peg.2674	CDS	node_148_[5]	66076	64931	1146	Protein export cytoplasm protein SecA ATPase RNA helicase (TC 3.A.5.1.1)	CBSS-393121.3.peg.2760	64931	66076
fig|1504.6.peg.2675	CDS	node_148_[5]	66872	66069	804	Phage protein	- none -	66069	66872
fig|1504.6.peg.2676	CDS	node_148_[5]	67283	67116	168	hypothetical protein	- none -	67116	67283
fig|1504.6.peg.2677	CDS	node_148_[5]	67411	67256	156	hypothetical protein	- none -	67256	67411
fig|1504.6.peg.2678	CDS	node_148_[5]	67813	67574	240	hypothetical protein	- none -	67574	67813
fig|1504.6.peg.2679	CDS	node_148_[5]	67899	68453	555	hypothetical protein	- none -	67899	68453
fig|1504.6.peg.2680	CDS	node_148_[5]	68758	68546	213	hypothetical protein	- none -	68546	68758
fig|1504.6.peg.2681	CDS	node_148_[5]	69012	68854	159	hypothetical protein	- none -	68854	69012
fig|1504.6.peg.2682	CDS	node_148_[5]	69292	69149	144	hypothetical protein	- none -	69149	69292
fig|1504.6.peg.2683	CDS	node_148_[5]	69425	69817	393	Transcriptional regulator, Cro/CI family	- none -	69425	69817
fig|1504.6.peg.2684	CDS	node_148_[5]	69966	69826	141	hypothetical protein	- none -	69826	69966

Feature ID	Type	Contig	Start	Stop	Length (bp)	Function	Subsystems	Begin	End
fig|1504.6.peg.2685	CDS	node_148_[5]	70290	70102	189	hypothetical protein	- none -	70102	70290
fig|1504.6.peg.2686	CDS	node_148_[5]	70452	72161	1710	Site-specific recombinases, DNA invertase Pin homolog	- none -	70452	72161
fig|1504.6.peg.2687	CDS	node_148_[5]	72932	72138	795	Fragment flavodoxin oxidoreductase	- none -	72138	72932
fig|1504.6.peg.2688	CDS	node_148_[5]	73921	72929	993	Electron transfer subunit protein	- none -	72929	73921
fig|1504.6.peg.2689	CDS	node_148_[5]	75235	74066	1170	D-alanyl-D-alanine carboxypeptidase (EC 3.4.16.4)	CBSS-84588.1.peg.1247, Metallocarboxypeptidases (EC 3.4.17.-), Murein Hydrolases	74066	75235
fig|1504.6.peg.2690	CDS	node_148_[5]	75374	75952	579	hypothetical protein	- none -	75374	75952
fig|1504.6.peg.2691	CDS	node_148_[5]	75962	76471	510	Sporulation protein YtfJ	- none -	75962	76471
fig|1504.6.peg.2692	CDS	node_148_[5]	76575	76892	318	Mobile element protein	- none -	76575	76892
fig|1504.6.peg.2693	CDS	node_148_[6]	217	1665	1449	hypothetical protein	- none -	217	1665
fig|1504.6.peg.2694	CDS	node_148_[6]	1702	1935	234	Hypothetical protein, CF-8 family	- none -	1702	1935
fig|1504.6.peg.2695	CDS	node_148_[6]	1951	2232	282	hypothetical protein	- none -	1951	2232
fig|1504.6.peg.2696	CDS	node_148_[6]	2302	3351	1050	N-acetylmuramoyl-L-alanine amidase (EC 3.5.1.28)	Murein Hydrolases, Recycling of Peptidoglycan Amino Acids	2302	3351
fig|1504.6.peg.2697	CDS	node_148_[6]	3602	4699	1098	hypothetical protein	- none -	3602	4699
fig|1504.6.peg.2698	CDS	node_148_[6]	4706	6247	1542	DNA double-strand break repair Rad50 ATPase	Rad50-Mre11 DNA repair cluster	4706	6247
fig|1504.6.peg.2699	CDS	node_148_[6]	6248	6607	360	hypothetical protein	- none -	6248	6607
fig|1504.6.peg.2700	CDS	node_148_[6]	6612	7346	735	Transcriptional regulator, HTH_3 family	- none -	6612	7346
fig|1504.6.peg.2701	CDS	node_148_[6]	7340	7951	612	hypothetical protein	- none -	7340	7951
fig|1504.6.peg.2702	CDS	node_148_[6]	8350	9570	1221	Transposase, mutator type	- none -	8350	9570
fig|1504.6.peg.2703	CDS	node_148_[6]	10010	9843	168	hypothetical protein	- none -	9843	10010
fig|1504.6.peg.2704	CDS	node_148_[6]	10162	10815	654	hypothetical protein	- none -	10162	10815
fig|1504.6.peg.2705	CDS	node_148_[6]	10884	11639	756	modification methylase dpniia, putative	- none -	10884	11639
fig|1504.6.peg.2706	CDS	node_148_[6]	12182	12799	618	FIG00531946: hypothetical protein	- none -	12182	12799
fig|1504.6.peg.2707	CDS	node_148_[6]	12911	13561	651	hypothetical protein	- none -	12911	13561

Feature ID	Type	Contig	Start	Stop	Length (bp)	Function	Subsystems	Begin	End
fig|1504.6.peg.2708	CDS	node_148_[6]	13756	14412	657	tRNA (guanine46-N7-)-methyltransferase (EC 2.1.1.33)	RNA methylation	13756	14412
fig|1504.6.peg.2709	CDS	node_148_[6]	15242	14466	777	Metal transporter, ZIP family	- none -	14466	15242
fig|1504.6.peg.2710	CDS	node_148_[6]	15472	16293	822	Esterase/lipase/thioesterase family protein	- none -	15472	16293
fig|1504.6.peg.2711	CDS	node_148_[6]	16340	17314	975	membrane protein	- none -	16340	17314
fig|1504.6.peg.2712	CDS	node_148_[6]	17560	18102	543	Substrate-specific component NiaX of predicted niacin ECF transporter	ECF class transporters, NAD and NADP cofactor biosynthesis global	17560	18102
fig|1504.6.peg.2713	CDS	node_148_[6]	18233	18790	558	Glycerol uptake operon antiterminator regulatory protein	- none -	18233	18790
fig|1504.6.peg.2714	CDS	node_148_[6]	18856	19224	369	Methylglyoxal synthase (EC 4.2.3.3)	Methylglyoxal Metabolism	18856	19224
fig|1504.6.peg.2715	CDS	node_148_[6]	19542	20003	462	hypothetical protein	- none -	19542	20003
fig|1504.6.peg.2716	CDS	node_148_[6]	20233	20502	270	ACT domain protein	- none -	20233	20502
fig|1504.6.peg.2717	CDS	node_148_[6]	20517	21872	1356	FIG00518792: hypothetical protein	- none -	20517	21872
fig|1504.6.peg.2718	CDS	node_148_[6]	22531	21905	627	Transcriptional regulator, GntR family	- none -	21905	22531
fig|1504.6.peg.2719	CDS	node_148_[6]	22905	24446	1542	Glycine betaine transporter OpuD	Choline and Betaine Uptake and Betaine Biosynthesis	22905	24446
fig|1504.6.peg.2720	CDS	node_148_[6]	24506	26782	2277	ATP-dependent DNA helicase, UvrD/REP family	- none -	24506	26782
fig|1504.6.peg.2721	CDS	node_148_[6]	26979	28151	1173	Probable flavoprotein	- none -	26979	28151
fig|1504.6.peg.2722	CDS	node_148_[6]	28359	29321	963	Inner membrane protein YrbG, predicted calcium/sodium:proton antiporter	- none -	28359	29321
fig|1504.6.peg.2723	CDS	node_148_[6]	29418	29552	135	hypothetical protein	- none -	29418	29552
fig|1504.6.peg.2724	CDS	node_148_[6]	29953	30090	138	hypothetical protein	- none -	29953	30090
fig|1504.6.peg.2725	CDS	node_148_[6]	30246	31859	1614	conserved protein (pathogens)	- none -	30246	31859
fig|1504.6.peg.2726	CDS	node_148_[6]	32429	31911	519	Cell surface protein, ErfK family	- none -	31911	32429
fig|1504.6.peg.2727	CDS	node_148_[6]	34552	32537	2016	Thymidylate kinase (EC 2.7.4.9)	CBSS-393133.3.peg.2787, pyrimidine conversions	32537	34552
fig|1504.6.peg.2728	CDS	node_148_[6]	35329	34706	624	putative sporulation protein YtaF	- none -	34706	35329
fig|1504.6.peg.2729	CDS	node_148_[6]	36282	35413	870	Cobalt-zinc-cadmium resistance protein	Cobalt-zinc-cadmium resistance	35413	36282

Feature ID	Type	Contig	Start	Stop	Length (bp)	Function	Subsystems	Begin	End
fig|1504.6.peg.2730	CDS	node_148_[6]	36527	36850	324	hypothetical protein	- none -	36527	36850
fig|1504.6.peg.2731	CDS	node_148_[6]	36990	37262	273	conserved hypothetical protein	- none -	36990	37262
fig|1504.6.peg.2732	CDS	node_148_[6]	37280	37675	396	hypothetical protein	- none -	37280	37675
fig|1504.6.peg.2733	CDS	node_148_[6]	38272	38069	204	hypothetical protein	- none -	38069	38272
fig|1504.6.peg.2734	CDS	node_148_[6]	38580	38783	204	Ortholog of S. aureus MRSA252 (BX571856) SAR1351	- none -	38580	38783
fig|1504.6.peg.2735	CDS	node_148_[6]	38798	39706	909	HPr kinase/phosphorylase (EC 2.7.1.-) (EC 2.7.4.-)	HPr catabolite repression system	38798	39706
fig|1504.6.peg.2736	CDS	node_148_[6]	39742	41133	1392	Probable M18-family aminopeptidase 1 (EC 3.4.11.-)	- none -	39742	41133
fig|1504.6.peg.2737	CDS	node_148_[6]	41221	41490	270	FIG00519079: hypothetical protein	- none -	41221	41490
fig|1504.6.peg.2738	CDS	node_148_[6]	42360	41533	828	COG0613, Predicted metal-dependent phosphoesterases (PHP family)	CBSS-314276.3.peg.1499	41533	42360
fig|1504.6.peg.2739	CDS	node_148_[6]	42511	43101	591	Para-aminobenzoate synthase, amidotransferase component (EC 2.6.1.85)	Chorismate: Intermediate for synthesis of Tryptophan, PAPA antibiotics, PABA, 3-hydroxyanthranilate and more., Folate Biosynthesis	42511	43101
fig|1504.6.peg.2740	CDS	node_148_[6]	43102	44457	1356	Para-aminobenzoate synthase, aminase component (EC 2.6.1.85)	Chorismate: Intermediate for synthesis of Tryptophan, PAPA antibiotics, PABA, 3-hydroxyanthranilate and more., Folate Biosynthesis	43102	44457
fig|1504.6.peg.2741	CDS	node_148_[6]	44457	45212	756	Aminodeoxychorismate lyase (EC 4.1.3.38)	Chorismate: Intermediate for synthesis of Tryptophan, PAPA antibiotics, PABA, 3-hydroxyanthranilate and more., Folate Biosynthesis	44457	45212
fig|1504.6.peg.2742	CDS	node_148_[6]	45212	45766	555	GTP cyclohydrolase I (EC 3.5.4.16) type 1	Folate Biosynthesis, Folate biosynthesis cluster, Molybdenum cofactor biosynthesis, Queuosine-Archaeosine Biosynthesis	45212	45766
fig|1504.6.peg.2743	CDS	node_148_[6]	45781	46254	474	Putative DHNTP pyrophosphatase	Folate Biosynthesis	45781	46254

Feature ID	Type	Contig	Start	Stop	Length (bp)	Function	Subsystems	Begin	End
fig|1504.6.peg.2744	CDS	node_148_[6]	46426	47619	1194	Acetate kinase (EC 2.7.2.1)	Ethanolamine utilization, Fermentations: Lactate, Fermentations: Mixed acid, Pyruvate metabolism II: acetyl-CoA, acetogenesis from pyruvate	46426	47619
fig|1504.6.peg.2745	CDS	node_148_[6]	47780	48826	1047	Galactose/methyl galactoside ABC transport system, D-galactose-binding periplasmic protein MglB (TC 3.A.1.2.3)	Lactose and Galactose Uptake and Utilization	47780	48826
fig|1504.6.peg.2746	CDS	node_148_[6]	48900	50399	1500	Galactose/methyl galactoside ABC transport system, ATP-binding protein MglA (EC 3.6.3.17)	Lactose and Galactose Uptake and Utilization	48900	50399
fig|1504.6.peg.2747	CDS	node_148_[6]	50415	51437	1023	Galactose/methyl galactoside ABC transport system, permease protein MglC (TC 3.A.1.2.3)	Lactose and Galactose Uptake and Utilization	50415	51437
fig|1504.6.peg.2748	CDS	node_148_[6]	51457	51603	147	hypothetical protein	- none -	51457	51603
fig|1504.6.peg.2749	CDS	node_148_[6]	51814	53424	1611	Two-component response regulator yesN, associated with MetSO reductase	- none -	51814	53424
fig|1504.6.peg.2750	CDS	node_148_[6]	53435	55243	1809	Two-component sensor kinase YesM (EC 2.7.3.-)	Fructooligosaccharides(FOS) and Raffinose Utilization	53435	55243
fig|1504.6.peg.2751	CDS	node_148_[6]	55243	56220	978	FIG00524186: hypothetical protein	- none -	55243	56220
fig|1504.6.peg.2752	CDS	node_148_[6]	56247	57287	1041	Galactose/methyl galactoside ABC transport system, D-galactose-binding periplasmic protein MglB (TC 3.A.1.2.3)	Lactose and Galactose Uptake and Utilization	56247	57287
fig|1504.6.peg.2753	CDS	node_148_[6]	57395	58147	753	FIG00589306: hypothetical protein	- none -	57395	58147
fig|1504.6.peg.2754	CDS	node_148_[6]	59633	58314	1320	Acetylornithine deacetylase (EC 3.5.1.16)	- none -	58314	59633
fig|1504.6.peg.2755	CDS	node_148_[6]	59832	60188	357	Dihydropyrimidinase (EC 3.5.2.2)	Hydantoin metabolism, Pyrimidine utilization	59832	60188
fig|1504.6.peg.2756	CDS	node_148_[6]	60270	61508	1239	Mobile element protein	- none -	60270	61508
fig|1504.6.peg.2757	CDS	node_148_[6]	61754	62746	993	Dihydropyrimidinase (EC 3.5.2.2)	Hydantoin metabolism, Pyrimidine utilization	61754	62746
fig|1504.6.peg.2758	CDS	node_148_[6]	62757	63215	459	glutathione-regulated potassium-efflux system protein	- none -	62757	63215
fig|1504.6.peg.2759	CDS	node_148_[6]	63244	64383	1140	Butyryl-CoA dehydrogenase (EC 1.3.99.2)	- none -	63244	64383

Feature ID	Type	Contig	Start	Stop	Length (bp)	Function	Subsystems	Begin	End
fig|1504.6.peg.2760	CDS	node_148_[6]	64436	65626	1191	L-carnitine dehydratase/bile acid-inducible protein F	- none -	64436	65626
fig|1504.6.peg.2761	CDS	node_148_[6]	65681	66130	450	3-aminobutyryl-CoA ammonia-lyase (EC 4.3.1.14)	- none -	65681	66130
fig|1504.6.peg.2762	CDS	node_148_[6]	66173	66565	393	3-aminobutyryl-CoA ammonia-lyase (EC 4.3.1.14)	- none -	66173	66565
fig|1504.6.peg.2763	CDS	node_148_[6]	66710	66883	174	hypothetical protein	- none -	66710	66883
fig|1504.6.peg.2764	CDS	node_148_[6]	67156	68409	1254	Pyridine nucleotide-disulphide oxidoreductase family protein	- none -	67156	68409
fig|1504.6.peg.2765	CDS	node_148_[6]	68409	69644	1236	Dihydropyrimidine dehydrogenase [NADP+] (EC 1.3.1.2)	Pyrimidine utilization	68409	69644
fig|1504.6.peg.2766	CDS	node_148_[6]	69769	70230	462	glutathione-regulated potassium-efflux system protein	- none -	69769	70230
fig|1504.6.peg.2767	CDS	node_148_[6]	70415	71146	732	N-acetylmannosaminyltransferase (EC 2.4.1.187)	Teichoic and lipoteichoic acids biosynthesis	70415	71146
fig|1504.6.peg.2768	CDS	node_148_[6]	71143	72678	1536	Membrane protein involved in the export of O-antigen, teichoic acid lipoteichoic acids	- none -	71143	72678
fig|1504.6.peg.2769	CDS	node_148_[6]	72687	73964	1278	TPR/glycosyl transferase domain protein	- none -	72687	73964
fig|1504.6.peg.2770	CDS	node_148_[6]	73971	75119	1149	Putative teichuronic acid biosynthesis glycosyl transferase TuaC	- none -	73971	75119
fig|1504.6.peg.2771	CDS	node_148_[6]	75132	75779	648	Formiminotetrahydrofolate cyclodeaminase (EC 4.3.1.4)	5-FCL-like protein, One-carbon metabolism by tetrahydropterines, Serine-glyoxylate cycle	75132	75779
fig|1504.6.peg.2772	CDS	node_148_[6]	76610	75822	789	Polysaccharide deacetylase	Polysaccharide deacetylases	75822	76610
fig|1504.6.peg.2773	CDS	node_148_[6]	76796	77893	1098	GTP-binding and nucleic acid-binding protein YchF	Universal GTPases	76796	77893
fig|1504.6.peg.2774	CDS	node_148_[6]	79390	77981	1410	Mobile element protein	- none -	77981	79390
fig|1504.6.peg.2775	CDS	node_148_[6]	79741	80169	429	Cell division protein MraZ	16S rRNA modification within P site of ribosome, Bacterial Cell Division, Bacterial Cytoskeleton	79741	80169
fig|1504.6.peg.2776	CDS	node_148_[6]	80181	81113	933	rRNA small subunit methyltransferase H	16S rRNA modification within P site of ribosome, Bacterial Cell Division	80181	81113

Feature ID	Type	Contig	Start	Stop	Length (bp)	Function	Subsystems	Begin	End
fig|1504.6.peg.2777	CDS	node_148_[6]	81148	81648	501	Cell division protein FtsL	16S rRNA modification within P site of ribosome, Bacterial Cell Division, Bacterial Cytoskeleton, Stationary phase repair cluster	81148	81648
fig|1504.6.peg.2778	CDS	node_148_[6]	81689	83884	2196	Cell division protein FtsI [Peptidoglycan synthetase] (EC 2.4.1.129)	16S rRNA modification within P site of ribosome, Bacterial Cell Division, Bacterial Cytoskeleton, CBSS-83331.1.peg.3039, Flagellum in Campylobacter	81689	83884
fig|1504.6.peg.2779	CDS	node_148_[6]	83991	85433	1443	UDP-N-acetylmuramoylalanyl-D-glutamate--2,6-diaminopimelate ligase (EC 6.3.2.13)	Peptidoglycan biosynthesis--gjo	83991	85433
fig|1504.6.peg.2780	CDS	node_148_[6]	85449	86813	1365	UDP-N-acetylmuramoylalanyl-D-glutamyl-2,6-diaminopimelate--D-alanyl-D-alanine ligase (EC 6.3.2.10)	Peptidoglycan biosynthesis--gjo	85449	86813
fig|1504.6.peg.2781	CDS	node_148_[6]	86849	87823	975	Phospho-N-acetylmuramoyl-pentapeptide-transferase (EC 2.7.8.13)	- none -	86849	87823
fig|1504.6.peg.2782	CDS	node_148_[6]	87848	88978	1131	Cell division protein FtsW	Bacterial Cell Division, Bacterial Cytoskeleton, cell division cluster containing FtsQ	87848	88978
fig|1504.6.peg.2783	CDS	node_148_[6]	89100	89849	750	Cell division protein FtsQ	Bacterial Cell Division, Bacterial Cytoskeleton, CBSS-227882.1.peg.6980, cell division cluster containing FtsQ, cell division core of larger cluster	89100	89849
fig|1504.6.peg.2784	CDS	node_148_[6]	89863	90582	720	Division initiation protein	CBSS-227882.1.peg.6980	89863	90582
fig|1504.6.peg.2785	CDS	node_148_[6]	90595	90948	354	FIG025307: hypothetical protein	CBSS-227882.1.peg.6980	90595	90948
fig|1504.6.peg.2786	CDS	node_148_[6]	90945	91676	732	Division initiation protein	CBSS-227882.1.peg.6980	90945	91676
fig|1504.6.peg.2787	CDS	node_148_[6]	91756	92412	657	Hypothetical protein YggS, proline synthase co-transcribed bacterial homolog PROSC	A Hypothetical Protein Related to Proline Metabolism	91756	92412
fig|1504.6.peg.2788	CDS	node_148_[6]	92424	92870	447	FIG001960: FtsZ-interacting protein related to cell division	- none -	92424	92870
fig|1504.6.peg.2789	CDS	node_148_[6]	93146	93916	771	FIG001583: hypothetical protein, contains S4-like RNA binding domain	- none -	93146	93916

Feature ID	Type	Contig	Start	Stop	Length (bp)	Function	Subsystems	Begin	End
fig|1504.6.peg.2790	CDS	node_148_[6]	93936	94532	597	Cell division initiation protein DivIVA	Bacterial Cell Division, Bacterial Cytoskeleton	93936	94532
fig|1504.6.peg.2791	CDS	node_148_[6]	94661	95572	912	Ribosomal large subunit pseudouridine synthase D (EC 4.2.1.70)	RNA pseudouridine syntheses, Ribosome biogenesis bacterial	94661	95572
fig|1504.6.peg.2792	CDS	node_148_[6]	95586	96125	540	Uracil phosphoribosyltransferase (EC 2.4.2.9) / Pyrimidine operon regulatory protein PyrR	De Novo Pyrimidine Synthesis, De Novo Pyrimidine Synthesis, pyrimidine conversions	95586	96125
fig|1504.6.peg.2793	CDS	node_148_[6]	96149	97306	1158	FIG001721: Predicted N6-adenine-specific DNA methylase	- none -	96149	97306
fig|1504.6.peg.2794	CDS	node_148_[6]	99113	97362	1752	Fibronectin/fibrinogen-binding protein	- none -	97362	99113
fig|1504.6.peg.2795	CDS	node_148_[6]	99366	100349	984	hypothetical protein	- none -	99366	100349
fig|1504.6.peg.2796	CDS	node_148_[6]	100455	101846	1392	Type IV fimbrial assembly, ATPase PilB	- none -	100455	101846
fig|1504.6.peg.2797	CDS	node_148_[6]	101815	102870	1056	Late competence protein ComGB, access of DNA to ComEA	- none -	101815	102870
fig|1504.6.peg.2798	CDS	node_148_[6]	102867	103313	447	hypothetical protein	- none -	102867	103313
fig|1504.6.peg.2799	CDS	node_148_[6]	103325	103777	453	hypothetical protein	- none -	103325	103777
fig|1504.6.peg.2800	CDS	node_148_[6]	103734	104237	504	hypothetical protein	- none -	103734	104237
fig|1504.6.peg.2801	CDS	node_148_[6]	104228	104704	477	hypothetical protein	- none -	104228	104704
fig|1504.6.peg.2802	CDS	node_148_[6]	104727	105401	675	hypothetical protein	- none -	104727	105401
fig|1504.6.peg.2803	CDS	node_148_[6]	105352	105744	393	hypothetical protein	- none -	105352	105744
fig|1504.6.peg.2804	CDS	node_148_[6]	105818	106105	288	hypothetical protein	- none -	105818	106105
fig|1504.6.peg.2805	CDS	node_148_[6]	106269	106826	558	Translation elongation factor P	Translation elongation factors bacterial	106269	106826
fig|1504.6.peg.2806	CDS	node_148_[6]	106951	107313	363	hypothetical protein	- none -	106951	107313
fig|1504.6.peg.2807	CDS	node_148_[6]	107470	108393	924	Stage III sporulation protein AA	Sporulation Cluster III A, Sporulation gene orphans	107470	108393
fig|1504.6.peg.2808	CDS	node_148_[6]	108381	108899	519	Stage III sporulation protein AB	Sporulation Cluster III A, Sporulation gene orphans	108381	108899
fig|1504.6.peg.2809	CDS	node_148_[6]	108916	109113	198	Stage III sporulation protein AC	Sporulation Cluster III A, Sporulation gene orphans	108916	109113
fig|1504.6.peg.2810	CDS	node_148_[6]	109123	109506	384	Stage III sporulation protein AD	Sporulation Cluster III A, Sporulation gene orphans	109123	109506

Feature ID	Type	Contig	Start	Stop	Length (bp)	Function	Subsystems	Begin	End
fig|1504.6.peg.2811	CDS	node_148_[6]	109516	110760	1245	Stage III sporulation protein AE	SpoVS protein family, Sporulation-associated proteins with broader functions, Sporulation Cluster III A, Sporulation gene orphans	109516	110760
fig|1504.6.peg.2812	CDS	node_148_[6]	110764	111345	582	Stage III sporulation protein AF	Sporulation Cluster III A, Sporulation gene orphans	110764	111345
fig|1504.6.peg.2813	CDS	node_148_[6]	111356	111964	609	Stage III sporulation protein AG	Sporulation Cluster III A, Sporulation gene orphans	111356	111964
fig|1504.6.peg.2814	CDS	node_148_[6]	112003	112566	564	Stage III sporulation protein AH	Sporulation Cluster III A, Sporulation gene orphans	112003	112566
fig|1504.6.peg.2815	CDS	node_148_[6]	112656	113042	387	Alkaline shock protein	- none -	112656	113042
fig|1504.6.peg.2816	CDS	node_148_[6]	113167	113571	405	Transcription termination protein NusB	Riboflavin synthesis cluster, Transcription factors bacterial	113167	113571
fig|1504.6.peg.2817	CDS	node_148_[6]	113602	114450	849	Methylenetetrahydrofolate dehydrogenase (NADP+) (EC 1.5.1.5) / Methenyltetrahydrofolate cyclohydrolase (EC 3.5.4.9)	5-FCL-like protein, One-carbon metabolism by tetrahydropterines, One-carbon metabolism by tetrahydropterines, Serine-glyoxylate cycle, Serine-glyoxylate cycle	113602	114450
fig|1504.6.peg.2818	CDS	node_148_[6]	114440	115639	1200	Exodeoxyribonuclease VII large subunit (EC 3.1.11.6)	DNA repair, bacterial, Purine salvage cluster	114440	115639
fig|1504.6.peg.2819	CDS	node_148_[6]	115653	115874	222	Exodeoxyribonuclease VII small subunit (EC 3.1.11.6)	DNA repair, bacterial, Purine salvage cluster	115653	115874
fig|1504.6.peg.2820	CDS	node_148_[6]	115858	116733	876	Octaprenyl diphosphate synthase (EC 2.5.1.90) / Dimethylallyltransferase (EC 2.5.1.1) / (2E,6E)-farnesyl diphosphate synthase (EC 2.5.1.10) / Geranylgeranyl diphosphate synthase (EC 2.5.1.29)	Isoprenoid Biosynthesis, Isoprenoid Biosynthesis, Isoprenoid Biosynthesis: Interconversions, Isoprenoinds for Quinones, Isoprenoinds for Quinones, Isoprenoinds for Quinones, Isoprenoinds for Quinones, Polyprenyl Diphosphate Biosynthesis, Polyprenyl Diphosphate Biosynthesis, Polyprenyl Diphosphate Biosynthesis	115858	116733

Feature ID	Type	Contig	Start	Stop	Length (bp)	Function	Subsystems	Begin	End
fig|1504.6.peg.2821	CDS	node_148_[6]	116755	118608	1854	1-deoxy-D-xylulose 5-phosphate synthase (EC 2.2.1.7)	Isoprenoid Biosynthesis, Nonmevalonate Branch of Isoprenoid Biosynthesis, Pyridoxin (Vitamin B6) Biosynthesis, Thiamin biosynthesis	116755	118608
fig|1504.6.peg.2822	CDS	node_148_[6]	118625	119434	810	RNA binding methyltransferase FtsJ like	- none -	118625	119434
fig|1504.6.peg.2823	CDS	node_148_[6]	119571	120422	852	NAD kinase (EC 2.7.1.23)	NAD and NADP cofactor biosynthesis global	119571	120422
fig|1504.6.peg.2824	CDS	node_148_[6]	120424	120873	450	Arginine pathway regulatory protein ArgR, repressor of arg regulon	Arginine and Ornithine Degradation	120424	120873
fig|1504.6.peg.2825	CDS	node_148_[6]	120895	122595	1701	DNA repair protein RecN	DNA-replication, DNA repair, bacterial	120895	122595
fig|1504.6.peg.2826	CDS	node_148_[6]	122771	123961	1191	Stage IV sporulation protein B	Sporulation gene orphans	122771	123961
fig|1504.6.peg.2827	CDS	node_148_[6]	125643	124252	1392	Multiple sugar ABC transporter, substrate-binding protein	Fructooligosaccharides(FOS) and Raffinose Utilization	124252	125643
fig|1504.6.peg.2828	CDS	node_148_[6]	127710	126301	1410	Mobile element protein	- none -	126301	127710
fig|1504.6.peg.2829	CDS	node_148_[6]	128517	128633	117	hypothetical protein	- none -	128517	128633
fig|1504.6.peg.2830	CDS	node_148_[6]	129138	129944	807	Stage 0 sporulation two-component response regulator (Spo0A)	Sporulation gene orphans	129138	129944
fig|1504.6.peg.2831	CDS	node_148_[6]	130747	131184	438	hypothetical protein	- none -	130747	131184
fig|1504.6.peg.2832	CDS	node_148_[6]	131196	131714	519	ADP-ribose pyrophosphatase (EC 3.6.1.13)	CBSS-216591.1.peg.168, NAD and NADP cofactor biosynthesis global, Nudix proteins (nucleoside triphosphate hydrolases), Ribosome post-transcriptional modification and chromosomal segregation cluster	131196	131714
fig|1504.6.peg.2833	CDS	node_148_[6]	131872	132507	636	Stage II sporulation protein M (SpoIIM)	Sporulation gene orphans	131872	132507
fig|1504.6.peg.2834	CDS	node_148_[6]	132577	133455	879	Tyrosine recombinase XerD	- none -	132577	133455
fig|1504.6.peg.2835	CDS	node_148_[6]	133484	134668	1185	Phosphopentomutase (EC 5.4.2.7)	Deoxyribose and Deoxynucleoside Catabolism	133484	134668

Feature ID	Type	Contig	Start	Stop	Length (bp)	Function	Subsystems	Begin	End
fig|1504.6.peg.2836	CDS	node_148_[6]	134713	136017	1305	Pyrimidine-nucleoside phosphorylase (EC 2.4.2.2)	Deoxyribose and Deoxynucleoside Catabolism, pyrimidine conversions	134713	136017
fig|1504.6.peg.2837	CDS	node_148_[6]	136118	137371	1254	D-alanyl-D-alanine carboxypeptidase (EC 3.4.16.4)	CBSS-84588.1.peg.1247, Metallocarboxypeptidases (EC 3.4.17.-), Murein Hydrolases	136118	137371
fig|1504.6.peg.2838	CDS	node_148_[6]	137486	138229	744	Segregation and condensation protein A	CBSS-314276.3.peg.1499, Ribosome post-transcriptional modification and chromosomal segregation cluster	137486	138229
fig|1504.6.peg.2839	CDS	node_148_[6]	138222	138833	612	Segregation and condensation protein B	CBSS-314276.3.peg.1499, Ribosome post-transcriptional modification and chromosomal segregation cluster	138222	138833
fig|1504.6.peg.2840	CDS	node_148_[6]	139219	139019	201	Transposase, mutator type	- none -	139019	139219
fig|1504.6.peg.2841	CDS	node_148_[7]	522	1025	504	2',3'-cyclic-nucleotide 2'-phosphodiesterase (EC 3.1.4.16)	Purine conversions, pyrimidine conversions	522	1025
fig|1504.6.peg.2842	CDS	node_148_[7]	1103	1876	774	hypothetical protein	- none -	1103	1876
fig|1504.6.peg.2843	CDS	node_148_[7]	2795	2034	762	Hydrolase (HAD superfamily)	- none -	2034	2795
fig|1504.6.peg.2844	CDS	node_148_[7]	3367	2921	447	PTS system, fructose-specific IIA component (EC 2.7.1.69) / PTS system, fructose-specific IIB component (EC 2.7.1.69) / PTS system, fructose-specific IIC component (EC 2.7.1.69)	Fructose utilization, Fructose utilization, Fructose utilization	2921	3367
fig|1504.6.peg.2845	CDS	node_148_[7]	4837	3425	1413	PTS system, fructose-specific IIB component (EC 2.7.1.69)	Fructose utilization	3425	4837
fig|1504.6.peg.2846	CDS	node_148_[7]	6808	4859	1950	Transcriptional antiterminator of lichenan operon, BglG family	Beta-Glucoside Metabolism	4859	6808
fig|1504.6.peg.2847	CDS	node_148_[7]	7062	7271	210	hypothetical protein	- none -	7062	7271
fig|1504.6.peg.2848	CDS	node_148_[7]	7380	7538	159	hypothetical protein	- none -	7380	7538
fig|1504.6.peg.2849	CDS	node_148_[7]	7607	7765	159	hypothetical protein	- none -	7607	7765
fig|1504.6.peg.2850	CDS	node_148_[7]	9109	7874	1236	Sensor histidine kinase	- none -	7874	9109
fig|1504.6.peg.2851	CDS	node_148_[7]	11402	10002	1401	Glycolate dehydrogenase (EC 1.1.99.14), subunit GlcD	- none -	10002	11402

Feature ID	Type	Contig	Start	Stop	Length (bp)	Function	Subsystems	Begin	End
fig|1504.6.peg.2852	CDS	node_148_[7]	12595	11405	1191	Electron transfer flavoprotein, alpha subunit	- none -	11405	12595
fig|1504.6.peg.2853	CDS	node_148_[7]	13396	12608	789	Electron transfer flavoprotein, beta subunit	- none -	12608	13396
fig|1504.6.peg.2854	CDS	node_148_[7]	14946	13426	1521	L-lactate permease	- none -	13426	14946
fig|1504.6.peg.2855	CDS	node_148_[7]	16025	15336	690	Lactate-responsive regulator LldR in Firmicutes, GntR family	- none -	15336	16025
fig|1504.6.peg.2856	CDS	node_148_[7]	16527	17789	1263	Immunoglobulin G-endopeptidase (IdeS) / Mac/ Secreted immunoglobulin binding protein (Sib38)	- none -	16527	17789
fig|1504.6.peg.2857	CDS	node_148_[7]	17906	19162	1257	Immunoglobulin G-endopeptidase (IdeS) / Mac/ Secreted immunoglobulin binding protein (Sib38)	- none -	17906	19162
fig|1504.6.peg.2858	CDS	node_148_[7]	19751	20446	696	Immunoglobulin G-endopeptidase (IdeS) / Mac/ Secreted immunoglobulin binding protein (Sib38)	- none -	19751	20446
fig|1504.6.peg.2859	CDS	node_148_[7]	20575	21831	1257	Immunoglobulin G-endopeptidase (IdeS) / Mac/ Secreted immunoglobulin binding protein (Sib38)	- none -	20575	21831
fig|1504.6.peg.2860	CDS	node_148_[7]	30450	21943	8508	Cyclic beta-1,2-glucan synthase (EC 2.4.1.-)	Synthesis of osmoregulated periplasmic glucans	21943	30450
fig|1504.6.peg.2861	CDS	node_148_[7]	31379	30714	666	ABC transporter, ATP-binding protein	- none -	30714	31379
fig|1504.6.peg.2862	CDS	node_148_[7]	32578	31379	1200	permease domain-containing protein	- none -	31379	32578
fig|1504.6.peg.2863	CDS	node_148_[7]	33725	32592	1134	ABC transporter, permease protein	- none -	32592	33725
fig|1504.6.peg.2864	CDS	node_148_[7]	36827	35532	1296	Aspartyl aminopeptidase (EC 3.4.11.21)	- none -	35532	36827
fig|1504.6.peg.2865	CDS	node_148_[7]	37007	38185	1179	Cobalt-zinc-cadmium resistance protein	Cobalt-zinc-cadmium resistance	37007	38185
fig|1504.6.peg.2866	CDS	node_148_[7]	38449	39264	816	hypothetical protein	- none -	38449	39264
fig|1504.6.peg.2867	CDS	node_148_[7]	39257	40057	801	hypothetical protein	- none -	39257	40057
fig|1504.6.peg.2868	CDS	node_148_[7]	40054	40839	786	hypothetical protein	- none -	40054	40839
fig|1504.6.peg.2869	CDS	node_148_[7]	40836	41462	627	ABC transporter, ATP-binding protein	- none -	40836	41462
fig|1504.6.peg.2870	CDS	node_148_[7]	42372	41671	702	Glycerol uptake facilitator protein	Glycerol and Glycerol-3-phosphate Uptake and Utilization, Osmoregulation	41671	42372

Feature ID	Type	Contig	Start	Stop	Length (bp)	Function	Subsystems	Begin	End
fig|1504.6.peg.2871	CDS	node_148_[7]	42843	44252	1410	Mobile element protein	- none -	42843	44252
fig|1504.6.peg.2872	CDS	node_148_[7]	44696	44343	354	FIG00513440: hypothetical protein	- none -	44343	44696
fig|1504.6.peg.2873	CDS	node_148_[7]	45992	44751	1242	Sarcosine oxidase alpha subunit (EC 1.5.3.1)	Choline and Betaine Uptake and Betaine Biosynthesis	44751	45992
fig|1504.6.peg.2874	CDS	node_148_[7]	47437	46004	1434	Glycerol-3-phosphate dehydrogenase (EC 1.1.5.3)	Glycerol and Glycerol-3-phosphate Uptake and Utilization, Glycerolipid and Glycerophospholipid Metabolism in Bacteria, Respiratory dehydrogenases 1	46004	47437
fig|1504.6.peg.2875	CDS	node_148_[7]	49136	47640	1497	Glycerol kinase (EC 2.7.1.30)	Glycerol and Glycerol-3-phosphate Uptake and Utilization, Glycerolipid and Glycerophospholipid Metabolism in Bacteria	47640	49136
fig|1504.6.peg.2876	CDS	node_148_[7]	52100	49557	2544	TETRATRICOPEPTIDE REPEAT FAMILY PROTEIN	- none -	49557	52100
fig|1504.6.peg.2877	CDS	node_148_[7]	53223	52276	948	Kinase similar to eukaryotic-like N-acetylglucosamine kinase	- none -	52276	53223
fig|1504.6.peg.2878	CDS	node_148_[7]	54334	53240	1095	Outer surface protein of unknown function, cellobiose operon	Beta-Glucoside Metabolism	53240	54334
fig|1504.6.peg.2879	CDS	node_148_[7]	55678	54410	1269	PTS system, cellobiose-specific IIC component (EC 2.7.1.69)	Beta-Glucoside Metabolism	54410	55678
fig|1504.6.peg.2880	CDS	node_148_[7]	56061	55753	309	PTS system, diacetylchitobiose-specific IIB component (EC 2.7.1.69)	Beta-Glucoside Metabolism	55753	56061
fig|1504.6.peg.2881	CDS	node_148_[7]	56608	56219	390	hypothetical protein	- none -	56219	56608
fig|1504.6.peg.2882	CDS	node_148_[7]	57761	56613	1149	Anhydro-N-acetylmuramic acid kinase (EC 2.7.1.-)	Recycling of Peptidoglycan Amino Sugars	56613	57761
fig|1504.6.peg.2883	CDS	node_148_[7]	58151	57834	318	PTS system, cellobiose-specific IIA component (EC 2.7.1.69)	Beta-Glucoside Metabolism	57834	58151
fig|1504.6.peg.2884	CDS	node_148_[7]	59090	58185	906	N-acetylmuramic acid 6-phosphate etherase	- none -	58185	59090
fig|1504.6.peg.2885	CDS	node_148_[7]	59131	60237	1107	Mobile element protein	- none -	59131	60237
fig|1504.6.peg.2886	CDS	node_148_[7]	60884	60648	237	hypothetical protein	- none -	60648	60884
fig|1504.6.peg.2887	CDS	node_148_[7]	61903	61067	837	Sialic acid utilization regulator, RpiR family	Sialic Acid Metabolism	61067	61903

Feature ID	Type	Contig	Start	Stop	Length (bp)	Function	Subsystems	Begin	End
fig|1504.6.peg.2888	CDS	node_148_[7]	62805	62035	771	hypothetical protein	- none -	62035	62805
fig|1504.6.peg.2889	CDS	node_148_[7]	63710	62988	723	amino acid ABC transporter, ATP-binding protein	- none -	62988	63710
fig|1504.6.peg.2890	CDS	node_148_[7]	64377	63697	681	Amino acid ABC transporter, amino acid-binding/permease protein	- none -	63697	64377
fig|1504.6.peg.2891	CDS	node_148_[7]	65271	64432	840	Amino acid ABC transporter, amino acid-binding/permease protein	- none -	64432	65271
fig|1504.6.peg.2892	CDS	node_148_[7]	65707	66789	1083	ATPase component BioM of energizing module of biotin ECF transporter	Biotin biosynthesis, ECF class transporters	65707	66789
fig|1504.6.peg.2893	CDS	node_148_[7]	66969	68318	1350	Methyl-accepting chemotaxis protein	- none -	66969	68318
fig|1504.6.peg.2894	CDS	node_148_[7]	68625	68461	165	hypothetical protein	- none -	68461	68625
fig|1504.6.peg.2895	CDS	node_148_[7]	71109	69004	2106	ATP-dependent DNA helicase rep (EC 3.6.1.-)	- none -	69004	71109
fig|1504.6.peg.2896	CDS	node_148_[7]	73159	71240	1920	Cell division protein FtsH (EC 3.4.24.-)	Bacterial Cell Division, Cell division-ribosomal stress proteins cluster, Folate biosynthesis cluster	71240	73159
fig|1504.6.peg.2897	CDS	node_148_[7]	73742	73176	567	Signal peptidase I (EC 3.4.21.89)	CBSS-176299.4.peg.1292, Signal peptidase	73176	73742
fig|1504.6.peg.2898	CDS	node_148_[7]	74303	73773	531	Signal peptidase I (EC 3.4.21.89)	CBSS-176299.4.peg.1292, Signal peptidase	73773	74303
fig|1504.6.peg.2899	CDS	node_148_[7]	74521	74303	219	no significant homology.	- none -	74303	74521
fig|1504.6.peg.2900	CDS	node_148_[7]	76031	74739	1293	Diaminopimelate decarboxylase (EC 4.1.1.20)	Lysine Biosynthesis DAP Pathway, Lysine Biosynthesis DAP Pathway, GJO scratch	74739	76031
fig|1504.6.peg.2901	CDS	node_148_[7]	76269	76141	129	hypothetical protein	- none -	76141	76269
fig|1504.6.peg.2902	CDS	node_148_[7]	77157	76486	672	probable enzyme with TIM-barrel fold	- none -	76486	77157
fig|1504.6.peg.2903	CDS	node_148_[7]	77380	78621	1242	Permeases of the major facilitator superfamily	- none -	77380	78621
fig|1504.6.peg.2904	CDS	node_148_[7]	78626	78970	345	hypothetical protein	- none -	78626	78970
fig|1504.6.peg.2905	CDS	node_148_[7]	80429	79191	1239	Mobile element protein	- none -	79191	80429
fig|1504.6.peg.2906	CDS	node_148_[7]	81047	80553	495	NADH pyrophosphatase (EC 3.6.1.22)	Nudix proteins (nucleoside triphosphate hydrolases)	80553	81047

Feature ID	Type	Contig	Start	Stop	Length (bp)	Function	Subsystems	Begin	End
fig|1504.6.peg.2907	CDS	node_148_[7]	81801	81106	696	Sugar/maltose fermentation stimulation protein homolog	Fermentations: Mixed acid	81106	81801
fig|1504.6.peg.2908	CDS	node_148_[7]	81818	82249	432	hypothetical protein	- none -	81818	82249
fig|1504.6.peg.2909	CDS	node_148_[7]	82405	83166	762	lmo0600	- none -	82405	83166
fig|1504.6.peg.2910	CDS	node_148_[7]	83166	84170	1005	hypothetical protein	- none -	83166	84170
fig|1504.6.peg.2911	CDS	node_148_[7]	84421	84236	186	hypothetical protein	- none -	84236	84421
fig|1504.6.peg.2912	CDS	node_148_[7]	84892	84590	303	hypothetical protein	- none -	84590	84892
fig|1504.6.peg.2913	CDS	node_148_[7]	85819	84956	864	hypothetical protein BH3604	CBSS-393121.3.peg.2760	84956	85819
fig|1504.6.peg.2914	CDS	node_148_[7]	86626	85979	648	putative acyl carrier protein phosphodiesterase	- none -	85979	86626
fig|1504.6.peg.2915	CDS	node_148_[7]	87532	86681	852	Spermidine synthase (EC 2.5.1.16)	Polyamine Metabolism	86681	87532
fig|1504.6.peg.2916	CDS	node_148_[7]	87955	87536	420	S-adenosylmethionine decarboxylase proenzyme (EC 4.1.1.50), prokaryotic class 1B	Polyamine Metabolism	87536	87955
fig|1504.6.peg.2917	CDS	node_148_[7]	89864	88224	1641	Sulfate permease	Cysteine Biosynthesis	88224	89864
fig|1504.6.peg.2918	CDS	node_148_[7]	91306	90119	1188	FIG00525398: hypothetical protein	- none -	90119	91306
fig|1504.6.peg.2919	CDS	node_148_[7]	91983	92687	705	response regulator, putative virR	- none -	91983	92687
fig|1504.6.peg.2920	CDS	node_148_[7]	92781	94415	1635	sensor histidine kinase, putative virS	- none -	92781	94415
fig|1504.6.peg.2921	CDS	node_148_[7]	94739	95707	969	hypothetical protein	- none -	94739	95707
fig|1504.6.peg.2922	CDS	node_148_[7]	97048	95828	1221	Transposase, mutator type	- none -	95828	97048
fig|1504.6.peg.2923	CDS	node_148_[7]	97138	97341	204	hypothetical protein	- none -	97138	97341
fig|1504.6.peg.2924	CDS	node_148_[7]	97972	97580	393	3-oxoacyl-[acyl-carrier protein] reductase (EC 1.1.1.100)	Fatty Acid Biosynthesis FASII	97580	97972
fig|1504.6.peg.2925	CDS	node_148_[8]	113	922	810	Dihydropteroate synthase (EC 2.5.1.15)	Folate Biosynthesis, Folate biosynthesis cluster	113	922
fig|1504.6.peg.2926	CDS	node_148_[8]	936	1763	828	Dihydroneopterin aldolase (EC 4.1.2.25) / 2-amino-4-hydroxy-6-hydroxymethyldihydropteridine pyrophosphokinase (EC 2.7.6.3)	Folate Biosynthesis, Folate Biosynthesis, Folate biosynthesis cluster, Folate biosynthesis cluster	936	1763
fig|1504.6.peg.2927	CDS	node_148_[8]	1884	3122	1239	Mobile element protein	- none -	1884	3122

Feature ID	Type	Contig	Start	Stop	Length (bp)	Function	Subsystems	Begin	End
fig|1504.6.peg.2928	CDS	node_148_[8]	3830	3342	489	Conserved protein	- none -	3342	3830
fig|1504.6.peg.2929	CDS	node_148_[8]	3951	4385	435	hypothetical protein	- none -	3951	4385
fig|1504.6.peg.2930	CDS	node_148_[8]	4489	5517	1029	Similar to pyruvate kinase	- none -	4489	5517
fig|1504.6.peg.2931	CDS	node_148_[8]	5586	6368	783	putative signalling component	- none -	5586	6368
fig|1504.6.peg.2932	CDS	node_148_[8]	6427	7215	789	ABC transporter ATP-binding protein	- none -	6427	7215
fig|1504.6.peg.2933	CDS	node_148_[8]	7217	8872	1656	ABC transporter, permease protein	- none -	7217	8872
fig|1504.6.peg.2934	CDS	node_148_[8]	9353	9036	318	hypothetical protein	- none -	9036	9353
fig|1504.6.peg.2935	CDS	node_148_[8]	9923	9381	543	Rubrerythrin	Oxidative stress, Rubrerythrin	9381	9923
fig|1504.6.peg.2936	CDS	node_148_[8]	10205	11578	1374	Na+ driven multidrug efflux pump	- none -	10205	11578
fig|1504.6.peg.2937	CDS	node_148_[8]	11825	12088	264	hypothetical protein	- none -	11825	12088
fig|1504.6.peg.2938	CDS	node_148_[8]	12138	12431	294	hypothetical protein	- none -	12138	12431
fig|1504.6.peg.2939	CDS	node_148_[8]	13161	13280	120	hypothetical protein	- none -	13161	13280
fig|1504.6.peg.2940	CDS	node_148_[8]	13264	14193	930	membrane protein	- none -	13264	14193
fig|1504.6.peg.2941	CDS	node_148_[8]	14316	14609	294	Mobile element protein	- none -	14316	14609
fig|1504.6.rna.70	RNA	node_148_[8]	15013	14933	81	tRNA-Leu-CAA	- none -	14933	15013
fig|1504.6.peg.2942	CDS	node_148_[8]	15261	15953	693	no significant homology.	- none -	15261	15953
fig|1504.6.peg.2943	CDS	node_148_[8]	15976	16977	1002	no significant homology.	- none -	15976	16977
fig|1504.6.peg.2944	CDS	node_148_[8]	17626	20244	2619	Mg(2+) transport ATPase, P-type (EC 3.6.3.2)	Magnesium transport	17626	20244
fig|1504.6.peg.2945	CDS	node_148_[8]	20457	21770	1314	Xanthine/uracil/thiamine/ascorbate permease family protein	Purine Utilization	20457	21770
fig|1504.6.peg.2946	CDS	node_148_[8]	22152	23582	1431	Probable transport protein	- none -	22152	23582
fig|1504.6.peg.2947	CDS	node_148_[8]	23812	24102	291	hypothetical protein	- none -	23812	24102
fig|1504.6.peg.2948	CDS	node_148_[8]	24179	25063	885	transcriptional regulator, MerR family	- none -	24179	25063
fig|1504.6.peg.2949	CDS	node_148_[8]	25164	26180	1017	Putative membrane protein YeiH	- none -	25164	26180
fig|1504.6.peg.2950	CDS	node_148_[8]	26438	27646	1209	Isocitrate dehydrogenase [NADP] (EC 1.1.1.42)	5-FCL-like protein	26438	27646
fig|1504.6.peg.2951	CDS	node_148_[8]	27723	27884	162	no significant homology.	- none -	27723	27884

Feature ID	Type	Contig	Start	Stop	Length (bp)	Function	Subsystems	Begin	End
fig|1504.6.peg.2952	CDS	node_148_[8]	28812	27910	903	Ribosome-associated endonuclease, involved in final steps of 23S rRNA maturation	- none -	27910	28812
fig|1504.6.peg.2953	CDS	node_148_[8]	30157	28925	1233	Aminopeptidase S (Leu, Val, Phe, Tyr preference) (EC 3.4.11.24)	Aminopeptidases (EC 3.4.11.-)	28925	30157
fig|1504.6.peg.2954	CDS	node_148_[8]	30324	31241	918	Glutaminase (EC 3.5.1.2)	Glutamine, Glutamate, Aspartate and Asparagine Biosynthesis	30324	31241
fig|1504.6.peg.2955	CDS	node_148_[8]	31405	34011	2607	DNA polymerase I (EC 2.7.7.7)	DNA-replication, DNA Repair Base Excision	31405	34011
fig|1504.6.peg.2956	CDS	node_148_[8]	34027	34626	600	Dephospho-CoA kinase (EC 2.7.1.24)	Coenzyme A Biosynthesis	34027	34626
fig|1504.6.peg.2957	CDS	node_148_[8]	34641	35186	546	Soluble lytic murein transglycosylase precursor (EC 3.2.1.-)	Murein Hydrolases	34641	35186
fig|1504.6.peg.2958	CDS	node_148_[8]	36180	35320	861	Ribosomal protein L11 methyltransferase (EC 2.1.1.-)	Heat shock dnaK gene cluster extended, Ribosome biogenesis bacterial	35320	36180
fig|1504.6.peg.2959	CDS	node_148_[8]	36918	36262	657	Flavoredoxin	- none -	36262	36918
fig|1504.6.peg.2960	CDS	node_148_[8]	38309	37029	1281	D-alanyl-D-alanine carboxypeptidase (EC 3.4.16.4)	CBSS-84588.1.peg.1247, Metallocarboxypeptidases (EC 3.4.17.-), Murein Hydrolases	37029	38309
fig|1504.6.peg.2961	CDS	node_148_[8]	38596	39231	636	Peptidoglycan N-acetylglucosamine deacetylase (EC 3.5.1.-)	Polysaccharide deacetylases	38596	39231
fig|1504.6.peg.2962	CDS	node_148_[8]	40078	39353	726	Putative amidotransferase similar to cobyric acid synthase	- none -	39353	40078
fig|1504.6.peg.2963	CDS	node_148_[8]	41451	40093	1359	proposed amino acid ligase found clustered with an amidotransferase	- none -	40093	41451
fig|1504.6.peg.2964	CDS	node_148_[8]	41655	42578	924	Lysophospholipase (EC 3.1.1.5); Monoglyceride lipase (EC 3.1.1.23); putative	Triacylglycerol metabolism, Triacylglycerol metabolism	41655	42578
fig|1504.6.peg.2965	CDS	node_148_[8]	43039	44655	1617	two-component sensor histidine kinase	- none -	43039	44655
fig|1504.6.peg.2966	CDS	node_148_[8]	44645	46633	1989	sensor histidine kinase	- none -	44645	46633
fig|1504.6.peg.2967	CDS	node_148_[8]	46693	47268	576	Benzodiazepine receptor TspO	- none -	46693	47268
fig|1504.6.peg.2968	CDS	node_148_[8]	47651	49840	2190	DNA topoisomerase III (EC 5.99.1.2)	DNA processing cluster, DNA topoisomerases, Type I, ATP-independent	47651	49840
fig|1504.6.peg.2969	CDS	node_148_[8]	50639	49935	705	LrgA-associated membrane protein LrgB	Murein hydrolase regulation and cell death	49935	50639

Feature ID	Type	Contig	Start	Stop	Length (bp)	Function	Subsystems	Begin	End
fig|1504.6.peg.2970	CDS	node_148_[8]	51013	50639	375	Antiholin-like protein LrgA	Murein hydrolase regulation and cell death	50639	51013
fig|1504.6.peg.2971	CDS	node_148_[8]	51152	52105	954	FIG00529298: hypothetical protein	- none -	51152	52105
fig|1504.6.peg.2972	CDS	node_148_[8]	52290	52547	258	ABC transporter, substrate-binding protein, putative	- none -	52290	52547
fig|1504.6.peg.2973	CDS	node_148_[8]	52672	53133	462	hypothetical protein	- none -	52672	53133
fig|1504.6.peg.2974	CDS	node_148_[8]	55096	53501	1596	cassette chromosome recombinase B	- none -	53501	55096
fig|1504.6.peg.2975	CDS	node_148_[8]	56476	55856	621	hypothetical protein	- none -	55856	56476
fig|1504.6.peg.2976	CDS	node_148_[8]	56922	56473	450	hypothetical protein	- none -	56473	56922
fig|1504.6.peg.2977	CDS	node_148_[8]	57852	56932	921	DNA polymerase III, epsilon subunit related 3'-5' exonuclease	- none -	56932	57852
fig|1504.6.peg.2978	CDS	node_148_[8]	58795	57881	915	Phage protein	- none -	57881	58795
fig|1504.6.peg.2979	CDS	node_148_[8]	59286	58912	375	Transcriptional regulator, Cro/CI family	- none -	58912	59286
fig|1504.6.peg.2980	CDS	node_148_[8]	59522	59695	174	hypothetical protein	- none -	59522	59695
fig|1504.6.peg.2981	CDS	node_148_[8]	59760	59951	192	hypothetical protein	- none -	59760	59951
fig|1504.6.peg.2982	CDS	node_148_[8]	60310	60486	177	hypothetical protein	- none -	60310	60486
fig|1504.6.peg.2983	CDS	node_148_[8]	60690	60824	135	hypothetical protein	- none -	60690	60824
fig|1504.6.peg.2984	CDS	node_148_[8]	61039	61338	300	hypothetical protein	- none -	61039	61338
fig|1504.6.peg.2985	CDS	node_148_[8]	61512	61625	114	hypothetical protein	- none -	61512	61625
fig|1504.6.peg.2986	CDS	node_148_[8]	62099	63076	978	N-acetylmuramoyl-L-alanine amidase (EC 3.5.1.28)	Murein Hydrolases, Recycling of Peptidoglycan Amino Acids	62099	63076
fig|1504.6.peg.2987	CDS	node_148_[8]	64952	63459	1494	Mobile element protein	- none -	63459	64952
fig|1504.6.peg.2988	CDS	node_148_[8]	66710	65685	1026	Mobile element protein	- none -	65685	66710
fig|1504.6.peg.2989	CDS	node_148_[8]	66750	66908	159	hypothetical protein	- none -	66750	66908
fig|1504.6.peg.2990	CDS	node_148_[8]	67286	67035	252	Spore coat protein F	- none -	67035	67286
fig|1504.6.peg.2991	CDS	node_148_[8]	67484	67299	186	hypothetical protein	- none -	67299	67484
fig|1504.6.peg.2992	CDS	node_148_[8]	67670	68341	672	Polypeptide composition of the spore coat protein CotJC	- none -	67670	68341
fig|1504.6.peg.2993	CDS	node_148_[8]	68776	70386	1611	Phage protein	- none -	68776	70386

Feature ID	Type	Contig	Start	Stop	Length (bp)	Function	Subsystems	Begin	End
fig|1504.6.peg.2994	CDS	node_148_[8]	70462	71250	789	ABC transporter substrate-binding protein	- none -	70462	71250
fig|1504.6.peg.2995	CDS	node_148_[8]	71344	72111	768	Hydroxymethylpyrimidine ABC transporter, ATPase component	Thiamin biosynthesis	71344	72111
fig|1504.6.peg.2996	CDS	node_148_[8]	72104	72892	789	Hydroxymethylpyrimidine ABC transporter, transmembrane component	Thiamin biosynthesis	72104	72892
fig|1504.6.peg.2997	CDS	node_148_[8]	73013	74746	1734	tetratricopeptide repeat domain protein	- none -	73013	74746
fig|1504.6.peg.2998	CDS	node_148_[8]	74810	75919	1110	Conserved protein	- none -	74810	75919
fig|1504.6.peg.2999	CDS	node_148_[8]	75995	76879	885	Undecaprenyl-diphosphatase (EC 3.6.1.27)	- none -	75995	76879
fig|1504.6.peg.3000	CDS	node_148_[8]	77106	78206	1101	6-phosphofructokinase (EC 2.7.1.11)	Glycolysis and Gluconeogenesis, N-Acetyl-Galactosamine and Galactosamine Utilization	77106	78206
fig|1504.6.peg.3001	CDS	node_148_[8]	78364	79143	780	Beta-lactamase (EC 3.5.2.6)	Beta-lactamase	78364	79143
fig|1504.6.peg.3002	CDS	node_148_[8]	80426	80548	123	hypothetical protein	- none -	80426	80548
fig|1504.6.peg.3003	CDS	node_148_[8]	82159	81938	222	hypothetical protein	- none -	81938	82159
fig|1504.6.peg.3004	CDS	node_148_[8]	82800	83720	921	Aspartate carbamoyltransferase (EC 2.1.3.2)	De Novo Pyrimidine Synthesis	82800	83720
fig|1504.6.peg.3005	CDS	node_148_[8]	83720	84145	426	Aspartate carbamoyltransferase regulatory chain (PyrI)	De Novo Pyrimidine Synthesis	83720	84145
fig|1504.6.peg.3006	CDS	node_148_[8]	84168	85364	1197	Dihydroorotase (EC 3.5.2.3)	De Novo Pyrimidine Synthesis	84168	85364
fig|1504.6.peg.3007	CDS	node_148_[8]	85375	86250	876	Orotidine 5'-phosphate decarboxylase (EC 4.1.1.23)	De Novo Pyrimidine Synthesis, Riboflavin synthesis cluster	85375	86250
fig|1504.6.peg.3008	CDS	node_148_[8]	86268	87005	738	Dihydroorotate dehydrogenase electron transfer subunit (EC 1.3.3.1)	De Novo Pyrimidine Synthesis	86268	87005
fig|1504.6.peg.3009	CDS	node_148_[8]	87025	87924	900	Dihydroorotate dehydrogenase, catalytic subunit (EC 1.3.3.1)	De Novo Pyrimidine Synthesis	87025	87924
fig|1504.6.peg.3010	CDS	node_148_[8]	88378	88055	324	no significant homology. 1 putative transmembrane region was found by PSORT	- none -	88055	88378
fig|1504.6.peg.3011	CDS	node_148_[8]	88753	88400	354	no significant homology. 1 putative transmembrane region was found by PSORT	- none -	88400	88753
fig|1504.6.peg.3012	CDS	node_148_[8]	88932	89780	849	hypothetical protein	- none -	88932	89780
fig|1504.6.peg.3013	CDS	node_148_[8]	91241	89814	1428	sodium:alanine symporter family protein	- none -	89814	91241
fig|1504.6.peg.3014	CDS	node_148_[8]	94127	91521	2607	Multimodular transpeptidase-transglycosylase (EC 2.4.1.129) (EC 3.4.-.-)	- none -	91521	94127

Feature ID	Type	Contig	Start	Stop	Length (bp)	Function	Subsystems	Begin	End
fig|1504.6.peg.3015	CDS	node_148_[8]	94353	94240	114	hypothetical protein	- none -	94240	94353
fig|1504.6.peg.3016	CDS	node_148_[8]	94388	94888	501	Conserved protein	- none -	94388	94888
fig|1504.6.peg.3017	CDS	node_148_[8]	95493	94963	531	Hypoxanthine-guanine phosphoribosyltransferase (EC 2.4.2.8)	Cell division-ribosomal stress proteins cluster, Folate biosynthesis cluster, Purine conversions	94963	95493
fig|1504.6.peg.3018	CDS	node_148_[8]	95627	97423	1797	GTP-binding protein HflX	Hfl operon, Universal GTPases	95627	97423
fig|1504.6.peg.3019	CDS	node_148_[8]	97461	98156	696	no significant homology	- none -	97461	98156
fig|1504.6.peg.3020	CDS	node_148_[8]	98221	99123	903	probable nucleotidyltransferase	- none -	98221	99123
fig|1504.6.peg.3021	CDS	node_148_[8]	99144	100547	1404	Transcriptional regulator, GntR family domain / Aspartate aminotransferase (EC 2.6.1.1)	CBSS-216591.1.peg.168, Glutamine, Glutamate, Aspartate and Asparagine Biosynthesis, Threonine and Homoserine Biosynthesis	99144	100547
fig|1504.6.peg.3022	CDS	node_148_[8]	100547	101194	648	FIG000605: protein co-occurring with transport systems (COG1739)	- none -	100547	101194
fig|1504.6.peg.3023	CDS	node_148_[8]	101315	102046	732	FIG000859: hypothetical protein YebC	Riboflavin, FMN and FAD metabolism in plants, RuvABC plus a hypothetical	101315	102046
fig|1504.6.peg.3024	CDS	node_148_[8]	102655	102194	462	no significant homology	- none -	102194	102655
fig|1504.6.peg.3025	CDS	node_148_[8]	103152	106694	3543	FIG00528563: hypothetical protein	- none -	103152	106694
fig|1504.6.peg.3026	CDS	node_148_[8]	106851	107894	1044	OB-fold nucleic acid binding domain protein	- none -	106851	107894
fig|1504.6.peg.3027	CDS	node_148_[8]	107985	109145	1161	membrane protein, YbiE/YbiF family	- none -	107985	109145
fig|1504.6.peg.3028	CDS	node_148_[8]	109347	111353	2007	two-component sensor histidine kinase	- none -	109347	111353
fig|1504.6.peg.3029	CDS	node_148_[8]	111641	113683	2043	2',3'-cyclic-nucleotide 2'-phosphodiesterase (EC 3.1.4.16) / 5'-nucleotidase (EC 3.1.3.5)	Purine conversions, Purine conversions, pyrimidine conversions, pyrimidine conversions	111641	113683
fig|1504.6.peg.3030	CDS	node_148_[8]	113788	114894	1107	probable peptidase	- none -	113788	114894
fig|1504.6.peg.3031	CDS	node_148_[8]	115482	114949	534	Molecular chaperone, DnaJ family (contain C-term. Zn finger domain)	- none -	114949	115482
fig|1504.6.peg.3032	CDS	node_148_[8]	115850	116728	879	Molybdenum cofactor biosynthesis enzyme and related Fe-S oxidoreductases	- none -	115850	116728

Feature ID	Type	Contig	Start	Stop	Length (bp)	Function	Subsystems	Begin	End
fig|1504.6.peg.3033	CDS	node_148_[8]	116753	117721	969	hypothetical protein	- none -	116753	117721
fig|1504.6.peg.3034	CDS	node_148_[8]	118091	119191	1101	Diaminohydroxyphosphoribosylaminopyrimidine deaminase (EC 3.5.4.26) / 5-amino-6-(5-phosphoribosylamino)uracil reductase (EC 1.1.1.193)	Riboflavin, FMN and FAD metabolism, Riboflavin, FMN and FAD metabolism, Riboflavin, FMN and FAD metabolism in plants, Riboflavin, FMN and FAD metabolism in plants, Riboflavin synthesis cluster, Riboflavin synthesis cluster	118091	119191
fig|1504.6.peg.3035	CDS	node_148_[8]	119216	119866	651	Riboflavin synthase eubacterial/eukaryotic (EC 2.5.1.9)	Riboflavin, FMN and FAD metabolism, Riboflavin, FMN and FAD metabolism in plants, Riboflavin synthesis cluster, riboflavin to FAD	119216	119866
fig|1504.6.peg.3036	CDS	node_148_[8]	119933	121120	1188	3,4-dihydroxy-2-butanone 4-phosphate synthase (EC 4.1.99.12) / GTP cyclohydrolase II (EC 3.5.4.25)	Molybdenum cofactor biosynthesis, Riboflavin, FMN and FAD metabolism, Riboflavin, FMN and FAD metabolism, Riboflavin, FMN and FAD metabolism in plants, Riboflavin, FMN and FAD metabolism in plants, Riboflavin synthesis cluster, Riboflavin synthesis cluster, riboflavin to FAD	119933	121120
fig|1504.6.peg.3037	CDS	node_148_[8]	121166	121630	465	6,7-dimethyl-8-ribityllumazine synthase (EC 2.5.1.78)	Riboflavin, FMN and FAD metabolism, Riboflavin, FMN and FAD metabolism in plants, Riboflavin synthesis cluster	121166	121630
fig|1504.6.peg.3038[12]	CDS	node_148_[8]	121797	125555	3759	Putative hemagglutinin/hemolysin-related protein	- none -	121797	125555
fig|1504.6.peg.3039	CDS	node_148_[8]	125700	125924	225	hypothetical protein	- none -	125700	125924
fig|1504.6.peg.3040	CDS	node_148_[8]	126039	126650	612	DNA-3-methyladenine glycosylase II (EC 3.2.2.21)	DNA Repair Base Excision	126039	126650
fig|1504.6.peg.3041	CDS	node_148_[8]	126733	127095	363	hypothetical protein	- none -	126733	127095
fig|1504.6.peg.3042	CDS	node_148_[8]	127221	128450	1230	tunicamycin resistance	- none -	127221	128450

Feature ID	Type	Contig	Start	Stop	Length (bp)	Function	Subsystems	Begin	End
fig|1504.6.peg.3043	CDS	node_148_[8]	128573	129439	867	DegV family protein	- none -	128573	129439
fig|1504.6.peg.3044	CDS	node_148_[8]	129529	130128	600	regulatory protein, TetR	- none -	129529	130128
fig|1504.6.peg.3045	CDS	node_148_[8]	130352	132445	2094	hypothetical protein	- none -	130352	132445
fig|1504.6.peg.3046	CDS	node_148_[8]	132451	134157	1707	hypothetical protein	- none -	132451	134157
fig|1504.6.peg.3047	CDS	node_148_[8]	134313	135542	1230	Repeated DNA sequence	- none -	134313	135542
fig|1504.6.peg.3048	CDS	node_148_[8]	135557	135748	192	hypothetical protein	- none -	135557	135748
fig|1504.6.peg.3049	CDS	node_148_[8]	135906	136514	609	Conserved protein	- none -	135906	136514
fig|1504.6.peg.3050	CDS	node_148_[8]	136603	137010	408	hypothetical protein	- none -	136603	137010
fig|1504.6.peg.3051	CDS	node_148_[8]	137182	137787	606	Holliday junction DNA helicase RuvA	DNA-replication, RuvABC plus a hypothetical	137182	137787
fig|1504.6.peg.3052	CDS	node_148_[8]	137798	138826	1029	Holliday junction DNA helicase RuvB	DNA-replication, RuvABC plus a hypothetical	137798	138826
fig|1504.6.peg.3053	CDS	node_148_[8]	138866	139891	1026	S-adenosylmethionine:tRNA ribosyltransferase-isomerase (EC 5.-.-.-)	CBSS-211586.1.peg.2832, Queuosine-Archaeosine Biosynthesis, tRNAmodification position 34	138866	139891
fig|1504.6.peg.3054	CDS	node_148_[8]	139923	141065	1143	tRNA-guanine transglycosylase (EC 2.4.2.29)	CBSS-211586.1.peg.2832, Queuosine-Archaeosine Biosynthesis, tRNAmodification position 34	139923	141065
fig|1504.6.peg.3055	CDS	node_148_[8]	141170	141439	270	Preprotein translocase subunit YajC (TC 3.A.5.1.1)	CBSS-211586.1.peg.2832	141170	141439
fig|1504.6.peg.3056	CDS	node_148_[8]	141491	141859	369	FIG00514125: hypothetical protein	- none -	141491	141859
fig|1504.6.peg.3057	CDS	node_148_[8]	142027	143295	1269	Protein-export membrane protein SecD (TC 3.A.5.1.1)	CBSS-211586.1.peg.2832	142027	143295
fig|1504.6.peg.3058	CDS	node_148_[8]	143288	144160	873	Protein-export membrane protein SecF (TC 3.A.5.1.1)	CBSS-211586.1.peg.2832	143288	144160
fig|1504.6.peg.3059	CDS	node_148_[8]	144300	145154	855	Single-stranded-DNA-specific exonuclease RecJ, clostridial paralog	DNA Repair Base Excision, DNA repair, bacterial RecFOR pathway	144300	145154
fig|1504.6.peg.3060	CDS	node_148_[8]	145243	145761	519	Adenine phosphoribosyltransferase (EC 2.4.2.7)	Purine conversions, cAMP signaling in bacteria	145243	145761

Feature ID	Type	Contig	Start	Stop	Length (bp)	Function	Subsystems	Begin	End
fig|1504.6.peg.3061	CDS	node_148_[8]	145874	148057	2184	GTP pyrophosphokinase (EC 2.7.6.5), (p)ppGpp synthetase I	CBSS-176299.4.peg.1292, Stringent Response, (p)ppGpp metabolism	145874	148057
fig|1504.6.peg.3062	CDS	node_148_[8]	148071	148520	450	D-tyrosyl-tRNA(Tyr) deacylase (EC 3.6.1.n1)	- none -	148071	148520
fig|1504.6.peg.3063	CDS	node_148_[8]	148535	149134	600	Hydroxyacylglutathione hydrolase (EC 3.1.2.6)	CBSS-228410.1.peg.134, CBSS-342610.3.peg.1536, Glutathione: Non-redox reactions, Methylglyoxal Metabolism	148535	149134
fig|1504.6.peg.3064	CDS	node_35_[3]	926	678	249	hypothetical protein	- none -	678	926
fig|1504.6.peg.3065	CDS	node_35_[3]	2129	1353	777	Heme transporter analogous to IsdDEF, ATP-binding protein	Heme, hemin uptake and utilization systems in GramPositives	1353	2129
fig|1504.6.peg.3066	CDS	node_35_[3]	3152	2163	990	Heme transporter IsdDEF, permease component IsdF	Heme, hemin uptake and utilization systems in GramPositives	2163	3152
fig|1504.6.peg.3067	CDS	node_35_[3]	4046	3171	876	Heme transporter IsdDEF, lipoprotein IsdE	Heme, hemin uptake and utilization systems in GramPositives	3171	4046
fig|1504.6.peg.3068	CDS	node_35_[3]	4789	4163	627	putative cell wall anchor domain protein	- none -	4163	4789
fig|1504.6.peg.3069	CDS	node_35_[3]	8184	4798	3387	Streptococcal cell surface hemoprotein receptor Shr	Heme, hemin uptake and utilization systems in GramPositives	4798	8184
fig|1504.6.peg.3070	CDS	node_35_[3]	9545	8571	975	Peptide chain release factor 2; programmed frameshift-containing	CBSS-393121.3.peg.2760, Programmed frameshift, Programmed frameshift, Translation termination factors bacterial	8571	9545
fig|1504.6.peg.3071	CDS	node_35_[3]	12240	9721	2520	Protein export cytoplasm protein SecA ATPase RNA helicase (TC 3.A.5.1.1)	CBSS-393121.3.peg.2760	9721	12240
fig|1504.6.peg.3072	CDS	node_35_[3]	12913	12389	525	Ribosomal subunit interface protein	Ribosome activity modulation	12389	12913
fig|1504.6.peg.3073	CDS	node_35_[3]	14006	13359	648	Competence protein F homolog, phosphoribosyltransferase domain; protein YhgH required for utilization of DNA as sole source of carbon and energy	Biotin biosynthesis Experimental, CBSS-216591.1.peg.168	13359	14006

- Coding sequences corresponding to known or potential toxins genes are highlighted (red rows)
  - [1]Putative hemolysin that is not the alpha toxin; may correspond with the delta toxin
  - [2]Putative deoxyribonuclease; may correspond with the beta toxin
  - [3]Putative hemolysin that is not the alpha toxin; may correspond with the delta toxin
  - [4]Putative leukocidin; may correspond with the beta toxin
  - [5]Hemagglutinin/hemolysin-related peptide; may correspond with the delta toxin
  - [6,7]Putative toxins; do not correspond with any of the known major toxins produced by *C. septicum*
  - [8,9]Putative hyaluronoglucosaminidase; may correspond with the gamma toxin
  - [10]Confirmed gene sequence for the *C. septicum* alpha toxin (CsA)
  - [11]Hyaluronoglucosaminidase precursor; may correspond with the gamma toxin
  - [12]Hemagglutinin/hemolysin-related peptide; may correspond with the delta toxin
- Coding sequences in the Beta-lactamase family are highlighted (blue rows); of interest because Penicillin is a commonly and effectively used in treatment and prevention of field outbreaks of clostridial dermatitis (cellulitis) in turkeys caused by *C. septicum*
- Coding sequences corresponding with phage proteins are highlighted (green rows)